BEILSTEIN JOURNAL OF ORGANIC CHEMISTRY

Natural products in synthesis and biosynthesis II

Edited by Jeroen S. Dickschat

Imprint

Beilstein Journal of Organic Chemistry
www.bjoc.org
ISSN 1860-5397
Email: journals-support@beilstein-institut.de

The *Beilstein Journal of Organic Chemistry* is published by the Beilstein-Institut zur Förderung der Chemischen Wissenschaften.

Beilstein-Institut zur Förderung der Chemischen Wissenschaften
Trakehner Straße 7–9
60487 Frankfurt am Main
Germany
www.beilstein-institut.de

BEILSTEIN JOURNAL OF ORGANIC CHEMISTRY

Natural products in synthesis and biosynthesis II

Jeroen S. Dickschat

Editorial

Open Access

Address:
Kekulé-Institut für Organische Chemie und Biochemie, Rheinische Friedrich-Wilhelms-Universität Bonn, Gerhard-Domagk-Straße 1, D-53121 Bonn, Germany

Email:
Jeroen S. Dickschat - dickschat@uni-bonn.de

Keywords:
biosynthesis; natural products; synthesis

Beilstein J. Org. Chem. **2016,** *12,* 413–414.
doi:10.3762/bjoc.12.44

Received: 12 February 2016
Accepted: 24 February 2016
Published: 03 March 2016

This article is part of the Thematic Series "Natural products in synthesis and biosynthesis II".

Guest Editor: J. S. Dickschat

As a continuation of the first two Thematic Series in the *Beilstein Journal of Organic Chemistry* on natural products in 2011 and 2013 [1,2], it is my pleasure to present the third issue on this topic. Natural products continue to be an inspiring field of research and an important source of potent biologically active compounds. This was recently highlighted by the fact that last year's Nobel Prize in Physiology and Medicine for the discovery of important drugs from natural sources that revolutionised the clinical treatment of parasite-borne infectious diseases was awarded to three natural product researchers: Youyou Tu (Academy of Chinese Medical Sciences) for the discovery of the terpenoid antimalaria drug artemisinin that is produced by the plant *Artemisia annua* [3], and to Satoshi Ōmura and William C. Campbell for the discovery of avermectins isolated from the actinobacterium *Streptomyces avermitilis* at the famous Kitasato Institute and for the development of derivatives that are used as highly potent anthelmintics both for animal and human welfare [4]. Currently, also in the pharmaceutical industry, natural products are experiencing a revival as viable drug candidates, which is a pleasing development since many infectious diseases continue to threaten human health. From the numerous articles in daily newspapers, it is obvious that politicians have also realised the urgent need for new drugs and the potential associated with natural products and their derivatives. Certainly, the recent technological advances in many fields related to natural products (including synthetic methodology, as exemplified by a review article by Thomas Magauer and co-workers in this Thematic Series [5]), analytical chemistry [6], gene synthesis, and genome sequencing and editing [7] offer an efficient toolbox to natural products chemists. In addition, classical methods such as isotopic labelling experiments [8] continue to be important.

I thank all contributors that participated in this third Thematic Series on natural product chemistry in the *Beilstein Journal of Organic Chemistry* and also the whole team at the Beilstein-Institut for their professional work. I wish the readers of the present Thematic Series joyful reading and hopefully new inspiration for their own research.

Jeroen S. Dickschat

Bonn, February 2016

References

1. Dickschat, J. S. *Beilstein J. Org. Chem.* **2011,** *7,* 1620–1621. doi:10.3762/bjoc.7.190

2. Dickschat, J. S. *Beilstein J. Org. Chem.* **2013,** *9,* 1897–1898. doi:10.3762/bjoc.9.223
3. Tu, Y. *Nat. Med.* **2011,** *17,* 1217–1220. doi:10.1038/nm.2471
4. Ōmura, S.; Crump, A. *Nat. Rev. Microbiol.* **2004,** *2,* 984–989. doi:10.1038/nrmicro1048
5. Huber, T.; Weisheit, L.; Magauer, T. *Beilstein J. Org. Chem.* **2015,** *11,* 2521–2539. doi:10.3762/bjoc.11.273
6. Dorrestein, P. C. *Nat. Prod. Rep.* **2014,** *31,* 704–705. doi:10.1039/c4np90016b
7. Travis, J. *Science* **2015,** *350,* 1456–1457. doi:10.1126/science.350.6267.1456
8. Rinkel, J.; Dickschat, J. S. *Beilstein J. Org. Chem.* **2015,** *11,* 2493–2508. doi:10.3762/bjoc.11.271

BEILSTEIN JOURNAL OF ORGANIC CHEMISTRY

Recent highlights in biosynthesis research using stable isotopes

Jan Rinkel and Jeroen S. Dickschat*

Review

Open Access

Address:
Kekulé-Institute of Organic Chemistry and Biochemistry, Gerhard-Domagk-Str. 1, 53121 Bonn, Germany

Email:
Jeroen S. Dickschat* - dickschat@uni-bonn.de

* Corresponding author

Keywords:
biosynthesis; enzyme mechanisms; isotopes; labeling experiments; natural products

Beilstein J. Org. Chem. **2015,** *11,* 2493–2508.
doi:10.3762/bjoc.11.271

Received: 24 September 2015
Accepted: 23 November 2015
Published: 09 December 2015

This article is part of the Thematic Series "Natural products in synthesis and biosynthesis II".

Associate Editor: A. Kirschning

Abstract

The long and successful history of isotopic labeling experiments within natural products research has both changed and deepened our understanding of biosynthesis. As demonstrated in this article, the usage of isotopes is not at all old-fashioned, but continues to give important insights into biosynthetic pathways of secondary metabolites. This review with 85 cited references is structured by separate discussions of compounds from different classes including polyketides, non-ribosomal peptides, their hybrids, terpenoids, and aromatic compounds formed via the shikimate pathway. The text does not aim at a comprehensive overview, but instead a selection of recent important examples of isotope usage within biosynthetic studies is presented, with a special emphasis on mechanistic surprises.

Introduction

This year may be seen as the 80th anniversary of using isotopes in biosynthetical and biochemical research. Since the first experiments performed by Schoenheimer and Rittenberg in 1935 using deuterated fatty acids and sterols to follow their fate in a living organism [1], a lot of new synthetic and analytical methods for the detection of isotopes have been developed that today allow for nearly unlimited applications in biosynthesis research. The basic principle of labeling an organic molecule in a way that is incognito for metabolism, but easy to follow for the researcher still remains the same. The first application of this idea probably was the investigation on fatty acid degradation by Knoop in 1904, even long before isotopes were discovered. He used “chemically labeled” fatty acids with a phenyl residue in ω-position bearing an odd or an even number of carbon atoms in the chain and fed it to dogs [2] to draw important conclusions on the β-oxidation of fatty acids [3] from the reisolated material. However, changing the chemical nature of the metabolite did not prove to be suitable for broader applica-

tions, and therefore, after the discovery of the isotopes by Frederick Soddy, for which he was awarded the Nobel prize in 1921, the first labeling experiments using isotopes quickly changed the way of investigating metabolic pathways and promoted a new dynamic view on biosynthesis research [4], leading to numerous breakthroughs such as the discovery of cholesterol biosynthesis [5]. With the rise of NMR and MS methods the usage of radioactive nuclei such as ^{14}C and ^{3}H shifted towards stable isotopes such as ^{13}C and ^{2}H [6], with the consequence that chemical degradation methods in natural products chemistry are almost vanished today. The usage of isotopically labeled precursors depends on careful interpretations of the incorporation pattern, which sometimes may lead to errors if unknown metabolic pathways are involved, as in the prominent example of the deoxyxylulose phosphate way in terpene biosynthesis [7,8]. Thus, a critical analysis of labeling experiments is required and may hint towards undiscovered metabolic pathways or enzyme functions [9]. As demonstrated in this article, the isotopic labeling technique continues to be an inspiring source of useful information in biosynthesis research. Isotopes have also found their way to many other applications, e.g., in systems biology including proteomics [10], lipidomics [11] and metabolomics [12], or for mapping isotopic fingerprints of whole organisms in metabolic flux studies [13], but these aspects will not be discussed here. Instead, this review highlights recent biosynthetic studies using isotopes from major classes of natural products including polyketides, non-ribosomal peptides, hybrids thereof, isoprenoids and a few aromatic compounds that arise via the shikimate pathway. It does not provide a comprehensive overview of all the work conducted, but tries to create a diversified picture of isotope usage in the study of selected interesting natural products. IUPAC nomenclature allows to distinguish isotopically substituted (every molecule in a sample is labeled at the designated position) and isotopically labeled compounds (a fraction of the molecules in a sample is labeled) by use of round or square brackets, respectively [14]. The assignments used in this article are based on the presentations in the original publications, even if the nomenclature in the original work may not precisely follow the IUPAC rules.

Review

Polyketides

Polyketide synthases (PKS) are multidomain enzymes that catalyze the formation of natural products via reaction steps similar to fatty acid biosynthesis, in which C_2-units are fused in Claisen condensations and modified in an iterative or modular fashion [15]. In contrast to fatty acid synthases (FAS), PKSs do not necessarily process the initially formed 3-keto functions through a complete reductive cycle, which leads to structurally diverse products as shown in Figure 1 for lovastatin (**1**), an inhibitor of 3-hydroxy-3-methylglutaryl CoA reductase [16], aflatoxin B_1 (**2**) [17] and the potent antifungal agent amphotericin B (**3**) [18], which affects membrane integrity.

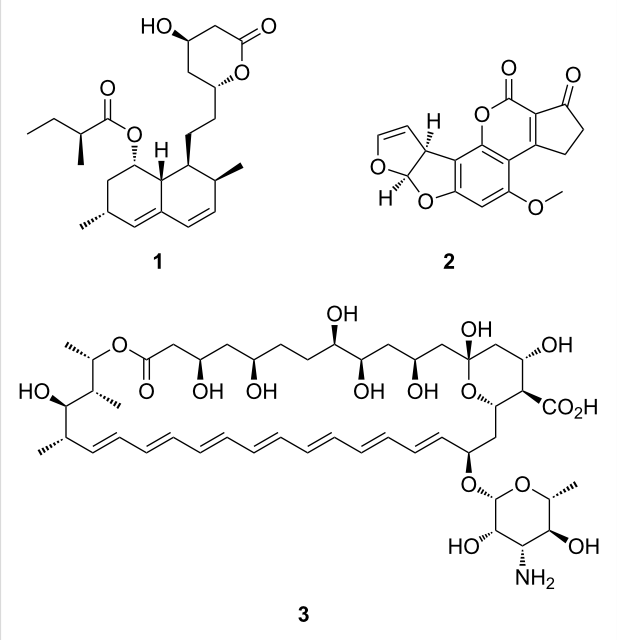

Figure 1: Structures of lovastatin (**1**), aflatoxin B_1 (**2**) and amphotericin B (**3**).

The products of polyketide synthases (PKS) belong to the first secondary metabolites that were investigated using isotopically labeled compounds [19]. Feeding experiments using (1,2-$^{13}C_2$)acetate and (1-^{13}C) or (2-^{13}C)acetate are a convenient and simple source of information on intact acetate units, chain direction and modifications of PKS derived natural products. Sensu stricto, polyketides (i.e., polymers of the "ketide" group $–CH_2–CO–$) are structurally made of malonyl-CoA building blocks leading to a linear chain assembly. However, many examples deviate from this rule, and the biological activities shown by these polyketides may in many cases especially depend on their branched side chains silhouetting them against the bulk of other PKS products [20]. Known reasons for branched polyketides at the α-position of the growing chain include the usage of different elongation units such as methylmalonyl-CoA, or methylation of the nucleophilic α-position by *S*-adenosyl methionine (SAM) [21]. Branching in the β-position is less common and proceeds through a β-aldol attack of an acetyl nucleophile at the growing chain. This mechanism is similar to the formation of hydroxymethylglutaryl-CoA along the mevalonate pathway in isoprenoid biosynthesis [22]. Recently, a different additional mechanism of β-branching was reported, in which a special PKS module is catalyzing the reaction [20]. It was investigated in the biosynthesis of the phytotoxin rhizoxin (**4**, Scheme 1), a potent antimitotic agent binding

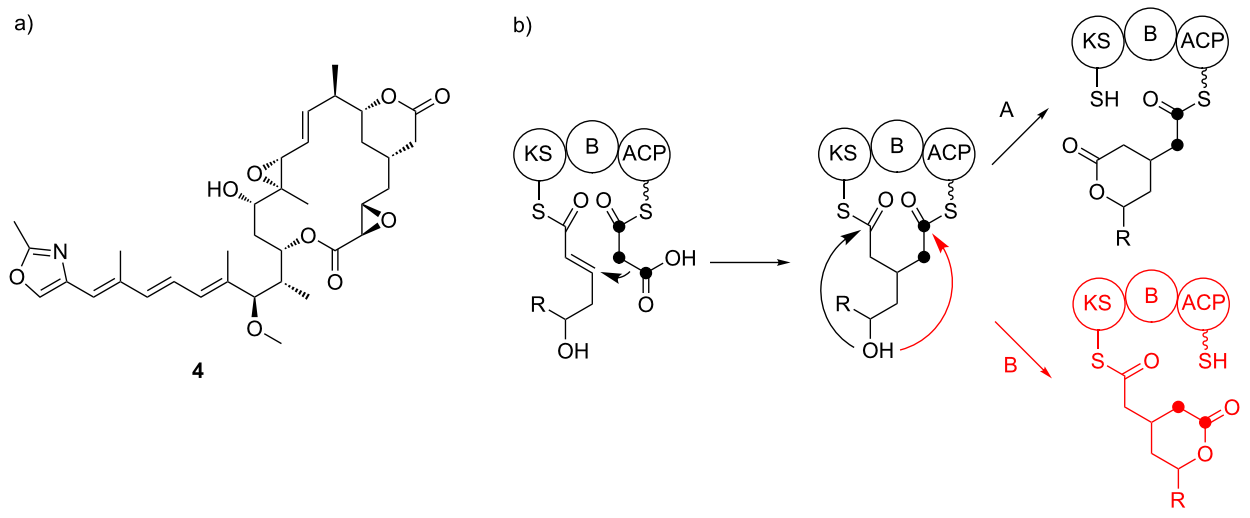

Scheme 1: a) Structure of rhizoxin (**4**). b) Two possible mechanisms of chain branching catalysed by a branching module. The ^{13}C-labeled carbons are annotated with black dots. KS: keto-synthase; B: branching domain; ACP: acyl carrier protein.

to β-tubulin from the bacterium *Burkholderia rhizoxinica*, which lives in symbiosis with the fungus *Rhizopus microsporus* [23]. The mechanism includes a Michael addition of a malonyl moiety to the α,β-unsaturated thioester bound to the keto-synthase domain (KS).

After this reaction, the polyketide chain is bound to the KS and the acyl carrier protein (ACP). The following lactonization to generate the δ-lactone structure in **4** can either proceed via nucleophilic attack of the δ-hydroxy function at the KS-bound (A) or at the ACP-bound thioester (B) with subsequent loading of the polyketide onto the ACP. To distinguish both mechanisms, ^{13}C-labeled malonyl-CoA and an *N*-acetylcysteamine (SNAC) thioester as synthetic analogon were used as substrates for an in vitro construct of the branching module. NMR experiments on the ACP-bound product unambiguously showed the labeled ^{13}C signals in the linear polyketide chain and not in the lactone ring, thus supporting mechanism A. Therefore, this labeling experiment took an important role on the road to a better understanding of this unusual mechanism.

An interesting feeding experiment was performed for the elucidation of both absolute configuration and biosynthesis of the polyketid alkaloid coelimycin P1 (**8**, Scheme 2). The compound was isolated from *Streptomyces coelicolor* M145 after genetically engineered increase of the metabolic flux and is the product of a polyketide biosynthetic gene cluster [24].

To test whether *N*-acetylcysteine could be a biosynthetic precursor of the unusual 1,5-oxathiocane structure, feeding experiments using both (2*S*)- and (2*R*)-*N*-((^{2}H$_3$)acetyl)cysteine

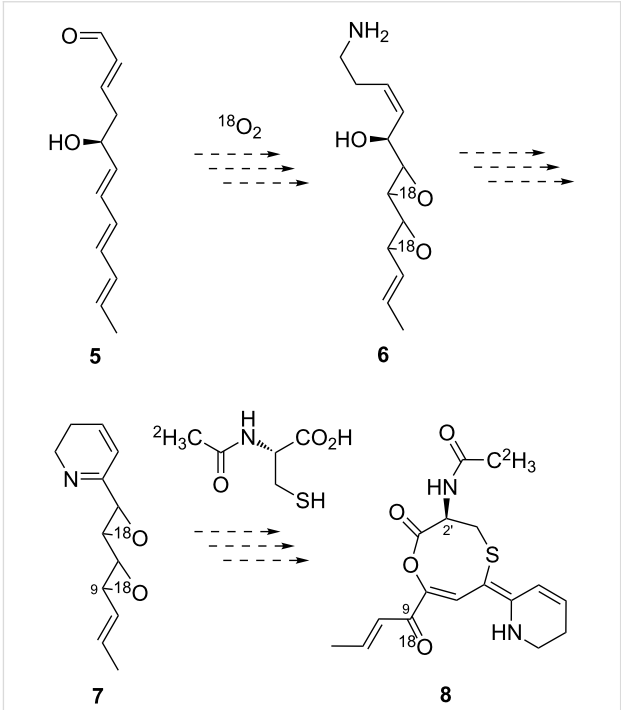

Scheme 2: Structure of coelimycin P1 (**8**) and proposed biosynthetic formation from the putative PKS produced aldehyde **5** via cyclized bisepoxide **7**.

were performed. The deuterium atoms of both precursors were incorporated into **8**, showing the direct biosynthetic relationship of the amino acid derivative and indicating that the addition of *N*-acetylcysteine might not be catalyzed by an enzyme. Exploiting the only stereocenter of **8** being located in the incorporated residue, also the absolute configuration of **8** could be

deduced from these labeling experiments as (2'*R*) via comparison of the retention times of both compounds to naturally occurring **8** on a homochiral stationary LC phase.

To investigate the proposed structure of **7**, which likely exhibits the antibiotic properties connected to the bacterial strain as a highly reactive bisepoxide, *S. coelicolor* M1157 was grown in an $^{18}O_2$ atmosphere. MS/MS measurements indicated a direct incorporation of ^{18}O at the C-9 carbonyl group. This result supports the activity of putative epoxidases processing the linear unsaturated PKS precursor **5** to amine **6**. Oxidation of the hydroxy function and subsequent ring closure would then lead to the proposed antibiotic **7**. The other oxygen atom is lost during biosynthesis und is therefore undetectable. This example shows how well-designed labeling experiments can support biosynthetic investigations especially on highly derivatized and altered polyketide products.

Emphasizing the same principle, the biosynthesis of trioxacarcin A (**9**, Scheme 3), a complex aromatic natural product originally isolated from *Streptomyces bottropensis* DO-45 and showing remarkable antibacterial and antitumor properties [25], was investigated using isotopically labeled precursors to gain insight into the used building blocks for the unusual polyketide core [26]. Compound **9** features a trisketal structure in addition

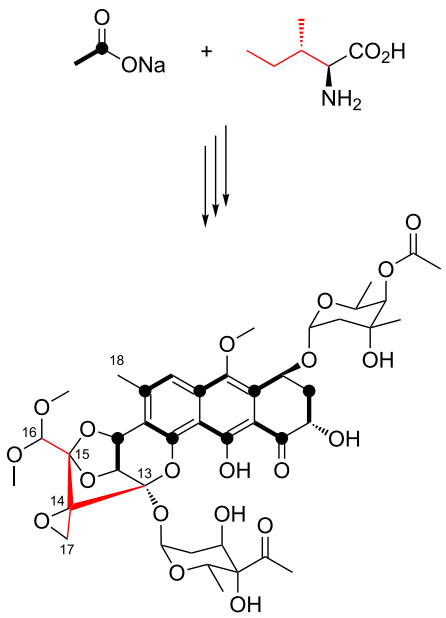

9

Scheme 3: Structure of trioxacarcin A (**9**) with highlighted carbon origins of the polyketide core from acetate (bold) and L-isoleucine (red) as deduced from labeling experiments. Labels introduced into the carbohydrates and methyl groups are omitted.

to the spiro-epoxide at C-14, which is believed to be the active part of the molecule for interaction with DNA. This was supported by the isolation of gutingimycin, a guanine-adduct of **9** [27]. However, very little was known about the biosynthetic assembly of the complex antibiotic. Feeding of [1-^{13}C]-, [2-^{13}C]- and [1,2-$^{13}C_2$]acetate to *S. bottropensis* and analysis of the produced **9** via ^{13}C NMR yielded the carbon origins of the polyketide core. The regular incorporation pattern in the tricyclic aromatic moiety suggests a normal PKS assembly line. Moreover, a decarboxylation step is indicated by incorporation of the acetate methyl carbon atom into C-18. In contrast, the origins of C-13 to C-17 remained unclear because of low incorporation of acetate into this part of the molecule.

The location of these five carbons at the end of the proposed linear PKS chain indicated the use of an unusual starter unit, most likely isoleucine-derived 2-methylbutyryl-CoA. Indeed, feeding of [U-$^{13}C_6$]-L-isoleucine resulted in a mass shift of +5 *m*/*z* compared to the unlabeled compound. In conclusion, these feeding experiments using isotopically labeled precursors supported the biosynthetic assembly from an unusual PKS starter unit which results in the remarkable scaffold for the bioactivity-generating functionalities.

A similar study showing the enduring significance of labeled acetate in PKS research deals with the fusion of the polycyclic aromatic pigment clostrubin A (**12**) from *Clostridium beijerinckii*, a strictly anaerobic bacterium [28]. The purple colored compound features a benzo[*a*]tetraphene skeleton, which is unique in known polyphenolic natural products. Moreover, feeding experiments using [1-^{13}C]- or [1,2-$^{13}C_2$]acetate revealed the PKS chain to build up an angucyclic scaffold (in **11**) first, which then probably fuses the fifth ring via reaction with acetoacetyl-CoA (Scheme 4), with folding of the linear PKS chain **10** downwards with respect to the D ring. For the A ring, C-9 and C-14 are connected. This folding differs from the biosynthesis of all known angucyclic cores, which are fused in an upwards folding connecting C-7 and C-12 for the formation of the A ring [29].

Despite the fact that the biosynthesis of this polyphenol cannot be deduced completely from labeled acetate feeding experiments, the results laid the ground for the discovery of the unusual chain folding and the loss of one carbon atom through the singly labeled C-2 position. These recent findings of Hertweck and co-workers are an interesting extension of the pioneering work by Bringmann et al. on the anthraquinone crysophanol, for which different folding modes in fungi (F type folding) and in bacteria (S type, "*Streptomyces*" type) were found by isotopic labeling experiments for one and the same compound [30].

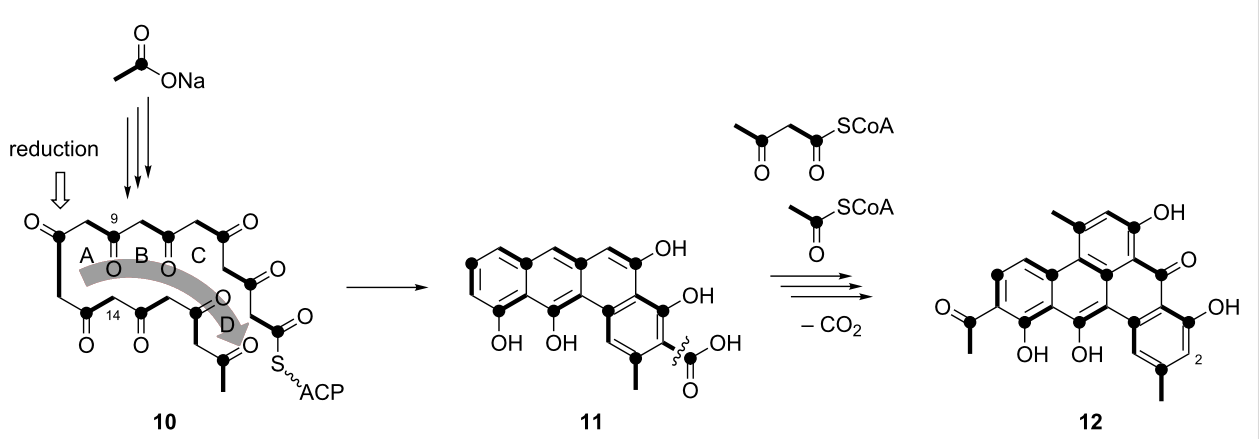

Scheme 4: Proposed biosynthetic assembly of clostrubin A (**12**). Bold bonds show intact acetate units.

As an additional concluding remark of this chapter, the role of isotopic labeling in the structure elucidation of complex polyketide natural products will be discussed. Especially in combination with two-dimensional NMR spectroscopic techniques, several powerful tools are becoming more interesting to natural products research. Production of new compounds in a labeled medium and analyzing the $^{13}C,^{13}C$-COSY spectrum of the resulting fully ^{13}C-labeled natural product as in case of forazoline A (**13**) can easily determine the carbon skeleton (Figure 2). This technique was also used for the elucidation of marine aromatic acids [31]. Even the nitrogen–carbon connectivities can be investigated by fermentation in a ^{15}N-labeled medium and analysis of the resulting product with $^{13}C,^{15}N$-HMQC [32]. These applications represent helpful additions to the repertoire for structure elucidation of complex natural products, which can be produced under laboratory conditions in sufficient amounts.

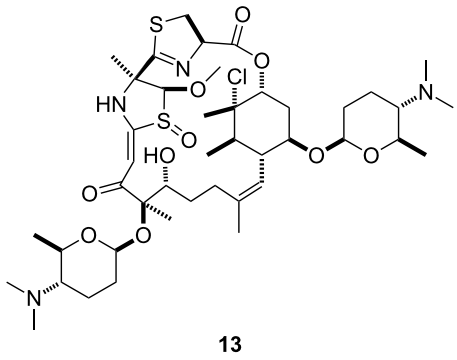

Figure 2: Structure of forazoline A (**13**).

Non-ribosomal peptides

Non-ribosomal peptides often exhibit a high bioactivity and are biosynthesized by non-ribosomal peptide synthethases (NRPS) [33], which work RNA-independent and catalyze the assembly of both proteinogenic and non-proteinogenic amino acids in a modular fashion. Moreover, NRPSs can contain additional modifying modules, e.g., epimerization domains, resulting in a greater structural variety than ribosomal peptides usually have. Two examples are the membrane disrupting decapeptide antibiotic tyrocidine A (**14**) [34] and teixobactin (**15**) [35], a recently discovered multi-target antibiotic rising high hopes in the treatment of resistant pathogens (Figure 3).

Producing an isotopologue of the desired compound by feeding of labeled precursors or growing the producing organism in labeled medium can simplify structure elucidation by giving access to the sum formula by mass spectrometry, which is not in all cases easily accessible for the unlabeled compound. In particular, advanced mass spectrometry techniques in combination with labeled amino acids catch a growing attention for the often challenging structure elucidation of NRPS products. To give insights into the assembled building blocks and the sum formula of the desired compound, either the traditional way of providing isotopically labeled amino acids to the NRPS can be used, or completely labeled media can be supplemented with non-labeled building blocks in an inverse feeding experiment [36]. The latter method is particularly advantageous, if the compound contains precursors that are not commercially available in a labeled way. Incorporation into the NRPS product [37-41] can be followed by MS^n that may even give information about the position of incorporation.

Another very interesting method for structure elucidation of NRPS products using isotopic labelings was recently developed by Bode and co-workers [36]. The method is designed to investigate the absolute configuration of the amino acid building blocks without hydrolysing the NRPS product, can be performed on minute amounts of material, and was first

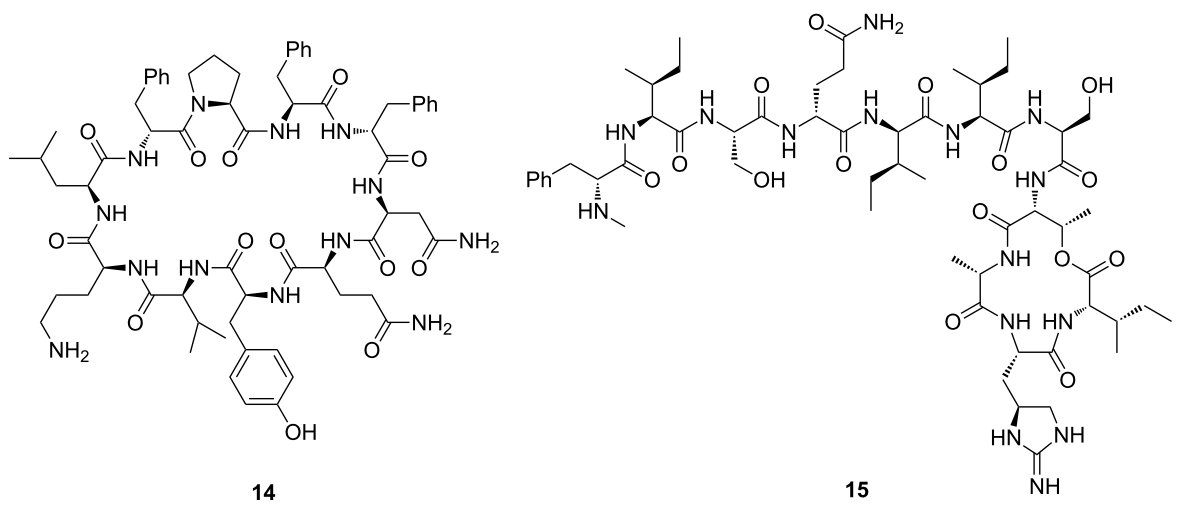

Figure 3: Structures of tyrocidine A (**14**) and teixobactin (**15**).

applied to different cyclic peptides from *Photorhabdus* and *Xenorhabdus* species [42] and for activity testing of heterologously expressed SAM-epimerases from various bacteria [43]. In a follow-up study the recently discovered NRPS product kollosin A (**16**, Figure 4) was investigated. This pentadecapeptide is made by the largest known NRPS that consists of 15 modules and is encoded by a single 49.1 kbp gene found in the entomopathogenic bacterium *Photorhabdus luminescens* [44]. Despite the non-detectable expression under various fermentation conditions, it was possible to express the machinery using a promoter exchange [45] in the native host.

Bioinformatics allowed for the annotation of several epimerization domains in the kollosin A NRPS, but it is hard to determine the actual activity of each of these functions. To overcome this problem, L-[$^2H_8$]valine, L-[$^2H_{10}$]leucin, L-[$^2H_7$,^{15}N]tyrosine und L-[$^2H_5$,^{15}N]threonine were fed to *P. luminescens*. The loss of one deuterium atom for an incorporated labeled amino acid (from C_α) directly supports an epimerase function within the corresponding NRPS module, and the incorporated building block can be assigned as D-configured. In this example, epimerization activity was shown for tyrosine and both threonine building blocks, marked by asterisks in Figure 4. Moreover, one leucine could be determined as D-configured according to incorporation in truncated fragments of **16**. For the elucidation of the second stereocenter in both threonines, solid phase synthesis of the peptide was performed, which confirmed the structure of **16** with two

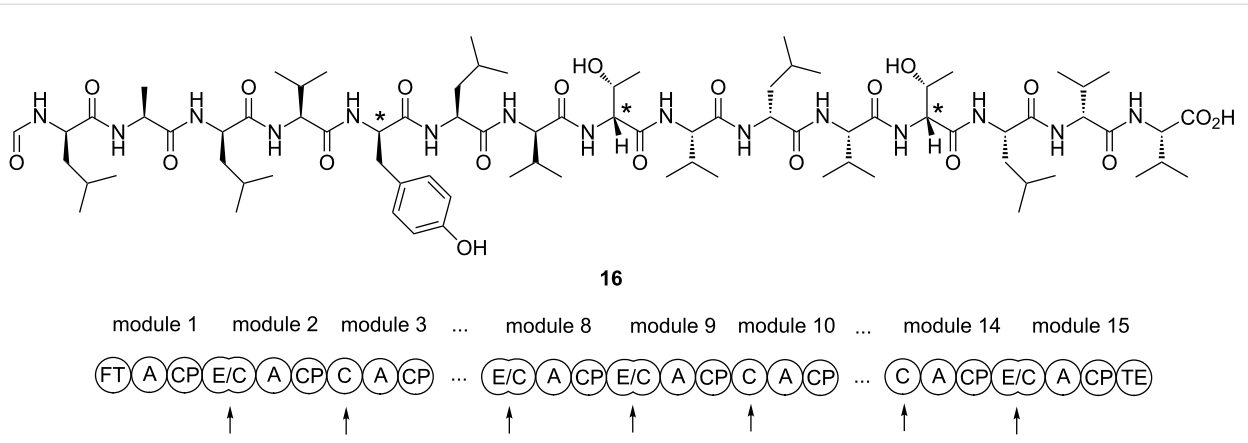

Figure 4: Top: Structure of the NRPS product kollosin A (**16**) with the sequence *N*-formyl-D-Leu-L-Ala-D-Leu-L-Val-D-Tyr-L-Leu-D-Val-D-aThr-L-Val-D-Leu-L-Val-D-aThr-L-Leu-D-Val-L-Val-OH (aThr: *allo*-threonine). Bottom: Domains of some of the 15 modules (FT: formyltransferase, A: adenylation, CP: peptidyl carrier protein, C: condensation, E/C: condensation + epimerization, TE: thioesterase). For the absolute configuration of incorporated amino acids relevant domains are highlighted with arrows. Modules not shown consist of alternating C and E/C. Asterisks indicate stereocenters deduced from labeling experiments.

allo-threonines. In conclusion, all bioinformatically assigned epimerization functions of the kollosin A NRPS were shown to be active, resulting in an alternating incorporation of L- and D-configured amino acids into kollosin A except for modules 8 and 9.

This example proves that the use of isotopically labeled compounds can be a valuable addition to the common repertoire of structure elucidation for minimal amounts of material and provides an interesting combination of bioinformatic, synthetic and labeling techniques.

NRPS products are frequently modified by tailoring enzymes. This can extend to a complexity, which obscures the initial building blocks to the eye of the observer. Labeling experiments can in these cases clarify the origins even if they seem to be obvious in the beginning. The structure of aspirochlorine (**20**, Scheme 5), a toxin from *Aspergillus oryzae*, provides an interesting example. Its importance arises from the use of the producing organism in Asian food industry [46]. The biosynthesis of **20** can be hypothesized from phenylalanine and glycine. To investigate this, (*ring*-$^2H_5$)Phe and (2-^{13}C)Gly were fed and incorporation of two ^{2}H and one ^{13}C atom was confirmed by MS analysis [47]. However, structure elucidation of the biosynthetic intermediates **18** and **19** that were isolated from deletion mutants suggested a different assembly from two Phe via the dimeric structure **17**, which was further supported by the incorporation of two ^{13}C atoms after feeding of (1-^{13}C)Phe. Therefore, ($^{13}C_2$,^{15}N)Gly was fed to *A. oryzae*, pointing to incorporation of one ^{13}C by MS analysis. To finally solve this riddle, feeding experiments with ($^{13}C_2$)Gly were performed on a preparative scale to unambiguously assign the ^{13}C-labeled positions via NMR. It turned out that the label was incorporated into the *N*-methoxy group, and not into the presumptive glycine unit of the diketopiperazine structure. In summary, these results support an unusual conversion of one phenylalanine-derived side chain to a glycin-like moiety.

The observed incorporation of labeled Gly into the methyl group was rationalized by glycine degradation, directing the labeling via tetrahydrofolate and SAM into aspirochlorine biosynthesis. The conversion of the Phe residue to Gly may proceed through either oxidative C–C bond cleavage or a retro-aldol reaction in **18**, in agreement with the detection of (*ring*-$^2H_5$)benzoic acid in culture extracts from labeling experiments with (*ring*-$^2H_5$)Phe. This interconversion of two proteinogenic amino acids in the biosynthesis of an NRPS compound from secondary metabolism is unprecedented and its discovery was strongly supported by the careful evaluation of feeding experiments with labeled precursors.

PKS/NRPS-Hybrids

The formation of interesting structural motifs in natural products is an exciting aspect in the field of biosynthetic research and gives insights to the synthetic abilities of nature fusing structures, whose formation usually requires sophisticated chemistry in organic laboratories. Prominent examples are [*n*]paracyclophane moieties in natural products such as haouamines [48] or fijiolides [49,50]. As for the [7]paracyclophane in haouamine A and B, a reasonable suggestion for compensating the high barrier of a bended benzene ring includes intermediate loss of aromaticity followed by rearomatization during the formation of the cyclophane ring [51]. However, a recently investigated example shows, that breaking the aromatic character of a phenyl ring is not necessary for building up a bended aryl ether in a biological scaffold. In this study, ^{13}C- and ^{18}O-labeled L-tyrosine was used to elucidate the biosynthesis of pyrrocidines such as pyrrocidine A (**24**, Scheme 6) bearing a [9]paracyclophane moiety in the fungus *Acremonium zeae* [52]. Compound **24** is the product of a mixed PKS and NRPS machinery containing nine acetate units, five methyl groups from SAM and one L-tyrosine [53]. Two possible mechanisms for the cyclization of the linear precursor **21** were hypothesized. In route A, an oxidation of the aromatic ring would lead to an electrophilic center at the quinone moiety in **22**, which can be attacked by the C-6 hydroxy group. The energy barrier of a distorted benzene ring would then be compensated by rearomatization in **23** after intramolecular Diels–Alder reaction. This mechanism would involve a 1,2-hydride shift and a nucleophilic attack of water at C-2'.

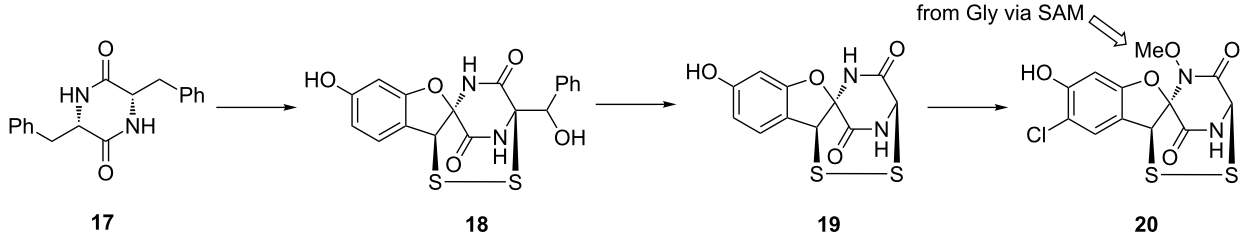

Scheme 5: Proposed biosynthesis of aspirochlorine (**20**) via **18** and **19**.

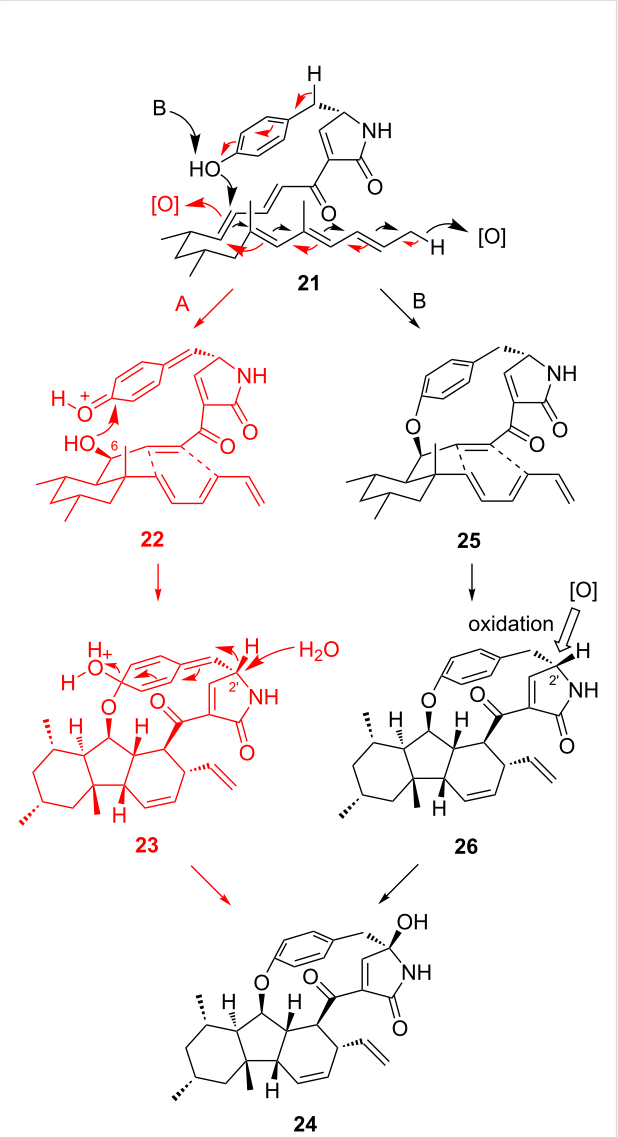

Scheme 6: Two different macrocyclization mechanisms in the biosynthesis of pyrrocidine A (**24**).

The second discussed route starts with a nucleophilic attack of the phenolic oxygen at C-6 to close the macrocycle in **25**. In this mechanism, the aromaticity of the phenol ring remains untouched. Intramolecular Diels–Alder reaction gives rise to the hexacyclic system **26**, which would then be oxidized to pyrrocidine A (**24**) at C-2'. In contrast to route A, the phenolic oxygen is conserved here. To distinguish between these mechanisms, (4'-hydroxy-^{18}O,1-^{13}C)-L-tyrosine was enantioselectively synthesized and fed to *A. zeae*. Both labels were incorporated into **24**, thus providing evidence for mechanism B and a paracyclophane formation without intermediate loss of aromaticity. This kind of tyrosine reporter might also prove useful in other biosynthetic studies.

Sometimes the biosynthesis of mixed PKS/NRPS/FAS natural products involves the discovery of surprising building blocks as recently shown for thiomarinol A (**27**, Figure 5) from the marine bacterium *Pseudoalteromonas* sp. SANK 73390 [54], which exhibits antibiotic activity against methicillin-resistant *Staphylococcus aureus* (MRSA) [55].

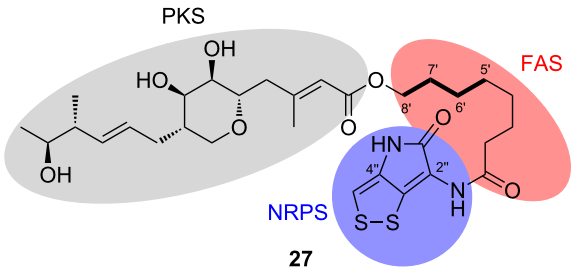

Figure 5: Structure of thiomarinol A (**27**). Bold bonds indicate carbon atoms derived from 4-hydroxybutyrate.

Particularly interesting results of feeding experiments with [1,2-$^{13}C_2$]-, [2-^{13}C]- and [1-^{13}C,$^{18}O_2$]acetate were the unexpectedly low incorporation into C-5' to C-8' of the octanoate side chain, whereas approximately the double incorporation rates were observed in the PKS part of the molecule. To test a hypothetical C_4-starter unit for the fatty acid synthase, [2,3-$^{13}C_2$]succinate was fed to *Pseudoalteromonas* SANK 73390, which showed an intact incorporation of labeling into C-6' and C-7' of **27**. Moreover, also [2,3-$^{13}C_2$]-4-hydroxybutyrate was incorporated with appearance of labeling in the same positions. The proposed origin of the pyrrothine unit from two cysteins was confirmed by feeding of [2,2'-$^{13}C_2$]cystine and detection of the label at C-2'' and C-4''. As deduced from these experiments in combination with genetic studies, the biosynthesis of thiomarinol A (**27**) proceeds via coupling of 4-hydroxybutyrate to the PKS product, two cycles of chain elongation and finally coupling with the NRPS product pyrrothine.

Terpenes

Terpenoids constitute the largest group of natural products and are remarkably diverse in structure, bioactivity, and use. Prominent examples such as the antimalaria drug artemisinin (**28**) from *Artemisia annua*, ingenol (**29**) and its derivatives from *Euphorbia ingens* [56], or the anticancer drug paclitaxel (**30**) feature highly functionalized polycyclic carbon skeletons (Figure 6).

The fascination of terpene biosynthesis arises from the complexity and variety of carbon scaffolds, terpene cyclases are able to build up using few linear oligoprenyl diphosphate precursors. This promotes investigations using isotopically

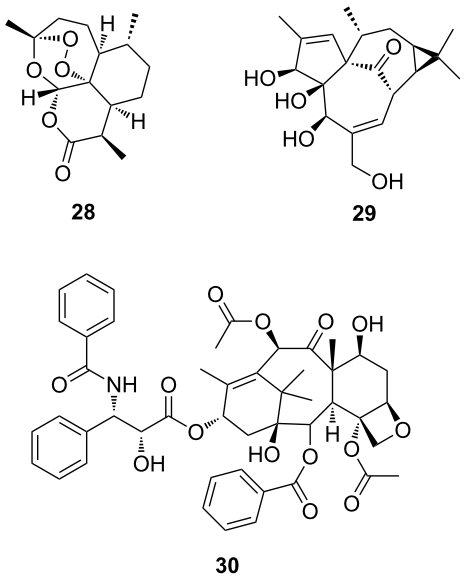

Figure 6: Structures of artemisinin (**28**), ingenol (**29**) and paclitaxel (**30**).

labeled compounds both on acetate- and mevalonate/deoxyxylulose-level for in vivo feeding experiments or oligoprenyl diphosphates for in vitro studies to understand the often complex cyclization cascades catalyzed by a single enzyme. In many cases, isotopes represent the only way of elucidating proposed hydride shifts, carbon–carbon rearrangements and cyclizations experimentally.

The structure elucidation of terpenoids can be challenging because of the multicyclic carbon skeletons with several contiguous stereocenters. The assistance of ^{13}C labels can in such cases be especially helpful, and if completely ^{13}C-labeled carbon backbones can be made accessible, $^{13}C,^{13}C$-COSY experiments are possible that allow for a comparably easy structure elucidation even for minimal amounts of material. As recently demonstrated for hypodoratoxide (**31**) from *Hypomyces odoratus* DSM 11934, such labeled products can be obtained by feeding of terpene precursors to an actively growing culture [57]. The application of $^{13}C,^{13}C$-COSY for hypodoratoxide led to a revision of the previously proposed structure **32** [58], showing the significance of this technique in comparison to unlabeled standard 2D NMR methods. Alternatively, a completely ^{13}C-labeled terpene can be made in vitro by usage of enzymes. This approach was used for investigating the structure of miltiradiene (**33**, Figure 7), a diterpene from *Selaginella moellendorffii*, starting from uniformly labeled mevalonate [59].

Despite the tools for structure elucidation, labeled compounds continue to offer interesting insights into terpene synthase catalyzed cyclizations. Labeled oligoprenyl diphosphates, the

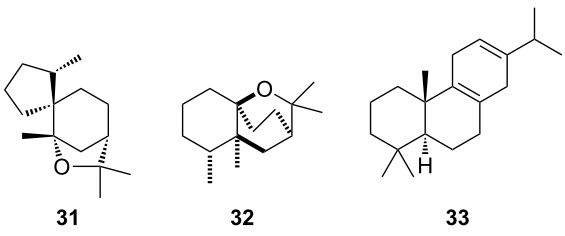

Figure 7: The revised (**31**) and the previously suggested (**32**) structure of hypodoratoxide and the structure of miltiradiene (**33**).

substrates for these enzymes, can be made available by synthesis and provide an excellent tool for such investigations, as recently demonstrated for sesquiterpenes by the synthesis of all 15 singly ^{13}C-labeled isotopomers of farnesyl diphosphate (FPP) [60]. These precursors were used to unambiguously assign both ^{13}C NMR and (via HSQC) ^{1}H NMR data of (1(10)*E*,4*E*)-germacradien-6-ol (**34**) from *Streptomyces pratensis*. The NMR spectra of this compound are complicated because of a mixture of conformers (Figure 8) that prevented a full assignment of NMR data by conventional methods.

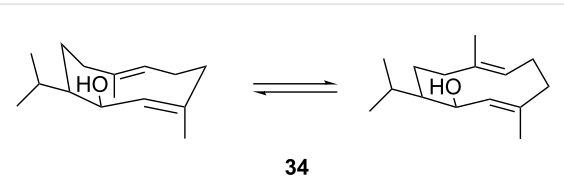

Figure 8: Structure of the two interconvertible conformers of (1(10)*E*,4*E*)-germacradien-6-ol (**34**) studied with extensive ^{13}C labeling experiments.

To correlate a conformational signal set, (U-$^{13}C_{15}$)FPP was synthesized and $^{13}C,^{13}C$-COSY showed the connected carbon skeleton for each conformer. The 15 obtained labeled natural products also allowed a detailed analysis of the EIMS-fragmentation reactions of **34** by comparison of the ^{13}C-including fragments.

Singly labeled FPP isotopomers also proved valuable to investigate reprotonation steps in sesquiterpene cyclization mechanisms by incubation in deuterium oxide. The biosynthesis of the recently discovered corvol ethers A (**42**) and B (**43**) provides an interesting example (Scheme 7) [61].

The proposed mechanism starts with isomerization of farnesyl diphoshate (FPP, **35**) to nerolidyl diphosphate (**36**) followed by 1,10-ring closure to the helminthogermacradienyl cation (**37**). A 1,3-hydride shift to the allylic cation **38** and attack of water gives the neutral intermediate germacrene D-4-ol (**39**). Reprotonation induces the formation of the bicyclic system **40**, which

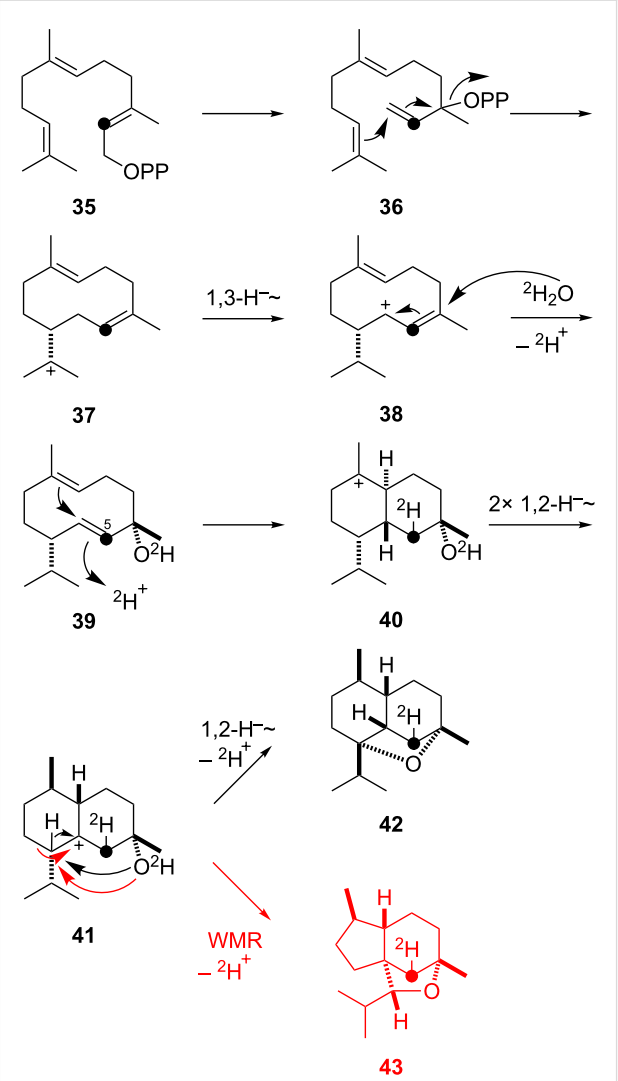

Scheme 7: Proposed cyclization mechanism of corvol ethers A (**42**) and B (**43**) with the investigated reprotonation using ^2H_2O. Black dots indicate ^{13}C-labeled carbon atoms.

can rearrange via two sequential 1,2-hydride shifts to the cation **41**. The attack of the hydroxy function and either a 1,2-hydride shift or a Wagner–Meerwein rearrangement in a concerted process leads to **42** and **43**. The protonation of C-5 was shown by using (2-^{13}C)FPP as a substrate for an in vitro incubation of the terpene synthase in D_2O leading to characteristic strongly enhanced triplets for the labeled carbons of **42** and **43** in the ^{13}C NMR spectrum. As an extension to these experiments, the stereochemical course of reprotonation of a neutral intermediate can be followed by comparing the HSQC spectra of the labeled and the unlabeled compounds, if combined with a NOESY based assignment of the signals for the relevant diastereotopic protons, as recently performed to investigate the mechanisms for intermedeol and neomeranol B biosynthesis [62].

Cyclooctat-9-en-7-ol (**52**), a member of the fusicoccane family of diterpenoids, is the biosynthetic precursor of cyclooctatin (**45**) [63], a potent inhibitor of lysophospholipase, which was isolated from *Streptomyces melanosporofaciens* [64]. The cyclization of geranylgeranyl diphosphate (GGPP, **44**) to **52** features an unexpected carbon backbone rearrangement, which was shown recently by Kuzuyama and co-workers using isotopically labeled glucose in vivo and labeled GGPP in vitro [65]. The reaction is catalysed by the enzyme CotB2, the first structurally characterized bacterial diterpene cyclase [66]. After identification of the biosynthetic gene cluster, a mechanism involving a deprotonation–reprotonation sequence and two 1,2-hydride shifts was proposed [67]. However, a simple feeding experiment performed with a *S. albus* transformant and [U-$^{13}C_6$]glucose revealed an unexpected labeling pattern in **45**, which could not be explained by the anticipated GGPP labeling following the deoxyxylulosephosphate pathway [68] and the initially suggested mechanism for GGPP cyclization (Scheme 8).

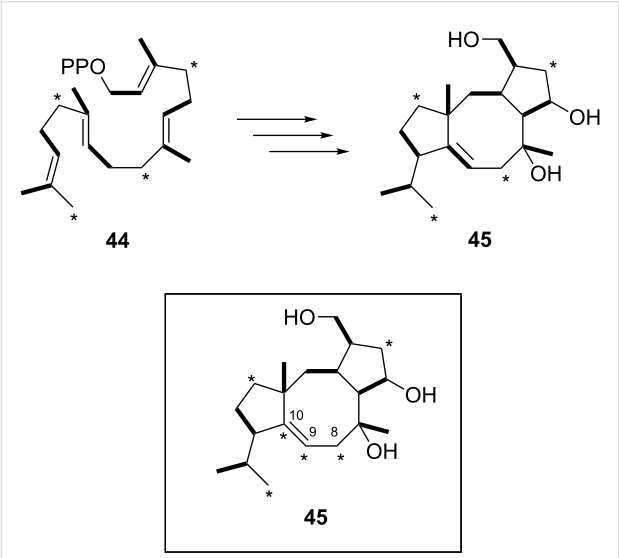

Scheme 8: Predicted (top) and observed (bottom) ^{13}C-labeling pattern in cyclooctatin (**45**) after feeding of [U-$^{13}C_6$]glucose to a *S. albus* transformant. Labeling in the resulting geranylgeranyl diphosphate (GGPP, **44**) is added for clarity. Bold bonds show intact C_2-fragments and asterisks indicate carbons without direct coupling. The carbon numbers shown for **45** derive from carbon numbers of GGPP (**44**).

The missing $^{13}C,^{13}C$-coupling between C-9 and C-10 excluded a simple mechanistic assembly of the tricyclic system. Instead, advanced NMR experiments focusing on $^2J_{C,C}$-couplings revealed that C-8 and C-10 originate from the same glucose molecule. To account for this surprising observation, a new mechanistic proposal was suggested involving a carbon–carbon-bond rearrangement and several hydride shifts, which were confirmed with elegant labeling experiments using

(9,9-$^2H_2$)GGPP (a), (10-^{2}H)GGPP (b), and (8,8-$^2H_2$)GGPP (c) in incubation experiments with recombinant CotB2 (Scheme 9).

A mechanism that is in line with all labeling experiments proceeds via GGPP cyclization to form the bicyclic cation **46**, followed by a second cyclization and a 1,5-hydride shift to yield **47**. This unusual hydride migration was experimentally supported by location of H^c at C-15 of **52**. A 1,3-hydride shift generates the allylic cation **48**, which can undergo another 1,5-hydride shift to the tertiary cation **49**. This step was elucidated using (10-^{2}H)GGPP to follow the transannular movement of H^b. Ring contraction leads to the tetracyclic cation **50**, which rearranges to **51** explaining the observed lost linkage between C-9 and C-10. Quenching of this cation with water leads to the diterpenoid product cyclooctat-9-en-7-ol (**52**). Further oxidation by the cytochrome P450-hydroxylases CotB3 and CotB4 yields the biologically active compound cyclooctatin (**45**) [67].

This outstanding study exemplifies the scope of isotopic labeling experiments in the elucidation of terpene biosynthesis by combined in vivo and in vitro labeling techniques to achieve a better understanding of nature's astonishing mechanistic toolbox utilized by terpene synthases. Additionally, the unexpected outcome of the initial feeding experiment gives an ideal example as to why isotopic labeling experiments are not at all old-fashioned, but rather still yield important mechanistic insights in biosynthetic pathways that would otherwise never be obtained.

Emphazising the same principle, feeding of even simpler precursors such as labeled acetate can give useful hints to carbon and hydrogen rearrangement, as shown for sesterfisherol (**59**, Scheme 10), the product of a bifunctional sesterterpene cyclase (C_{25}) from *Neosartorya fischeri* [69]. In this case, [1-^{13}C,$^2H_3$]acetate was fed and the resulting labeling pattern of an epoxidation product was analyzed by ^{13}C NMR, revealing a loss of deuterium from carbons C-2, C-6 and C-10 by hydride shifts during terpene cyclization that was concluded from missing upfield-shifted ^{13}C NMR signals of the neighboring ^{13}C-labeled carbons C-1, C-5 and C-9, while corresponding upfield-shifted signals were observed for all other expected cases (C-3, C-7, C-11, C-13, C-15, C-17, C-19).

These results are in line with the proposed cyclization mechanism starting from geranylfarnesyl diphosphate (GFPP, **53**), which undergoes two cyclizations yielding cation **54**. A 1,5-hydride shift at C-12 to C-19 leads to the allylic cation **55**. Additional ring closure fuses the tricyclic system **56**, which rearranges to the tertiary cation **57** by two sequential 1,2-hydride shifts and another cyclization. Two 1,2-hydride

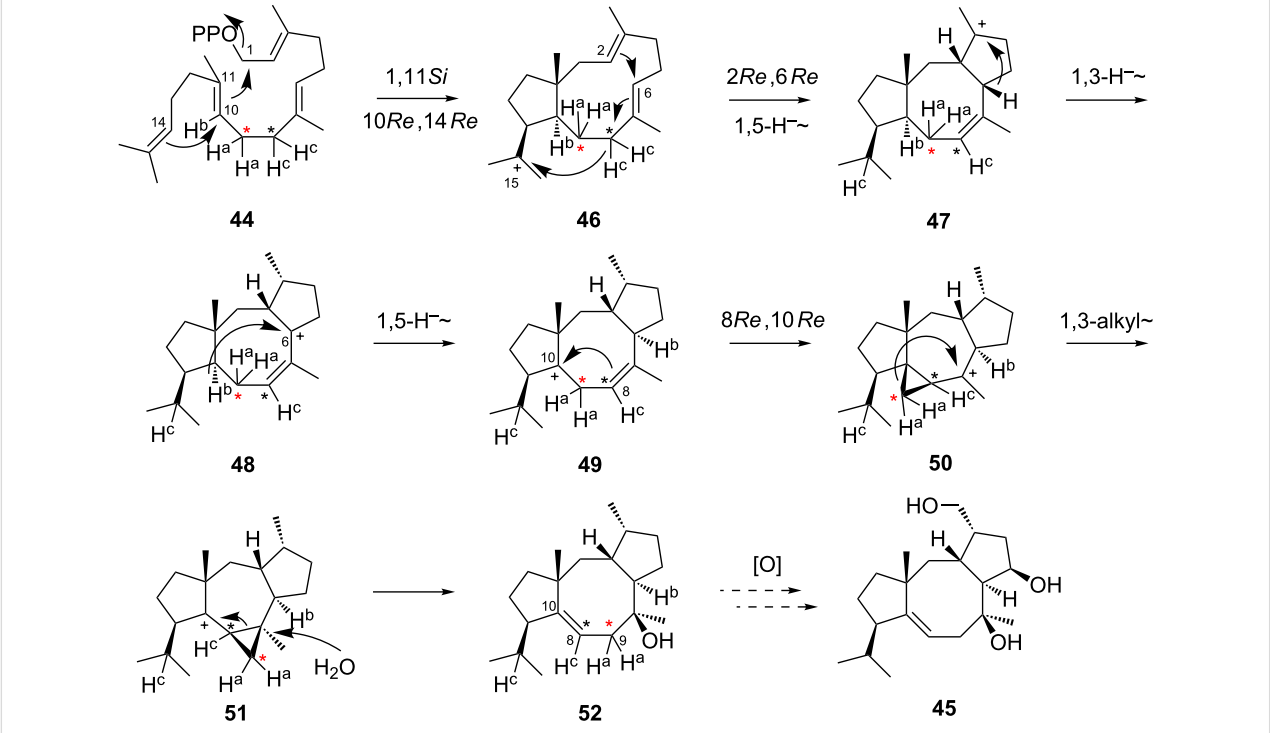

Scheme 9: Proposed mechanism of the cyclooctat-9-en-7-ol (**52**) biosynthesis catalysed by CotB2. Annotated hydrogen atoms (a–c) were investigated by deuterium labeling. Asterisks are used to follow the rearrangement of C-8 and C-9 (carbon numbers as for GGPP).

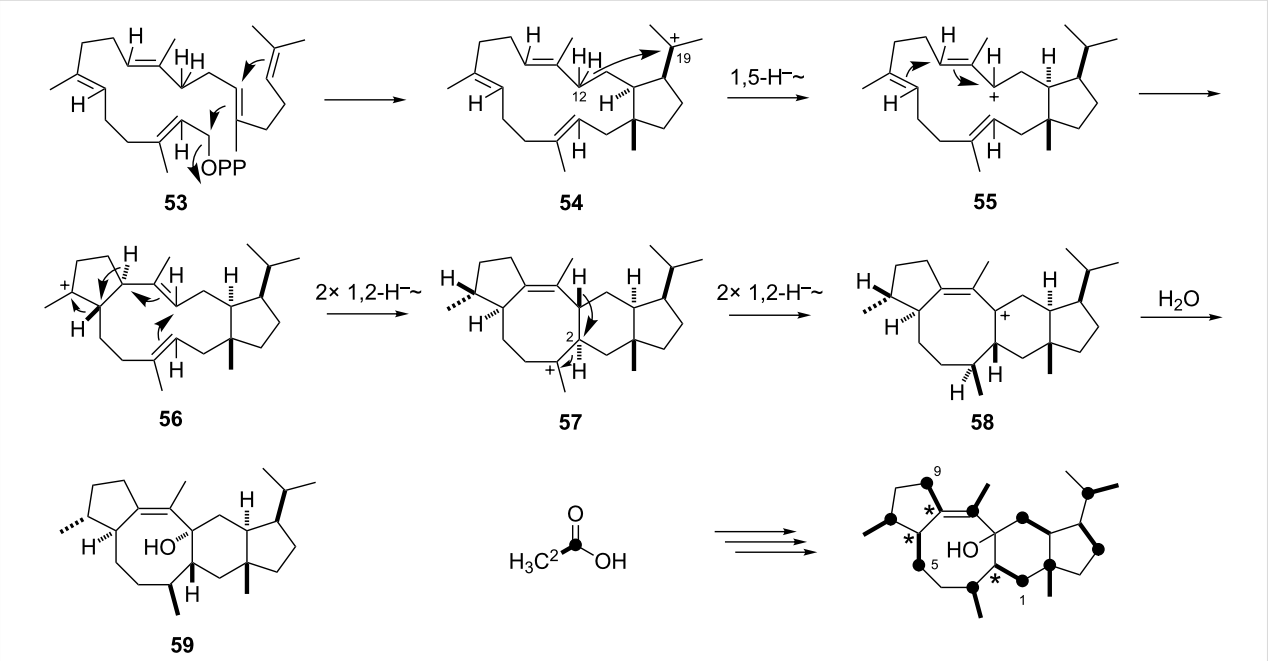

Scheme 10: Cyclization mechanism of sesterfisherol (**59**). Bold lines indicate acetate units; black circles represent C-1 of acetate. Asterisks show positions with lost deuterium labels.

shifts yield the allylic cation **58**, which is finally quenched by water to the sesterterpene product **59**. The involved 1,2-hydride shifts along this pathway explain the missing upfield-shifted ^{13}C signals mentioned above. To investigate the 1,5-hydride shift, (8,8-$^2H_2$)GGPP and IPP were used for an in vitro reaction with the recombinant terpene synthase, utilizing the bifunctional character of the enzyme to form (12,12-$^2H_2$)GFPP and its subsequent cyclization to ($^2H_2$)-**59**. NMR data of the obtained labeled product indicated a migration of the C-12 deuterium atoms to C-19 and to C-2, thus proving evidence for the proposed hydride migrations from **54** to **55** and from **57** to **58**.

The application of isotopes in mechanistic investigations is by far not limited to following atoms through the biosynthetic assembly of natural product. Also the kinetic isotope effect can be used to probe mechanistic proposals, as elegantly shown for the pentalenene (**65**) cyclization mechanism. Pentalenene synthase is one of the first and best investigated bacterial terpene cyclases both structurally [70] and functionally [71]. The initially suggested mechanism of building up its tricyclic structure is shown in Scheme 11 as pathway A and involves a 1,11-cyclization of FPP to the humulyl cation **60**. A deprotonation–reprotonation sequence leads to cation **61**, which is converted to a bicyclic secoillud-6-en-3-yl cation (**62**). A subsequent 1,2-hydride migration to **63** followed by ring closure gives **64**, which is deprotonated to give pentalenene (**65**). Quantum chemical calculations led to the suggestion of the protoilludyl cation **66** as central intermediate between **61** and **64** (pathway B), which is directly formed from **61** [72]. Interestingly, this proposal is also in line with all previously conducted labeling experiments.

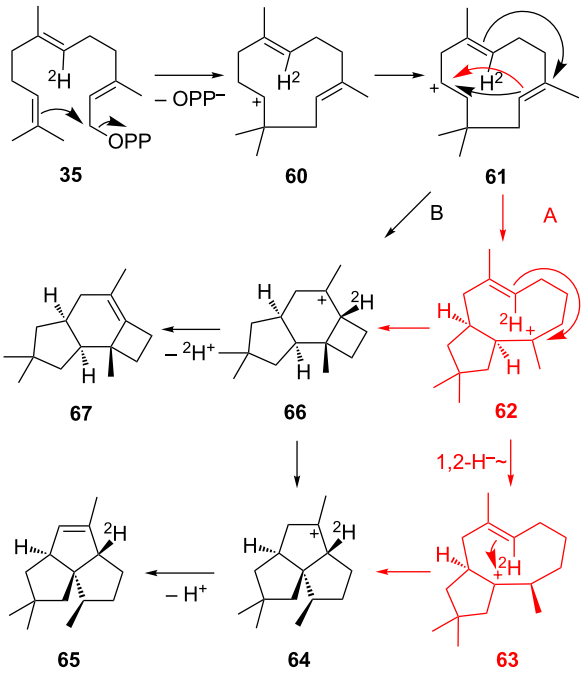

Scheme 11: Cyclization mechanisms to pentalenene (**65**) and protoillud-6-ene (**67**).

To address this mechanistic question experimentally, an elegant approach was recently presented in a collaborative work by the groups of Tantillo, Peters and Cane [73]. A H309A mutant of pentalenene synthase produces both **65** and the side product protoillud-6-ene (**67**). Using this mutant, experiments with (6-^{2}H)FPP were performed to exploit the different branching points of both mechanisms towards **65** and **67**. Assuming there is no fast equilibrium between cations **62** and **66**, cyclization via pathway B should influence the product ratio of **65** and **67** due to the easier loss of protium in comparison to deuterium in the deprotonation to **67**, whereas for pathway A no such influence would be expected. Indeed, the observed product ratio shifted towards pentalenene in the experiment with the labeled precursor, supporting the mechanism via cation **66**. This isotopically sensitive branching experiment shows the usefulness of labeling studies even in cases where two possible mechanisms lead to the same atom arrangement in the natural product.

Aromatic compounds via the shikimate pathway

Recently, a series of $H_2{}^{18}O$-based labeling experiments were used by Andexer et al. to elucidate the mechanism of chorismatases [74]. Biochemically, chorismate (**68**) plays an important role at the border of primary and secondary metabolism for many natural products made from aromatic building blocks [75]. Chorismatases were, e.g., found to be involved in the formation of the starter unit 3,4-*trans*-dihydroxycyclohexa-1,5-dienecarboxylate (**69**) for biosynthesis of the important immunosuppressants FK506, FK520 and rapamycin [76]. This family of enzymes catalyzes the conversion of chorismate (**68**) to different hydroxybenzoates and dihydrohydroxybenzoates (Scheme 12).

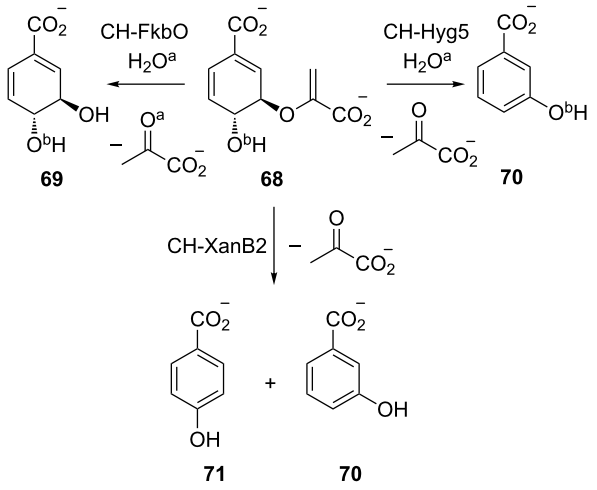

Scheme 12: Reactions of chorismate catalyzed by three different enzyme subfamilies. Oxygen atoms originating from water are labeled as O^a, whereas ^{18}O labels in the hydroxy group of chorismate are annotated as O^b. The XanB2-reaction was not investigated (missing label).

The FkbO-subfamily catalyses the formation of 3,4-*trans*-dihydroxycyclohexa-1,5-dienecarboxylate (**69**). This reaction is thought to occur via a protonation of the terminal double bond in the enol pyruvate moiety and subsequent attack of water at the cationic position to induce the cleavage of pyruvate. To support this mechanism, the enzymatic reaction was performed in ^{18}O-labeled water to yield labeled pyruvate as expected. However, conducting the same experiment for the Hyg5-subfamily of chorismatases, which produce 3-hydroxybenzoate (**70**), did not yield in any labeled pyruvate. This surprising result contradicts an elimination mechanism in the formation of **70** and demands for a new mechanistic proposal. Alternatively, an intramolecular attack at C-3 by the neighbouring hydroxy group at C-4 to cleave the activated pyruvate via an oxirane intermediate can be thought of. To test this hypothesis, chorismate with an ^{18}O label in its hydroxy function was prepared enzymatically starting from isochorismate. This label was retained during the reaction supporting the oxirane intermediate. The mechanism was also proposed for the XanB2-subfamily, which shows an unselective opening of the oxirane ring to produce both **70** and 4-hydroxybenzoate (**71**). This study created an interesting example of ^{18}O usage to distinguish two different mechanisms of action within the same family of enzymes.

Due to the poor availability of isotopically labeled sulfur compounds, corresponding labeling experiments are rare, but can provide interesting insights into the biosynthesis of sulfur containing natural products. Besides the recently presented synthetic developments towards ^{36}S-labeled SAM and methionine [77], also [^{34}S]cysteine has been made accessible by synthesis from elemental $^{34}S_8$ and used to study the sulfur source in tropodithietic acid (TDA, **74**, Scheme 13) biosynthesis [78]. TDA is a marine antibiotic which was originally isolated from *Pseudomonas* species [79] showing no observable resistance in important pathogens up to now [80]. The biosynthesis of the tropone core proceeds via the phenylalanine degradation pathway, as was shown by labeling experiments with (^{13}C)Phe and [$^{13}C_6$]glucose, and incorporation into phenylacetate [81] and TDA [82]. To resolve the sulfur precursor of TDA, (^{34}S)Cys (**72**) was synthesized and fed to *Phaeobacter inhibens* to observe an incorporation rate of 87% into both sulfur atoms of TDA. This result together with mutations of relevant genes of the primary sulfur metabolism pointed towards an introduction of sulfur from Cys via (*S*)-thiocysteine (**73**) into TDA.

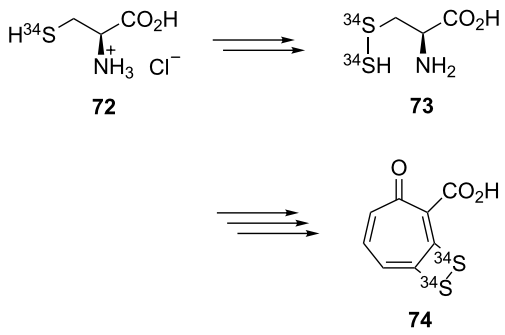

Scheme 13: Incorporation of sulfur into tropodithietic acid (**72**) via cysteine.

Antimycins such as antimycin A1 (**79**) are known for their inhibitory effect on the respiratory chain [83] and are widely used as antibiotics in fish farming industry. All compounds from this class feature a nine-membered dilactone core and a 3-formamidosalicylic acid moiety [84]. The latter provides an interesting biosynthetic rearrangement starting from tryptophan, which was investigated both by isotopic labeling experiments and by using fluorine as a positional label of the aromatic structure [85]. The formamido-residue in antimycine A1 (**79**, $R^1 = R^2 = H$, Scheme 14) is located in the *meta*-position with respect to the carboxylic acid moiety, whereas in the precursor molecule **76**, derived from tryptophan (**75**) via the well-known

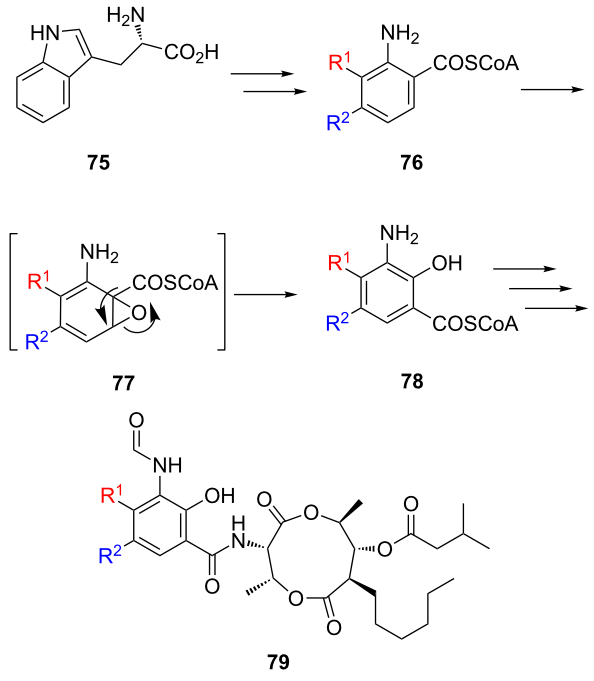

Scheme 14: Biosynthetic proposal for the starter unit of antimycin biosynthesis. The hydrogens at positions R^1 and R^2 were replaced by fluorine in the feeding experiments with fluoroanthranilic acids.

Trp degradation pathway, the corresponding amino group is found in the *ortho*-position. An unusual 1,2-shift via the oxirane intermediate **77** was proposed for the formation of the starter unit **78**.

Using fluorine as a non-reactive anchor on the benzene ring in feeding experiments with different isomers of fluoroanthranilic acid, the fate of the amino and the carboxylic acid group in the biosynthesis of antimycins could be followed [85]. Incorporation of 3-fluoro ($R^1 = F$) and 4-fluoroanthranilic acid ($R^2 = F$) into antimycins was observed with retention of the position for the amino group, but migration of the carboxylic acid group relative to the fluorine label. This example shows that chemical labelings that are usually much cheaper than isotopic labelings can in special cases be useful to address biosynthetic problems, as was impressively demonstrated in the cutting-edge experiments by Knoop more than one century ago.

Conclusion

The examples of isotope usage presented in this review article emphasize the important role of labeling methods on the road to a better understanding of nature's ways to assemble complex molecular structures. Although the principle of isotopic labeling itself did not change throughout 80 years of biochemical applications, isotopes are continuing to inspire biosynthetic studies to generate tailored methods for the specific problems evolved by natural products. As delineated here, labeling techniques are especially powerful in combination with other chemical and biological methods to give rise to a complete picture of biosynthetic conversions, both on enzymatic and molecular level. Some surprising results would probably still remain uncovered without the carefully designed usage of isotopes. Despite the exclusivity isotopic labeling techniques have lost to a lot of new bioinformatical, biotechnological and biological methods in the study of biosynthetic pathways, they still represent an indispensable tool in natural product research.

References

1. Schoenheimer, R.; Rittenberg, D. *Science* **1935,** *82,* 156–157. doi:10.1126/science.82.2120.156
2. Knoop, F. *Beitr. Chem. Physiol. Pathol.* **1904,** *6,* 150–162.
3. Ghisla, S. *Eur. J. Biochem.* **2004,** *271,* 459–461. doi:10.1046/j.1432-1033.2003.03952.x
4. Kennedy, E. P. *J. Biol. Chem.* **2001,** *276,* 42619–42631. doi:10.1074/jbc.R100051200
5. Liscum, L. Cholesterol biosynthesis. In *Biochemistry of Lipids, Lipoproteins and Membranes;* Vance, J. E.; Vance, D. E., Eds.; Elsevier: Amsterdam, 2008; pp 399–421. doi:10.1016/B978-044453219-0.50016-7
6. Simpson, T. J. *Nat. Prod. Rep.* **2014,** *31,* 1247–1252. doi:10.1039/C4NP00065J
7. Rohmer, M. *Nat. Prod. Rep.* **1999,** *16,* 565–574. doi:10.1039/a709175c

8. Eisenreich, W.; Schwarz, M.; Cartayrade, A.; Arigoni, D.; Zenk, M. H.; Bacher, A. *Chem. Biol.* **1998,** *5,* R221–R233. doi:10.1016/S1074-5521(98)90002-3
9. Mahmud, T. *J. Labelled Compd. Radiopharm.* **2007,** *50,* 1039–1051. doi:10.1002/jlcr.1391
10. Julka, S.; Regnier, F. *J. Proteome Res.* **2004,** *3,* 350–363. doi:10.1021/pr0340734
11. Postle, A. D.; Hunt, A. N. *J. Chromatogr., B* **2009,** *877,* 2716–2721. doi:10.1016/j.jchromb.2009.03.046
12. Chokkathukalam, A.; Kim, D.-H.; Barrett, M. P.; Breitling, R.; Creek, D. J. *Bioanalysis* **2014,** *6,* 511–524. doi:10.4155/bio.13.348
13. Tang, J. K.-H.; You, L.; Blankenship, R. E.; Tang, Y. J. *J. R. Soc., Interface* **2012,** *9,* 2767–2780. doi:10.1098/rsif.2012.0396
14. IUPAC. *Pure Appl. Chem.* **1979,** *51,* 353–380. doi:10.1351/pac197951020353
15. Hertweck, C. *Angew. Chem., Int. Ed.* **2009,** *48,* 4688–4716. doi:10.1002/anie.200806121
16. Witter, D. J.; Vederas, J. C. *J. Org. Chem.* **1996,** *61,* 2613–2623. doi:10.1021/jo952117p
17. Do, J. H.; Choi, D.-K. *Biotechnol. Bioprocess Eng.* **2007,** *12,* 585–593. doi:10.1007/BF02931073
18. McNamara, C. M.; Box, S.; Crawforth, J. M.; Hickman, B. S.; Norwood, T. J.; Rawlings, B. J. *J. Chem. Soc., Perkin Trans. 1* **1998,** 83–88. doi:10.1039/a704545j
19. Bentley, R. *Crit. Rev. Biotechnol.* **1999,** *19,* 1–40. doi:10.1080/0738-859991229189
20. Bretschneider, T.; Heim, J. B.; Heine, D.; Winkler, R.; Busch, B.; Kusebauch, B.; Stehle, T.; Zocher, G.; Hertweck, C. *Nature* **2013,** *502,* 124–128. doi:10.1038/nature12588
21. Wilson, M. C.; Moore, B. S. *Nat. Prod. Rep.* **2012,** *29,* 72–86. doi:10.1039/C1NP00082A
22. Calderone, C. T. *Nat. Prod. Rep.* **2008,** *25,* 845–853. doi:10.1039/b807243d
23. Scherlach, K.; Partida-Martinez, L. P.; Dahse, H.-M.; Hertweck, C. *J. Am. Chem. Soc.* **2006,** *128,* 11529–11536. doi:10.1021/ja062953o
24. Gomez-Escribano, J. P.; Song, L.; Fox, D. J.; Yeo, V.; Bibb, M. J.; Challis, G. L. *Chem. Sci.* **2012,** *3,* 2716–2720. doi:10.1039/c2sc20410j
25. Tamaoki, T.; Shirahata, K.; Iida, T.; Tomita, F. *J. Antibiot.* **1981,** *34,* 1525–1530. doi:10.7164/antibiotics.34.1525
26. Zhang, M.; Hou, X.-F.; Qi, L.-H.; Yin, Y.; Li, Q.; Pan, H.-X.; Chen, X.-Y.; Tang, G.-L. *Chem. Sci.* **2015,** *6,* 3440–3447. doi:10.1039/C5SC00116A
27. Maskey, R. P.; Sevvana, M.; Usón, I.; Helmke, E.; Laatsch, H. *Angew. Chem., Int. Ed.* **2004,** *43,* 1281–1283. doi:10.1002/anie.200352312
28. Pidot, S.; Ishida, K.; Cyrulies, M.; Hertweck, C. *Angew. Chem., Int. Ed.* **2014,** *53,* 7856–7859. doi:10.1002/anie.201402632
29. Fritzsche, K.; Ishida, K.; Hertweck, C. *J. Am. Chem. Soc.* **2008,** *130,* 8307–8316. doi:10.1021/ja800251m
30. Bringmann, G.; Noll, T. F.; Gulder, T. A. M.; Grüne, M.; Dreyer, M.; Wilde, C.; Pankewitz, F.; Hilker, M.; Payne, G. D.; Jones, A. L.; Goodfellow, M.; Fiedler, H.-P. *Nat. Chem. Biol.* **2006,** *2,* 429–433. doi:10.1038/nchembio805
31. Ellis, G. A.; Wyche, T. P.; Fry, C. G.; Braun, D. R.; Bugni, T. S. *Mar. Drugs* **2014,** *12,* 1013–1022. doi:10.3390/md12021013
32. Wyche, T. P.; Piotrowski, J. S.; Hou, Y.; Braun, D.; Deshpande, R.; McIlwain, S.; Ong, I. M.; Myers, C. L.; Guzei, I. A.; Westler, W. M.; Andes, D. R.; Bugni, T. S. *Angew. Chem., Int. Ed.* **2014,** *53,* 11583–11586. doi:10.1002/anie.201405990
33. Finking, R.; Marahiel, M. A. *Annu. Rev. Microbiol.* **2004,** *58,* 453–488. doi:10.1146/annurev.micro.58.030603.123615
34. Mootz, H. D.; Marahiel, M. A. *J. Bacteriol.* **1997,** *179,* 6843–6850.
35. Ling, L. L.; Schneider, T.; Peoples, A. J.; Spoering, A. L.; Engels, I.; Conlon, B. P.; Mueller, A.; Schäberle, T. F.; Hughes, D. E.; Epstein, S.; Jones, M.; Lazarides, L.; Steadman, V. A.; Cohen, D. R.; Felix, C. R.; Fetterman, K. A.; Millett, W. P.; Nitti, A. G.; Zullo, A. M.; Chen, C.; Lewis, K. *Nature* **2015,** *517,* 455–459. doi:10.1038/nature14098
36. Bode, H. B.; Reimer, D.; Fuchs, S. W.; Kirchner, F.; Dauth, C.; Kegler, C.; Lorenzen, W.; Brachmann, A. O.; Grün, P. *Chem. – Eur. J.* **2012,** *18,* 2342–2348. doi:10.1002/chem.201103479
37. Fuchs, S. W.; Proschak, A.; Jaskolla, T. W.; Karas, M.; Bode, H. B. *Org. Biomol. Chem.* **2011,** *9,* 3130–3132. doi:10.1039/c1ob05097d
38. Zhou, Q.; Dowling, A.; Heide, H.; Wöhnert, J.; Brandt, U.; Baum, J.; ffrench-Constant, R.; Bode, H. B. *J. Nat. Prod.* **2012,** *75,* 1717–1722. doi:10.1021/np300279g
39. Zhou, Q.; Grundmann, F.; Kaiser, M.; Schiell, M.; Gaudriault, S.; Batzer, A.; Kurz, M.; Bode, H. B. *Chem. – Eur. J.* **2013,** *19,* 16772–16779. doi:10.1002/chem.201302481
40. Kronenwerth, M.; Bozhüyük, K. A. J.; Kahnt, A. S.; Steinhilber, D.; Gaudriault, S.; Kaiser, M.; Bode, H. B. *Chem. – Eur. J.* **2014,** *20,* 17478–17487. doi:10.1002/chem.201403979
41. Reimer, D.; Nollmann, F. I.; Schultz, K.; Kaiser, M.; Bode, H. B. *J. Nat. Prod.* **2014,** *77,* 1976–1980. doi:10.1021/np500390b
42. Kegler, C.; Nollmann, F. I.; Ahrendt, T.; Fleischhacker, F.; Bode, E.; Bode, H. B. *ChemBioChem* **2014,** *15,* 826–828. doi:10.1002/cbic.201300602
43. Morinaka, B. I.; Vagstad, A. L.; Helf, M. J.; Gugger, M.; Kegler, C.; Freeman, M. F.; Bode, H. B.; Piel, J. *Angew. Chem., Int. Ed.* **2014,** *53,* 8503–8507. doi:10.1002/anie.201400478
44. Bode, H. B.; Brachmann, A. O.; Jadhav, K. B.; Seyfarth, L.; Dauth, C.; Fuchs, S. W.; Kaiser, M.; Waterfield, N. R.; Sack, H.; Heinemann, S. H.; Arndt, H.-D. *Angew. Chem., Int. Ed.* **2015,** *54,* 10352–10355. doi:10.1002/anie.201502835
45. Bode, E.; Brachmann, A. O.; Kegler, C.; Simsek, R.; Dauth, C.; Zhou, Q.; Kaiser, M.; Klemmt, P.; Bode, H. B. *ChemBioChem* **2015,** *16,* 1115–1119. doi:10.1002/cbic.201500094
46. Bourdichon, F.; Casaregola, S.; Farrokh, C.; Frisvad, J. C.; Gerds, M. L.; Hammes, W. P.; Harnett, J.; Huys, G.; Laulund, S.; Ouwehand, A.; Powell, I. B.; Prajapati, J. B.; Seto, Y.; Ter Schure, E.; van Boven, A.; Vankerckhoven, V.; Zgoda, A.; Tuijtelaars, S.; Hansen, E. B. *Int. J. Food Microbiol.* **2012,** *154,* 87–97. doi:10.1016/j.ijfoodmicro.2011.12.030
47. Chankhamjon, P.; Boettger-Schmidt, D.; Scherlach, K.; Urbansky, B.; Lackner, G.; Kalb, D.; Dahse, H.-M.; Hoffmeister, D.; Hertweck, C. *Angew. Chem., Int. Ed.* **2014,** *53,* 13409–13413. doi:10.1002/anie.201407624
48. Garrido, L.; Zubía, E.; Ortega, M. J.; Salvá, J. *J. Org. Chem.* **2003,** *68,* 293–299. doi:10.1021/jo020487p
49. Nam, S.-J.; Gaudêncio, S. P.; Kauffman, C. A.; Jensen, P. R.; Kondratyuk, T. P.; Marler, L. E.; Pezzuto, J. M.; Fenical, W. *J. Nat. Prod.* **2010,** *73,* 1080–1086. doi:10.1021/np100087c
50. Heinz, C.; Cramer, N. *J. Am. Chem. Soc.* **2015,** *137,* 11278–11281. doi:10.1021/jacs.5b07964
51. Matveenko, M.; Liang, G.; Lauterwasser, E. M. W.; Zubía, E.; Trauner, D. *J. Am. Chem. Soc.* **2012,** *134,* 9291–9295. doi:10.1021/ja301326k
52. Ear, A.; Amand, S.; Blanchard, F.; Blond, A.; Dubost, L.; Buisson, D.; Nay, B. *Org. Biomol. Chem.* **2015,** *13,* 3662–3666. doi:10.1039/C5OB00114E
53. Oikawa, H. *J. Org. Chem.* **2003,** *68,* 3552–3557. doi:10.1021/jo0267596

54. Murphy, A. C.; Gao, S.-S.; Han, L.-C.; Carobene, S.; Fukuda, D.; Song, Z.; Hothersall, J.; Cox, R. J.; Crosby, J.; Crump, M. P.; Thomas, C. M.; Willis, C. L.; Simpson, T. *J. Chem. Sci.* **2014,** *5,* 397–402. doi:10.1039/C3SC52281D
55. Shiozawa, H.; Kagasaki, T.; Kinoshita, T.; Haruyama, H.; Domon, H.; Utsui, Y.; Kodama, K.; Takahashi, S. *J. Antibiot.* **1993,** *46,* 1834–1842. doi:10.7164/antibiotics.46.1834
56. Kuwajima, I.; Tanino, K. *Chem. Rev.* **2005,** *105,* 4661–4670. doi:10.1021/cr040636z
57. Barra, L.; Ibrom, K.; Dickschat, J. S. *Angew. Chem., Int. Ed.* **2015,** *54,* 6637–6640. doi:10.1002/anie.201501765
58. Kühne, B.; Hanssen, H.-P.; Abraham, W.-R.; Wray, V. *Phytochemistry* **1991,** *30,* 1463–1465. doi:10.1016/0031-9422(91)84187-W
59. Sugai, Y.; Ueno, Y.; Hayashi, K.-i.; Oogami, S.; Toyomasu, T.; Matsumoto, S.; Natsume, M.; Nozaki, H.; Kawaide, H. *J. Biol. Chem.* **2011,** *286,* 42840–42847. doi:10.1074/jbc.M111.302703
60. Rabe, P.; Barra, L.; Rinkel, J.; Riclea, R.; Citron, C. A.; Klapschinski, T. A.; Janusko, A.; Dickschat, J. S. *Angew. Chem., Int. Ed.* **2015,** *54,* 13448–13451. doi:10.1002/anie.201507615
61. Rabe, P.; Pahirulzaman, K. A. K.; Dickschat, J. S. *Angew. Chem., Int. Ed.* **2015,** *54,* 6041–6045. doi:10.1002/anie.201501119
62. Rabe, P.; Rinkel, J.; Klapschinski, T. A.; Barra, L.; Dickschat, J. S. *Org. Biomol. Chem.* **2015,** in press. doi:10.1039/C5OB01998B
63. Aoyama, T.; Naganawa, H.; Muraoka, Y.; Aoyagi, T.; Takeuchi, T. *J. Antibiot.* **1992,** *45,* 1703–1704. doi:10.7164/antibiotics.45.1703
64. Aoyagi, T.; Aoyama, T.; Kojima, F.; Hattori, S.; Honma, Y.; Hamada, M.; Takeuchi, T. *J. Antibiot.* **1992,** *45,* 1587–1591. doi:10.7164/antibiotics.45.1587
65. Meguro, A.; Motoyoshi, Y.; Teramoto, K.; Ueda, S.; Totsuka, Y.; Ando, Y.; Tomita, T.; Kim, S.-Y.; Kimura, T.; Igarashi, M.; Sawa, R.; Shinada, T.; Nishiyama, M.; Kuzuyama, T. *Angew. Chem., Int. Ed.* **2015,** *54,* 4353–4356. doi:10.1002/anie.201411923
66. Janke, R.; Görner, C.; Hirte, M.; Brück, T.; Loll, B. *Acta Crystallogr., Sect. D* **2014,** *70,* 1528–1537. doi:10.1107/S1399004714005513
67. Kim, S.-Y.; Zhao, P.; Igarashi, M.; Sawa, R.; Tomita, T.; Nishiyama, M.; Kuzuyama, T. *Chem. Biol.* **2009,** *16,* 736–743. doi:10.1016/j.chembiol.2009.06.007
68. Rohmer, M.; Knani, M.; Simonin, P.; Sutter, B.; Sahm, H. *Biochem. J.* **1993,** *295,* 517–524. doi:10.1042/bj2950517
69. Ye, Y.; Minami, A.; Mandi, A.; Liu, C.; Taniguchi, T.; Kuzuyama, T.; Monde, K.; Gomi, K.; Oikawa, H. *J. Am. Chem. Soc.* **2015,** *137,* 11846–11853. doi:10.1021/jacs.5b08319
70. Lesburg, C. A.; Zhai, G.; Cane, D. E.; Christianson, D. W. *Science* **1997,** *277,* 1820–1824. doi:10.1126/science.277.5333.1820
71. Cane, D. E.; Sohng, J.-K.; Lamberson, C. R.; Rudnicki, S. M.; Wu, Z.; Lloyd, M. D.; Oliver, J. S.; Hubbard, B. R. *Biochemistry* **1994,** *33,* 5846–5857. doi:10.1021/bi00185a024
72. Gutta, P.; Tantillo, D. J. *J. Am. Chem. Soc.* **2006,** *128,* 6172–6179. doi:10.1021/ja058031n
73. Zu, L.; Xu, M.; Lodewyk, M. W.; Cane, D. E.; Peters, R. J.; Tantillo, D. J. *J. Am. Chem. Soc.* **2012,** *134,* 11369–11371. doi:10.1021/ja3043245
74. Hubrich, F.; Juneja, P.; Müller, M.; Diederichs, K.; Welte, W.; Andexer, J. N. *J. Am. Chem. Soc.* **2015,** *137,* 11032–11037. doi:10.1021/jacs.5b05559
75. Floss, H. G. *Nat. Prod. Rep.* **1997,** *14,* 433–452. doi:10.1039/np9971400433
76. Andexer, J. N.; Kendrew, S. G.; Nur-e-Alam, M.; Lazos, O.; Foster, T. A.; Zimmermann, A.-S.; Warneck, T. D.; Suthar, D.; Coates, N. J.; Koehn, F. E.; Skotnicki, J. S.; Carter, G. T.; Gregory, M. A.; Martin, C. J.; Moss, S. J.; Leadlay, P. F.; Wilkinson, B. *Proc. Natl. Acad. Sci. U. S. A.* **2011,** *108,* 4776–4781. doi:10.1073/pnas.1015773108
77. Poulin, M. B.; Du, Q.; Schramm, V. L. *J. Org. Chem.* **2015,** *80,* 5344–5347. doi:10.1021/acs.joc.5b00608
78. Brock, N. L.; Nikolay, A.; Dickschat, J. S. *Chem. Commun.* **2014,** *50,* 5487–5489. doi:10.1039/c4cc01924e
79. Kintaka, K.; Ono, H.; Tsubotani, S.; Harada, S.; Okazaki, H. *J. Antibiot.* **1984,** *37,* 1294–1300. doi:10.7164/antibiotics.37.1294
80. Harrington, C.; Reen, F. J.; Mooij, M. J.; Stewart, F. A.; Chabot, J.-B.; Guerra, A. F.; Glöckner, F. O.; Nielsen, K. F.; Gram, L.; Dobson, A. D. W.; Adams, C.; O'Gara, F. *Mar. Drugs* **2014,** *12,* 5960–5978. doi:10.3390/md12125960
81. Berger, M.; Brock, N. L.; Liesegang, H.; Dogs, M.; Preuth, I.; Simon, M.; Dickschat, J. S.; Brinkhoff, T. *Appl. Environ. Microbiol.* **2012,** *78,* 3539–3551. doi:10.1128/AEM.07657-11
82. Cane, D. E.; Wu, Z.; van Epp, J. E. *J. Am. Chem. Soc.* **1992,** *114,* 8479–8483. doi:10.1021/ja00048a019
83. Tappel, A. L. *Biochem. Pharmacol.* **1960,** *3,* 289–296. doi:10.1016/0006-2952(60)90094-0
84. Seipke, R. F.; Hutchings, M. I. *Beilstein J. Org. Chem.* **2013,** *9,* 2556–2563. doi:10.3762/bjoc.9.290
85. Schoenian, I.; Paetz, C.; Dickschat, J. S.; Aigle, B.; Leblond, P.; Spiteller, D. *ChemBioChem* **2012,** *13,* 769–773. doi:10.1002/cbic.201200033

License and Terms

BEILSTEIN JOURNAL OF ORGANIC CHEMISTRY

Synthesis of *Xenia* diterpenoids and related metabolites isolated from marine organisms

Tatjana Huber‡, Lara Weisheit‡ and Thomas Magauer*

Review

Open Access

Address:
Department of Chemistry and Pharmacy, Ludwig-Maximilians-University Munich, Butenandtstraße 5–13, 81377 Munich, Germany

Email:
Thomas Magauer* - thomas.magauer@lmu.de

* Corresponding author ‡ Equal contributors

Keywords:
asymmetric synthesis; natural products; total synthesis; Xenia diterpenoids; xenicanes

Beilstein J. Org. Chem. **2015,** *11,* 2521–2539.
doi:10.3762/bjoc.11.273

Received: 13 October 2015
Accepted: 27 November 2015
Published: 10 December 2015

This article is part of the Thematic Series "Natural products in synthesis and biosynthesis II".

Guest Editor: J. S. Dickschat

Abstract

This review describes strategies for the chemical synthesis of xenicane diterpenoids and structurally related metabolites. Selected members from the four different subclasses of the *Xenia* diterpenoid family, the xenicins, xeniolides, xeniaphyllanes and xeniaethers, are presented. The synthetic strategies are discussed with an emphasis on the individual key reactions for the construction of the uncommon nine-membered carbocycle which is the characteristic structural feature of these natural products. Additionally, the putative biosynthetic pathway of xenicanes is illustrated.

Introduction

Terpenoids are a large group of structurally diverse secondary metabolites. Among these natural products, *Xenia* diterpenoids or xenicanes represent a unique family with intriguing structural features and diverse biological activities. Many xenicanes display significant cytotoxic and antibacterial activity and are therefore of great interest for drug discovery, especially for their application as anticancer agents [1]. Marine soft corals of the genus *Xenia* (order *Alcyonacea*, family *Xeniidae*) are known to be rich in xenicane diterpenoids. The first reported member of these metabolites was xenicin (**1**), isolated from the soft coral *Xenia elongata* in Australia, whose structure was elucidated in 1977 by Schmitz and van der Helm (Figure 1a) [2]. The common numbering of the xenicane skeleton shown in Figure 1b is used throughout this review.

Since then, several further xenicanes with various modifications of the cyclononane ring and isoprenyl side chain in their structure have been isolated. In general, the common structural feature of xenicanes is a bicyclic framework consisting of an A ring which is trans-fused to a nine-membered carbocyclic B ring. The family of *Xenia* diterpenoids was originally divided into three subfamilies: the xenicins (containing an 11-oxabi-

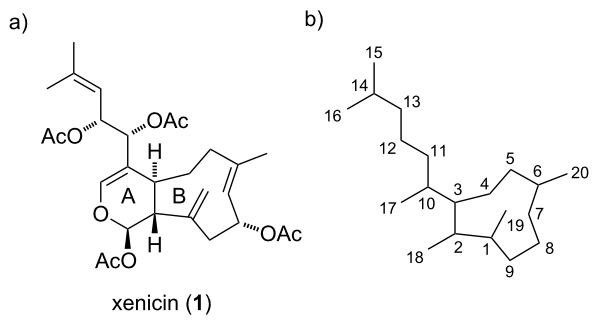

Figure 1: a) Structure of xenicin (**1**) and b) numbering of the xenicane skeleton according to Schmitz and van der Helm.

cyclo[7.4.0]tridecane ring system with an acetal functionality) [2], the xeniolides (containing an 11-oxabicyclo[7.4.0]tridecane ring system with a lactone functionality) [3] and the xeniaphyllanes (with a bicyclo[7.2.0]undecane ring system) [4]. Later, an additional subfamily was discovered and named xeniaethers [5] (containing an 11-oxabicyclo[7.3.0]dodecane ring system). An overview of representative members of these subfamilies is depicted in Figure 2.

Xenicanes are closely related to a number of metabolites which also feature the characteristic cyclononene framework (Figure 3). For example, a class of bicyclic sesquiterpenes, caryophyllenes [21], exhibit the same bicyclo[7.2.0]undecane skeleton as xeniaphyllanes. Furthermore, while monocyclic azamilides [22] are seco-A-ring diterpenoids that are acylated with fatty acids, *Dictyota* diterpenes [23,24] either bear a similar seco-ring fragment, as observed for dictyodiol (**24**), or comprise a fused γ-butyrolactone moiety, as in dictyolactone (**25**, Figure 3).

This review intends to provide a comprehensive overview of research covering xenicane diterpenoids and related natural products. In the following section, we present a biosynthetic proposal, discuss various synthetic approaches towards xenicane diterpenoids and highlight successful total syntheses.

Review

Biosynthetic hypothesis

The proposed biogenesis of xenicanes (Scheme 1) is suggested to be similar to the reported biosynthesis of the structurally related caryophyllene sesquiterpenes [25]. *Xenia* diterpenoids are believed to originate from the common diterpenoid precursor geranylgeranyl pyrophosphate (GGPP, **28**), which is assembled from the two terpene units, isoprenyl pyrophosphate (IPP, **26**) and dimethylallyl pyrophosphate (DMAPP, **27**) [26]. Initial loss of a diphosphate anion from GGPP generates an allylic cation in **29** which is intramolecularly trapped by nucleophilic attack of the C3,C10-double bond, forming the secondary cation **30**. Attack of the newly generated C1,C2-double bond with simultaneous loss of a proton then affords the bicyclo[7.2.0]undecane ring system **31** as found in xeniaphyllanes [3]. Finally, double C–H oxidation furnishes the β-hydroxy aldehyde **32** which can undergo a retro-aldol reaction with concomitant opening of the cyclobutane ring to form dialdehyde **33** as the common biogenetic precursor of xenicins, xeniolides and xeniaethers.

An alternative biosynthetic pathway proposed by Schmitz and van der Helm involves the direct formation of the nine-membered carbocyclic ring via oxidative cyclization of geranyllinalool (**34**) [2], which is formed from GGPP (**28**) by enzymatic hydrolysis of the pyrophosphate unit and allylic rearrangement (Scheme 2).

Synthetic strategies

The unusual molecular structures and the potential of xenicanes to act as chemotherapeutic agents make these natural products attractive targets for synthetic chemists. Although more than 100 different *Xenia* diterpenoids are known to date, only a few total syntheses of xeniolides have been reported in the last two decades. Surprisingly, since the discovery of xenicin in 1977 [2], no total synthesis of a member of this subclass has been accomplished.

The synthesis of nine-membered rings is challenging, especially when they contain an *E*-configured double bond. Different strategies for the construction of *E*- or *Z*-cyclononenes have been reported to date and common reactions are summarized in Scheme 3. Transition metal-catalyzed ([M] = Ru, Mo, W) ring-closing metathesis (RCM) reactions of 1,10-dienes **A** can be employed for the synthesis of cyclononenes. The *E*/*Z*-selectivity of the olefin depends on the ring-size and the choice of catalyst. As a consequence of avoiding ring strain, small- and medium-sized rings are generally obtained with *Z*-configuration of the alkene. The Grob fragmentation reaction of fused 6,5-bicycles **B** is usually a concerted process that affords cyclononenes in a stereospecific manner [27]. The relative configuration of the leaving group (LG = OTs, OMs, Hal, NR_3^+) and the adjacent substituent determine the *E*/*Z*-geometry of the olefin. A *cis*-geometry leads to the formation of the *E*-configured double bond. In general, the Grob fragmentation is the most commonly employed method for the synthesis of cyclononenes due to the predictability of the stereochemical outcome of the product. The construction of cyclononenes can furthermore be achieved by thermal [3,3]-sigmatropic rearrangements of 1,5-dienes **C**. When the reaction proceeds via a chairlike transition state, the substituents are oriented with minimal steric hindrance to give the *E*,*E*-configured nine-

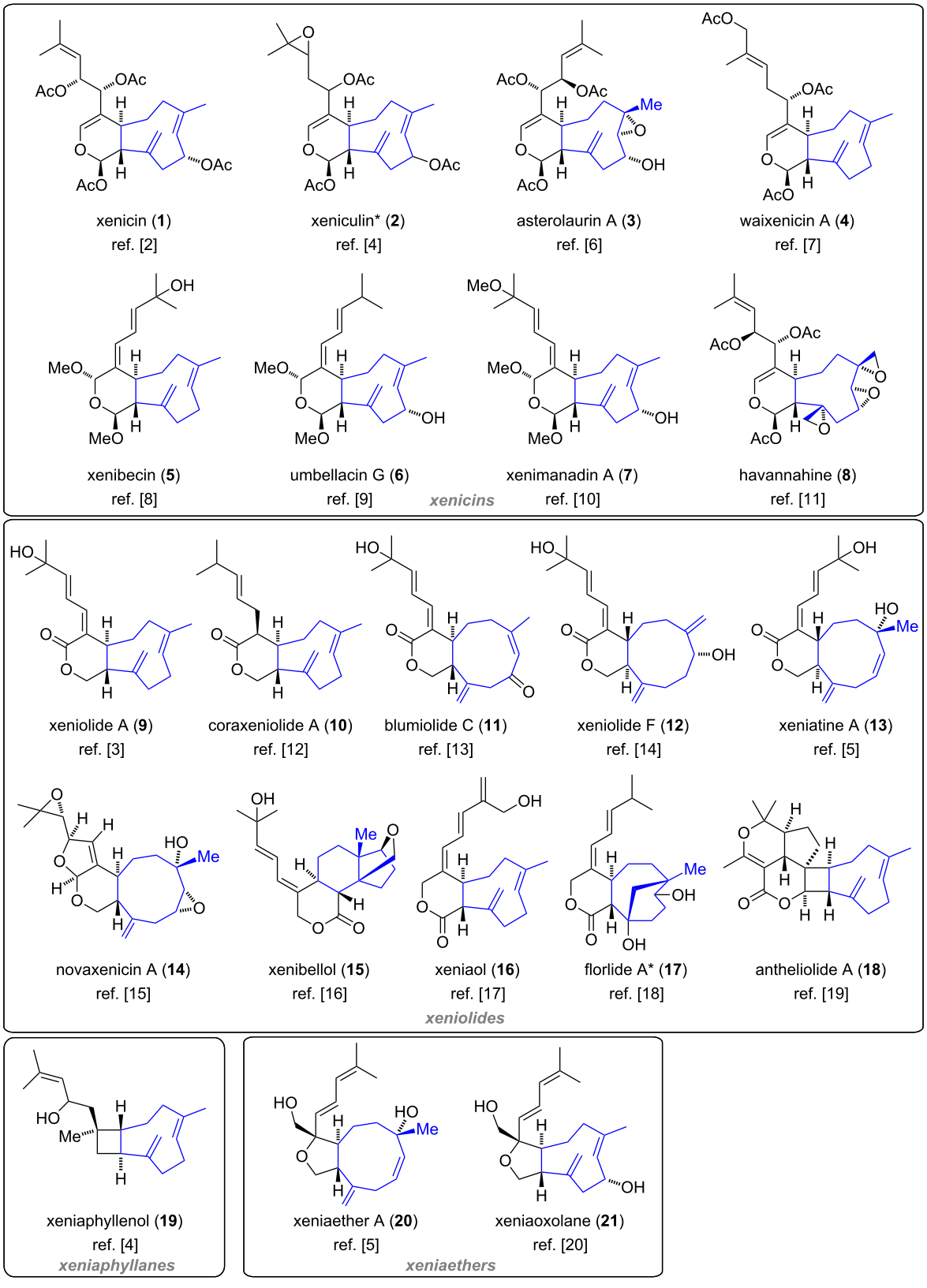

Figure 2: Overview of selected Xenia diterpenoids according to the four subclasses [2-20]. The nine-membered carbocyclic rings are highlighted in blue. *Stereochemistry not determined.

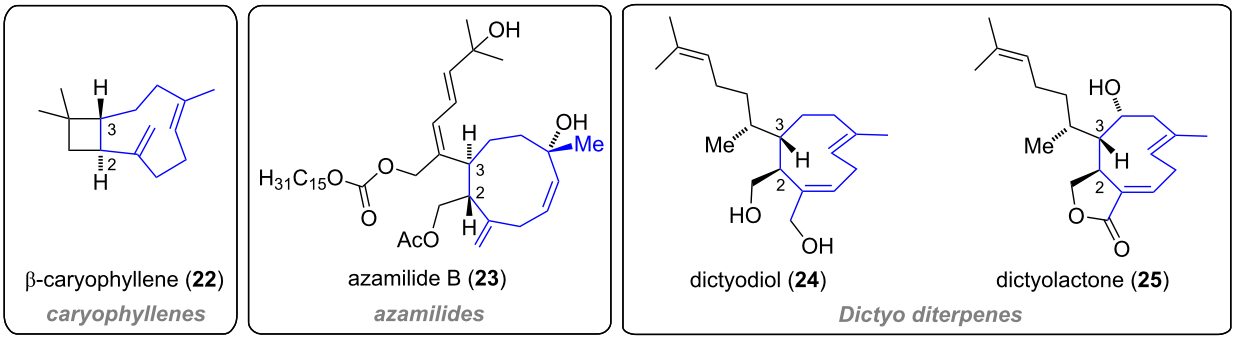

Figure 3: Representative members of the caryophyllenes, azamilides and *Dictyota* diterpenes.

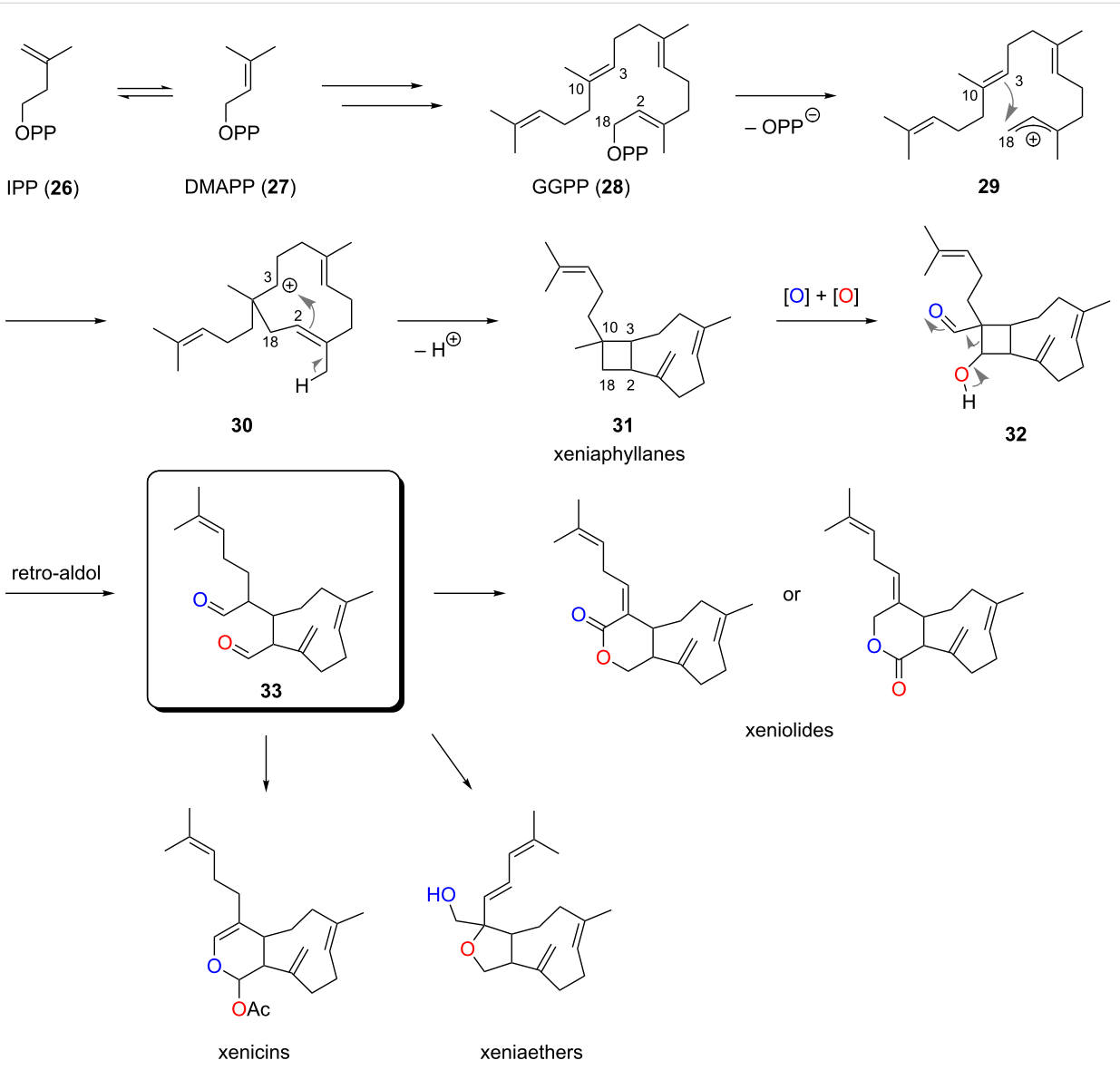

Scheme 1: Proposed biosynthesis of *Xenia* diterpenoids (OPP = pyrophosphate, GGPP = geranylgeranyl pyrophosphate, IPP = isoprenyl pyrophosphate, DMAPP = dimethylallyl pyrophosphate).

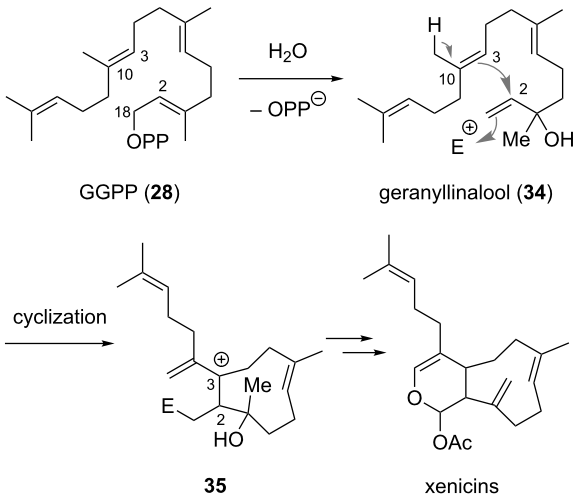

Scheme 2: Direct synthesis of the nine-membered carbocycle as proposed by Schmitz and van der Helm (E = electrophilic oxygen species) [2].

membered ring. Ring contraction reactions of 13-membered lactams afford cyclononenes via intramolecular acyl transfer reactions. The configuration of the double bond derives from precursor **D** and thus allows the formation of *E*- or *Z*-configured cyclononenes. Additionally, the intramolecular palladium-catalyzed cyclization of haloalkenes with organoboranes affords cyclononenes with retention of the double bond configuration [28]. The corresponding allylic alcohols can be prepared by a Nozaki–Hiyama–Kishi coupling of haloalkenes with aldehydes.

The first synthesis of the unusual nine-membered carbocyclic ring was reported by Corey for the total synthesis of β-caryophyllene in 1963 (Scheme 4) [29-31]. Starting with a photochemical [2 + 2] cycloaddition between 2-cyclohexen-1-one (**37**) and isobutene (**36**), an isomeric mixture of *trans*- and *cis*-fused [4.2.0]octanone was obtained (*trans*-**38**/*cis*-**39** = 4:1). The more stable *cis*-bicycle **39** could be obtained by isomerization of *trans*-**38** with base. Acylation with sodium hydride and dimethyl carbonate followed by methylation furnished β-keto ester **40**. Addition of lithium acetylide **41** to the keto group led to acetal **42**. Hydrogenation of the triple bond under basic

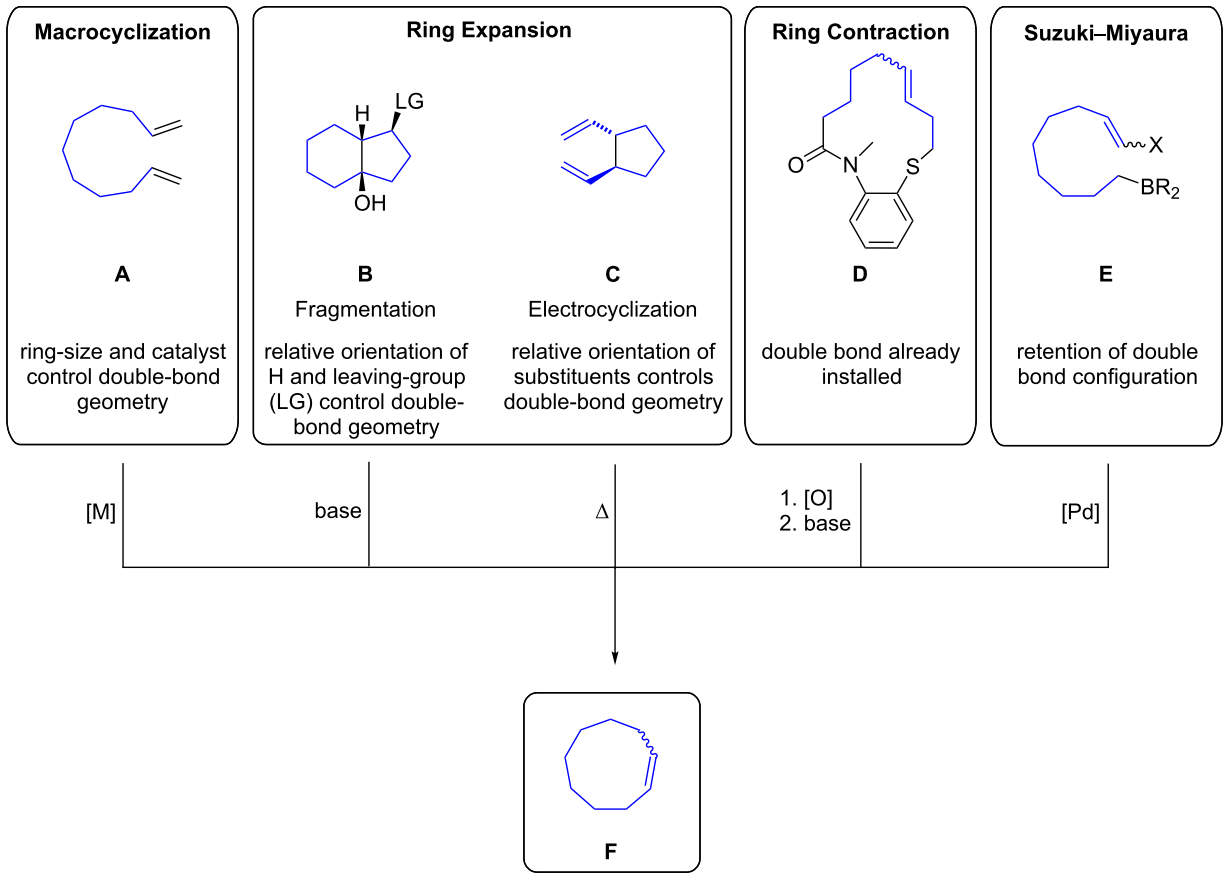

Scheme 3: The construction of *E*- or *Z*-cyclononenes.

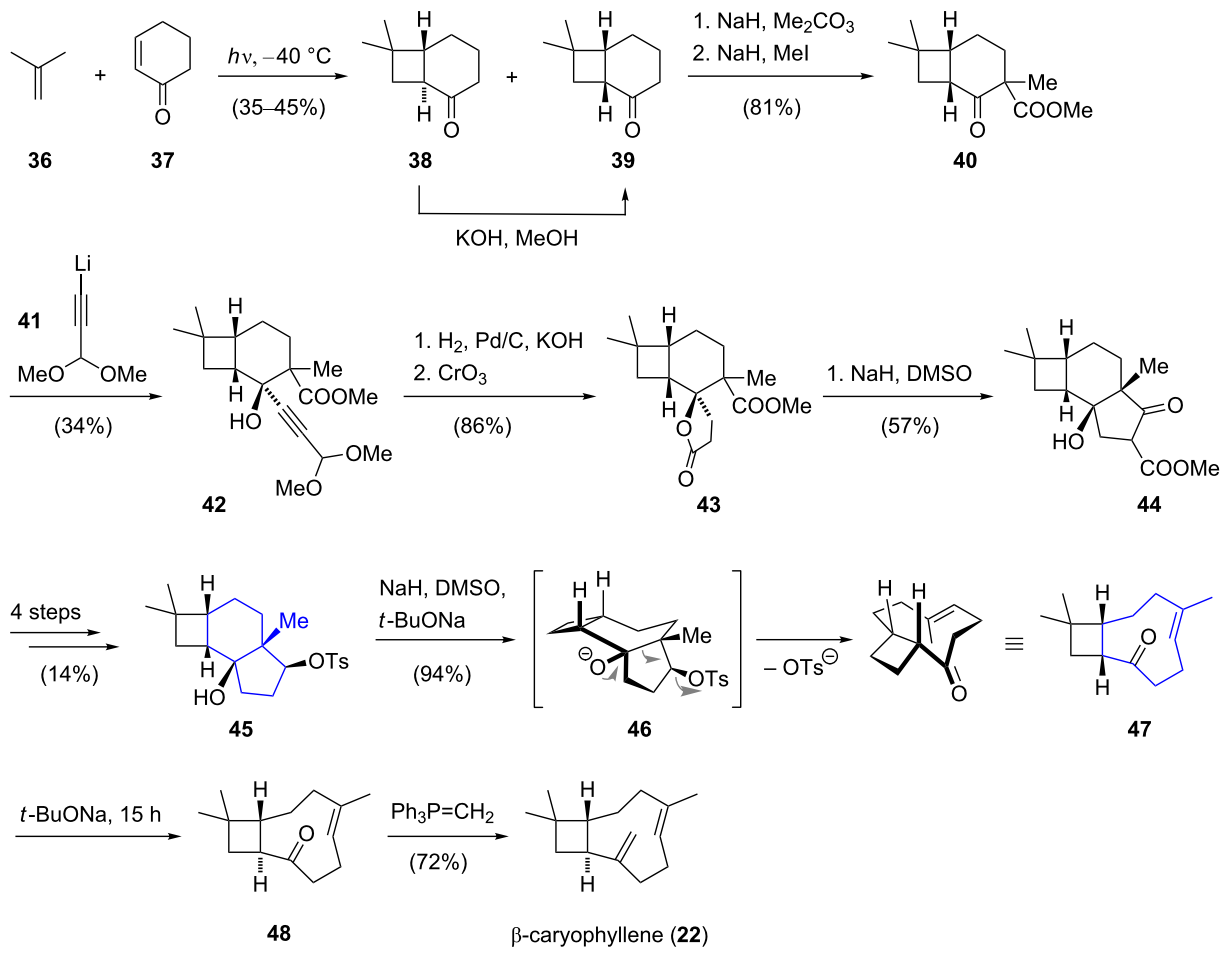

Scheme 4: Total synthesis of racemic β-caryophyllene (**22**) by Corey.

conditions resulted in cleavage of the acetal and ring closure to the corresponding lactol which was oxidized with chromic acid to furnish γ-lactone **43**. An ensuing Dieckmann condensation [32] of **43** afforded a 4,6,5-tricycle which was converted to the fragmentation precursor **45** in four further steps. A base-mediated Wharton-type Grob fragmentation [33] then served as the key step to construct the cyclononene motif of bicycle **47**. Prolonged exposure of the resulting *cis*-fused 4,9-bicycle **47** to sodium *tert*-butoxide gave rise to the epimerized *trans*-isomer **48**. Finally, the exocyclic double bond was introduced by olefination of ketone **48** and thus completed the racemic total synthesis of β-caryophyllene (**22**) in 13 steps. This elegant synthesis received considerable attention and revealed already at that time the great potential of modern synthetic organic chemistry.

More than 20 years later, in 1984, Oishi and co-workers reported a different strategy which culminated in the total synthesis of racemic β-caryophyllene (**22**) (Scheme 5) [34]. Their synthesis commenced with conjugate addition of ethyl (phenylsulfonyl)acetate, a methylsulfonyl anion equivalent, to cyclobutene ester **49** followed by a sequence consisting of saponification, regioselective decarboxylation and reesterification to afford methyl ester **50**. The ester group was reduced with lithium aluminum hydride and the resulting alcohol was converted to the corresponding silyl ether. Next, alkylation of the metalated sulfone with allylic chloride **51** afforded alcohol **52** after desilylation. Subsequent desulfonylation with sodium amalgam and Jones oxidation of the primary alcohol furnished carboxylic acid **53**. The corresponding tertiary amide was then formed by sequential reaction of carboxylic acid **53** with oxalyl chloride and *N*-methylaniline derivative **54**. The following two-step debenzylation sequence afforded alcohol **55** which was converted to the corresponding mesylate, serving as a key intermediate for the construction of the nine-membered carbocyclic ring. Treatment of this intermediate with potassium *tert*-

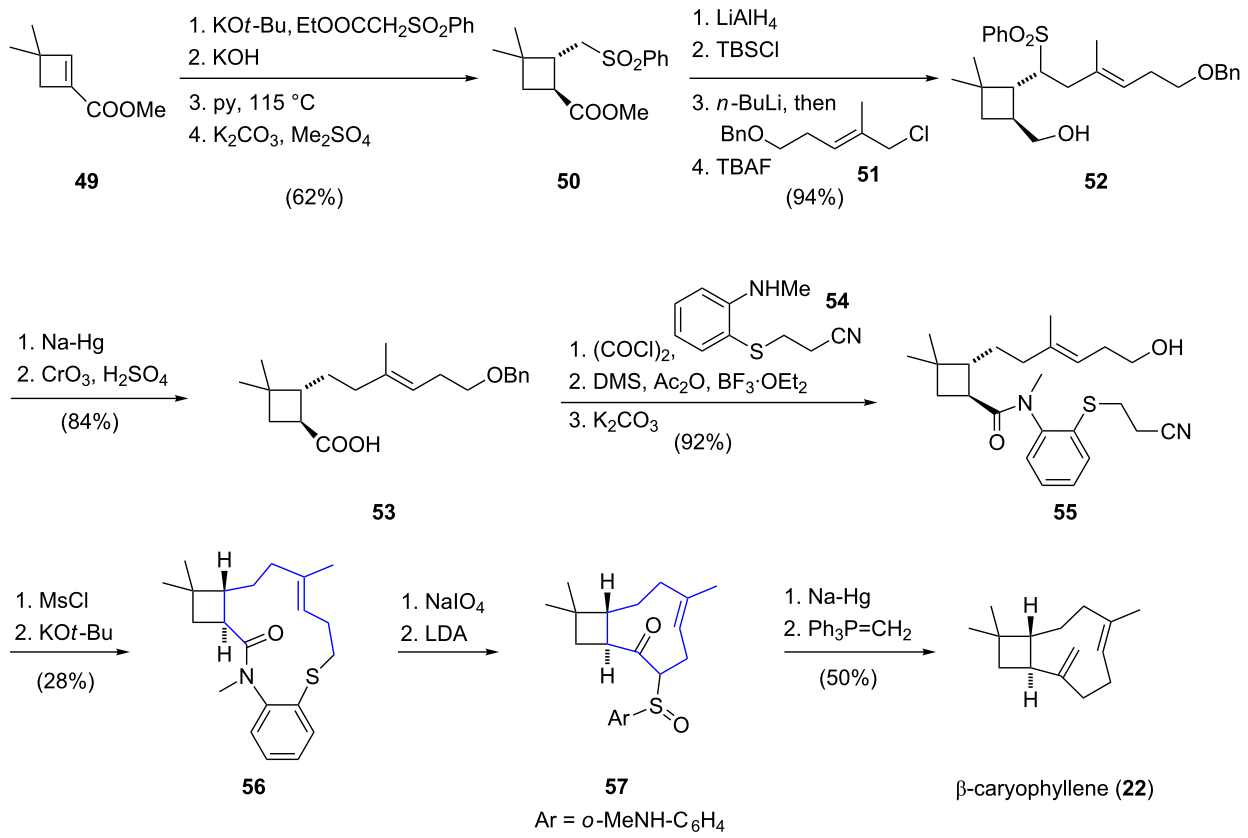

Scheme 5: Total synthesis of racemic β-caryophyllene (**22**) by Oishi.

butoxide led to the cleavage of the 2-cyanoethylsulfide moiety and the generation of a thiolate anion, which underwent S_N2 displacement of the primary mesylate, affording the 13-membered lactam **56**. The stage was now set for the key intramolecular acyl transfer reaction to form the cyclononene motif. After sodium periodate oxidation of sulfide **56** to the corresponding sulfoxide, addition of lithium diisopropylamide initiated the intramolecular acyl transfer and led to formation of cyclononene **57** in quantitative yield. Reductive desulfonylation and a final Wittig olefination of the ketone then afforded racemic β-caryophyllene (**22**). In summary, the total synthesis of β-caryophyllene was achieved in 19 steps with an overall yield of 6.3%. Although the key intramolecular acyl transfer reaction for construction of the cyclononene ring could be realized in quantitative yield, the low-yielding formation of the macrocyclic thioether reduced the overall efficiency of the presented synthetic route. Based on a similar strategy and using the corresponding *Z*-isomer of cyclization precursor **39**, Oishi and co-workers reported a total synthesis of racemic isocaryophyllene, the *cis* double bond isomer of caryophyllene. Further total syntheses of isocaryophyllene have also been reported by Kumar [35,36], Miller [37] and Bertrand [38].

In 1995, Pfander reported the synthesis of an important building block [24] for the total synthesis of coraxeniolide A (**10**) [12], starting from chiral (−)-Hajos–Parrish diketone (**58**) [39]. Based on Pfander's seminal work, the first total synthesis of a xenicane diterpenoid was then accomplished by Leumann in 2000 (Scheme 6) [40]. Starting from enantiopure (−)-Hajos–Parrish diketone (**58**), allylic alcohol **59** was prepared by regioselective reduction of the carbonyl group, silylation of the resulting alcohol and further reduction of the enone moiety. An ensuing transetherification of alcohol **59** with ethyl vinyl ether gave an allyl vinyl ether, which underwent a magnesium perchlorate-promoted [1,3]-sigmatropic rearrangement [41] to afford an aldehyde that was converted to dimethylacetal **60**. The following epoxidation proceeded with good stereoselectivity (α/β ≈ 11:1) and the regioselective opening of the epoxide moiety using lithium cyanide afforded a β-hydroxy nitrile in a *trans*-diaxial arrangement. Under basic conditions, the configuration of the nitrile group at C2 was inverted, furnishing the thermodynamically more stable **61**. Nitrile **61** was then converted to lactol **62** in seven further steps. Next, the cyclononene ring of **63** was constructed via a Grob fragmentation of 6,6,5-tricycle **62**, affording the bicyclic product **63** in very good yield,

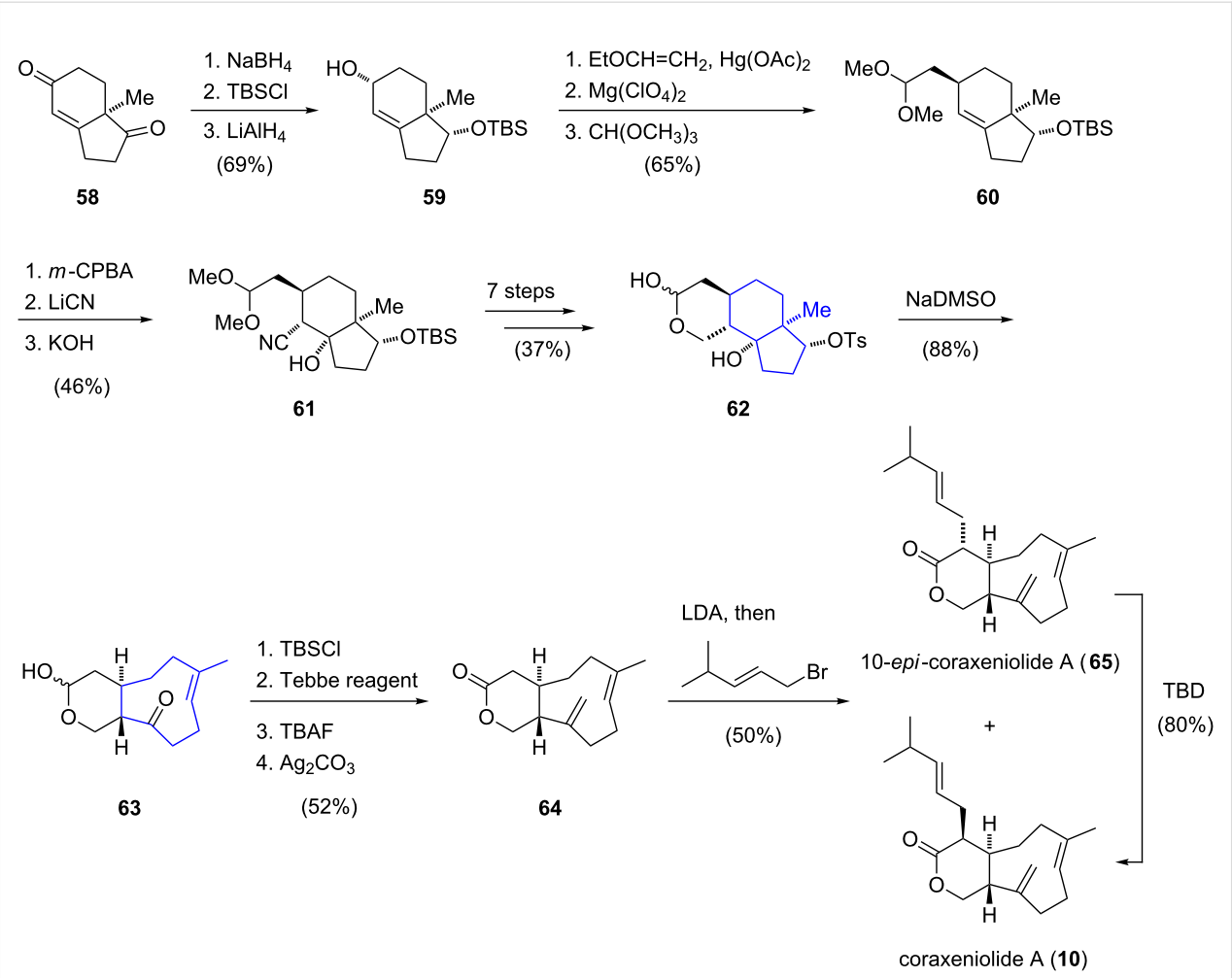

Scheme 6: Total synthesis of coraxeniolide A (**10**) by Leumann.

however, as a mixture of lactol epimers (α/β ≈ 56:44). Silyl protection of the lactol and subsequent Tebbe olefination [42] of the ketone group installed the exocyclic double bond of the nine-membered carbocycle. Desilylation followed by oxidation with silver carbonate then afforded lactone **64**. For the introduction of the side chain, the enolate derived from lactone **64** was treated with 1-bromo-4-methylpent-2-ene, giving a 1:6 mixture of coraxeniolide A (**10**) and its epimer **65**. By equilibration with triazabicyclodecene (TBD), the ratio of **10**:**65** could be inverted to 3:1. In summary, coraxeniolide A (**10**) was synthesized in a longest linear sequence of 23 steps with an overall yield of 1.4%.

The most complex xenicane diterpenoid synthesized to date is pentacyclic antheliolide A (**18**) [18] by Corey (Scheme 7) [43]. The linear precursor **68** was prepared from vinyl bromide **66** and aldehyde **67** in six steps in 34% yield. After saponification of the ester functionality, treatment with tosyl chloride and trimethylamine resulted in the formation of a ketene that underwent a diastereoselective intramolecular [2 + 2] cycloaddition to provide bicyclic ketone **69**. Addition of TMS cerium acetylide to the carbonyl group of **69**, followed by desilylation under basic conditions gave rise to (±)-ethynylcarbinol, which was separated by chiral HPLC. The desired diastereomer was then transformed to benzene sulfinate ester **70**. A palladium-catalyzed [2,3]-sigmatropic rearrangement formed an isomeric allenic sulfone [44] which, upon conjugate addition of diethyl amine followed by hydrolysis afforded a β-ketosulfone. For the following ring closure, the primary alcohol was desilylated and converted to the corresponding allylic carbonate **71**. The cyclononene structure **72** was then assembled via a palladium-catalyzed and base-mediated cyclization of carbonate **71** [45]. Reductive cleavage of the sulfone using aluminium amalgam afforded a ketone, which was converted to an exocyclic double bond by treatment with Tebbe's reagent [42]. In order to convert the methoxy acetal to the corresponding lactone,

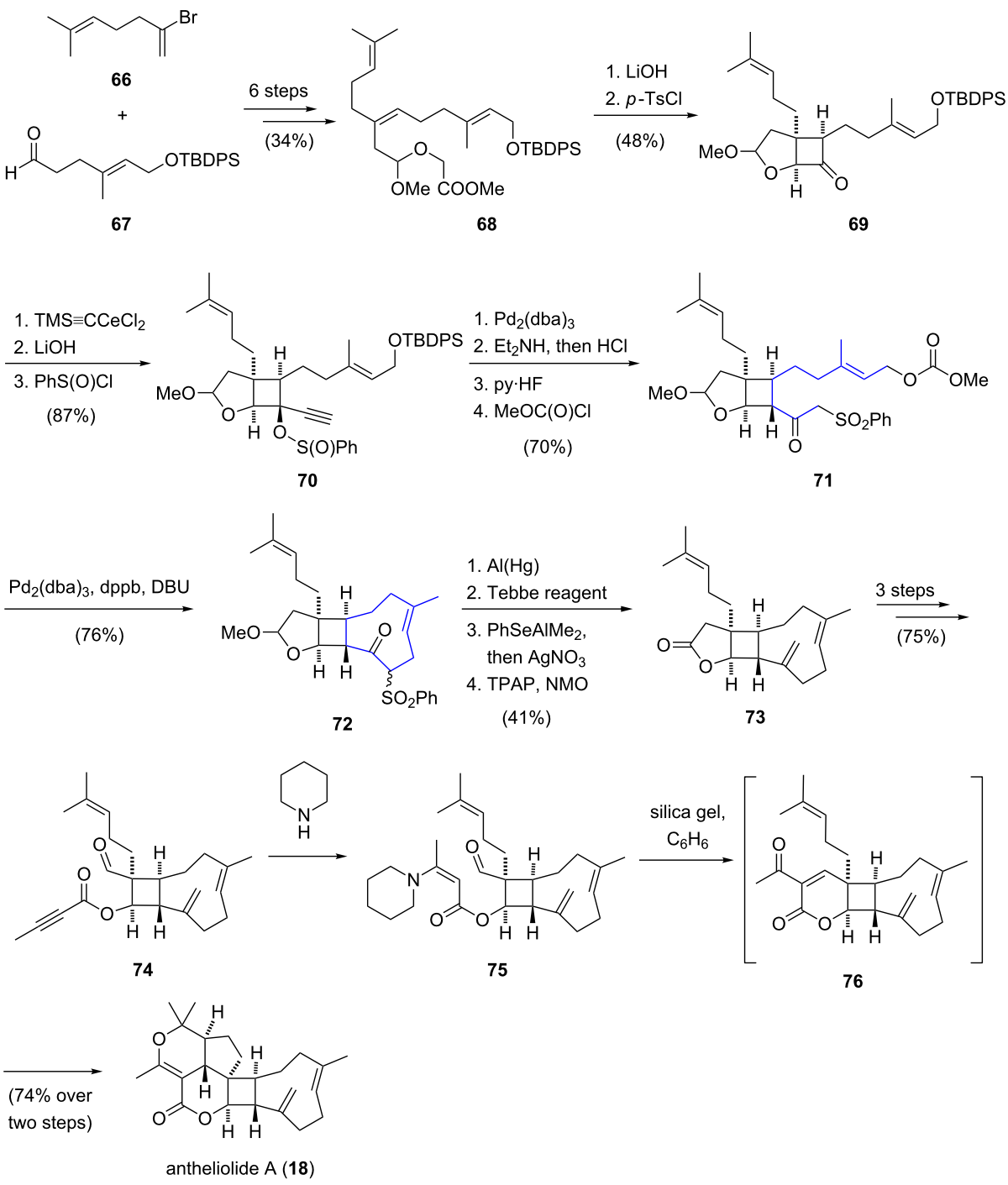

Scheme 7: Total synthesis of antheliolide A (**18**) by Corey.

without affecting the sensitive caryophyllene-like subunit, the methoxy group was replaced with a phenylseleno moiety, which was converted to the alcohol and finally oxidized to lactone **73**. In three further steps, lactone **73** was converted to aldehyde ester **74**, which upon treatment with piperidine gave a β-enamino ester **75**. Finally, an elegant cascade reaction involving an aldol condensation, followed by a hetereo Diels–Alder reaction closed the last three rings and antheliolide A (**18**) was obtained in 74% yield. In summary, the successful total synthesis of antheliolide A proceeded in 25 linear steps with an overall yield of 1.7%.

The total syntheses of coraxeniolide A (**10**) and β-caryophyllene (**22**) reported by Corey [46] in 2008 are based on Pfander's

idea [24] to construct the cyclononene fragment from (−)-Hajos–Parrish diketone (**58**) [39] (Scheme 8). Chiral hydroxy dione **77** was synthesized according to a literature-known procedure [47]. Regioselective reduction with sodium borohydride, followed by dehydration under Mitsunobu conditions and silylation of the tertiary alcohol furnished trimethylsiloxy ketone **78**. The ketone functionality was then diastereoselectively reduced under Corey–Bakshi–Shibata conditions [48] and an ensuing desilylation furnished a diol. In order to introduce a leaving group for the following key step, the secondary hydroxy group was tosylated to afford **79**. Once again, a stereospecific Grob fragmentation of tosylate **79** served as the key step for the synthesis of the enantiomerically pure and configurationally stable nine-membered *E*,*Z*-dienone **80**. The synthesis of the enantiomer of dienone **80**, *ent*-**80**, was accomplished by a route parallel to that presented in Scheme 8a, starting from *ent*-**77**. The highly efficient construction of these versatile intermediates provides a basis to synthesize a variety of natural products containing this macrocyclic structural motif. Based on chiral enone **80** and its enantiomer, *ent*-**80**, coraxeniolide A (**10**) and β-caryophyllene (**22**) were synthesized in five and four further steps, respectively. The synthesis of **10** continued with a trityl perchlorate-catalyzed conjugate addition of silyl ketene acetal **81a** to enone *ent*-**80**. Deprotonation and trapping of the resulting enolate with formaldehyde furnished lactone **82** in a regio- and stereoselective fashion. Introduction of the exocyclic double bond proved to be challenging and therefore salt-free, highly reactive methylenetriphenylphosphorane was used. Finally, α-alkylation of the lactone with iodide **83** provided coraxeniolide A (**10**) and its epimer in a 1:6 ratio which could be reversed to 4:1 by base-mediated equilibration. Purification by column chromatography, allowed the two epimers to be separated and afforded coraxeniolide A (**10**) in 38% yield over three steps.

Additionally, the enantioselective total synthesis of β-caryophyllene was realized starting from key intermediate **80**. The route commenced with conjugate addition of silyl ketene acetal **81b** to enone **80** from the sterically less hindered re-face. The ester group was selectively reduced and desilylation afforded alcohol **84**. The generated primary alcohol was tosylated and regioselective deprotonation followed by intramolecular α-alkylation stereoselectively formed the cyclobutane ring. A final Wittig methylenation introduced the exocyclic double bond and afforded (−)-β-caryophyllene (**22**), for the first time in an enantioselective manner. In conclusion, Corey's protocol for

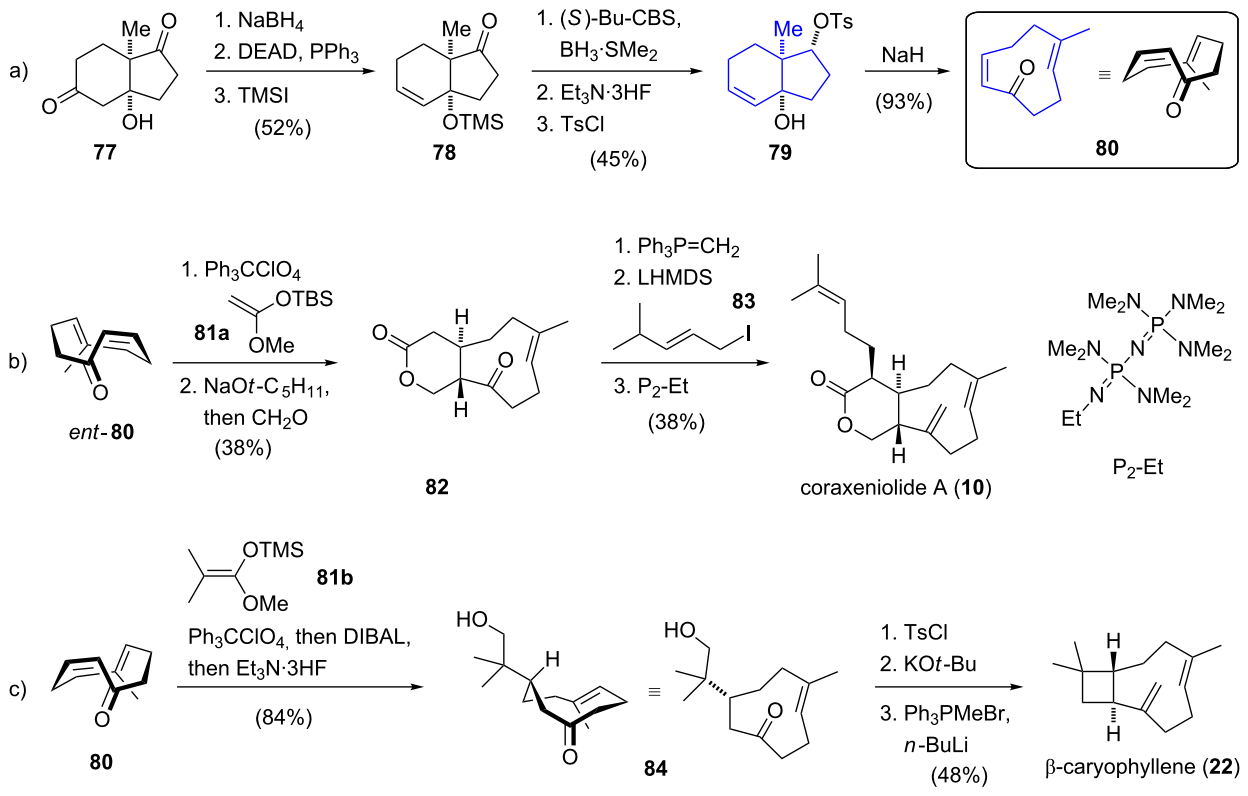

Scheme 8: a) Synthesis of enantiomer **80**, b) total syntheses of coraxeniolide A (**10**) and c) β-caryophyllene (**22**) by Corey.

the synthesis of a highly versatile building block represents a valuable platform for the construction of many different metabolites containing the nine-membered carbocyclic ring segment. The application of this useful intermediate was elegantly demonstrated in the synthesis of coraxeniolide A proceeding in 14% yield over five steps.

Altmann and co-workers disclosed the total synthesis of blumiolide C (**11**) [20] employing a *Z*-selective ring-closing metathesis reaction for construction of the cyclononene unit [49]. The synthesis started with a diastereoselective Evans syn-aldol reaction between substituted propanal **86** and *E*-crotonyl-oxazolidinone **85** (Scheme 9). The resulting secondary alcohol was silylated and the chiral auxiliary was cleaved with lithium borohydride. Acylation with acryloyl chloride gave ester **87** and a ring-closing metathesis reaction using Grubbs second generation catalyst [50] furnished an α,β-unsaturated lactone. Subsequent 1,4-addition of the cuprate derived from alkylmagnesium chloride **88** provided the *trans*-product with excellent diastereoselectivity and thus installed the required stereocenter at the C3 position of the natural product. After deprotection of the sterically less hindered silyl ether, the resultant primary alcohol was oxidized to give aldehyde **89**. By treatment with in situ generated divinylzinc, aldehyde **89** was transformed to an allylic alcohol which was converted to the corresponding *para*-methoxybenzyl ether **90** using Bundle's reagent [51]. In the key step of the synthesis, the nine-membered carbocyclic ring was constructed via a ring-closing metathesis reaction. Under optimized conditions, Hoveyda–Grubbs second generation catalyst [52] selectively converted diene **90** to the bicyclic ring system **91** in 66% yield. For the installation of the exocyclic double bond, bicycle **92** was treated with Martin sulfurane [53]. Subsequent hydrolysis of the acetal functionality and oxidation of the resulting lactol restored the lactone function in bicycle **93**. The side chain of blumiolide C was introduced by an aldol reaction between lactone **93** and aldehyde **94**. In the final sequence, blumiolide C (**11**) was obtained via stereospecific dehydration, removal of the *para*-methoxybenzyl ether and oxidation. In summary, the total synthesis of blumiolide C was accomplished in an overall yield of 0.63%.

In 2005, Hiersemann and co-workers reported an approach towards the synthesis of xeniolide F [13] employing a catalytic asymmetric Claisen rearrangement to set the crucial stereocen-

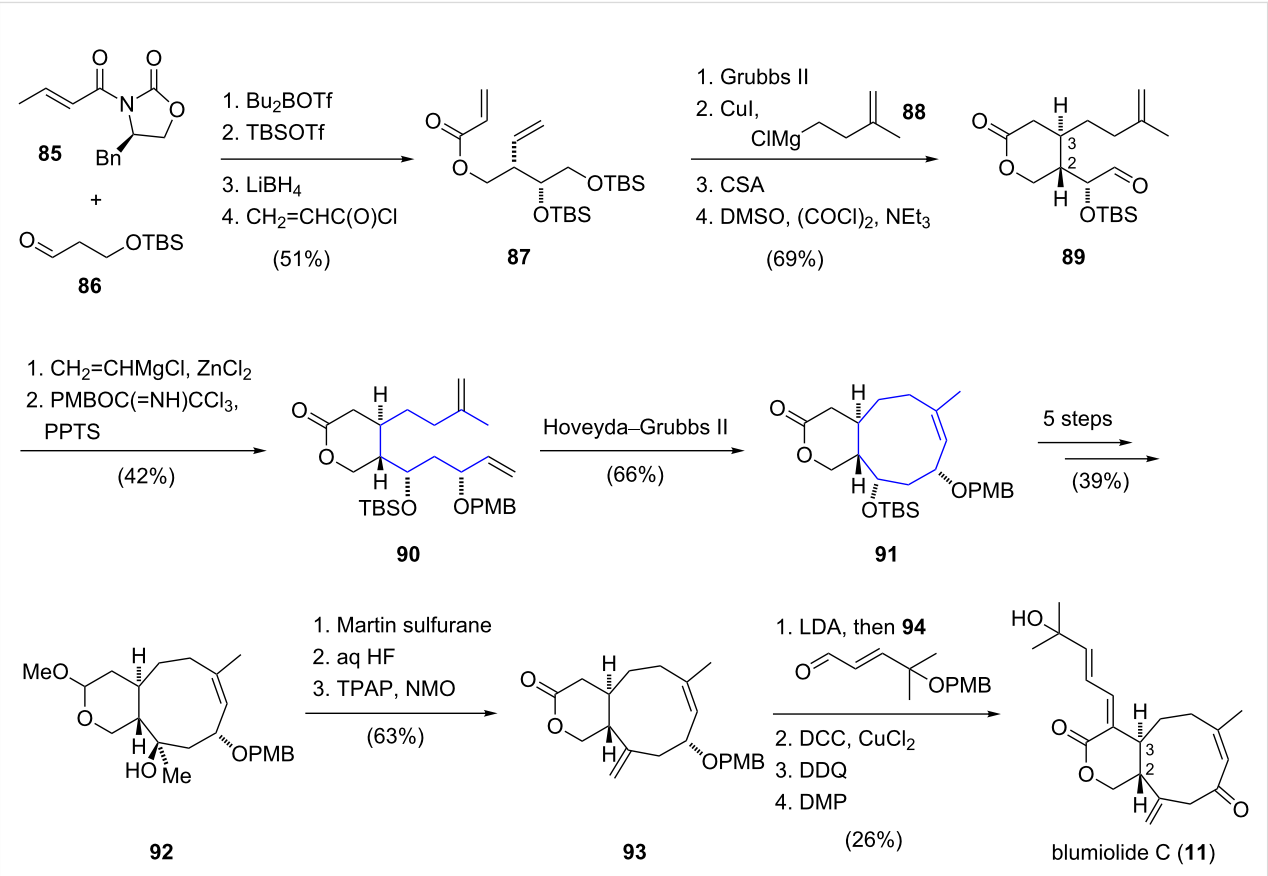

Scheme 9: Total synthesis of blumiolide C (**11**) by Altmann.

ters at the C2 and C3 positions (Scheme 10) [54]. The synthesis commenced with the preparation of diol **96** by a palladium-catalyzed hydrostannylation of 2-butyne-1,4-diol (**95**). Regioselective silylation with *tert*-butyldimethylsilyl chloride of the sterically less hindered alcohol, iodination and silylation of the primary alcohol with trimethylsilyl chloride gave vinyl iodide **97**. The following palladium-catalyzed B-alkyl Suzuki–Miyaura cross coupling between the borane derived from alkene **98** and vinyl iodide **97** furnished a *Z*-configured alkene. Deprotection of the trimethylsilyl ether then afforded alcohol **99**. A rhodium(II)-catalyzed O–H insertion reaction of the rhodium carbenoid derived from diazophosphonoacetate **100** and alcohol **99** afforded intermediate **101** which was treated with lithium diisopropylamide and aldehyde **102** to afford alkene **103** with high *E*-selectivity. The following asymmetric copper(II)-catalyzed Claisen rearrangement [55], which is postulated to proceed via the chair-like transition state **104**, afforded key intermediate **105** with high diastereo- and enantioselectivity. Preparation of the δ-lactone **106** of the A ring of xeniolide F was then realized by treatment of Claisen product **105** with the methylene Wittig reagent, followed by desilylation and lactonization. Although a successful synthetic approach leading to lactone **106** was thus established, further efforts to complete the total synthesis of xeniolide F (**12**) have yet to be reported.

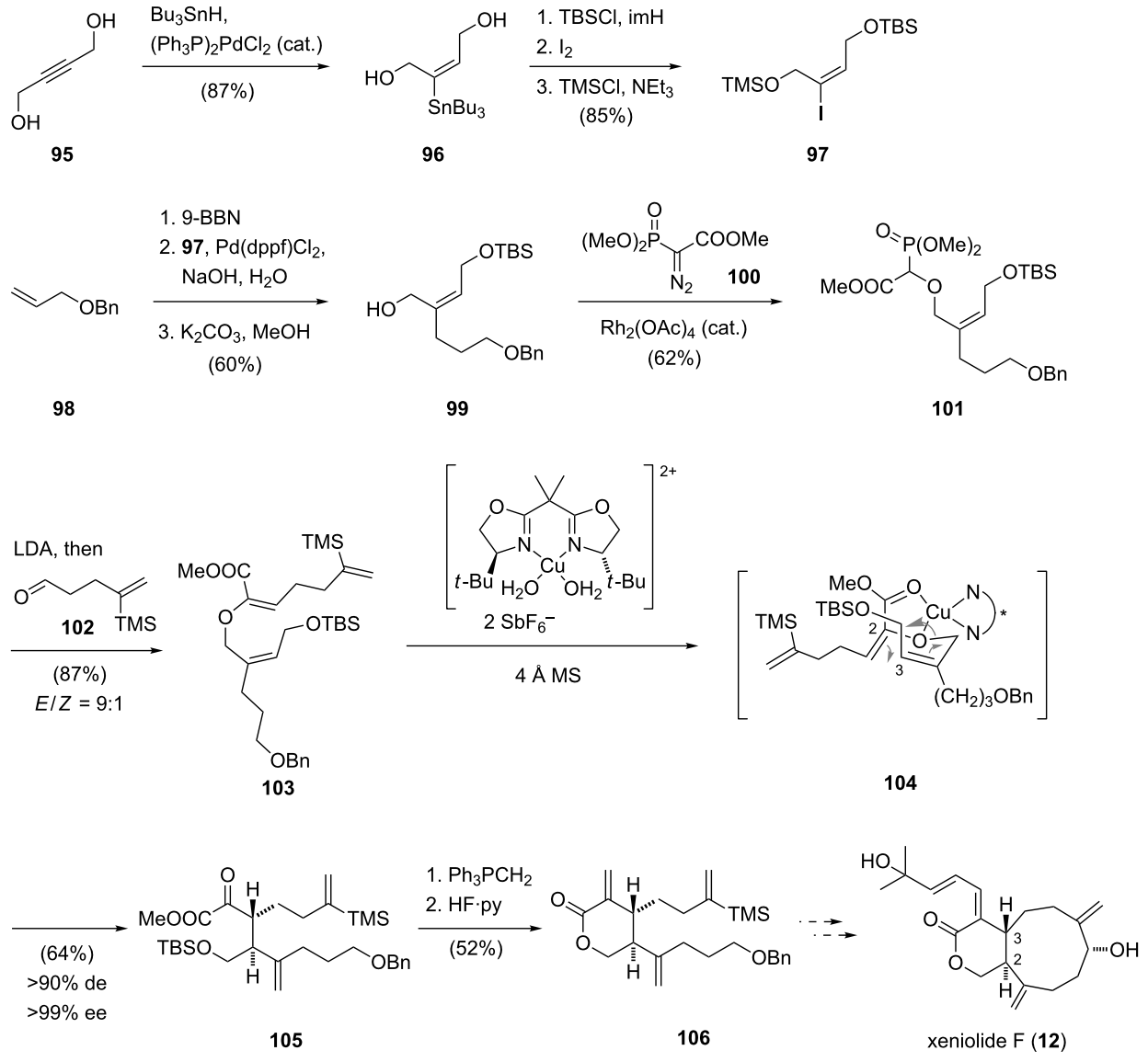

Scheme 10: Synthesis of a xeniolide F precursor by Hiersemann.

Efforts aimed at constructing the core structure of xenibellol A (**15**) [15] and umbellacetal (**114**) [56] employing a 2,3-Wittig–Still rearrangement as the key step were reported by Danishefsky and co-workers (Scheme 11) [57]. In contrast to other xenicanes mentioned above, xenibellol A (**15**) does not possess the characteristic nine-membered carbocyclic ring but rather features a 6,5,5-ring system, containing an unusual oxolane bridge between C1 and C7. Hajos–Parrish diketone (**107**) [39] served as the starting material for the preparation of key intermediate **112**. Selective reduction of the ketone and silylation of the resulting alcohol furnished enone **108**. α-Carboxylation of the enone with magnesium methyl carbonate and a global reduction of the carbonyl functionalities afforded allylic alcohol **109**. The precursor for the key reaction was obtained by formation of the methoxymethyl (MOM) ether from primary alcohol **109** and subsequent conversion of the allylic alcohol to stannane **110**. The following 2,3-Wittig–Still rearrangement [58] employing *n*-butyllithium afforded primary alcohol **111** in 31% yield and enabled the installation of the C1 quaternary stereocenter. According to the authors, a competing 1,2-Wittig rearrangement and reduction pathway posed a significant challenge in this transformation. Desilylation and regioselective tosylation of the primary alcohol **111** set the stage for the construction of the oxolane via Williamson etherification, which was realized by treatment with potassium hydride. Surprisingly, the following deprotection of the MOM ether using standard reaction conditions (1 N aqueous hydrochloric acid) led to opening of the oxolane ring and afforded tricycle **113** which features the carbon framework of structurally related umbellacetal (**114**). Gratifyingly, when magnesium bromide and ethanethiol were used as a mild alternative for the cleavage of the MOM ether, the xenibellol core could be obtained. Although the key 2,3-Wittig–Still rearrangement proceeded in low yield and further improvements are necessary, a promising route towards the synthesis of umbellacetal (**114**) and xenibellol (**15**) was thus established.

Yao and co-workers have investigated a synthetic approach towards the soft coral metabolite plumisclerin A by Pauson–Khand annulation and SmI_2-mediated radical cyclization [59]. The xenicane-related diterpenoid (isolated from the same marine organism as xenicin **116**) possesses a complex ring

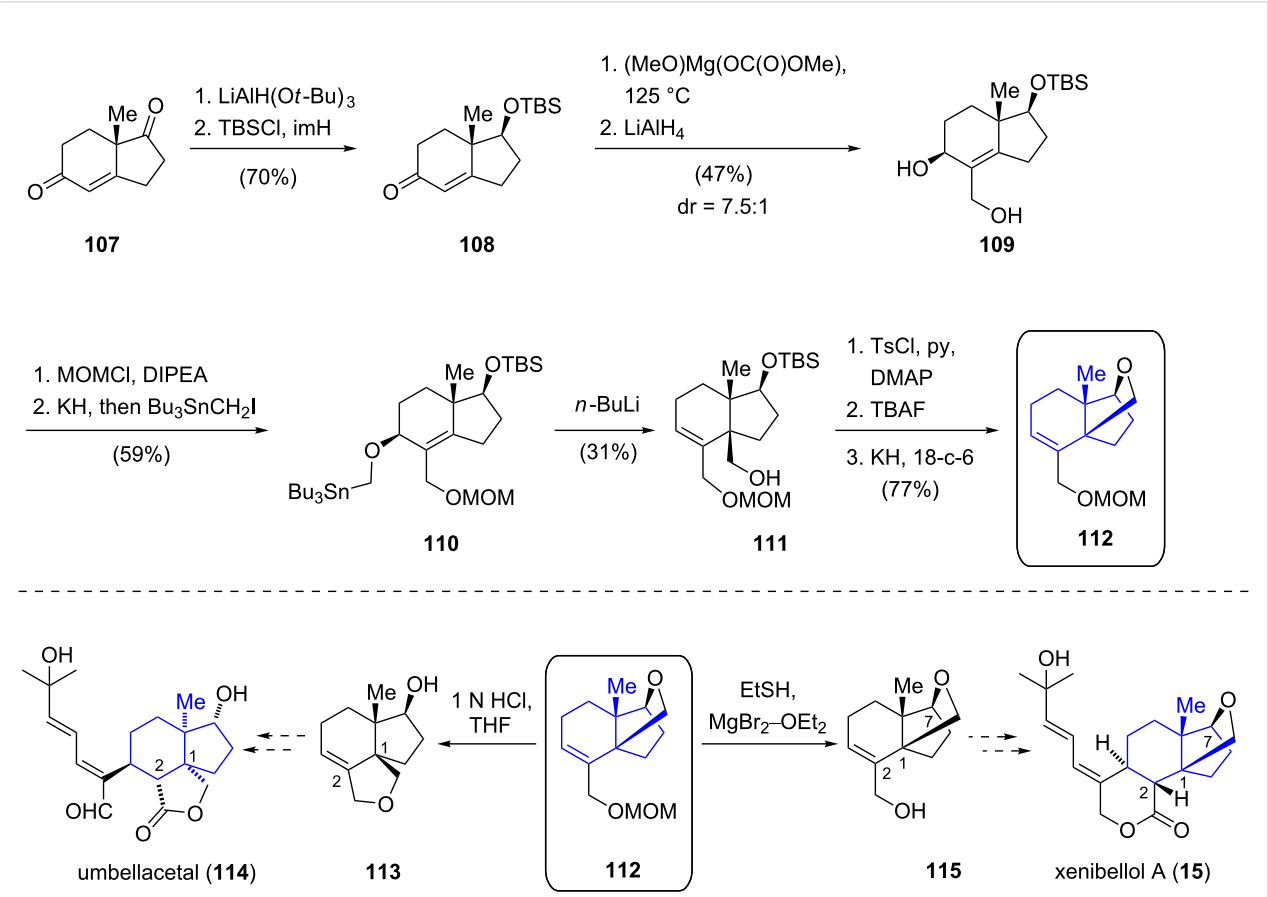

Scheme 11: Synthesis of the xenibellol (**15**) and the umbellacetal (**114**) core by Danishefsky.

system that is proposed to be biosynthetically derived from the xenicin diterpenoid **116** by an intramolecular [2 + 2] cycloaddition (Scheme 12) [60].

The synthetic route commenced with known aldehyde **119** which was converted to triol **120** in five steps (Scheme 13). The introduction of the benzyl ether next to the alkyne moiety was necessary to control the stereochemical outcome of the key annulation, and further three steps enabled preparation of the annulation precursor **121**. The following Pauson–Khand reaction [61] for the construction of the fused bicyclic structure **122** was performed by treatment of **121** with dicobaltoctacarbonyl in the presence of cyclohexylamine. Hydrolysis of the acetonide, chemoselective silylation and oxidation afforded aldehyde **123**. Next, the formation of the cyclobutanol ring was realized by an intramolecular samarium diiodide-mediated radical conjugate addition to afford tricycle **124** in 60% yield. Introduction of the dihydropyran ring of plumisclerin A (**118**) was envisioned to be carried out at a late stage of the synthesis, but efforts towards its construction have yet to be reported.

In 2009, the enantioselective total synthesis of 4-hydroxydictyolactone (**137**) was reported by Williams and co-workers (Scheme 14) [62]. Starting from α,β-unsaturated ester **125**, allylic alcohol **126** was synthesized in four steps. Esterification with (*R*)-(+)-citronellic acid (**127**) yielded a single diastereomer of ester **128**. Addition of lithium diisopropylamide to a mixture of **128**, trimethylsilyl chloride and triethylamine initiated an Ireland–Claisen rearrangement [63] which gave carboxylic acid **129** in 85% yield and with high diastereoselectivity (dr = 94:6). Carboxylic acid **129** was then converted to intermediate **130** in seven further steps. An intramolecular coupling between the formate ester and the allylic bromide provided lactol **131** in excellent stereoselectivity (dr > 95:5). The preparation of sec-

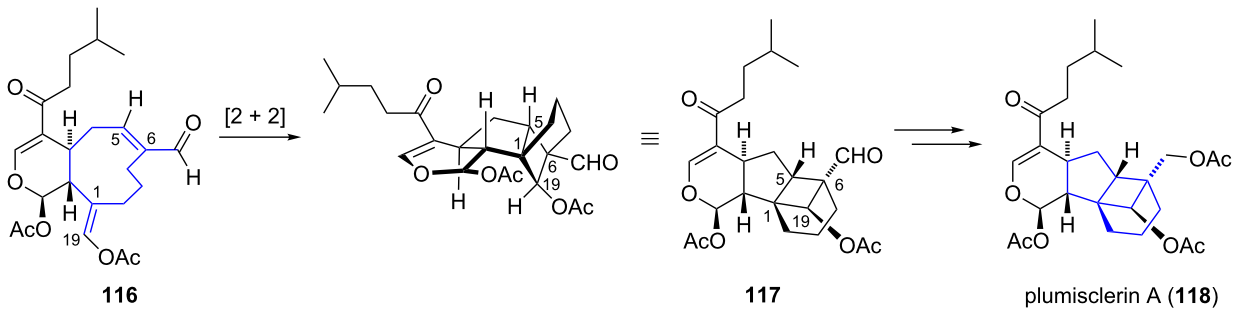

Scheme 12: Proposed biosynthesis of plumisclerin A (**118**).

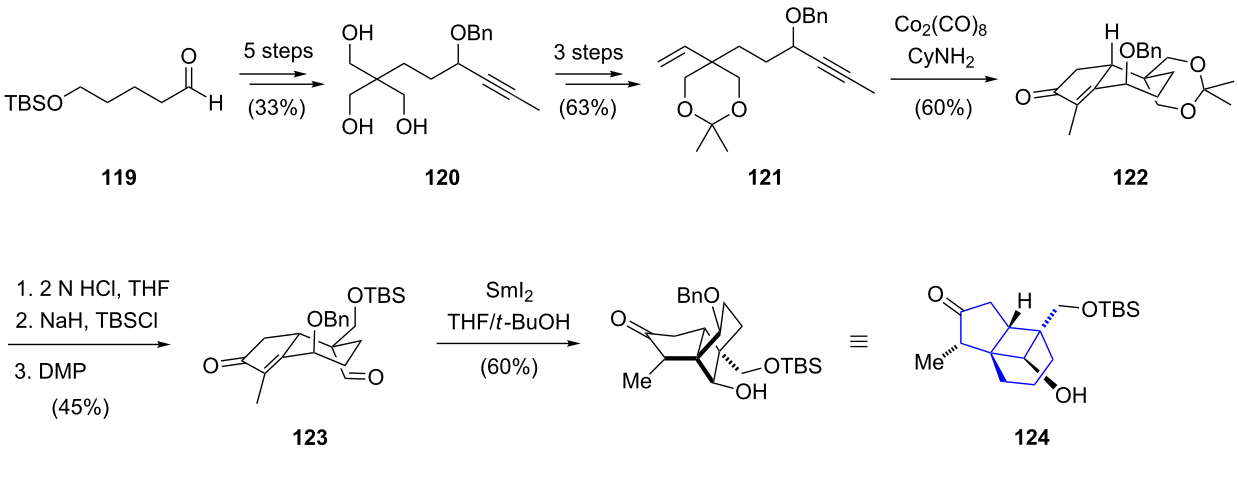

Scheme 13: Synthesis of the tricyclic core structure of plumisclerin A by Yao.

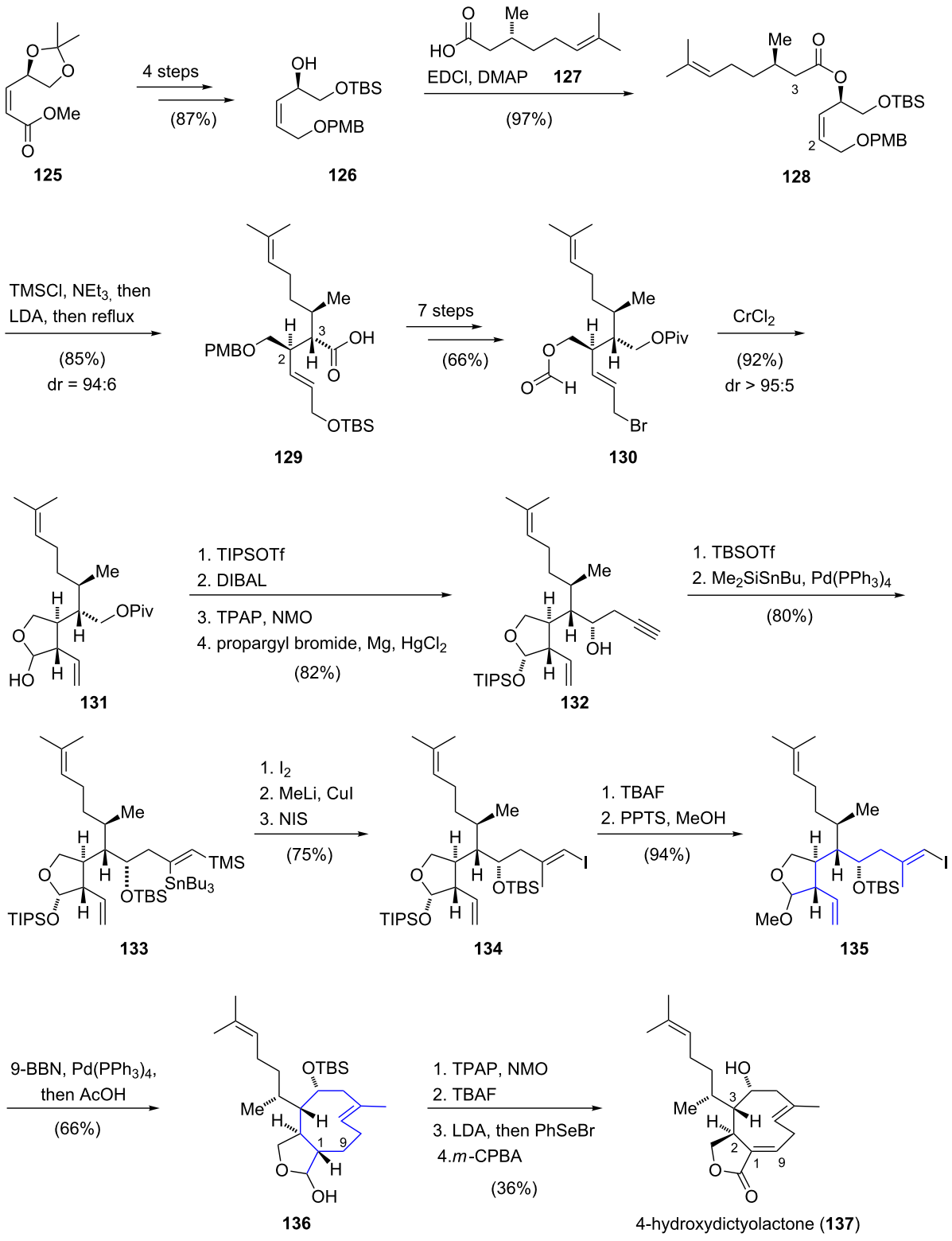

Scheme 14: Total synthesis of 4-hydroxydictyolactone (**137**) by Williams.

ondary alcohol **132** was accomplished by cleavage of the pivaloate ester, oxidation under Ley–Griffith oxidation [64] and subsequent addition of propargylmagnesium bromide. *O*-Silylation of the propargylic alcohol followed by a regioselective palladium-catalyzed *syn*-silylstannylation yielded product **133**. After employing a three-step protocol for the sequential replacement of the stannyl and silyl substituents, *E*-vinyl iodide **134** was obtained with retention of the olefin geometry. The following intramolecular key coupling step between the vinyl iodide and the terminal alkene for the formation of the nine-membered carbocycle was realized via a B-alkyl Suzuki–Miyaura cross-coupling reaction. Optimization studies of this key ring closure with different protecting groups on the lactol functionality revealed methyl acetal **135** as the most efficient substrate for this transformation. The challenging key step was finally realized in 66% yield and gave, after hydrolysis of the acetal with acetic acid, a mixture of *trans*-fused diastereomers **136**. Finally, a sequence consisting of oxidation, deprotection of the silyl ether and selenoxide elimination introduced the C1,C9 double bond to furnish 4-hydroxydictyolactone (**137**). In summary, the total synthesis of 4-hydroxydictyolactone was successfully completed in 30 linear steps with an overall yield of 4.8%.

Paquette and co-workers disclosed the enantioselective total synthesis of the *Xenia* diterpenoid related crenulatane (+)-acetoxycrenulide (**151**) [65-67]. The skeleton of crenulatanes, which features an eight-membered carbocyclic ring fused to a cyclopropane ring, may be the product of a photoisomerization of xenicanes. This hypothesis was further supported by the fact that crenulatanes usually co-occur with xenicanes in brown seaweeds of the family *Dictyotaceae*. Evidence for this proposed biogenetic origin of crenulatanes has been provided by Guella and Pietra who showed that irradiation of 4-hydroxydictyolactone (**137**) with ultraviolet light (254 nm) led to the formation of 4-hydroxycrenulide (**138**) (Scheme 15) [68]. Although this transformation remains mechanistically unclear, the authors suggested that either a free radical process or a photoinduced double bond isomerization (C9,C1 to C1,C2) followed by an [1,3]H shift might lead to the formation of 4-hydroxycrenulide (**138**).

The total synthesis of (+)-acetoxycrenulide (**151**) commenced with preparation of butenolide **140** from (*R*)-citronellol (**139**) in an 11-step sequence. Next, the two stereocenters at C2 and C3 position were installed by stereoselective conjugate addition of enantiopure α-allylphosphonamide **141** to butenolide **140**. After cleavage of the chiral auxiliary by ozonolysis, aldehyde **142** was protected as the dimethoxy acetal and reduction of the lactone followed by olefination furnished alkene **143**. The lactone fragment of the natural product was then installed by acidic hydrolysis of the acetal functionality and subsequent oxidation gave γ-lactone **144**. Ozonolysis of the terminal alkene and addition of (phenylseleno)methyllithium to the resulting aldehyde afforded secondary alcohol **145**. Temporary protection of the alcohol followed by an aldol reaction of the lactone with *E*-crotonaldehyde led to an inseparable mixture (dr = 1:1) of β-hydroxy lactone **146**. The synthesis of the key precursor for formation of the cyclooctene core was achieved via an acid-catalyzed cyclization to form tetrahydropyran **147**. The following key sequence consisted of a thermal selenoxide 1,2-elimination to generate allyl vinyl ether **148** which underwent a stereoselective Claisen rearrangement [69] to furnish cyclooctenone **149** in 55% yield. A highly stereoselective Simmons–Smith reaction [70] delivered the cyclopropyl ring exclusively from the accessible α-face to give **150**. The synthesis of (+)-acetoxycrenulide (**151**) was completed in seven further steps and in summary proceeded in 33 steps (longest linear sequence) and in 1% overall yield (Scheme 16).

In addition to the presented strategies for the synthesis of *Xenia* diterpenoids, total syntheses of the *Xenia* sesquiterpenes xenitorin B and C were also reported [71].

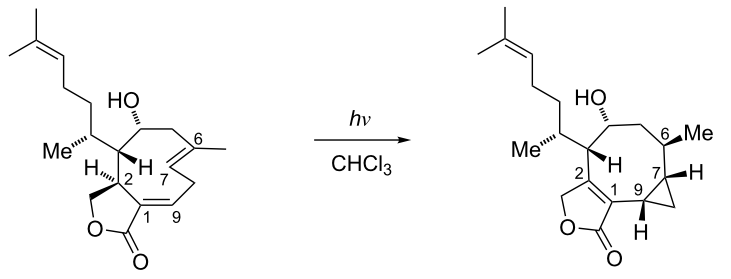

4-hydroxydictyolactone (**137**) 4-hydroxycrenulide (**138**)

Scheme 15: Photoisomerization of 4-hydroxydictyolactone (**137**) to 4-hydroxycrenulide (**138**).

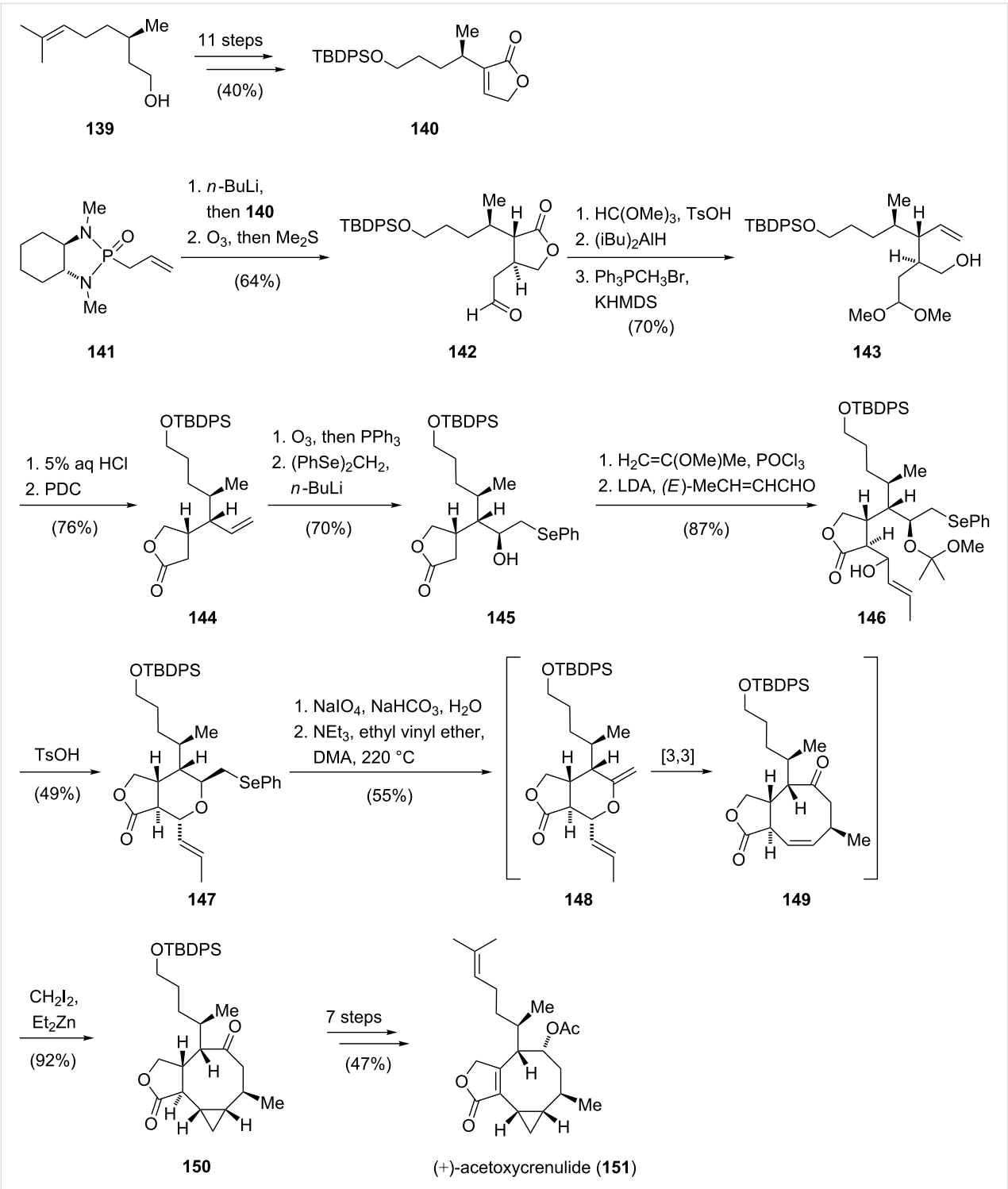

Scheme 16: The total synthesis of (+)-acetoxycrenulide (**151**) by Paquette.

Conclusion

This review has presented various synthetic approaches towards xenicane and xenicane-related diterpenoids. Additionally, total syntheses of xeniolides and of a crenulatane natural product were illustrated. It has been shown that the rare structural features of *Xenia* diterpenoids represent an enduring challenge for the total synthesis of these fascinating metabolites. For these reasons, several strategies for the preparation of the characteristic nine-membered carbocyclic ring structures have been developed. The synthetic strategies are typically based on ring

expansion (Grob-type fragmentation and sigmatropic rearrangements), ring closing (metathesis and transition metal-catalyzed coupling) and ring contracting reactions. The choice of tactic is dependent on the individual substitution pattern of the target compound. However, many of the presented strategies rely on long synthetic sequences that cannot provide large amounts of synthetic material which is required for further investigations of the biological activity of these natural products, and ultimately for drug discovery. The development of short and efficient synthetic routes towards xenicane natural products therefore remains a great challenge of this exciting research field.

Acknowledgements

We gratefully acknowledge financial support from the FCI (Sachkostenzuschuss to T.M.), the DFG (SFB TRR 152 and Emmy Noether Fellowship to T.M.) and the German National Academic Foundation (Research Fellowship to T.H.). We thank M.Sc. Cedric L. Hugelshofer for helpful discussions during the preparation of the manuscript.

References

1. Elshamy, A. I.; Nassar, M. I. *J. Biol. Act. Prod. Nat.* **2015,** *5,* 78–107. doi:10.1080/22311866.2015.1015611
2. Vanderah, D. J.; Steudler, P. A.; Ciereszko, L. S.; Schmitz, F. J.; Ekstrand, J. D.; van der Helm, D. *J. Am. Chem. Soc.* **1977,** *99,* 5780–5784. doi:10.1021/ja00459a040
3. Kashman, Y.; Groweiss, A. *Tetrahedron Lett.* **1978,** *19,* 4833–4836. doi:10.1016/S0040-4039(01)85745-2
4. Groweiss, A.; Kashman, Y. *Tetrahedron Lett.* **1978,** *19,* 2205–2208. doi:10.1016/S0040-4039(01)86846-5
5. Iwagawa, T.; Amano, Y.; Hase, T.; Shiro, M. *Chem. Lett.* **1995,** *24,* 695–696. doi:10.1246/cl.1995.695
6. Lin, Y.-S.; Eid Fazary, A.; Chen, C.-H.; Kuo, Y.-H.; Shen, Y.-C. *Chem. Biodiversity* **2011,** *8,* 1310–1317. doi:10.1002/cbdv.201000173
7. Coval, S. J.; Scheuer, P. J.; Matsumoto, G. K.; Clardy, J. *Tetrahedron* **1984,** *40,* 3823–3828. doi:10.1016/S0040-4020(01)88813-X
8. Duh, C.-Y.; El-Gamal, A. A. H.; Chiang, C.-Y.; Chu, C.-J.; Wang, S.-K.; Dai, C.-F. *J. Nat. Prod.* **2002,** *65,* 1882–1885. doi:10.1021/np020268z
9. El-Gamal, A. A. H.; Wang, S. K.; Duh, C. Y. *J. Nat. Prod.* **2006,** *69,* 338–341. doi:10.1021/np058093r
10. Fattorusso, E.; Romano, A.; Taglialatela-Scafati, O.; Achmad, M. J.; Bavestrello, G.; Cerrano, C. *Tetrahedron* **2008,** *64,* 3141–3146. doi:10.1016/j.tet.2008.01.120
11. Almourabit, A.; Ahond, A.; Poupat, C.; Potier, P. *J. Nat. Prod.* **1990,** *53,* 894–908. doi:10.1021/np50070a017
12. Schwartz, R. E.; Scheuer, P. J.; Zabel, V.; Watson, W. H. *Tetrahedron* **1981,** *37,* 2725–2733. doi:10.1016/S0040-4020(01)92338-5
13. Anta, C.; González, N.; Santafé, G.; Rodríguez, J.; Jiménez, C. *J. Nat. Prod.* **2002,** *65,* 766–768. doi:10.1021/np010488x
14. Bishara, A.; Rudi, A.; Goldberg, I.; Benayahu, Y.; Kashman, Y. *Tetrahedron* **2006,** *62,* 12092–12097. doi:10.1016/j.tet.2006.09.050
15. El-Gamal, A. A. H.; Wang, S.-K.; Duh, C.-Y. *Org. Lett.* **2005,** *7,* 2023–2025. doi:10.1021/ol0505205
16. Miyaoka, H.; Nakano, M.; Iguchi, K.; Yamada, Y. *Tetrahedron* **1999,** *55,* 12977–12982. doi:10.1016/S0040-4020(99)00806-6
17. Iwagawa, T.; Nakamura, K.; Hirose, T.; Okamura, H.; Nakatani, M. *J. Nat. Prod.* **2000,** *63,* 468–472. doi:10.1021/np990470a
18. Smith III, A. B.; Carroll, P. J.; Kashman, Y.; Green, D. *Tetrahedron Lett.* **1989,** *30,* 3363–3364. doi:10.1016/S0040-4039(00)99245-1
19. Miyaoka, H.; Mitome, H.; Nakano, M.; Yamada, Y. *Tetrahedron* **2000,** *56,* 7737–7740. doi:10.1016/S0040-4020(00)00689-X
20. El-Gamal, A. A. H.; Chiang, C. Y.; Huang, S. H.; Wang, S. K.; Duh, C. Y. *J. Nat. Prod.* **2005,** *68,* 1336–1340. doi:10.1021/np058047r
21. Tkachev, A. V. *Chem. Nat. Compd.* **1987,** *23,* 393–412. doi:10.1007/BF00597793
22. Iwagawa, T.; Amano, Y.; Nakatani, M.; Hase, T. *Bull. Chem. Soc. Jpn.* **1996,** *69,* 1309–1312. doi:10.1246/bcsj.69.1309
23. Finer, J.; Clardy, J.; Fenical, W.; Minale, L.; Riccio, R.; Battaile, J.; Kirkup, M.; Moore, R. E. *J. Org. Chem.* **1979,** *44,* 2044–2047. doi:10.1021/jo01326a040
24. Liu, G.; Smith, T. C.; Pfander, H. *Tetrahedron Lett.* **1995,** *36,* 4979–4982. doi:10.1016/0040-4039(95)00938-9
25. Cane, D. E. *Acc. Chem. Res.* **1985,** *18,* 220–226. doi:10.1021/ar00115a005
26. Kashman, Y.; Rudi, A. *Phytochem. Rev.* **2004,** *3,* 309–323. doi:10.1007/s11101-004-8062-x
27. Prantz, K.; Mulzer, J. *Chem. Rev.* **2010,** *110,* 3741–3766. doi:10.1021/cr900386h
28. Miyaura, N.; Suzuki, A. *Chem. Rev.* **1995,** *95,* 2457–2483. doi:10.1021/cr00039a007
29. Corey, E. J.; Mitra, R. B.; Uda, H. *J. Am. Chem. Soc.* **1963,** *85,* 362–363. doi:10.1021/ja00886a037
30. Corey, E. J.; Mitra, R. B.; Uda, H. *J. Am. Chem. Soc.* **1964,** *86,* 485–492. doi:10.1021/ja01057a040
31. Corey, E. J.; Cheng, X.-M. *The Logic of Chemical Synthesis;* John Wiley & Sons: New York, 1995.
32. Dieckmann, W.; Kron, A. *Ber. Dtsch. Chem. Ges.* **1908,** *41,* 1260–1278. doi:10.1002/cber.190804101236
33. Grob, C. A.; Baumann, W. *Helv. Chim. Acta* **1955,** *38,* 594–610. doi:10.1002/hlca.19550380306
34. Ohtsuka, Y.; Niitsuma, S.; Tadokoro, H.; Hayashi, T.; Oishi, T. *J. Org. Chem.* **1984,** *49,* 2326–2332. doi:10.1021/jo00187a006
35. Kumar, A.; Singh, A.; Devaprabhakara, D. *Tetrahedron Lett.* **1976,** *17,* 2177–2178. doi:10.1016/S0040-4039(00)93151-4
36. Kumar, A.; Devaprabhakara, D. *Synthesis* **1976,** *1976,* 461–462. doi:10.1055/s-1976-24082
37. Mc Murry, J. E.; Miller, D. D. *Tetrahedron Lett.* **1983,** *24,* 1885–1888. doi:10.1016/S0040-4039(00)81797-9
38. Bertrand, M.; Gras, J.-L. *Tetrahedron* **1974,** *30,* 793–796. doi:10.1016/S0040-4020(01)97168-6
39. Hajos, Z. G.; Parrish, D. R. *J. Org. Chem.* **1974,** *39,* 1615–1621. doi:10.1021/jo00925a003
40. Renneberg, D.; Pfander, H.; Leumann, C. J. *J. Org. Chem.* **2000,** *65,* 9069–9079. doi:10.1021/jo005582h
41. Grieco, P. A.; Clark, J. D.; Jagoe, C. T. *J. Am. Chem. Soc.* **1991,** *113,* 5488–5489. doi:10.1021/ja00014a069
42. Tebbe, F. N.; Parshall, G. W.; Reddy, G. S. *J. Am. Chem. Soc.* **1978,** *100,* 3611–3613. doi:10.1021/ja00479a061
43. Mushti, C. S.; Kim, J.; Corey, E. J. *J. Am. Chem. Soc.* **2006,** *128,* 14050–14052. doi:10.1021/ja066336b
44. Hiroi, K.; Kato, F. *Tetrahedron* **2001,** *57,* 1543–1550. doi:10.1016/S0040-4020(00)01111-X
45. Hu, T.; Corey, E. J. *Org. Lett.* **2002,** *4,* 2441–2443. doi:10.1021/ol026205p

46. Larionov, O. V.; Corey, E. J. *J. Am. Chem. Soc.* **2008,** *130,* 2954–2955. doi:10.1021/ja8003705
47. Hajos, Z. G.; Parish, D. R. *Org. Synth.* **1985,** *63,* 26. doi:10.15227/orgsyn.063.0026
48. Corey, E. J.; Shibata, S.; Bakshi, R. K. *J. Org. Chem.* **1988,** *53,* 2861–2863. doi:10.1021/jo00247a044
49. Hamel, C.; Prusov, E. V.; Gertsch, J.; Schweizer, W. B.; Altmann, K. H. *Angew. Chem., Int. Ed.* **2008,** *47,* 10081–10085. doi:10.1002/anie.200804004
50. Scholl, M.; Trnka, T. M.; Morgan, J. P.; Grubbs, R. H. *Tetrahedron Lett.* **1999,** *40,* 2247–2250. doi:10.1016/S0040-4039(99)00217-8
51. Iversen, T.; Bundle, D. R. *J. Chem. Soc., Chem. Commun.* **1981,** 1240–1241. doi:10.1039/c39810001240
52. Garber, S. B.; Kingsbury, J. S.; Gray, B. L.; Hoveyda, A. H. *J. Am. Chem. Soc.* **2000,** *122,* 8168–8179. doi:10.1021/ja001179g
53. Martin, J. C.; Arhart, R. J. *J. Am. Chem. Soc.* **1971,** *93,* 4327–4329. doi:10.1021/ja00746a059
54. Pollex, A.; Hiersemann, M. *Org. Lett.* **2005,** *7,* 5705–5708. doi:10.1021/ol052462t
55. Abraham, L.; Czerwonka, R.; Hiersemann, M. *Angew. Chem., Int. Ed.* **2001,** *40,* 4700–4703. doi:10.1002/1521-3773(20011217)40:24<4700::AID-ANIE4700>3.0.CO;2-6
56. El-Gamal, A. A. H.; Wang, S.-K.; Duh, C.-Y. *Tetrahedron Lett.* **2005,** *46,* 6095–6096. doi:10.1016/j.tetlet.2005.06.168
57. Kim, W. H.; Angeles, A. R.; Lee, J. H.; Danishefsky, S. J. *Tetrahedron Lett.* **2009,** *50,* 6440–6441. doi:10.1016/j.tetlet.2009.08.131
58. Still, W. C.; Mitra, A. *J. Am. Chem. Soc.* **1978,** *100,* 1927–1928. doi:10.1021/ja00474a049
59. Chen, J.-P.; He, W.; Yang, Z.-Y.; Yao, Z.-J. *Org. Lett.* **2015,** *17,* 3379–3381. doi:10.1021/acs.orglett.5b01563
60. Martín, M. J.; Fernández, R.; Francesch, A.; Amade, P.; de Matos-Pita, S. S.; Reyes, F.; Cuevas, C. *Org. Lett.* **2010,** *12,* 912–914. doi:10.1021/ol902802h
61. Khand, I. U.; Knox, G. R.; Pauson, P. L.; Watts, W. E. *J. Chem. Soc. D* **1971,** *1,* 36a. doi:10.1039/c2971000036a
62. Williams, D. R.; Walsh, M. J.; Miller, N. A. *J. Am. Chem. Soc.* **2009,** *131,* 9038–9045. doi:10.1021/ja902677t
63. Ireland, R. E.; Mueller, R. H. *J. Am. Chem. Soc.* **1972,** *94,* 5897–5898. doi:10.1021/ja00771a062
64. Ley, S. V.; Norman, J.; Griffith, W. P.; Marsden, S. P. *Synthesis* **1994,** *1994,* 639–666. doi:10.1055/s-1994-25538
65. Wang, T. Z.; Pinard, E.; Paquette, L. A. *J. Am. Chem. Soc.* **1996,** *118,* 1309–1318. doi:10.1021/ja9533609
66. He, W.; Pinard, E.; Paquette, L. A. *Helv. Chim. Acta* **1995,** *78,* 391–402. doi:10.1002/hlca.19950780210
67. Paquette, L. A.; Wang, T.-Z.; Pinard, E. *J. Am. Chem. Soc.* **1995,** *117,* 1455–1456. doi:10.1021/ja00109a041
68. Guella, G.; Pietra, F. *J. Chem. Soc., Chem. Commun.* **1993,** 1539. doi:10.1039/c39930001539
69. Ezquerra, J.; He, W.; Paquette, L. A. *Tetrahedron Lett.* **1990,** *31,* 6979–6982. doi:10.1016/S0040-4039(00)97221-6
70. Simmons, H. E.; Smith, R. D. *J. Am. Chem. Soc.* **1958,** *80,* 5323–5324. doi:10.1021/ja01552a080
71. Chang, W.-S.; Shia, K.-S.; Liu, H.-J.; Wei Ly, T. *Org. Biomol. Chem.* **2006,** *4,* 3751–3753. doi:10.1039/b610427d

License and Terms

BEILSTEIN JOURNAL OF ORGANIC CHEMISTRY

Natural products from microbes associated with insects

Christine Beemelmanns*[1], Huijuan Guo[1], Maja Rischer[1] and Michael Poulsen[2]

Review

Open Access

Address:
[1]Leibniz Institute for Natural Product Research and Infection Biology e.V., Beutenbergstrasse 11a, 07745 Jena, Germany and [2]Centre for Social Evolution, Section for Ecology and Evolution, Department of Biology, University of Copenhagen, Universitetsparken 15, Building 3, 1st floor, 2100 Copenhagen East, Denmark

Email:
Christine Beemelmanns* - christine.beemelmanns@hki-jena.de

* Corresponding author

Keywords:
biosynthesis; chemical ecology; natural products; secondary metabolism; structure elucidation; symbiosis

Beilstein J. Org. Chem. **2016,** *12,* 314–327.
doi:10.3762/bjoc.12.34

Received: 08 December 2015
Accepted: 02 February 2016
Published: 19 February 2016

This article is part of the Thematic Series "Natural products in synthesis and biosynthesis II".

Guest Editor: J. S. Dickschat

Abstract

Here we review discoveries of secondary metabolites from microbes associated with insects. We mainly focus on natural products, where the ecological role has been at least partially elucidated, and/or the pharmaceutical properties evaluated, and on compounds with unique structural features. We demonstrate that the exploration of specific microbial–host interactions, in combination with multidisciplinary dereplication processes, has emerged as a successful strategy to identify novel chemical entities and to shed light on the ecology and evolution of defensive associations.

Introduction

Although natural products represent the most consistently successful drug leads [1,2], many pharmaceutical companies eliminated their natural product research during the past decades due to diminishing returns from this discovery platform. Instead they intensely focused on screening efforts and combinatorial chemistry to find and develop novel drug candidates.

This approach of target-focused screening of synthetic compound libraries to counteract a declining number of new antibiotic entities in the drug development pipeline has largely failed [3], and the current poor repertoire represents a ”ticking time bomb”. Societies face, as a consequence of the rapid globalization and intensive use of antibiotics, an increasing threat of multidrug-resistant pathogens, which are responsible for the growing numbers of lethal infections [4,5]. The urge to discover novel lead-like antibiotic compounds and to refill the industrial antibiotic pipeline to meet current and future societal challenges has never been greater [6].

Nowadays the major drawback of natural products research and drug discovery represents the re-isolation of known compounds and the random nature – in terms of organisms explored – by which this research is performed. Most compounds are still isolated from random sources and tested against random targets to find more or less useful bioactivities. More rational

approaches are necessary to enhance the efficacy, efficiency, and speed of drug discovery in general and antibiotic discovery in particular. In recent years, the exploration of the chemical basis of specific and well-described bacteria–host or fungal–host interactions in combination with analytical dereplication processes has emerged as a powerful strategy to identify novel chemical entities (Figure 1) [7,8].

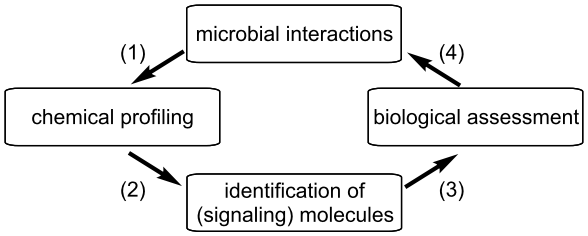

Figure 1: Flow chart of the typical characterization of chemical signals from microbial interactions. (1) Chemical profiling of microbial interactions using analytical techniques. (2) Dereplication leads to potentially new small molecules. (3) Optimization of the isolation protocol based on biological assessment of the activity of the isolated compounds. (4) General conclusions about ecological role and evolution of interactions.

Since their initial appearance, natural products and the respective complex biosynthetic machineries have been in a constant state of evolutionary-based refinement for at least a billion years [9-11]. They function as chemical modulators and signaling molecules for intra- and interkingdom interactions such as defense, protection, behavior, virulence, and central physiological functions; thereby generating evolutionary benefits for the producer in natural habitats [12-17]. Recent developments in analytical chemistry, genome sequencing and molecular biology facilitate the analyse of minute amounts of biological material and enable a more efficient interaction-to-molecule discovery approach [18-23]. These studies also place the natural products into a genomic, regulatory, functional, and ecological context, and might allow drawing more general conclusions about the biosynthetic origins, the ecology and evolution of symbiotic associations. However, even in this ecological context natural product chemistry is highly capricious, because so far, we are not able to calculate or predict which molecular structures are responsible for a certain biological function. Despite this aspect, natural products originating from insect–microbial symbioses have a vast biochemical diversity which is a powerful resource for drug discovery [24-27].

Below we provide an overview of natural products isolated from microbial symbionts of insects, and the analytical dereplication methods when these have been applied to identify the molecules. The (potential) ecological function of the identified natural products will be discussed. We will not go into details about biosynthetic origins and assembly lines of the respective compounds, which have partially been reviewed in detail previously [28-32]. We are building on existing excellent reviews [12-17,24-26], and apologize in advance to the many researchers whose research might not be covered.

Review

Insects as host systems

Insects, the most diverse groups of animals on Earth [12-17], originated about 480 million years ago, at about the same time period when terrestrial plants evolved [33]. Since their initial appearance, insects have occupied almost every environmental niche while in the meantime, symbiotic and/or pathogenic microorganisms have adapted specifically to insects as host systems (Figure 2) [34-36]. As an immediate response, insects were colonized by symbiotic microorganisms that are often required by the insect host to provide necessary nutritional and immunological effectors (obligate symbiont) [37]. The microbiota may account for 1–10% of the insect biomass, implying that the insect, as well as any other higher organism, can be regarded as a multi-organismal entity [38]. Due to specialized lifestyles and feeding behavior, insects are often prone to exploitation and pathogen infestation. In particular, life in large communities (social insects), the mass provisioning of nutrients to the offspring, and the construction of brooding chambers are threatened by invading and predatory species [12-17].

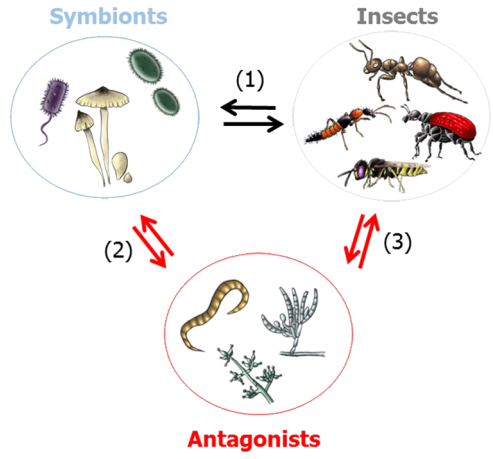

Figure 2: Multilateral microbe–insect interactions. (1) Insect–symbiont interactions with both partners benefiting from the interactions. (2) Antagonistic microbial interactions (e.g., competition for nutrients and space). (3) Antagonistic microbe–insect interactions (e.g., entomopathogenic microbes).

As a response to these threats, many insects have evolved defensive strategies, including mechanical and behavioral defense, complex immune systems, and the use of bioactive

secondary metabolites produced by residing mutualists [12-17,24-26]. The occurrence of these metabolites in often subinhibitory concentrations indicates that they might not primarily function as antimicrobials. Rather they work as signaling molecules leading to modulation of gene expression in the target organism, to alteration in factors contributing to the virulence or persistence of bacterial pathogens, or to the development and persistence of microbial communities [39-41]. Nowadays it is hypothesized that the evolution and diversification of the microbial biosynthetic machinery may have evolved secondarily in interactions with other organisms, and microbial–insect interaction and regulation mechanisms are likely to be more complex than previously expected.

Defensive bacterial symbionts of insects

Kaltenpoth and co-workers described one of the most intriguing examples of an insect–bacteria symbiosis and symbiont conferred protection [42-44]. Predatory females of the solitary digger wasp European beewolf (*Philanthus triangulum*), catch and paralyze honeybees and use the insect prey as food source for their larvae. To protect the offspring, beewolves cultivate the endosymbiont "*Candidatus* Streptomyces philanthi" in antennal glands. By inoculation of the soil of the brood cell with the protective symbiont, beewolf females ensure that the larvae take up the symbionts from the surrounding soil while spinning the cocoon. Using high resolution mass spectrometry (HRMS) and nuclear magnetic resonance (NMR) spectroscopy, the protective secondary metabolites were identified as piericidin derivatives (e.g., piericidin A_1 (**1**), Figure 3) and the chlorinated indole derivative streptochlorin (**2**). Imaging analysis based on a combination of laser desorption/ionization (LDI)–time of flight (TOF) mass spectrometry imaging visualized the spatial distribution of the antibiotics on the outer cocoon surface. Subsequent gas chromatography–mass spectrometry (GC–MS) analyses and expression studies revealed that the production of both antibiotics peaked within the first two weeks after cocoon spinning [45]. Although expression levels decreased shortly afterwards, the antibiotic substances were detectable on the cocoon surface for months during hibernation.

Structurally, piericidins consist of a pyridone core attached to polyene side chains of variable size, a structural and physiochemical feature of ubiquinone. Therefore, it is not surprising that piericidins are potent inhibitors of mitochondrial and bacterial NADH–ubiquinone oxidoreductase (complex I) [46]. Streptochlorin (**2**), on the other side, belongs to the natural compound class of 5-(3-indolyl)oxazoles, and has been isolated from many different (marine) Actinobacteria species. Streptochlorin and closely related derivatives have been shown to possess a variety of biological activities, such as antibiotic, antifungal and antiproliferative activity [47]. The combination of the antibiotic properties of piericidins and streptochlorin is most likely the reason for the effective inhibition of various entomopathogenic microbes, indicating a "first chemical defense line" and "long term prophylaxis" of *P. triangulum* ensuring protection and enhanced survival rates of the offspring.

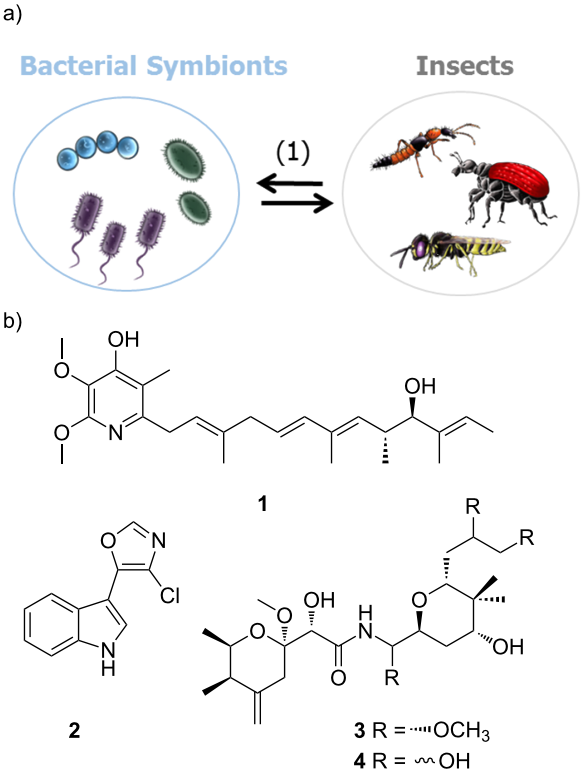

Figure 3: a) Interactions between bacterial (endo)symbionts and insects with both partners benefiting from the interactions (1). b) Defensive secondary metabolites isolated from bacterial symbionts: piericidin A1 (**1**), streptochlorin (**2**), pederin (**3**), and diaphorin (**4**).

In a similar study, a detailed chemical analysis of rove beetles (*Paederus* spp.) led to the isolation of the complex polyketide pederin (**3**), a potent toxin that can ward of natural predators such as wolf spiders [48]. The initial isolation of pederin (**3**) included the collection and chemical analysis of 250,000 beetles. Later, the true producer was found to be an endosymbiotic *Pseudomonas* sp. within the female beetle which was identified by molecular analysis of the biosynthetic gene cluster of pederin (**3**) [49-52]. Beetle larvae hatching from pederin-containing eggs were less prone to predation by wolf spiders than pederin-free larvae, indicating the ecological significance of this secondary metabolite [53]. The biosynthetic gene cluster analysis also revealed that pederin is formed by an enzyme belonging to a functionally and evolutionarily novel group termed trans-acyltransferase PKSs (trans-AT PKSs) [24,52].

The structurally related compound diaphorin (**4**) was later found in a study of the defensive symbiosis between the Asian citrus psyllid and the β-proteobacterium "*Candidatus* Profftella armatura" [54,55]. A genome analysis of *Profftella*, which resides in a symbiotic organ called the bacteriome, revealed that 15% of the drastically reduced genome encoded horizontally acquired genes for the biosynthesis of the polyketide toxin indicating an ancient and mutually obligatory association with the host. In another model system, it was also found that the aphid symbiont, *Hamiltonella defensa*, harbors a prophage that encodes proteinaceous toxins (Shiga-like toxin, cytolethal distending toxin, YD-repeat toxin), which is believed to protect aphids from the parasitic wasp *Aphidius ervi*. [56,57].

Various other protective functions of bacterial endosymbionts have been characterized, but the molecular basis of these interactions still remains elusive. Examples include defensive bacterial symbionts of aphids and their activity against entomopathogenic fungi [58], and the defensive character of *Spiroplasma* species (Tenericutes phylum) associated with *Drosophila* species [59,60].

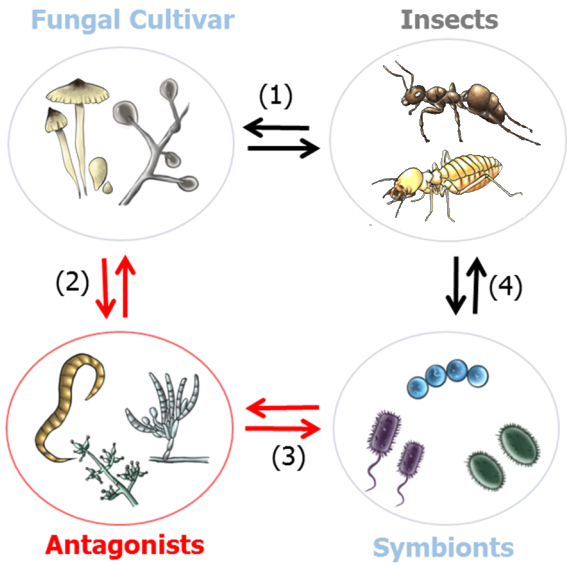

Figure 4: Multilateral microbial interactions in fungus-growing insects. (1) Insect cultivar: protects and shares habitat and nutrients. (2) Cultivar antagonist: competition for nutrients and habitat. (3) Antagonist mutualist: competition for nutrients and habitat; detrimental infestation by antagonist. (4) Symbiont insect: (beneficial) coexistence by sharing and protecting habitat and nutrients.

Defensive bacterial symbionts of fungus-growing insects

Insects, such as ants [61,62], termites [63], beetles [64], and even some bees [65] engage in fungi culture [66]. Fungus-growing insects create fungal gardens underground or in wooden galleys in which they grow an obligate food fungus that they supply with organic matter (Figure 4). The nutrient-rich fungus gardens are prone to exploitation by parasitic microorganisms, nematodes and other predators (e.g., other insects), rendering a high selective pressure on the insect to evolve effective (chemical) defenses [12,13,67,68].

Fungus-growing ants

One of the best-studied defensive symbiosis are leaf-cutting ants [69,70]. The symbiotic relationship between ants and fungus is particularly challenged by invading fungal species such as *Escovopsis*, *Fusarium*, and *Trichoderma* (Ascomycota). To clean the garden, ants apply mechanical grooming [71] and secrete antimicrobial compounds, such as 3-hydroxydecanoic acid, from their metapleural glands [72]. As a second line of defense, the ants are associated with protective Actinobacteria belonging in most attine ant genera to the genus *Pseudonocardia*, which grow on species-specific areas of the cuticle [73-76]. In vitro bioassay-guided screening of one of the *Pseudonocardia* symbionts afforded the antimicrobial cyclic depsipeptide dentigerumycin (**5**) that selectively inhibits the growth of the nest parasite *Escovopsis* but not the ants' mutualistic fungus at micromolar concentrations [77]. Dentigerumycin bears an unusual amino acid core skeleton including three piperazic acids, β-hydroxyleucine, *N*-hydroxyalanine, and a polyketide-derived moiety with a pyran ring. A follow-up study via genomic analysis and metabolomic profiles revealed that piperazic acid-containing cyclic depsipeptides are very common in this ecological niche of ant-associated bacteria. Fermentation and purification of metabolite extracts of three ant-associated *Pseudonocardia* derived from different geological places (Panama and Costa Rica) lead to the isolation of additional dentigerumycin-like molecules (e.g., gerumycin A (**6**) and gerumycin C (**7**), Figure 5) [78].

Gerumycins lack the polyketide-derived moiety, but contain e.g. a modified piperazic acid moiety carrying an additional chlorine and/or hydroxy substituent. In contrast to dentigerumycin, gerumycins do not exhibit significant antifungal activity in vitro against dentigerumycin-sensitive *Escovopsis* strains. A detailed biosynthetic analysis of gerumycins revealed that the biosynthetic gene clusters are encoded within variable genetic architectures and greatly differ between the three producing bacteria that it is not possible to deduce an evolutionary relation [78]. Over the last decade, the chemical investigation of *Pseudonocardia* and other Actinobacteria from fungus-growing ant species has led to the isolation and identification of many, including known, antimicrobial compounds. Among the reported structures are candicidin derivatives (e.g., candicidin D (**8**)) [79-81], actinomycin derivatives (e.g., actinomycin D (**9**)) [82], antimycin derivatives (e.g., antimycin A1 (**10**)), and novel

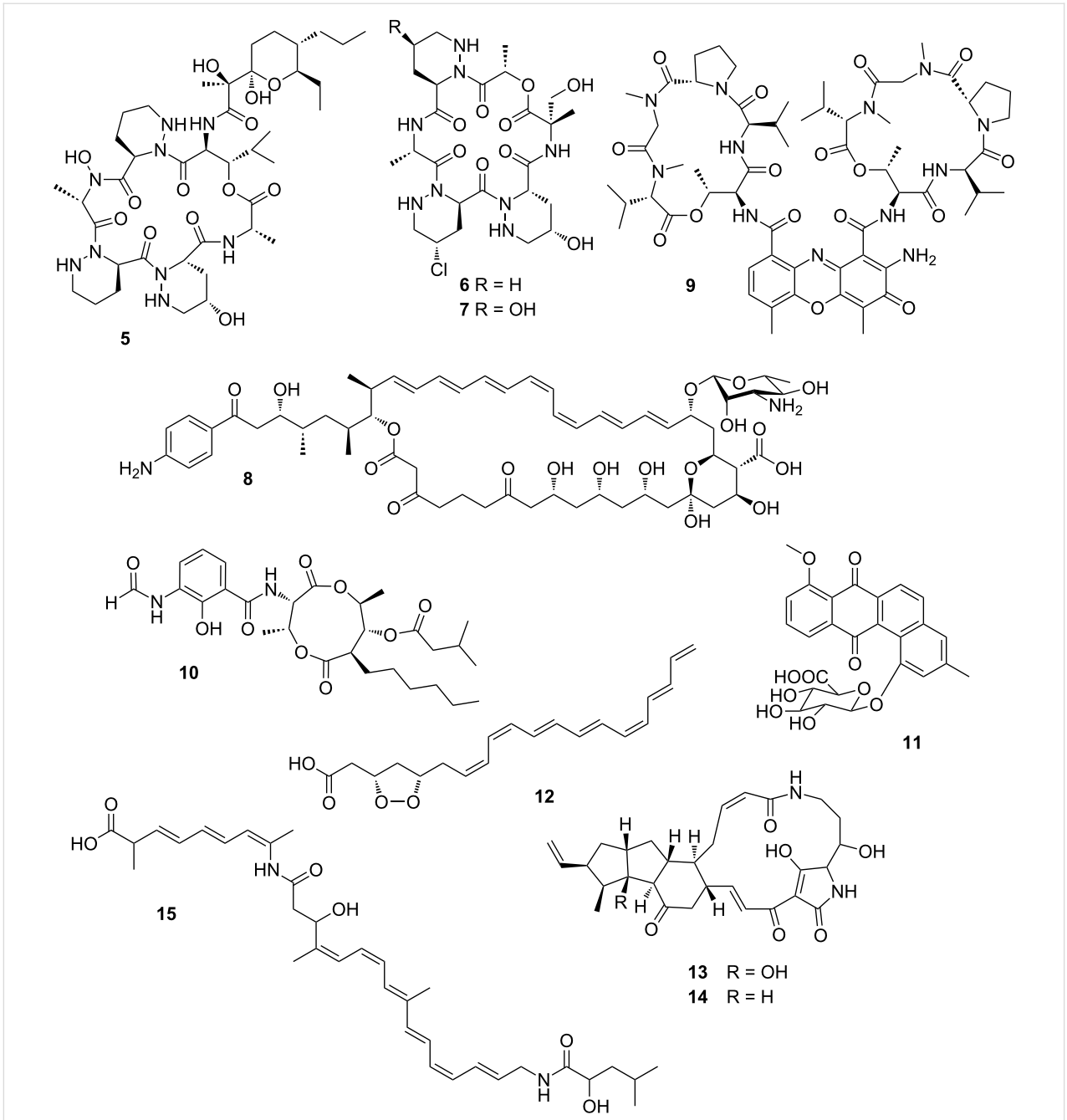

Figure 5: Small molecules (chemical mediators) play key roles in maintaining garden homeostasis in fungus-growing insects: dentigerumycin (**5**), gerumycin A (**6**), gerumycin C (**7**), candicidin D (**8**), actinomycin D (**9**), antimycin A1 (**10**), pseudonocardone B (**11**), mycangimycin (**12**), frontalamide A (**13**), frontalamide B (**14**), and bacillaene A (**15**).

quinones (e.g., pseudo-nocardone B (**11**)) [83] as depicted in Figure 5. This reflects the defensive role of Actinobacteria against fungus garden invaders and demonstrates their enormous biosynthetic potential as producers of antimicrobial compounds. Despite intensive research efforts, the specificity and evolutionary history of the ant–*Pseudonocardia* association still remains controversial [84,85]. It has been hypothesized that many of the isolated soil-dwelling Actinobacteria may have also been recruited from the environment by horizontal transmission, without having tight evolutionary bonds to the insect host.

Fungus-growing beetles

Bark beetles like the Southern Pine beetles (*Dendroctonus frontalis*) are responsible for widespread destruction of trees in parts of the United States [64]. They engage in an obligate symbiosis with the fungus *Entomocorticium* sp. A (Ascomy-

cota), which serves as nutrition for the beetle larvae, but also eventually causes the death of the tree. To propagate the fungus, adult beetles carry *Entomocorticium* sp. A in a specialized storage compartment called a mycangium from which the galleries within the inner bark of the host pine tree, housing the beetle larvae, are inoculated. The symbiosis is threatened by an antagonistic fungus *Ophiostoma minus*, which is able to overgrow *Entomocorticium* sp. A. To counteract this threat, *D. frontalis* house defensive bacterial symbionts within the galleries as well as inside the mycangia that appear to suppress the antagonistic fungus *Ophiostoma*.

Using symbiont pairing bioassays and chemical analysis one of the major isolates *Streptomyces thermosacchari* was shown to produce the fungicide mycangimycin (**12**), which inhibits the growth of the antagonist *O. minus*. Mycangimycin is an unusual carboxylic acid derivative with an endoperoxide unit and a conjugated heptaene moiety [86,87]. Subsequent chemical analysis of another *Streptomyces* strain associated with the southern pine beetle led to the discovery of two new members of polyketide-derived polycyclic tetramate macrolactams named frontalamides A (**13**) and B (**14**) (Figure 5) [88,89], which also displayed negative effects on the growth of the antagonistic fungus *O. minus*. By genetic analysis and manipulation of the producing *Streptomyces* strain the respective biosynthetic gene cluster could be identified. It encodes a hybrid polyketide synthase–non-ribosomal peptide synthase (PKS–NRPS), and resembles iterative enzymes normally only found in fungi. Subsequently, genomes of phylogenetically diverse bacteria from various environments were screened for the biosynthetic pathways of frontalamide-like compounds using a degenerate primer-based PCR screen. The respective gene clusters were broadly distributed in environmental Actinobacteria and the presence of the compounds was confirmed by chemical analysis of the bacterial cultures by LC–MS. Once again, these examples show that antibiotic-producing Actinobacteria may be commonly maintained as defensive microbes.

Fungus-growing termites

The monophyletic termite subfamily Macrotermitinae propagates a basidiomycete fungal cultivar *Termitomyces*, which serves as a major food source for the termite colony [90]. The domestication of *Termitomyces* facilitates an increase in carbohydrate decomposition capacity relative to that of other higher termites [91]. In turn, the termites cultivate and clean the fungus gardens; thus, protecting them from infestation by invasive species (e.g., mycoparasitic *Trichoderma* species). Despite targeted efforts, strong evidence for defensive microbial symbionts has remained elusive [92]. Only one study showed that the fungus-growing termite *Macrotermes natalensis* harbors a *Bacillus* strain, which produces a single major antibiotic, bacillaene A (**15**) (Figure 5), that inhibits putatively competitive or antagonistic fungi of *Termitomyces* suggesting a defensive property [93]. In various other studies, *Streptomyces* have been isolated from fungus-growing termite workers and combs, and some of these have been investigated for their chemical potential despite their so far largely undefined role in the symbiosis. Bugni and co-workers prioritized *Streptomyces* isolates from fungus-growing termites based on a HRMS-based principle component analysis (PCA) to rapidly identify unique natural product producers [94]. Based on this strategy, Clardy and co-workers then performed detailed chemical investi-

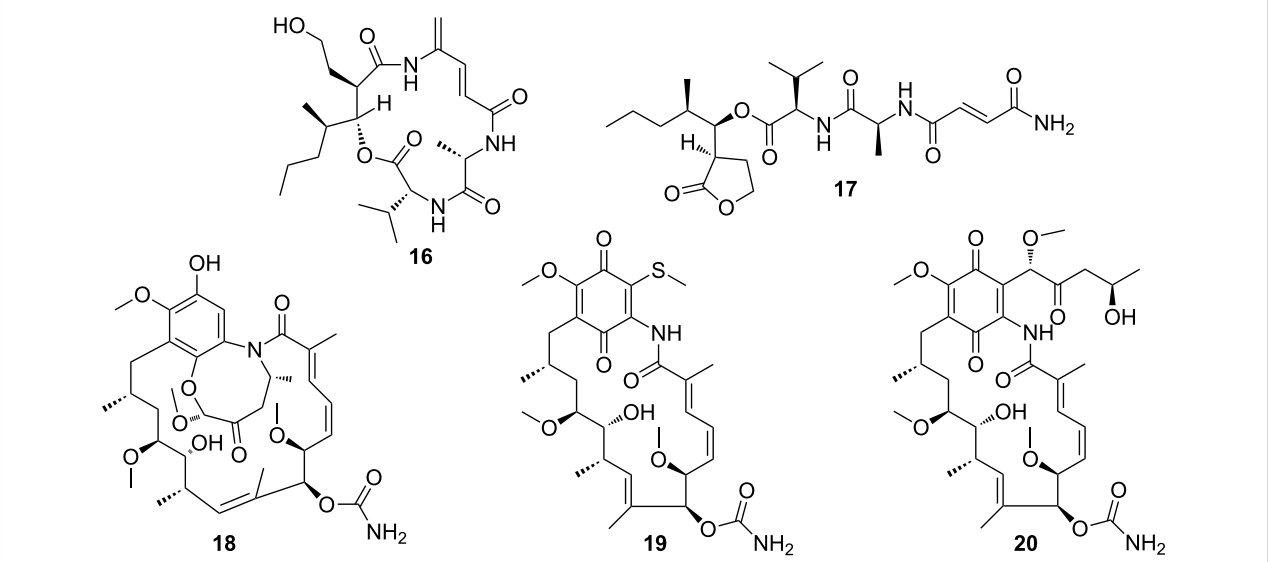

Figure 6: Secondary metabolites isolated from Actinobacteria from fungus-growing termites. Microtermolide A (**16**), microtermolide B (**17**), natalamycin A (**18**), 19-*S*-methylgeldanamycin (**19**), and 19-[(1*S*,4*R*)-4-hydroxy-1-methoxy-2-oxopentyl]geldanamycin (**20**).

gations of strains with an unique metabolomic profile, which led to the isolation, characterization, and reassignment of microtermolides A (**16**) and B (**17**) (Figure 6), products by an unusual hybrid non-ribosomal–polyketide pathway [95]. In a follow-up study, a *Streptomyces* isolate with exceptional high antifungal activity was investigated, and an unusual geldanamycin-derived natalamycin A (**18**), 19-*S*-methylgeldanamycin (**19**), and a geldanamycin analog with an unusual side chain modification (**20**) were isolated (Figure 6) [96]. The structure of **18** was elucidated using a combination of NMR spectroscopy, X-ray crystallography and additional quantum chemical NMR calculations.

Bacterial mutualists

Streptomyces and other Actinobacteria are well adapted to living in symbiosis with invertebrates, and have been isolated from many different parts of different insect species [12]. To further illuminate the importance of Actinobacteria as producers of valuable small molecules, we provide below additional examples of novel bioactive secondary metabolites originating from Actinobacteria–insect interactions, despite lack of clarity regarding the specificity and evolutionary history of these associations [97-99].

As described by Poulsen et al. a large number of morphologically, phylogenetically, and chemically diverse *Streptomyces* strains were isolated from two solitary wasp species (*Sceliphron caementarium* and *Chalybion californicum*, Hymenoptera, Sphecidae) [100]. Based on a pre-screening of bacterial extracts, the detailed chemical analysis of selected strains revealed not only a broad range of known bioactive compounds, such as bafilomycins (e.g., bafilomycin A1 (**21**) and B1 (**22**), Figure 7), but also a novel polyunsaturated and polyoxygenated 26-membered macrolactam named sceliphrolactam (**23**)

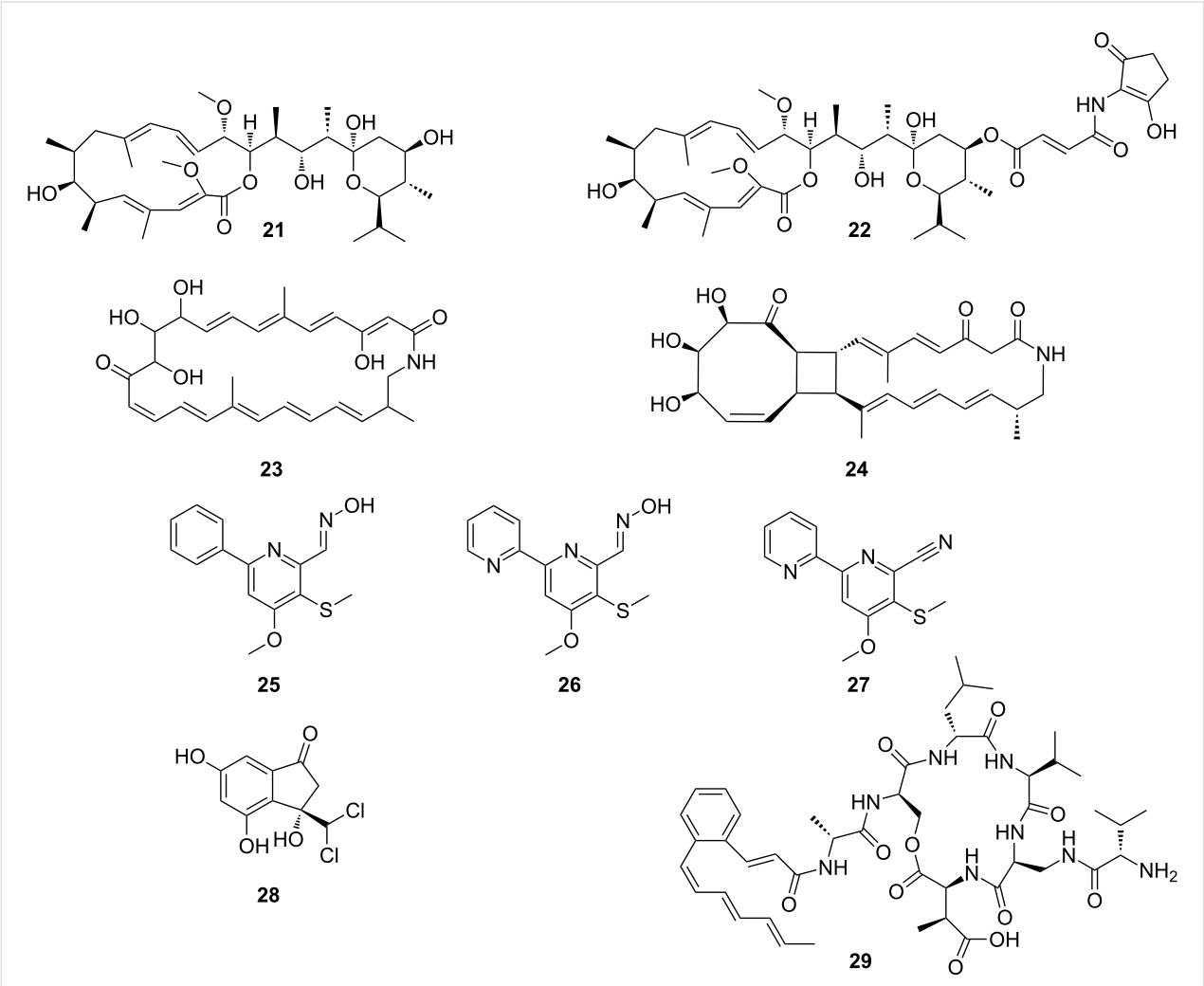

Figure 7: Secondary metabolites from bacterial mutualists of solitary insects. Bafilomycin A1 (**21**), bafilomycin B1 (**22**), sceliphrolactam (**23**), tripartilactam (**24**), coprismycin A (**25**), collismycin A (**26**), dipyridine SF2738D (**27**), tripartin (**28**), and coprisamide A (**29**).

(Figure 7) [101]. Sceliphrolactam showed strong antifungal activity against amphotericin B-resistant *Candida albicans*, but its functional role in vivo remains enigmatic.

In another study, Oh and co-workers chemically investigated a diverse population of Actinobacteria from the indigenous soil-dwelling Korean dung beetle (*Copris tripartitus*), its larvae and dung balls [102,103]. Dung beetles are prime contributors to the cyclic breakdown of organic waste material, and their life cycle is tightly dependent on herbivore faeces [104,105]. Based on unique metabolomic profiles (UV chromatogram) and HRMS data, several of the isolated *Streptomyces* strains were selected for large scale fermentation. Detailed chemical analysis of an organic culture extract led to the isolation of a new tricyclic macrolactam named tripartilactam (**24**) [103]. Tripartilactam (**24**) contains an unprecedented cyclobutane moiety, which links the 8- and 18-membered rings, and it is most likely derived from a photochemically [2 + 2] cycloaddition reaction of the corresponding macrocyclic 26-membered lactam precursor. Although compound **24** lacks any significant antimicrobial and anticancer activity, it was shown to act as a Na^+/K^+ ATPase inhibitor.

Subsequent studies by the same group lead to the isolation of phenylpyridines (e.g., coprismycin A (**25**)), dipyridines (e.g., collismycin A (**26**), SF2738D (**27**)) [102], and a dichlorinated indanone tripartin (**28**) [106]. Recently, the same group isolated new cyclic heptapeptides, named coprisamides (e.g., coprisamide A (**29**)) from a *Streptomyces* strain isolated from the gut of *C. tripartitus*. The cyclic heptapeptides contain unusual amino acid units (e.g., β-methylaspartic acid and 2,3-diaminopropanoic acid) and a previously unreported 2-hepta-trienyl cinnamoyl chain unit [107]. Dung beetle larvae are prone to bacterial and fungal infestations during their development inside the faeces balls. Although the direct involvement of defensive microbial symbionts has not been described yet, the presence of highly productive Actinobacteria might provide an indirect protection against parasites and pathogens as suggested in the termite symbiosis.

Fungal symbionts

Fungi co-evolved with various different insects over millions of years, thereby serving as a food source to fungal grazers, or competing with saprophagous insects, and attacking insects as hosts for growth and reproduction [108]. The cross-kingdom interactions and long-time co-evolution are assumed to be responsible for the genetic accumulation of biosynthetic gene clusters encoding for bioactive secondary metabolites. The respective natural products are predicted to play key roles as chemical signals or virulence factors mediating the interactions with the respective insect host [108-111].

Despite the fact that a few examples exist, fungi as (defensive) symbionts have not nearly been explored to the same extent as bacterial protagonists, which is surprising as fungi have a vast biosynthetic potential and are a rich source of antibiotics (Figure 8).

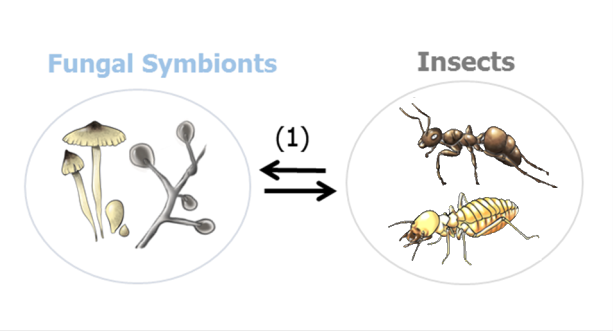

Figure 8: Beneficial interactions (1) between fungal symbionts and insects.

As early as 1982, Nakashima et al. investigated the fungal cultivar (*Fusarium* sp.) of the ambrosia beetle *Euwalecea validus*. The chemical analysis of culture extracts revealed the antifungal secondary metabolites cerulenin (**30**) and the nortriterpenoid helvolic acid (**31**) (Figure 9), which inhibit the growth of mold fungi in vitro and are assumed to suppress bacterial contaminations [112]. Slightly earlier, in 1979, Nair et al. had described the isolation of an antibacterial chlorinated lactol, lepiochlorin (**32**), from liquid cultures of a *Lepiota* species, a fungus cultivated by fungus-growing ants (*Cyphomyrmex costatus*) [113]. Nearly twenty years later, Clardy and co-workers explored the symbiotic interactions between the fungus *Tyridiomyces formicarum* of the fungus-growing ant *Cyphomyrmex minutus*, as part of the seminal "biorationale" approach in the search for novel compounds. The fungus is unique among the attine fungi because it grows as a yeast form (unicellular) and not in the mycelial form which is typical for all other attine ant fungi. The fungus was found to produce several antifungal diketopiperazines (e.g., **33**) [114]. In another study, also reported by Clardy and co-workers, the secondary metabolite profile of the symbiotic fungus *Bionectria* sp. associated with the fungus-growing ant *Apterostigma dentigerum*, was investigated [115]. Again, a chemical analysis of an organic culture extract led to the isolation of a new polyketide bionectriol A (**34**), a glycosylated, polyunsaturated polyol, with so far undetermined ecological function. More recently, Wang et al. showed that the solitary leaf-rolling weevil *Euops chinensis* (Attelabidae) undergoes a protofarming symbiosis with the polysaccharide-degrading *Penicillium herquei* (family *Trichocomaceae*), which is planted on leave roles containing eggs and larvae to protect the offspring. *P. herquei* was shown to produce the antibiotic polyketide (+)-

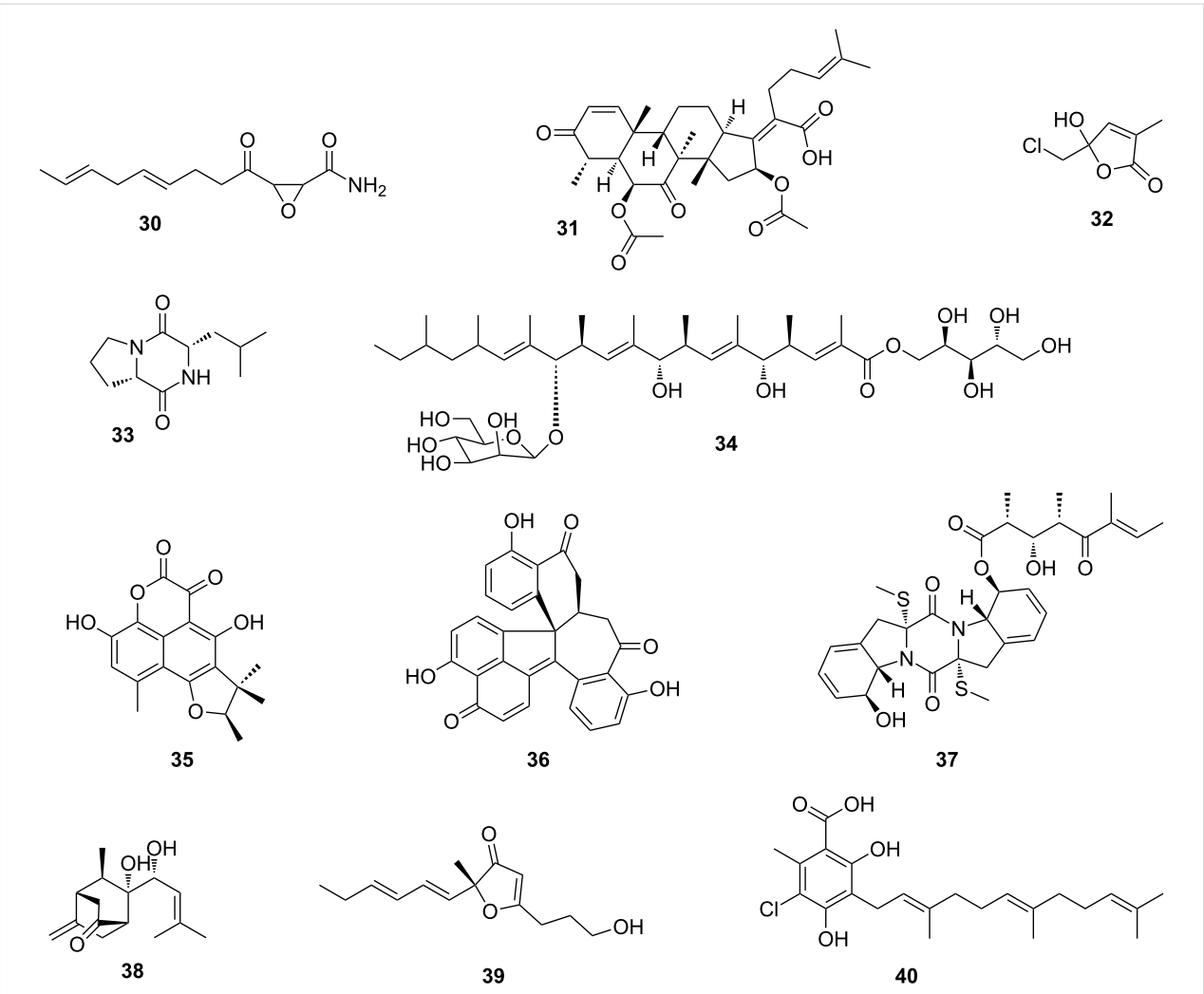

Figure 9: Secondary metabolites isolated from fungal symbionts. Cerulenin (**30**), helvolic acid (**31**), lepiochlorin (**32**), cyclo-(L-Pro-L-Leu) (**33**), bionectriol A (**34**), (+)-scleroderolide (**35**), dalesconol A (**36**), boydine B (**37**), boydene A (**38**), paraconfuranone A (**39**), and ilicicolinic acid A (**40**).

scleroderolide (**35**), which can inhibit the growth of several bacterial and fungal pathogens in competition assays on plates and keeps larval brood chambers free of other microbes [116,117].

Although the ecological roles of the compounds produced by the investigated fungi remain elusive, the following examples show that associated fungi are valuable sources for novel bioactive secondary metabolites with high pharmacological potential.

In 2008, Tan and co-workers discovered the unusual polyketide dalesconol A (**36**) from extracts of the fungus *Daldinia eschscholzii* isolated from the gut of the mantis *Tenodera aridifolia* [118,119]. Additional insights into the dalesconol biosynthesis was gained from a characterization of minor dalesconols and biosynthetic intermediates only present in chemical extracts prepared from a large-scale fermentation. The ascomycete fungus *Pseudallescheria boydii*, isolated from the gut of the larvae of the beetle *Holotrichia parallela*, showed also a broad range of bioactive secondary metabolites including epipolythiodioxopiperazines, named boydines (e.g., boydine B, (**37**)) [120]. Boydines significantly inhibit clinically relevant anaerobic bacterial strains (e.g., *Bifidobacterium* sp., *Veillonella parvula*, *Anaerosterptococcus* sp., *Bacteroides vulgatus*, and *Peptostreptococcus* sp.), suggesting a potential ecological role as defensive symbiont in addition to interesting pharmacological properties. Further analysis of the same fermentation extracts afforded boydenes (e.g., boydene A, (**38**)), sesquiterpenes with an unprecedented carbon skeleton that are most likely built up by an enzymatic Aldol addition.

In a similar example, new cytotoxic furanone analogues (e.g., paraconfuranone A (**39**)) were obtained from the fungus *Para-*

coniothyrium brasiliense isolated from the gut of the grasshopper *Acrida cinerea* [121]. Antibacterial ilicicolinic acids (e.g., ilicicolinic acid A (**40**)) were detected in a fungus *Neonectria discophora* isolated from a soil-feeding and wood-damaging termite nest (*Nasutitermes corniger*) in the North Amazon (French Guiana). Ilicicolinic acids show good inhibitory effects against several human pathogens [122].

Entomopathogenic fungi

More than 700 known fungal species from 100 genera have adopted an entomopathogenic lifestyle (Figure 10) [123,124]. Entomopathogenic fungi release infective spores which attach to the insect cuticle; once the spore germinates, the developing hyphae penetrate the insect integument and start the infection process. Apart from a variety of secreted proteases that digest the chitin-containing cuticle of the insect, secreted toxic metabolites are assumed to assist in overcoming host defenses and killing the host. Some entomopathogenic species, such as *Beauveria bassiana* and *Metarhizium anisopliae*, have a broad host range encompassing over 1,000 insect species from more than 50 different insect families. These fungi are used as biocontrol agents for invertebrate pest control, a commercial alternative to chemical pesticides [125-127]. Other entomopathogenic fungi, such as different *Cordiceps* species, are also known to be prolific producers of highly active secondary metabolites, but with a relatively narrow host range and geographic distribution [108,124]. Recent comparative genomic analyses of *Metarhizium* sp. and *Beauveria* sp. indicate that over 80% of the genes associated with putative secondary metabolites have no identified specific products, and even sequences are unique to this group of organisms [124]. Despite the enormous chemical potential, only a few studies to date have unequivocally demonstrated the exact role of the respective compounds. Here, we briefly summarize compounds for which an ecological role has been identified.

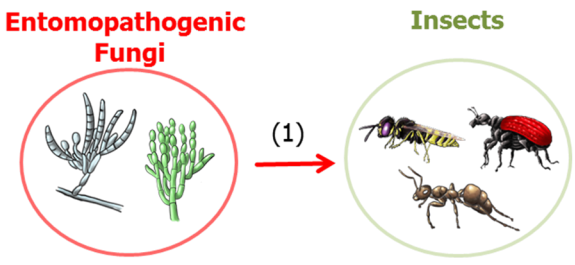

Figure 10: Predatory interactions, (1) entomopathogenic fungi use insect as prey.

One of the most prominent secondary metabolites of *M. anisopliae* are the cyclic hexadepsipeptides named destruxins (e.g., destruxin A (**41**), Figure 11). Destruxins are composed of an α-hydroxy acid and five amino acid residues, and they exhibit a wide range of interesting biological properties, such as insecticidal, cytotoxic, and moderate antibiotic activity [128]. The secretion of destruxins is weakly correlated to fungal virulence and insecticidal activity, because injection, ingestion or topical application of these compounds resulted in tetanic paralysis in many insects, caused by destruxin-mediated opening of calcium channels and resulting membrane depolarization.

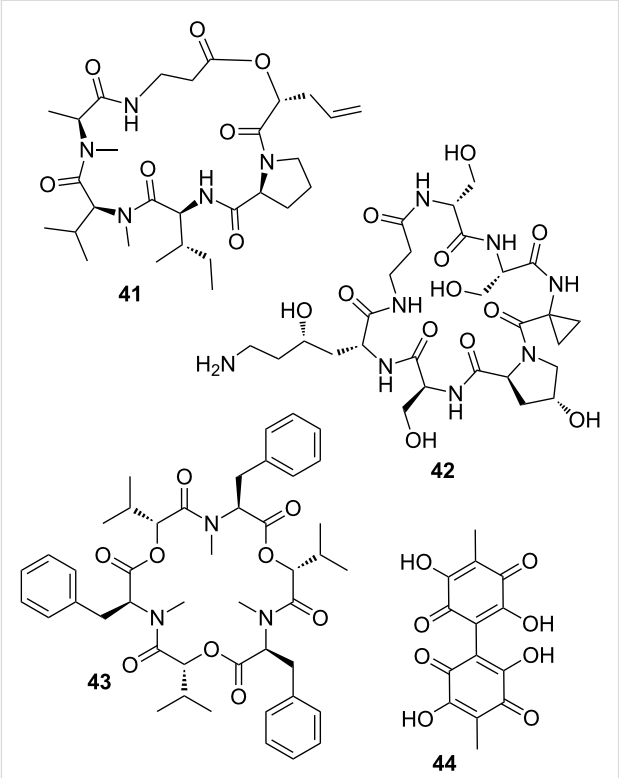

Figure 11: Entomopathogenic fungi use secondary metabolites as insecticidal compounds to kill their prey. Destruxin A (**41**), serinocyclin A (**42**), beauvericin (**43**), and oosporein (**44**).

In another study, the cyclic heptapeptide serinocyclins (e.g., serinocyclin A (**42**)) were isolated from conidia harvested on agar surface cultures of *M. anisopliae*, a commercial biocontrol product called Green Muscle [129]. Serinocyclin A contains several non-proteinogenic amino acids. Among them are the uncommon 1-aminocyclopropane-1-carboxylic acid, (2*R*,4*S*)-4-hydroxylysine, and the more frequently encountered hydroxyproline, β-alanine, and D-serine. Due to the presence in conidia, serinocyclines have also been hypothesized to play a role in the virulence of *M. anisopliae*.

Chemical analysis of the entomopathogenic fungus *B. bassiana* yielded beauvericin (**43**), a depsipeptide with alternating methylphenylalanyl and hydroxyisovaleryl residues. Beauvericin has antibacterial, antifungal, and insecticidal activities,

in addition to its potent cytotoxic activity against human cell lines [130]; attributes which indicate a crucial role in the infection process. The red 1,4-bibenzoquinone derivative oosporein (**44**) was first identified in the 1960s [131], and exhibits similar antibiotic [132], antiviral [133], antifungal [134], and insecticidal activities [135]. Oosporein (**44**) production in *B. bassiana* is correlated to the fungal virulence due to the inhibition of host immunity, which facilitates fungal propagation in insects [136].

In summary, entomopathogenic fungi are rich in secondary metabolite gene clusters, some of which have been genetically characterized. However, the vast majority of the encoded compounds, as well as their biological role(s) remain uncovered [137]. In light of the rapidly declining costs for -omic technologies, in vivo infection studies coupled with methods such as RNA sequencing, can lead to further insights into the role and expression levels of potentially new secondary metabolites.

Conclusion

Insects provide experimentally tractable and cost-effective model systems to investigate the evolutionary development and chemical basis of animal–bacterial interactions, and symbiosis in particular. Bacterial and fungal symbionts represent an extraordinary discovery opportunity for both biology and chemistry. Studying these interactions will shed light on equivalent processes in other animals, including humans. The in-depth investigations of a small number of insect–microbe interactions have already led to the discovery of a number of secondary metabolites with new and structurally diverse chemical core structures. Unfortunately, the identification of chemical mediators has so far been mainly restricted to in vitro analyses, but efforts should be directed towards identifying the presence and activity of candidate compounds in situ. The examination of bacterial secondary metabolisms and the respective small molecules secretome, can give insights into the up or down-regulation of (cryptic) biosynthetic pathways. This in turn can lead to the discovery of new metabolic pathways that would otherwise be silent or undetected under typical laboratory cultivation conditions. In recent years many successful analytical methods including UHPLC–DAD and UHPLC–MS-based techniques, imaging mass spectrometry (IMS) [138,139] and high resolution NMR systems have been developed and optimized [7,18]. These technologies allow the identification in minute concentrations of the chemical entities moderating insect–microbial interactions and at least partially eliminate the need for bioassay-guided fractionation for the identification of key compounds. We are still scratching the surface of the chemical potential of the microbial world, but chemical investigations of microbial interactions will undoubtedly expand the list of new bioactive secondary metabolites in the near future.

Acknowledgements

We thank the anonymous referees for their constructive comments, which helped to improve the manuscript. We are also grateful for financial support from the German National Academy of Sciences Leopoldina (LPDS 2011-2) and the Daimler Benz foundation for a postdoctoral fellowship to CB, and the Villum Kann Rasmussen foundation for a Young Investigator Fellowship (10101) to MP. MR was supported by the graduate school Jena School for Microbial Communication (JSMC) financed by the Deutsche Forschungsgemeinschaft.

References

1. Newman, D. J.; Cragg, G. M. *J. Nat. Prod.* **2012,** *75,* 311–335. doi:10.1021/np200906s
2. Gerwick, W. H.; Moore, B. S. *Chem. Biol.* **2012,** *19,* 85–98. doi:10.1016/j.chembiol.2011.12.014
3. Lewis, K. *Nat. Rev. Drug Discovery* **2013,** *12,* 371–387. doi:10.1038/nrd3975
4. Fair, R. J.; Tor, Y. *Perspect. Med. Chem.* **2014,** *6,* 25–64. doi:10.4137/PMC.S14459
5. Trevino, S. E.; Kollef, M. H. *Clin. Chest Med.* **2015,** *36,* 531–541. doi:10.1016/j.ccm.2015.05.007
6. *Nat. Rev. Drug Discovery* **2013,** *12,* 494. doi:10.1038/nrd4074
7. Tawifke, A. F.; Viegelmann, C.; Edrada-Ebel, R. *Methods Mol. Biol.* **2013,** *1055,* 227–244. doi:10.1007/978-1-62703-577-4_17
8. Gaudêncio, S. P.; Pereira, P. *Nat. Prod. Rep.* **2015,** *32,* 779–810. doi:10.1039/C4NP00134F
9. Fischbach, M. A.; Walsh, C. T.; Clardy, J. *Proc. Natl. Acad. Sci. U. S. A.* **2008,** *105,* 4601–4608. doi:10.1073/pnas.0709132105
10. Fischbach, M. A. *Curr. Opin. Microbiol.* **2009,** *12,* 520–527. doi:10.1016/j.mib.2009.07.002
11. Jenke-Kodama, H.; Dittmann, E. *Phytochemistry* **2009,** *70,* 1858–1866. doi:10.1016/j.phytochem.2009.05.021
12. Kaltenpoth, M. *Trends Microbiol.* **2009,** *17,* 529–535. doi:10.1016/j.tim.2009.09.006
13. Bode, H. B. *Angew. Chem., Int. Ed.* **2009,** *48,* 6394–6396. doi:10.1002/anie.200902152
14. Brownlie, J. C.; Johnson, K. N. *Trends Microbiol.* **2009,** *17,* 348–354. doi:10.1016/j.tim.2009.05.005
15. Douglas, A. E. *Cell Host Microbe* **2011,** *10,* 359–367. doi:10.1016/j.chom.2011.09.001
16. Brachmann, A. O.; Bode, H. B. Identification and Bioanalysis of Natural Products from Insect Symbionts and Pathogens. In *Yellow Biotechnology I;* Vilcinskas, A., Ed.; Advances in Biochemical Engineering/Biotechnology, Vol. 135; Springer: Berlin, Heidelberg; pp 123–155. doi:10.1007/10_2013_192
17. Oliver, K. M.; Smith, A. H.; Russell, J. A. *Funct. Ecol.* **2014,** *28,* 341–355. doi:10.1111/1365-2435.12133
18. Kuhlisch, C.; Pohnert, G. *Nat. Prod. Rep.* **2015,** *32,* 937–955. doi:10.1039/C5NP00003C
19. Davies, J. *Curr. Opin. Chem. Biol.* **2011,** *15,* 5–10. doi:10.1016/j.cbpa.2010.11.001
20. Zotchev, S. B.; Sekurova, O. N.; Katz, L. *Curr. Opin. Biotechnol.* **2012,** *23,* 941–947. doi:10.1016/j.copbio.2012.04.002
21. Vizcaino, M. I.; Guo, X.; Crawford, J. M. *J. Ind. Microbiol. Biotechnol.* **2014,** *41,* 285–299. doi:10.1007/s10295-013-1356-5

22. Harvey, A. L.; Edrada-Ebel, R.; Quinn, R. J. *Nat. Rev. Drug Discovery* **2015,** *14,* 111–129. doi:10.1038/nrd4510
23. Johnston, C. W.; Skinnider, M. A.; Wyatt, M. A.; Li, X.; Ranieri, M. R. M.; Yang, L.; Zechel, D. L.; Ma, B.; Magarvey, N. A. *Nat. Commun.* **2015,** *6,* No. 8421. doi:10.1038/ncomms9421
24. Piel, J. *Nat. Prod. Rep.* **2009,** *26,* 338–362. doi:10.1039/b703499g
25. Crawford, J. M.; Clardy, J. *Chem. Commun.* **2011,** *47,* 7559–7566. doi:10.1039/c1cc11574j
26. Traxler, M. F.; Kolter, R. *Nat. Prod. Rep.* **2015,** *32,* 956–970. doi:10.1039/C5NP00013K
27. Challinor, V. L.; Bode, H. B. *Ann. N. Y. Acad. Sci.* **2015,** *1354,* 82–97. doi:10.1111/nyas.12954
28. Fischbach, M. A.; Walsh, C. T. *Chem. Rev.* **2006,** *106,* 3468–3496. doi:10.1021/cr0503097
29. Hertweck, C. *Angew. Chem., Int. Ed.* **2009,** *48,* 4688–4716. doi:10.1002/anie.200806121
30. Piel, J. *Nat. Prod. Rep.* **2010,** *27,* 996–1047. doi:10.1039/b816430b
31. Wang, H.; Fewer, D. P.; Holm, L.; Rouhiainen, L.; Sivonen, K. *Proc. Natl. Acad. Sci. U. S. A.* **2014,** *111,* 9259–9264. doi:10.1073/pnas.1401734111
32. Hertweck, C. *Trends Biochem. Sci.* **2015,** *40,* 189–199. doi:10.1016/j.tibs.2015.02.001
33. Misof, B.; Liu, S.; Meusemann, K.; Peters, R. S.; Donath, A.; Mayer, C.; Frandsen, P. B.; Ware, J.; Flouri, T.; Beutel, R. G.; Niehuis, O.; Petersen, M.; Izquierdo-Carrasco, F.; Wappler, T.; Rust, J.; Aberer, A. J.; Aspöck, U.; Aspöck, H.; Bartel, D.; Blanke, A.; Berger, S.; Böhm, A.; Buckley, T. R.; Calcott, B.; Chen, J.; Friedrich, F.; Fukui, M.; Fujita, M.; Greve, C.; Grobe, P.; Gu, S.; Huang, Y.; Jermiin, L. S.; Kawahara, A. Y.; Krogmann, L.; Kubiak, M.; Lanfear, R.; Letsch, H.; Li, Y.; Li, Z.; Li, J.; Lu, H.; Machida, R.; Mashimo, Y.; Kapli, P.; McKenna, D. D.; Meng, G.; Nakagaki, Y.; Navarrete-Heredia, J. L.; Ott, M.; Ou, Y.; Pass, G.; Podsiadlowski, L.; Pohl, H.; von Reumont, B. M.; Schütte, K.; Sekiya, K.; Shimizu, S.; Slipinski, A.; Stamatakis, A.; Song, W.; Su, X.; Szucsich, N. U.; Tan, M.; Tan, X.; Tang, M.; Tang, J.; Timelthaler, G.; Tomizuka, S.; Trautwein, M.; Tong, X.; Uchifune, T.; Walzl, M. G.; Wiegmann, B. M.; Wilbrandt, J.; Wipfler, B.; Wong, T. K.; Wu, Q.; Wu, G.; Xie, Y.; Yang, S.; Yang, Q.; Yeates, D. K.; Yoshizawa, K.; Zhang, Q.; Zhang, R.; Zhang, W.; Zhang, Y.; Zhao, J.; Zhou, C.; Zhou, L.; Ziesmann, T.; Zou, S.; Li, Y.; Xu, X.; Zhang, Y.; Yang, H.; Wang, J.; Wang, J.; Kjer, K. M.; Zhou, X. *Science* **2014,** *346,* 763–767. doi:10.1126/science.1257570
34. McFall-Ngai, M.; Hadfield, M. G.; Bosch, T. C. G.; Carey, H. V.; Domazet-Lošo, T.; Douglas, A. E.; Dubilier, N.; Eberl, G.; Fukami, T.; Gilbert, S. F.; Hentschel, U.; King, N.; Kjelleberg, S.; Knoll, A. H.; Kremer, N.; Mazmanian, S. K.; Metcalf, J. L.; Nealson, K.; Pierce, N. E.; Rawls, J. F.; Reid, A.; Rudy, E. G.; Rumpho, M.; Sanders, J. G.; Tautz, D.; Wernegreen, J. J. *Proc. Natl. Acad. Sci. U. S. A.* **2013,** *110,* 3229–3236. doi:10.1073/pnas.1218525110
35. Su, Q.; Zhou, X.; Zhang, Y. *Commun. Integr. Biol.* **2013,** *6,* e23804. doi:10.4161/cib.23804
36. Engel, M. S. *Curr. Biol.* **2015,** *25,* R868–R872. doi:10.1016/j.cub.2015.07.059
37. Douglas, A. E. *J. Mol. Biol.* **2014,** *426,* 3830–3837. doi:10.1016/j.jmb.2014.04.005
38. Douglas, A. E. *Annu. Rev. Entomol.* **2015,** *60,* 17–34. doi:10.1146/annurev-ento-010814-020822
39. Yim, G.; Wang, H. H.; Davies, J. *Philos. Trans. R. Soc., B* **2007,** *362,* 1195–1200. doi:10.1098/rstb.2007.2044
40. Clardy, J.; Fischbach, M. A.; Currie, C. R. *Curr. Biol.* **2009,** *19,* R437–R441. doi:10.1016/j.cub.2009.04.001
41. Romero, D.; Traxler, M. F.; López, D.; Kolter, R. *Chem. Rev.* **2011,** *111,* 5492–5505. doi:10.1021/cr2000509
42. Kaltenpoth, M.; Göttler, W.; Herzner, G.; Strohm, E. *Curr. Biol.* **2005,** *15,* 475–479. doi:10.1016/j.cub.2004.12.084
43. Kaltenpoth, M.; Göttler, W.; Dale, C.; Stubblefield, J. W.; Herzner, G.; Röser-Müller, K.; Strohm, E. *Int. J. Syst. Evol. Microbiol.* **2006,** *56,* 1403–1411. doi:10.1099/ijs.0.64117-0
44. Kroiss, J.; Kaltenpoth, M.; Schneider, B.; Schwinger, M.-G.; Hertweck, C.; Maddula, R. K.; Strohm, E.; Svatoš, A. *Nat. Chem. Biol.* **2010,** *6,* 261–263. doi:10.1038/nchembio.331
45. Koehler, S.; Doubský, J.; Kaltenpoth, M. *Front. Zool.* **2013,** *10,* No. 3. doi:10.1186/1742-9994-10-3
46. Darrouzet, E.; Issartel, J. P.; Lunardi, J.; Dupuis, A. *FEBS Lett.* **1998,** *431,* 34–38. doi:10.1016/S0014-5793(98)00719-4
47. Zhang, M.-Z.; Chen, Q.; Xie, C.-H.; Mulholland, N.; Turner, S.; Irwin, D.; Gu, Y.-C.; Yang, G.-F.; Clough, J. *Eur. J. Med. Chem.* **2015,** *92,* 776–783. doi:10.1016/j.ejmech.2015.01.043
48. Kellner, R. L. L.; Dettner, K. *J. Chem. Ecol.* **1995,** *21,* 1719–1733. doi:10.1007/BF02033672
49. Kellner, R. L. L. *J. Insect Physiol.* **2001,** *47,* 475–483. doi:10.1016/S0022-1910(00)00140-2
50. Kellner, R. L. L. *Chemoecology* **2001,** *11,* 127–130. doi:10.1007/PL00001842
51. Kellner, R. L. L. *Insect Biochem. Mol. Biol.* **2002,** *32,* 389–395. doi:10.1016/S0965-1748(01)00115-1
52. Piel, J. *Proc. Natl. Acad. Sci. U. S. A.* **2002,** *99,* 14002–14007. doi:10.1073/pnas.222481399
53. Kellner, R. L. L.; Dettner, K. *Oecologia* **1996,** *107,* 293–300. doi:10.1007/BF00328445
54. Nakabachi, A.; Ueoka, R.; Oshima, K.; Teta, R.; Mangoni, A.; Gurgui, M.; Oldham, N. J.; van Echten-Deckert, G.; Okamura, K.; Yamamota, K.; Inoue, H.; Ohkuma, M.; Hongoh, Y.; Miyagishima, S.; Hattori, M.; Piel, J.; Fukatsu, T. *Curr. Biol.* **2013,** *23,* 1478–1484. doi:10.1016/j.cub.2013.06.027
55. The structure of diaphorin (**4**) is based on comparative NMR analysis, but no additional proof of the stereochemistry at positions 7, 10 and 17 are given.
56. Oliver, K. M.; Moran, N. A.; Hunter, M. S. *Proc. Natl. Acad. Sci. U. S. A.* **2005,** *102,* 12795–12800. doi:10.1073/pnas.0506131102
57. Degnan, P. H.; Moran, N. A. *Appl. Environ. Microbiol.* **2008,** *74,* 6782–6791. doi:10.1128/AEM.01285-08
58. Łukasik, P.; van Asch, M.; Guo, H.; Ferrari, J.; Godfray, H. C. J. *Ecol. Lett.* **2013,** *16,* 214–218. doi:10.1111/ele.12031
59. Xie, J.; Vilchez, I.; Mateos, M. *PLoS One* **2010,** *5,* e12149. doi:10.1371/journal.pone.0012149
60. Jaenike, J.; Unckless, R.; Cockburn, S. N.; Boelio, L. M.; Perlman, S. J. *Science* **2010,** *329,* 212–215. doi:10.1126/science.1188235
61. Currie, C. R. *Annu. Rev. Microbiol.* **2001,** *55,* 357–380. doi:10.1146/annurev.micro.55.1.357
62. Mueller, U. G.; Schultz, T. R.; Currie, C. R.; Adams, R. M. M.; Malloch, D. *Q. Rev. Biol.* **2001,** *76,* 169–197. doi:10.1086/393867
63. Aanen, D. K.; Eggleton, P.; Rouland-Lefèvre, C.; Guldberg-Frøslev, T.; Rosendahl, S.; Boomsma, J. J. *Proc. Natl. Acad. Sci. U. S. A.* **2002,** *99,* 14887–14892. doi:10.1073/pnas.222313099
64. Six, D. L. *Insects* **2012,** *3,* 339–366. doi:10.3390/insects3010339

65. Menezes, C.; Vollet-Neto, A.; Marsaioli, A. J.; Zampieri, D.; Fontoura, I. C.; Luchessi, A. D.; Imperatriz-Fonseca, V. L. *Curr. Biol.* **2015,** *25,* 2851–2855. doi:10.1016/j.cub.2015.09.028
66. Mueller, U. G.; Gerardo, N. M.; Aanen, D. K.; Six, D. L.; Schultz, T. R. *Annu. Rev. Ecol. Evol. Syst.* **2005,** *36,* 563–595. doi:10.1146/annurev.ecolsys.36.102003.152626
67. Ramadhar, T. R.; Beemelmanns, C.; Currie, C. R.; Clardy, J. *J. Antibiot.* **2014,** *67,* 53–58. doi:10.1038/ja.2013.77
68. Aylward, F. O.; Suen, G.; Biedermann, P. H. W.; Adams, A. S.; Scott, J. J.; Malfatti, S. A.; Glavina del Rio, T.; Tringe, S. G.; Poulsen, M.; Raffa, K. F.; Klepzig, K. D.; Currie, C. R. *mBio* **2014,** *5,* e02077–14. doi:10.1128/mBio.02077-14
69. Currie, C. R.; Bot, A. N. M.; Boomsma, J. J. *Oikos* **2003,** *101,* 91–102. doi:10.1034/j.1600-0706.2003.12036.x
70. Poulsen, M.; Currie, C. R. *PLoS One* **2010,** *5,* e8748. doi:10.1371/journal.pone.0008748
71. Currie, C. R.; Stuart, A. E. *Proc. R. Soc. London, Ser. B* **2001,** *268,* 1033–1039. doi:10.1098/rspb.2001.1605
72. Bot, A. N. M.; Ortius-Lechner, D.; Finster, K.; Maile, R.; Boomsma, J. J. *Insectes Soc.* **2002,** *49,* 363–370. doi:10.1007/PL00012660
73. Currie, C. R.; Scott, J. A.; Summerbell, R. C.; Malloch, D. *Nature* **1999,** *398,* 701–704. doi:10.1038/19519
74. Currie, C. R.; Poulsen, M.; Mendenhall, J.; Boomsma, J. J.; Billen, J. *Science* **2006,** *311,* 81–83. doi:10.1126/science.1119744
75. Cafaro, M. J.; Poulsen, M.; Little, A. E.; Price, S. L.; Gerardo, N. M.; Wong, B.; Stuart, A. E.; Larget, B.; Abbot, P.; Currie, C. R. *Proc. R. Soc. London, Ser. B* **2011,** *278,* 1814–1822. doi:10.1098/rspb.2010.2118
76. Caldera, E. J.; Currie, C. R. *Am. Nat.* **2012,** *180,* 604–617. doi:10.1086/667886
77. Oh, D.-C.; Poulsen, M.; Currie, C. R.; Clardy, J. *Nat. Chem. Biol.* **2009,** *5,* 391–393. doi:10.1038/nchembio.159
78. Sit, C. S.; Ruzzini, A. C.; van Arnam, E. B.; Ramadhar, T. R.; Currie, C. R.; Clardy, J. *Proc. Natl. Acad. Sci. U. S. A.* **2015,** *112,* 13150–13154. doi:10.1073/pnas.1515348112
79. Haeder, S.; Wirth, R.; Herz, H.; Spiteller, D. *Proc. Natl. Acad. Sci. U. S. A.* **2009,** *106,* 4742–4746. doi:10.1073/pnas.0812082106
80. Barke, J.; Seipke, R. F.; Grüschow, S.; Heavens, D.; Drou, N.; Bibb, M. J.; Goss, R. J. M.; Yu, D. W.; Hutchings, M. I. *BMC Biol.* **2010,** *8,* No. 109. doi:10.1186/1741-7007-8-109
81. Seipke, R. F.; Barke, J.; Brearley, C.; Hill, L.; Yu, D. W.; Goss, R. J. M.; Hutchings, M. I. *PLoS One* **2011,** *6,* e22028. doi:10.1371/journal.pone.0022028
82. Schoenian, I.; Spiteller, M.; Ghaste, M.; Wirth, R.; Herz, H.; Spiteller, D. *Proc. Natl. Acad. Sci. U. S. A.* **2011,** *108,* 1955–1960. doi:10.1073/pnas.1008441108
83. Carr, G.; Derbyshire, E. R.; Caldera, E.; Currie, C. R.; Clardy, J. *J. Nat. Prod.* **2012,** *75,* 1806–1809. doi:10.1021/np300380t
84. Kost, C.; Lakatos, T.; Böttcher, I.; Arendholz, W.-R.; Redenbach, M.; Wirth, R. *Naturwissenschaften* **2007,** *94,* 821–828. doi:10.1007/s00114-007-0262-y
85. Mueller, U. G. *Curr. Opin. Microbiol.* **2012,** *15,* 269–277. doi:10.1016/j.mib.2012.03.001
86. Scott, J. J.; Oh, D.-C.; Yuceer, M. C.; Klepzig, K. D.; Clardy, J.; Currie, C. R. *Science* **2008,** *322,* 63–65. doi:10.1126/science.1160423
87. Oh, D.-C.; Scott, J. J.; Currie, C. R.; Clardy, J. *Org. Lett.* **2009,** *11,* 633–636. doi:10.1021/ol802709x
88. Cao, S.; Blodgett, J. A. V.; Clardy, J. *Org. Lett.* **2010,** *12,* 4652–4654. doi:10.1021/ol1020064
89. Blodgett, J. A. V.; Oh, D.-C.; Cao, S.; Currie, C. R.; Kolter, R.; Clardy, J. *Proc. Natl. Acad. Sci. U. S. A.* **2010,** *107,* 11692–11697. doi:10.1073/pnas.1001513107
90. Aanen, D. K.; de Fine Licht, H. H.; Debets, A. J. M.; Kerstes, N. A. G.; Hoekstra, R. F.; Boomsma, J. J. *Science* **2009,** *326,* 1103–1106. doi:10.1126/science.1173462
91. Poulsen, M.; Hu, H.; Li, C.; Chen, Z.; Xu, L.; Otani, S.; Nygaard, S.; Nobre, T.; Klaubauf, S.; Schindler, P. M.; Hauser, F.; Pan, H.; Yang, Z.; Sonnenberg, A. S. M.; de Beer, Z. W.; Zhang, Y.; Wingfield, M. J.; Grimmelikhuijzen, C. J. P.; de Vriese, R. P.; Korb, J.; Aanen, D. K.; Wang, J.; Boomsma, J. J.; Zhang, G. *Proc. Natl. Acad. Sci. U. S. A.* **2014,** *111,* 14500–14505. doi:10.1073/pnas.1319718111
92. Visser, A. A.; Nobre, T.; Currie, C. R.; Aanen, D. K.; Poulsen, M. *Microb. Ecol.* **2012,** *63,* 975–985. doi:10.1007/s00248-011-9987-4
93. Um, S.; Fraimout, A.; Sapountzis, P.; Oh, D.-C.; Poulsen, M. *Sci. Rep.* **2013,** *3,* No. 3250. doi:10.1038/srep03250
94. Hou, Y.; Braun, D. R.; Michel, C. R.; Klassen, J. L.; Adnani, N.; Wyche, T. P.; Bugni, T. S. *Anal. Chem.* **2012,** *84,* 4277–4283. doi:10.1021/ac202623g
95. Carr, G.; Poulsen, M.; Klassen, J. L.; Hou, Y.; Wyche, T. P.; Bugni, T. S.; Currie, C. R.; Clardy, J. *Org. Lett.* **2012,** *14,* 2822–2825. doi:10.1021/ol301043p
96. Kim, K. H.; Ramadhar, T. R.; Beemelmanns, C.; Cao, S.; Poulsen, M.; Currie, C. R.; Clardy, J. *Chem. Sci.* **2014,** *5,* 4333–4338. doi:10.1039/C4SC01136H
97. Hopwood, D. A. *Streptomyces in Nature and Medicine: The Antibiotic Makers;* Oxford University Press: New York, USA, 2007.
98. Baltz, R. H. *Curr. Opin. Pharmacol.* **2008,** *8,* 557–563. doi:10.1016/j.coph.2008.04.008
99. Jose, P. A.; Jebakumar, S. R. D. *Front. Microbiol.* **2013,** *4,* No. 240. doi:10.3389/fmicb.2013.00240
100. Poulsen, M.; Oh, D.-C.; Clardy, J.; Currie, C. R. *PLoS One* **2011,** *6,* e16763. doi:10.1371/journal.pone.0016763
101. Oh, D.-C.; Poulsen, M.; Currie, C. R.; Clardy, J. *Org. Lett.* **2011,** *13,* 752–755. doi:10.1021/ol102991d
102. Kim, S.-H.; Ko, H.; Bang, H.-S.; Park, S.-H.; Kim, D.-G.; Kwon, H. C.; Kim, S. Y.; Shin, J.; Oh, D.-C. *Bioorg. Med. Chem. Lett.* **2011,** *21,* 5715–5718. doi:10.1016/j.bmcl.2011.08.023
103. Park, S.-H.; Moon, K.; Bang, H.-S.; Kim, S.-H.; Kim, D.-G.; Oh, K.-B.; Shin, J.; Oh, D.-C. *Org. Lett.* **2012,** *14,* 1258–1261. doi:10.1021/ol300108z
104. Fincher, G. T. *J. Ga. Entomol. Soc.* **1981,** *16,* 316–333.
105. Kang, A. R.; Kim, K.-G.; Park, J. W.; Kim, I. *Entomol. Res.* **2012,** *42,* 247–261. doi:10.1111/j.1748-5967.2012.00470.x
106. Kim, S.-H.; Kwon, S. H.; Park, S.-H.; Lee, J. K.; Bang, H.-S.; Nam, S.-J.; Kwon, H. C.; Shin, J.; Oh, D.-C. *Org. Lett.* **2013,** *15,* 1834–1837. doi:10.1021/ol4004417
107. Um, S.; Park, S. H.; Kim, J.; Park, H. J.; Ko, K.; Bang, H.-S.; Lee, S. K.; Shin, J.; Oh, D.-C. *Org. Lett.* **2015,** *17,* 1272–1275. doi:10.1021/acs.orglett.5b00249
108. Spiteller, P. *Nat. Prod. Rep.* **2015,** *32,* 971–993. doi:10.1039/C4NP00166D
109. Isaka, M.; Kittakoop, P.; Thebtaranonth, Y. Secondary metabolites of clavicipitalean fungi. In *Claviciptialean Fungi: Evolutionary Biology, Chemistry, Biocontrol, and Cultural Impacts;* White, J. F.; Bacon, C. W.; Hywel-Jones, N. L.; Spatafora, J. W., Eds.; Mycology, Vol. 19; CRC Press: New York, 2003; pp 355–397.

110. Isaka, M.; Kittakoop, P.; Kirtikara, K.; Hywel-Jones, N. L.; Thebtaranonth, Y. *Acc. Chem. Res.* **2005,** *38,* 813–823. doi:10.1021/ar040247r
111. Molnár, I.; Gibson, D. M.; Krasnoff, S. B. *Nat. Prod. Rep.* **2010,** *27,* 1241–1275. doi:10.1039/C001459C
112. Nakashima, T.; Lizuka, T.; Ogura, K.; Maeda, M.; Tanaka, T. *J. Fac. Agric., Hokkaido Univ.* **1982,** *61,* 60–72.
113. Nair, M. S. R.; Hervey, A. *Phytochemistry* **1979,** *18,* 326–327. doi:10.1016/0031-9422(79)80085-0
114. Wang, Y.; Mueller, U. G.; Clardy, J. *J. Chem. Ecol.* **1999,** *25,* 935–941. doi:10.1023/A:1020861221126
115. Freinkman, E.; Oh, D.-C.; Scott, J. J.; Currie, C. R.; Clardy, J. *Tetrahedron Lett.* **2009,** *50,* 6834–6837. doi:10.1016/j.tetlet.2009.09.120
116. Wang, L.; Feng, Y.; Tian, J.; Xiang, M.; Sun, J.; Ding, J.; Yin, W.-B.; Stadler, M.; Che, Y.; Liu, X. *ISME J.* **2015,** *9,* 1793–1801. doi:10.1038/ismej.2014.263
117. Kobayashi, C.; Fukasawa, Y.; Hirose, D.; Kato, M. *Evol. Ecol.* **2008,** *22,* 711–722. doi:10.1007/s10682-007-9196-2
118. Zhang, Y. L.; Ge, H. M.; Zhao, W.; Dong, H.; Xu, Q.; Li, S. H.; Li, J.; Zhang, J.; Song, Y. C.; Tan, R. X. *Angew. Chem., Int. Ed.* **2008,** *47,* 5823–5826. doi:10.1002/anie.200801284
119. Zhang, Y. L.; Zhang, J.; Jiang, N.; Lu, Y. H.; Wang, L.; Xu, S. H.; Wang, W.; Zhang, G. F.; Xu, Q.; Ge, H. M.; Ma, J.; Song, Y. C.; Tan, R. X. *J. Am. Chem. Soc.* **2011,** *133,* 5931–5940. doi:10.1021/ja110932p
120. Wu, Q.; Jiang, N.; Han, W. B.; Mei, Y. N.; Ge, H. M.; Guo, Z. K.; Wen, N. S.; Tan, R. X. *Org. Biomol. Chem.* **2014,** *12,* 9405–9412. doi:10.1039/C4OB01494D
121. Liu, C.-X.; Wang, L.; Chen, J.-F.; Guo, Z.-Y.; Tu, X.; Deng, Z.-S.; Zou, K. *Magn. Reson. Chem.* **2015,** *53,* 317–322. doi:10.1002/mrc.4197
122. Nirma, C.; Eparvier, V.; Stien, D. *J. Nat. Prod.* **2015,** *78,* 159–162. doi:10.1021/np500080m
123. Rohlfs, M.; Churchill, A. C. L. *Fungal Genet. Biol.* **2011,** *48,* 23–34. doi:10.1016/j.fgb.2010.08.008
124. Gibson, D. M.; Donzelli, B. G. G.; Krasnoff, S. B.; Keyhani, N. O. *Nat. Prod. Rep.* **2014,** *31,* 1287–1305. doi:10.1039/C4NP00054D
125. Hajek, A. E.; Wraight, S. P.; Vanderberg, J. D. Control of arthropods using pathogenic fungi. In *Bioexploitation of filamentous fungi;* Pointing, S. B.; Hyde, K. D., Eds.; Fungal Diversity Research, Vol. 6; Fungal Diversity Press: Hong Kong, 2001; pp 309–347.
126. Hajek, A. E.; McManus, M. L.; Delalibera Júnior, I. *BioControl* **2007,** *41,* 1–13. doi:10.1016/j.biocontrol.2006.11.003
127. Li, Z.; Alves, S. B.; Roberts, D. W.; Fan, M.; Delalibera Júnior, I.; Tang, J.; Lopes, R. B.; Faria, M.; Rangel, D. E. N. *Biocontrol Sci. Technol.* **2010,** *20,* 117–136. doi:10.1080/09583150903431665
128. Pedras, M. S. C.; Zaharia, L. I.; Ward, D. E. *Phytochemistry* **2002,** *59,* 579–596. doi:10.1016/S0031-9422(02)00016-X
129. Krasnoff, S. B.; Keresztes, I.; Gillilan, R. E.; Szebenyi, D. M.; Donzelli, B. G. G.; Churchill, A. C. L.; Gibson, D. M. *J. Nat. Prod.* **2007,** *70,* 1919–1924. doi:10.1021/np070407i
130. Wang, Q.; Xu, L. *Molecules* **2012,** *17,* 2367–2377. doi:10.3390/molecules17032367
131. Vining, L. C.; Kelleher, W. J.; Schwarting, A. E. *Can. J. Microbiol.* **1962,** *8,* 931–933. doi:10.1139/m62-122
132. Brewer, D.; Jen, W.-C.; Jones, G. A.; Taylor, A. *Can. J. Microbiol.* **1984,** *30,* 1068–1072. doi:10.1139/m84-166
133. Terry, B. J.; Liu, W.-C.; Cianci, C. W.; Proszynski, E.; Fernandes, P.; Bush, K.; Meyers, E. *J. Antibiot.* **1992,** *45,* 286–288. doi:10.7164/antibiotics.45.286
134. Nagaoka, T.; Nakata, K.; Kouno, K.; Ando, T. *Z. Naturforsch., C* **2004,** *59,* 302–304.
135. Amin, G. A.; Youssef, N. A.; Bazaid, S.; Saleh, W. D. *World J. Microbiol. Biotechnol.* **2010,** *26,* 2263–2268. doi:10.1007/s11274-010-0416-5
136. Feng, P.; Shang, Y.; Cen, K.; Wang, C. *Proc. Natl. Acad. Sci. U. S. A.* **2015,** *112,* 11365–11370. doi:10.1073/pnas.1503200112
137. Boomsma, J. J.; Jensen, A. B.; Meyling, N. V.; Eilenberg, J. *Annu. Rev. Entomol.* **2014,** *59,* 467–485. doi:10.1146/annurev-ento-011613-162054
138. Esquenazi, E.; Yang, Y.-L.; Watrous, J.; Gerwick, W. H.; Dorrestein, P. C. *Nat. Prod. Rep.* **2009,** *26,* 1521–1534. doi:10.1039/B915674G
139. Luzzatto-Knaan, T.; Melnik, A. V.; Dorrestein, P. C. *Analyst* **2015,** *140,* 4949–4966. doi:10.1039/C5AN00171D

License and Terms

BEILSTEIN JOURNAL OF ORGANIC CHEMISTRY

Dynamic behavior of rearranging carbocations – implications for terpene biosynthesis

Stephanie R. Hare and Dean J. Tantillo*

Review

Open Access

Address:
Department of Chemistry, University of California–Davis, 1 Shields Avenue, Davis, CA 95616, USA

Email:
Dean J. Tantillo* - djtantillo@chem.ucdavis.edu

* Corresponding author

Keywords:
carbocation; density functional theory; dynamics; mechanism; terpene

Beilstein J. Org. Chem. **2016,** *12,* 377–390.
doi:10.3762/bjoc.12.41

Received: 21 December 2015
Accepted: 15 February 2016
Published: 29 February 2016

This article is part of the Thematic Series "Natural products in synthesis and biosynthesis II".

Guest Editor: J. S. Dickschat

Abstract

This review describes unexpected dynamical behaviors of rearranging carbocations and the modern computational methods used to elucidate these aspects of reaction mechanisms. Unique potential energy surface topologies associated with these rearrangements have been discovered in recent years that are not only of fundamental interest, but also provide insight into the way Nature manipulates chemical space to accomplish specific chemical transformations. Cautions for analyzing both experimental and theoretical data on carbocation rearrangements are included throughout.

Review

Introduction to terpene forming carbocation rearrangements

Terpene natural products display a striking range of molecular architectures, varying in size and complexity (Figure 1) [1-5]. Some terpenes sport multiple stereogenic centers and multiple carbocyclic rings. These complex hydrocarbon frameworks are derived, however, from simple precursors lacking stereogenic centers and rings that are transformed in only one or two enzyme-promoted reactions. These reactions involve generation of a carbocation by protonation or loss of a diphosphate group followed by cyclization, alkyl shift, hydride shift and/or proton transfer reactions to generate new, more complex, carbocations. Ultimately these carbocations are either trapped by a nucleophile (e.g., water, diphosphate) or deprotonated to form alkenes.

The details of terpene-forming carbocation cyclization/rearrangement processes have been of interest for decades [1-6]. Although much has been learned, new observations continue to surprise researchers in the natural products field. For instance, recent computational/theoretical studies have focused on the inherent dynamical behavior of carbocations involved in these reactions – the subject of this review article. These studies have

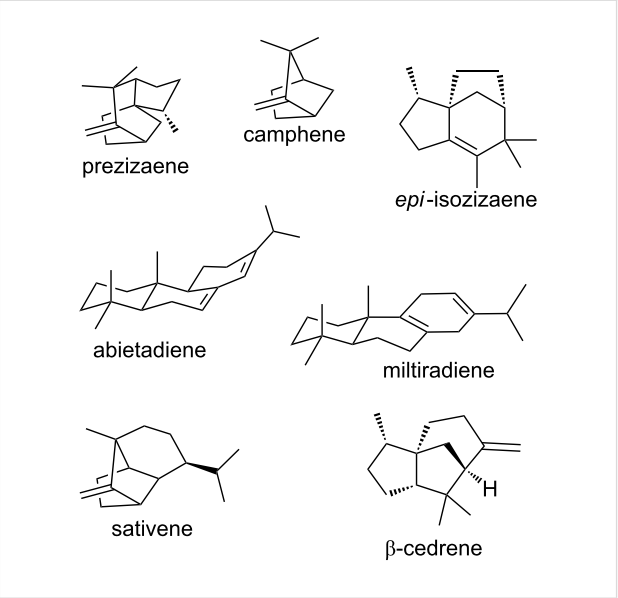

Figure 1: Representative terpenes.

revealed that inherent dynamical tendencies, i.e., the dynamical behavior of carbocations in the absence of an enzyme, tend to be reflected in product distributions for enzyme-promoted reactions. Consequently, the problem of elucidating the role of terpene synthase enzymes in terpene formation has been redefined. In addition, these studies have pointed to the possibility that inherent dynamical tendencies of reactive intermediates may play important roles in enzyme evolution.

Here we review key studies on the dynamical behavior of carbocations. First we provide an introduction to dynamical behavior and how it is examined using modern theoretical tools. Then we describe studies dealing with carbocations that are not involved in terpene formation, but which reveal reactivity principles that may have implications for terpene biosynthesis. This is followed by descriptions of the relatively few studies published so far that are concerned with dynamical behavior of carbocations involved in terpene-forming reactions. In each section, we highlight important take home messages.

Dynamical behavior – a brief tutorial

The reactivity of a molecule often ties back to a single characteristic: its energy (in particular, its free energy). Computational and synthetic chemists are most often interested in potential energy because selective conversion of the potential energy associated with chemical bonds is the basis of chemical reaction design. The surface representing how the potential energy of a molecule is affected by geometrical (and subsequently electronic) changes is called (unsurprisingly) the molecule's potential energy surface (PES). Technically, there are $3N$ dimensions in which geometrical changes can occur, where N is the number of atoms in the molecule each moving in 3 dimensions. When all N atoms move in the x, y, or z directions, the molecule is translating. Similarly, if all N atoms are rotating along the x, y, or z axes, the entire molecule is rotating. This leaves $3N - 6$, or $3N - 5$ if a molecule is linear, vibrational degrees of freedom that contribute to the molecule's internal energy. Being able to visualize how each of these changes affects the energy of the molecule would require the ability to visualize $(3N - 6) + 1$-dimensional space. However, $(3N - 6) + 1$ dimensions can be reduced to two dimensions by looking only at the minimum energy pathway (MEP) between two minima on the PES, which is also referred to as the intrinsic reaction coordinate (IRC; Figure 2, left) [7,8]. It is the IRC that is typically used to make arguments for reactivity observed experimentally.

The IRC contains a wealth of information about the behavior of a particular system, but not all chemical phenomena can be explained by analyzing this pathway alone. The most common characteristic of an IRC that is used to make arguments for relative reaction rates leading to chemo-, regio-, or stereoselectivity of a reaction is the energy difference between the reactant and the relevant transition state structure (TSS) along the IRC. Traditional static approaches, transition state theories (TSTs) [9-13] and the Rice–Ramsperger–Kassel–Marcus theory (RRKM) [14-17], that relate activation barriers to reaction rates rely on the assumption that the molecule will follow the IRC at all times during a chemical reaction (sometimes referred to as "quasi-equilibrium conditions"). Importantly, this pathway lies on the PES and thus neglects the kinetic energy of the system. Kinetic energy becomes particularly important when the PES topology exhibits certain features that can make the system deviate from the IRC, such as: (1) when a reaction pathway involves a shallow intermediate (particularly when the preceding TSS is high in energy) and (2) when a single TSS leads directly to multiple minima, sometimes called an "ambimodal" TSS [18], without intervening minima; this scenario is referred to as a pathway with one or more post-transition state bifurcations (PTSB) [19-26]. For a detailed discussion of unique PES features that lead to deviations from IRC behavior, see Birney's review on PESs of pericyclic and pseudopericyclic reactions [27].

These two scenarios are visualized by way of an analogy in Figure 3. First, consider scenario (1). Imagine a snowboarder riding down a mountain. If the mountain is very tall and there is a mogul on the way to the bottom (Figure 3, right), the snowboarder is more able to easily pass the small hill than if he or she started from the base of the mogul. At the molecular level, this scenario can result in bypassed intermediates, i.e., an IRC having a minimum calculated along the pathway to the product, but with a lifetime that is not long enough to allow for equili-

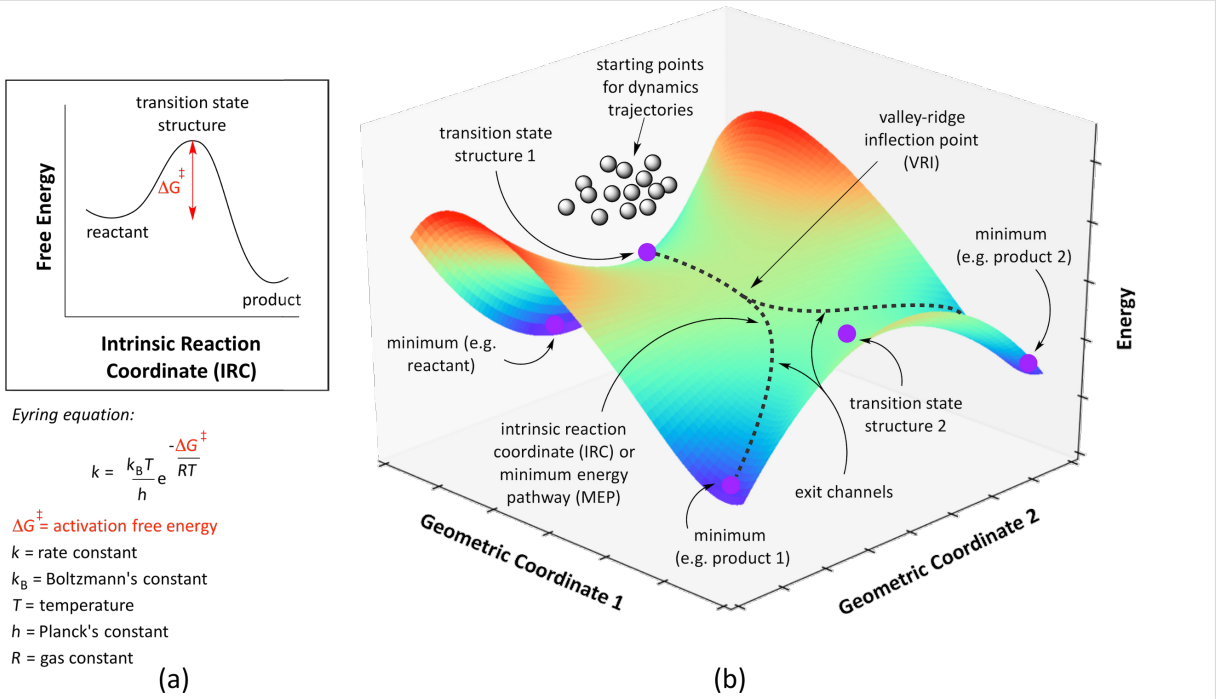

Figure 2: Two different models showing how energy evolves throughout the course of a reaction: (a) a two-dimensional plot, where the reactant follows a single path through the TSS to the product at a rate governed by the Eyring equation [9] and (b) a three-dimensional hypothetical PES exhibiting the features of a PTSB and a qualitative representation of the starting points for dynamics trajectories. The function $z = 2x^5 - 5x^2 - 5xy + y^2 + 2$ was used to generate this hypothetical surface.

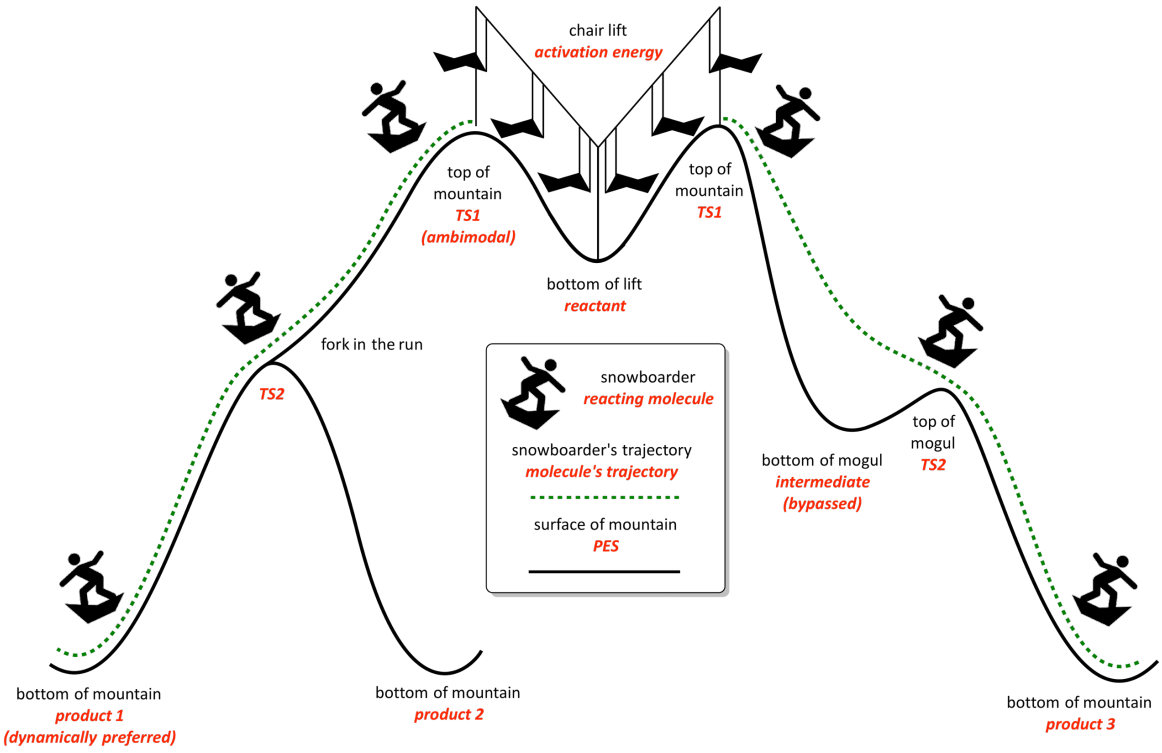

Figure 3: A depiction of the "snowboarder" analogy for reactions displaying non-statistical dynamic effects. Features of a PES that correspond to features found on the slopes are highlighted in red. This figure illustrates two independent phenomena: Left: formation of a preferred product following an ambimodal TSS due to dynamic matching. Right: an intermediate that is rapidly passed through or bypassed as a result of dynamic matching.

bration; some pathways/trajectories will also skirt past the deepest parts of the energy well. Additionally, if the initial path down the mountain splits into two paths to the bottom of the mountain (i.e., at the molecular level, having an ambimodal TSS; Figure 3, left), it will be easier for the snowboarder to take the path that requires fewer changes in direction, unless he or she is leaning heavily toward the other path. In both scenarios, where the snowboarder (molecule) came from and how it was behaving (vibrating) on its way to the shallow valley (minimum) or fork in the path (PTSB) influences the path ultimately taken and the time associated with doing so. This concept, at the molecular level, is referred to as "dynamic matching" [28]. Molecules similarly retain momentum within particular vibrational modes if the timescale of the reaction is too short for the molecule's kinetic energy to be distributed statistically throughout all vibrational modes. Reactions that undergo generation of reactive intermediates often meet this criterion and exhibit what are called "non-statistical dynamic effects", that is, product distributions that cannot be rationalized by traditional TST [19,29,30]. These effects (highlighted through the examples discussed below) are typically described using classical mechanics (i.e., solving either Newton's or Hamilton's classical equations of motion to propagate nuclear positions), but there have been cases reported where *quantum* dynamic effects have been found to be important, particularly when tunneling effects contribute significantly to the reaction rate [31-34].

To acquire evidence for non-statistical dynamic effects, molecular dynamics (MD) simulations are run for a statistically relevant number of trajectories (typically on the order of hundreds or thousands, depending on the system and the starting point for trajectories) [35,36]. The most common modern technique for computing dynamics trajectories for organic reactions is the method of direct dynamics. With direct dynamics, instead of solving for a PES analytically, each point along a trajectory is calculated numerically "as needed" or "on-the-fly". A quantum chemical program capable of ab initio or density functional theory (DFT) calculations is used to calculate either (1) force constants (via frequency calculation) along the trajectory, either at every point or in periodic increments, or (2) the gradient of the potential energy, depending on the specific integrator chosen to integrate the equations of motion. The calculation of gradients rather than force constants is significantly faster, but requires a smaller time step to achieve the same calculation accuracy. The calculations are run under the Born–Oppenheimer Approximation, which is why they are also called Born–Oppenheimer Molecular Dynamics (BOMD) calculations, so that nuclear motion and electronic structure are calculated separately, the former propagated classically and the latter determined using quantum mechanics.

As with any computational (or experimental) study, there will always be a tradeoff between sampling a sufficient amount of the relevant chemical space and completing the study in a reasonable amount of time. Different strategies can be used to achieve a compromise between these factors, depending on the size of the system of interest and the accuracy required to answer the relevant chemical questions. MD simulations have been employed to answer two different questions about the chemical reactions discussed below: (1) what mechanism(s) is energetically viable? and (2) do (non-statistical) dynamic effects exert control over product distributions? While trajectories can be started from anywhere on a PES, it is most common to initiate trajectories either from a structure that is a minimum (usually the reactant for the reaction of interest) – used when exploring possible mechanisms – or a TSS – used when assessing the impact of dynamic effects for a particular mechanism. In both cases, each atom in the molecule is given a random initial velocity and each vibrational mode is displaced a random distance, such that the total kinetic and potential energy of the molecule is equal to the amount of energy available at the specified temperature. The problem with initiating trajectories from a minimum, however, is that there is no guarantee the trajectories are going to be "productive". This creates an operational problem in most cases because, relative to the optimization of stationary points on a PES, MD trajectories are very computationally expensive, a result of having to repeatedly calculate force constants. For a 1 ps long direct dynamics trajectory with a time step of 1 fs where force constants are calculated at each point, the nuclear and electronic structure of the molecule will need to be recalculated a total of 1000 times, which equates to a great deal of computer time, even in 2016. There is a (somewhat controversial) method to facilitate barrier crossing in which a "biased potential" is employed to "push" a reactant up and toward the barrier of interest in an MD simulation [37-39]. The controversy arises from the question of whether such a biased method leads to biased results, so using a biased method requires testing against unbiased methods and/or experimental data to ensure accuracy. The complication of having unproductive trajectories is mitigated when initiating trajectories from a transition state, but of course this leads to the most biased strategy of all because a pre-determined TSS is the starting point for such a calculation. This strategy cannot be used to explore a large variety of possible mechanisms, but is effective for determining the magnitude of dynamic effects associated with falling downhill from a particular TSS. Therefore, one can make the assumption that the system always passes through the transition state region when only "reactive" trajectories are of interest. Notably, this makes the assumption that quasi-equilibrium conditions are followed up until the transition state region. For most systems, this is a reasonable assumption, but careful consideration of any chemical steps in the reac-

tion preceding the transition state from which trajectories are initiated should be made, since any dynamical effects preceding the transition state would be neglected and would have to be treated separately if of interest. Studies involving trajectories initiated from minima and transition states have both been carried out on carbocations [25] and examples of each are described below. While many different quantum chemical methods can be used to carry out trajectory calculations, standard density functional theory (DFT) approaches are most commonly used [35-40]. In particular, the B3LYP and mPW1PW91 functionals, along with small to medium sized basis sets have seen the most use in studying carbocation rearrangements of relevance to biosynthesis [6].

Using molecular dynamics trajectories to rationalize experimental results is still not standard practice, but the potential for the utility of dynamics simulations in a variety of systems has certainly been demonstrated. The studies detailed below primarily highlight situations where molecular dynamics simulations were used to quantify "non-IRC" behavior, but the value of dynamics simulations does not stop there. For example, Bogle and Singleton used dynamics trajectories to gather evidence for whether the tetramethylbromonium ion existed as a single C_{2v}-symmetric bridged structure or rapidly interconverted between two β-bromocarbenium ion structures (Figure 4) [41]. Experimental evidence for which of these two types of scenarios is present is generally obtained using the "isotopic perturbation" method pioneered by Saunders [42-44]. In this method, isotopic labels are added (e.g., L = D in Figure 4) and NMR spectra are acquired. The ^{13}C NMR spectrum of the resultant system would be expected to exhibit a large difference in signals (Δ) between carbons with H versus D substituents, whereas essentially no difference in signals between carbons would be expected if there was no equilibrium to affect. Ohta et al. [45] experimentally determined a large Δ (3.61 ppm) for the system shown in Figure 4, concluding that the two β-bromocarbenium ion structures interconvert in solution. However, by running dynamics simulations on the system and calculating NMR chemical shifts at each point, Bogle and Singleton were able to gather evidence that this effect instead can be attributed to geometrical changes of a bridged ion resulting from the isotopic substitution. They concluded that it cannot be assumed that a large Δ resulting from isotopic labeling guarantees rapid equilibration between two unlabeled structures. While the cases described below are focused on reaction pathways, similar cautions on interpretation are presented throughout. We hope these cautions will encourage a healthy skepticism in the interpretation of all data, experimental and computational alike.

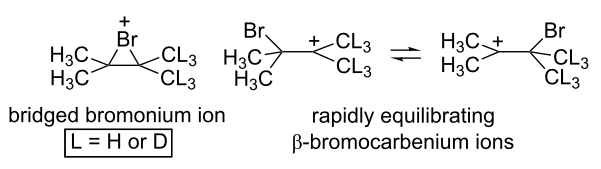

Figure 4: The tetramethylbromonium ion system [14].

Take home messages:

• A PES can reveal important information about a system, but complicating features on some PESs make analyses using traditional TST incomplete.

• Two common examples of these complicating features are (1) highly exergonic steps leading to bypassed intermediates and (2) PTSBs.

• Molecular dynamics simulations can be used in these contexts to provide evidence for the pathways that are accessible to the molecular system given a particular amount of initial kinetic energy. These simulations can be initiated from the region of the reactant or TSS, but which is appropriate for a specific case depends on the nature of the chemical questions to be answered.

Non-biological carbocation rearrangements

Generation of carbocations via protonated alcohols – the concerted vs stepwise spectrum

The seminal work of Dupuis and co-workers in running dynamics simulations to elucidate the nature of the dehydration-rearrangement mechanism of protonated pinacolyl alcohol (Figure 5, R = CH_3) was instrumental in bringing the issue of dynamic effects to a wide audience [46]. The question addressed in this work was ostensibly simple: is the mechanism of dehydration/alkyl migration of a protonated alcohol a concerted or stepwise process? The IRC for the process revealed a concerted mechanism (Figure 5, blue), with no secondary carbocation found as a stationary point on the PES. However, molecular dynamics simulations initiated from the reactant revealed trajectories that predominantly followed a stepwise mechanism (Figure 5, green), with a lifetime of the secondary carbocation of up to 4000 fs. This is the opposite of the situation illustrated on the right side of Figure 3; instead of an intermediate structure being rapidly bypassed due to dynamic effects, the reacting molecule gets stuck in a region of the PES where there is no minimum. In total, 50 trajectories were run where, after 500 fs, 20 trajectories went to the secondary carbocation, only one trajectory went directly to the rearranged product (concerted mechanism), and one remained in the secondary carbocation region before eventually affording the rearranged product. The remaining 28 trajectories remained in the reactant region, illustrating the complication associated with

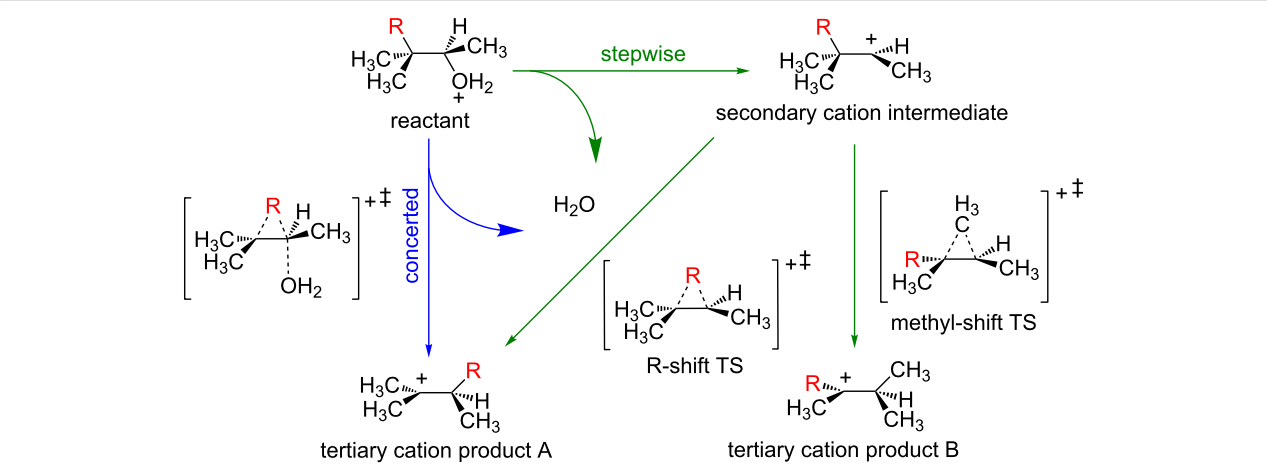

Figure 5: The reaction mechanisms of interest in the PES and dynamics studies of Dupuis and co-workers (R = CH_3) and de Souza et al. (R = CH_3, Et, iPr). Note: in the case of R = CH_3, tertiary cation products A and B are equivalent. Adapted from Dupuis and co-workers and de Souza et al. [46,55].

initiating dynamics trajectories from a minimum on the PES mentioned above. Though this number of productive trajectories would not be considered sufficient to make definitive conclusions regarding the experimental behavior of this system (especially given the computational power available today), this study paved the way for future dynamics studies and correctly predicted that "similar findings will arise for many other reactions … and interpretation of reaction mechanisms ought to consider the effects of dynamics explicitly" [46]. In light of more recent studies (e.g., see below), the results just described could be anticipated. The IRC for the dehydration-rearrangement reaction actually proceeds through the region where the secondary carbocation resides, even though this structure is not a PES minimum. The curvature of the IRC in this region would likely have indicated the presence of a "hidden intermediate" [47-51], i.e., a structure along the IRC that is not a minimum but is associated with an energy plateau and may have a substantial lifetime. Such IRCs have subsequently been observed for many reactions for which secondary carbocations are putative intermediates [52-54].

More recently, de Souza et al. revisited these systems and conducted a study looking at the rearrangement behavior of a series of protonated alcohols using TST, a "static" approach, and a slightly different variation of molecular dynamics simulations compared to that used by Dupuis and co-workers [55]. Additionally, replacing R in Figure 5 with a non-methyl substituent opened up the possibility of the formation of two different products resulting from migration of different alkyl groups (tertiary carbocation products A and B in Figure 5). While these differences led to results that were quantitatively different from those described in the Dupuis study, they were qualitatively the same and led the authors to essentially the same conclusions. The authors emphasized that, in reality, all mechanisms are on a spectrum, where "concerted" and "stepwise" define limiting cases, in line with previous descriptions of carbocation reactions as existing on a "continuum" [56,57]. In the case of the dehydration-rearrangements of protonated alcohols, the most intense "band" in the spectrum of possible reaction types involves the formation of a secondary carbocation structure prior to formation of the rearranged product, as revealed by molecular dynamics simulations.

Take home messages:

• *Dynamics simulations can reveal behavior not readily apparent in IRC calculations* [58].

• *The terms "concerted" and "stepwise" define the limiting cases of a spectrum/continuum of mechanistic possibilities.*

Norborn-2-en-7-ylmethyl cation – memory effects

Dynamic effects are often suspected when a stereochemical result is observed experimentally that is inconsistent with a proposed mechanism, despite other evidence supporting the proposed mechanism. For example, Berson et al. discovered that solvolysis of *syn*- and *anti*-norborn-2-en-7-ylmethyl-X diastereomers ($\mathbf{I_s}$ and $\mathbf{I_a}$, Figure 6; X is a leaving group) both led to the same two products, but in different ratios, despite sharing a common intermediate (in different conformations; **V**, Figure 6) [59]. The major product generated from the solvolysis of $\mathbf{I_a}$ was the acetate of carbocation **L**, with a small amount of the acetate of carbocation **G** also observed. Solvolysis of $\mathbf{I_s}$ also led to the acetate of carbocation **L**, but this time accompanied by a significant amount of the acetate of carbocation **G**. This difference in product distribution (whose magnitude varied with leaving

group identity) was ascribed to a "memory effect". Put simply, product ratios were skewed from what would be expected by simply comparing activation barriers, because the reacting molecule "remembers" the conformation from which it came; this is a hallmark of dynamic matching. Additionally, the memory effect can be decreased by "leakage" when one conformation of the common intermediate rapidly converts to the other conformation (essentially the equilibration expected for a reaction not displaying non-statistical dynamic effects).

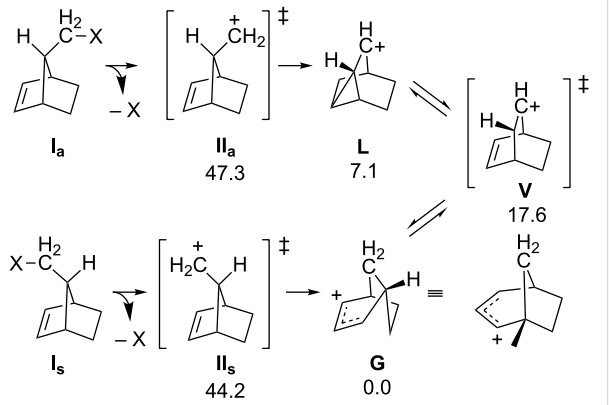

Figure 6: The portion of the norborn-2-en-7-ylmethyl cation PES examined by Ghigo et al. [60]. Energies reported are electronic energies, including zero-point corrections (ZPE), at the B3LYP/6-31G(d) level of theory and are all relative to that of **G** [61-63].

Ghigo et al. set out to explore the memory effect phenomenon computationally [60]. The relevant PES for this transformation (key points shown in Figure 6) was examined using several DFT methods. The portion of the PES prior to formation of TSSs $\mathbf{II_a}$ and $\mathbf{II_s}$ was also explored, but it was assumed that all structures were required to go through TSSs $\mathbf{II_a}$ and $\mathbf{II_s}$ in order to make the products; consequently, dynamics trajectories were initiated from the regions of these TSSs (using a lower level of theory so that 250 trajectories from each transition state could be obtained in a reasonable amount of time; the influence of the leaving group on dynamical behavior was not explored). The results from the dynamics simulations were in qualitative agreement with the experimental results: trajectories initiated from $\mathbf{II_s}$ generated almost equal amounts of cations **G** and **L**, while trajectories initiated from $\mathbf{II_a}$ go predominantly to cation **L**.

Take home message:

- *"Memory effects" can result from dynamic matching.*

2-Norbornyl and other highly delocalized cations – a caution on complexity

When exploring carbocation rearrangement mechanisms using MD simulations, one should remember that MD simulations are inherently statistical. That is, there are times when a systematic approach to exploring mechanistic pathways is preferable to MD simulations, which use random sampling techniques. This point is illustrated by two studies on the isomerization of the infamous 2-norbornyl cation to the 1,3-dimethylcyclopentenyl cation ($DMCP^+$) (Figure 7) [64,65].

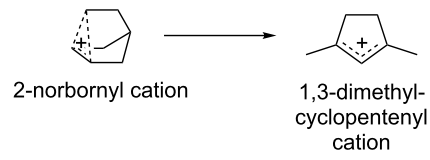

Figure 7: The transformation of 2-norbornyl cation to 1,3-dimethylcyclopentyl cation.

After an attempt by Mosley et al. to study the experimental IR spectrum of the 2-norbornyl cation in the gas phase revealed a structural rearrangement to $DMCP^+$, Jalife et al. set out to determine the isomerization mechanism using modern computational methods [64]. BOMD simulations using DFT were employed, with trajectories initiated from the equilibrium geometry of the 2-norbornyl cation (i.e., the reactant structure) with random velocities assigned to all atoms. When a trajectory formed $DMCP^+$, key points on the PES for the pathway observed in that trajectory were optimized. Two complex pathways to $DMCP^+$ were found that had energy barriers that were reasonable given the experimental conditions used for generation of the 2-norbornyl cation. Both pathways involve a retro-Lawton–Bartlett "π-route" norbornyl ring-opening process [66,67]. The shorter mechanism was found to involve nine discrete chemical steps and had an overall predicted activation barrier of 33 kcal/mol, while the longer pathway involved 16 steps with an overall barrier of 37 kcal/mol. Similar results have been obtained for other complex carbocations: the same group used molecular dynamics to explore the homocubyl cation's rearrangement behavior [68], and East et al. used "rising-temperature" molecular dynamics to determine the carbocation branching behavior of molecules relevant to petroleum chemistry [69-71].

Lobb also attempted to answer the same mechanistic question using a different strategy [65]. Instead of using BOMD simulations to explore possible pathways, Lobb wanted to "systematize" the mechanistic search to explore all possible isomerization pathways and predict their barriers. Lobb used simple algebraic tools, similar to a strategy employed by Johnson and others [72-76], to systematically generate a vast set of possible isomers of $C_7H_{11}^+$ and rank them by their energies (calculated with DFT) [65,77]. The connectivity of each of the generated molecules was examined for isomorphism, ultimately leading to

a set of 1254 distinct groups of isomers involved in possible rearrangements. This number is only an estimation of the full set of isomers, however, due to limitations of the automated methods. $DMCP^+$ was found to be the global minimum for this set of isomers, consistent with experimental results [77]. The mechanistic pathways between isomers were explored by optimizing putative TSSs corresponding to breaking of each bond within a ring (if the molecule contains one) and hydride shifts. The 4500 unique TSSs optimized were then connected to the isomers they interconvert, connecting 1179 out of the 1254 carbocation isomers, to generate various pathways that led to the final product. A huge number of possible pathways were found, the shortest of which are summarized in Table 1.

Table 1: The number of pathways found by Lobb corresponding to a certain number of steps in the mechanism and the lowest overall activation barrier necessary for a pathway with that number of steps [65].

Number of steps	Number of paths	Lowest activation barrier (kcal/mol)
2	1	110.7
3	14	54.7
4	406	31.0
5	8460	29.3
6	171050	27.4

Though the MD strategy used by Jalife et al. uncovered two reasonable mechanistic pathways, the systematic approach taken by Lobb revealed 5 orders of magnitude more pathways that were shorter than those proposed by Jalife, many of which had a lower overall activation barrier, any number of which could be operative in the rearrangements of the 2-norbornyl cation to $DMCP^+$. While a systematic search of all possible isomerization pathways should always be considered for carbocation rearrangements, it is often unnecessary (and prohibitively time-consuming) in the case of carbocation rearrangements that occur in Nature. Thankfully, enzyme-catalyzed carbocation rearrangements are often subject to conformational constraints that make analysis of the possible rearrangement pathways more tractable. Further discussion of enzymatic carbocation rearrangements is found below.

Take home messages:

• Sometimes there are many, many pathways that are energetically viable for the isomerization of a carbocation.

• In some cases, a systematic, rather than statistical, approach to determining all possible isomerization pathways is necessary to ensure that all energetically viable pathways have been explored.

• There is no "one-size-fits-all" strategy to "determine" a reaction mechanism using computations; however, coupled examination of PESs and simulations of dynamic effects can provide nearly (one hopes) exhaustive pictures of the transformation of reactants to products.

Carbocation rearrangements that lead to terpenes

Camphene, sativene and prezizaene – lifetimes and electrostatic effects

Portions of the $C_{10}H_{17}^+$ and $C_{15}H_{25}^+$ PESs (in the absence of enzyme) relevant to the formation of camphene [21,22,78], sativene [79] and prezizaene [54,80] (and related terpenes) were examined in detail using several DFT methods. For each of these systems, secondary carbocations were found along reaction coordinates, but they were not minima; rather, these structures resided in regions near to TSSs for concerted reactions involving the merging, asynchronously, of alkyl shift and/or cyclization events (Figure 8, red) [56,57]. Direct dynamics trajectory calculations were run on each of these systems, with trajectories initiated near the TSSs, i.e., the secondary carbocations. Trajectories (>100 for each system) were run in both forward and reverse directions. Based on the results of these calculations, average lifetimes for the secondary cations were found to range between 35 and 100 fs (with standard deviations between 10 and 35 fs), a time window on the same order as that for a single bond stretch. This lifetime could be increased significantly (by a factor of 2–3 for the bornyl cation, based on the preliminary calculations described) if the secondary carbocation engages in noncovalent interactions with electron rich groups (e.g., C–H···X hydrogen bonds [81]), thereby increasing the probability of trapping these species by deprotonation or addition of a nucleophile. Although some secondary carbocations have been found as minima in terpene-forming carbocation cyclization/rearrangement reactions [57], most are found near TSSs along reaction coordinates and therefore, as this study showed, can be expected to have exceedingly brief lifetimes in the absence of specifically oriented noncovalent interactions with groups in terpene synthase active sites. Molecular dynamics calculations using the full bornyl diphosphate synthase enzyme were also carried out (here using a combination of DFT and molecular mechanics) [21,22]. These simulations indicated that the bornyl cation also has a short lifetime in the active site of the enzyme, but one – 185 fs on average – that is longer (by approximately a factor of 4) than in the absence of the enzyme and complexed diphosphate.

Take home messages:

• Secondary carbocations, which often correspond to structures in the vicinity of transition states, tend to have short

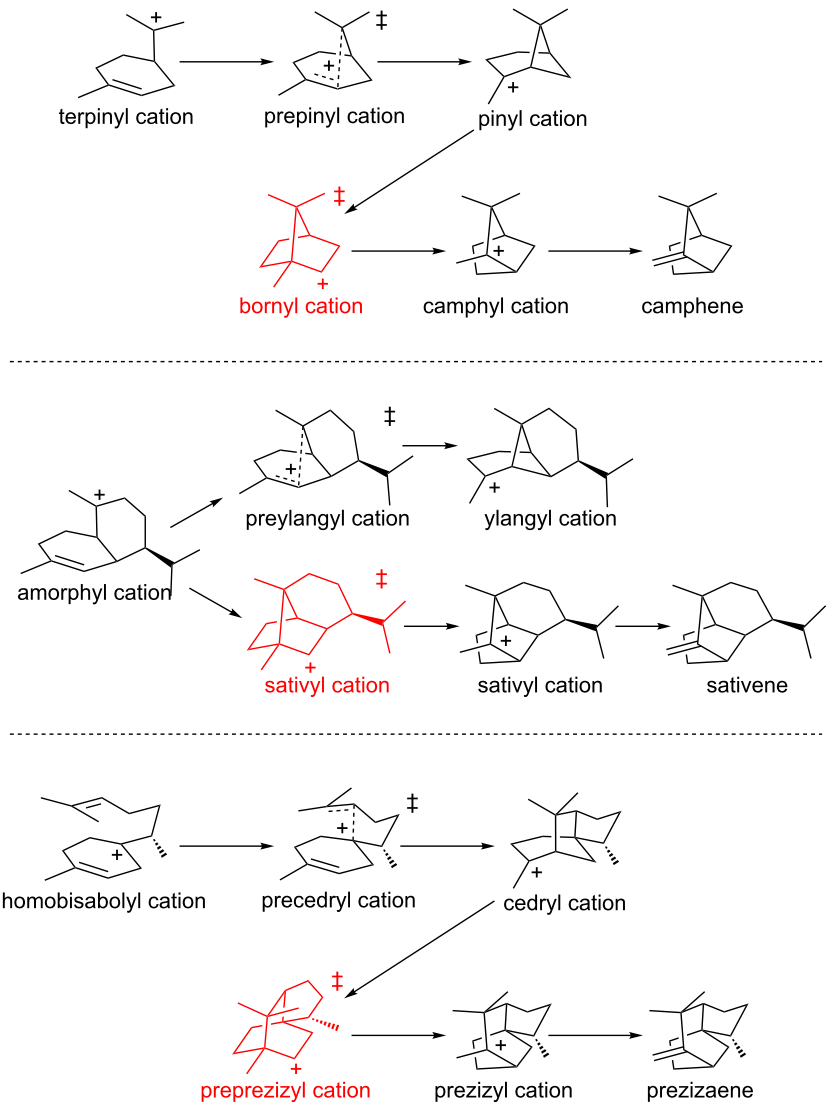

Figure 8: Carbocation rearrangements for which trajectory calculations were used to estimate lifetimes of secondary carbocations.

lifetimes, on the order of the period of a single-bond stretching vibration.

• *These lifetimes can be increased via noncovalent interactions with electron-rich groups.*

Abietadiene – navigating past forks in the road

Pathways to abietadiene [82-90] have also been examined computationally [91-93]. First, the portion of the $C_{20}H_{33}^{+}$ PES corresponding to the reactions depicted in Figure 9 was examined with several DFT methods [91]. This study revealed, quite unexpectedly, that intramolecular proton transfer in the pimar-15-en-8-yl cation can lead to a PTSB – one branch of which leads to the carbocation precursor to abietadiene (Figure 9, green), but the other branch of which leads to a rearranged skeleton, not yet reported for any diterpenes/diterpenoids from Nature (Figure 9, red). Interconversion of these two carbocations proceeds via a TSS that resembles the secondary carbocation expected to be formed upon proton translocation (Figure 9, purple), i.e., the secondary carbocation again corresponds to a TSS rather than a minimum. Direct dynamics trajectories were run from the 1,5-proton transfer transition state region, using both small model carbocations and full-sized structures and using several theoretical methods [92,93], and a ratio of trajectories leading to the abietadiene precursor versus the rearranged carbocation of 1.1–1.7:1 was found. These results first indicate that there is an inherent dynamical tendency built into the substrate (an enzyme was not present during the simula-

tions) for formation of the observed natural product. Second, these results indicate that the inherent dynamical preference is not large enough to rationalize why abietadiene synthase produces 95% abietadiene (and simple diene isomers) [87], setting the stage for future studies aimed at elucidating the means by which abietadiene synthase steers its reaction away from rearrangement and at engineering abietadiene synthase so that it selectively forms rearranged products.

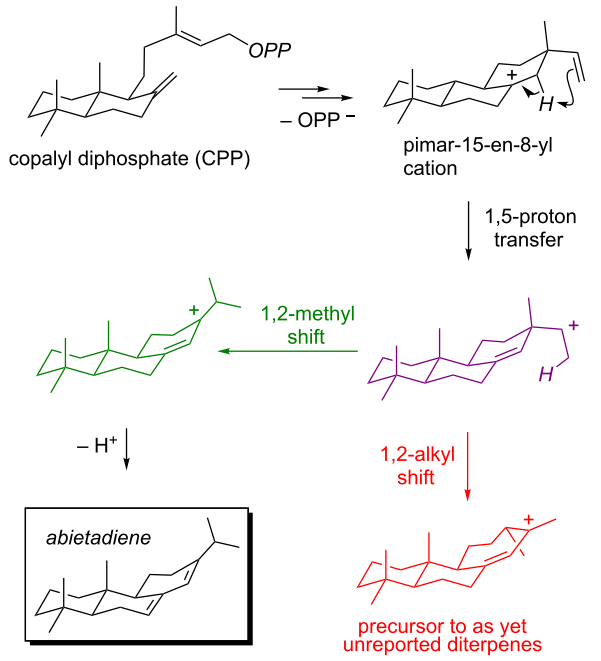

Figure 9: Carbocation rearrangements involved in abietadiene formation.

Take home messages:

• *PTSBs can occur in biosynthetically-relevant carbocation rearrangements.*

• *There is an inherent dynamical tendency of the carbocations involved in abietadiene formation to form abietadiene, even in the absence of an enzyme.*

• *There is also an inherent dynamical tendency of the carbocations involved in abietadiene formation to form a rearranged product, that has not yet been observed in Nature, in a similar magnitude.*

• *Direct enzymatic intervention is likely necessary to overcome the latter tendency, although the nature of this intervention has not yet been characterized.*

Miltiradiene – multiple sesquential bifurcations and testable predictions

The PES associated with formation of miltiradiene (Figure 10) [94], interrogated with a variety of DFT methods, was also found to involve a PTSB following a proton transfer TSS [26]. Surprisingly, however, this bifurcation was associated with a complex PES with flat regions and multiple additional sequential bifurcations. As a result, direct pathways from the 1,6-proton transfer TSS to eight products, without the intermediacy of any PES minima, were found. This is an unusual reactivity problem for an enzyme to tackle! How is one carbon skeleton obtained in high yield when barrierless pathways to eight different skeletons emanate from the same TSS? Direct dynamics trajectory calculations were again applied, with trajectories initiated in the region of the 1,6-proton transfer TSS (specifically for proton transfer to the *re* face of the C=C double bond) [95]. Although pathways to many products exist on the PES, only two products were formed to any appreciable extent in the dynamics calculations – the carbocation precursor to miltiradiene (Figure 10, green) and, similar to the scenario described above for abietadiene, a rearranged carbocation with a skeleton not yet reported in any natural products (Figure 10, red). These two carbocations were predicted to form in approximately a 1:1 ratio. Again, there is an inherent dynamical tendency for the substrate to form the observed natural product, but again this

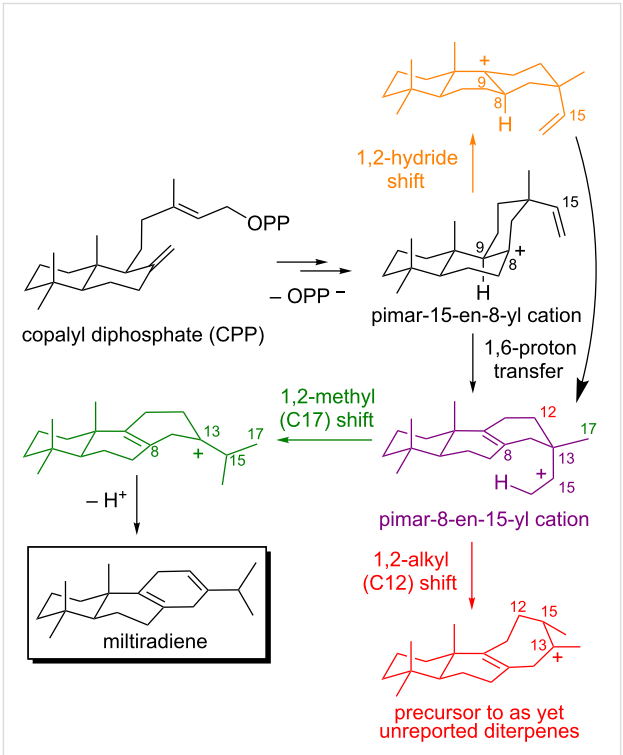

Figure 10: Carbocation rearrangements involved in miltiradiene formation.

tendency is not strong enough to preclude formation of a rearranged product. In addition, the dynamics calculations indicated that the 1,2-methyl (C17) shift that forms the abietadiene precursor should occur specifically to one face of the carbocation carbon (C15), a prediction that could be tested through substrate labeling. If only trajectories that lead to the pimar-15-en-8-yl cation are considered, then a product ratio of approximately 2:1, in favor of miltiradiene formation, is found, i.e., some trajectories actually connect to a carbocation formed by a 1,2-hydride shift of the pimar-15-en-8-yl cation (Figure 10, orange). This result suggests that preorganization of the substrate into a conformation that disfavors the 1,2-hydride shift actually promotes miltiradiene formation. Finally, when dynamics trajectories were initiated from the region of the 1,6-proton transfer transition state associated with proton migration to the *si* face of the C=C double bond, the carbocation precursor to abietadiene was formed <1% of the time. This result implies that the pimar-15-en-8-yl cation is bound in a conformation that allows for proton transfer specifically to the *re* face of the C=C double bond. This study serves to redefine the problem faced by miltiradiene synthase in controlling selectivity, makes firm predictions about the bound conformation of the substrate and the stereochemical course of the enzymatic reaction from calculations that did not include the enzyme, and again sets the stage for future rational reengineering efforts.

Take home messages:

• *Multiple sequential PTSBs can occur in biosynthetically-relevant carbocation rearrangements.*

• *The PES for miltiradiene formation (in the absence of an enzyme) involves direct pathways from a single TSS to many products.*

• *There is, however, an inherent dynamical tendency of the carbocations involved in miltiradiene formation (in the absence of an enzyme) to form almost exclusively miltiradiene and a rearranged product that has not yet been observed in Nature in comparable amounts.*

• *Direct enzymatic intervention is likely necessary to reduce the dynamical tendency to form the rearranged product. Although the nature of this intervention has not yet been deduced, it likely involves conformational restrictions that suppress a possible 1,2-hydride shift in the first-formed carbocation and prevent proton transfer to the si face of the C=C π-bond.*

epi-Isozizaene – shape selection

DFT calculations on the pathway for formation of the sesquiterpene *epi*-isozizaene [96-101] (Figure 11) showed that several expected chemical steps were merged into concerted processes [80]. For example, conversion of the homobisabolyl cation to the acorenyl cation (Figure 11, step 7) is barrierless for many conformers of the homobisabolyl cation. In addition, conversion of the cedryl cation to the prezizyl cation involves the combination of two alkyl shift events into a concerted process that avoids formation of a secondary carbocation as a PES minimum (Figure 11, step 9, a "dyotropic" rearrangement) [102]. Direct dynamics trajectory calculations were run for this system starting from the region of the TSS for the 1,2-hydride shift that converts the bisabolyl cation to the homobisabolyl cation (Figure 11, step 6). The goal of this study was to assess how far along the reaction coordinate trajectories would proceed without becoming "trapped" in an intermediate energy well. For some conformers of the bisabolyl cation, many trajectories proceeded to the cedryl cation without significant delay in the regions of the homobisabolyl and acorenyl cations. Subsequent automated docking calculations of carbocations (specifically, those derived from the conformer of the bisabolyl cation that most readily formed the cedryl cation in the dynamics simulations) into the crystallographically-determined structure of *epi*-isozizaene synthase revealed that some carbocations along the reaction coordinate were bound more strongly than others. Of particular note was the prediction that the TSS for conversion of the cedryl cation to the prezizyl cation (Figure 11, step 9) and for the conversion of the prezizyl cation to the zizyl cation (Figure 11, step 10) are bound more strongly than the carbocations that immediately precede them, implying that shape selection by the enzyme can lower the barriers for these steps (Figure 11, bottom), thereby making it more likely that trajectories will proceed to product.

Take home message:

• *Shape selection by epi-isozizaene synthase can lower barriers for steps in the epi-isozizaene-forming carbocation cascade reaction, thereby increasing the likelihood of direct formation of epi-isozizaene over byproducts.*

Outlook

Clearly, non-statistical dynamic effects play important roles in carbocation rearrangement reactions. Neglecting such dynamic effects may lead to incorrect conclusions about lifetimes of particular structures and product distributions – not merely for reactions of academic interest, but for reactions that occur in Nature during the biosynthesis of complex natural products. While characterizing the dynamical behavior of reactive species is challenging, it can be accomplished using modern computational approaches. We look forward to many more studies that do so. We believe as predicted so presciently by Lionel Salem four and a half decades ago, "…the beautiful mechanistic

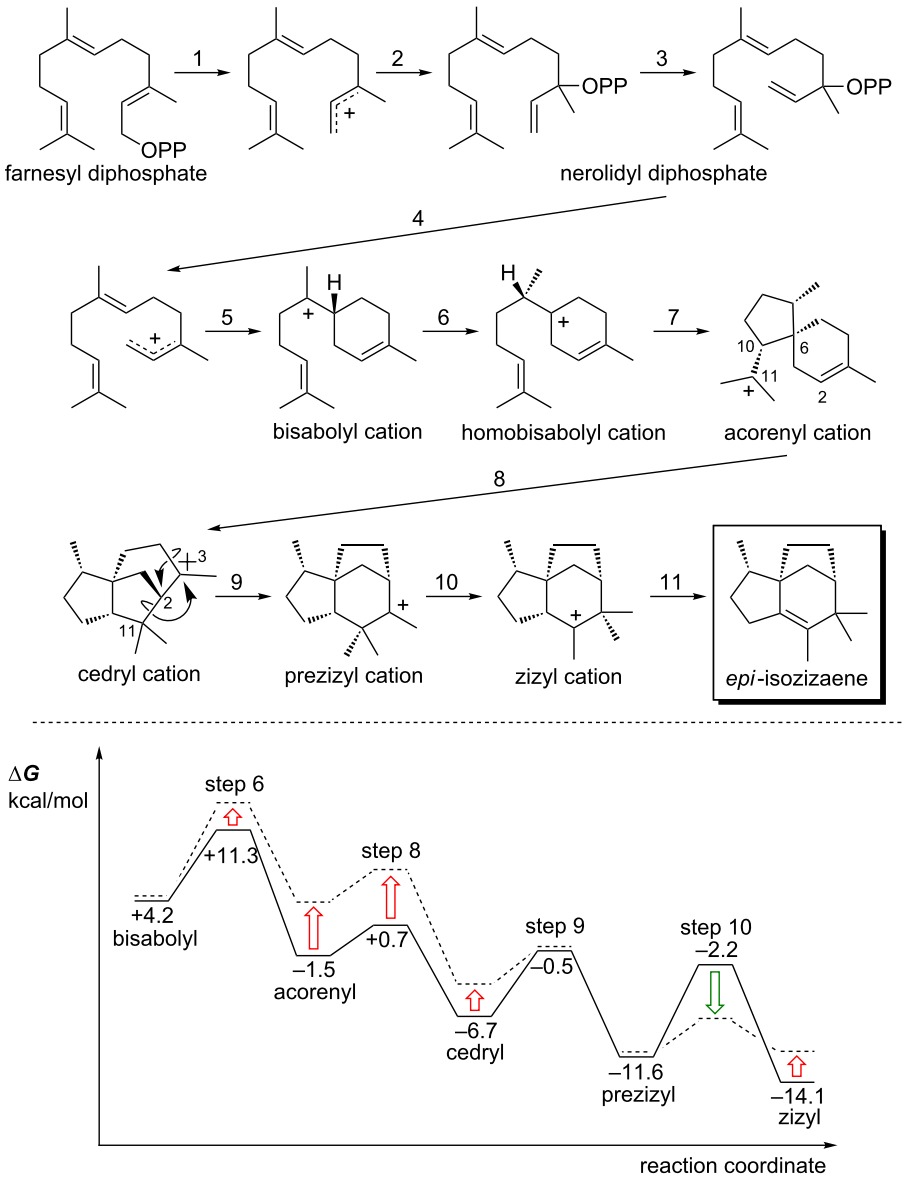

Figure 11: Top: carbocation rearrangements involved in *epi*-isozizaene formation. Bottom: reaction coordinate diagram for conversion of the bisabolyl cation to the zizyl cation in the absence (solid lines; computed relative energies in kcal/mol) and presence (broken lines) of *epi*-isozizaene synthase.

schemes used by organic chemists to interpret reactions will slowly be supplemented and may eventually be replaced by a detailed picture of the dynamic behavior of the reacting species on a complex potential energy surface" [103].

Acknowledgements

We gratefully acknowledge the National Science Foundation, including its XSEDE program, for support of the projects from the Tantillo lab described herein and support from the US Department of Education's GAANN program.

References

1. Christianson, D. W. *Curr. Opin. Chem. Biol.* **2008,** *12,* 141–150. doi:10.1016/j.cbpa.2007.12.008
2. Christianson, D. W. *Chem. Rev.* **2006,** *106,* 3412–3442. doi:10.1021/cr050286w
3. Davis, E. M.; Croteau, R. Cyclization Enzymes in the Biosynthesis of Monoterpenes, Sesquiterpenes, and Diterpenes. In *Biosynthesis;* Leeper, F. J.; Vederas, J. C., Eds.; Topics in Current Chemistry, Vol. 209; Springer: Berlin, Heidelberg, 2000; pp 53–95. doi:10.1007/3-540-48146-X_2

4. Cane, D. E. *Compr. Nat. Prod. Chem.* **1999,** *2,* 155–200. doi:10.1016/B978-0-08-091283-7.00039-4
5. Cane, D. E. *Chem. Rev.* **1990,** *90,* 1089–1103. doi:10.1021/cr00105a002
6. Tantillo, D. J. *Nat. Prod. Rep.* **2011,** *28,* 1035–1053. doi:10.1039/c1np00006c
7. Fukui, K. *Acc. Chem. Res.* **1981,** *14,* 363–368. doi:10.1021/ar00072a001
8. Maeda, S.; Harabuchi, Y.; Ono, Y.; Taketsugu, T.; Morokuma, K. *Int. J. Quantum Chem.* **2015,** *115,* 258–269. doi:10.1002/qua.24757
9. Eyring, H. *J. Chem. Phys.* **1935,** *3,* 107. doi:10.1063/1.1749604
10. Fernández-Ramos, A.; Miller, J. A.; Klippenstein, S. J.; Truhlar, D. G. *Chem. Rev.* **2006,** *106,* 4518–4584. doi:10.1021/cr050205w
11. Truhlar, D. G.; Garrett, B. C.; Klippenstein, S. J. *J. Phys. Chem.* **1996,** *100,* 12771–12800. doi:10.1021/jp953748q
12. Laidler, K. J.; King, M. C. *J. Phys. Chem.* **1983,** *87,* 2657–2664. doi:10.1021/j100238a002
13. Pechukas, P. *Annu. Rev. Phys. Chem.* **1981,** *32,* 159–177. doi:10.1146/annurev.pc.32.100181.001111
14. Marcus, R. A. *J. Chem. Phys.* **1952,** *20,* 352–354. doi:10.1063/1.1700422
15. Marcus, R. A. *J. Chem. Phys.* **1952,** *20,* 355–359. doi:10.1063/1.1700423
16. Kassel, L. S. *Chem. Rev.* **1932,** *10,* 11–25. doi:10.1021/cr60035a002
17. Rice, O. K.; Ramsperger, H. C. *J. Am. Chem. Soc.* **1927,** *49,* 1617–1629. doi:10.1021/ja01406a001
18. Pham, H. V.; Houk, K. N. *J. Org. Chem.* **2014,** *79,* 8968–8976. doi:10.1021/jo502041f
19. Collins, P.; Carpenter, B. K.; Ezra, G. S.; Wiggins, S. *J. Chem. Phys.* **2013,** *139,* 154108. doi:10.1063/1.4825155
20. Ess, D. H.; Wheeler, S. E.; Iafe, R. G.; Xu, L.; Çelebi-Ölçüm, N.; Houk, K. N. *Angew. Chem., Int. Ed.* **2008,** *47,* 7592–7601. doi:10.1002/anie.200800918
21. Weitman, M.; Major, D. T. *J. Am. Chem. Soc.* **2010,** *132,* 6349–6360. doi:10.1021/ja910134x
22. Major, D. T.; Weitman, M. *J. Am. Chem. Soc.* **2012,** *134,* 19454–19462. doi:10.1021/ja308295p
23. Gonzalez, C.; Schlegel, H. B. *J. Phys. Chem.* **1990,** *94,* 5523–5527. doi:10.1021/j100377a021
24. Davies, H. M. L.; Lian, Y. *Acc. Chem. Res.* **2012,** *45,* 923–935. doi:10.1021/ar300013t
25. Pemberton, R. P.; Hong, Y. J.; Tantillo, D. J. *Pure Appl. Chem.* **2013,** *85,* 1949–1957. doi:10.1351/pac-con-12-11-22
26. Hong, Y. J.; Tantillo, D. J. *Nat. Chem.* **2014,** *6,* 104–111. doi:10.1038/nchem.1843
27. Birney, D. M. *Curr. Org. Chem.* **2010,** *14,* 1658–1668. doi:10.2174/138527210793563260
28. Carpenter, B. K. *J. Am. Chem. Soc.* **1995,** *117,* 6336–6344. doi:10.1021/ja00128a024
29. Lourderaj, U.; Hase, W. L. *J. Phys. Chem. A* **2009,** *113,* 2236–2253. doi:10.1021/jp806659f
30. Carpenter, B. K. *Annu. Rev. Phys. Chem.* **2005,** *56,* 57–89. doi:10.1146/annurev.physchem.56.092503.141240
31. Klinman, J. P. *Procedia Chem.* **2011,** *3,* 291–305. doi:10.1016/j.proche.2011.08.037
32. Klinman, J. P.; Kohen, A. *Annu. Rev. Biochem.* **2013,** *82,* 471–496. doi:10.1146/annurev-biochem-051710-133623
33. Klinman, J. P. *Acc. Chem. Res.* **2015,** *48,* 449–456. doi:10.1021/ar5003347
34. Antoniou, D.; Caratzoulas, S.; Kalyanaraman, C.; Mincer, J. S.; Schwartz, S. D. *Eur. J. Biochem.* **2002,** *269,* 3103–3112. doi:10.1046/j.1432-1033.2002.03021.x
35. Bachrach, S. M. *Computational organic chemistry,* 2nd ed.; John Wiley & Sons: Hoboken, New Jersey, 2014. doi:10.1002/9781118671191
36. Lourderaj, U.; Park, K.; Hase, W. L. *Int. Rev. Phys. Chem.* **2008,** *27,* 361–403. doi:10.1080/01442350802045446
37. Fleming, K. L.; Tiwary, P.; Pfaendtner, J. *J. Phys. Chem. A* **2016,** *120,* 299–305. doi:10.1021/acs.jpca.5b10667
38. Voter, A. F.; Montalenti, F.; Germann, T. C. *Annu. Rev. Mater. Res.* **2002,** *32,* 321–346. doi:10.1146/annurev.matsci.32.112601.141541
39. Xiao, P.; Duncan, J.; Zhang, L.; Henkelman, G. *J. Chem. Phys.* **2015,** *143,* 244104. doi:10.1063/1.4937393
40. Cramer, C. J. *Essentials of computational chemistry: theories and models;* John Wiley & Sons: West Sussex, England, 2002.
41. Bogle, X. S.; Singleton, D. A. *J. Am. Chem. Soc.* **2011,** *133,* 17172–17175. doi:10.1021/ja2084288
42. Saunders, M.; Telkowski, L.; Kates, M. R. *J. Am. Chem. Soc.* **1977,** *99,* 8070–8071. doi:10.1021/ja00466a060
43. Saunders, M.; Kates, M. R. *J. Am. Chem. Soc.* **1977,** *99,* 8071–8072. doi:10.1021/ja00466a061
44. Saunders, M.; Kates, M. R.; Wiberg, K. B.; Pratt, W. *J. Am. Chem. Soc.* **1977,** *99,* 8072–8073. doi:10.1021/ja00466a062
45. Ohta, B. K.; Hough, R. E.; Schubert, J. W. *Org. Lett.* **2007,** *9,* 2317–2320. doi:10.1021/ol070673n
46. Ammal, S. C.; Yamataka, H.; Aida, M.; Dupuis, M. *Science* **2003,** *299,* 1555–1557. doi:10.1126/science.1079491
47. Roca-López, D.; Polo, V.; Tejero, T.; Merino, P. *Eur. J. Org. Chem.* **2015,** *2015,* 4143–4152. doi:10.1002/ejoc.201500447
48. Kraka, E.; Cremer, D. *Acc. Chem. Res.* **2010,** *43,* 591–601. doi:10.1021/ar900013p
49. Cremer, D.; Wu, A.; Kraka, E. *Phys. Chem. Chem. Phys.* **2001,** *3,* 674–687. doi:10.1039/b007733j
50. Duarte, F.; Gronert, S.; Kamerlin, S. C. L. *J. Org. Chem.* **2014,** *79,* 1280–1288. doi:10.1021/jo402702m
51. Joo, H.; Kraka, E.; Quapp, W.; Cremer, D. *Mol. Phys.* **2010,** *105,* 2697–2717. doi:10.1080/00268970701620677
52. Hong, Y. J.; Tantillo, D. J. *Org. Lett.* **2011,** *13,* 1294–1297. doi:10.1021/ol103079v
53. Hong, Y. J.; Tantillo, D. J. *J. Am. Chem. Soc.* **2010,** *132,* 5375–5386. doi:10.1021/ja9084786
54. Hong, Y. J.; Tantillo, D. J. *J. Am. Chem. Soc.* **2009,** *131,* 7999–8015. doi:10.1021/ja9005332
55. de Souza, M. A. F.; Ventura, E.; do Monte, S. A.; Riveros, J. M.; Longo, R. L. *Chem. – Eur. J.* **2014,** *20,* 13742–13754. doi:10.1002/chem.201402617
56. Tantillo, D. J. *J. Phys. Org. Chem.* **2008,** *21,* 561–570. doi:10.1002/poc.1320
57. Tantillo, D. J. *Chem. Soc. Rev.* **2010,** *39,* 2847–2854. doi:10.1039/b917107j
58. Sun, L.; Song, K.; Hase, W. L. *Science* **2002,** *296,* 875–878. doi:10.1126/science.1068053
59. Berson, J. A.; Wege, D.; Clarke, G. M.; Bergman, R. G. *J. Am. Chem. Soc.* **1969,** *91,* 5594–5601. doi:10.1021/ja01048a029
60. Ghigo, G.; Maranzana, A.; Tonachini, G. *J. Org. Chem.* **2013,** *78,* 9041–9050. doi:10.1021/jo401188e
61. Becke, A. D. *J. Chem. Phys.* **1993,** *98,* 1372–1377. doi:10.1063/1.464304
62. Becke, A. D. *J. Chem. Phys.* **1993,** *98,* 5648. doi:10.1063/1.464913

63. Ditchfield, R.; Hehre, W. J.; Pople, J. A. *J. Chem. Phys.* **1971,** *54,* 724–728. doi:10.1063/1.1674902
64. Jalife, S.; Martínez-Guajardo, G.; Zavala-Oseguera, C.; Fernández-Herrera, M. A.; von Ragué Schleyer, P.; Merino, G. *Eur. J. Org. Chem.* **2014,** 7955–7959. doi:10.1002/ejoc.201403146
65. Lobb, K. A. *Eur. J. Org. Chem.* **2015,** 5370–5380. doi:10.1002/ejoc.201500518
66. Lawton, R. G. *J. Am. Chem. Soc.* **1961,** *83,* 2399. doi:10.1021/ja01471a047
67. Bartlett, P. D.; Bank, S.; Crawford, R. J.; Schmid, G. H. *J. Am. Chem. Soc.* **1965,** *87,* 1288–1297. doi:10.1021/ja01084a025
68. Jalife, S.; Wu, J. I.; Martinez-Guajardo, G.; von Ragué Schleyer, P.; Fernandez-Herrera, M. A.; Merino, G. *Chem. Commun.* **2015,** *51,* 5391–5393. doi:10.1039/C4CC08071H
69. East, A. L. L.; Bucko, T.; Hafner, J. *J. Phys. Chem. A* **2007,** *111,* 5945–5947. doi:10.1021/jp072327t
70. East, A. L. L.; Bučko, T.; Hafner, J. *J. Chem. Phys.* **2009,** *131,* 104314. doi:10.1063/1.3230603
71. Sandbeck, D. J. S.; Markewich, D. J.; East, A. L. L. *J. Org. Chem.* **2016,** *81,* 1410–1415. doi:10.1021/acs.joc.5b02553
72. Johnson, C. K.; Collins, C. J. *J. Am. Chem. Soc.* **1974,** *96,* 2514–2523. doi:10.1021/ja00815a033
73. Collins, C. J.; Johnson, C. K. *J. Am. Chem. Soc.* **1973,** *95,* 4766–4768. doi:10.1021/ja00795a057
74. Collins, C. J.; Johnson, C. K.; Raaen, V. F. *J. Am. Chem. Soc.* **1974,** *96,* 2524–2531. doi:10.1021/ja00815a034
75. Tratch, S. S.; Molchanova, M. S.; Zefirov, N. S. *Croat. Chem. Acta* **2006,** *79,* 339–353.
76. Sorensen, T. S. *Acc. Chem. Res.* **1976,** *9,* 257–265. doi:10.1021/ar50103a003
77. Mosley, J. D.; Young, J. W.; Agarwal, J.; Schaefer, H. F., III; von Ragué Schleyer, P.; Duncan, M. A. *Angew. Chem., Int. Ed.* **2014,** *53,* 5888–5891. doi:10.1002/anie.201311326
78. Hong, Y. J.; Tantillo, D. J. *Org. Biomol. Chem.* **2010,** *8,* 4589–4600. doi:10.1039/c0ob00167h
79. Lodewyk, M. W.; Gutta, P.; Tantillo, D. J. *J. Org. Chem.* **2008,** *73,* 6570–6579. doi:10.1021/jo800868r
80. Pemberton, R. P.; Ho, K. C.; Tantillo, D. J. *Chem. Sci.* **2015,** *6,* 2347–2353. doi:10.1039/C4SC03782K
81. Hong, Y. J.; Tantillo, D. J. *Chem. Sci.* **2013,** *4,* 2512–2518. doi:10.1039/c3sc50571e
82. Lafever, R. E.; Vogel, B. S.; Croteau, R. *Arch. Biochem. Biophys.* **1994,** *313,* 139–149. doi:10.1006/abbi.1994.1370
83. Peters, R. J.; Flory, J. E.; Jetter, R.; Ravn, M. M.; Lee, H.-J.; Coates, R. M.; Croteau, R. B. *Biochemistry* **2000,** *39,* 15592–15602. doi:10.1021/bi001997l
84. Peters, R. J.; Croteau, R. B. *Proc. Natl. Acad. Sci. U. S. A.* **2002,** *99,* 580–584. doi:10.1073/pnas.022627099
85. Peters, R. J.; Ravn, M. M.; Coates, R. M.; Croteau, R. B. *J. Am. Chem. Soc.* **2001,** *123,* 8974–8978. doi:10.1021/ja010670k
86. Funk, C.; Croteau, R. *Arch. Biochem. Biophys.* **1994,** *308,* 258–266. doi:10.1006/abbi.1994.1036
87. Ravn, M. M.; Peters, R. J.; Coates, R. M.; Croteau, R. *J. Am. Chem. Soc.* **2002,** *124,* 6998–7006. doi:10.1021/ja017734b
88. Ravn, M. M.; Coates, R. M.; Jetter, R.; Croteau, R. B. *Chem. Commun.* **1998,** 21–22. doi:10.1039/a706202h
89. Ravn, M. M.; Coates, R. M.; Flory, J. E.; Peters, R. J.; Croteau, R. *Org. Lett.* **2000,** *2,* 573–576. doi:10.1021/ol991230p
90. Wilderman, P. R.; Peters, R. J. *J. Am. Chem. Soc.* **2007,** *129,* 15736–15737. doi:10.1021/ja074977g
91. Hong, Y. J.; Tantillo, D. J. *Nat. Chem.* **2009,** *1,* 384–389. doi:10.1038/nchem.287
92. Siebert, M. R.; Zhang, J.; Addepalli, S. V.; Tantillo, D. J.; Hase, W. L. *J. Am. Chem. Soc.* **2011,** *133,* 8335–8343. doi:10.1021/ja201730y
93. Siebert, M. R.; Manikandan, P.; Sun, R.; Tantillo, D. J.; Hase, W. L. *J. Chem. Theory Comput.* **2012,** *8,* 1212–1222. doi:10.1021/ct300037p
94. Gao, W.; Hillwig, M. L.; Huang, L.; Cui, G.; Wang, X.; Kong, J.; Yang, B.; Peters, R. J. *Org. Lett.* **2009,** *11,* 5170–5173. doi:10.1021/ol902051v
95. Hong, Y. J.; Tantillo, D. J. *J. Am. Chem. Soc.* **2015,** *137,* 4134–4140. doi:10.1021/ja512685x
96. Aaron, J. A.; Lin, X.; Cane, D. E.; Christianson, D. W. *Biochemistry* **2010,** *49,* 1787–1797. doi:10.1021/bi902088z
97. Lin, X.; Hopson, R.; Cane, D. E. *J. Am. Chem. Soc.* **2006,** *128,* 6022–6023. doi:10.1021/ja061292s
98. Zhao, B.; Lin, X.; Lei, L.; Lamb, D. C.; Kelly, S. L.; Waterman, M. R.; Cane, D. E. *J. Biol. Chem.* **2008,** *283,* 8183–8189. doi:10.1074/jbc.M710421200
99. Lin, X.; Cane, D. E. *J. Am. Chem. Soc.* **2009,** *131,* 6332–6333. doi:10.1021/ja901313v
100. Li, R.; Chou, W. K. W.; Himmelberger, J. A.; Litwin, K. M.; Harris, G. G.; Cane, D. E.; Christianson, D. W. *Biochemistry* **2014,** *53,* 1155–1168. doi:10.1021/bi401643u
101. Belhassen, E.; Baldovini, N.; Brevard, H.; Meierhenrich, U. J.; Filippi, J.-J. *Chem. Biodiversity* **2014,** *11,* 1821–1842. doi:10.1002/cbdv.201400079
102. Gutierrez, O.; Tantillo, D. J. *J. Org. Chem.* **2012,** *77,* 8845–8850. doi:10.1021/jo301864h
103. Salem, L. *Acc. Chem. Res.* **1971,** *4,* 322–328. doi:10.1021/ar50045a005

License and Terms

BEILSTEIN JOURNAL OF ORGANIC CHEMISTRY

Biosynthesis of α-pyrones

Till F. Schäberle

Review

Open Access

Address:
Institute for Pharmaceutical Biology, University of Bonn, Nußallee 6, 53115 Bonn, Germany

Email:
Till F. Schäberle - till.schaeberle@uni-bonn.de

Keywords:
α-pyrones; biological activity; interconnecting ketosynthases; natural product; polyketides

Beilstein J. Org. Chem. **2016,** *12,* 571–588.
doi:10.3762/bjoc.12.56

Received: 28 December 2015
Accepted: 02 March 2016
Published: 24 March 2016

This article is part of the Thematic Series "Natural products in synthesis and biosynthesis II".

Guest Editor: J. S. Dickschat

Abstract

The α-pyrone moiety is a structural feature found in a huge variety of biologically active metabolites. In recent times new insights into additional biosynthetic mechanisms, yielding in such six-membered unsaturated ester ring residues have been obtained. The purpose of this mini-review is to give a brief overview of α-pyrones and the mechanisms forming the basis of their natural synthesis. Especially the chain interconnecting enzymes, showing homology to ketosynthases which catalyze Claisen-like condensation reactions, will be presented.

Introduction

α-Pyrones (**1**, also 2-pyrones) represent a moiety widespread in nature (Figure 1). The motif of a six-membered cyclic unsaturated ester is present in a large number of natural products, and molecules containing α-pyrones can be found in all three kingdoms of life. Additionally α-pyrones, especially the structurally simple ones, i.e., triacetic acid lactone (**2**) and tetraacetic acid lactone (**3**) (Figure 1), represent widely exploited building blocks in synthetic chemistry. Examples are the syntheses of compounds like α-chymotrypsin, coumarins, pheromones, and solanopyrones [1]. Known biological functions reach from intermediates and end products in primary metabolism to signaling molecules and molecules which are applied for defense against competitors and predators. The biological activities these compounds exhibit is immense, including antimicrobial [2], antitumor [3,4], and cytotoxic activities [5]. Aflatoxins, produced by several *Aspergillus* species, are known to cause food poisoning due to their cytotoxic activity. They can regularly be found in improperly stored food, hence, entering the food supply chain [6]. Further coumarin derivatives, e.g., umbelliferone (**4**), esculetin (**5**), and scopoletin (**6**), are subject of investigation due to their pharmacological properties, i.e., anticancer effects (Figure 1) [7]. α-Pyrones have also been shown to be HIV protease [8-10] and selective COX-2 inhibitors [11,12], and further, signaling functions were attributed to them. Already in the 1990s an unusual dialkyl-substituted α-pyrone (supellapyrone, **7**) was detected to be the cockroach sex pheromone [13], and recently it was reported that so called photopyrones (**8**–**15**) act as signaling molecules in the cell–cell communication system of the bacterium *Photorhabdus luminescens* (Figure 1) [14].

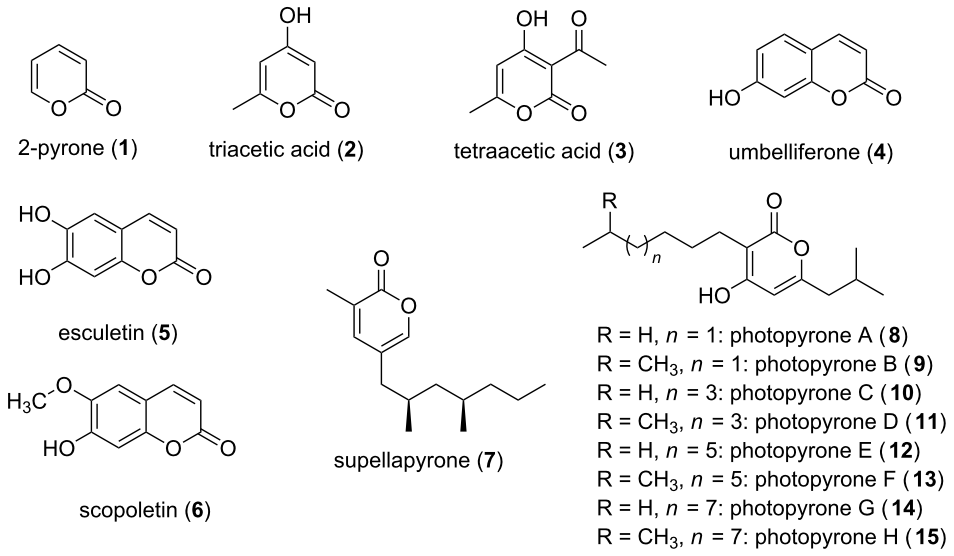

Figure 1: Selected monocyclic and monobenzo α-pyrone structures.

Since the biological activities of α-pyrones are very diverse, these compounds are in the focus of synthetic chemists [15]. Hence, the phenomenal abundance of natural products and of chemically synthesized derivatives therefrom justifies several reviews, and comprehensive articles exist [1,16]. However, in the present review the diverse biosynthesis of α-pyrones will be the focus. Different mechanisms for the biosynthesis of these mostly polyketide-derived structures exist, thus it is assumed that the route towards α-pyrones has been developed several times in evolution. They can be built up by the catalytic activities of the different types of polyketide synthase (PKS) systems, and especially the final ring formation yielding in the α-pyrone moiety can be accomplished in different ways. The different biosynthetic routes towards an α-pyrone ring will be presented. The biosynthetic mechanisms to yield saturated lactones, like the statin drug lovastatin, which is in application for lowering cholesterol, will not be discussed.

Review

1 Occurrence and activities

In this chapter special sub-types of α-pyrones will be described. The compounds are grouped into three categories depending on their structural features: (i) dibenzo-α-pyrones, (ii) monocyclic α-pyrones, and (iii) monobenzo-α-pyrones.

1.1 Dibenzo-α-pyrones

Dibenzo-α-pyrones (**16**) harbor the α-pyrone moiety in the middle part and consist of three ring structures (Figure 2). Aromatic rings are fused to edge c and e of the central 2-pyrone, yielding the basic structure of **16**.

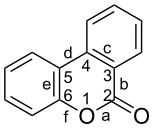

Figure 2: The basic core structure of dibenzo-α-pyrones.

Many dibenzo-α-pyrone-producing fungi have been described. However, it seems that they are mainly distributed in the *Alternaria* species and mycobionts. Especially endophytic fungi can be regarded as source organisms. Alternariol (**17**), altenuene (**18**), and alternariol 9-methyl ether (**19**) have been described from *Alternaria* sp. [17], botrallin (**20**) from *Hyalodendriella* sp. [18], and graphislactone A (**21**) from *Cephalosporium acremonium* IFB-E007 (Figure 3) [19]. These compounds show toxic effects in plants and animals. In addition, *Alternaria* spp. have been involved in the contamination of food, even in refrigerated stocks, since the fungi is able to grow also at low temperature. *Alternaria* spp. had also been linked to a poultry disease outbreak called poultry hemorrhagic syndrome. However, the main toxic effects seem to be linked to other toxins produced, e.g., the non pyrone metabolite tenuazonic acid [20]. Nevertheless, alternariol (**17**) and altenuene (**18**) were studied for their toxicity using different assays. Toxicity to *Artemia salina* larvae was examined by measuring the optical motility and resulted in IC_{50} values of 150 µg/mL [21]. A comparable result was obtained using the disk method of inoculation, whereby the IC_{50} values were 100 µg/mL for **17** and 375 µg/mL for **18** [22].

Further, alternariol (**17**) and derivatives were tested against L5178Y mouse lymphoma cells. Here **17** was the most active compound with an EC_{50} value of 1.7 μg/mL [23]. In another in vitro assay, this time a biochemical assay using protein kinase, the IC_{50} values were determined, and **17** inhibited 10 out of the 24 kinases tested. The results of the MTT and the kinase assay showed a similar pattern, and hence it was concluded that protein kinase inhibition should be one mechanism leading to the cytotoxicity of **17**. In a study using human colon carcinoma cells to elucidate the cell death mode and the pathways triggered by **17**, the induction of an apoptotic process was revealed. Further investigations showed that cell death was mediated through a mitochondria-dependent pathway [24]. In murine hepatoma cells it was shown that **17** and its methyl ether **19** interfere with the transcription factor and by inducing the so-called aryl hydrocarbon receptor, apoptosis is mediated by inducing cytochrome P450 1A1 [25]. For alternariol 9-methyl ether (**19**) and the graphislactone A (**21**) cytotoxic effects against the human cancer cell line SW1116 with IC_{50} values between 8.5 and 21 μg/mL were reported [26].

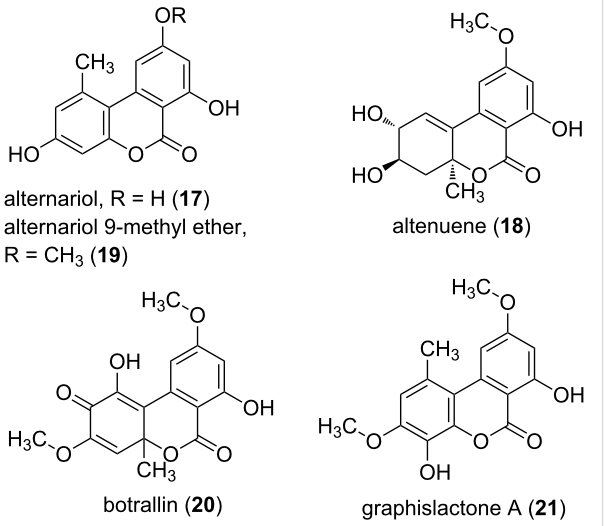

Figure 3: Selected dibenzo-α-pyrones.

These toxic fungi-derived metabolites are often pathogenic to plants, and are therefore called phytotoxins. Phytotoxins are divided into host-specific and host non-specific toxins, whereby the here named *Alternaria*-derived dibenzo-α-pyrones **17**, **18**, and **19** represent host-specific phytotoxins [26].

Several dibenzo-α-pyrones have been isolated from plant parts. Purified from roots, bulbi, heartwood, or whole plant material, the origin of some plant-derived pyrones is not finally clarified, since the production by endophytic fungi cannot be excluded. Djalonensone was isolated from *Anthocleista djalonensis* (*Loganiaceae*) roots, but is identical to alternariol 9-methyl ether (the corresponding bioactivities are described above.) The latter was isolated from a series of fungi including endophytic species. Thus, the possibility that a fungus is the real producer cannot be ruled out. In addition, production by a fungus and modification of the metabolites by plant enzymes is also possible. Further α-pyrone plant secondary metabolites are ellagitannins and ellagic acid (**22**) [27] (Figure 4). These metabolites are important constituents of different foods, e.g., berries, nuts, medicinal plants and tisanes, as well as of grapes and oak-aged wines. These natural products are not absorbed in the intestinal tract; rather they are metabolized by intestinal bacteria, yielding so called urolithins (**23**–**27**, Figure 4). Therefore, it can be assumed that the urolithins are responsible for the biological activities related to the intake of ellagitannins by higher organisms. Such urolithins show different phenolic hydroxylation patterns and have been isolated from animal feces.

Concerning the activity urolithin A (**23**), urolithin B (**24**), and isourolithin A (**27**), all isolated from fruits of *Trapa natans* (water chestnut) showed antioxidant activity [28]. Testing urolithins A, B, C, D (**23**–**26**) in an assay using myelomonocytic HL-60 cells showed antioxidant activities for **23**, **25** and **26**. These three derivatives inhibited the reactive oxygen species (ROS)-dependent oxygenation of the non-fluorescent 2',7'-dichlorodihydrofluorescein (DCFH) to the fluorescent 2',7'-dichlorofluorescein (DCF) [29]. This antioxidant activity

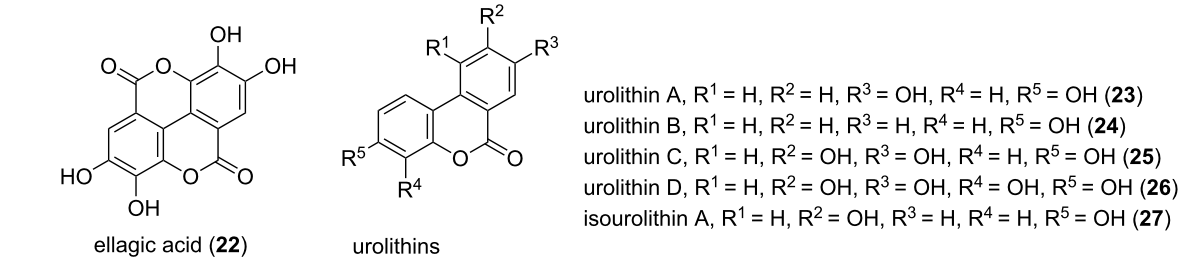

Figure 4: Structure of ellagic acid and of the urolithins, the latter metabolized from ellagic acid by intestinal bacteria.

was also linked to anti-inflammatory effects by testing the in vivo effects of **23** in a carrageenan-induced paw edema assay. Oral administration of **23** to mice prior to carrageenan injection resulted in a significant decrease in paw edema, compared to the control group [30]. Further, weak antiallergic activity in the mM range was indicated for urolithin A (**23**), urolithin B (**24**), and isourolithin A (**27**), by testing the influences of these compounds on the activity of the enzyme hyaluronidase. The latter is involved in inflammation reactions. The authors isolated **23**, **24** and **27** from the feces of *Trogopterus xanthipes* (flying squirrel) by bioactivity-guided fractionation, and determined IC_{50} values for the pure compounds to be in the low mM range (1.33, 1.07 and 2.33 mM, respectively) [31]. Also estrogenic and antiestrogenic activities in a dose-dependent manner were shown for **23** and **24**. Thus, the authors suggested further research to evaluate the possible role of ellagitannins and ellagic acid as dietary "pro-phytoestrogens" [32].

Even though many α-pyrones have been isolated from bacteria, only one dibenzo variant was described, i.e., murayalactone (**28**) isolated from *Streptomyces murayamaensis* (Figure 5) [33].

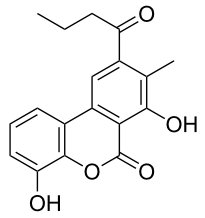

murayalactone (**28**)

Figure 5: Structure of murayalactone, the only dibenzo-α-pyrone described from bacteria.

1.2 Monocyclic α-pyrones

In addition to the aforementioned examples also the simplest α-pyrones show remarkable biological effects. Isolated from several fungi, e.g., *Trichoderma viride*, 6-pentyl-α-pyrone (**29**) showed antifungal activity against *Rhizoctonia cerealis*, *Gaeumannomyces graminis* and *Botrytis cinerea* (Figure 6) [34]. The structural related trichopyrone (**30**) instead showed no antimicrobial activity [35]. For compound **29** it was further revealed that it represents the prominent headspace volatile of *Trichoderma asperellum* IsmT5 [36]. Deeper investigation of the volatiles released by *Trichoderma* species revealed the complexity of the volatile mixture consisting of many derivatives [37]. Several alkylated and alkenylated α-pyrones with length variations in the side chain and different positions of olefinic double bonds were isolated in the headspace extracts and unambiguously assigned by comparison to authentic standards [37]. Co-cultivation experiments of *T. asperellum* and *Arabidopsis thaliana* without physical contact resulted in smaller but vital and robust plants. Therefore, **29** was applied to *A. thaliana*, and the growth and defense reactions were verified. *A. thaliana* pre-exposed to **29** showed significantly reduced symptoms when challenged with *B. cinerea* and *Alternaria brassicicola* [36].

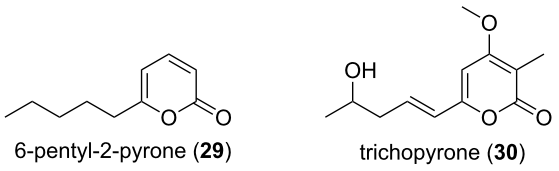

Figure 6: Structures of the 6-pentyl-2-pyrone (**29**) and of trichopyrone (**30**). Only **29** showed antifungal activity.

Beside the examples of simple substituted α-pyrone derivatives, such as triacetic acid lactone (**2**), tetraacetic acid lactone (**3**), and 6-pentyl-2-pyrone (**29**) also more complex systems, e.g., bufalin (**31**) [38], fusapyrones (**32,33**) [39], or the α-pyrone antibiotics corallopyronins (**34,35**) [40] and myxopyronins (**36,37**) [41], exist in the group of monocyclic α-pyrones (Figure 7).

The bufadienolides are an important group of steroids containing an α-pyrone moiety. The α-pyrone ring is here connected to a steroid nucleus, as exemplified in bufalin (**31**, Figure 7). These α-pyrones were detected in several plants, as well as in animals. The vast amount of derivatives shows also very diverse biological activities. The bufadienolides from succulent plants of the family Crassulaceae cause the symptoms of cardiac poisoning in animals. Animal sources are the name giving toad genus *Bufo* and others, e.g., *Photinus* (fireflies) and *Rhabdophis* (snake). The abundance of bufadienolides in some *Bufo* species is extremely high, and all together, over eighty derivatives have already been isolated, e.g., the epoxide-containing resibufogenin (**38**, Figure 7) was isolated from the Chinese toad skin extract drug Ch´an Su. It showed growth inhibition effects on human oral epidermoid carcinoma KB cells and murine leukemia MH-60 cells [42].

Testing the inhibitory effect of corallopyronin A (**34**) against various microorganisms revealed promising activity against Gram-positive bacteria, but no relevant effect on Gram-negative bacteria (only at concentrations >100 µg/mL activity was observed). Against *Staphylococcus aureus* a MIC of 0.097 µg/mL and against *Bacillus megaterium* of 0.39 µg/mL was obtained [40]. Myxopyronin B (**37**), the most active derivative of the myxopyronins, showed comparable activities, e.g., MIC of 0.3 and 0.8 µg/mL against *S. aureus* and *B. megaterium*, respectively [43]. In addition corallopyronin A was also

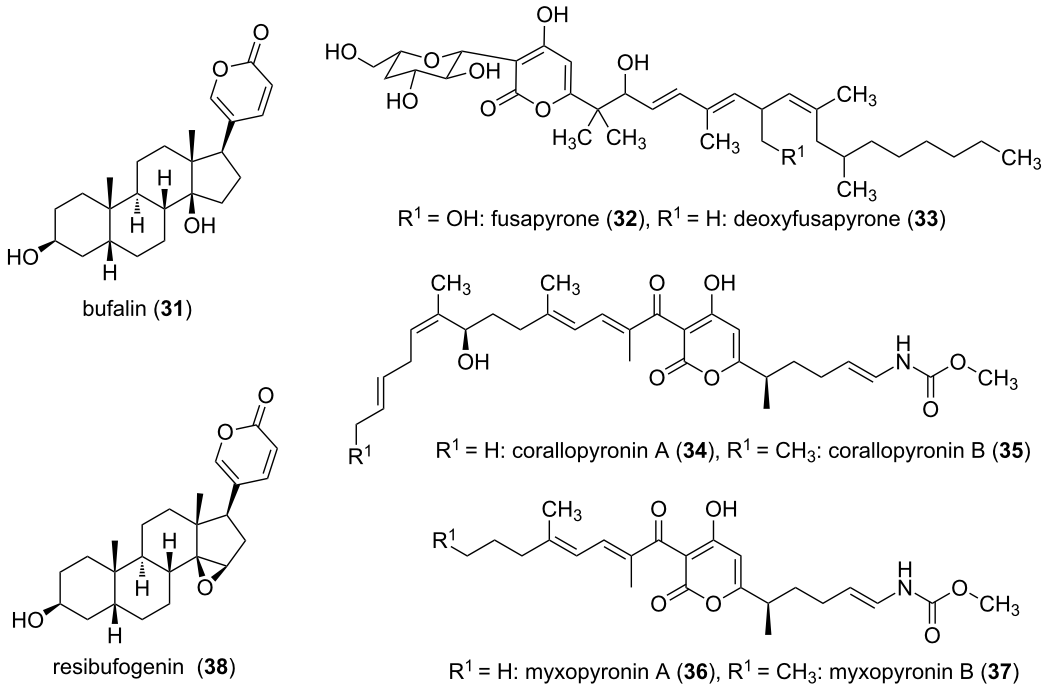

Figure 7: Selected monocyclic α-pyrones.

tested successfully using an in vivo mouse model for the treatment of infections with filarial nematodes [44]. Such antibiotics produced by heterotroph bacteria, e.g., marine and terrestrial myxobacteria which can feed on other bacteria, are suggested as predatory weapons to paralyze and kill their prey [45,46].

Fusapyrone (**32**) and the derivative deoxyfusapyrone (**33**) had been isolated from *Fusarium semitectum* [39]. These compounds show considerable antifungal activity, e.g., a minimum inhibitory concentration against *Botrytis cinerea*, *Aspergillus parasiticus*, and *Penicillium brevi-compactum* in the range of 0.78–6.25 µg/mL [47]. Testing the zootoxicity of **32** and **33**, using brine shrimp assays, revealed that only approximately 50-fold higher concentrations had a negative effect. Therefore, it was concluded that these compounds might be used together with biocontrol yeasts to control crop diseases which can occur while storing the crops [47]. From another strain of this fungal genus, i.e., *Fusarium fujikuroi*, the gibepyrones A–F (**39**–**44**) were isolated (Figure 8) [48]. The activity of these compounds was tested against bacterial and fungal strains. However, the activities were extremely low, e.g. gibepyrone A inhibited *B. subtilis* and *S. cerevisiae* at 100 µg/mL.

The diastereomeric pair of phomenin A (**45**) and phomenin B (**46**) was isolated from the phytopathogenic fungus *Phoma tracheiphila*,[49] and from *Alternaria infectoria* (Figure 9) [50]. Further, the same compound **45** was isolated from *Leptosphaeria maculans* and named phomapyrone A, as well as from the mediterranean ascoglossan mollusc *Ercolania fune-*

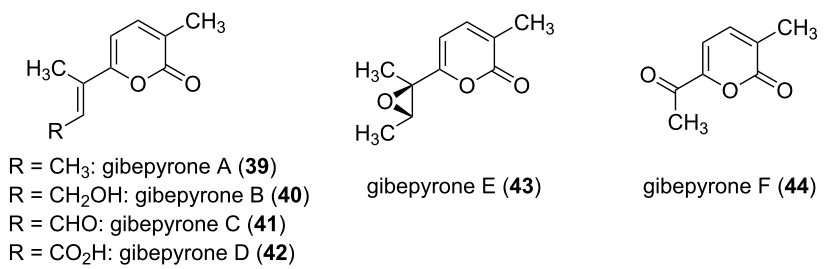

Figure 8: Structures of the gibepyrones A–F.

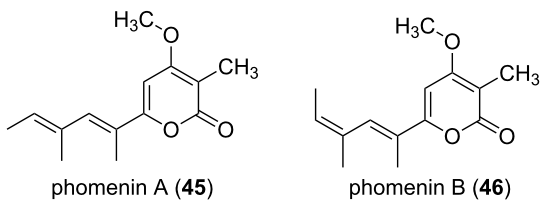

phomenin A (**45**) phomenin B (**46**)

Figure 9: Structures of the phomenins A and B.

real, described as cyercene [51]. Phomenin A displayed phytotoxicity at a concentration of 100 µg/mL. Chemical synthesis approaches enabled then to investigate many more α-pyrone derivatives for their antimicrobial and cytotoxic properties [2].

The volatile α-pyrone 5-(2,4-dimethylheptyl)-3-methyl-2*H*-pyran-2-one (**7**, Figure 1), also named supellapyrone) is used by female brownbanded cockroaches to attract males [13]. It is known that cockroaches use pheromones in many aspects of influencing interacting behavior between individuals. Hence, such volatiles are used in courtship behavior to find mating partners. Also another α-pyrone fulfilling pheromone function in insects is known, i.e., the queen recognition pheromone of the red imported fire ant, 6-(1-pentenyl)-2*H*-pyran-2-one (**47**, Figure 10) [52].

Also antitumor activities of α-pyrones had been shown. Thus, pironetin (**47**, Figure 10) induced apoptosis in a dose- and time-dependent manner, and tubulin assembly was inhibited in vitro [53]. The natural product was isolated from *Streptomyces* sp. NK10958 [54], and its biosynthesis was investigated using various ^{13}C-labeled precursors [55]. Hence, it was concluded that beside four acetate units also two propionate units and one butyrate unit form the backbone, while the *O*-methylation is S-adenosyl-methionine dependent.

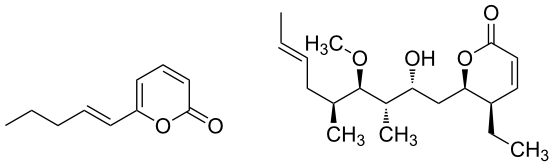

6-(1-pentenyl)-2*H*-pyran-2-one (**47**) pironetin (**48**)

Figure 10: Structures of monocyclic α-pyrones showing pheromone (**47**) and antitumor activity (**48**), respectively.

Also cyclooxygenase-2 (COX-2) inhibitors are an interesting target of research, due to the fact that the progression of Alzheimer's disease was slowed down by using anti-inflammatory drugs. Thus, selective COX-2 inhibitors, anti-inflammatory compounds themselves, might have beneficial effects in vivo. Several derivatives of 6-alkyl (alkoxy or alkylthio)-4-aryl-3-(4-methanesulfonylphenyl)pyrones **49** had been synthesized to get insights into structure activity relationships, whereby 6-methyl-3-(4-methanesulfonylphenyl)-4-phenylpyran-2-one (**50**) showed the best combination of inhibitory concentration and selectivity (IC_{50} = 0.68 µM, SI = 904; Figure 11) [56].

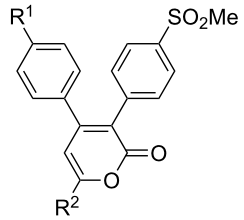

6-alkyl (alkoxy or alkylthio)-4-aryl-3-(4-methanesulfonylphenyl)pyran-2-ones (**49**)
R^1 = H; R^2 = CH_3: 6-methyl-3-(4-methanesulfonylphenyl)-4-phenylpyran-2-one (**50**)

Figure 11: Structures of 6-alkyl (alkoxy or alkylthio)-4-aryl-3-(4-methanesulfonylphenyl)pyrones.

A further group of compounds are the kavalactones **51** (Figure 12), e.g., yangonin (**52**, Figure 12), which have been isolated from *Piper methysticum* [57]. At various regions of the Pacific Ocean the roots of the plant have been used for a long time to produce a drink with sedative and anesthetic properties. The α-pyrones responsible for the influence on the nervous system have a wide variety of effects including amnestic, analgesic, anticonvulsant, anxiolytic, nootropic, and sedative/hypnotic activities [58].

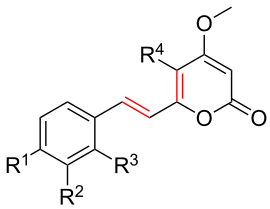

general structure of kavalactones (**51**)
marked C=C double bonds can be reduced to C–C
R^1 = OCH_3, R^2 = H, R^3 = H, R^4 = H: yangonin (**52**)

Figure 12: Structures of kavalactones.

Highly active α-pyrones, i.e., germicidins (**53**, **54**, Figure 13), were isolated from *Streptomyces viridochromogenes* NRRL B-1551, whereby the compounds had been detected in the supernatant of germinated spores, as well as in the supernatant of the submerged culture [59]. The excretion of these compounds prevents the germination of the spores too close to the

parent culture. Germination of *S. viridochromogenes* NRRL B-1551 spores is inhibited at pM concentrations, i.e., 200 pM (40 pg/mL). A comparable effect was also observed by applying **53** and **54** to seeds, however, only at much higher concentrations. Germination of *Lepidium sativum* (garden cress) seeds was clearly retarded. An additional in vitro effect was inhibition of porcine Na^+/K^+-activated ATPase. Germicidin was the first known autoregulative inhibitor of spore germination in the genus *Streptomyces* [59]. Influence on plant germination was also shown for further lactones. An inhibiting effect was proven for 3,4-dimethylpentan-4-olid from the plant pathogenic fungus *Hymenoscyphus pseudoalbidus*, which inhibited germination of *Fraxinus excelsior* (European ash) seeds [60]. In contrast, 3-methyl-2*H*-furo[2,3-*c*]pyran-2-one, a component of smoke derived from burning plant material, promotes seed germination [61].

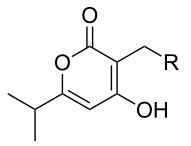

R = CH_3: germicin A (**53**)
R = H: germicin D (**54**)

Figure 13: Strutures of germicins.

Recently, a further regulatory function for α-pyrones within bacteria was discovered. The so called photopyrones (**8**–**15**, Figure 1) represent extracellular signals involved in cell–cell communication [14]. *Photorhabdus luminescens*, an entomopathogenic bacterium species, excretes these molecules, and binding of the latter to the respective receptor, i.e., the PluR protein, leads to the activation of the *Photorhabdus* clumping factor (PCF) operon (*pcfABCDEF*). The phenotypic change observed due to PCF expression was cell clumping, which in turn contributed to insect toxicity [14]. Structurally related are the pseudopyronines A (**55**), B (**56**), and C (**57**, Figure 14), which have been isolated from different *Pseudomonas* strains [62,63]. Compounds **55** and **56** had been initially tested positive for antimycobacterial and antiparasitic activities and both inhibited fatty acid biosynthesis [62]. The new derivative **57**, possessing a longer eastern acyl moiety, was identified in *Pseudomonas* sp. GM30, and it was subsequently proven by heterologous expression experiments with ketosynthase which is responsible for the biosynthesis of these derivatives [63].

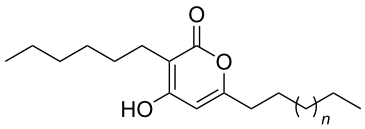

n = 1: pseudopyronine A (**55**)
n = 3: pseudopyronine B (**56**)
n = 5: pseudopyronine C (**57**)

Figure 14: Structures of the pseudopyronines.

1.3 Monobenzo-α-pyrones

Synthetic derivatives of the natural product 4-hydroxycoumarin are widely used as anticoagulant drugs. Warfarin (**58**, Figure 15) – initially introduced as a pesticide against rats and mice – is the most described oral anticoagulant drug in North America. The derivative phenprocoumon (**59**, Figure 15) is the most commonly used anticoagulant in Germany. Phenprocoumon was further identified as a lead template with HIV protease inhibitory activity, i.e., K_i = 1 μM [64]. However, the prototype of these anticoagulant drugs was dicoumarol (**60**), which was in use until it was replaced by other derivatives, e.g., **58** and **59** [65].

Aflatoxins are poisonous and cancer-causing monobenzo-α-pyrones [6]. Several derivatives exist, whereby aflatoxin B_1 (**61**, Figure 16) represents the most poisonous compound. Usually these toxins are ingested, but **61** can also permeate through the skin. The aflatoxins are PKS-derived molecules which undergo an extreme rearrangement [66]. The cytotoxic effects of the coumarin derivatives umbelliferone (**4**, Figure 1), esculetin (**5**, Figure 1), and scopoletin (**6**, Figure 1) are subject of anticancer research [67]. Marmesin (**62**) was first isolated from the fruits of *Ammi majus* [67], and is currently under investigation as an agent for the treatment of angiogenesis-related diseases, e.g., cancer [68]. A structurally related compound, i.e., isopim-

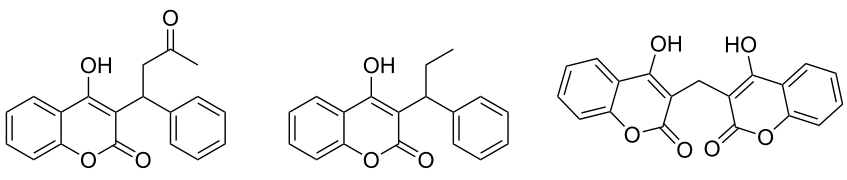

warfarin (**58**) phenprocoumon (**59**) dicoumarol (**60**)

Figure 15: The structures of the monobenzo-α-pyrone anticoagulant drugs warfarin and phenprocoumon.

pinellin (**63**), was also first isolated from fruits of *Ammi majus* [69]. It was shown that **63** blocks DNA adduct formation and skin tumor initiation in mice [70]. Psoralen (**64**), isolated from plants, e.g., *Ficus carica*, had been used against skin diseases due to its mutagenic effect [71].

Bacterial monobenzo-α-pyrones were isolated from the myxobacterium *Stigmatella aurantiaca* MYX-030. Myxocoumarins A (**65**) and B (**66**) were identified, and **65** was tested for antifungal activity [72]. It showed a promising activity against agronomically important pathogens, e.g., complete inhibition of *Magnaporthe grisea* and *Phaeosphaeria nodorum* at 67 μg/mL, and *Botrytis cinerea* was inhibited at 200 μg/mL.

2 Biosynthesis

Even though the α-pyrones possessing interesting activities were in the focus of chemical synthesis approaches for a long time, for most of them the clarification of the biosynthesis remained unknown for many years.

An early example for a biosynthetic hypothesis is the biosynthesis of the simple 6-pentyl-α-pyrone (**29**), which was hypothesized to start with the C-18 linoleic acid. This acid is then shortened by β-oxidation reactions to a C-10 intermediate, i.e., 5-hydroxy-2,4-decenoic acid (**72**), which undergoes lactonization to yield **29** (Figure 17) [34]. This hypothesis is based on the fact that feeding studies with *Trichoderma harzianum* and *T. viride* using [U-^{14}C]linoleic acid or [5-^{14}C]sodium mevalonate revealed the incorporation of these labelled compounds into 6-pentyl-α-pyrone (**29**). Labelled sodium mevalonate was used to test for the possible link between the isoprenic pathway and biosynthesis of **29**. The experiments revealed that the incorporation of labelled linoleic acid reached within the first 24 hours 18-fold higher ratios than labelled sodium mevalonate. Therefore, the authors suggested that β-oxidation of linoleic acid is a probable main step in the biosynthetic pathway of **29** in *Trichoderma* species [34]. The incorporation of labelled sodium mevalonate is hypothesized to be due to degradation to acetate with following polymerization to fatty acids [34].

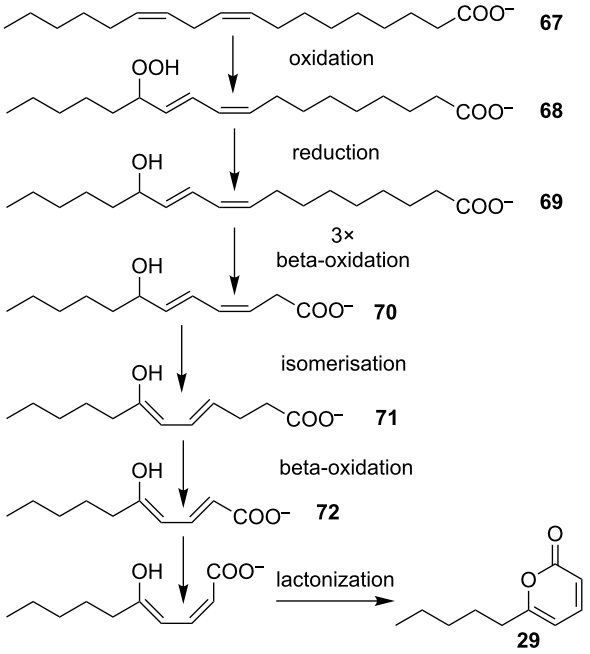

Figure 17: Hypothetical pathway of **29** generation from linoleic acid [34].

Now, it is generally accepted that most α-pyrones are synthesized via the polyketide pathway. Solely for plant-derived ellagitannins another biosynthetic origin was described. Via the shikimate pathway gallic acid is generated, which represents the precursor in ellagitannin biosynthesis [73]. The ellagitannins

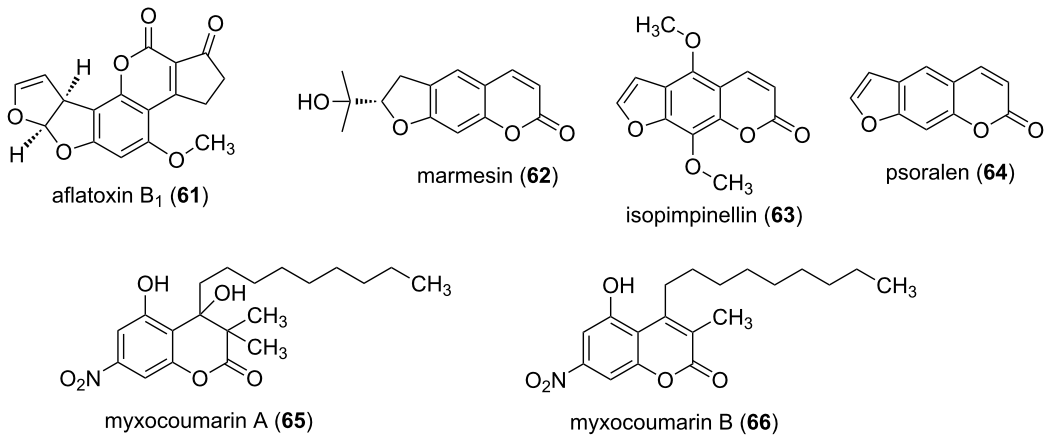

Figure 16: Structures of selected monobenzo-α-pyrones.

can then be hydrolyzed to ellagic acid (**22**), and subsequently converted to urolithins (**23**–**27**). In microorganisms the PKS-derived origin was independently postulated for numerous compounds. The polyketide biosynthesis has much in common with fatty acid biosynthesis: The mechanisms of chain elongation resemble each other, and simple building blocks, e.g., acetyl-CoA and malonyl-CoA, are used to build up the molecule [74]. In general both, polyketides and fatty acids are assembled by repeating Claisen-condensations between an activated acyl-starter unit and malonyl-CoA-derived extender units. This process is catalyzed by the concerted action of a ketosynthase (KS), an acyltransferase (AT), and either a phosphopantetheinylated acyl carrier protein (ACP), or CoA to which the nascent chain is attached. After each elongation step the β-keto functionality can be reduced by further enzymes involved. In fatty acid biosynthesis usually a complete reductive cycle takes place, i.e., a ketoreductase (KR) generates a hydroxy group, a dehydratase (DH) reduces to an alkene double bond, and an enoyl reductase (ER) yields a completely saturated acyl-backbone. These reductive steps are optional in PKS biosynthesis, and considering the pyrone ring formation, an unsaturated PKS chain residue attached to the carrier is essential. This general PKS catalyzed mechanism is accomplished by different enzymatic machineries. In the following section the three PKS types which can be responsible for the biosynthesis of the polyketide chain are described. A strong indication was that in the genome of the alternariol producer *Alternaria alternate* two PKS genes, i.e., *pksJ* and *pksH*, had been identified, whose expression pattern was in correlation with alternariol (**17**) production [75]. Mutant strains with downregulated expression level for these PKSI systems were constructed and suggested that PksJ is the PKS required for the biosynthesis of **17**. PksH downregulation affected *pksJ* expression and in that way influenced biosynthesis of **17** as well. The initially postulated biosynthesis via norlichexanthone was ruled out by incorporation studies in *Alternaria tenuis* using [1-^{13}C, $^{18}O_2$]-labeled acetate. This resulted in high incorporation of acetate-derived oxygen into all the oxygen-bearing carbons [76]. A proposed biosynthetic pathway of **17** [77] (by aromatization of a polyketide), and of derivatives (by post-PKS reactions) is shown in Figure 18. The authors suggested that seven malonyl-CoA building blocks are connected via Claisen-condensation reactions, followed by aldol-type cyclizations between C-2 and C-7, as well as between C-8 and C-13. The subsequent lactonization yields alternariol (**17**). However, it can be assumed that the starter molecule should be acetyl-CoA. Through subsequent chain elongation by six malonyl-CoA extender units the linear chain is assembled. It has to be mentioned, that there is still an ongoing debate about the real alternariol-producing PKS in *A. alternate*, but the building blocks and the general mechanism are accepted [78].

2.1 Biosynthesis by PKSI systems

The biosynthesis of an α-pyrone by a modular PKSI system will be showcased using the phenylnannolone (**73**–**75**, Figure 19) pathway (Figure 20) [79]. The aromatic starter is cinnamic acid, which is elongated by a butyrate moiety. Subsequently three further elongation steps, this time using malonate as extender units, follow. This results in the incorporation of acetate units via Claisen-condensation reactions. The reductive domains, i.e., ketoreductase (KR) and dehydration (DH) domains, present in the distinct modules reduce the keto group in a stepwise manner to the hydroxy group and the C=C double bond. Subsequently, the KR present in the terminal module catalyzes the reduction of the β-keto group to an L-hydroxy group. This hydroxy is then further reduced by the catalytic activity of the DH in the

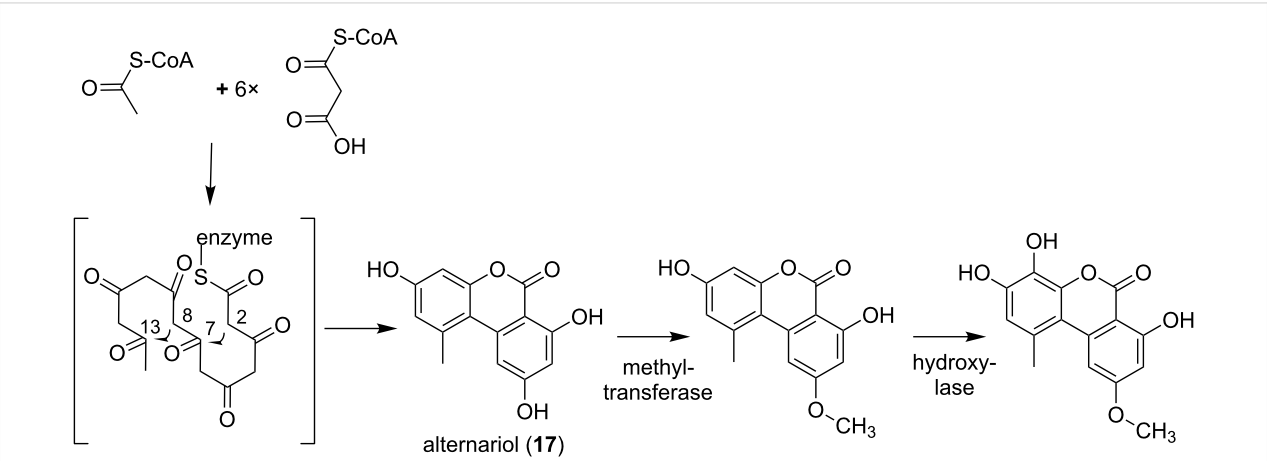

Figure 18: Proposed biosynthetic pathway of alternariol (modified from [77]). Malonyl-CoA building blocks are applied to build up the enzyme-bound polyketide chain. Cyclization between C-2, C-7 and C-8, C-13, as well as lactonization takes place, resulting in alternariol (**17**). Subsequently, a methylation and a hydroxylation reaction occur, catalyzed by the respective enzymes.

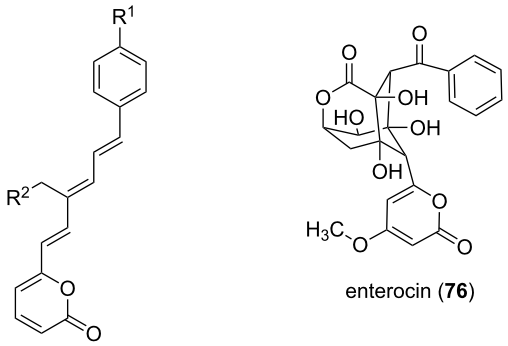

phenylnannolone A: R^1 = H, R^2 = CH_3 (**73**)
phenylnannolone B: R^1 = H, R^2 = H (**74**)
phenylnannolone C: R^1 = OH, R^2 = CH_3 (**75**)

Figure 19: Structures of phenylnannolones and of enterocin, both biosynthesized via polyketide synthase systems.

terminal module, which results in a *cis*-configured double bond. Through the formation of the *cis* double bond the sterical arrangement of the nascent chain favors the lactone ring closure which results in the α-pyrone moiety. Hence, the polyketide is released from the assembly line, whereby the thioesterase (TE) domain catalyzes the ring-closure and therewith also the off-loading from the PKSI system [79]. A comparable mechanism, in which a TE is involved in off-loading the nascent chain from the PKS assembly line by lactonization, was described for other natural products, e.g., the isochromanone ring formation for the ajudazols A and B in *Chondromyces crocatus* Cm c5 [80].

2.2 Biosynthesis by PKSII systems

In the type II PKS-catalyzed biosynthesis, the subunit type of such megaenzyme systems, the starter molecule and the extender units, mostly malonate molecules, are assembled at the same ACP. A lactonization at the ACP-bound terminus yields the pyrone ring. As an example the enterocin (**76**, Figure 19) biosynthesis will be regarded (Figure 20). In the marine bacterium *Streptomyces maritimus* a gene cluster corresponding to enterocin (*enc*) biosynthesis was identified [81]. The minimal *enc* PKS, EncABC, is encoded by a set of genes architecturally similar to most other type II PKS clusters. EncA represents the KSα, EncB the KSβ, and EncC the ACP domain. First, an uncommon benzoate starter unit gets elongated by seven malonate molecules. This nascent carbon chain undergoes a rare Favorskii-like rearrangement and lactonization to yield the polyketide **76**.

2.3 Biosynthesis by PKSIII systems

Type III PKSs are relatively small molecules, since in contrast to the PKSs of type I and II they solely consist of a single ketosynthase. A single KS connects the CoA-bound starter and extender units; and also in this system the final lactonization of the peptide-bound polyketide chain results in the pyrone ring. Type III systems synthesize a variety of aromatic polyketides. First discovered in plants, later PKS III systems have also been described in fungi and bacteria. BpsA (for *Bacillus* pyrone synthase) was analyzed in vivo and in vitro [82]. These experiments revealed BpsA to be indeed the enzyme responsible for the synthesis of triketide pyrones. The substrates used by BpsA are long-chain fatty acyl-CoAs and malonyl-CoAs – either as starter or as elongation building blocks, respectively (Figure 20). Generating *B. subtilis* mutant strains, overexpressing the *bpsA* gene, yielded in triketide pyrenes. Once the adjacent gene *bpsB*, the latter coding for a methyltransferase, was co-overexpressed, the methylated variants, i.e., triketide pyrone methyl ethers, were synthesized. The pyrone-forming activity of BpsA was also proven in vitro, using heterologously expressed protein. Thereby, the chain length of the acyl residue had only minor influence on the pyrone formation, since many substrates had been accepted. This could be expected, since the α-pyrone formation takes place at the enzyme-tethered end of the nascent chain, resulting in off-loading.

2.4 Biosynthesis by free-standing ketosynthases

In contrast to the α-pyrone formation by intramolecular cyclization reactions, also the condensation of two polyketide chains can result in a pyrone ring. Such a mechanism was indicated by feeding experiments for the antibiotically active compounds **36** [83] and **34** [84]. The resulting labeling pattern clearly showed that the central α-pyrone ring of the molecule was not the result of a usual intramolecular reaction. Rather, an interconnection of two independent chains should form the central ring structure. In addition further molecules, e.g., photopyrones (**8**–**15**) from *Photorhabdus luminescens* are synthesized by such a head-to-head condensation of two acyl moieties [60]. Also the csypyrones (**79**–**81**, Figure 21), first reported from *Aspergillus oryzae*, are composed of two independent chains which are interconnected thereafter [85]. Recently, the biosynthetic origin of the pseudopyronines A (**55**) and B (**56**) in *Pseudomonas putida* BW11M1 was clarified – and again two chains are fused to yield the final products [86]. Thus, it can be assumed that this mechanism is exemplified quite often in natural products. Therefore, in the next paragraph the chain interconnecting mechanism will be described.

For α-pyrone antibiotics, the corallopyronin and myxopyronin derivatives, free-standing KSs encoded in the respective cluster, i.e., CorB and MxnB, were suggested as the chain-interconnecting enzymes [84,87]. These enzymes have now been investigated in detail.

In vitro assays using NAC thioesters of the western and eastern chains in the biosynthesis of **36** [88], as well as simplified sub-

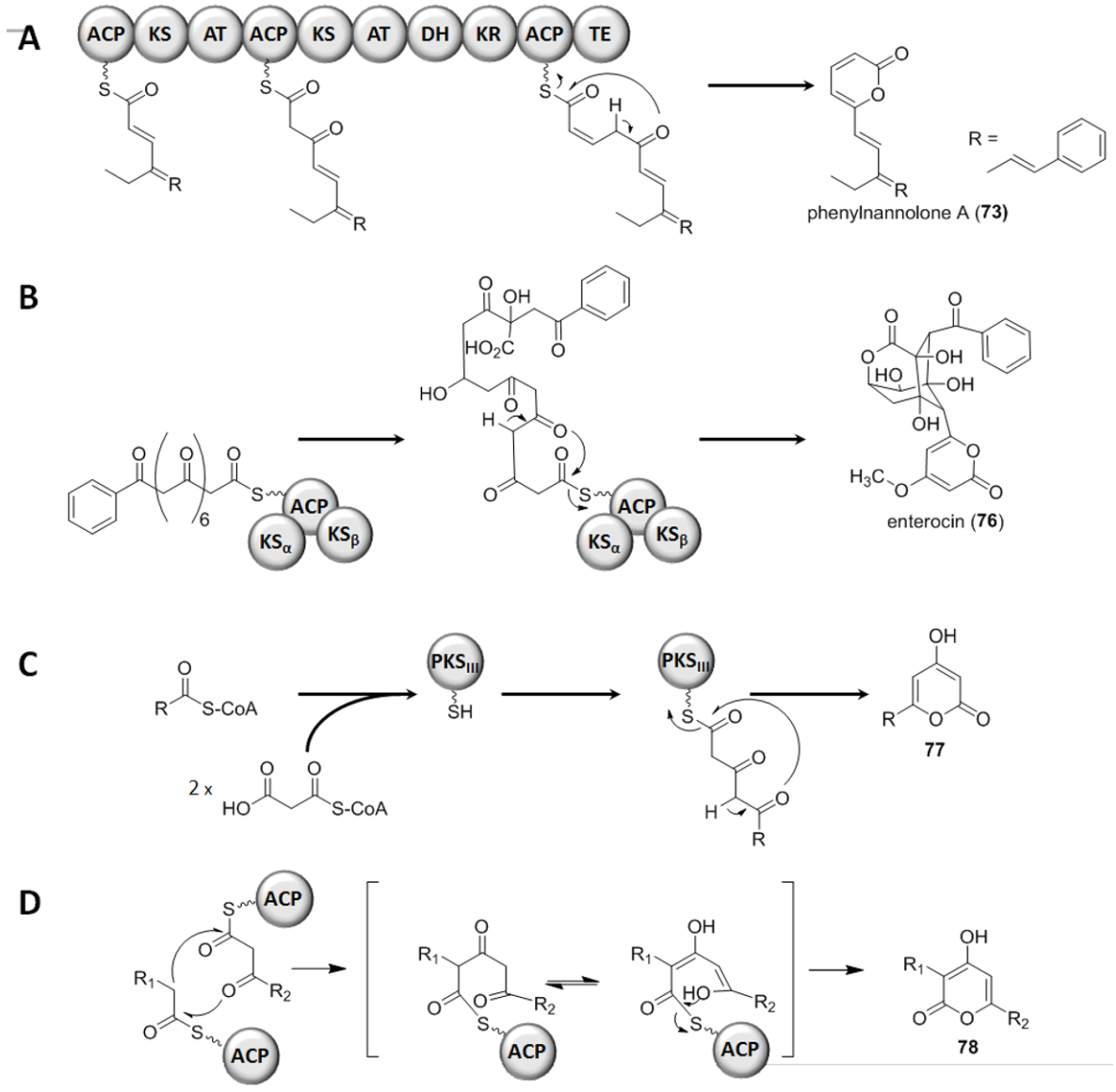

Figure 20: Pyrone ring formation. Examples for the three types of PKS systems are shown in A–C. In D the mechanism catalyzed by a free-standing ketosynthase is depicted. Herein the keto–enol tautomerism is shown. A) Polyketide synthase (PKS) type I: The end part of the phenylnannolone A biosynthesis is given. The ACP-tethered nascent chain gets elongated by the incorporation of acetate units. The corresponding reductive domains (ketoreductase, KR; and dehydratase, DH) reduce the β-keto group to a *cis* double bond. The chain is then released from the assembly line through pyrone ring formation catalyzed by the thioesterase (TE) domain, resulting in **73**. B) PKS type II: The precursor of the enterocin biosynthesis, comprising the uncommon benzoate starter unit, is shown attached to the ACP domain, which forms a complex with the KS_α and the KS_β domain. Modification, rearrangement and lactonization of this bound precursor yield enterocin (**77**). C) PKS type III: The starter molecule, e.g., a CoA-activated fatty acid, gets loaded to the PKS III enzyme. Two rounds of chain elongation via malonyl-CoA take place before the molecule is released by pyrone ring formation, resulting in **77**. D) The two ACP-tethered chains are interconnected by the catalytic activity of a free-standing KS. In the second step the lactonization takes place, facilitated by the keto–enol tautomerism. Thereby the α-pyrone **78** is formed.

strate mimics of both antibiotics [88,89] provided experimental evidence that the free-standing ketosynthases are responsible for the α-pyrone ring formation. In both publications non-enzymatic condensation was ruled out, since in the absence of the respective protein no product formation was detectable. For MxnB it was further shown that in vitro conditions can be optimized by applying carrier-protein-bound substrates instead of the SNAC-coupled substrates, i.e., this resulted in a 12-fold increase of product formation. This is an additional hint that protein–protein interactions represent an important factor in PKS systems. Further, it seemed that the carrier proteins conferred specificity for α-pyrone ring formation, since once the carrier proteins were primed in each case with the other substrate (mimic), the production rate decreased significantly.

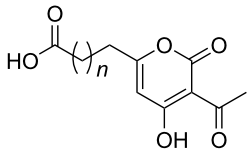

csypyrone B1: *n* = 1 (**79**)
csypyrone B2: *n* = 2 (**80**)
csypyrone B3: *n* = 3 (**81**)

Figure 21: Structures of csypyrones.

However, a certain degree of flexibility in α-pyrone ring formation was proven by the in vitro experiments using the ketosynthases CorB and MxnB. In addition, the substrate specificity was analyzed in vivo in a mutasynthesis study employing a *Myxococcus fulvus* mutant unable to biosynthesize the western chain. This study revealed that MxnB is capable of condensing a wide variety of activated synthetic western chains with the carrier protein bound native eastern chain [90].

The two proposed mechanism for CorB and MxnB closely resembles each other, but certain differences have also been proposed, as will be discussed here. First, one chain is transferred and covalently linked to the active-site cysteine. This results in an activation of the cysteine-tethered chain. In the second step, the other chain is placed into the proximal cavity, orienting the α-carbon in a position suitable for the nucleophilic attack by the cysteine-tethered, activated chain. Thereby, the second chain is still attached to the ACP, the phosphopantetheine residue reaching into the T-shaped catalytic cavity, enabling the placement of the two chains in opposite directions (Figure 22 and Figure 23). In that way a nucleophilic attack of the enzyme-bound chain onto the carbonyl carbon of the ACP-tethered chain is facilitated. Hence, a diketothioester is formed, which results in chain interconnection and the release of the catalytic cysteine. Subsequently, lactonization can take place. It is assumed that an enolate exists as an intermediate in the formation of the C–O bond [88]. Even though for both enzymes no experimental evidences for the chronological order of the two condensation reactions exist, it can be expected that the C–C

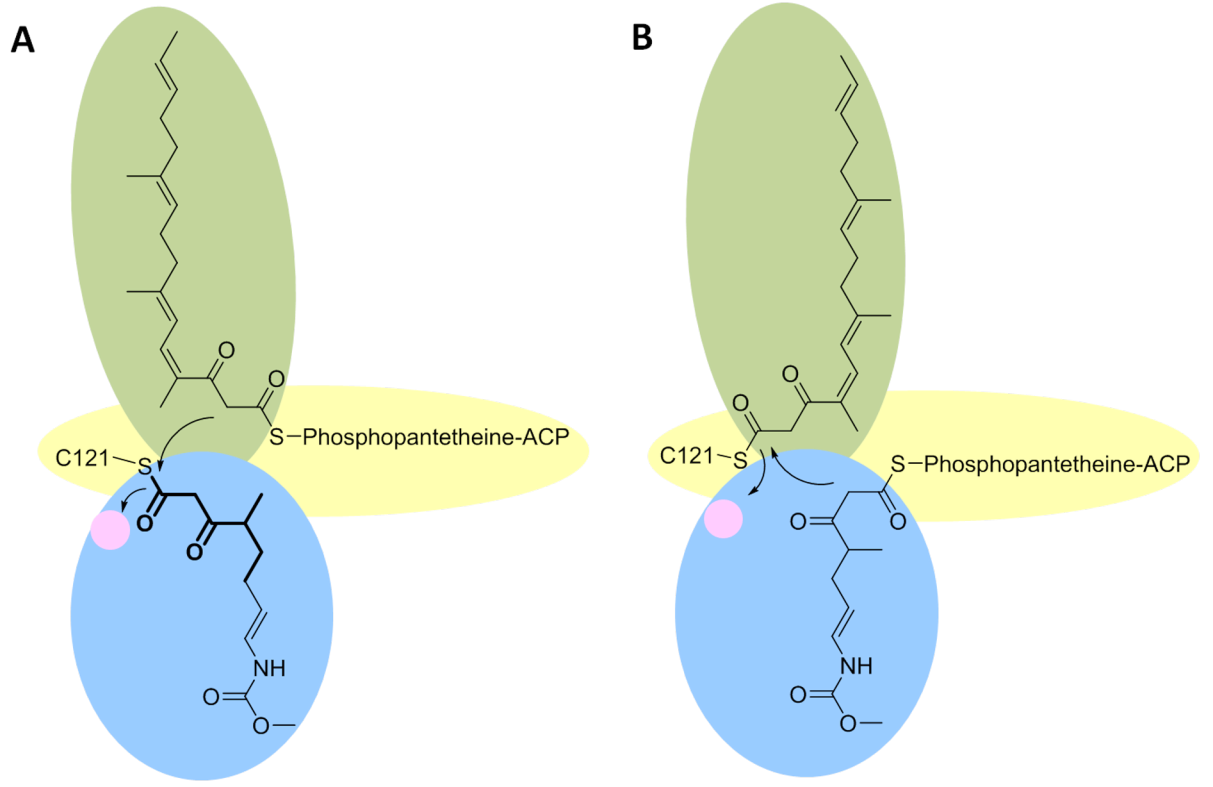

Figure 22: Schematic drawing of the T-shaped catalytic cavities of the related enzymes CorB and MxnB. The two cavities, each harboring one chain are depicted in green and blue, respectively. The phosphopantetheine arm of the ACP reaches into the T-shaped catalytic cavity through a third hydrophobic channel. The oxyanion hole is highlighted by a pink circle. In that way the two chains are positioned face to face. A) Transacylation of the eastern chain to C_{121} of CorB. The simplified mimic of the eastern chain (shown in bold) was placed into the active site on the basis of its unbiased (F_0–F_c)-difference electron density. The remaining portion of the eastern chain was modeled into the cavity. B) Transacylation of the western chain to the catalytic C_{121} of MxnB. In vitro experiments assaying MxnB together with substrate mimics indicate the transacylation of the western chain as the natural mechanism. It can be assumed that different chains alter the binding preferences for CorB and MxnB.

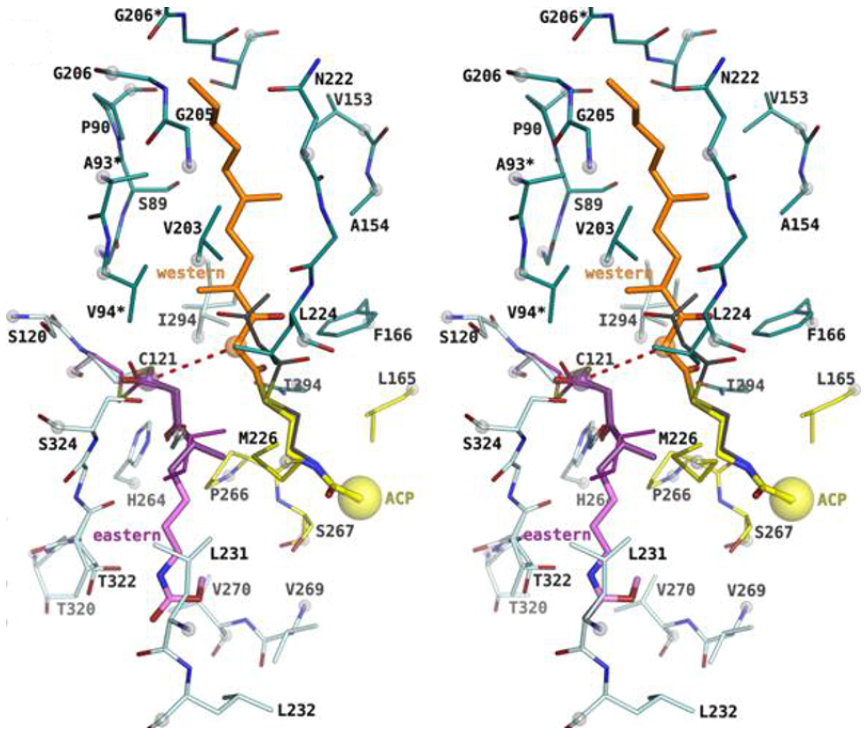

Figure 23: Stereo representation of the CorB binding situation (modified from [89]). The substrate mimic (dark violet) was placed into the active site on the basis of its unbiased (F_0–F_c)-difference electron density and the remaining portion of the eastern chain (light magenta) was modeled into the cavity. The western chain was modeled into the proximal cavity on the basis of a homologue α-pyrone synthase using the pantotheine entity as an anchor point.

bond is formed prior to lactonization [88]. For the following lactonization process a spontaneous reaction can be anticipated, which takes place once the two chains are interconnected, since thereby the atoms needed for lactonization are positioned in close proximity to each other. The sterical requirements within the catalytic cavity of CorB and MxnB do not favor the ring closure, thus the second step might take place in solution [90].

It has to be mentioned that the results between CorB and MxnB differ slightly. The in vitro results obtained for MxnB imply that the western chain gets covalently attached, prior to condensation with the second chain. The transfer of the western chain from the corresponding ACP to MxnB occurred much faster than the transfer of the eastern chain [88]. However, concerning CorB it was possible to observe a substantial positive electron density at the catalytic cysteine as a result of substrate incubation prior to crystallization. This was only possible with a very short substrate mimic which renders more similarity to the eastern chain. Using the longer western chain mimic no suitable crystals for structure determination could be produced (neither for CorB, nor for MxnB). Thus, in the CorB model the eastern chain was covalently attached. These inconsistent results indicate that the use of different chains could alter the binding preference.

Also CsyB from *Aspergillus oryzae* catalyzes the condensation of two β-ketoacyl-CoAs [85]. However, this mechanism to form 3-acetyl-4-hydroxy-6-alkyl-α-pyrones (**79–81**) significantly differs from the one catalyzed by the myxobacterial ketosynthases described before [89]. CsyB is indeed an up to now unexemplified case of a type III PKS with dual function. First, CsyB catalyzes chain elongation – as many other PKS III enzymes. Secondly, it catalyzes the condensation of two β-ketoacyl units – a mechanism comparable to the enzymes described in the previous paragraph. It possesses two β-ketoacyl-CoA coupling activities to synthesize acylalkylpyrone. The initially proposed mechanism for the formation of 3-acetyl-4-hydroxy-6-alkyl-α-pyrone by CysB was the coupling of a β-keto fatty acid acyl intermediate with acetoacetyl-CoA, followed by pyrone ring formation (Figure 24 A) [85]. Then, as the crystal structure was solved the authors proposed the detailed mechanism as follows [91]: First, acetoacetyl-CoA is loaded onto the catalytic cysteine residue. Subsequently, the thioester bond is cleaved by the nucleophilic water molecule, which itself is activated through hydrogen bonding to the catalytic cysteine and a histidine residue. Thereby, the β-keto acid intermediate is generated. This intermediate is proposed to be placed within the novel pocket, a cavity accessible from the conventional elongation/cyclization pocket. After the replacement of the first β-keto acid, the second

β-ketoacyl unit is produced. The catalytic cavity of CysB is loaded with a fatty acyl-CoA which is elongated with one molecule of malonyl-CoA, yielding the second β-ketoacyl chain. Condensation of the two chains generates the final product, whereby first the two chains are interconnected due to a nucleophilic attack, and subsequently an intramolecular lactonization takes place. In that way the ring closure results in the elimination of a water molecule, yielding the csypyrones harboring four *O*-atoms. The first step of the proposed mechanism was deligated from a set of in vitro assays, which indicated that the ^{18}O atom of the $H_2{}^{18}O$ molecule – which should be activated by hydrogen bonds networks with a histidine and the catalytic cysteine residue – is enzymatically incorporated into the final product (Figure 24 B). However, this mechanism is hard to prove, because ^{18}O incorporation into the molecule can occur due to spontaneous exchange. Anyway, CysB clearly differs from CorB and MxnB. The latter condense two β-ketoacyl chains in a Claisen-like reaction to form the α-pyrone, while CysB should first generate a β-keto acid intermediate by hydrolysis of the thioester bond. Then the starter of the second chain is loaded onto the free catalytic cysteine, gets elongated by a malonyl-CoA before the nucleophilic attack of the first chain. In that way the thioester bond is cleaved and subsequently lactonization takes place, yielding in the final product (Figure 24 B).

In *Photorhabdus luminescens* it was shown that α-pyrones act as bacterial signaling molecules at low nanomolar concentrations [14]. A similar mechanism for the biosynthesis of these photopyrones as for the above mentioned α-pyrone antibiotics myxo- and corallopyronin was expected. To identify the gene corresponding to the biosynthesis of these so-called photopyrones, all ketosynthases which are not part of the usual fatty acid biosynthesis had been identified in the genome of *P. luminescens*. Thereby the ketosynthases neighbored by genes related to fatty acid synthesis had not been considered. Insertion mutants were generated and the influence on photopyrone production was analyzed. Thus, the gene *ppyS* (for photopyrone synthase) was identified, since all other disruption mutants did not yield in a photopyrone negative strain. Heterologous expres-

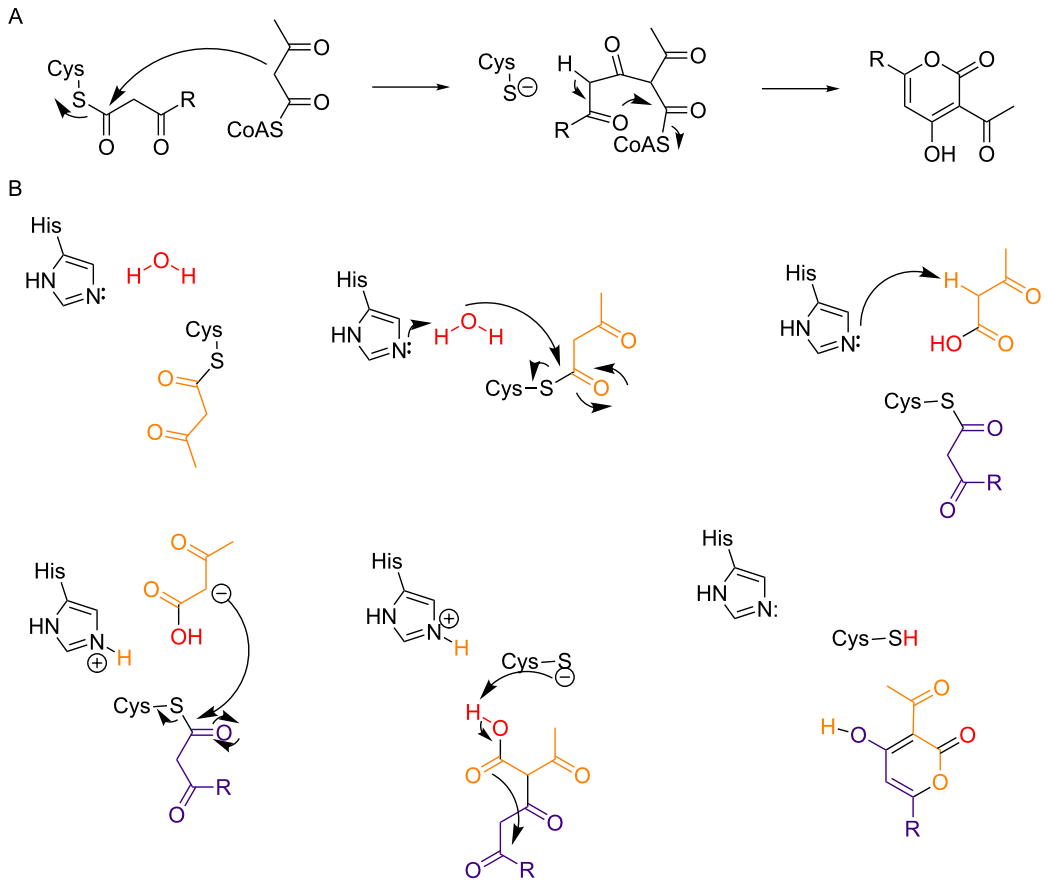

Figure 24: Proposed mechanism for the CsyB enzymatic reaction. A) Coupling reaction of the β-keto fatty acyl intermediate with acetoacetyl-CoA followed by pyrone ring formation (modified from [85]). B) Detailed mechanism; the two chains are color coded (orange and violet), as well as the water molecule (red) whose oxygen atom is incorporated into the α-pyrone (modified from [91]).

sion of *ppyS* in *E. coli*, together with the *bkdABC* operon (encoding the branched chain α-ketoacid dehydrogenase (Bkd) complex) and *ngrA* (encoding a phosphopantetheinyl-transferase which is essential to generate the *holo*-acyl carrier protein BkdB) for the biosynthesis of branched-chain iso-fatty acid, resulted in the production of photopyrone derivatives. This was a functional proof that PpyS catalyzes the formation of α-pyrones, as indicated before by feeding experiments with stable isotope-labeled precursors. PpyS should connect 5-methyl-3-oxohexanoyl thioester and different thioesters of straight-chain and iso-branched chain fatty acids [14]. The mechanism proposal also includes the catalytic cysteine. The first chain, i.e., thioester-activated 9-methyldecanoic acid, gets covalently tethered to that important residue within the active site. This reflects the same mechanism as for the other KS-like enzymes described. Also for PpyS the proposal postulates that the α-carbon of the enzyme-bound chain acts as a nucleophile. Thus, this activated carbon executes a nucleophilic attack on the carbonyl carbon of chain two, i.e., 5-methyl-3-oxohexanoyl thioester, which is itself synthesized by the Bkd complex. In that way a C–C bond is formed, and both chains are still attached to the catalytic cysteine residue. This bound intermediate undergoes a further deprotonation, which enables the formation of the α-pyrone ring. Through the ring closure the α-pyrone is released from PpyS. This second deprotonation can occur spontaneously, or enzyme catalyzed. In contrast to the cases of myxopyronins **36** and **37** and corallopyronins **34** and **35**, no PKSI system provides the ACP-bound chains. Therefore, the substrates for the chain interconnection might be either ACP or CoA bound. This would be depending on their origin in the cell, either fatty acid biosynthesis or degradation. The flexibility of the system in regard to the first chain to be bound to PpyS was already shown by the photopyrones A–H, which differ in the chain length and in the either branched or unbranched starting unit.

No crystal structure for PpyS exists. Therefore, the structure was modeled using OleA from *Xanthomonas campestris*, which is showing the highest sequence identity (27%) of all available PDB-deposited crystal structures as template. Using the generated homodimeric model of PpyS, docking studies of the substrates onto the catalytic cysteine were performed. The resulting model suggested that a glutamate residue, which reaches into the catalytic cavity of the respectively other homodimer, acts as a base by forming a hydrogen bond with the α-carbon of the covalently bound substrate (Figure 25). Indeed, the exchange of this glutamate against an alanine residue resulted in an inactive version of the protein. Further an arginine residue, which could be involved in dimerization, was mutated to an aspartate. Also this mutant lost its catalytic activity, indicating that dimerization is essential [63].

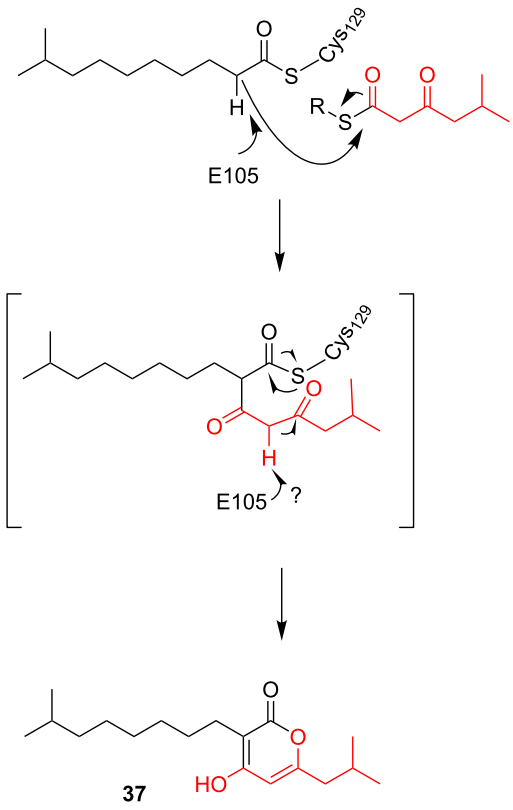

Figure 25: Proposed biosynthesis of photopyrone D (**37**) by the enzyme PpyS from *P. luminescens* (modified from [63]). The catalytic cysteine and the glutamate residue postulated to be involved in the biosynthesis are indicated. The two chains are colored in red and black, respectively.

The pseudopyronine synthase PyrS represents a homologue of PpyS. Using PpyS from *Pseudomonas* sp. GM30, it was analyzed if this KS is also involved in the formation of α-pyrones. The two pseudopyronines A (**55**) and B (**56**) have been up to now isolated from different *Pseudomonas* strains. Recently, in an independent publication **55** and **56** have been rediscovered from the banana rhizobacterium *Pseudomonas putida* BW11M1 [86]. Feeding studies with isotopically labelled precursors supported the biosynthesis from two chains. Subsequent analysis of the draft genome of the strain revealed a *ppyS* homologue. However, instead of the syntenic genomic region where pseudomonads usually harbor the *ppyS* homologue, it appeared that the gene has inserted between genes belonging to carbohydrate metabolism in *P. putida* BW11M1. An in-frame deletion mutant of the *ppyS* homologue was constructed and yielded in a strain which lost the opportunity for pseudopyronine biosynthesis [86]. Despite the similar mechanism for α-pyrone formation by PpyS homologues in the different *Pseudomonas* strains, a phylogenetic analysis revealed that different clades of PpyS exist. These different clades reflect also different locations in the genome sequences of the differ-

ent *Pseudomonas* species: On a taxonomic level closely related strains harbor the *ppyS* homologue in the same region of their genome. Therefore, it can be assumed that the genetic information coding for the enzyme needed to synthesize pseudopyronines was acquired several times. Hence, Pseudomonas species from different habitats, e.g., rhizosphere, soil, water, acquired the gene set independently [86].

In summary different types of chain-interconnecting KSs which catalyze α-pyrone ring formation were identified in the last years. One mechanism is to fuse two ketoacyl moieties, as exemplified by CorB and MxnB. Another mechanism is the fusion of one ketoacyl moiety with one acyl moiety, as shown for PpyS-like KSs. All evolved from FabH-type KSs, but form different clades in phylogenetic analyses. PpyS-like enzymes show the conserved glutamate residue – indicating a mechanism distinct from the ketoacyl–ketoacyl-connecting KSs – and were identified in different bacterial genera, i.e., *Burkholderia, Legionella, Nocardia, Microcystis* and *Streptomyces*, therewith also in clinically relevant pathogens [63]. Future work will reveal which natural products are biosynthesized by such KSs, and which relevance these products have.

Conclusion

The α-pyrones show an extraordinary wide variation in biological activities, independently if structurally simple or complex, naturally or non-naturally synthesized. Therefore, α-pyrones represent a rich source for isolation studies and lead discovery. Now, new insights into the biosynthesis of these molecules through chain interconnecting ketosynthases were obtained. This opens up the possibility to use these enzymes as tools; both, in bio- as well as in semi-synthetic approaches. The potential of these enzymes in combinatorial biosynthesis has to be further evaluated in the future.

Acknowledgements

The German Federal Ministry of Education and Research is thanked for funding.

References

1. McGlacken, G. P.; Fairlamb, I. J. S. *Nat. Prod. Rep.* **2005,** *22,* 369–385. doi:10.1039/b416651p
2. Fairlamb, I. J. S.; Marrison, L. R.; Dickinson, J. M.; Lu, F.-J.; Schmidt, J. P. *Bioorg. Med. Chem.* **2004,** *12,* 4285–4299. doi:10.1016/j.bmc.2004.01.051
3. Suzuki, K.; Kuwahara, A.; Yoshida, H.; Fujita, S.; Nishikiori, T.; Nakagawa, T. *J. Antibiot.* **1997,** *50,* 314–317. doi:10.7164/antibiotics.50.314
4. Kondoh, M.; Usui, T.; Kobayashi, S.; Tsuchiya, K.; Nishikawa, K.; Nishikiori, T.; Mayumi, T.; Osada, H. *Cancer Lett.* **1998,** *126,* 29–32. doi:10.1016/S0304-3835(97)00528-4
5. Calderón-Montaño, J. M.; Burgos-Morón, E.; Orta, M. L.; Pastor, N.; Austin, C. A.; Mateos, S.; López-Lázaro, M. *Toxicol. Lett.* **2013,** *222,* 64–71. doi:10.1016/j.toxlet.2013.07.007
6. Villers, P. *Front. Microbiol.* **2014,** *5,* No. 158. doi:10.3389/fmicb.2014.00158
7. Musa, M. A.; Cooperwood, J. S.; Khan, M. O. F. *Curr. Med. Chem.* **2008,** *15,* 2664–2679. doi:10.2174/092986708786242877
8. Thaisrivongs, S.; Romero, D. L.; Tommasi, R. A.; Janakiraman, M. N.; Strohbach, J. W.; Turner, S. R.; Biles, C.; Morge, R. R.; Johnson, P. D.; Aristoff, P. A.; Tomich, P. K.; Lynn, J. C.; Horng, M.-M.; Chong, K.-T.; Hinshaw, R. R.; Howe, W. J.; Finzel, B. C.; Watenpaugh, K. D. *J. Med. Chem.* **1996,** *39,* 4630–4642. doi:10.1021/jm960228q
9. Poppe, S. M.; Slade, D. E.; Chong, K. T.; Hinshaw, R. R.; Pagano, P. J.; Markowitz, M.; Ho, D. D.; Mo, H.; Gorman, R. R., III; Dueweke, T. J.; Thaisrivongs, S.; Tarpley, W. G. *Antimicrob. Agents Chemother.* **1997,** *41,* 1058–1063.
10. Turner, S. R.; Strohbach, J. W.; Tommasi, R. A.; Aristoff, P. A.; Johnson, P. D.; Skulnick, H. I.; Dolak, L. A.; Seest, E. P.; Tomich, P. K.; Bohanon, M. J.; Horng, M.-M.; Lynn, J. C.; Chong, K.-T.; Hinshaw, R. R.; Watenpaugh, K. D.; Janakiraman, M. N.; Thaisrivongs, S. *J. Med. Chem.* **1998,** *41,* 3467–3476. doi:10.1021/jm9802158
11. Yeh, P.-P.; Daniels, D. S. B.; Cordes, D. B.; Slawin, A. M. Z.; Smith, A. D. *Org. Lett.* **2014,** *16,* 964–967. doi:10.1021/ol403697h
12. Liaw, C.-C.; Yang, Y.-L.; Lin, C.-K.; Lee, J.-C.; Liao, W.-Y.; Shen, C.-N.; Sheu, J.-H.; Wu, S.-H. *Org. Lett.* **2015,** *17,* 2330–2333. doi:10.1021/acs.orglett.5b00739
13. Charlton, R. E.; Webster, F. X.; Zhang, A.; Schal, C.; Liang, D.; Sreng, I.; Roelofs, W. L. *Proc. Natl. Acad. Sci. U. S. A.* **1993,** *90,* 10202–10205. doi:10.1073/pnas.90.21.10202
14. Brachmann, A. O.; Brameyer, S.; Kresovic, D.; Hitkova, I.; Kopp, Y.; Manske, C.; Schubert, K.; Bode, H. B.; Heermann, R. *Nat. Chem. Biol.* **2013,** *9,* 573–578. doi:10.1038/nchembio.1295
15. Lee, J. S. *Mar. Drugs* **2015,** *13,* 1581–1620. doi:10.3390/md13031581
16. Dickinson, J. M. *Nat. Prod. Rep.* **1993,** *10,* 71–98. doi:10.1039/np9931000071
17. Harvan, D. J.; Pero, R. W. *Adv. Chem. Ser.* **1976,** *149,* 344–355. doi:10.1021/ba-1976-0149.ch015
18. Luo, H.; Liu, H.; Cao, Y.; Xu, D.; Mao, Z.; Mou, Y.; Meng, J.; Lai, D.; Liu, Y.; Zhou, L. *Molecules* **2014,** *19,* 14221–14234. doi:10.3390/molecules190914221
19. Song, Y. C.; Huang, W. Y.; Sun, C.; Wang, F. W.; Tan, R. X. *Biol. Pharm. Bull.* **2005,** *28,* 506–509. doi:10.1248/bpb.28.506
20. Griffin, G. F.; Chu, F. S. *Appl. Environ. Microbiol.* **1983,** *46,* 1420–1422.
21. Zajkowski, P.; Grabarkiewicz-Szcesna, J.; Schmidt, R. *Mycotoxin Res.* **1991,** *7,* 11–15. doi:10.1007/BF03192158
22. Panigrahi, S.; Dallin, S. *J. Sci. Food Agric.* **1994,** *66,* 493–496. doi:10.1002/jsfa.2740660411
23. Aly, A. H.; Edrada-Ebel, R.; Indriani, I. D.; Wray, V.; Müller, W. E. G.; Totzke, F.; Zirrgiebel, U.; Schächtele, C.; Kubbutat, M. H. G.; Lin, W. H.; Proksch, P.; Ebel, R. *J. Nat. Prod.* **2008,** *71,* 972–980. doi:10.1021/np070447m
24. Bensassi, F.; Gallerne, C.; Sharaf El Dein, O.; Hajlaoui, M. R.; Bacha, H.; Lemaire, C. *Toxicol. In Vitro* **2012,** *26,* 915–923. doi:10.1016/j.tiv.2012.04.014
25. Schreck, I.; Deigendesch, U.; Burkhardt, B.; Marko, D.; Weiss, C. *Arch. Toxicol.* **2012,** *86,* 625–632. doi:10.1007/s00204-011-0781-3
26. Mao, Z.; Sun, W.; Fu, L.; Luo, H.; Lai, D.; Zhou, L. *Molecules* **2014,** *19,* 5088–5108. doi:10.3390/molecules19045088

27. Grasser, G. *Synthetic Tannins;* Crosby Lockwood & Son: London, 1922.
28. Yoshiaki, S.; Shizuo, T. *Nat. Med.* **2001,** *55,* 247–250.
29. Bialonska, D.; Kasimsetty, S. G.; Khan, S. I.; Ferreira, D. *J. Agric. Food Chem.* **2009,** *57,* 10181–10186. doi:10.1021/jf9025794
30. Ishimoto, H.; Shibata, M.; Myojin, Y.; Ito, H.; Sugimoto, Y.; Tai, A.; Hatano, T. *Bioorg. Med. Chem. Lett.* **2011,** *21,* 5901–5904. doi:10.1016/j.bmcl.2011.07.086
31. Jeong, S.-J.; Kim, N.-Y.; Kim, D.-H.; Kang, T.-H.; Ahn, N.-H.; Miyamoto, T.; Higuchi, R.; Kim, Y.-C. *Planta Med.* **2000,** *66,* 76–77. doi:10.1055/s-0029-1243114
32. Larrosa, M.; González-Sarrías, A.; García-Conesa, M. T.; Tomás-Barberán, F. A.; Espín, J. C. *J. Agric. Food Chem.* **2006,** *54,* 1611–1620. doi:10.1021/jf0527403
33. Melville, C. R.; Gould, S. J. *J. Nat. Prod.* **1994,** *57,* 597–601. doi:10.1021/np50107a005
34. Serrano-Carreon, L.; Hathout, Y.; Bensoussan, M.; Belin, J. M. *Appl. Environ. Microbiol.* **1993,** *59,* 2945–2950.
35. Abdel-Lateff, A.; Fisch, K.; Wright, A. D. *Z. Naturforsch., C* **2009,** *64,* 186–192.
36. Kottb, M.; Gigolashvili, T.; Großkinsky, D. K.; Piechulla, B. *Front. Microbiol.* **2015,** *6,* No. 995. doi:10.3389/fmicb.2015.00995
37. Wickel, S. M.; Citron, C. A.; Dickschat, J. S. *Eur. J. Org. Chem.* **2013,** 2906–2913. doi:10.1002/ejoc.201300049
38. Pettit, G. R.; Houghton, L. E.; Knight, J. C.; Bruschweiler, F. *J. Org. Chem.* **1970,** *35,* 2895–2898. doi:10.1021/jo00834a008
39. Evidente, A.; Conti, L.; Altomare, C.; Bottalico, A.; Sindona, G.; Segre, A. L.; Logrieco, A. *Nat. Toxins* **1994,** *2,* 4–13. doi:10.1002/nt.2620020103
40. Irschik, H.; Jansen, R.; Höfle, G.; Gerth, K.; Reichenbach, H. *J. Antibiot.* **1985,** *38,* 145–152. doi:10.7164/antibiotics.38.145
41. Irschik, H.; Gerth, K.; Höfle, G.; Kohl, W.; Reichenbach, H. *J. Antibiot.* **1983,** *36,* 1651–1658. doi:10.7164/antibiotics.36.1651
42. Kamano, Y.; Nogawa, T.; Yamashita, A.; Hayashi, M.; Inoue, M.; Drašar, P.; Pettit, G. R. *J. Nat. Prod.* **2002,** *65,* 1001–1005. doi:10.1021/np0200360
43. Schäberle, T. F.; Lohr, F.; Schmitz, A.; König, G. M. *Nat. Prod. Rep.* **2014,** *31,* 953–972. doi:10.1039/c4np00011k
44. Schiefer, A.; Schmitz, A.; Schäberle, T. F.; Specht, S.; Lämmer, C.; Johnston, K. L.; Vassylyev, D. G.; König, G. M.; Hoerauf, A.; Pfarr, K. *J. Infect. Dis.* **2012,** *206,* 249–257. doi:10.1093/infdis/jis341
45. Dávila-Céspedes, A.; Hufendiek, P.; Crüsemann, M.; Schäberle, T. F.; König, G. M. *Beilstein J. Org. Chem.* submitted.
46. Korp, J.; Vela Gurovic, M. S.; Nett, M. *Beilstein J. Org. Chem.* **2016,** *12,* in press.
47. Altomare, C.; Pengue, R.; Favilla, M.; Evidente, A.; Visconti, A. *J. Agric. Food Chem.* **2004,** *52,* 2997–3001. doi:10.1021/jf035233z
48. Barrero, A. F.; Oltra, J. E.; Herrador, M. M.; Cabrera, E.; Sanchez, J. F.; Quílez, J. F.; Rojas, F. J.; Reyes, J. F. *Tetrahedron* **1993,** *49,* 141–150. doi:10.1016/S0040-4020(01)80514-7
49. Tringali, C.; Parisi, A.; Piatelli, M.; di San Lio, G. M. *Nat. Prod. Lett.* **1993,** *3,* 101–106. doi:10.1080/10575639308043845
50. Ivanova, L.; Petersen, D.; Uhlig, S. *Toxicon* **2010,** *55,* 1107–1114. doi:10.1016/j.toxicon.2009.12.017
51. Vardaro, R. R.; Di Marzo, V.; Marin, A.; Cimino, G. *Tetrahedron* **1992,** *48,* 9561–9566. doi:10.1016/S0040-4020(01)88324-1
52. Rocca, J. R.; Tumlinson, J. H.; Glancey, B. M.; Lofgren, C. S. *Tetrahedron Lett.* **1983,** *24,* 1889–1892. doi:10.1016/S0040-4039(00)81798-0
53. Kondoh, M.; Usui, T.; Nishikiori, T.; Mayumi, T.; Osada, H. *Biochem. J.* **1999,** *340,* 411–416. doi:10.1042/bj3400411
54. Kobayashi, S.; Tsuchiya, K.; Harada, T.; Nishide, M.; Kurokawa, T.; Nakagawa, T.; Shimada, N.; Kobayashi, K. *J. Antibiot.* **1994,** *47,* 697–702. doi:10.7164/antibiotics.47.697
55. Kobayashi, S.; Tsuchiya, K.; Nishide, M.; Nishikiori, T.; Nakagawa, T.; Shimada, N. *J. Antibiot.* **1995,** *48,* 893–895. doi:10.7164/antibiotics.48.893
56. Rao, P. N. P.; Amini, M.; Li, H.; Habeeb, A. G.; Knaus, E. E. *J. Med. Chem.* **2003,** *46,* 4872–4882. doi:10.1021/jm0302391
57. Bilia, A. R.; Scalise, L.; Bergonzi, M. C.; Vincieri, F. F. *J. Chromatogr. B: Anal. Technol. Biomed. Life Sci.* **2004,** *812,* 203–214. doi:10.1016/S1570-0232(04)00644-0
58. Sarris, J.; Kavanagh, D. J. *J. Altern. Complementary Med.* **2009,** *15,* 827–836. doi:10.1089/acm.2009.0066
59. Petersen, F.; Zähner, H.; Metzger, J. W.; Freund, S.; Hummel, R.-P. *J. Antibiot.* **1993,** *46,* 1126–1138. doi:10.7164/antibiotics.46.1126
60. Citron, C. A.; Junker, C.; Schulz, B.; Dickschat, J. S. *Angew. Chem., Int. Ed.* **2014,** *53,* 4346–4349. doi:10.1002/anie.201402290
61. Flematti, G. R.; Ghisalberti, E. L.; Dixon, K. W.; Trengove, R. D. *Science* **2004,** *305,* 977. doi:10.1126/science.1099944
62. Giddens, A. C.; Nielsen, L.; Boshoff, H. I.; Tasdemir, D.; Perozzo, R.; Kaiser, M.; Wang, F.; Sacchettini, J. C.; Copp, B. R. *Tetrahedron* **2008,** *64,* 1242–1249. doi:10.1016/j.tet.2007.11.075
63. Kresovic, D.; Schempp, F.; Cheikh-Ali, Z.; Bode, H. B. *Beilstein J. Org. Chem.* **2015,** *11,* 1412–1417. doi:10.3762/bjoc.11.152
64. Thaisrivongs, S.; Tomich, P. K.; Watenpaugh, K. D.; Chong, K.-T.; Howe, W. J.; Yang, C.-P.; Strohbach, J. W.; Turner, S. R.; McGrath, J. P.; Bohanon, M. J.; Lynn, J. C.; Mulichak, A. M.; Spinelli, P. A.; Hinshaw, R. A.; Pagano, P. J.; Moon, J. B.; Ruwart, M. J.; Wilkinson, K. F.; Rush, B. D.; Zipp, G. L.; Dalga, R. J.; Schwende, F. J.; Howard, G. M.; Padbury, G. E.; Toth, L. N.; Zhao, Z.; Koeplinger, K. A.; Kakuk, T. J.; Cole, S. L.; Zaya, R. M.; Piper, R. C.; Jeffrey, P. *J. Med. Chem.* **1994,** *37,* 3200–3204. doi:10.1021/jm00046a002
65. Richards, R. K. *Science* **1943,** *97,* 313. doi:10.1126/science.97.2518.313
66. Townsend, C. A. *Nat. Prod. Rep.* **2014,** *31,* 1260–1265. doi:10.1039/C4NP00092G
67. Balbaa, S. I.; Hilal, S. H.; Haggag, M. Y. *Planta Med.* **1973,** *23,* 191–195. doi:10.1055/s-0028-1099432
68. Kim, J. H.; Kim, J.-K.; Ahn, E.-K.; Ko, H.-J.; Cho, Y.-R.; Lee, C. H.; Kim, Y. K.; Bae, G.-U.; Oh, J. S.; Seo, D.-W. *Cancer Lett.* **2015,** *369,* 323–330. doi:10.1016/j.canlet.2015.09.021
69. Abdel-Hay, F. M.; Abu-Mustafa, E. A.; Fayez, M. B. E. *Naturwissenschaften* **1966,** *53,* 406. doi:10.1007/BF00625773
70. Kleiner, H. E.; Vulimiri, S. V.; Starost, M. F.; Reed, M. J.; DiGiovanni, J. *Carcinogenesis* **2002,** *23,* 1667–1675. doi:10.1093/carcin/23.10.1667
71. George, W. M.; Burks, J. W., Jr. *AMA Arch. Dermatol.* **1955,** *71,* 14–18. doi:10.1001/archderm.1955.01540250016004
72. Gulder, T. A. M.; Neff, S.; Schüz, T.; Winkler, T.; Gees, R.; Böhlendorf, B. *Beilstein J. Org. Chem.* **2013,** *9,* 2579–2585. doi:10.3762/bjoc.9.293
73. Werner, R. A.; Rossmann, A.; Schwarz, C.; Bacher, A.; Schmidt, H.-L.; Eisenreich, W. *Phytochemistry* **2004,** *65,* 2809–2813. doi:10.1016/j.phytochem.2004.08.020
74. Hertweck, C. *Angew. Chem., Int. Ed.* **2009,** *48,* 4688–4716. doi:10.1002/anie.200806121

75. Saha, D.; Fetzner, R.; Burkhardt, B.; Podlech, J.; Metzler, M.; Dang, H.; Lawrence, C.; Fischer, R. *PLoS One* **2012,** *7,* e40564. doi:10.1371/journal.pone.0040564
76. Dasenbrock, J.; Simpson, T. J. *J. Chem. Soc., Chem. Commun.* **1987,** 1235–1236. doi:10.1039/C39870001235
77. Sun, J.; Awakawa, T.; Noguchi, H.; Abe, I. *Bioorg. Med. Chem. Lett.* **2012,** *22,* 6397–6400. doi:10.1016/j.bmcl.2012.08.063
78. Throckmorton, K.; Wiemann, P.; Keller, N. P. *Toxins* **2015,** *7,* 3572–3607. doi:10.3390/toxins7093572
79. Bouhired, S. M.; Crüsemann, M.; Almeida, C.; Weber, T.; Piel, J.; Schäberle, T. F.; König, G. M. *ChemBioChem* **2014,** *15,* 757–765. doi:10.1002/cbic.201300676
80. Buntin, K.; Weissman, K. J.; Müller, R. *ChemBioChem* **2010,** *11,* 1137–1146. doi:10.1002/cbic.200900712
81. Piel, J.; Hertweck, C.; Shipley, P. R.; Hunt, D. M.; Newman, M. S.; Moore, B. S. *Chem. Biol.* **2000,** *7,* 943–955. doi:10.1016/S1074-5521(00)00044-2
82. Nakano, C.; Ozawa, H.; Akanuma, G.; Funa, N.; Horinouchi, S. *J. Bacteriol.* **2009,** *191,* 4916–4923. doi:10.1128/JB.00407-09
83. Kohl, W.; Irschik, H.; Reichenbach, H.; Höfle, G. *Liebigs Ann. Chem.* **1984,** 1088–1093. doi:10.1002/jlac.198419840605
84. Erol, Ö.; Schäberle, T. F.; Schmitz, A.; Rachid, S.; Gurgui, C.; El Omari, M.; Lohr, F.; Kehraus, S.; Piel, J.; Müller, R.; König, G. M. *ChemBioChem* **2010,** *11,* 1253–1265. doi:10.1002/cbic.201000085
85. Hashimoto, M.; Koen, T.; Takahashi, H.; Suda, C.; Kitamoto, K.; Fujii, I. *J. Biol. Chem.* **2014,** *289,* 19976–19984. doi:10.1074/jbc.M114.569095
86. Bauer, J. S.; Ghequire, M. G. K.; Nett, M.; Josten, M.; Sahl, H.-G.; De Mot, R.; Gross, H. *ChemBioChem* **2015,** *16,* 2491–2497. doi:10.1002/cbic.201500413
87. Sucipto, H.; Wenzel, S. C.; Müller, R. *ChemBioChem* **2013,** *14,* 1581–1589. doi:10.1002/cbic.201300289
88. Sucipto, H.; Sahner, J. H.; Prusov, E.; Wenzel, S. C.; Hartmann, R. W.; Koehnke, J.; Müller, R. *Chem. Sci.* **2015,** *6,* 5076–5085. doi:10.1039/C5SC01013F
89. Zocher, G.; Vilstrup, J.; Heine, D.; Hallab, A.; Goralski, E.; Hertweck, C.; Stahl, M.; Schäberle, T. F.; Stehle, T. *Chem. Sci.* **2015,** *6,* 6525–6536. doi:10.1039/C5SC02488A
90. Sahner, J. H.; Sucipto, H.; Wenzel, S. C.; Groh, M.; Hartmann, R. W.; Müller, R. *ChemBioChem* **2015,** *16,* 946–953. doi:10.1002/cbic.201402666
91. Mori, T.; Yang, D.; Matsui, T.; Hashimoto, M.; Morita, H.; Fujii, I.; Abe, I. *J. Biol. Chem.* **2015,** *290,* 5214–5225. doi:10.1074/jbc.M114.626416

License and Terms

BEILSTEIN JOURNAL OF ORGANIC CHEMISTRY

Antibiotics from predatory bacteria

Juliane Korp[1], María S. Vela Gurovic[2] and Markus Nett[*1,3]

Review

Open Access

Address:
[1]Leibniz Institute for Natural Product Research and Infection Biology – Hans-Knöll-Institute, Beutenbergstr. 11, 07745 Jena, Germany, [2]Centro de Recursos Naturales Renovables de la Zona Semiárida (CERZOS) -CONICET- Carrindanga Km 11, Bahía Blanca 8000, Argentina and [3]Department of Biochemical and Chemical Engineering, Technical Biology, Technical University Dortmund, Emil-Figge-Strasse 66, 44227 Dortmund, Germany

Email:
Markus Nett[*] - markus.nett@bci.tu-dortmund.de

* Corresponding author

Keywords:
antibiotics; genome mining; *Herpetosiphon*; myxobacteria; predation

Beilstein J. Org. Chem. **2016,** *12,* 594–607.
doi:10.3762/bjoc.12.58

Received: 29 January 2016
Accepted: 11 March 2016
Published: 30 March 2016

This article is part of the Thematic Series "Natural products in synthesis and biosynthesis II".

Guest Editor: J. S. Dickschat

Abstract

Bacteria, which prey on other microorganisms, are commonly found in the environment. While some of these organisms act as solitary hunters, others band together in large consortia before they attack their prey. Anecdotal reports suggest that bacteria practicing such a wolfpack strategy utilize antibiotics as predatory weapons. Consistent with this hypothesis, genome sequencing revealed that these micropredators possess impressive capacities for natural product biosynthesis. Here, we will present the results from recent chemical investigations of this bacterial group, compare the biosynthetic potential with that of non-predatory bacteria and discuss the link between predation and secondary metabolism.

Introduction

Microorganisms are major contributors to primary biomass production and nutrient cycling in nature. The composition of a microbial community shapes an ecosystem, but is also responsive to biotic and environmental cues. Predation is among the ecological forces, which drive the diversity and dynamics of microbial consortia [1-3]. While protozoa and nematodes are widely known as bacterivores [4,5], the existence of predatory prokaryotes is often neglected despite the abundance of the latter and their early occurrence in the history of life, likely preceding eukaryotic predators [6-9].

Predatory behavior is in fact not uncommon for bacteria. It can be observed in many different species, which are found in the actinobacteria (e.g., *Agromyces ramosus*) [10], the chloroflexi (e.g., *Herpetosiphon* spp.) [11,12], the proteobacteria (e.g., *Bdellovibrio bacteriovorus*, *Myxococcus xanthus*, *Ensifer*

adhaerens, *Cupriavidus necator*, *Lysobacter* spp.) [13-17], the bacteroidetes (e.g., *Saprospira grandis*, *Tenacibaculum* spp.) [18,19], and even in the cyanobacteria (e.g., *Vampirovibrio chlorellavorus*) [20]. Depending on their feeding behavior, that is, whether or not their diet relies exclusively on prey consumption, these bacteria have been classified as obligate or facultative predators [6]. While obligate predators can only survive by consuming other bacteria, facultative predators readily switch to a saprophytic lifestyle in the absence of appropriate preys [21]. Another division of predatory bacteria is based on their hunting strategies [22]. Epibiotic predation involves attachment to the outer surface of the prey, which is then followed by a degradation of the prey's cell wall and assimilation of cell components through specialized structures [23]. Other predatory bacteria are known to directly penetrate the prey cell in a process called diacytosis [24,25] or to selectively invade the periplasm of Gram-negative bacteria [26]. The corresponding behaviors are referred to as endobiotic and periplasmic predation, respectively [22]. Another strategy, which is called group or 'wolfpack' predation, is only practiced by facultative predators. A prerequisite for this collaborative type of hunting is a quorum of predatory cells, which pool hydrolytic enzymes, proteases or nucleases in order to lyse and feed on nearby prey [22].

Group predation occurs predominantly in bacteria, which also display social swarming behavior, gliding motility and sophisticated communication systems. Illustrative examples include the myxobacteria, as well as *Lysobacter* and *Herpetosiphon* species [6,27-29]. Members of these taxa are further characterized by their large genome sizes and their striking potential for the production of structurally diverse natural products with antimicrobial activities [12,30-35]. For many years, it has been speculated whether antibiotic biosynthesis is functionally linked to the predatory lifestyle of these organisms [27,36]. In this review, we will address this unresolved question both from a genomic perspective and on the basis of chemical investigations. Terrestrial myxobacteria and the genus *Herpetosiphon* will be in the focus of our analysis, whereas *Lysobacter* spp., which have just been the subject of a comparative metabolomics study [37], are not covered. For information on marine myxobacteria, readers are referred to the review article by König et al. in this Thematic Series [38].

Review

Biology and biosynthetic potential of myxobacteria

Myxobacteria are ubiquitous soil bacteria with a complex life cycle, which involves the coordinated differentiation from individual cells into multicellular fruiting bodies under starvation conditions [39,40]. Furthermore, myxobacteria are distinguished by their unique gliding motility allowing a rapid swarming dispersal [41], which likely also benefits their predation strategy. Considering their highly sophisticated developmental program and their manifold social interactions, it is not surprising that fruiting myxobacteria are among the prokaryotes with the largest genomes. Their genomes typically range from 9 up to 15 Mbp in size and contain between 7,285 (*Myxococcus fulvus* HW-1) and 11,599 (*Sorangium cellulosum* So0157-2) protein-coding sequences (Table 1) [42-47]. In comparison, the genome of the standard laboratory bacterium *Escherichia coli* comprises only 4.6 Mbp of DNA [48]. With a single exception, all myxobacterial genomes that have been sequenced to date consist of a single circular chromosome and feature no plasmids [42-47,49,50]. To evaluate the biosynthetic capabilities of the myxobacterial strains listed in Table 1, their genome sequences were scanned for the presence of putative secondary metabolite gene clusters using the publicly available online tool antiSMASH 3.0 [51]. This analysis revealed that all strains possess extraordinary capacities for natural product assembly. Interestingly, however, the number of biosynthetic loci is not linearly correlated with the genome size. The largest number of secondary metabolite gene clusters was found in *Corallococcus coralloides* DSM 2259 and not in the two *Sorangium cellulosum* strains, although the latter feature significantly larger genomes (Table 1). When the number of detected loci is related to the genome size, it becomes obvious that the Cystobacterineae strains consistently possess more biosynthesis gene clusters per Mbp of DNA than the analyzed Sorangiineae and that they also devote a larger percentage of their total nucleotides to natural product biosynthesis. Noteworthy in this context, the genera *Myxococcus* and *Corallococcus*, on the one hand, as well as the genus *Sorangium*, on the other, represent different nutritional types among the myxobacteria. Only the former are bacteriolytic and attack other microorganisms, whereas the latter live as cellulose degraders [36,52-54]. Although mere numbers of biosynthesis gene clusters provide no information about the identity or biological role of the associated natural products, we note that predatory myxobacteria possess a higher density of secondary metabolite gene clusters in their genomes than their non-predatory relatives.

But are these clusters indicators for predatory behavior? – To answer this question, we will take a closer look at their metabolic products using *Myxococcus xanthus* DK1622 as an example. This strain, a model organism for the analysis of myxobacterial fruiting body development and motility, feeds on a number of different soil bacteria upon direct contact by a mechanism called predatory rippling [14,55]. Although the biology of *M. xanthus* DK1622 had been thoroughly investigated for decades, the bacterium did not come into the focus of natural product chemists until the sequencing of its genome. Bioinfor-

Table 1: Taxonomic assignment, nutrition, genomic and biosynthetic features of myxobacterial strains.

	Myxococcus fulvus HW-1	*Myxococcus xanthus* DK1622	*Corallococcus coralloides* DSM 2259	*Myxococcus stipitatus* DSM 14675	*Sorangium cellulosum* So ce56	*Sorangium cellulosum* So0157-2
Suborder	Cystobacterineae	Cystobacterineae	Cystobacterineae	Cystobacterineae	Sorangiineae	Sorangiineae
Family	Myxococcaceae	Myxococcaceae	Myxococcaceae	Myxococcaceae	Polyangiaceae	Polyangiaceae
Nutrition	saprotrophic predatory	saprotrophic predatory	saprotrophic predatory	saprotrophic predatory	saprotrophic, cellulolytic	saprotrophic, cellulolytic
Genome size [bp]	9,003,593	9,139,763	10,080,619	10,350,586	13,033,779	14,782,125
Protein-coding sequences	7,285	7,388	8,033	8,043	9,367	11,599
GenBank accession no.	CP002830	CP000113	CP003389	CP004025	AM746676	CP003969
Reference	[42]	[43]	[44]	[45]	[46]	[47]
# of biosynthesis gene clusters[a]	25	24	36	29	31	34
# of biosynthesis gene clusters per Mbp	2.78	2.63	3.57	2.80	2.38	2.30
Combined length of biosynthesis clusters [bp][a]	1,147,796	1,329,413	1,571,607	1,672,930	1,199,901	1,450,537
Genome portion devoted to biosynthesis [%]	12.75	14.55	15.59	16.16	9.21	9.81

[a]Numbers and size of biosynthesis loci were determined using antiSMASH [50].

matic analysis of the DK1622 chromosome with antiSMASH indicated the presence of 24 gene clusters, which are involved in the secondary metabolism (Table 2).

Until now, six loci have been associated with isolated natural products on the basis of biosynthetic precedence and extensive metabolome analyses (Figure 1) [56,57]. While some of the retrieved compounds from *M. xanthus* DK1622 are also known from different myxobacterial species, as exemplified by the myxochelins [58-60] and myxochromides [61,62], others were initially discovered in this strain, such as the myxoprincomides [57] and the DKxanthenes [63].

The known secondary metabolites of *M. xanthus* DK1622 show a wide range of biological activities and can hence be expected to fulfill different ecological functions. The yellow DKxanthenes, for instance, play a crucial role in spore maturation during fruiting body formation [63]. They were also shown to possess antioxidative properties and might thus confer resistance towards oxidative stress [63]. Structurally, the DKxanthenes harbor a hydrophilic asparagine moiety attached to a hydrophobic polyene chain bearing an additional oxazoline and pyrrol ring system. Their production seems to be universal among *Myxococcus* strains and several derivatives varying in their polyene chain length as well as extent of methyl branching have been identified [63-65]. The myxochromides represent another pigment family commonly encountered in myxobacteria [61,65,66]. While their chemistry and biosynthesis have been thoroughly explored [62,67], the biological function of these cyclic depsipeptides is still not clear. In contrast, the myxochelins primarily serve as siderophores for *M. xanthus* DK1622, as evidenced by their iron-responsive production and complexing properties [58,59]. Recent studies also unveiled specific enzymatic targets for these natural products [60,68], which are not due to their iron affinity [69]. Myxalamids [70-73] and myxovirescins [74-79] are distinguished by their potent antimicrobial activities. The former are inhibitors of electron transport in the respiratory chain. They were shown to block the electron flow at complex I of mitochondria (NADH:ubiquinone oxidoreductase) in a competitive manner, but do not act on bacterial complex I [71,72]. This explains why the myxalamids are mainly active against fungi [71].

Table 2: Biosynthetic gene clusters in the genome of *M. xanthus* DK1622 and their predicted or known products.[a]

No.	Cluster location	Type	Actual or predicted product	Estimated size [kb]
1	MXAN_0889-MXAN_0906	terpene	carotenoid	21.0
2	MXAN_1276-MXAN_1312	NRPS	dipeptide	46.3
3	MXAN_1508-MXAN_1543	other	unknown	44.4
4	MXAN_1588-MXAN_1624	NRPS	hexapeptide	64.6
5	MXAN_2782-MXAN_2814	NRPS/PKS (type I)	unknown	51.8
6	MXAN_2847-MXAN_2864	lantipeptide	class II lantipeptide	23.3
7	MXAN_3447-MXAN_3479	PKS (type I)	unknown	46.7
8	MXAN_3551-MXAN_3559	bacteriocin	bacteriocin	10.9
9	MXAN_3602-MXAN_3658	NRPS/PKS (type I) + NRPS	lipopeptide + **myxochelin**	168.4
10	MXAN_3763-MXAN_3797	NRPS/PKS (type I)	**myxoprincomide**	82.8
11	MXAN_3917-MXAN_3957	*trans*-AT-PKS/NRPS	**myxovirescin**	109.6
12	MXAN_3986-MXAN_4020	NRPS/PKS (type I)	lipopeptide	70.3
13	MXAN_4057-MXAN_4100	PKS (type I)/NRPS	**myxochromide**	69.0
14	MXAN_4156-MXAN_4166	bacteriocin	bacteriocin	11.7
15	MXAN_4271-MXAN_4312	PKS (type I)/NRPS	**DKxanthene**	76.9
16	MXAN_4384-MXAN_4402	NRPS/PKS (type I)	unknown	48.2
17	MXAN_4404-MXAN_4438	NRPS/PKS (type I)	lipopeptide	70.0
18	MXAN_4508-MXAN_4549	NRPS/PKS (type I)	**myxalamide**	92.7
19	MXAN_4545-MXAN_4561	lantipeptide	lantipeptide	26.2
20	MXAN_4578-MXAN_4618	NRPS	lipopeptide	79.4
21	MXAN_4951-MXAN_4960	bacteriocin	bacteriocin	10.8
22	MXAN_6241-MXAN_6257	terpene	geosmin	22.2
23	MXAN_6377-MXAN_6414	lantipeptide/ladderane/ PKS (type II)	unknown	41.1
24	MXAN_6618-MXAN_6659	PKS (type III)	alkylresorcinol	41.1

[a]All predictions are according to [50], except for the assignment of the myxochelin gene cluster.

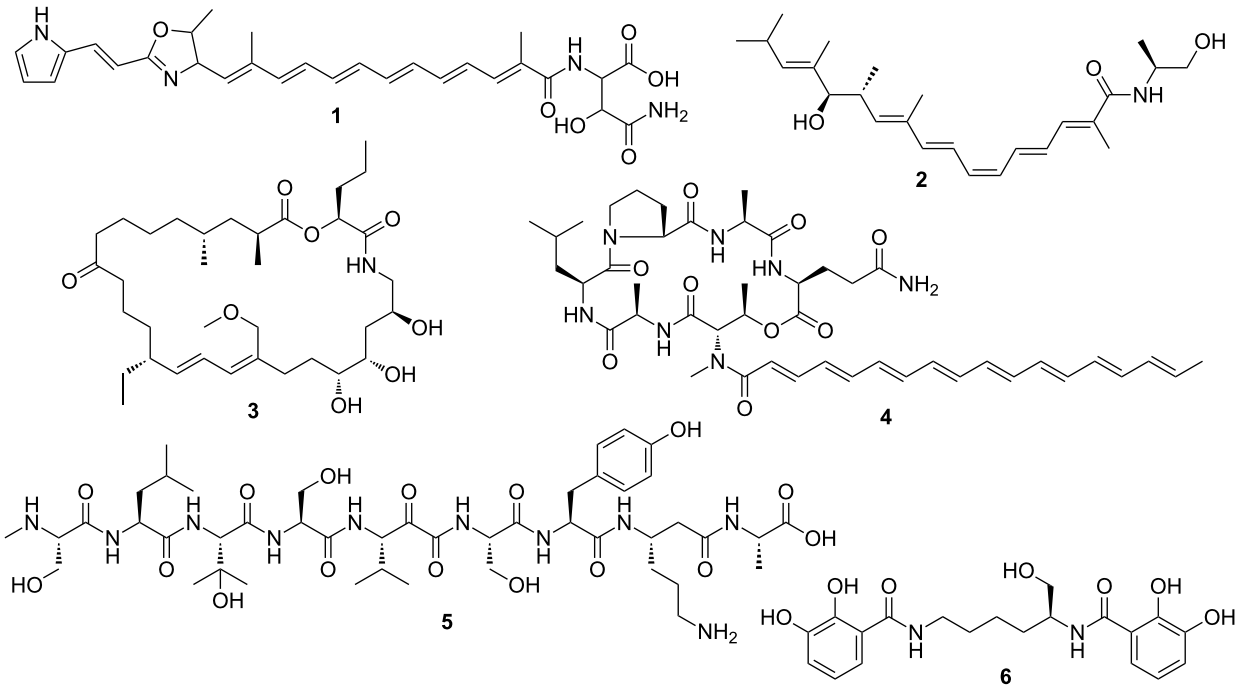

Figure 1: Natural products isolated from *M. xanthus* DK1622. DKxanthene-534 (**1**); myxalamid B (**2**); myxovirescin A_1 (**3**); myxochromide A_3 (**4**); myxoprincomide (**5**); myxochelin A (**6**).

The myxovirescins comprise a family of closely related antibiotics featuring a distinctive 28-membered macrolide ring. First discovered by Rosenberg et al. in *M. xanthus* TA [74], the myxovirescins were later also reported from other myxobacterial isolates, including strain DK1622 [75-79]. Myxovirescins are excreted during late exponential and early stationary growth phase and display strong inhibitory activities on growing bacterial cells, even when applied at concentrations less than 5 µg/mL. Toxicity against eukaryotic cells was not observed [74,80]. Myxovirescin A_1 was found to be particularly effective against enterobacteria with a minimal inhibitory concentration (MIC) of 1 µg/mL [75]. Its mode of action was deduced after genetic characterization of myxovirescin-resistant *E. coli* mutants [81]. The antibiotic interferes with cell-wall biosynthesis by inhibiting a novel target, i.e., the type II signal peptidase LspA, which is involved in the maturation of lipoproteins required for murein biosynthesis [81].

Myxovirescin A_1 (also known as antibiotic TA) and its derivatives seem to be of particular importance for the predatory lifestyle of *M. xanthus* DK1622. Gene deletion experiments demonstrated that a loss of myxovirescin biosynthesis significantly affects the ability of the myxobacterium to kill actively growing *E. coli* cells [82]. Furthermore, myxovirescin-resistant *E. coli* strains were shown to be largely resistant against predation by DK1622, demonstrating for the first time a clear link between antibiotic production and predation. However, myxovirescins cannot be considered as universal predatory weapons for *M. xanthus* DK1622, as the macrolides have no effects on the Gram-positive prey bacterium *Micrococcus luteus* [82]. It remains unclear whether as yet unidentified antibiotics from the DK1622 metabolome complement the bioactivity of myxovirescins and, thereby, expand the prey spectrum. Alternatively, it is possible that the killing of *M. luteus* involves a different predation strategy (e.g., attack with hydrolytic enzymes).

In any case, the coordinate production of antibiotics, such as myxovirescin A, requires a tight regulatory network in predatory myxobacteria [80]. This is also reflected in the genome of *M. xanthus* DK1622, which features an unusual high duplication frequency of genes encoding regulatory proteins like serine-threonine kinases and enhancer binding proteins (EBPs) [43]. EBPs are regulatory proteins influencing the transcription by binding to a specific enhancer-like element (ELE) sequence located in close vicinity to the corresponding promoter in a δ54 dependent manner [83]. Two EBPs of *M. xanthus* DK1622, namely HsfA and MXAN4899, have recently been identified as transcriptional regulators of secondary metabolism via DNA–protein pull-down assays [84]. Knock-out studies revealed that both EBPs are necessary for the formation of intact fruiting body and sporulation. DKxanthene biosynthesis was strongly influenced by HsfA and MXAN4899, respectively, which is in good agreement with the biological function of this compound class [63]. Furthermore, the two EBPs were linked to the regulation of the myxovirescin pathway and motility. While HsfA acted as a repressor of the myxovirescin production, MXAN4899 could exert enhancing or inhibitory effects depending on the nutrition status of the myxobacterium. The findings of this study attested a complex regulatory network to *M. xanthus* DK1622, in which development, predation, and motility are clearly connected to secondary metabolism [84].

Lastly, it should be mentioned that genomic data might also provide the explanation for the predatory behavior of some myxobacteria. Nutritional studies had shown that *M. xanthus* cannot be grown in the absence of branched-chain amino acids [85]. Consistent with these results, the genome of strain DK1622 lacks *ilvC* and *ilvD* genes, which are required for the biosynthesis of these amino acids. It was hence speculated that predation might compensate for this deficiency [43]. Analysis of the other myxobacterial genomes now lends support to this assumption. We found the absence of *ilvC* and *ilvD* to be a consistent trait in the bacteriolytic *Myxococcus* and *Corallococcus* strains, whereas the genomes of the cellulolytic *Sorangium* strains harbor well-conserved homologs of both genes.

Antibiotics from myxobacteria with a possible role in predation

The following listing highlights few selected antibiotics from myxobacteria in the context of predation. For a comprehensive overview of bioactive compounds from myxobacteria and their modes of action, the reader is referred to the excellent review articles by König et al. [33] and Müller et al. [86].

Gulmirecins: The gulmirecins were found in a culture broth of the predatory myxobacterium *Pyxidicoccus fallax* HKI 727 (Figure 2) [87]. Their discovery is an illustrative example on how new antibiotics can be retrieved from predatory bacteria. The isolation of predatory bacteria from soil is typically achieved by means of baiting techniques. For this, a pea-sized sample is placed on a nutrient-poor agar medium, that was previously inoculated with potential prey microbes [88-90]. These organisms serve as attractants that will allow the enrichment of any predators present in the soil sample. Baiting techniques have proven to be particularly useful for the recovery of bacteriolytic myxobacteria, as swarming and fruiting body formation facilitate the separation from other microorganisms [91]. If the isolation procedure is repeated with varying "food organisms", it becomes possible to select for myxobacteria that can be distinguished by their preference for certain prey bacteria. This

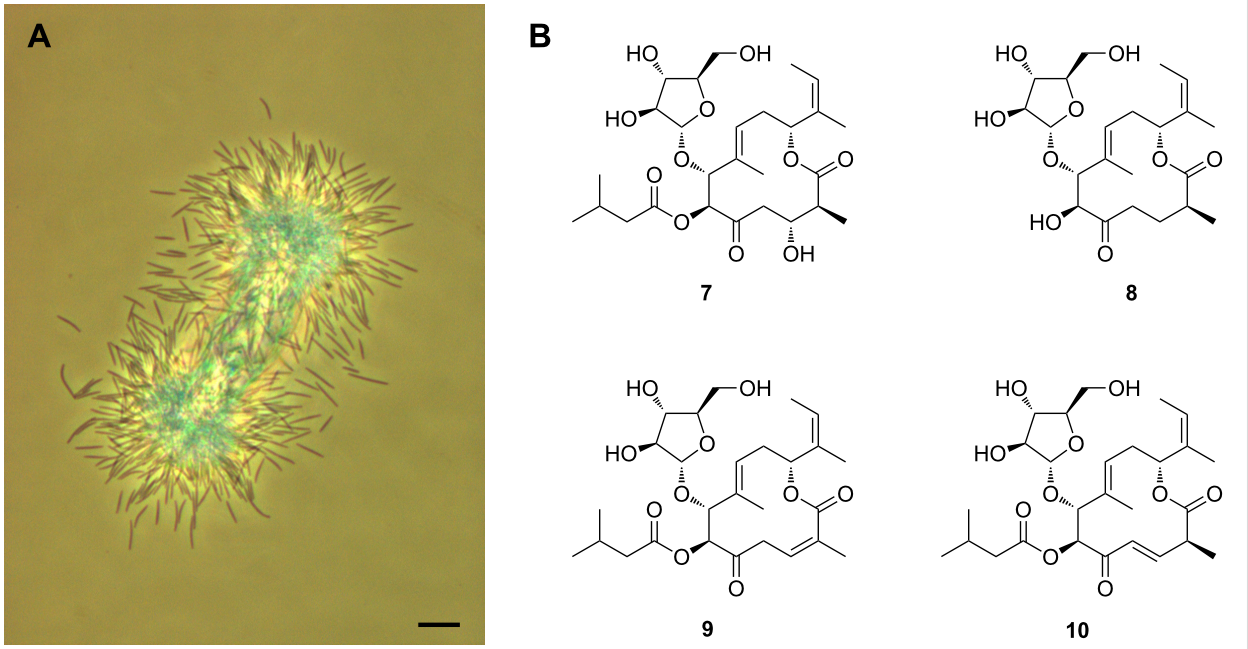

Figure 2: Vegetative cells of *P. fallax* HKI 727 under a phase-contrast microscope (K. Martin, unpublished). Bar is 10 µm (A). Structures of gulmirecin A (**7**), gulmirecin B (**8**), disciformycin A (**9**), and disciformycin B (**10**) (B).

approach was also used during the isolation of strain HKI 727, which readily consumed the prey bacterium *Bacillus subtilis*, but not *Escherichia coli*. Further tests revealed that *P. fallax* HKI 727 exhibits a prey range that is restricted to Gram-positive bacteria. Culture extracts of strain HKI 727 showed a consistent antimicrobial profile, i.e., they were highly active against Gram-positive bacteria. Bioactivity-guided fractionation then led to the identification of the gulmirecins as the active principles [87].

Chemically, the gulmirecins form a novel class of antibiotics together with the disciformycins [92], which were discovered in a different *P. fallax* strain upon a large-scale screening. The distinctive 12-membered macrolide scaffold in these natural products features an arabinose moiety (Figure 2), which is only rarely observed in bacterial polyketides. The main difference between gulmirecins A and B is the presence or absence of an isovalerate substituent. Comparison with the bioactivity data of the disciformycins suggests that the isovalerate motive is important for the antibacterial activity. Due to their potent effects against human pathogenic staphylococci as well as negligible toxicity, gulmirecins A and disciformycin B have become promising candidate compounds for the design of new antibiotics [93,94]. Since the gene loci that are involved in their biosyntheses have been identified [87,92], it might even be possible to genetically engineer further derivatives in the future. The close correlation between the activity profile of the gulmirecins and the prey range of strain HKI 727 further suggests that isolation procedures for predatory bacteria can be directed in order to obtain strains producing antibiotics against specific pathogens.

Myxopyronins and corallopyronins: The myxopyronins were first reported in 1983 from a culture supernatant of *Myxococcus fulvus* Mxf50 [95,96]. Later, the structurally related corallopyronins were found in different strains of *Corallococcus coralloides* [97-99]. Myxopyronins and corallopyronins share a common scaffold composed of a central pyrone ring carrying two flexible side chains (Figure 3). Structural variability manifests in the so-called western side chain, which ranges from 10 (myxopyronin A) up to 18 carbon atoms (corallopyronin B). In contrast, the eastern chain is conserved among all members and features a terminal methyl carbamate moiety. Differences in the architectures of the respective biosynthetic assembly lines were recently shown to account for the diverging frameworks of the western chain [100-102].

Myxopyronins and corallopyronins turned out to be highly active against Gram-positive bacteria with MIC values between 0.1 and 1.0 µg/mL for *Staphylococcus aureus*, whereas their inhibitory effects on Gram-negative strains are in general much weaker. Gram-negative bacteria of the genus *Wolbachia*, which have emerged as a new target for filariasis control, constitute a significant exception [103]. Already in the 1980s, incorporation studies with labeled precursors revealed the inhibition of prokaryotic RNA polymerase (RNAP) as mode of action for myxopyronins and corallopyronins [95,97]. Later on, mutagen-

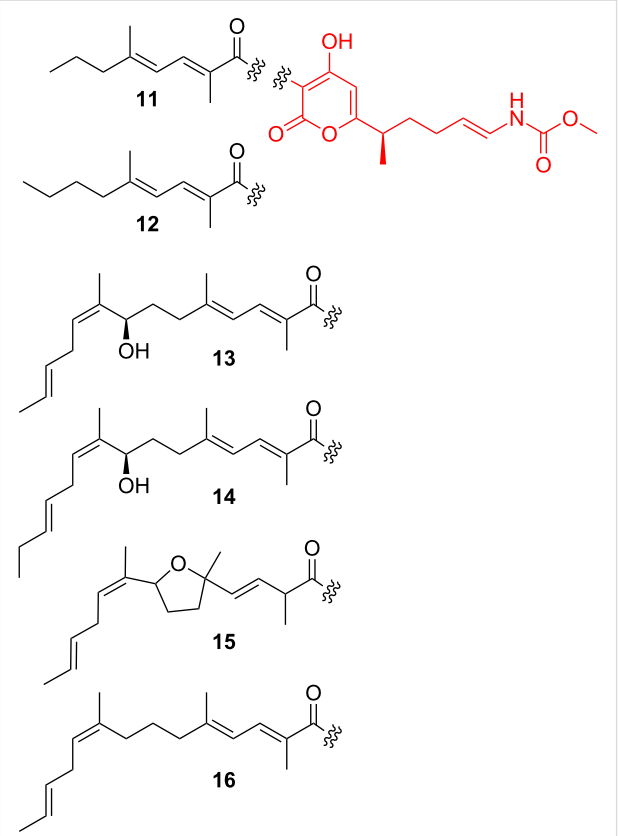

Figure 3: Structures of myxopyronins A (**11**) and B (**12**), corallopyronins A (**13**), B (**14**) and C (**15**), as well as precorallopyronin A (**16**).

esis experiments as well as binding studies indicated that the antibiotics interact with the RNAP switch region [104,105], which acts as a hinge mediating conformational changes during transcription [106]. During early stages of transcriptional initiation, the RNAP clamp possesses an opened form in order to allow binding of the promoter DNA to the active-center cleft. At late transcriptional initiation and elongation, the clamp changes into a closed position to retain the DNA inside the active-center cleft. After binding to the switch region, myxopyronins and corallopyronins prevent the opening of the clamp [104,105].

Prey bacteria that develop resistance against corallopyronin, e.g., due to a *rpoB* mutation, also become resistant towards predation by *C. coralloides* [82]. It is thus likely that corallopyronin is produced by myxobacteria to facilitate feeding on other bacteria.

Althiomycin: The antibiotic althiomycin (Figure 4) had been initially discovered in cultures of *Streptomyces althioticus* [107], before it was also reported from strains of *Myxococcus virescens, M. xanthus, and Cystobacter fuscus* [108]. The pentapeptide is broadly active against Gram-positive as well as Gram-negative bacteria and was shown to selectively inhibit bacterial protein synthesis. Its specific site of inhibition is the 50S subunit of the ribosome, where althiomycin interferes with the peptidyl transferase reaction [109,110]. The althiomycin biosynthetic gene cluster was recently identified in *M. xanthus* DK897 by a combination of retrobiosynthetic analysis and gene inactivation [111]. Two open reading frames (ORFs) encoding for a nonribosomal peptide synthetase (NRPS) and a NRPS/polyketide synthase (PKS) hybrid were found to be involved in the assembly of the core structure. Furthermore, the cluster included four additional ORFs that have specific roles in tailoring reactions and drug resistance [111].

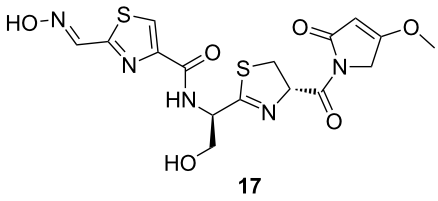

Figure 4: Structure of althiomycin (**17**).

Unlike the ubiquitous DKxanthenes or myxochelins, althiomycin is only produced by a few members of the species *M. xanthus* [65]. For instance, the model strain DK1622 lacks the althiomycin biosynthesis genes and is even sensitive against this antibiotic [111]. In a comprehensive chemical analysis of 98 different *M. xanthus* strains, althiomycin was never observed together with myxovirescins [65]. It is hence very tempting to speculate that the predatory weapon myxovirescin could have been replaced by another potent antibiotic. Considering the dispersal of althiomycin biosynthesis genes in many taxonomically unrelated bacteria [112], it appears possible that some myxobacteria acquired the respective locus via horizontal gene transfer.

Cystobactamids: The cystobactamids were recently isolated from a *Cystobacter* sp. and represent a novel class of NRPS-derived antimicrobial peptides [113]. Cystobactamids 919-1 and 919-2 (Figure 5) display an unusual aromatic scaffold composed of *p*-nitrobenzoic acid and four *p*-aminobenzoic acid (PABA)-derived moieties. The latter vary in their oxidation and substitution pattern, which may even comprise rare isopropoxy groups. The two unmodified PABA residues in compounds 919-1 and 919-2 are connected via an *iso*-β-methoxyasparagine or a β-methoxyasparagine unit, respectively. In contrast, the tripeptidic cystobactamid 507 seems to be either a biosynthetic byproduct or a degradation fragment of its larger congeners. All cystobactamids lack antifungal and cytotoxic properties, but they exhibit significant antibacterial activities. Especially deriv-

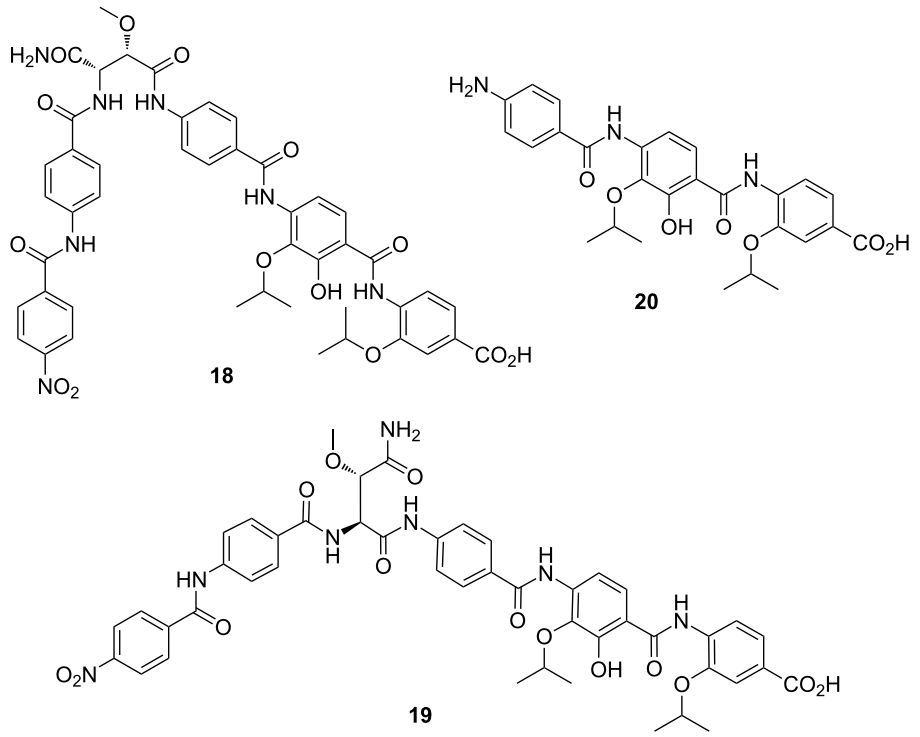

Figure 5: Structures of cystobactamids 919-1 (**18**), 919-2 (**19**), and 507 (**20**).

ative 919-2 (**19**) possesses strong inhibitory effects on the growth of Gram-positive and Gram-negative bacteria. Susceptible bacteria include *Acinetobacter baumannii*, which is a frequent inhabitant of soil, but has received even more attention as a causative agent of hard-to-treat nosocomial infections [113].

Analysis of the cystobactamid biosynthesis gene cluster led to the identification of a gene encoding a putative resistance factor. This discovery was the starting point for resolving the molecular target of these antibiotics. Subsequent assays confirmed that the cystobactamids act as bacterial DNA gyrase inhibitors [113]. Whether or not the cystobactamids are involved in predation has not been investigated yet. Their potent activity at nanomolar concentrations against a broad range of bacteria would undoubtedly make them excellent molecules for hunting down prey.

Biology and biosynthetic potential of *Herpetosiphon* spp.

Taxonomically, the genus *Herpetosiphon* belongs to the class Chloroflexi within the homonymous phylum. Members of this phylum are metabolically highly diverse, including dehalorespiring anaerobes besides aerobic CO-oxidizing thermophiles, chlorophototrophs and chemoheterotrophs [114-116]. Characteristic features in the class Chloroflexi comprise a filamentous morphology and gliding motility. The associated bacteria stain Gram-negative, albeit lacking a lipopolysaccharide-containing outer membrane [117], and they typically grow phototrophically under anoxic conditions [118]. In stark contrast to its relatives, *Herpetosiphon* is not capable of photosynthesis. It has been proposed that the genus diverged from the major lineage upon loss of its photosystem and has shifted to a saprophytic, facultative predatory lifestyle [114]. *Herpetosiphon* spp. seem to be widely distributed in soil and freshwater environments [119], where they attack and digest a multitude of bacteria [11]. Akin to myxobacteria, they are assumed to practice group predation [6]. Actually, the genus only includes two validly described species, namely *H. aurantiacus* and *H. geysericola*. The genome of *H. aurantiacus* 114-95^T, which is the type species of the entire genus, was fully sequenced and annotated [12]. Furthermore, a draft genome sequence of *H. geysericola* has recently become available [120]. The circular chromosomes of the two *Herpetosiphon* strains are of comparable size, i.e., 6.35 and 6.14 Mbp, whereas their phototrophic relatives have smaller replicons that range from 4.68 to 5.80 Mbp [12]. It thus appears as if there has been an enlargement of the predator's genomes. Some of the expansion that is evident results from the acquisition of genes involved in secondary metabolism [121]. While the potential of *Chloroflexus* and *Roseiflexus* spp. for the production of natural products is negligible [122], the *Herpetosiphon* genomes contain a signifi-

cant number of biosynthetic loci (Table 3). Unlike actinomycete genomes, which are particularly rich in polyketide pathways [123], the *Herpetosiphon* chromosomes were found to be dominated by NRPS or mixed NRPS/PKS clusters. This situation is hence quite similar to myxobacteria [56]. An unexpected finding, however, was the discovery of an enediyne PKS gene in *H. aurantiacus* 114-95^T. Enediynes are highly potent antibiotics, causing DNA-strand scissions. Although an impressive number of 87 enediyne clusters could be identified in sequencing projects over the past years, comparatively few loci were retrieved from microbes outside the actinobacteria [124]. This suggests an event of horizontal gene transfer (HGT) in *H. aurantiacus* 114-95^T. Analysis of a large NRPS/PKS cluster in the same strain yielded even more compelling evidence for HGT. Not only is the respective cluster enclosed by a number of transposon fragments, it also features an above-average G+C content of ≈66% (the genome standard is 50.9%) as well as significant G+C shifts in its border regions [12]. The observation that HGT is in part responsible for the accumulation of biosynthesis genes is again reminiscent of the predatory myxobacteria [43].

Natural products from *Herpetosiphon* spp.

While myxobacteria are already known as a promising source for natural product research [31,32], the genus *Herpetosiphon* has been almost completely ignored in the field. It is therefore no surprise that to date only three classes of secondary metabolites have been reported from this genus (Figure 6). Siphonazole and its *O*-methyl derivative were the first natural products to be isolated from a *Herpetosiphon* strain [125]. The two compounds exhibit an unusual molecular architecture featuring two oxazole rings connected by a two-carbon tether and a terminal 2,4-pentadienylamine moiety. Feeding experiments as well as biosynthetic reasoning indicated that the siphonazoles originate from a mixed PKS/NRPS pathway [125]. Both bisoxazoles were found to possess anticancer properties, but they lack antimicrobial activities [126]. In case the siphonazoles should contribute to the predatory behavior of the producing strain, they must exert more subtle effects than those described for myxovirescins and gulmirecins.

Efforts to identify secondary metabolites from the *H. aurantiacus* type strain 114-95^T led to the discovery of auriculamide (**22**) [127]. This natural product is composed of a 2-hydroxy-3-methylvalerate and a 2-amino-1-(3-chloro-4-hydroxy-phenyl)pentan-3-one residue. A retrobiosynthetic analysis allowed the assignment of the gene cluster, which is responsible for the production of auriculamide. According to the current biosynthetic model, the scaffold of auriculamide is assembled on an NRPS/PKS enzyme complex. A decarboxyl-

Table 3: Taxonomic assignment, nutrition, genomic and biosynthetic features of Chloroflexi bacteria.

	Herpetosiphon aurantiacus 114-95^T	*Herpetosiphon geysericola* GC-42	*Chloroflexus aurantiacus* J-10-fl	*Chloroflexus aggregans* DSM 9485	*Roseiflexus castenholzii* DSM 13941	*Roseiflexus* sp. RS-1
Order	Herpetosiphonales	Herpetosiphonales	Chloroflexales	Chloroflexales	Chloroflexales	Chloroflexales
Nutrition	saprotrophic predatory	saprotrophic predatory	phototrophic	phototrophic	phototrophic	phototrophic
Chromosome size [bp]	6,346,587	6,140,412 (draft)	5,258,541	4,684,931	5,723,298	5,801,598
Protein-coding sequences	5,577	4,688	3,853	3,679	4,492	4,639
GenBank accession no.	CP000875	NZ_ LGKP00000000	CP000909	CP001337	CP000804	CP000686
Reference	[12]	[120]	[122]	GenBank	GenBank	GenBank
# of biosynthesis gene clusters[a]	14	9	2	4	4	4
# of biosynthesis gene clusters per Mbp	2.21	1.47	0.38	0.43	0.70	0.69
Combined length of biosynthesis clusters [bp][a]	821,829	300,554	42,182	42,170	117,838	117,958
Genome portion devoted to biosynthesis [%]	12.95	4.89	0.80	0.90	2.06	2.03

[a]Numbers and size of biosynthesis loci were determined using antiSMASH [50].

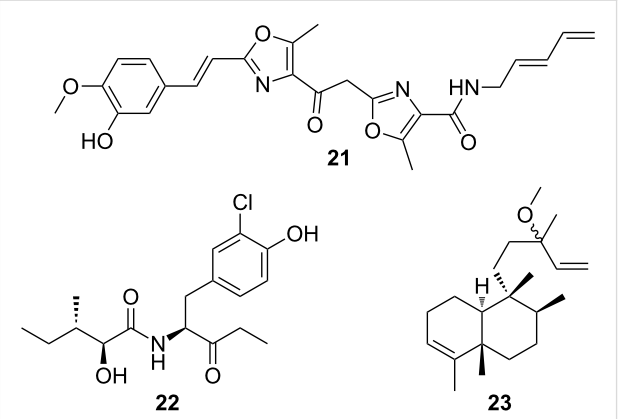

Figure 6: Structures of natural products isolated from *Herpetosiphon* spp.: siphonazole (**21**); auriculamide (**22**); (+)-*O*-methylkolavelool (**23**).

ation reaction was proposed to shorten the off-loaded carboxylic acid and to give rise to the unusual end group of the natural product [127]. Whether auriculamide possesses antibiotic properties is still open. The low fermentation yield prevented biological testing of the isolated compound.

More recently, the terpenome of *H. aurantiacus* 114-95^T received some attention. Researchers found two genes in the chromosome, the enzymatic products of which exhibited high sequence similarity to proteins that are responsible for the biosynthesis of tuberculosinol and isotuberculosinol in *Mycobacterium tuberculosis* [128]. Following in vitro studies of the two *Herpetosiphon* enzymes as well as a reconstitution of the entire associated pathway, (+)-*O*-methylkolavelool was identified as a metabolic product. Subsequent GC–MS analyses confirmed that this previously unknown diterpene is actually produced by the predatory bacterium [128].

From genomic data, it is evident that the genus *Herpetosiphon* harbors a significant potential for the biosynthesis of natural products. The fact that no antibiotics have been described from this bacterium yet is in our opinion most likely due to a lack of adequate studies. Similar to other neglected producer organisms [129], the genus *Herpetosiphon* can be expected to yield many previously unknown natural products.

Conclusion

Bacteria practicing group predation possess comparatively large replicons with an average size of 6.0 to 6.3 Mbp in case of *Lysobacter* and *Herpetosiphon* spp., or 9.6 Mbp in case of *Myxococcus* and *Corallococcus* spp. [12,37,49]. Although the genome size must not necessarily exceed the most closely related non-predatory species, as shown for the myxobacteria, a distinctive feature between predatory and non-predatory strains is the density of biosynthetic loci. In other words, families of genes encoding the production of secondary metabolites were consistently found to be overrepresented in the genomes of predatory bacteria. This observation may reflect a need for specialized molecules that coordinate swarm formation or mediate prey killing. The assumption that the extended biosynthetic capacities are due to the predatory lifestyle can, however, not be verified, because only a small fraction of the corresponding secondary metabolomes have been explored. Even in case of model organisms, which were subject of extensive chemical investigations, such as *M. xanthus* DK1622, the products of most biosynthetic pathways await their discovery. On the other hand, there is now strong evidence that compounds, such as the myxovirescins or corallopyronins, are used by their producers to enable feeding on certain prey bacteria [82]. The loss of these antibiotics or, alternatively, a resistance development of the prey organism could not be compensated by the predator and always resulted in a restricted prey spectrum [82]. Regarding the available information on the chemistry of predatory myxobacteria, it seems likely that every strain has the potential to produce at least a single class of natural products with potent antibacterial activity. The high recovery rate of myxovirescins and corallopyronins in strains of *Myxococcus xanthus* and *Corallococcus coralloides* [65,100] suggests a correlation between taxonomy and secondary metabolism. The discovery of the structurally related gulmirecins and disciformycins in different strains of *Pyxidicoccus fallax* [87,92] further supports the idea of species-specific antibiotics. Is the analysis of new *M. xanthus* isolates hence futile in terms of antibiotic discovery? – The observation of *M. xanthus* strains producing althiomycin instead of myxovirescins indicates the opposite, although the chance for retrieving antibiotics other than myxovirescins from this species might be low [65]. However, it should not be ignored that the activity profile of the identified antibiotics from *M. xanthus* does not cover the entire prey spectrum of this predator.

In summary, predatory bacteria are a promising source to find antibiotics, as these compounds confer a clear advantage to feed on prey organisms. New compound classes can most likely be expected from hardly studied genera and species. Also, it seems advisable to consider the prey preference of a bacterial hunter when searching for antibiotics that are active against selected pathogens.

Acknowledgements

M.N. gratefully acknowledges the Bundesministerium für Bildung und Forschung for supporting the research involving the discovery of antibiotics from predatory bacteria (03ZZ0808A) within the program InfectControl 2020. We thank Karin Martin (Hans-Knöll-Institute Jena) for providing the micrograph of *Pyxidicoccus fallax* HKI 727.

References

1. Matz, C.; Kjelleberg, S. *Trends Microbiol.* **2005,** *13,* 302–307. doi:10.1016/j.tim.2005.05.009
2. Pernthaler, J. *Nat. Rev. Microbiol.* **2005,** *3,* 537–546. doi:10.1038/nrmicro1180
3. Chesson, P. *Annu. Rev. Ecol. Syst.* **2000,** *31,* 343–366. doi:10.1146/annurev.ecolsys.31.1.343
4. Jousset, A. *Environ. Microbiol.* **2012,** *14,* 1830–1843. doi:10.1111/j.1462-2920.2011.02627.x
5. Rønn, R.; Vestergård, M.; Ekelund, F. *Acta Protozool.* **2012,** *51,* 223–235.
6. Jurkevitch, E. *Microbe* **2007,** *2,* 67–73.
7. Davidov, Y.; Jurkevitch, E. *BioEssays* **2009,** *31,* 748–757. doi:10.1002/bies.200900018
8. Guerrero, R.; Esteve, I.; Pedrós-Alió, C.; Gaju, N. *Ann. N. Y. Acad. Sci.* **1987,** *503,* 238–250. doi:10.1111/j.1749-6632.1987.tb40611.x
9. Bengtson, S. *Paleontol. Soc. Pap.* **2002,** *8,* 289–318.
10. Casida, L. E. *Appl. Environ. Microbiol.* **1983,** *46,* 881–888.
11. Quinn, G. R.; Skerman, V. B. D. *Curr. Microbiol.* **1980,** *4,* 57–62. doi:10.1007/BF02602893
12. Kiss, H.; Nett, M.; Domin, N.; Martin, K.; Maresca, J. A.; Copeland, A.; Lapidus, A.; Lucas, S.; Berry, K. W.; Del Rio, T. G.; Dalin, E.; Tice, H.; Pitluck, S.; Richardson, P.; Bruce, D.; Goodwin, L.; Han, C.; Detter, J. C.; Schmutz, J.; Brettin, T.; Land, M.; Hauser, L.; Kyrpides, N. C.; Ivanova, N.; Göker, M.; Woyke, T.; Klenk, H.-P.; Bryant, D. A. *Stand. Genomic Sci.* **2011,** *5,* 356–370. doi:10.4056/sigs.2194987
13. Sockett, R. E. *Annu. Rev. Microbiol.* **2009,** *63,* 523–539. doi:10.1146/annurev.micro.091208.073346
14. Morgan, A. D.; MacLean, R. C.; Hillesland, K. L.; Velicer, G. J. *Appl. Environ. Microbiol.* **2010,** *76,* 6920–6927. doi:10.1128/AEM.00414-10
15. Casida, L. E., Jr. *Int. J. Syst. Bacteriol.* **1982,** *32,* 339–345. doi:10.1099/00207713-32-3-339
16. Makkar, N. S.; Casida, L. E. *Int. J. Syst. Evol. Microbiol.* **1987,** *37,* 323–326.
17. Seccareccia, I.; Kost, C.; Nett, M. *Appl. Environ. Microbiol.* **2015,** *81,* 7098–7105. doi:10.1128/AEM.01781-15
18. Lewin, R. A. *Microb. Ecol.* **1997,** *34,* 232–236. doi:10.1007/s002489900052
19. Banning, E. C.; Casciotti, K. L.; Kujawinski, E. B. *FEMS Microbiol. Ecol.* **2010,** *73,* 254–270. doi:10.1111/j.1574-6941.2010.00897.x
20. Soo, R. M.; Woodcroft, B. J.; Parks, D. H.; Tyson, G. W.; Hugenholtz, P. *PeerJ* **2015,** *3,* e968. doi:10.7717/peerj.968
21. Casida, L. E., Jr. *Microb. Ecol.* **1988,** *15,* 1–8. doi:10.1007/BF02012948
22. Martin, M. O. *J. Mol. Microbiol. Biotechnol.* **2002,** *4,* 467–477.
23. Esteve, I.; Guerrero, R.; Montesinos, E.; Abellà, C. *Microb. Ecol.* **1983,** *9,* 57–64. doi:10.1007/BF02011580
24. Guerrero, R.; Pedrós-Alió, C.; Esteve, I.; Mas, J.; Chase, D.; Margulis, L. *Proc. Natl. Acad. Sci. U. S. A.* **1986,** *83,* 2138–2142. doi:10.1073/pnas.83.7.2138
25. Moulder, J. W. *Microbiol. Rev.* **1985,** *49,* 298–337.
26. Sockett, R. E.; Lambert, C. *Nat. Rev. Microbiol.* **2004,** *2,* 669–675. doi:10.1038/nrmicro959
27. Berleman, J. E.; Kirby, J. R. *FEMS Microbiol. Rev.* **2009,** *33,* 942–957. doi:10.1111/j.1574-6976.2009.00185.x
28. Cao, P.; Dey, A.; Vassallo, C. N.; Wall, D. *J. Mol. Biol.* **2015,** *427,* 3709–3721. doi:10.1016/j.jmb.2015.07.022
29. Mendes-Soares, H.; Velicer, G. J. *Microb. Ecol.* **2013,** *65,* 415–423. doi:10.1007/s00248-012-0135-6
30. Bode, H. B., Jr.; Müller, R. *Angew. Chem., Int. Ed.* **2005,** *44,* 6828–6846. doi:10.1002/anie.200501080
31. Nett, M.; König, G. M. *Nat. Prod. Rep.* **2007,** *24,* 1245–1261. doi:10.1039/b612668p
32. Müller, R.; Wink, J. *Int. J. Med. Microbiol.* **2014,** *304,* 3–13. doi:10.1016/j.ijmm.2013.09.004
33. Schäberle, T. F.; Lohr, F.; Schmitz, A.; König, G. M. *Nat. Prod. Rep.* **2014,** *31,* 953–972. doi:10.1039/c4np00011k
34. Hayward, A. C.; Fegan, N.; Fegan, M.; Stirling, G. R. *J. Appl. Microbiol.* **2010,** *108,* 756–770. doi:10.1111/j.1365-2672.2009.04471.x
35. Xie, Y.; Wright, S.; Shen, Y.; Du, L. *Nat. Prod. Rep.* **2012,** *29,* 1277–1287. doi:10.1039/c2np20064c
36. Reichenbach, H.; Höfle, G. *Biotechnol. Adv.* **1993,** *11,* 219–277. doi:10.1016/0734-9750(93)90042-L
37. de Bruijn, I.; Cheng, X.; de Jager, V.; Gómez Expósito, R.; Watrous, J.; Patel, N.; Postma, J.; Dorrestein, P. C.; Kobayashi, D.; Raaijmakers, J. M. *BMC Genomics* **2015,** *16,* No. 991. doi:10.1186/s12864-015-2191-z
38. König, G. M.; Dávila-Céspedes, A.; Hufendiek, P.; Crüsemann, M.; Schäberle, T. F. *Beilstein J. Org. Chem.* **2016,** submitted.
39. Kaiser, D.; Robinson, M.; Kroos, L. *Cold Spring Harbor Perspect. Biol.* **2010,** *2,* a000380. doi:10.1101/cshperspect.a000380
40. Claessen, D.; Rozen, D. E.; Kuipers, O. P.; Søgaard-Andersen, L.; van Wezel, G. P. *Nat. Rev. Microbiol.* **2014,** *12,* 115–124. doi:10.1038/nrmicro3178
41. Nan, B.; Zusman, D. R. *Annu. Rev. Genet.* **2011,** *45,* 21–39. doi:10.1146/annurev-genet-110410-132547
42. Li, Z.-F.; Li, X.; Liu, H.; Liu, X.; Han, K.; Wu, Z.-H.; Hu, W.; Li, F.-F.; Li, Y.-Z. *J. Bacteriol.* **2011,** *193,* 5015–5016. doi:10.1128/JB.05516-11
43. Goldman, B. S.; Nierman, W. C.; Kaiser, D.; Slater, S. C.; Durkin, A. S.; Eisen, J. A.; Ronning, C. M.; Barbazuk, W. B.; Blanchard, M.; Field, C.; Halling, C.; Hinkle, G.; Iartchuk, O.; Kim, H. S.; Mackenzie, C.; Madupu, R.; Miller, N.; Shvartsbeyn, A.; Sullivan, S. A.; Vaudin, M.; Wiegand, R.; Kaplan, H. B. *Proc. Natl. Acad. Sci. U. S. A.* **2006,** *103,* 15200–15205. doi:10.1073/pnas.0607335103
44. Huntley, S.; Zhang, Y.; Treuner-Lange, A.; Kneip, S.; Sensen, C. W.; Søgaard-Andersen, L. *J. Bacteriol.* **2012,** *194,* 3012–3013. doi:10.1128/JB.00397-12
45. Huntley, S.; Kneip, S.; Treuner-Lange, A.; Søgaard-Andersen, L. *Genome Announc.* **2013,** *1,* e00100-13. doi:10.1128/genomeA.00100-13
46. Schneiker, S.; Perlova, O.; Kaiser, O.; Gerth, K.; Alici, A.; Altmeyer, M. O.; Bartels, D.; Bekel, T.; Beyer, S.; Bode, E.; Bode, H. B.; Bolten, C. J.; Choudhuri, J. V.; Doss, S.; Elnakady, Y. A.; Frank, B.; Gaigalat, L.; Goesmann, A.; Groeger, C.; Gross, F.; Jelsbak, L.; Jelsbak, L.; Kalinowski, J.; Kegler, C.; Knauber, T.; Konietzny, S.; Kopp, M.; Krause, L.; Krug, D.; Linke, B.; Mahmud, T.; Martinez-Arias, R.; McHardy, A. C.; Merai, M.; Meyer, F.; Mormann, S.; Muñoz-Dorado, J.; Perez, J.; Pradella, S.; Rachid, S.; Raddatz, G.; Rosenau, F.; Rückert, C.; Sasse, F.; Scharfe, M.; Schuster, S. C.; Suen, G.; Treuner-Lange, A.; Velicer, G. J.; Vorhölter, F.-J.; Weissman, K. J.; Welch, R. D.; Wenzel, S. C.; Whitworth, D. E.; Wilhelm, S.; Wittmann, C.; Blöcker, H.; Pühler, A.; Müller, R. *Nat. Biotechnol.* **2007,** *25,* 1281–1289. doi:10.1038/nbt1354

47. Han, K.; Li, Z.-F.; Peng, R.; Zhu, L.-P.; Zhou, T.; Wang, L.-G.; Li, S.-G.; Zhang, X.-B.; Hu, W.; Wu, Z.-H.; Qin, N.; Li, Y.-Z. *Sci. Rep.* **2013,** *3,* No. 2101. doi:10.1038/srep02101
48. Blattner, F. R.; Plunkett, G., III; Bloch, C. A.; Perna, N. T.; Burland, V.; Riley, M.; Collado-Vides, J.; Glasner, J. D.; Rode, C. K.; Mayhew, G. F.; Gregor, J.; Davis, N. W.; Kirkpatrick, H. A.; Goeden, M. A.; Rose, D. J.; Mau, B.; Shao, Y. *Science* **1997,** *277,* 1453–1462. doi:10.1126/science.277.5331.1453
49. Huntley, S.; Hamann, N.; Wegener-Feldbrügge, S.; Treuner-Lange, S.; Kube, M.; Reinhardt, R.; Klages, S.; Müller, R.; Ronning, C. M.; Nierman, W. C.; Søgaard-Andersen, L. *Mol. Biol. Evol.* **2011,** *28,* 1083–1097. doi:10.1093/molbev/msq292
50. Chen, X.-J.; Han, K.; Feng, J.; Zhuo, L.; Li, Y.-J.; Li, Y.-Z. *Stand. Genomic Sci.* **2016,** *11,* No. 1. doi:10.1186/s40793-015-0121-y
51. Weber, T.; Blin, K.; Duddela, S.; Krug, D.; Kim, H. U.; Bruccoleri, R.; Lee, S. Y.; Fischbach, M. A.; Müller, R.; Wohlleben, W.; Breitling, R.; Takano, E.; Medema, M. H. *Nucleic Acids Res.* **2015,** *43,* W237–W243. doi:10.1093/nar/gkv437
52. Garcia, R.; Müller, R. The Family *Polyangiaceae*. In *The Prokaryotes;* Rosenberg, E.; DeLong, E. F.; Lory, S.; Stackebrandt, E.; Thompson, F., Eds.; Springer: Berlin, Heidelberg, 2014; pp 247–279. doi:10.1007/978-3-642-39044-9_308
53. Garcia, R.; Gerth, K.; Stadler, M.; Dogma, I. J., Jr.; Müller, R. *Mol. Phylogenet. Evol.* **2010,** *57,* 878–887. doi:10.1016/j.ympev.2010.08.028
54. Garcia, R.; Pistorius, D.; Stadler, M.; Müller, R. *J. Bacteriol.* **2011,** *193,* 1930–1942. doi:10.1128/JB.01091-10
55. Berleman, J. E.; Chumley, T.; Cheung, P.; Kirby, J. R. *J. Bacteriol.* **2006,** *188,* 5888–5895. doi:10.1128/JB.00559-06
56. Wenzel, S. C.; Müller, R. *Nat. Prod. Rep.* **2009,** *26,* 1385–1407. doi:10.1039/b817073h
57. Cortina, N. S.; Krug, D.; Plaza, A.; Revermann, O.; Müller, R. *Angew. Chem., Int. Ed.* **2012,** *51,* 811–816. doi:10.1002/anie.201106305
58. Kunze, B.; Bedorf, N.; Kohl, W.; Höfle, G.; Reichenbach, H. *J. Antibiot.* **1989,** *42,* 14–17. doi:10.7164/antibiotics.42.14
59. Silakowski, B.; Kunze, B.; Nordsiek, G.; Blöcker, H.; Höfle, G.; Müller, R. *Eur. J. Biochem.* **2000,** *267,* 6476–6485. doi:10.1046/j.1432-1327.2000.01740.x
60. Schieferdecker, S.; König, S.; Koeberle, A.; Dahse, H.-M.; Werz, O.; Nett, M. *J. Nat. Prod.* **2015,** *78,* 335–338. doi:10.1021/np500909b
61. Wenzel, S. C.; Meiser, P.; Binz, T. M.; Mahmud, T.; Müller, R. *Angew. Chem., Int. Ed.* **2006,** *45,* 2296–2301. doi:10.1002/anie.200503737
62. Ohlendorf, B.; Kehraus, S.; König, G. M. *J. Nat. Prod.* **2008,** *71,* 1708–1713. doi:10.1021/np800319v
63. Meiser, P.; Bode, H. B.; Müller, R. *Proc. Natl. Acad. Sci. U. S. A.* **2006,** *103,* 19128–19133. doi:10.1073/pnas.0606039103
64. Meiser, P.; Weissman, K. J.; Bode, H. B.; Krug, D.; Dickschat, J. S.; Sandmann, A.; Müller, R. *Chem. Biol.* **2008,** *15,* 771–781. doi:10.1016/j.chembiol.2008.06.005
65. Krug, D.; Zurek, G.; Revermann, O.; Vos, M.; Velicer, G. J.; Müller, R. *Appl. Environ. Microbiol.* **2008,** *74,* 3058–3068. doi:10.1128/AEM.02863-07
66. Trowitzsch-Kienast, W.; Gerth, K.; Wray, V.; Reichenbach, H.; Höfle, G. *Liebigs Ann. Chem.* **1993,** 1233–1237. doi:10.1002/jlac.1993199301200
67. Wenzel, S. C.; Kunze, B.; Höfle, G.; Silakowski, B.; Scharfe, M.; Blöcker, H.; Müller, R. *ChemBioChem* **2005,** *6,* 375–385. doi:10.1002/cbic.200400282
68. Miyanaga, S.; Sakurai, H.; Saiki, I.; Onaka, H.; Igarashi, Y. *Bioorg. Med. Chem.* **2009,** *17,* 2724–2732. doi:10.1016/j.bmc.2009.02.040
69. Korp, J.; König, S.; Schieferdecker, S.; Dahse, H.-M.; König, G. M.; Werz, O.; Nett, M. *ChemBioChem* **2015,** *16,* 2445–2450. doi:10.1002/cbic.201500446
70. Jansen, R.; Reifenstahl, G.; Gerth, K.; Reichenbach, H.; Höfle, G. *Liebigs Ann. Chem.* **1983,** 1081–1095. doi:10.1002/jlac.198319830702
71. Gerth, K.; Jansen, R.; Reifenstahl, G.; Höfle, G.; Irschik, H.; Kunze, B.; Reichenbach, H.; Thierbach, G. *J. Antibiot.* **1983,** *36,* 1150–1156. doi:10.7164/antibiotics.36.1150
72. Friedrich, T.; Van Heek, P.; Leif, H.; Ohnishi, T.; Forche, E.; Kunze, B.; Jansen, R.; Trowitzsch-Kienast, W.; Höfle, G.; Reichenbach, H.; Weiss, H. *Eur. J. Biochem.* **1994,** *219,* 691–698. doi:10.1111/j.1432-1033.1994.tb19985.x
73. Bode, H. B.; Meiser, P.; Klefisch, T.; Cortina, N. S. D. J.; Krug, D.; Göhring, A.; Schwär, G.; Mahmud, T.; Elnakady, Y. A.; Müller, R. *ChemBioChem* **2007,** *8,* 2139–2144. doi:10.1002/cbic.200700401
74. Rosenberg, E.; Vaks, B.; Zuckerberg, A. *Antimicrob. Agents Chemother.* **1973,** *4,* 507–513. doi:10.1128/AAC.4.5.507
75. Gerth, K.; Irschik, H.; Reichenbach, H.; Trowitzsch, W. *J. Antibiot.* **1982,** *35,* 1454–1459. doi:10.7164/antibiotics.35.1454
76. Trowitzsch, W.; Wray, V.; Gerth, K.; Höfle, G. *J. Chem. Soc., Chem. Commun.* **1982,** 1340–1342. doi:10.1039/C39820001340
77. Onishi, N.; Izaki, K.; Takahashi, H. *J. Antibiot.* **1984,** *37,* 13–19. doi:10.7164/antibiotics.37.13
78. Takayama, S.; Yamanaka, S.; Miyashiro, S.; Yokokawa, Y.; Shibai, H. *J. Antibiot.* **1988,** *41,* 429–445. doi:10.7164/antibiotics.41.439
79. Simunovic, V.; Zapp, J.; Rachid, S.; Krug, D.; Meiser, P.; Müller, R. *ChemBioChem* **2006,** *7,* 1206–1220. doi:10.1002/cbic.200600075
80. Rosenberg, E.; Dworkin, M. *J. Ind. Microbiol.* **1996,** *17,* 424–431. doi:10.1007/BF01574773
81. Xiao, Y.; Gerth, K.; Müller, R.; Wall, D. *Antimicrob. Agents Chemother.* **2012,** *56,* 2014–2021. doi:10.1128/AAC.06148-11
82. Xiao, Y.; Wei, X.; Ebright, R.; Wall, D. *J. Bacteriol.* **2011,** *193,* 4626–4633. doi:10.1128/JB.05052-11
83. Morett, E.; Segovia, L. *J. Bacteriol.* **1993,** *175,* 6067–6074.
84. Volz, C.; Kegler, C.; Müller, R. *Chem. Biol.* **2012,** *19,* 1447–1459. doi:10.1016/j.chembiol.2012.09.010
85. Bretscher, A. P.; Kaiser, D. *J. Bacteriol.* **1978,** *133,* 763–768.
86. Weissman, K. J.; Müller, R. *Nat. Prod. Rep.* **2010,** *27,* 1276–1295. doi:10.1039/c001260m
87. Schieferdecker, S.; König, S.; Weigel, C.; Dahse, H.-M.; Werz, O.; Nett, M. *Chem. – Eur. J.* **2014,** *20,* 15933–15940. doi:10.1002/chem.201404291
88. Zhang, L.; Wang, H.; Fang, X.; Stackebrandt, E.; Ding, Y. *J. Microbiol. Methods* **2003,** *54,* 21–27. doi:10.1016/S0167-7012(02)00257-9
89. Schieferdecker, S.; Exner, T. E.; Gross, H.; Roth, M.; Nett, M. *J. Antibiot.* **2014,** *67,* 519–525. doi:10.1038/ja.2014.31
90. Mohr, K. I.; Stechling, M.; Wink, J.; Wilharm, E.; Stadler, M. *MicrobiologyOpen* **2016**. doi:10.1002/mbo3.325
91. Dawid, W. *FEMS Microbiol. Rev.* **2000,** *24,* 403–427. doi:10.1111/j.1574-6976.2000.tb00548.x
92. Surup, F.; Viehrig, K.; Mohr, K. I.; Herrmann, J.; Jansen, R.; Müller, R. *Angew. Chem., Int. Ed.* **2014,** *53,* 13588–13591. doi:10.1002/anie.201406973

93. Hille-Rehfeld, A. *Chem. Unserer Zeit* **2015,** *49,* 90–91. doi:10.1002/ciuz.201580017
94. Holzgrabe, U. *Pharmakon* **2015,** *3,* 181–183.
95. Irschik, H.; Gerth, K.; Höfle, G.; Kohl, W.; Reichenbach, H. *J. Antibiot.* **1983,** *36,* 1651–1658. doi:10.7164/antibiotics.36.1651
96. Kohl, W.; Irschik, H.; Reichenbach, H.; Höfle, G. *Liebigs Ann. Chem.* **1983,** 1656–1667. doi:10.1002/jlac.198319831003
97. Irschik, H.; Jansen, R.; Höfle, G.; Gerth, K.; Reichenbach, H. *J. Antibiot.* **1985,** *38,* 145–152. doi:10.7164/antibiotics.38.145
98. Jansen, R.; Höfle, G.; Irschik, H.; Reichenbach, H. *Liebigs Ann. Chem.* **1985,** 822–836. doi:10.1002/jlac.198519850418
99. Schäberle, T. F.; Schmitz, A.; Zocher, G.; Schiefer, A.; Kehraus, S.; Neu, E.; Roth, M.; Vassylyev, D. G.; Stehle, T.; Bierbaum, G.; Hoerauf, A.; Pfarr, K.; König, G. M. *J. Nat. Prod.* **2015,** *78,* 2505–2509. doi:10.1021/acs.jnatprod.5b00175
100. Erol, Ö.; Schäberle, T. F.; Schmitz, A.; Rachid, S.; Gurgui, C.; El Omari, M.; Lohr, F.; Kehraus, S.; Piel, J.; Müller, R.; König, G. M. *ChemBioChem* **2010,** *11,* 1253–1265. doi:10.1002/cbic.201000085
101. Sucipto, H.; Wenzel, S. C.; Müller, R. *ChemBioChem* **2013,** *14,* 1581–1589. doi:10.1002/cbic.201300289
102. Schäberle, T. F. *Beilstein J. Org. Chem.* **2016,** *12,* 571–588. doi:10.3762/bjoc.12.56
103. Schäberle, T. F.; Schiefer, A.; Schmitz, A.; König, G. M.; Hoerauf, A.; Pfarr, K. *Int. J. Med. Microbiol.* **2014,** *304,* 72–78. doi:10.1016/j.ijmm.2013.08.010
104. Mukhopadhyay, J.; Das, K.; Ismail, S.; Koppstein, D.; Jang, M.; Hudson, B.; Sarafianos, S.; Tuske, S.; Patel, J.; Jansen, R.; Irschik, H.; Arnold, E.; Ebright, R. H. *Cell* **2008,** *135,* 295–307. doi:10.1016/j.cell.2008.09.033
105. Srivastava, A.; Talaue, M.; Liu, S.; Degen, D.; Ebright, R. Y.; Sineva, E.; Chakraborty, A.; Druzhinin, S. Y.; Chatterjee, S.; Mukhopadhyay, J.; Ebright, Y. W.; Zozula, A.; Shen, J.; Sengupta, S.; Niedfeldt, R. R.; Xin, C.; Kaneko, T.; Irschik, H.; Jansen, R.; Donadio, S.; Connell, N.; Ebright, R. H. *Curr. Opin. Microbiol.* **2011,** *14,* 532–543. doi:10.1016/j.mib.2011.07.030
106. Cramer, P. *Curr. Opin. Struct. Biol.* **2002,** *12,* 89–97. doi:10.1016/S0959-440X(02)00294-4
107. Yamaguchi, H.; Nakayama, Y.; Takeda, K.; Tawara, K.; Maeda, K.; Takeuchi, T.; Umezawa, H. *J. Antibiot.* **1957,** *10,* 195–200.
108. Kunze, B.; Reichenbach, H.; Augustiniak, H.; Höfle, G. *J. Antibiot.* **1982,** *35,* 635–636. doi:10.7164/antibiotics.35.635
109. Fujimoto, H.; Kinoshita, T.; Suzuki, H.; Umezawa, H. *J. Antibiot.* **1970,** *23,* 271–275. doi:10.7164/antibiotics.23.271
110. Pestka, S. Althiomycin. In *Mechanism of Action of Antimicrobial and Antitumor Agents;* Corcoran, J. W.; Hahn, F. E., Eds.; Springer: Berlin, Heidelberg, New York, 1975; pp 323–326. doi:10.1007/978-3-642-46304-4_21
111. Cortina, N. S.; Revermann, O.; Krug, D.; Müller, R. *ChemBioChem* **2011,** *12,* 1411–1416. doi:10.1002/cbic.201100154
112. Gerc, A. J.; Song, L.; Challis, G. L.; Stanley-Wall, N. R.; Coulthurst, S. J. *PLoS One* **2012,** *7,* e44673. doi:10.1371/journal.pone.0044673
113. Baumann, S.; Herrmann, J.; Raju, R.; Steinmetz, H.; Mohr, K. I.; Hüttel, S.; Harmrolfs, K.; Stadler, M.; Müller, R. *Angew. Chem., Int. Ed.* **2014,** *53,* 14605–14609. doi:10.1002/anie.201409964
114. Garrity, G. M.; Holt, J. G.; Castenholtz, R. W.; Pierson, B. K.; Keppen, O. I.; Gorlenko, V. M. Phylum BVI. *Chloroflexi* phy. nov. In *Bergey's Manual of Systematic Bacteriology,* 2nd ed.; Garrity, G. M.; Boone, D. R.; Castenholz, R. W., Eds.; Springer: New York, 2001; Vol. 1, pp 427–446. doi:10.1007/978-0-387-21609-6_23
115. Hugenholtz, P.; Stackebrandt, E. *Int. J. Syst. Evol. Microbiol.* **2004,** *54,* 2049–2051. doi:10.1099/ijs.0.03028-0
116. Gupta, R. S.; Chander, P.; George, S. *Antonie van Leeuwenhoek* **2013,** *103,* 99–119. doi:10.1007/s10482-012-9790-3
117. Sutcliffe, I. C. *Trends Microbiol.* **2010,** *18,* 464–470. doi:10.1016/j.tim.2010.06.005
118. Frigaard, N.-U.; Bryant, D. A. *Arch. Microbiol.* **2004,** *182,* 265–276. doi:10.1007/s00203-004-0718-9
119. Lee, N.; Reichenbach, H. The genus *Herpetosiphon*. In *The Prokaryotes,* 3rd ed.; Dworkin, M.; Falkow, S.; Rosenberg, E.; Schleifer, K.-H.; Stackebrandt, E., Eds.; Springer: New York, 2006; Vol. 7, pp 854–877. doi:10.1007/0-387-30747-8_36
120. Ward, L. M.; Hemp, J.; Pace, L. A.; Fischer, W. W. *Genome Announc.* **2015,** *3,* e01352-15.
121. Kastner, S.; Müller, S.; Natesan, L.; König, G. M.; Guthke, R.; Nett, M. *Arch. Microbiol.* **2012,** *194,* 557–566. doi:10.1007/s00203-012-0789-y
122. Tang, K.-H.; Barry, K.; Chertkov, O.; Dalin, E.; Han, C. S.; Hauser, L. J.; Honchak, B. M.; Karbach, L. E.; Land, M. L.; Lapidus, A.; Larimer, F. W.; Mikhailova, N.; Pitluck, S.; Pierson, B. K.; Blankenship, R. E. *BMC Genomics* **2011,** *12,* No. 334. doi:10.1186/1471-2164-12-334
123. Nett, M.; Ikeda, H.; Moore, B. S. *Nat. Prod. Rep.* **2009,** *26,* 1362–1384. doi:10.1039/b817069j
124. Rudolf, J. D.; Yan, X.; Shen, B. *J. Ind. Microbiol. Biotechnol.* **2016,** *43,* 261–276. doi:10.1007/s10295-015-1671-0
125. Nett, M.; Erol, Ö.; Kehraus, S.; Köck, M.; Krick, A.; Eguereva, E.; Neu, E.; König, G. M. *Angew. Chem., Int. Ed.* **2006,** *45,* 3863–3867. doi:10.1002/anie.200504525
126. Zhang, J.; Polishchuk, E. A.; Chen, J.; Ciufolini, M. A. *J. Org. Chem.* **2009,** *74,* 9140–9151. doi:10.1021/jo9018705
127. Schieferdecker, S.; Domin, N.; Hoffmeier, C.; Bryant, D. A.; Roth, M.; Nett, M. *Eur. J. Org. Chem.* **2015,** 3057–3062. doi:10.1002/ejoc.201500181
128. Nakano, C.; Oshima, M.; Kurashima, N.; Hoshino, T. *ChemBioChem* **2015,** *16,* 772–781. doi:10.1002/cbic.201402652
129. Pidot, S. J.; Coyne, S.; Kloss, F.; Hertweck, C. *Int. J. Med. Microbiol.* **2014,** *304,* 14–22. doi:10.1016/j.ijmm.2013.08.011

License and Terms

BEILSTEIN JOURNAL OF ORGANIC CHEMISTRY

Muraymycin nucleoside-peptide antibiotics: uridine-derived natural products as lead structures for the development of novel antibacterial agents

Daniel Wiegmann‡, Stefan Koppermann‡, Marius Wirth, Giuliana Niro, Kristin Leyerer and Christian Ducho*

Review

Open Access

Address:
Department of Pharmacy, Pharmaceutical and Medicinal Chemistry, Saarland University, Campus C2 3, 66123 Saarbruecken, Germany

Email:
Christian Ducho* - christian.ducho@uni-saarland.de

* Corresponding author ‡ Equal contributors

Keywords:
antibiotics; natural products; nucleosides; peptides; structure–activity relationship

Beilstein J. Org. Chem. **2016,** *12,* 769–795.
doi:10.3762/bjoc.12.77

Received: 21 December 2015
Accepted: 24 February 2016
Published: 22 April 2016

This article is part of the Thematic Series "Natural products in synthesis and biosynthesis II" and is dedicated to Professor Wittko Francke on the occasion of his 75th birthday.

Guest Editor: J. S. Dickschat

Abstract

Muraymycins are a promising class of antimicrobial natural products. These uridine-derived nucleoside-peptide antibiotics inhibit the bacterial membrane protein translocase I (MraY), a key enzyme in the intracellular part of peptidoglycan biosynthesis. This review describes the structures of naturally occurring muraymycins, their mode of action, synthetic access to muraymycins and their analogues, some structure–activity relationship (SAR) studies and first insights into muraymycin biosynthesis. It therefore provides an overview on the current state of research, as well as an outlook on possible future developments in this field.

Introduction

The treatment of infectious diseases caused by bacteria is a severe issue. With multiresistant bacterial strains rendering well-established therapeutic procedures ineffective, the exploration of novel antimicrobial agents is of growing significance. The discovery of penicillin [1] and the proof of its in vivo efficacy [2] marked the starting point for the research on antibacterial drugs during the so-called "golden age" of antibiotics. Despite the early occurrence of first resistances [3-5], an innovation gap followed from the 1960s onwards, during which only few antibiotics were introduced into the market. Most of them were modifications of established substances already in clinical use. Current and future developments will have to consider these improved 2nd and 3rd generation antibiotics [6] alongside the search for completely unknown structures. For such novel agents, natural products appear to be a promising source [7-9].

Bacteria deploy different mechanisms to escape the toxic effect of an antibacterial drug [10-12]. These include the structural modification and degradation of a drug, as it is reported for aminoglycoside-modifying proteins [13], and alteration of the drug target, as can be found in macrolide-resistant bacteria that contain mutations in the bacterial ribosome [14]. Further mechanisms are an increased efflux [15] and a change in permeability of the cell wall [16,17]. Due to the evolutionary pressure exerted by antibiotics, bacteria featuring the aforementioned mutations survive, proliferate and may even develop resistances against multiple drug classes. Excessive application of antibiotics fuels the emergence of multiresistant strains such as hospital and community-associated methicillin-resistant *Staphylococcus aureus* (MRSA) [18,19] and vancomycin-resistant *Enterococcus* (VRE) [20]. This development raises the demand for antibiotics exploiting yet unused modes of action. Potential targets within bacteria include peptidoglycan biosynthesis, protein biosynthesis, DNA and RNA replication and folate metabolism [21].

Promising candidates meeting the requirements for new drugs are nucleoside antibiotics, i.e., uridine-derived compounds that address the enzyme translocase I (MraY) as a novel target, thereby interfering with a membrane-associated intracellular step of peptidoglycan biosynthesis. This review will focus on muraymycins as a subclass of nucleoside antibiotics, covering their mode of action, synthetic approaches as well as SAR studies on several derivatives. Furthermore, first insights into the biosynthesis of these *Streptomyces*-produced secondary metabolites will be discussed.

Review

Structures of naturally occurring muraymycins

The muraymycins were first isolated in 2002 from a broth of a *Streptomyces* sp. [22]. McDonald et al. discovered and characterised 19 naturally occurring muraymycins (Figure 1). These compounds belong to the family of nucleoside antibiotics which have a uridine-derived core structure in common. Their antibiotic potency is based on the inhibition of MraY, thereby blocking a membrane-associated intracellular step of bacterial cell-wall biosynthesis. The structure elucidation was carried out using one- and two-dimensional NMR experiments as well as FT mass spectrometry [22].

Muraymycins have a glycyl-uridine motif, which is connected via an aminopropyl linker to a urea peptide moiety consisting of L-leucine or L-hydroxyleucine, L-epicapreomycidine (a non-proteinogenic cyclic arginine derivative) and L-valine. The uridine structure is glycosylated in its 5'-position with an aminoribose unit and in some cases a lipophilic side chain is attached to the hydroxyleucine residue. The 19 compounds are divided into four different series (A–D) which mainly vary in the leucine residue and the lipophilic side chain or the amino sugar (Figure 1). The aminoribose is missing in muraymycins A5 and C4, which may eventually be hydrolysis products. The series A and B have lipophilic side chains with varying chain lengths, which are either ω-functionalised with a guanidino or hydroxyguanidino-function in case of series A or unfunctionalised but terminally branched in case of series B. Muraymycins of series C contain unfunctionalised L-hydroxyleucine while in series D proteinogenic L-leucine occurs instead.

Muraymycin A1 is one of the most active members of this family and shows good activity mainly against Gram-positive (*Staphylococcus* MIC: 2–16 μg/mL, *Enterococcus* MIC: 16–64 μg/mL) but also a few Gram-negative bacteria (*E. coli* MIC: down to 0.03 μg/mL). Since the activity against wild-type *E. coli* is clearly lower (MIC > 128 μg/mL) [22], it is assumed that this might be an effect resulting from low membrane permeability.

There are other naturally occurring nucleoside antibiotics which address the same biological target, thereby inhibiting peptidoglycan biosynthesis. Figure 2 shows the structures of selected other classes of nucleoside antibiotics, with structural similarities being highlighted. A broad overview of antimicrobial nucleoside antibiotics blocking peptidoglycan biosynthesis is given by Bugg et al. in two review articles [23,24] and by Ichikawa et al. in a recent review [25].

Representing the first discovered nucleoside antibiotics, the tunicamycins were isolated in 1971 from *Streptomyces lysosuperficus* nov. sp. by Takatsuki and Tamura et al. [26-28]. They contain a uridine moiety, two *O*-glycosidically linked sugars, the so-called tunicamine and a fatty acid moiety, which typically is terminally branched and unsaturated. Two closely related nucleoside antibiotics were isolated later on and named streptoviridins (isolated in 1975 from *Streptomyces griseoflavus* subsp. *thuringiensis* [29-31]) and corynetoxins (isolated in 1981 from *Corynebacterium rathayi* [32]). These classes have merely the uracil nucleoside core structure in common with the muraymycins and the terminally branched lipophilic side chain resembles the acyl moiety in muraymycins of group B.

Capuramycin, a nucleoside antibiotic isolated in 1986 from *Streptomyces griseus*, shares the uracil-derived nucleoside moiety with the muraymycins [33,34]. The antibiotic FR-900493, which is structurally closely related to muraymycins, was isolated from *Bacillus cereus* and characterised in 1990 [35]. In comparison to the muraymycins, only the urea peptide moiety and the lipopeptidyl motif are absent.

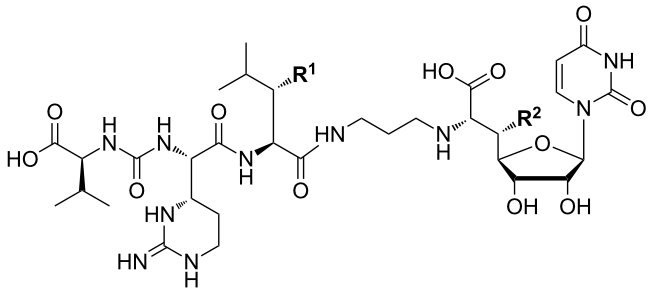

	R1	R2	R3		R1	R2	R3
A1	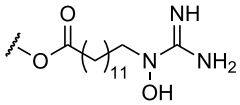	Arib	-OMe	B6	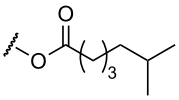	Arib	-OMe
A2	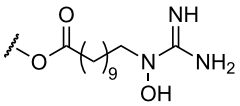	Arib	-OMe	B7	like B6	Arib	-OH
A3	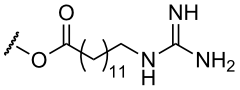	Arib	-OMe	C1	-OH	Arib	-OMe
A4	like A1	Arib	-OH	C2	-OH	Arib	-OH
A5	like A1	-OH		C3	-OH	Arib	-H
B1	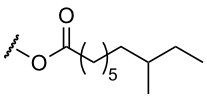	Arib	-OMe	C4	-OH	-OH	
B2	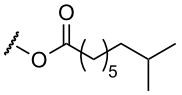	Arib	-OMe	D1	-H	Arib	-OMe
B3	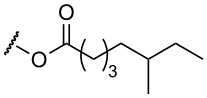	Arib	-OMe	D2	-H	Arib	-OH
B4	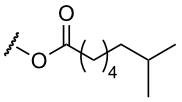	Arib	-OMe	D3	-H	Arib	-H
B5	like B4	Arib	-OH				

Figure 1: Structures of the naturally occurring muraymycins isolated by McDonald et al. [22].

The mureidomycins [36-38] and pacidamycins [39-41], both reported in 1989, the napsamycins (1994) [42] and the sansanmycins (2007) [43,44] are structurally closely related. They consist of a 3'-deoxyuridine unit with a unique enamide linkage and the non-proteinogenic *N*-methyl-2,3-diaminobutyric acid, which branches into two peptide moieties. They differ in the amino acid residues AA_2, AA_4 and AA_5, with AA_2 and AA_5 being aromatic in all four classes. The amino acid residue AA_4 is either methionine for mureidomycins, napsamycins and sansanmycins or alanine in case of pacidamycins. Remarkably, these natural products share a urea peptide motif with the muraymycins. They are mainly active against Gram-negative bacteria, which is a noteworthy difference to the muraymycins and other related nucleoside antibiotics.

The liposidomycins (isolated in 1985) [45] and the related caprazamycins (isolated in 2003) [46,47] have a unique diazepanone ring, and in case of the caprazamycins a per-

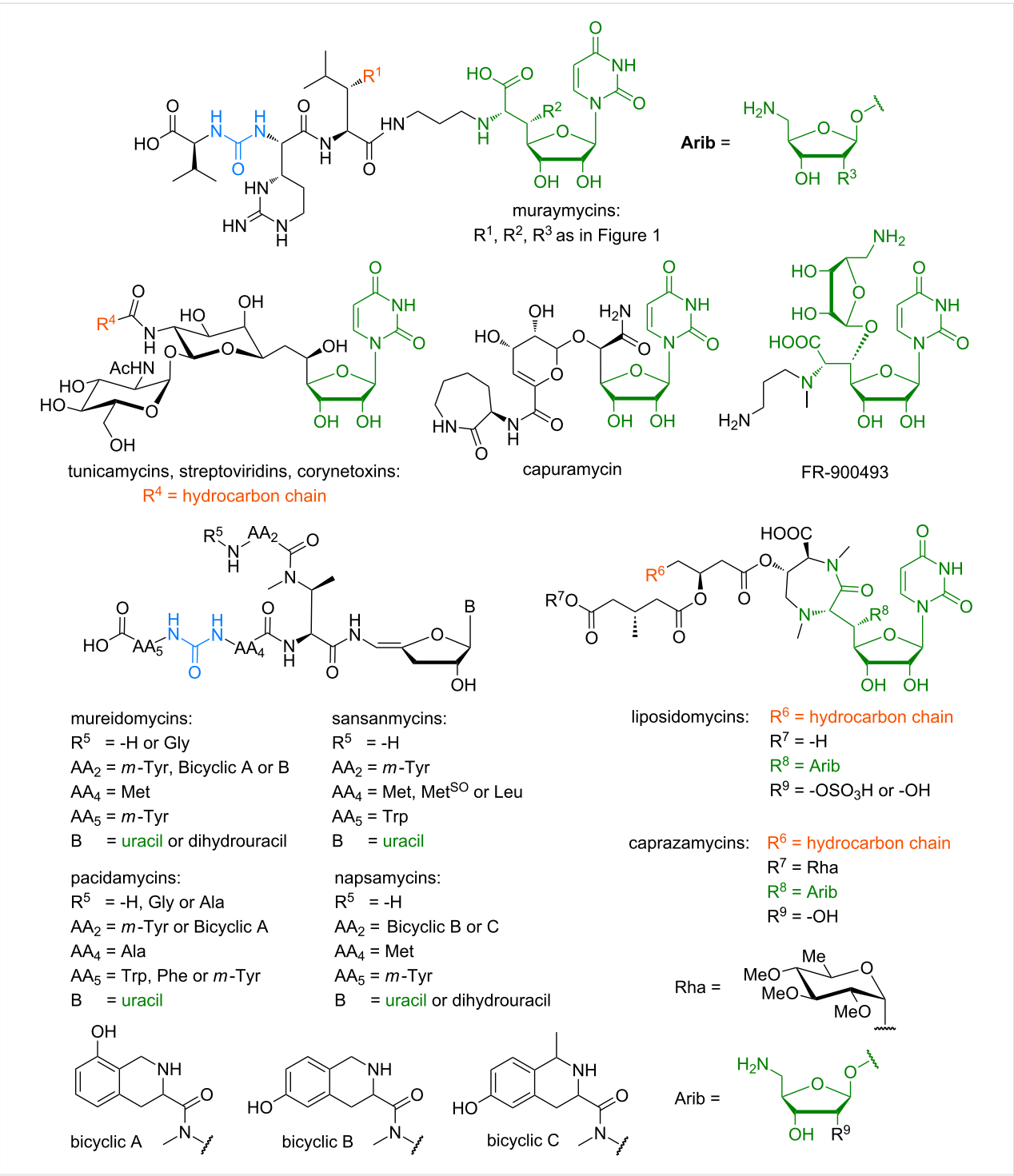

Figure 2: Structures of selected classes of nucleoside antibiotics. Similarities to the muraymycins are highlighted in different colours.

methylated rhamnose residue. They resemble the muraymycins in their uridine-derived core structure, which is also glycosylated in 5'-position with an aminoribose unit, and they contain a fatty acid moiety as well. Caprazamycins also display noteworthy antimicrobial activity against *M. tuberculosis* as well as most Gram-positive bacteria (Table 1) [46,48].

All aforementioned nucleoside antibiotics address the same biological target and most likely have the same mode of action by inhibiting MraY (see below), but their in vitro activity differs significantly. It is important to notice that a comprehensive comparison of minimum inhibitory concentrations (MIC values) is difficult because naturally occurring nucleoside antibiotics

Table 1: Comparison of the antimicrobial activities of selected representative compounds of different classes of nucleoside antibiotics against selected bacterial species.[a]

	Gram-positive			Gram-negative	
	S. aureus	*B. subtilis*	*M. smegmatis*	*E. coli*	*P. aeruginosa*
Muraymycin A1	++	n.r.	n.r.	++/+[b]	+/−
Tunicamycin	−	++	−	−	−
Capuramycin	−	−	++	−	−
FR-900493	++	++	n.r.	n.r.	n.r.
Mureidomycin C	−	n.r.	n.r.	−	++
Caprazamycin B	++	++/+	++	−	++
Liposidomycin A	−	−	n.r.[c]	−	n.r.

[a]++: good activity (MIC < 10 μg/mL), +: moderately active (10 μg/mL < MIC < 32 μg/mL), −: no notable activity (MIC > 32 μg/mL), n.r.: not reported. [b]Not active against wild-type *E. coli*. [c]Active against *M. phlei*.

have been tested against different bacterial strains. However, synthetic analogues of the nucleoside antibiotics listed in Table 1 have been tested against some of the listed bacterial species. It can therefore be assumed that the parent natural products display similar activities even though there are no data available. Furthermore, the activity of a compound against different strains of a bacterial species can vary. Nonetheless, there are certain trends and differences that can be observed. Muraymycin A1 is mainly active against Gram-positive bacteria such as *S. aureus* or *E. faecalis*, but also against some Gram-negative *E. coli* strains [49]. Tunicamycin, capuramycin and FR-900493 only show antimicrobial activity against Gram-positive strains. For mureidomycin C (R^5 = Gly, AA_2 = AA_5 = *m*-Tyr, AA_4 = Met, B = uracil, see Figure 2) as a representative compound, no activity against Gram-positive bacteria was observed, but it displayed pronounced antibacterial activity against *P. aeruginosa*. This remarkable finding distinguishes the mureidomycins, pacidamycins, sansanmycins and napsamycins from other nucleoside antibiotics. On the other hand, caprazamycin B shows good activity against Gram-positive bacteria, *Pseudomonas* and *M. tuberculosis* [48]. The related liposidomycins display good activity against *M. phlei*, while they are not active against a range of other bacteria [45].

Mode of action

To develop an effective antibiotic one needs to choose a target that is essential for bacterial survival or growth and offers selectivity to strike only bacterial cells (without cytotoxicity to human cells). There are mainly four classical target processes for antibiotics: bacterial cell wall biosynthesis, bacterial protein biosynthesis, DNA replication and folate metabolism [21]. Novel approaches that differ from these established modes of action are under investigation, but many new compounds in development still address bacterial cell wall biosynthesis. They are accompanied by a rich variety of prominent antibiotics in clinical use such as the penicillins [23,50,51]. All bacteria, i.e., Gram-positive and Gram-negative congeners, have a cell wall as part of their cell envelope. While its thickness differs among bacteria – Gram-positive strains usually have a thicker cell wall relative to Gram-negative ones – the principle molecular structure remains identical: Bacterial cell walls consist of peptidoglycan, a heteropolymer with long chains of alternating units of *N*-acetylmuramic acid (Mur*N*Ac) and *N*-acetylglucosamine (Glc*N*Ac) that are cross-linked through peptide chains attached to the muramic acid sugar (Figure 3) [52].

The biosynthesis of peptidoglycan is illustrated in Figure 4 and has been described in detail in several reviews (e.g., [51,53-57]). It can be divided into three parts: first, the formation of the monomeric building blocks in the cytosol (Figure 4, step A); second, the membrane-bound steps with the attachment to the lipid linker, transformation to a disaccharide and transport to the extracellular side of the membrane (Figure 4, steps B, C); finally, polymerisation to long oligosaccharide chains and cross-linking occur (Figure 4, steps D, F).

In the cytosol, uridine diphosphate-*N*-acetylglucosamine (UDP-Glc*N*Ac), that is formed from fructose-6-phosphate in four steps, is transformed into UDP-Mur*N*Ac-pentapeptide in a number of enzyme-catalysed reactions (Figure 4, step A). The exact composition of the peptide chain varies in different organisms. Examples given in Figure 3 are frequently occurring ones and a more comprehensive list has been reported elsewhere [52].

The membrane-associated steps commence with the transfer of UDP-Mur*N*Ac-pentapeptide to the lipid carrier undecaprenyl phosphate, catalysed by translocase I (MraY), to give lipid I (Figure 4, product of step B). The glycosyltransferase MurG attaches a Glc*N*Ac sugar to furnish lipid II (Figure 4, product of step C). This building block is then transported to the extracel-

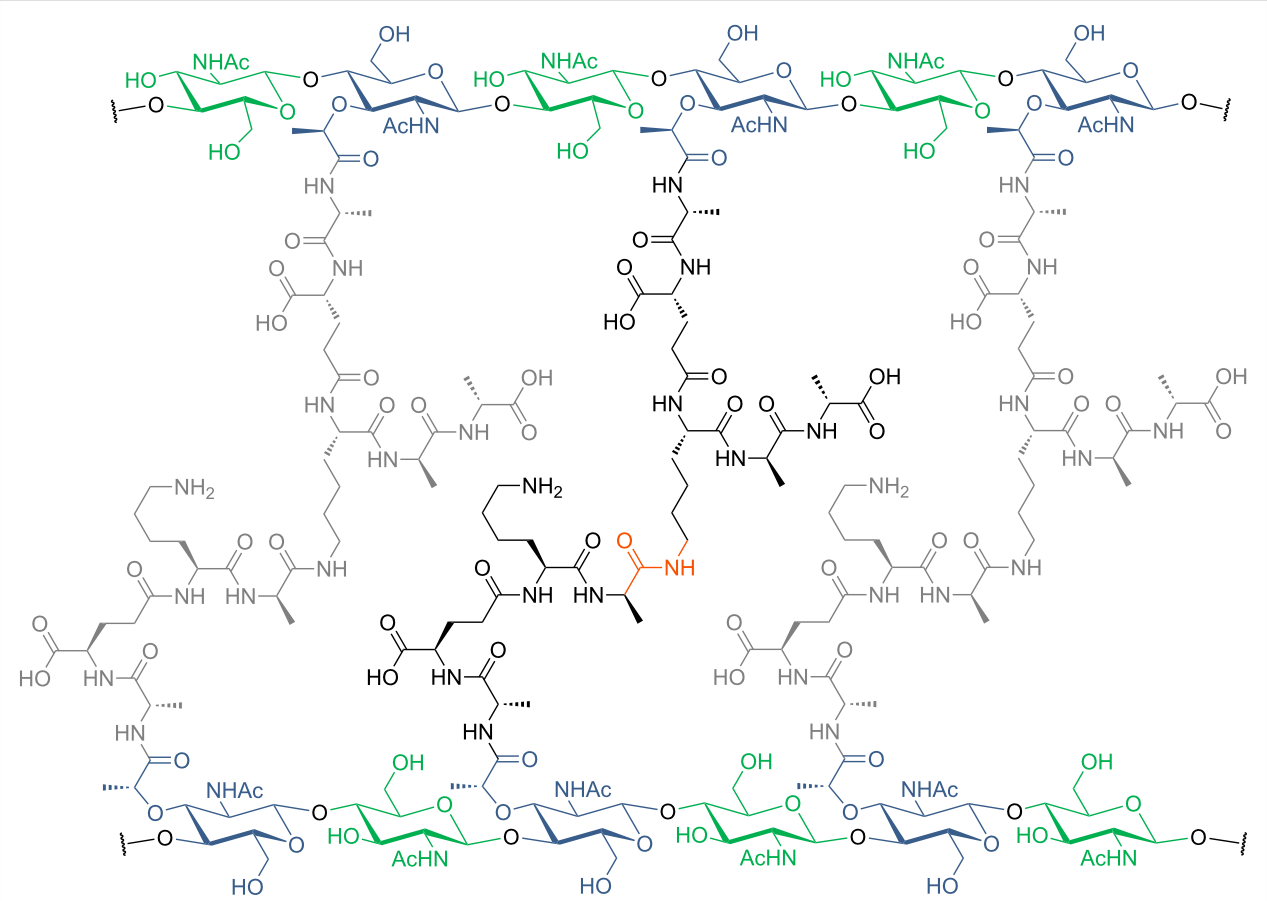

Figure 3: Structure of peptidoglycan. Long chains of glycosides (alternating Glc*N*Ac (green) and Mur*N*Ac (blue)) are cross-linked through the Mur*N*Ac peptide chain. The exact composition of the peptide chain varies among different bacterial species.

lular side of the membrane. It is speculated that there might be some kind of 'flippase' involved but this particular step is still unclear and requires further investigation [55]. On the extracellular side of the membrane, the building blocks are connected by transglycosylases to form long chains (Figure 4, step D) and then are cross-linked by transpeptidases (Figure 4, step E). Both enzymes are members of the family of penicillin-binding proteins [23].

As mentioned above, there are many antibiotics in clinical use that target at least one step of bacterial cell wall biosynthesis. Prominent examples besides penicillins are cephalosporins, cycloserine, vancomycin, fosfomycin and daptomycin [9]. All of them (except fosfomycin and cycloserine) inhibit late, extracellular steps of cell wall formation. Thus, there are still many steps not addressed by clinically used drugs, which implies that cell wall biosynthesis still offers promising novel targets for the development of antibiotics with new modes of action. Muraymycins and other nucleoside antibiotics target translocase I (MraY) that represents such a potential novel molecular target [22].

Overexpression of the *mraY* gene, identified in an *mra* (murein region A) cluster, led to an increase of UDP-*N*-acetylmuramoyl-pentapeptide: undecaprenyl phosphate phospho-*N*-acetylmuramoyl-pentapeptide transferase activity [58]. Gene knockout experiments revealed the MraY-catalysed reaction in cell wall biosynthesis to be an essential process for bacterial viability and growth [59-63].

The chemical transformation catalysed by MraY is shown in Figure 5. The cytosolic precursor UDP-Mur*N*Ac-pentapeptide is linked to undecaprenyl phosphate, a C_{55}-isoprenoid lipid carrier that is located in the cellular membrane. With concomitant release of uridine monophosphate (UMP), this furnishes a diphosphate linkage between the two substrates. The reaction is reversible and MraY accelerates the adjustment of the equilibrium state. Whereas this reaction was known for a long time [64,65], the structure of the MraY protein remained unclear. The mechanism of the MraY-catalysed reaction was investigated by kinetic studies by Heydanek, Neuhaus et al. in the 1960s. They proposed a two-step mechanism for lipid I formation that was later revised (Figure 6A) [55,66-69].

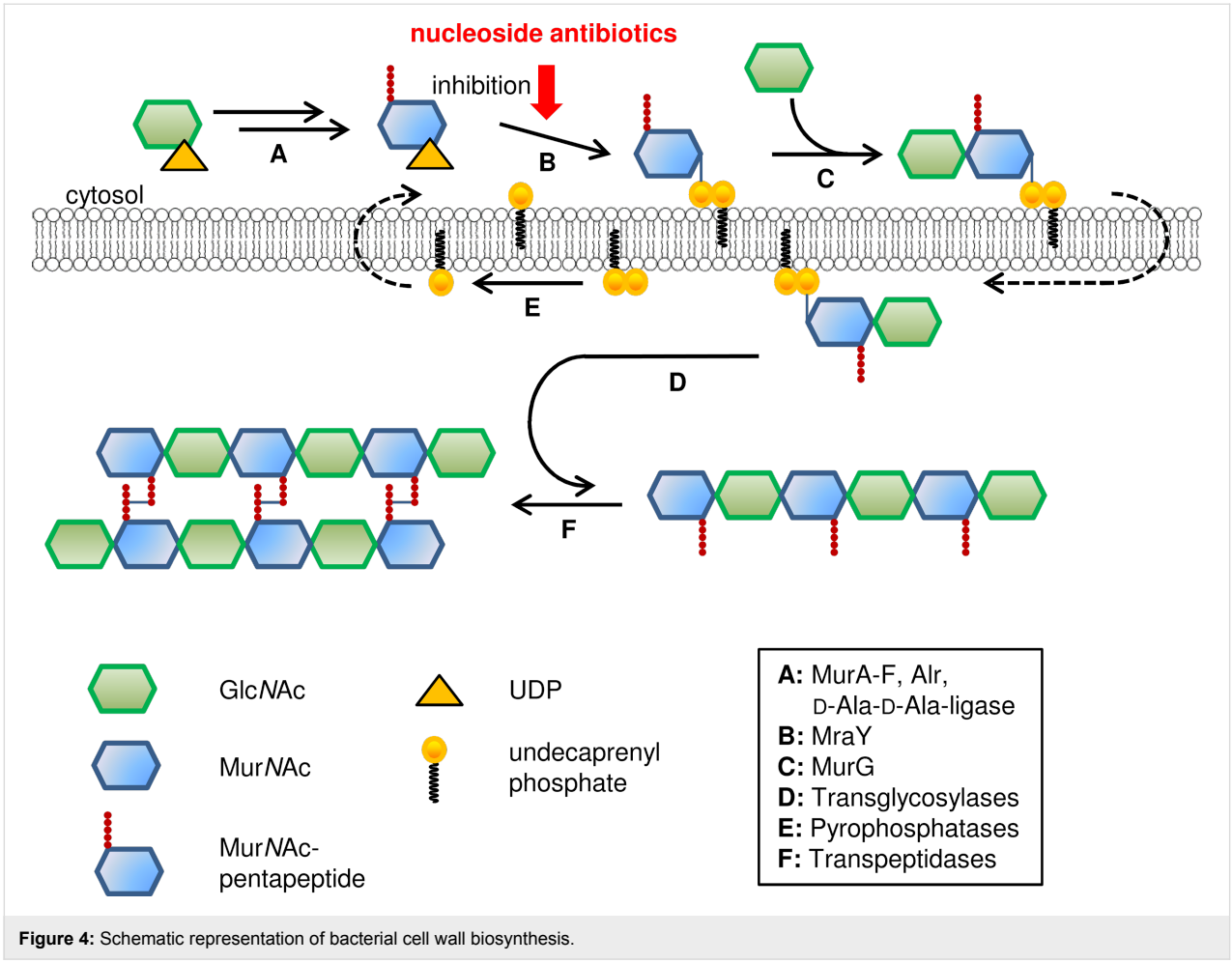

Figure 4: Schematic representation of bacterial cell wall biosynthesis.

The identification of the *mraY* gene [58] facilitated the alignment of MraY homologue sequences by van Heijenoort et al. and resulted in a two-dimensional topology model of MraY from *E. coli*, among others [70]. Bugg et al. identified three conserved residues with nucleophilic side chains within the superfamily of polyisoprenyl-phosphate *N*-acetyl hexosamine 1-phosphate transferases (PNPT). Mutation of these three aspartate residues (D115, D116 and D267 in the *E. coli* protein) resulted in a complete loss of catalytic activity. This led to a proposed model for the active site of MraY in accordance with previous findings [66]: D115 and D116 bind a Mg^{2+}-cofactor, UDP-Mur*N*Ac-pentapeptide also binds the Mg^{2+}-cofactor and D267 acts as a nucleophile within the proposed two-step mechanism (Figure 6) [68]. In a study with purified MraY from *B. subtilis*, Bouhss et al. found small remaining activity in the D231N mutant (corresponding to D267 in MraY from *E. coli*). They assumed that this would contradict the two-step mechanism as a nucleophilic residue is essential for the previously proposed mechanism. They found D98 to be crucial for activity and proposed its role to deprotonate undecaprenyl phosphate. This was speculated to be followed by a one-step nucleophilic attack of the C_{55}-alkyl phosphate at the UDP-Mur*N*Ac-pentapeptide (Figure 6B) [69].

In 2013, Lee et al. reported an X-ray crystal structure (3.3 Å resolution) of MraY from *Aquifex aeolicus* ($MraY_{AA}$) as the first structure of a member of the PNPT superfamily. $MraY_{AA}$ crystallised as a dimer and additional experiments showed that it also exists as a dimer in detergent micelles and membranes [71]. The previously proposed models are in agreement with the solved structure showing ten transmembrane helices and five cytoplasmic loops. The authors identified a cleft at the cytoplasmic side of the membrane that showed the highest conservation in sequence mapping. Furthermore, it is also the region where most of the previously identified, functionally important residues [69] are located [71]. The location and binding mode of the Mg^{2+} ion in the crystal does not support the proposed model for a two-step mechanism [68]. In experiments with Mn^{2+} exchange no interaction of the metal with D117 and D118 could be detected. Surface calculation of $MraY_{AA}$ showed an inverted U-shaped groove that could harbour the undecaprenyl phosphate co-substrate. The locations of this groove, the Mg^{2+}

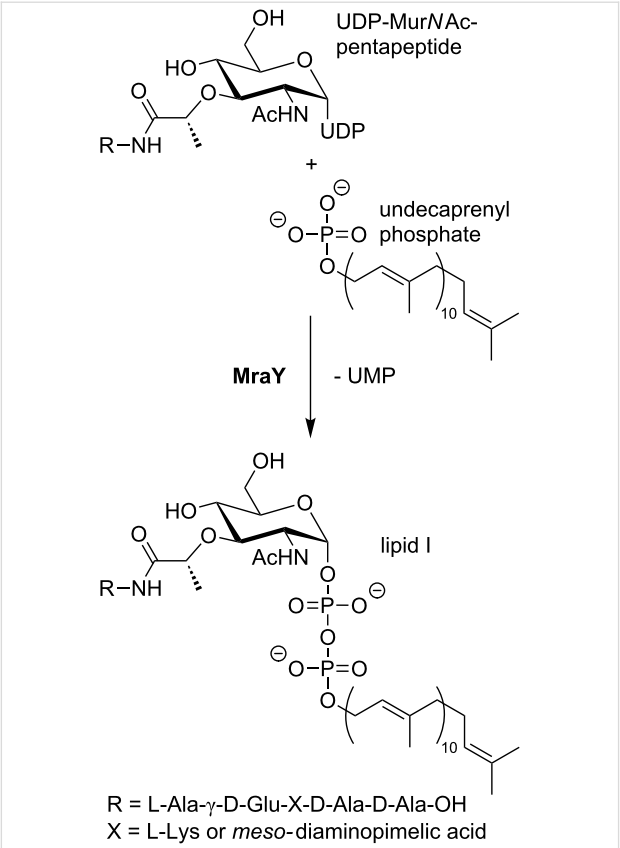

Figure 5: Translocase I (MraY) catalyses the reaction of UDP-Mur*N*Ac-pentapeptide with undecaprenyl phosphate towards lipid I.

and D265 do at least not contradict the proposed one-step mechanism. Nevertheless, there is still a need for further studies to fully understand the MraY-catalysed reaction at the molecular level [71].

In the context of a different MraY inhibitor, i.e., lysis protein E from bacteriophage ϕX174, Bugg et al. reported a different site of inhibition in pronounced distance to the proposed active site. It has been demonstrated before that mutation of phenylalanine 288 (F288L) in helix 9 of MraY caused resistance against lysis protein E [72,73]. An interaction between F288 and glutamic acid 287 (E287) with the peptide motif arginine-tryptophan-x-x-tryptophan (RWxxW, x represents an arbitrary amino acid) was found. Mutants F288L and E287A showed reduced or no detectable enzyme inhibition, thus indicating a secondary binding site for potential MraY inhibitors. Nevertheless, it remains unclear how binding at helix 9 can inhibit MraY function and further studies are probably inevitable [74].

In order to investigate the biological potencies of MraY inhibitors such as the muraymycins, in vitro assay systems are needed. A widely used and universal method to evaluate the in vitro activity of potential agents against certain bacteria is the determination of minimum inhibitory concentrations (MIC). MICs are defined as the lowest concentration at which a potential antimicrobial agent inhibits the visible growth of a microorganism [75]. They are easily determined and reflect several effects such as target interaction, cellular uptake and potential resistance mechanisms of the microorganism. MIC values are therefore widely used, also in studies on muraymycin analogues (e.g., [22,76-78]) and have been the basis of many structure–activity relationship studies (see below).

This bacterial growth assay, however, does not elucidate the inhibitory potency of the potential antimicrobial solely against the target protein MraY. Thus, another assay system that is not based on the interaction with whole cells but only with the

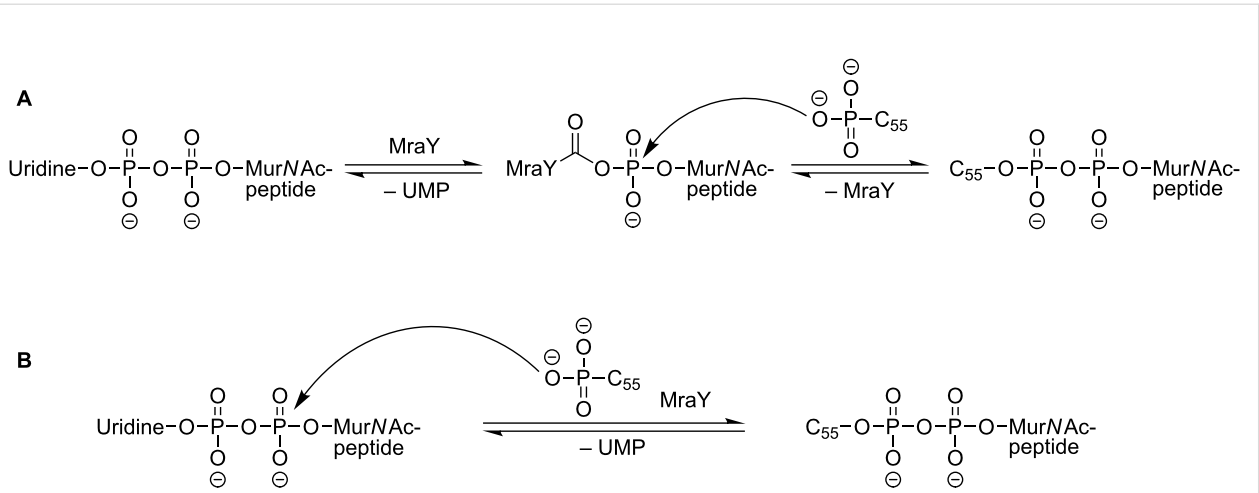

Figure 6: Proposed mechanisms for the MraY-catalysed reaction. A: Two-step mechanism postulated by Heydanek et al. [66]; B: one-step mechanism postulated by Bouhss et al. [69].

target protein is required. For MraY, there are three different assays available that provide such inhibition data: i) a fluorescence-based and ii) a radioactivity-based assay as well as iii) a relatively new Förster resonance energy transfer (FRET)-based method.

The fluorescence-based assay was developed by Bugg et al. [79,80] and uses a fluorescently labelled (dansylated) analogue of the MraY substrate UDP-Mur*N*Ac-pentapeptide. The reaction of this substrate analogue with undecaprenyl phosphate leads to an increase in fluorescence intensity that can be used as a measure for enzymatic activity (e.g., [74,78]). The assay reported by Bouhss et al. [81] uses a radioactively labelled UDP-Mur*N*Ac-pentapeptide and thin layer chromatography (TLC) separation of undecaprenyl-linked Mur*N*Ac-pentapeptide from unreacted substrate (e.g., [77,82]). The third assay was introduced in 2012 by Shapiro et al. and uses a FRET system with the FRET donor attached to the UDP-Mur*N*Ac-pentapeptide and the FRET acceptor in a detergent or detergent/lipid micelle that also hosts the MraY protein [83].

The overexpression and purification of the transmembrane protein MraY is challenging. MraY from different bacterial strains was heterologous overexpressed in *E. coli* and was used in assays mentioned above as a crude cellular membrane preparation or as a detergent-solubilised membrane protein mixture [79,84]. A purification to homogeneity was reported for MraY from *B. subtilis* by Bouhss et al. in 2004 [81] and for the congener from *Aquifex aeolicus* by Lee et al. in 2013 [71]. Wang, Bernhard et al. achieved a cell-free production of MraY from *B. subtilis* and *E. coli*, also experiencing the need of pronounced adjustments in expression conditions [85].

Synthetic access

Following the isolation of muraymycins [22], a group of scientists from Wyeth reported the semisynthetic access towards 16 derivatives of muraymycin C1 for structure–activity relationship (SAR) studies [86]. At the same time, a first set of fully synthetic structurally simplified muraymycin analogues was described [76]. Starting from uridine (**1**), protected uridine-5'-aldehyde **2** was prepared in four steps (Scheme 1) [87,88]. This

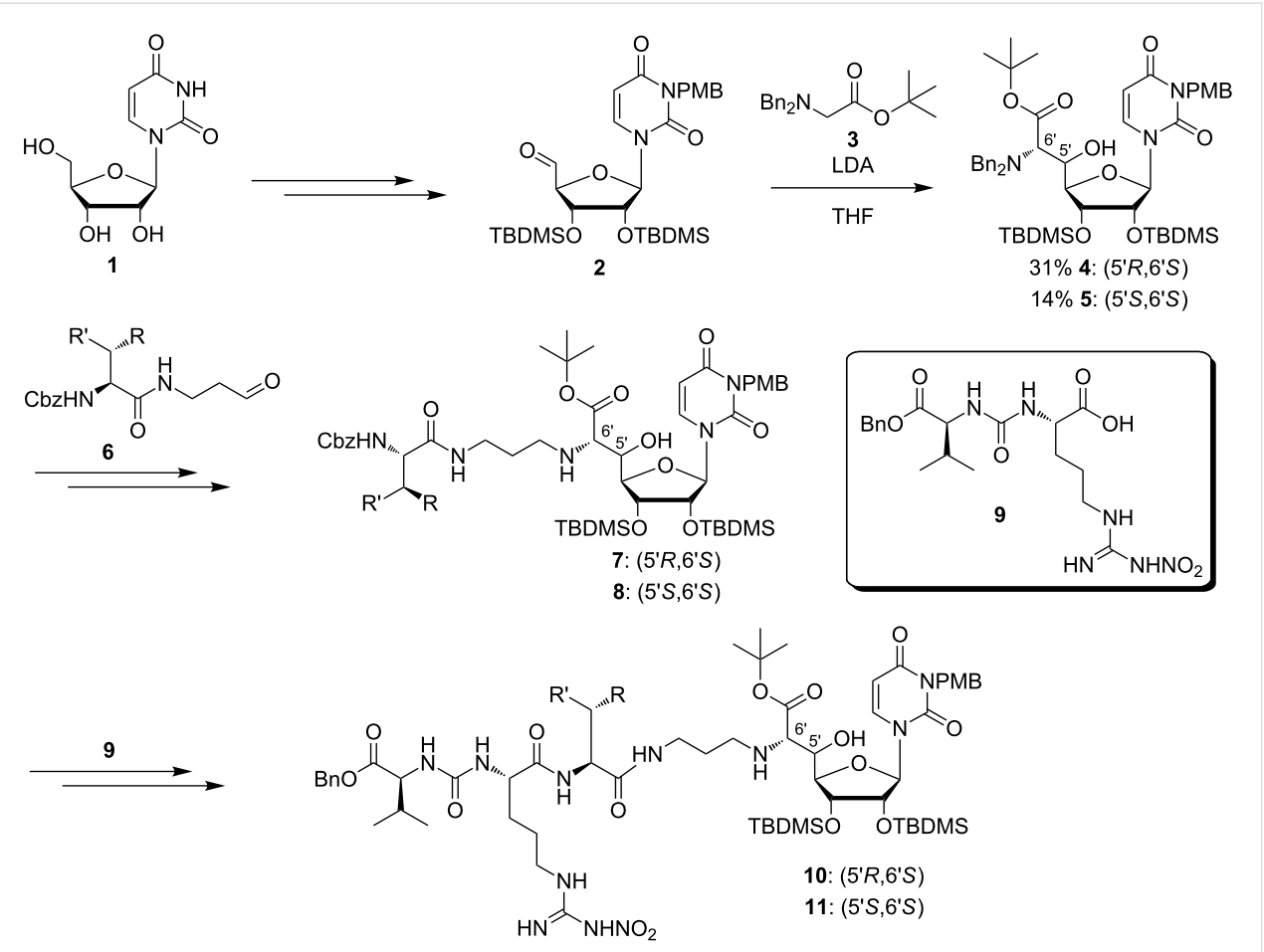

Scheme 1: First synthetic access towards simplified muraymycin analogues as reported by Yamashita et al. [76].

was followed by an aldol reaction of aldehyde **2** with *N*,*N*-dibenzylglycine *tert*-butyl ester (**3**) [89] and LDA as a key step of the synthesis (Scheme 1). The resultant products were the two 5'-epimers **4** (5'*R*,6'*S*) in 31% yield and **5** (5'*S*,6'*S*) in 14% yield, which could be separated by column chromatography. After debenzylation, the resultant primary amines were connected with amido aldehydes **6** substituted with different moieties R and R' by reductive amination with R being either a hydroxy group or a hydrogen and R' representing an alkyl, allyl, ester or a protected amino moiety. This led to many truncated muraymycin analogues based on the structures **7** and **8** [76]. Cbz deprotection and subsequent peptide coupling with the L-arginine-L-valine-derived urea dipeptide **9** gave various full-length muraymycin analogues **10** and **11** [76]. Some of the truncated and the full-length compounds were able to inhibit lipid II formation. These active compounds are discussed in the section on structure–activity relationship (SAR) studies.

In 2005, Ichikawa, Matsuda et al. reported the synthesis of (+)-caprazol [90-92] which contains the same uridine-derived core structure as the muraymycins. The latest and optimised synthesis is shown in Scheme 2 [92]. Oxidation of the isopropylidene-protected uridine **12** to the 5'-aldehyde and a Wittig reaction [93] gave olefin **13**. The key step was a subsequent asymmetric Sharpless aminohydroxylation [94] furnishing (5'*S*,6'*S*)-nucleosyl amino acid **14** in 96% yield (98% de)

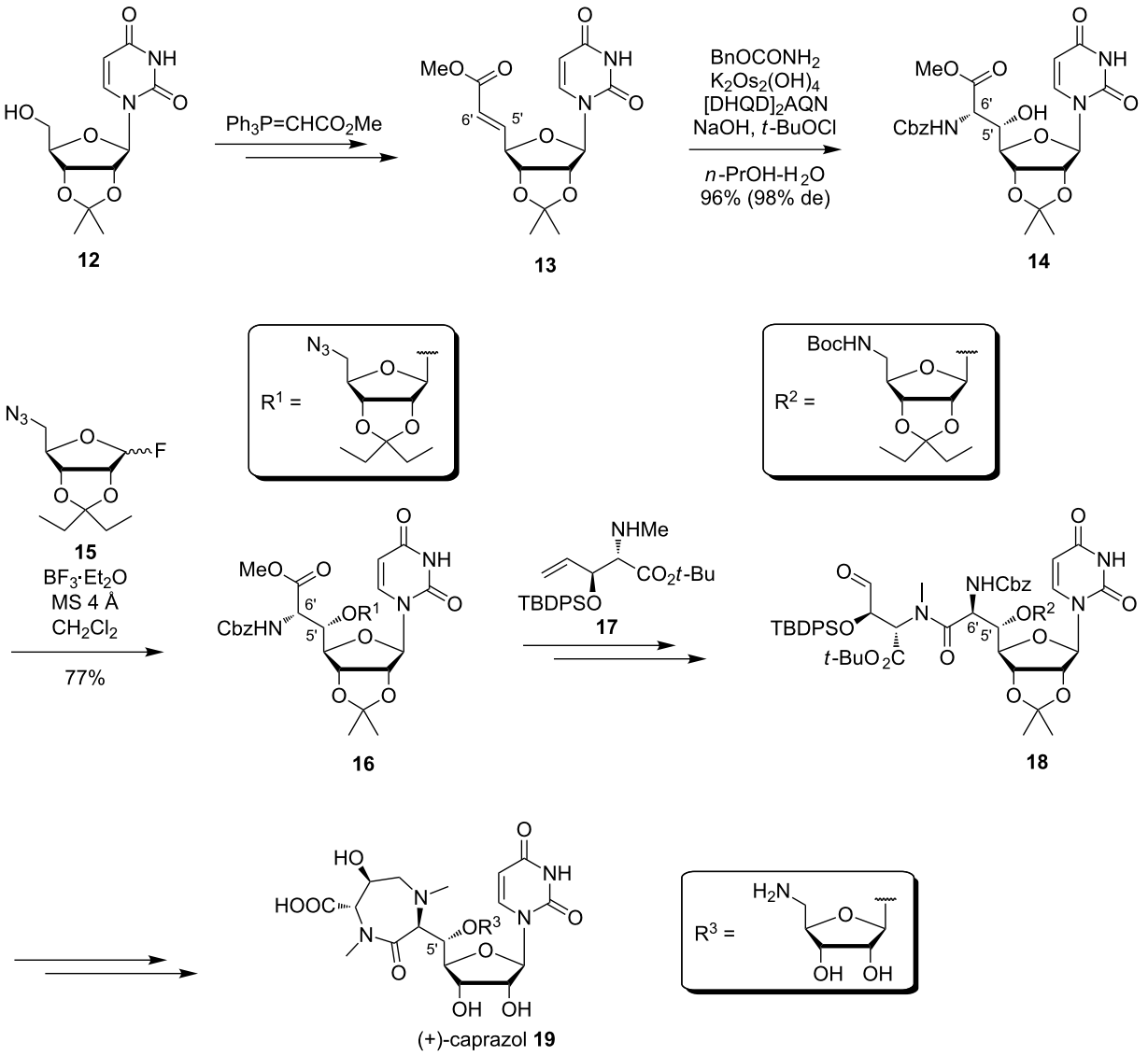

Scheme 2: Synthesis of (+)-caprazol (**19**) reported by Ichikawa, Matsuda et al. [92].

[92,95]. A novel β-selective glycosylation of the 5'-hydroxy group was also established. Thus, **14** was reacted with the ribosyl fluoride **15** and $BF_3{\cdot}Et_2O$, which afforded the glycosylated product **16** in 77% yield and with a β/α-selectivity of 24:1 [91,92]. This reaction was followed by an azide reduction, Boc protection, saponification of the ester, peptide coupling with the amino acid **17**, oxidative cleavage of the double bond to give **18** and an intramolecular reductive amination in order to construct the seven-membered ring. Methylation with subsequent acidic global deprotection led to the target compound (+)-caprazol (**19**) [90,92].

For the synthesis of muraymycins, Ichikawa, Matsuda et al. furthermore developed a new route towards the epicapreomycidine-containing urea dipeptide unit via C–H activation (Scheme 3) [96,97]. For this purpose, the commercially available δ-*N*-Boc-α-*N*-Cbz-L-ornithine (**20**) was transformed into sulfamate **21**. Subsequently, the C–H insertion representing the key step of this synthesis was examined with two different catalysts and different reaction conditions. Despite different ratios in the outcome of the C–H insertion in favour of the unwanted diastereomer **22**, the synthesis was finished with the desired minor component **23**. Boc deprotection followed by reaction with guanidinylation reagent **24** gave bicyclic compound **25**. The next steps included a desulfonylation and the reaction with **26** leading to protected epicapreomycidine-containing urea dipeptide **27** [96,97].

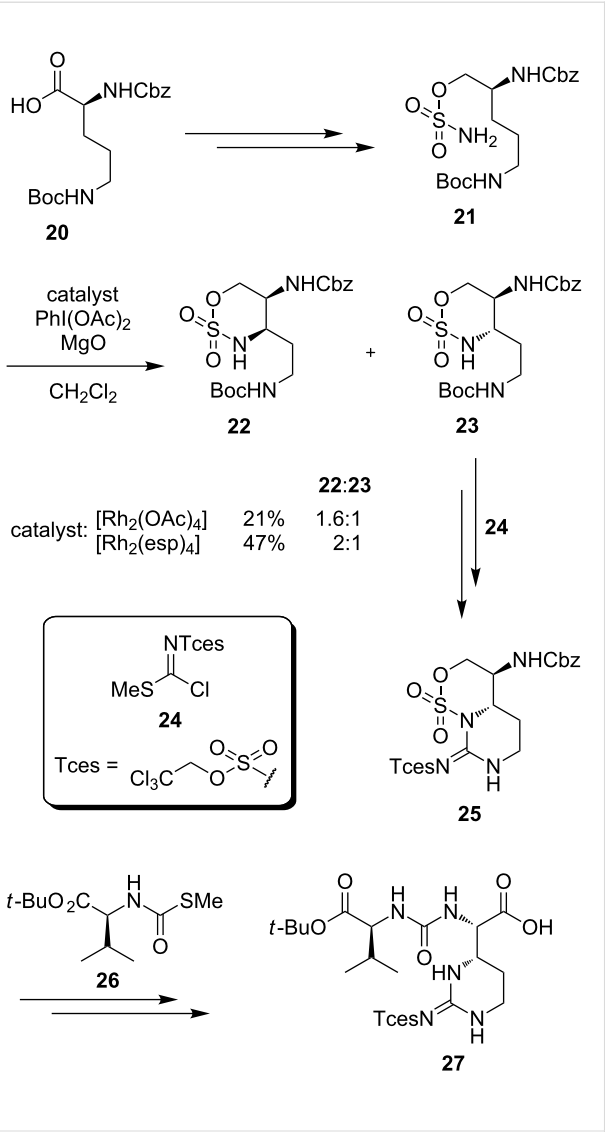

Scheme 3: Synthesis of the epicapreomycidine-containing urea dipeptide via C–H activation [96,97].

Starting from the uridine derivative **28** used in the synthesis of (+)-caprazol, Ichikawa and Matsuda built up muraymycin D2 and its epimer (Scheme 4). They used an Ugi four-component reaction with an isonitrile derivative **29** obtained from the uridine-derived core structure **28**, aldehyde **30**, amine **31** and the urea dipeptide building block **27**. A two-step global deprotection then gave the desired muraymycin D2 and its epimer which could be separated by HPLC [96,97].

In 2012, Kurosu et al. also reported the synthesis of potential key intermediates for the total synthesis of muraymycins (Scheme 5) [98]. A fully protected ureidomuraymycidine tripeptide was prepared through lactone opening followed by urea formation and a final Mitsunobu ring closure as key steps. A Strecker reaction of the benzylimine **34** followed by several steps afforded the alcohol **35**. A thermal lactonisation as a first key step of the synthesis led to a 1:1 mixture of the two epimers **36** and **37**, and the undesired lactone **37** could be epimerised and converted into **36** by treatment with DBU [98]. Epimerisation and simultaneous lactone opening could be achieved in another key step using L-valine *tert*-butyl ester. Acetylation of the thus formed primary alcohol resulted in compound **38**. This was followed by benzyl and Cbz deprotection and the subsequent urea formation with the imidazolium salt **39** to furnish tripeptide **40**. After Boc deprotection, the resultant amine was guanidinylated using isothiourea **41**. The thus obtained precursor **42** was treated with DIAD and PPh_3 in a final step for an intramolecular Mitsunobu ring closure to finish the synthesis of the fully protected ureidomuraymycidine **43** (Scheme 5) [98].

In 2010, Ducho et al. reported an alternative synthesis of the naturally occurring uridine-derived muraymycin core structure (Scheme 6) [78,99]. The key step of their route was a sulfur-ylide reaction with high substrate-controlled diastereoselectivity [100-102]. This epoxide-forming sulfur-ylide reaction had been established before by Sarabia et al. [103,104]. After some initial confusion regarding the stereochemical configuration of the epoxide product, it could be unambiguously proven that the

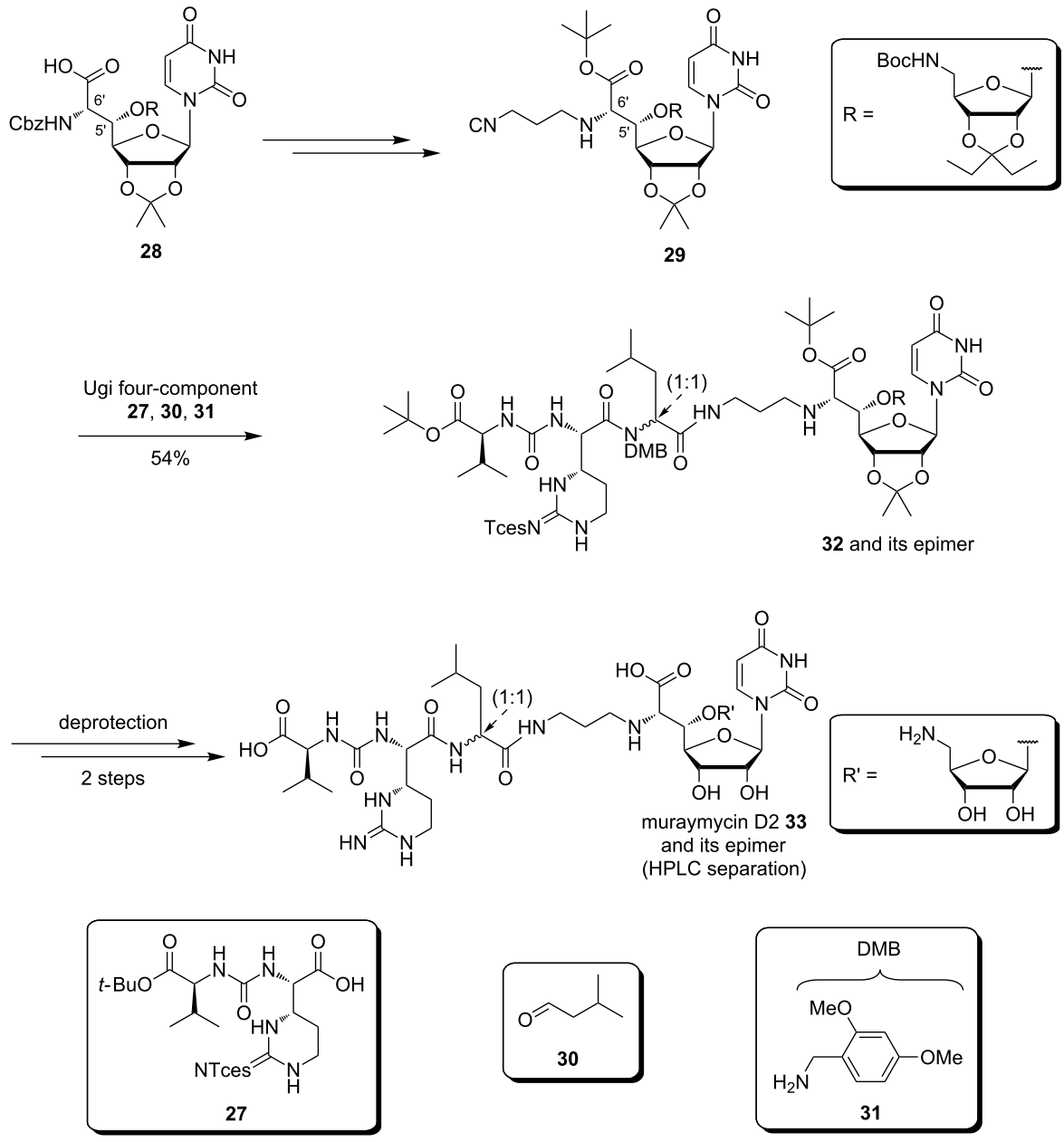

Scheme 4: Synthesis of muraymycin D2 and its epimer reported by Ichikawa, Matsuda et al. [96,97].

transformation of uridine-5'-aldehyde **44** with sulfonium salt **45** under basic conditions furnished epoxide **46** with high diastereoselectivity (Scheme 6). Subsequent ring opening of this epoxide with Bu_4NBr resulted in bromohydrine **47**, followed by levulinyl (Lev) protection of the hydroxy group (product **48**). Nucleophilic substitution at the 6'-position with Bu_4NN_3 gave the naturally occurring (5'*S*,6'*S*)-stereochemistry of the uridine core structure in a double inversion manner [78,99]. DDQ oxidation then provided indolamide **49**. Hydrolysis of the amide, formation of the synthetically more versatile *tert*-butyl ester, azide reduction and final Cbz protection resulted in the uridine-derived building block **50** for the synthesis of naturally occurring muraymycins (Scheme 6). Furthermore, 5'- and 6'-*epi* analogues of muraymycins were also synthesised via suitable epoxide precursors by Ducho et al. [105].

Ducho's synthesis of epicapreomycidine (Scheme 7) started from the (*R*)-configured Boc-protected Garner aldehyde **51** [106], which was transformed into the *N*-benzylimine **52**. The latter was then diastereoselectively converted with a Grignard

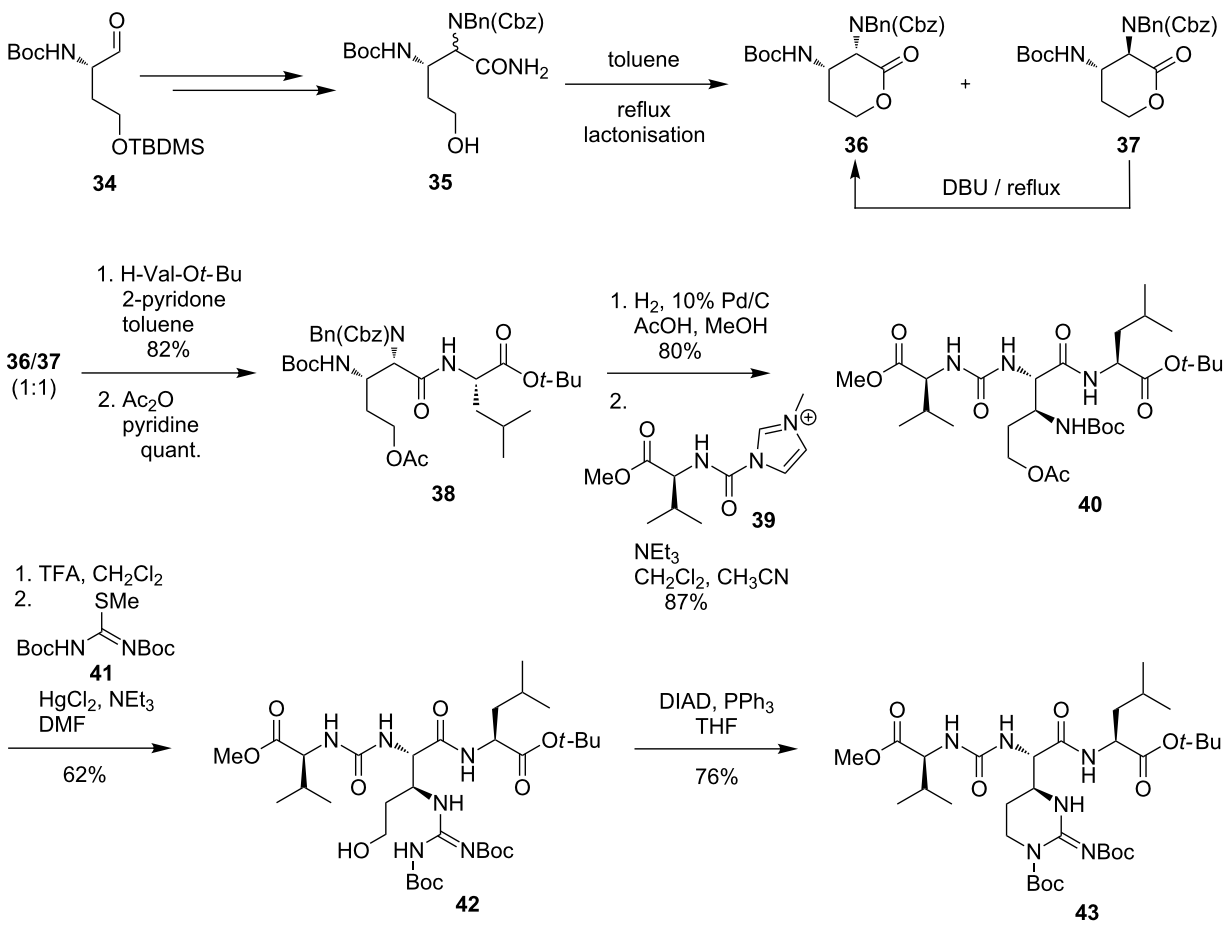

Scheme 5: Synthesis of the urea tripeptide unit as a building block for muraymycins reported by Kurosu et al. [98].

reagent into the amine **53** as a key step of the synthesis [78]. Cbz protection followed by ozonolysis with subsequent reductive amination and hydrogenolysis led to the 1,3-diamine **54**. The cyclisation to the guanidine functionality was achieved with the novel guanidinylation reagent **55**. With the protected epicapreomycidine precursor **56** in hand, the Boc and acetonide protecting groups were removed. Urea formation with the valine derivative **57** with final oxidation of the primary hydroxy function afforded the desired dipeptide **58** [78] (Scheme 7).

Furthermore, Ducho et al. synthesised the hydroxyleucine moiety found in naturally occurring muraymycins of classes A to C (Scheme 8) [107]. Adapting a strategy developed by Zhu et al., D-serine (**59**) was stereoselectively converted into the protected amino alcohol **60** [108]. Key intermediate **60** was then Cbz- and acetonide protected to give **61**. A sequence of desilylation and oxidation furnished the acid **62**. Peptide coupling with amine **63** and acidic deprotection then afforded the desired aldehyde **64**, which already contained the muraymycin linker unit (Scheme 8) [107]. Together with the uridine core structure **50** and the urea dipeptide **58**, the aldehyde **64** was the third building block of Ducho's envisioned stereocontrolled tripartite route towards muraymycins, in contrast to Ichikawa's and Matsuda's modular multicomponent, but non-stereocontrolled approach (see above).

This novel tripartite approach was then used by Ducho et al. to synthesise the structurally simplified natural product analogue 5'-deoxy muraymycin C4 (**65**), which formally differs from the parent natural product only by absence of one oxygen atom (Scheme 9) [78,109,110]. Starting from protected uridine-5'-aldehyde **44**, the first key step of the synthesis was a (*Z*)-selective Wittig–Horner reaction with phosphonate **66** [111] in order to obtain the didehydro amino acid **67**. The next important step of this route was an asymmetric catalytic hydrogenation [112,113] with the chiral Rh(I)–DuPHOS catalyst **68** to prepare the (6'*S*)-configured product **69** [109,110]. Subsequent hydrogenolytic cleavage of the Cbz group gave the nucleosyl amino acid **70**. To complete the tripartite approach, the reductive amination with the aldehyde **64** furnished **71**, and Cbz

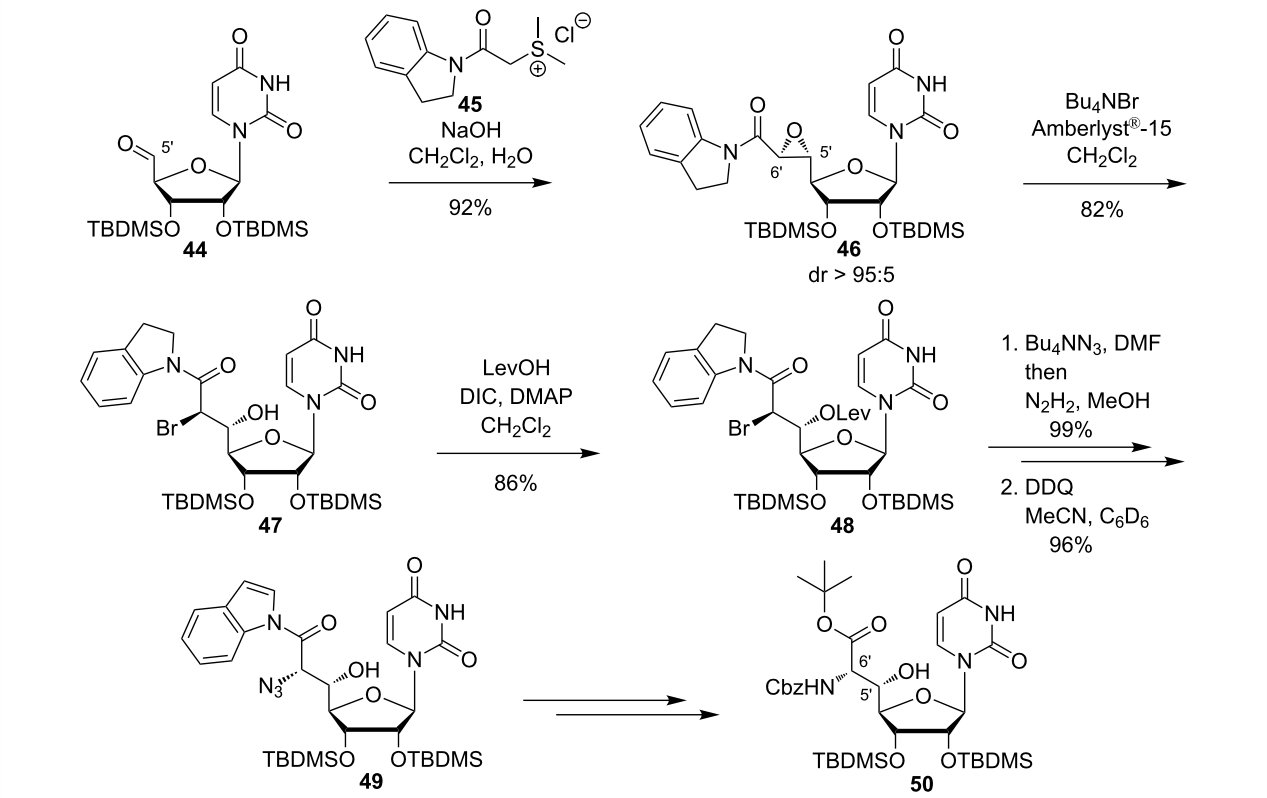

Scheme 6: Synthesis of the uridine-derived core structure of naturally occuring muraymycins reported by Ducho et al. [78,99].

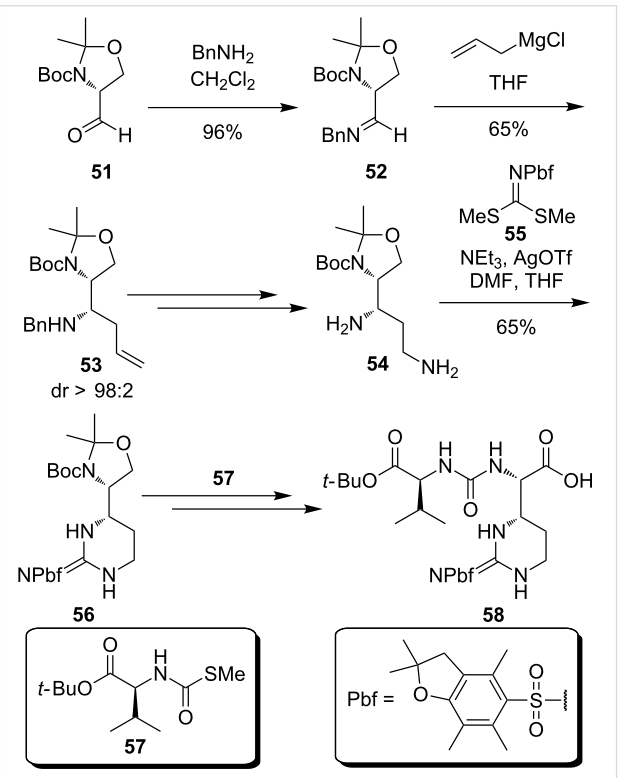

Scheme 7: Synthesis of the epicapreomycidine-containing urea dipeptide from Garner's aldehyde reported by Ducho et al. [78].

deprotection and peptide coupling with the epicapreomycidine-containing urea dipeptide **58**, followed by acidic global deprotection, gave the desired 5'-deoxy muraymycin C4 (**65**) (Scheme 9) [78].

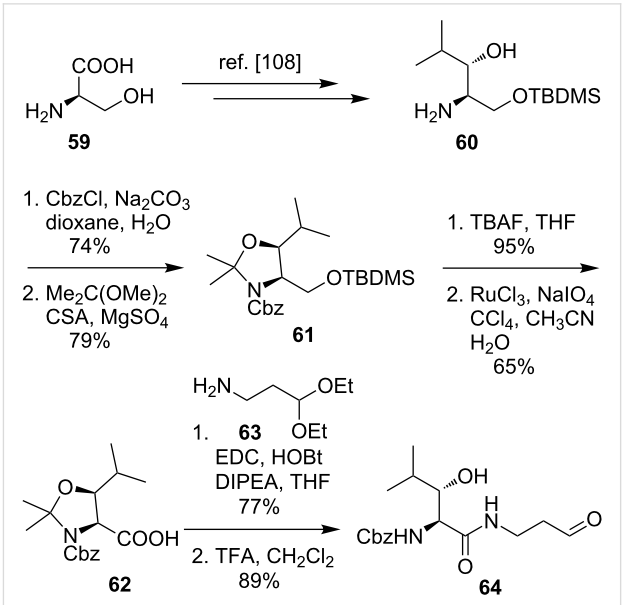

Scheme 8: Synthesis of a hydroxyleucine-derived aldehyde building block reported by Ducho et al. [107].

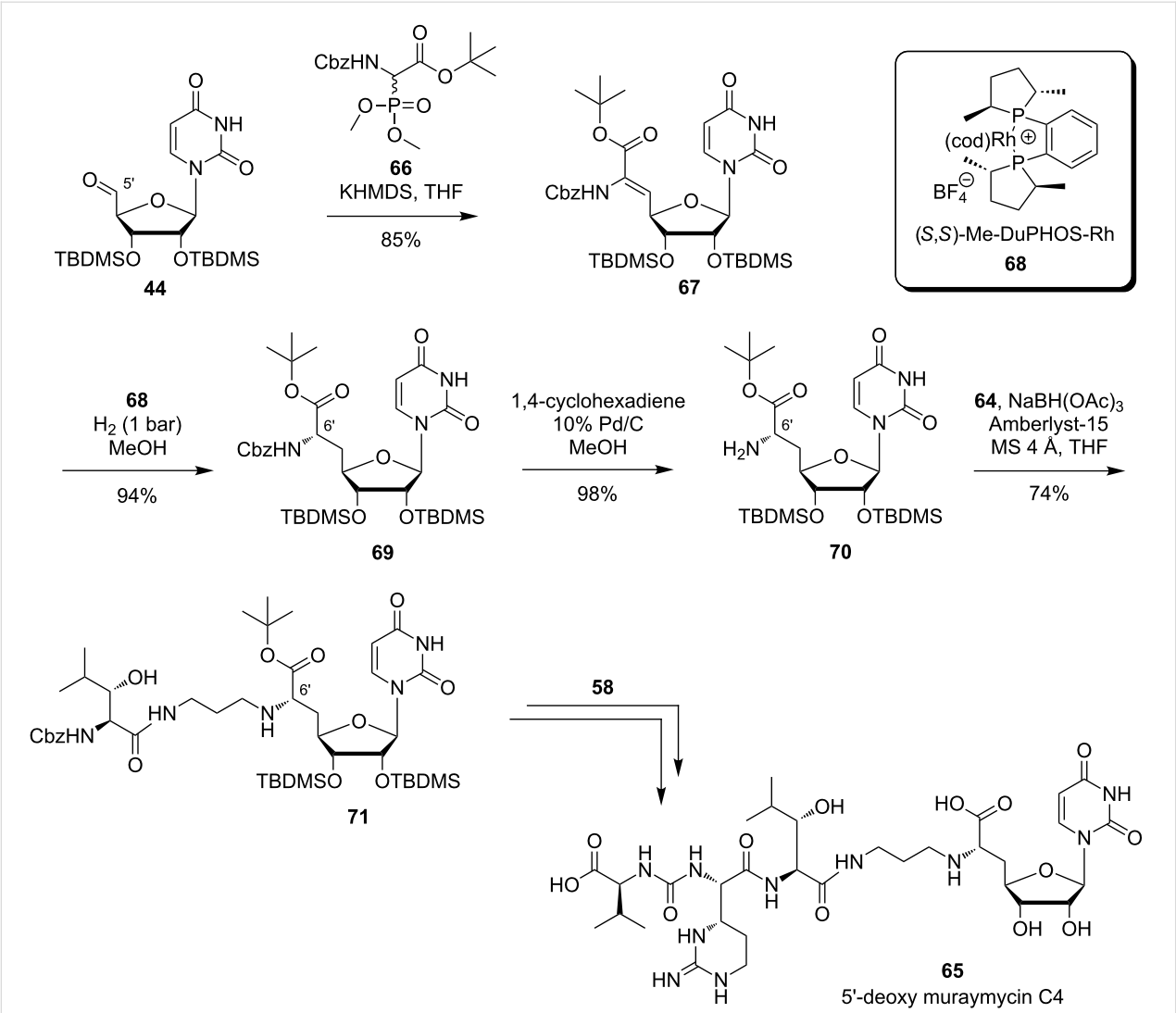

Scheme 9: Synthesis of 5'-deoxy muraymycin C4 (**65**) as a closely related natural product analogue [78,109,110].

In addition to the described synthetic routes, a range of other muraymycin analogues has been prepared. In the interest of conciseness, this synthetic work is not discussed here, but the biological properties of such analogues will be summarised in the following section on SAR studies.

Structure–activity relationship studies

With various structurally diverse compounds at hand, the stage has been set for SAR studies on muraymycins. The antimicrobial activities found by McDonald et al. introduced muraymycins as a promising subject of study [22]. The naturally occurring muraymycins isolated from *Streptomyces* guided first insights into the structural features essential for MraY inhibition. For the most active member of the family, i.e., muraymycin A1, antibiotic activity could be found against various bacteria ranging from *Staphylococci* with MIC values of 2 to 16 μg/mL, *Enterococci* with 16 μg/mL and higher to some Gram-negative bacteria (8 μg/mL). Against an *E. coli* mutant with increased membrane permeability, an MIC value below 0.03 μg/mL was obtained, suggesting that inhibition is a matter of cellular uptake of the compound. In vivo efficacy was demonstrated for muraymycin A1 with an ED_{50} of 1.1 mg/kg in *Staphylococcus aureus*-infected mice.

Five of the 19 naturally occurring compounds (i.e., muraymycins A1, A5, B6, C2 and C3) were capable of inhibiting both MraY and peptidoglycan synthesis at the lowest concentration tested (IC_{50} = 0.027 μg/mL), which represented activities comparable to those of liposidomycin C (0.05 μg/mL) and mureidomycin A (0.03 μg/mL). As a general trend, higher antimicrobial activities were found for acylated compounds, in particular with longer and functionalised fatty acid side chains.

Lin et al. employed a semisynthetic approach for modifications of muraymycin C1 as starting point of their SAR studies (Figure 7) [86]. In accordance with the results reported by McDonald et al., their work was based on the assumption that the cellular uptake required for MraY inhibition is mainly dependent on fatty acids connected to the hydroxyleucine moiety. The attachment of lipophilic groups on either the primary or both the primary and secondary amino function was supposed to have similar effects. The muraymycin derivatives **72**–**86** were thus evaluated against the target in a coupled MraY–MurG in vitro assay employing radiolabelled UDP-*N*-acetylglucosamine. Disubstituted analogues were not active at the concentrations tested, suggesting that one free amino group is vital for activity. Hydantoin-derived compounds **79** with $C_{12}H_{25}$ and **80** with $PhCH_2$ as residues R at the hydantoin moiety gave the best results with inhibition of lipid II formation at 6.25 µg/mL, which is comparable to muraymycin C1. Good activity was also found for hydantoin derivative **77** with the 4-FC_6H_4 substituent, showing inhibition of lipid II formation at 25 µg/mL. The only *N*-alkylated derivative inhibiting in the same order of magnitude was **83** with *n*-$C_{11}H_{23}$ substitution. However, activities of the other compounds within this group also coincided with the previous observation that lipophilic compounds were more active. Overall, the tested monosubstituted hydantoin derivatives confirmed the assumed correlation between inhibitory activities and lipophilicity of the substituent.

Yamashita et al. studied truncated muraymycin analogues lacking the lipophilic side chain as described in the section on synthetic access (compounds of type **7**, **8** and **10**) [76]. The ac-

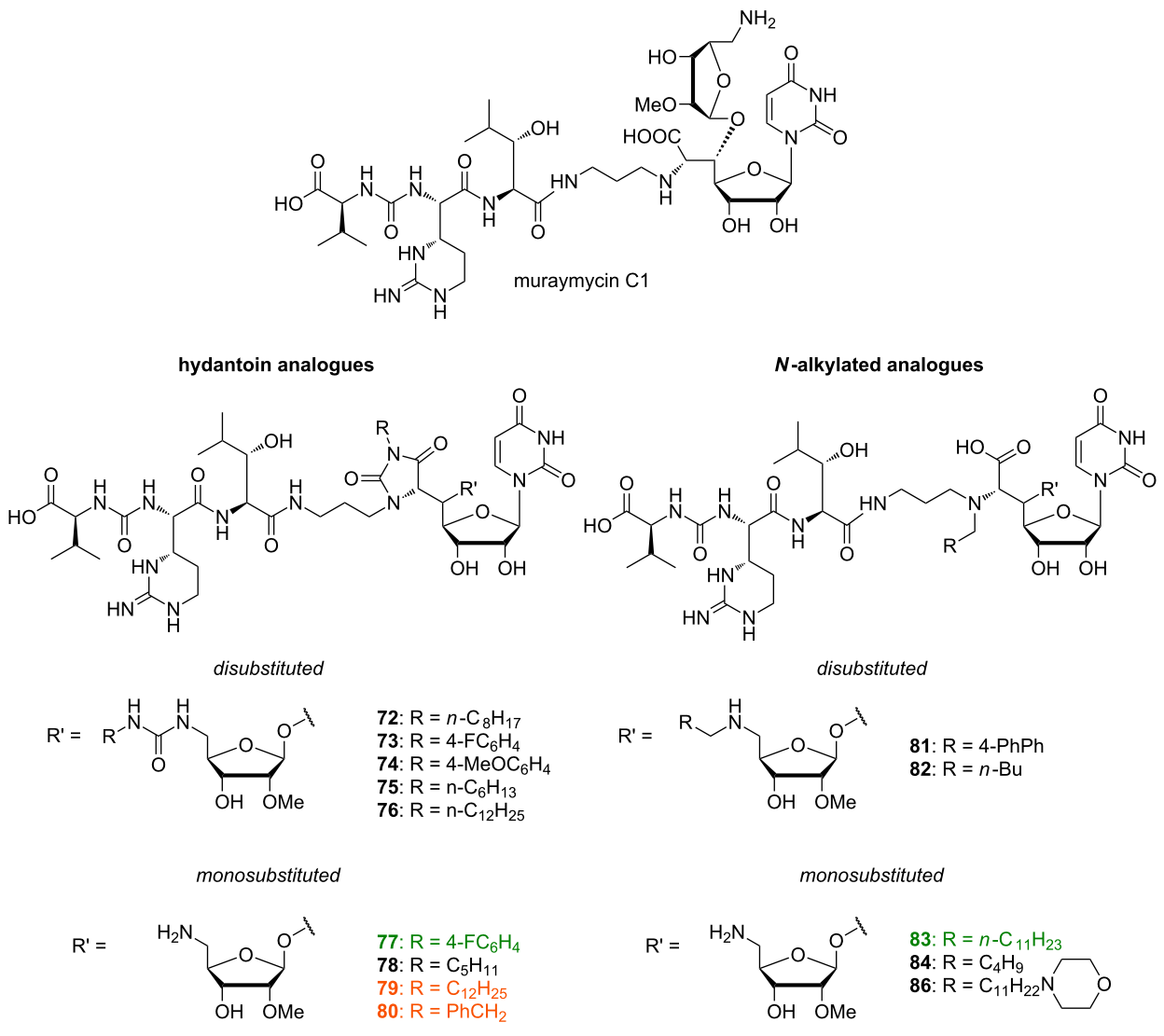

Figure 7: Summary of modifications on semisynthetic muraymycin analogues tested by Lin et al. [86]. Most active compounds are highlighted (in vitro inhibition of lipid II formation at 6.25 µg/mL: orange; 25–50 µg/mL: green).

tivities measured in a soluble peptidoglycan assay indicated a stereochemical preference for the (5'*S*)-configuration, contrary to the results of MIC value determination. Further studies were then carried out with (5'*R*)-derivatives only, i.e., with 5'-epimers of the parent natural products. The influence of protecting groups was examined applying a strategy of stepwise deprotection. This led to the observation that fully protected compounds were not active at all, as well as the completely deprotected analogues. Remarkably, some partially protected congeners **87**–**90** with the free terminal amino group were found to show good inhibition (MIC = 1–16 μg/mL) of the growth of Gram-positive bacteria including *S. aureus* and *E. faecalis* strains, with best results obtained for **88** (Figure 8). Evaluation of the inhibition of lipid II formation revealed the importance of the substitution pattern of the terminal amino acid.

In 2010 and 2011, Ichikawa, Matsuda et al. published SAR studies with a range of synthetic muraymycin analogues [77,114]. The IC_{50} values were measured in an in vitro assay mentioned above to examine the inhibitory activity of the prepared analogues against the target enzyme. MIC values were determined against several bacterial strains. The inhibitory activities of the synthesised muraymycin D2 **33** (with an L-leucine unit) and its epimer (with a D-leucine unit) on the purified MraY enzyme from *B. subtilis* were determined. Both compounds showed good inhibitory activities with IC_{50} values of 0.01 μM and 0.09 μM, respectively. However, their antibacterial activities against several Gram-positive bacteria (*S. aureus, E. faecalis, E. faecium*) were low (MIC values up to 64 μg/mL). In comparison to the analogues of the A and B series, which showed good antibacterial activities (see above), muraymycin D2 (**33**) and its epimer lack the hydrophobic side chain at the leucine moiety [22]. It was postulated that this lipophilic side chain may not be necessary for target inhibition, but for cellular uptake through the lipid bilayer of the cytoplasmic membrane, as an increased lipophilicity is advantageous for this [77,114].

Consequently, several lipophilic derivatives **91a**–**d** were prepared (Figure 9). Long-chain lipophilic amino acids were incorporated into the muraymycin core structure as a simplified replacement of the *O*-acylated hydroxyleucine moiety. Compound **91a** (highlighted in orange) with the pentadecyl side chain showed the best activity as an MraY inhibitor (IC_{50} = 0.33 μM (with L-leucine moiety), IC_{50} = 0.74 μM (with D-leucine moiety)), but relative to muraymycin D2 and its epimer, this implied a 33-fold and 8-fold, respectively, decrease of inhibitory activity. In bacterial growth assays, the analogue **91a** exhibited the best MIC values ranging between 0.25 μg/mL and 4 μg/mL (see Table 2). These values were comparable to those of the naturally occurring congeners of the A and B series [22]. Generally, derivatives with the naturally occurring L-configuration in the leucine moiety showed slightly better activities. These lipophilic analogues were also tested for cytotoxicity towards Hep G2 cells and showed no cytotoxicity (IC_{50} > 100 μg/mL) [114].

In another series of analogues with different peptide units, the pentadecyl side chain of **91a** was kept. The L-epicapreomycidine (L-*epi*-Cpm) unit of **91a** was replaced by L-capreomyci-

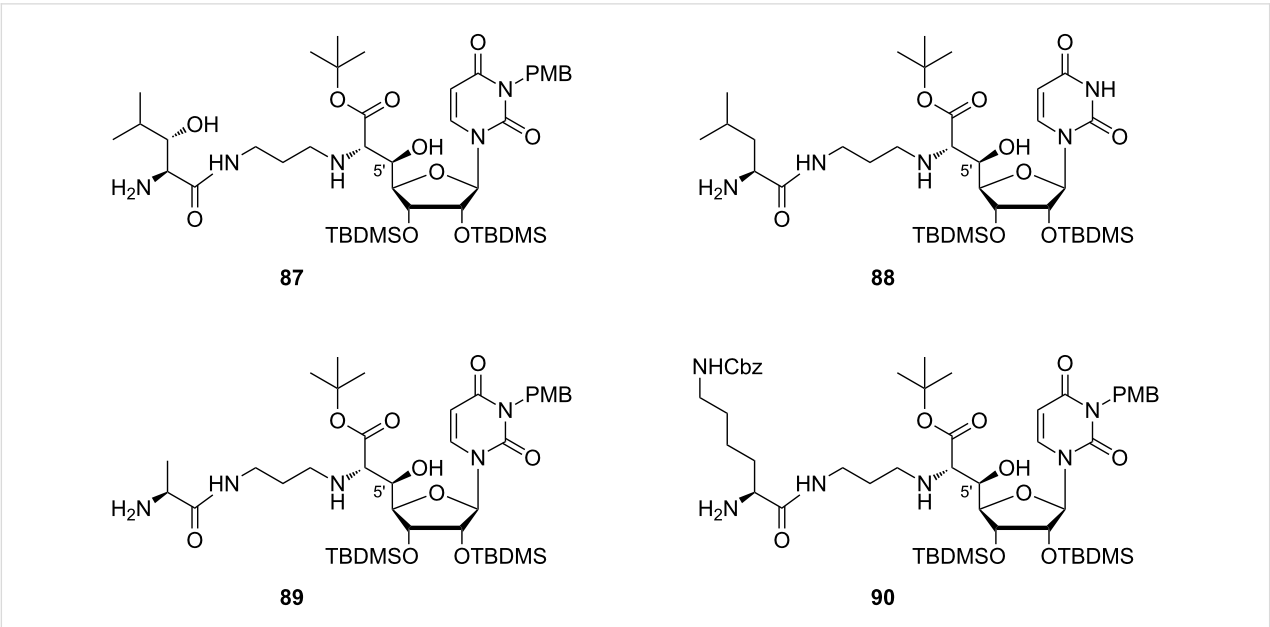

Figure 8: Bioactive muraymycin analogues identified by Yamashita et al. [76].

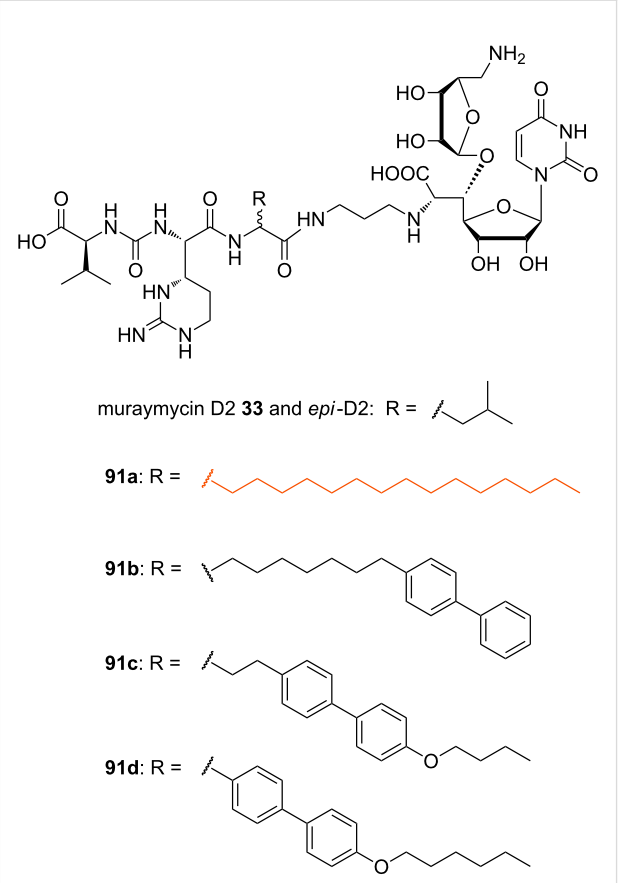

Figure 9: Muraymycin D2 and several non-natural lipidated analogues **91a–d** [77,114].

Table 2: Inhibitory (against MraY) and antibacterial activities of non-natural lipophilic muraymycin analogues [77,114].

Compound	(L-Leu) (D-Leu)	IC_{50} (μM)[a]	MIC (μg/mL)[b]
muraymycin D2 (**33**)		0.01 0.09	>64 >64
91a		0.33 0.74	2–4 0.25–4
91b		n.d.	4–16 4–16
91c		n.d.	16–64 4–64
91d		n.d.	4–8 4–16
92a		n.d.	2–4 2–4
92b		n.d.	1–2 2–4
92c		n.d.	2–8 4–8
92d		n.d.	4–8 4–8
92e		n.d.	4–8 4–8
Compound (L-Leu)		IC_{50} (μM)[a]	MIC (μg/mL)[b]
92f		n.d.	4–8
92g		n.d.	4
92h		n.d.	4–8
93		5	32 to ≥64

[a]Inhibitory activities were determined against purified MraY enzyme from *B. subtilis* [77]; [b]MIC values were determined for different strains of *S. aureus*, *E. faecalis* and *E. facium* including some multiresistant strains [77]; n.d. = not determined.

dine (L-Cpm, **92a**), L-arginine (L-Arg, **92b**) and L-ornithine (L-Orn, **92c**) in order to investigate the role of the cyclic guanidine functionality (Figure 10) [77].

These compounds were all active against MRSA and VRE with varying MIC values (Table 2). The most active analogues of this series were **92a** and **92b** (Figure 10, highlighted in orange) with MIC values between 1 μg/mL and 4 μg/mL. Derivatives with unnatural D-stereochemistry in the pentadecyl glycine motif possessed a similar antibacterial activity (potency within factor 2). Truncated analogues lacking the L-valine urea terminus (Cbz-protected **92d** and N-terminally unprotected **92e**) showed only a minor loss of activity (MIC = 4–8 μg/mL) (Table 2). These results indicated that the guanidine motif of analogues **91a**, **92a** and **92b** (MICs between 0.25 μg/mL and 4 μg/mL) is preferred, but that amino analogues **92c** and **92f** still show good activity (MICs between 2 μg/mL to 8 μg/mL). The different stereochemistry at the central leucine unit and the terminal truncation had no crucial effects on the antibacterial activity (Table 2). Truncated derivatives **92f**–**h** (Figure 10) without the L-valine urea terminus contained L-ornithine (L-Orn, **92f**), L-arginine (L-Arg, **92g**) and L-methionine (L-Met, **92h**), respectively. They were also tested and showed reasonable activity against some bacterial strains (MIC = 4–8 μg/mL), which further indicated that significant variations in the peptide moiety are tolerated. The truncated analogue **93** (Figure 10) only consisted of the *N*-alkylated nucleoside core structure. Its inhibitory activity was 6 to 12-fold reduced (IC_{50} = 5 μM) and the antibacterial activity decreased with MIC values between 32 μg/mL and 64 μg/mL. In summary, these systematic SAR studies demonstrated the importance of the lipophilic side chain for the antibacterial activity. The urea dipeptide motif is important for antibacterial activity as well, but it could be diversified with simpler amino acids as well as being truncated in order to provide bioactive analogues. A graphical summary of these results is provided in Figure 11.

In 2014, Ichikawa, Matsuda et al. continued their SAR studies with respect to urgently needed anti-*Pseudomonas* agents [115]. These Gram-negative bacteria possess an outer membrane

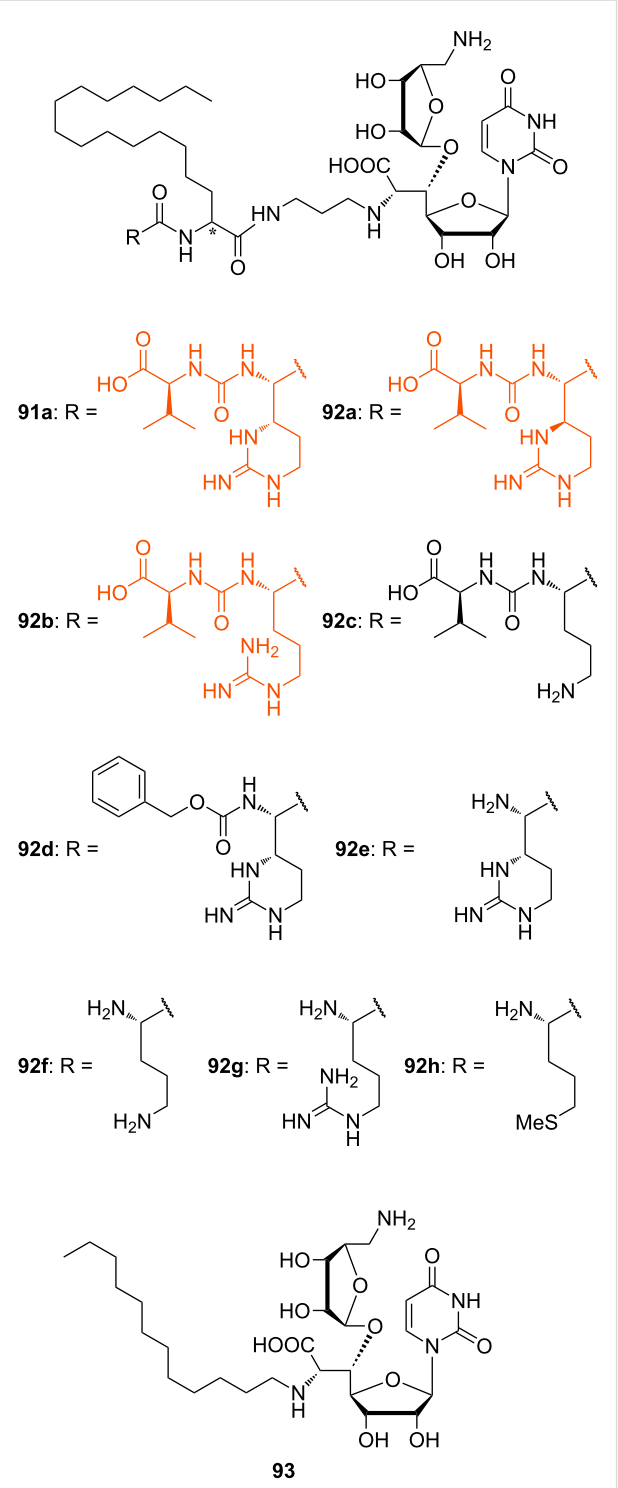

Figure 10: Non-natural muraymycin analogues with varying peptide structures [77,114].

which acts as an additional permeability barrier, making them generally less sensitive to antibacterial agents. In this context, the aforementioned muraymycin analogues (**91a**, **92a**–**h**) were tested for MraY inhibitory activity again, with MraY enzyme from *S. aureus* (Table 3). However, antibacterial activities against several *Pseudomonas* strains were moderate to low with MICs between 8 μg/mL and >64 μg/mL. Analogue **92g** was the most active congener in this series with MIC values between 8 μg/mL and 32 μg/mL. Compounds **92e** and **92f** showed nearly no activity (MIC = 32 to >64 μg/mL). More lipophilic truncated analogues **94** without the urea dipeptide unit (Figure 12) were synthesised and tested, but they all showed nearly no activity.

These results indicated the importance of the presence of a guanidine residue and a lipophilic side chain for potential antibacterial activity against *Pseudomonas* strains. Hence, several derivatives were prepared in which the positions and numbers of the guanidine groups and the lipophilic side chains were varied in order to optimise their relative orientation for best biological activity. This strategy resulted in the bioactive analogues **95**–**98** (Figure 12). Analogue **95** with an interconversion of the lipid side chain and the guanidine group had a slightly reduced activity compared to lipidated analogue **92g**. Analogue **96** showed an increased antibacterial activity towards some of the tested *Pseudomonas* strains. Analogue **97** is an interconverted version of **96** and displayed a comparatively poor activity. The most active analogue was compound **98** which is a hybrid type of the aforementioned analogues **95**–**97**. The results indicate that a lipophilic side chain and guanidine groups are necessary for antibacterial potency. Compounds **95**–**98** showed antibacterial activity, with the branched-type compound **96** (MIC values between 8 μg/mL and 16 μg/mL) and the hybrid-type compound **98** (MIC between 4 μg/mL and 8 μg/mL) being the most active congeners. A limitation of both analogues **96** and **98** is their increased cytotoxicity against HepG2 cells with IC_{50} values of 4.5 μg/mL and 34 μg/mL, respectively. Further, the metabolic stability was studied in vitro for the analogues **95**, **96** and **98** using human or rat liver microsomes and all of them proved to be reasonably stable [115].

In 2014, Ducho et al. reported the synthesis of 5'-deoxy muraymycin C4 (**65**, see above) [78]. Biological assays revealed that **65** inhibited the MraY enzymes of *E. coli* and *S. aureus* with potencies in the range of tunicamycins. The antibacterial activity of **65** was tested against some selected *E. coli* and *S. aureus* strains although the lack of a lipophilic moiety indicated that the compound should not be a potent antibiotic. However, an unexpected moderate activity against *E. coli* DH5 alpha was observed, whereas **65** was weakly active against *E. coli* strain ΔtolC but not active against the *S. aureus* Newman strain. Further studies indicated excellent plasma and metabolic stability and no cytotoxicity. Overall, the structurally simplified 5'-deoxy muraymycin scaffold **65** may therefore be useful for further antibacterial development. It should also be noticed that

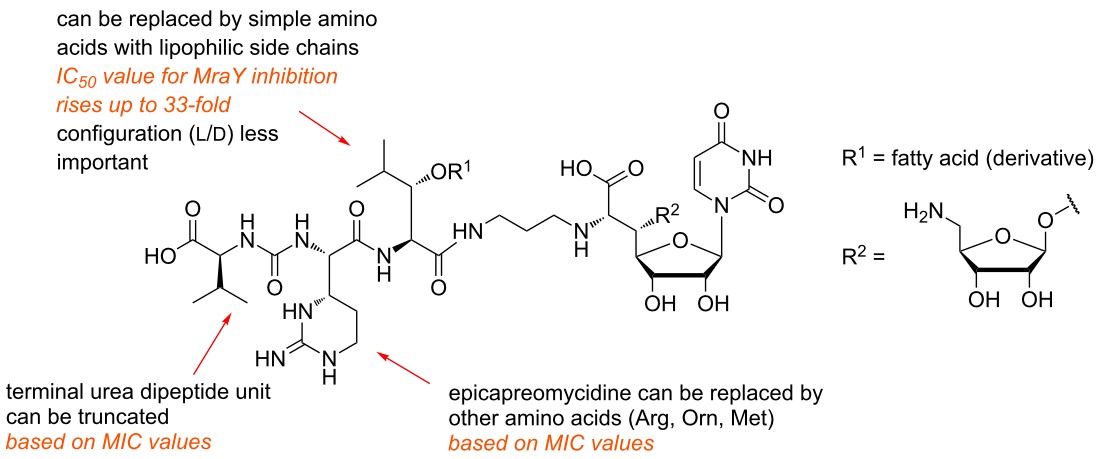

Figure 11: SAR results for several structural variations of the muraymycin scaffold.

Table 3: Inhibitory (against MraY) and antibacterial activities of non-natural muraymycin analogues against *Pseudomonas aeruginosa* [115].

Compound	IC_{50} (nM)[a]	MIC (μg/mL)[b]
91a, **92a–d**	0.7–4.2	≥ 64
92e,**f**	2.4–3.8	32 to ≥ 64
92g	2.2	8–32
92h	8.5	16 to ≥ 64
94 (R^1 = -H or -$COCH_3$)	2.6–2.7	32 to ≥ 64
94 (R^1 = -CO(het)aryl)	6.4–105	≥ 64
95	1.6	8–32
96	0.14	8–16
97	12.2	16–32
98	0.60	4–8

[a]Inhibitory activities were determined against MraY enzyme from *S. aureus* [115]; [b]MIC values were determined for several *P. aeruginosa* strains [115].

it has inspired the design of a novel oligonucleotide backbone modification [116,117].

Biosynthesis

So far, there are only limited insights into muraymycin biosynthesis. The biosynthetic gene cluster for the formation of muraymycins in *Streptomyces* sp. NRRL 30471 has been identified by Chen, Deng et al. in 2011 [118]. The sequence analysis revealed the cluster to contain 33 open reading frames (ORFs) with 26 of them being involved in muraymycin formation. Based on their elucidation of the gene cluster and sequence homologies, Chen, Deng et al. proposed an outline pathway for muraymycin biosynthesis (Scheme 10).

According to this biosynthetic proposal, uridine (**1**) is enzymatically oxidised to give uridine-5'-aldehyde **99**. Aldehyde **99** then supposedly undergoes an aldol addition with glycine **100** as the enol(ate) component, thus furnishing the amino acid–nucleoside hybrid 5'-*C*-glycyluridine (GlyU, **101**). Alkylation of the 6'-amino group is then achieved by reaction with *S*-adenosyl methionine (SAM), and the resultant intermediate **102** is decarboxylated to provide diamine **103**. Attachment of the aminoribosyl moiety (which is supposedly also derived from uridine (**1**) over several enzymatic steps) finally affords the aminopropyl-substituted 5'-*O*-aminoribosylated GlyU core structure **104**. Transformation of **104** with the thioester-activated peptide moiety **105** then gives muraymycin C2 (Scheme 10), which is speculated to serve as an intermediate en route to other muraymycins, in particular towards *O*-lipidated congeners of the A and B series (see Figure 2).

A fragmented non-ribosomal peptide synthetase (NRPS) system appears to be responsible for the assembly of the urea tripeptide building block **105**. However, the non-proteinogenic amino

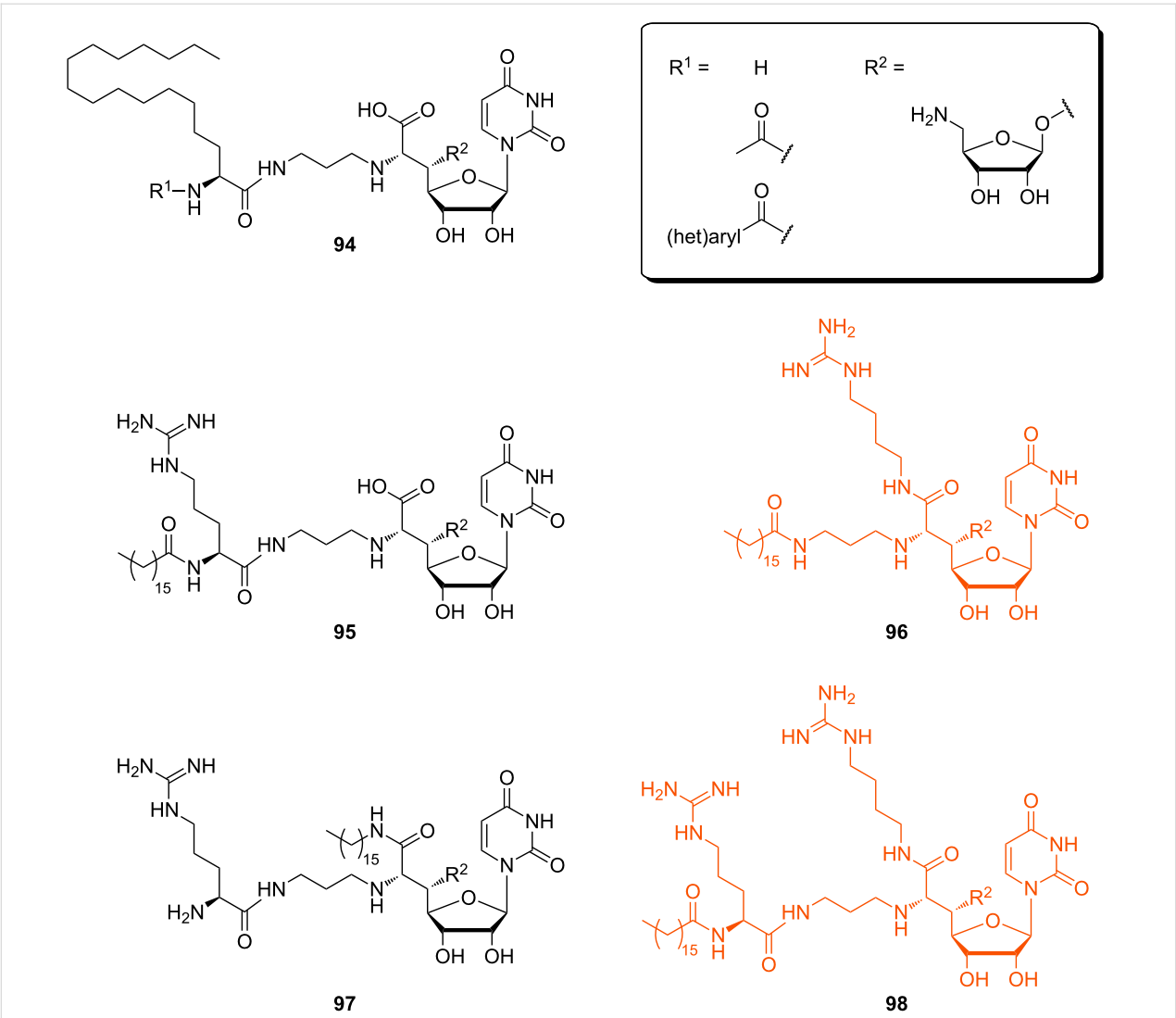

Figure 12: Muraymycin analogues designed for potential anti-*Pseudomonas* activity (most active analogues are highlighted in orange) [115].

acids need to be formed first. It has been proposed that L-arginine (**106**) undergoes 3-hydroxylation (giving 3-hydroxy-L-arginine (**107**)) and subsequent ring closure to furnish L-epicapreomycidine ((2*S*,3*S*)-capreomycidine, **108**), that is then activated as thioester **109** (Scheme 10). This proposal is based on the elucidated formation of the epimeric amino acid L-capreomycidine ((2*S*,3*R*)-capreomycidine) as part of viomycin biosynthesis in *Streptomyces vinaceus*. In this producing organism, L-arginine is diastereoselectively hydroxylated to afford (3*S*)-3-hydroxy-L-arginine. The ring-closure reaction then occurs with formal inversion of the β-stereocenter (but quite likely through an aza-Michael addition to the α,β-unsaturated intermediate) [119-121]. The exact stereochemical course of epicapreomycidine formation in muraymycin biosynthesis is unclear though as the stereochemical configuration at C-3 of the intermediate 3-hydroxy-L-arginine (**107**) has not been identified yet. It cannot be ruled out that an epimerisation reaction might be involved in the biosynthesis of **108**, in particular with respect to other epimerisation steps in bacterial biosynthetic pathways [122]. Consequently, synthetic routes towards both 3-epimers of 3-hydroxy-L-arginine have been developed which would also enable the preparation of isotopically labelled congeners for biosynthetic studies [123,124]. It should also be noted that a biomimetic domino guanidinylation–aza-Michael-addition reaction for the synthesis of the capreomycidine scaffold has been developed, which only furnished the target structures as stereoisomeric mixtures though [125].

The epicapreomycidine-derived thioester **109** is proposed to be converted into the urea dipeptide motif with valine derivative **110** and possibly hydrogen carbonate as a C_1-building block for urea formation, thus furnishing **111**. The 3-hydroxy-L-leucine

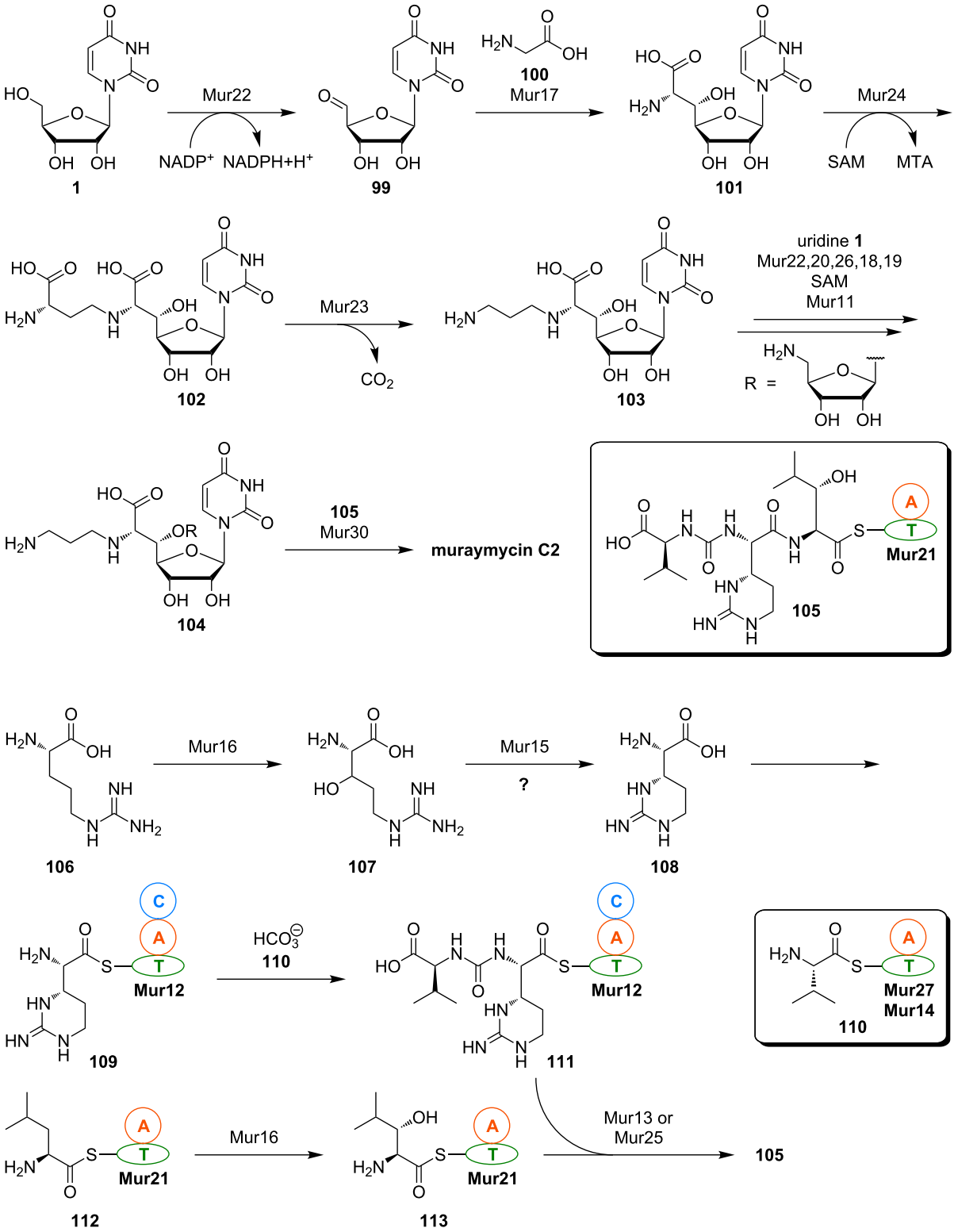

Scheme 10: Proposed outline pathway for muraymycin biosynthesis based on the analysis of the biosynthetic gene cluster by Chen, Deng et al. [118]. MTA = 5'-deoxy-5'-(methylthio)adenosine.

moiety might be obtained by stereoselective enzymatic β-hydroxylation of thioester-activated L-leucine **112**, which leads to the formation of **113**. Finally, peptide formation by condensation of **111** with **113** affords the complete thioester-activated urea tripeptide unit **105** (Scheme 10). One interesting aspect of this biosynthetic proposal by Chen, Deng et al. is that they assume the putative dioxygenase Mur16 to catalyse β-hydroxylations of two structurally distinct amino acid substrates, i.e., L-arginine (**106**) and thioester-activated L-leucine **112**.

As pointed out, there is a lack of experimental insights into muraymycin biosynthesis beyond the elucidation of its gene cluster. However, Van Lanen et al. have studied the early steps of the biosynthesis of A-90289 nucleoside antibiotics in detail (Scheme 11) [126]. The A-90289 subclass is structurally closely related to caprazamycins and liposidomycins, and its aminoribosylated nucleoside core is identical to that of muraymycins (Figure 2). This supports the assumption that the early steps of the biosynthesis of all these subclasses are probably highly similar, if not identical. For the A-90289 nucleoside antibiotics, Van Lanen et al. have demonstrated that uridine monophosphate (UMP, **114**) is the actual source of uridine-5'-aldehyde **99**, which is furnished in an oxidative transformation of UMP **114** with the 2-oxoglutarate (2-OG)-dependent non-haem Fe(II)-oxygenase LipL [127]. This result challenges the proposal by Chen, Deng et al. that aldehyde **99** might be formed by oxidation of uridine (**1**) in muraymycin biosynthesis. Aldehyde **99** then undergoes the aforementioned aldol-type transformation to GlyU **101**, catalysed by the enzyme LipK. However, aldehyde **99** also serves as a source of the aminoribosyl moiety. Thus, it is converted into 5'-amino-5'-deoxyuridine (**115**) in a transamination reaction mediated by LipO. This is followed by the LipP-catalysed displacement of the uracil with a phosphate moiety to afford 5-amino-5-deoxyribose-1-phosphate (**116**). The LipM-mediated reaction of ribosyl phosphate **116** with a nucleoside triphosphate (NTP) then yields nucleoside diphosphate (NDP)-aminoribose **117**. Finally, aminoribosylation of **101** with glycosyl donor **117**, catalysed by glycosyltransferase LipN, furnishes the complete nucleoside core structure **118** (Scheme 11). The order of 6'-*N*-(3-aminopropyl) attachment and 5'-*O*-aminoribosylation is not fully clear yet, i.e., it is not elucidated if **101** or 6'-*N*-aminoalkyl intermediate **103** (see Scheme 10) act as the glycosyl acceptor in the aminoribosylation step.

Van Lanen et al. then studied the LipK-catalysed aldol-type formation of GlyU **101** in more detail [128]. Surprisingly and in contrast to Chen's and Deng's proposal, L-threonine (**119**) turned out to be the source of the enol(ate) component instead of glycine (**100**). Hence, LipK was revealed to be a transaldolase mediating a retro-aldol reaction of L-threonine (**119**) towards the enol(ate) and acetaldehyde (**120**), followed by a

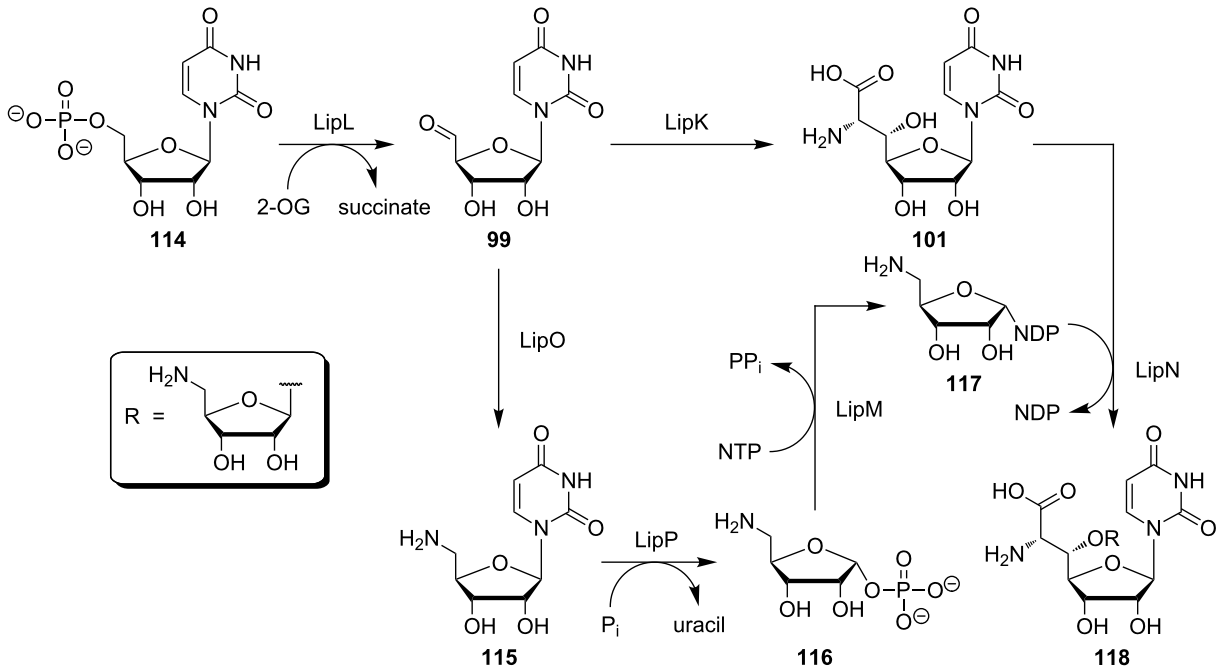

Scheme 11: Biosynthesis of the nucleoside core structure of A-90289 antibiotics (which is identical to the muraymycin nucleoside core) according to the studies of Van Lanen et al. [126]. 2-OG = 2-oxoglutarate.

stereoselective aldol addition of the former to uridine-5'-aldehyde **99** (Scheme 12). Using synthetic reference compounds, it could be proven that (5'*S*,6'*S*)-GlyU **101** is the stereoisomer furnished in this reaction, so that no epimerisation at a later stage of the biosynthetic route is required for the formation of the A-90289 nucleoside antibiotics.

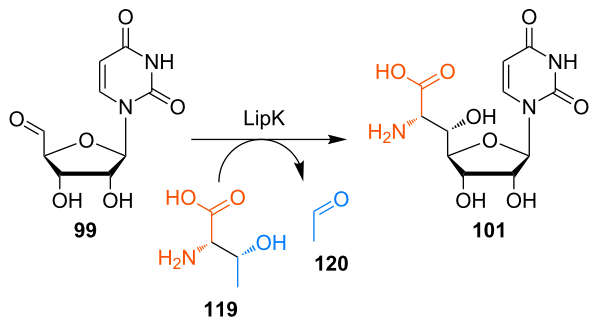

Scheme 12: Transaldolase-catalysed formation of the key intermediate GlyU **101** in the biosynthesis of muraymycin-related A-90289 antibiotics [128].

Based on the elucidation of the LipK-mediated reaction, Van Lanen et al. then performed a PCR-based screening of a collection of ≈2500 actinomycete strains for similar transaldolase-encoding genes [129]. They could identify the gene *sphJ* from a *Sphaerisporangium* sp., which encoded the transaldolase SphJ having 51% amino acid sequence identity with LipK. Following detailed characterisation of this enzyme, the *sphJ* gene was employed as a probe to clone the entire genetic locus consisting of 34 putative ORFs. The expression of three selected genes (including *sphJ*) was monitored under different growth conditions. Under the thereby identified optimal conditions, the actinomycete produced a set of four unprecedented MraY-inhibiting nucleoside antibiotics named sphaerimicin A to D [129]. Hence, detailed studies on LipK-like transaldolases led to the discovery of novel antimicrobially active secondary metabolites.

It remains to be proven that the results obtained for the early steps of A-90289 and sphaerimicin biosynthesis are also valid for the biosynthetic formation of muraymycins. Bioinformatic analyses of the biosynthetic gene clusters of A-90289 antibiotics, caprazamycins and muraymycins revealed six shared ORFs overall [128]. A sequence comparison of a range of transaldolases gave 47% identity and 78% similarity of Mur17 with LipK [129]. Overall, these insights suggest that the formation of the GlyU intermediate **101** and very likely also of the whole aminoribosylated nucleoside core structure occur in a conserved manner. Further studies on muraymycin biosynthesis are still pending.

Conclusion

In summary, this review describes a promising class of antimicrobially active natural products, the uridine-derived muraymycins. Muraymycins are one subclass of nucleoside antibiotics inhibiting the membrane protein translocase I (MraY), a key enzyme in the intracellular part of peptidoglycan formation. Synthetic methodology for the preparation of muraymycins and their analogues has been established, and first SAR insights revealed that the design of structurally simplified, biologically active muraymycin analogues is an auspicious approach. However, further SAR studies as well as investigations on the interplay of target inhibition and cellular uptake for the antibiotic activity are surely desirable. Studies on muraymycin biosynthesis may not only be of academic interest, but could also lead to semi- or mutasynthetic methodology for the preparation of novel muraymycin analogues. Several laboratories around the world currently perform research on muraymycins and other uridine-derived nucleoside antibiotics. Hopefully, this work will contribute to the development of urgently needed novel antimicrobial drugs.

Acknowledgements

We thank the Deutsche Forschungsgemeinschaft (DFG, SFB 803 "Functionality controlled by organization in and between membranes") and the Fonds der Chemischen Industrie (FCI, Sachkostenzuschuss) for financial support of our research on muraymycin antibiotics. G. N. is grateful for a doctoral fellowship of the Fonds der Chemischen Industrie, and D. W. is grateful for a doctoral fellowship of the Konrad-Adenauer-Stiftung.

References

1. Fleming, A. *Bull. W. H. O.* **2001,** *79,* 780–790.
2. Chain, E.; Florey, H. W.; Gardner, A. D.; Heatley, N. G.; Jennings, M. A.; Orr-Ewing, J.; Sanders, A. G. *Lancet* **1940,** *236,* 226–228. doi:10.1016/S0140-6736(01)08728-1
3. Abraham, E. P.; Chain, E. *Nature* **1940,** *146,* 837. doi:10.1038/146837a0
4. Kirby, W. M. M. *Science* **1944,** *99,* 452–453. doi:10.1126/science.99.2579.452
5. Levy, S. B.; Marshall, B. *Nat. Med.* **2004,** *10,* S122–S129. doi:10.1038/nm1145
6. Bush, K. *Curr. Opin. Pharmacol.* **2012,** *12,* 527–534. doi:10.1016/j.coph.2012.06.003
7. O'Connell, K. M. G.; Hodgkinson, J. T.; Sore, H. F.; Welch, M.; Salmond, G. P. C.; Spring, D. R. *Angew. Chem., Int. Ed.* **2013,** *52,* 10706–10733. doi:10.1002/anie.201209979
Angew. Chem. **2013,** *125,* 10904–10932. doi:10.1002/ange.201209979
8. von Nussbaum, F.; Brands, M.; Hinzen, B.; Weigand, S.; Häbich, D. *Angew. Chem., Int. Ed.* **2006,** *45,* 5072–5129. doi:10.1002/anie.200600350
Angew. Chem. **2006,** *118,* 5194–5254. doi:10.1002/ange.200600350
9. Butler, M. S.; Buss, A. D. *Biochem. Pharmacol.* **2006,** *71,* 919–929. doi:10.1016/j.bcp.2005.10.012

10. Alekshun, M. N.; Levy, S. B. *Cell* **2007,** *128,* 1037–1050. doi:10.1016/j.cell.2007.03.004
11. Walsh, C. *Nature* **2000,** *406,* 775–781. doi:10.1038/35021219
12. Wright, G. D. *Curr. Opin. Chem. Biol.* **2003,** *7,* 563–569. doi:10.1016/j.cbpa.2003.08.004
13. Wright, G. D. *Curr. Opin. Microbiol.* **1999,** *2,* 499–503. doi:10.1016/S1369-5274(99)00007-7
14. Katz, L.; Ashley, G. W. *Chem. Rev.* **2005,** *105,* 499–528. doi:10.1021/cr030107f
15. Li, X.-Z.; Nikaido, H. *Drugs* **2009,** *69,* 1555–1623. doi:10.2165/11317030-000000000-00000
16. Denyer, S. P.; Maillard, J.-Y. *J. Appl. Microbiol.* **2002,** *92,* 35S–45S. doi:10.1046/j.1365-2672.92.5s1.19.x
17. Lambert, P. A. *J. Appl. Microbiol.* **2002,** *92,* 46S–54S. doi:10.1046/j.1365-2672.92.5s1.7.x
18. Barrett, J. F. *Expert Opin. Ther. Targets* **2004,** *8,* 515–519. doi:10.1517/14728222.8.6.515
19. Otto, M. *Int. J. Med. Microbiol.* **2013,** *303,* 324–330. doi:10.1016/j.ijmm.2013.02.007
20. Bonten, M. J. M.; Willems, R.; Weinstein, R. A. *Lancet Infect. Dis.* **2001,** *1,* 314–325. doi:10.1016/S1473-3099(01)00145-1
21. Walsh, C. *Nat. Rev. Microbiol.* **2003,** *1,* 65–70. doi:10.1038/nrmicro727
22. McDonald, L. A.; Barbieri, L. R.; Carter, G. T.; Lenoy, E.; Lotvin, J.; Petersen, P. J.; Siegel, M. M.; Singh, G.; Williamson, R. T. *J. Am. Chem. Soc.* **2002,** *124,* 10260–10261. doi:10.1021/ja017748h
23. Kimura, K.; Bugg, T. D. H. *Nat. Prod. Rep.* **2003,** *20,* 252–273. doi:10.1039/b202149h
24. Winn, M.; Goss, R. J. M.; Kimura, K.; Bugg, T. D. H. *Nat. Prod. Rep.* **2010,** *27,* 279–304. doi:10.1039/B816215H
25. Ichikawa, S.; Yamaguchi, M.; Matsuda, A. *Curr. Med. Chem.* **2015,** *22,* 3951–3979. doi:10.2174/0929867322666150818103502
26. Takatsuki, A.; Arima, K.; Tamura, G. *J. Antibiot.* **1971,** *24,* 215–223. doi:10.7164/antibiotics.24.215
27. Takatsuki, A.; Tamura, G. *J. Antibiot.* **1971,** *24,* 224–231. doi:10.7164/antibiotics.24.224
28. Takatsuki, A.; Tamura, G. *J. Antibiot.* **1971,** *24,* 785–794. doi:10.7164/antibiotics.24.785
29. Eckardt, K.; Thrum, H.; Bradler, G.; Tonew, E.; Tonew, M. *J. Antibiot.* **1975,** *28,* 274–279. doi:10.7164/antibiotics.28.274
30. Thrum, H.; Eckardt, K.; Bradler, G.; Fügner, R.; Tonew, E.; Tonew, M. *J. Antibiot.* **1975,** *28,* 514–521. doi:10.7164/antibiotics.28.514
31. Eckardt, K.; Ihn, W.; Tresselt, D.; Krebs, D. *J. Antibiot.* **1981,** *34,* 1631–1632. doi:10.7164/antibiotics.34.1631
32. Vogel, P.; Petterson, D. S.; Berry, P. H.; Frahn, J. L.; Anderton, N.; Cockrum, P. A.; Edgar, J. A.; Jago, M. V.; Lanigan, G. W.; Payne, A. L.; Culvenor, C. C. J. *Aust. J. Exp. Biol. Med. Sci.* **1981,** *59,* 455–467. doi:10.1038/icb.1981.39
33. Seto, H.; Otake, N.; Sato, S.; Yamaguchi, H.; Takada, K.; Itoh, M.; Lu, H. S. M.; Clardy, J. *Tetrahedron Lett.* **1988,** *29,* 2343–2346. doi:10.1016/S0040-4039(00)86055-4
34. Yamaguchi, H.; Sato, S.; Yoshida, S.; Takada, K.; Itoh, M.; Seto, H.; Otake, N. *J. Antibiot.* **1986,** *39,* 1047–1053. doi:10.7164/antibiotics.39.1047
35. Ochi, K.; Ezaki, M.; Iwami, M.; Komori, T.; Kohsaka, M. FR-900493 substance, a process for its production and a pharmaceutical composition containing the same. U.S. Patent US4950605 A, Aug 21, 1990.
36. Inukai, M.; Isono, F.; Takahashi, S.; Enokita, R.; Sakaida, Y.; Haneishi, T. *J. Antibiot.* **1989,** *42,* 662–666. doi:10.7164/antibiotics.42.662
37. Isono, F.; Inukai, M.; Takahashi, S.; Haneishi, T.; Kinoshita, T.; Kuwano, H. *J. Antibiot.* **1989,** *42,* 667–673. doi:10.7164/antibiotics.42.667
38. Isono, F.; Katayama, T.; Inukai, M.; Haneishi, T. *J. Antibiot.* **1989,** *42,* 674–679. doi:10.7164/antibiotics.42.674
39. Karwowski, J. P.; Jackson, M.; Theriault, R. J.; Chen, R. H.; Barlow, G. J.; Maus, M. L. *J. Antibiot.* **1989,** *42,* 506–511. doi:10.7164/antibiotics.42.506
40. Chen, R. H.; Buko, A. M.; Whittern, D. N.; McAlpine, J. B. *J. Antibiot.* **1989,** *42,* 512–520. doi:10.7164/antibiotics.42.512
41. Fernandes, P. B.; Swanson, R. N.; Hardy, D. J.; Hanson, C. W.; Coen, L.; Rasmussen, R. R.; Chen, R. H. *J. Antibiot.* **1989,** *42,* 521–526. doi:10.7164/antibiotics.42.521
42. Chatterjee, S.; Nadkarni, S. R.; Vijayakumar, E. K. S.; Patel, M. V.; Ganguli, B. N.; Fehlhaber, H.-W.; Vertesy, L. *J. Antibiot.* **1994,** *47,* 595–598. doi:10.7164/antibiotics.47.595
43. Xie, Y.; Chen, R.; Si, S.; Sun, C.; Xu, H. *J. Antibiot.* **2007,** *60,* 158–161. doi:10.1038/ja.2007.16
44. Xie, Y.; Xu, H.; Si, S.; Sun, C.; Chen, R. *J. Antibiot.* **2008,** *61,* 237–240. doi:10.1038/ja.2008.34
45. Isono, K.; Uramoto, M.; Kusakabe, H.; Kimura, K.-I.; Izaki, K.; Nelson, C. C.; McCloskey, J. A. *J. Antibiot.* **1985,** *38,* 1617–1621. doi:10.7164/antibiotics.38.1617
46. Igarashi, M.; Nakagawa, N.; Doi, N.; Hattori, S.; Naganawa, H.; Hamada, M. *J. Antibiot.* **2003,** *56,* 580–583. doi:10.7164/antibiotics.56.580
47. Igarashi, M.; Takahashi, Y.; Shitara, T.; Nakamura, H.; Naganawa, H.; Miyake, T.; Akamatsu, Y. *J. Antibiot.* **2005,** *58,* 327–337. doi:10.1038/ja.2005.41
48. Naganawa, H.; Hamada, M.; Igarashi, M.; Takeuchi, T. Antibiotic caprazamycins and process for producing the same. Canadian Patent CA2388050 A1, Feb 22, 2001.
49. Carter, G. T.; Lotvin, J. A.; McDonald, L. A. Antibiotics AA-896. WO Patent WO2002085310 A3, Nov 20, 2003.
50. Bugg, T. D. H.; Walsh, C. T. *Nat. Prod. Rep.* **1992,** *9,* 199–215. doi:10.1039/np9920900199
51. van Heijenoort, J. *Nat. Prod. Rep.* **2001,** *18,* 503–519. doi:10.1039/a804532a
52. Vollmer, W.; Blanot, D.; De Pedro, M. A. *FEMS Microbiol. Rev.* **2008,** *32,* 149–167. doi:10.1111/j.1574-6976.2007.00094.x
53. Osborn, M. J. *Annu. Rev. Biochem.* **1969,** *38,* 501–538. doi:10.1146/annurev.bi.38.070169.002441
54. Barreteau, H.; Kovač, A.; Boniface, A.; Sova, M.; Gobec, S.; Blanot, D. *FEMS Microbiol. Rev.* **2008,** *32,* 168–207. doi:10.1111/j.1574-6976.2008.00104.x
55. Bouhss, A.; Trunkfield, A. E.; Bugg, T. D. H.; Mengin-Lecreulx, D. *FEMS Microbiol. Rev.* **2008,** *32,* 208–233. doi:10.1111/j.1574-6976.2007.00089.x
56. Gautam, A.; Vyas, R.; Tewari, R. *Crit. Rev. Biotechnol.* **2011,** *31,* 295–336. doi:10.3109/07388551.2010.525498
57. Egan, A. J. F.; Vollmer, W. *Ann. N. Y. Acad. Sci.* **2013,** *1277,* 8–28. doi:10.1111/j.1749-6632.2012.06818.x
58. Ikeda, M.; Wachi, M.; Jung, H. K.; Ishino, F.; Matsuhashi, M. *J. Bacteriol.* **1991,** *173,* 1021–1026.
59. Boyle, D. S.; Donachie, W. D. *J. Bacteriol.* **1998,** *180,* 6429–6432.

60. Branstrom, A. A.; Midha, S.; Longley, C. B.; Han, K.; Baizman, E. R.; Axelrod, H. R. *Anal. Biochem.* **2000,** *280,* 315–319. doi:10.1006/abio.2000.4530
61. Barbosa, M. D. F. S.; Ross, H. O.; Hillman, M. C.; Meade, R. P.; Kurilla, M. G.; Pompliano, D. L. *Anal. Biochem.* **2002,** *306,* 17–22. doi:10.1006/abio.2001.5691
62. Thanassi, J. A.; Hartman-Neumann, S. L.; Dougherty, T. J.; Dougherty, B. A.; Pucci, M. J. *Nucleic Acids Res.* **2002,** *30,* 3152–3162. doi:10.1093/nar/gkf418
63. Lara, B.; Mengin-Lecreulx, D.; Ayala, J. A.; van Heijenoort, J. *FEMS Microbiol. Lett.* **2005,** *250,* 195–200. doi:10.1016/j.femsle.2005.07.005
64. Struve, W. G.; Neuhaus, F. C. *Biochem. Biophys. Res. Commun.* **1965,** *18,* 6–12. doi:10.1016/0006-291X(65)90873-9
65. Anderson, J. S.; Matsuhashi, M.; Haskin, M. A.; Strominger, J. L. *Proc. Natl. Acad. Sci. U. S. A.* **1965,** *53,* 881–889. doi:10.1073/pnas.53.4.881
66. Heydanek, M. G., Jr.; Struve, W. G.; Neuhaus, F. C. *Biochemistry* **1969,** *8,* 1214–1221. doi:10.1021/bi00831a056
67. Pless, D. D.; Neuhaus, F. C. *J. Biol. Chem.* **1973,** *248,* 1568–1576.
68. Lloyd, A. J.; Brandish, P. E.; Gilbey, A. M.; Bugg, T. D. H. *J. Bacteriol.* **2004,** *186,* 1747–1757. doi:10.1128/JB.186.6.1747-1757.2004
69. Al-Dabbagh, B.; Henry, X.; Ghachi, M. E.; Auger, G.; Blanot, D.; Parquet, C.; Mengin-Lecreulx, D.; Bouhss, A. *Biochemistry* **2008,** *47,* 8919–8928. doi:10.1021/bi8006274
70. Bouhss, A.; Mengin-Lecreulx, D.; Le Beller, D.; van Heijenoort, J. *Mol. Microbiol.* **1999,** *34,* 576–585. doi:10.1046/j.1365-2958.1999.01623.x
71. Chung, B. C.; Zhao, J.; Gillespie, R. A.; Kwon, D.-Y.; Guan, Z.; Hong, J.; Zhou, P.; Lee, S.-Y. *Science* **2013,** *341,* 1012–1016. doi:10.1126/science.1236501
72. Bernhardt, T. G.; Roof, W. D.; Young, R. *Proc. Natl. Acad. Sci. U. S. A.* **2000,** *97,* 4297–4302. doi:10.1073/pnas.97.8.4297
73. Bernhardt, T. G.; Struck, D. K.; Young, R. *J. Biol. Chem.* **2001,** *276,* 6093–6097. doi:10.1074/jbc.M007638200
74. Rodolis, M. T.; Mihalyi, A.; O'Reilly, A.; Slikas, J.; Roper, D. I.; Hancock, R. E. W.; Bugg, T. D. H. *ChemBioChem* **2014,** *15,* 1300–1308. doi:10.1002/cbic.201402064
75. Andrews, J. M. *J. Antimicrob. Chemother.* **2001,** *48,* 5–16. doi:10.1093/jac/48.suppl_1.5
76. Yamashita, A.; Norton, E.; Petersen, P. J.; Rasmussen, B. A.; Singh, G.; Yang, Y.; Mansour, T. S.; Ho, D. M. *Bioorg. Med. Chem. Lett.* **2003,** *13,* 3345–3350. doi:10.1016/S0960-894X(03)00671-1
77. Tanino, T.; Al-Dabbagh, B.; Mengin-Lecreulx, D.; Bouhss, A.; Oyama, H.; Ichikawa, S.; Matsuda, A. *J. Med. Chem.* **2011,** *54,* 8421–8439. doi:10.1021/jm200906r
78. Spork, A. P.; Büschleb, M.; Ries, O.; Wiegmann, D.; Boettcher, S.; Mihalyi, A.; Bugg, T. D. H.; Ducho, C. *Chem. – Eur. J.* **2014,** *20,* 15292–15297. doi:10.1002/chem.201404775
79. Brandish, P. E.; Burnham, M. K.; Lonsdale, J. T.; Southgate, R.; Inukai, M.; Bugg, T. D. H. *J. Biol. Chem.* **1996,** *271,* 7609–7614. doi:10.1074/jbc.271.13.7609
80. Brandish, P. E.; Kimura, K.; Inukai, M.; Southgate, R.; Lonsdale, J. T.; Bugg, T. D. *Antimicrob. Agents Chemother.* **1996,** *40,* 1640–1644.
81. Bouhss, A.; Crouvoisier, M.; Blanot, D.; Mengin-Lecreulx, D. *J. Biol. Chem.* **2004,** *279,* 29974–29980. doi:10.1074/jbc.M314165200
82. Fer, M. J.; Bouhss, A.; Patrão, M.; Le Corre, L.; Pietrancosta, N.; Amoroso, A.; Joris, B.; Mengin-Lecreulx, D.; Calvet-Vitale, S.; Gravier-Pelletier, C. *Org. Biomol. Chem.* **2015,** *13,* 7193–7222. doi:10.1039/C5OB00707K
83. Shapiro, A. B.; Jahić, H.; Gao, N.; Hajec, L.; Rivin, O. *J. Biomol. Screening* **2012,** *17,* 662–672. doi:10.1177/1087057112436885
84. Mengin-Lecreulx, D.; Parquet, C.; Desviat, L. R.; Plá, J.; Flouret, B.; Ayala, J. A.; van Heijenoort, J. *J. Bacteriol.* **1989,** *171,* 6126–6134.
85. Ma, Y.; Münch, D.; Schneider, T.; Sahl, H.-G.; Bouhss, A.; Ghoshdastider, U.; Wang, J.; Dötsch, V.; Wang, X.; Bernhard, F. *J. Biol. Chem.* **2011,** *286,* 38844–38853. doi:10.1074/jbc.M111.301085
86. Lin, Y.-I.; Li, Z.; Francisco, G. D.; McDonald, L. A.; Davis, R. A.; Singh, G.; Yang, Y.; Mansour, T. S. *Bioorg. Med. Chem. Lett.* **2002,** *12,* 2341–2344. doi:10.1016/S0960-894X(02)00469-9
87. Zhu, X.-F.; Williams, H. J.; Scott, A. I. *J. Chem. Soc., Perkin Trans. 1* **2000,** 2305–2306. doi:10.1039/B003562I
88. Myers, A. G.; Gin, D. Y.; Rogers, D. H. *J. Am. Chem. Soc.* **1994,** *116,* 4697–4718. doi:10.1021/ja00090a018
89. Banfi, L.; Cardani, S.; Potenza, D.; Scolastico, C. *Tetrahedron* **1987,** *43,* 2317–2322. doi:10.1016/S0040-4020(01)86816-2
90. Hirano, S.; Ichikawa, S.; Matsuda, A. *Angew. Chem., Int. Ed.* **2005,** *44,* 1854–1856. doi:10.1002/anie.200462439
Angew. Chem. **2005,** *117,* 1888–1890. doi:10.1002/ange.200462439
91. Hirano, S.; Ichikawa, S.; Matsuda, A. *J. Org. Chem.* **2007,** *72,* 9936–9946. doi:10.1021/jo701699h
92. Hirano, S.; Ichikawa, S.; Matsuda, A. *J. Org. Chem.* **2008,** *73,* 569–577. doi:10.1021/jo702264e
93. Kimura, J.; Kobayashi, H.; Miyahara, O.; Mitsunobu, O. *Bull. Chem. Soc. Jpn.* **1986,** *59,* 869–874. doi:10.1246/bcsj.59.869
94. Tao, B.; Schlingloff, G.; Sharpless, K. B. *Tetrahedron Lett.* **1998,** *39,* 2507–2510. doi:10.1016/S0040-4039(98)00350-5
95. Ichikawa, S.; Hayashi, R.; Hirano, S.; Matsuda, A. *Org. Lett.* **2008,** *10,* 5107–5110. doi:10.1021/ol8018743
96. Tanino, T.; Hirano, S.; Ichikawa, S.; Matsuda, A. *Nucleic Acids Symp. Ser.* **2008,** *52,* 557–558. doi:10.1093/nass/nrn282
97. Tanino, T.; Ichikawa, S.; Shiro, M.; Matsuda, A. *J. Org. Chem.* **2010,** *75,* 1366–1377. doi:10.1021/jo9027193
98. Aleiwi, B. A.; Schneider, C. M.; Kurosu, M. *J. Org. Chem.* **2012,** *77,* 3859–3867. doi:10.1021/jo300205b
99. Spork, A. P.; Koppermann, S.; Dittrich, B.; Herbst-Irmer, R.; Ducho, C. *Tetrahedron: Asymmetry* **2010,** *21,* 763–766. doi:10.1016/j.tetasy.2010.03.037
100. Aggarwal, V. K.; Ford, J. G.; Thompson, A.; Jones, R. V. H.; Standen, M. C. H. *J. Am. Chem. Soc.* **1996,** *118,* 7004–7005. doi:10.1021/ja961144+
101. Aggarwal, V. K.; Harvey, J. N.; Richardson, J. *J. Am. Chem. Soc.* **2002,** *124,* 5747–5756. doi:10.1021/ja025633n
102. Spork, A. P.; Koppermann, S.; Ducho, C. *Synlett* **2009,** *15,* 2503–2507. doi:10.1055/s-0029-1217742
103. Sarabia, F.; Martín-Ortiz, L.; López-Herrera, F. J. *Org. Lett.* **2003,** *5,* 3927–3930. doi:10.1021/ol0355074
104. Sarabia, F.; Martín-Ortiz, L. *Tetrahedron* **2005,** *61,* 11850–11865. doi:10.1016/j.tet.2005.09.086
105. Spork, A. P.; Ducho, C. *Synlett* **2013,** *24,* 343–346. doi:10.1055/s-0032-1318117
106. Dondoni, A.; Perrone, D. *Org. Synth.* **2000,** *77,* 64–70. doi:10.15227/orgsyn.077.0064

107. Ries, O.; Büschleb, M.; Granitzka, M.; Stalke, D.; Ducho, C. *Beilstein J. Org. Chem.* **2014,** *10,* 1135–1142. doi:10.3762/bjoc.10.113
108. Laïb, T.; Chastanet, J.; Zhu, J. *J. Org. Chem.* **1998,** *63,* 1709–1713. doi:10.1021/jo971468w
109. Spork, A. P.; Ducho, C. *Org. Biomol. Chem.* **2010,** *8,* 2323–2326. doi:10.1039/c003092a
110. Spork, A. P.; Wiegmann, D.; Granitzka, M.; Stalke, D.; Ducho, C. *J. Org. Chem.* **2011,** *76,* 10083–10098. doi:10.1021/jo201935w
111. Schmidt, U.; Lieberknecht, A.; Schanbacher, U.; Beuttler, T.; Wild, J. *Angew. Chem., Int. Ed.* **1982,** *21,* 776–777. doi:10.1002/anie.198207761
Angew. Chem. **1982,** *94,* 797–798. doi:10.1002/ange.19820941027
112. Burk, M. J. *J. Am. Chem. Soc.* **1991,** *113,* 8518–8519. doi:10.1021/ja00022a047
113. Masquelin, T.; Broger, E.; Müller, K.; Schmid, R.; Obrecht, D. *Helv. Chim. Acta* **1994,** *77,* 1395–1411. doi:10.1002/hlca.19940770518
114. Tanino, T.; Ichikawa, S.; Al-Dabbagh, B.; Bouhss, A.; Oyama, H.; Matsuda, A. *ACS Med. Chem. Lett.* **2010,** *1,* 258–262. doi:10.1021/ml100057z
115. Takeoka, Y.; Tanino, T.; Sekiguchi, M.; Yonezawa, S.; Sakagami, M.; Takahashi, F.; Togame, H.; Tanaka, Y.; Takemoto, H.; Ichikawa, S.; Matsuda, A. *ACS Med. Chem. Lett.* **2014,** *5,* 556–560. doi:10.1021/ml5000096
116. Schmidtgall, B.; Spork, A. P.; Wachowius, F.; Höbartner, C.; Ducho, C. *Chem. Commun.* **2014,** *50,* 13742–13745. doi:10.1039/C4CC06371F
117. Schmidtgall, B.; Höbartner, C.; Ducho, C. *Beilstein J. Org. Chem.* **2015,** *11,* 50–60. doi:10.3762/bjoc.11.8
118. Cheng, L.; Chen, W.; Zhai, L.; Xu, D.; Huang, T.; Lin, S.; Zhou, X.; Deng, Z. *Mol. BioSyst.* **2011,** *7,* 920–927. doi:10.1039/C0MB00237B
119. Yin, X.; Zabriskie, T. M. *ChemBioChem* **2004,** *5,* 1274–1277. doi:10.1002/cbic.200400082
120. Yin, X.; McPhail, K. L.; Kim, K.; Zabriskie, T. M. *ChemBioChem* **2004,** *5,* 1278–1281. doi:10.1002/cbic.200400187
121. Ju, J.; Ozanick, S. G.; Shen, B.; Thomas, M. G. *ChemBioChem* **2004,** *5,* 1281–1285. doi:10.1002/cbic.200400136
122. Hamed, R. B.; Gomez-Castellanos, J. R.; Henry, L.; Ducho, C.; McDonough, M. A.; Schofield, C. J. *Nat. Prod. Rep.* **2013,** *30,* 21–107. doi:10.1039/C2NP20065A
123. Lemke, A.; Büschleb, M.; Ducho, C. *Tetrahedron* **2010,** *66,* 208–214. doi:10.1016/j.tet.2009.10.102
124. Lemke, A.; Ducho, C. *Eur. J. Org. Chem.* **2016,** *2016,* 87–98. doi:10.1002/ejoc.201501109
125. Büschleb, M.; Granitzka, M.; Stalke, D.; Ducho, C. *Amino Acids* **2012,** *43,* 2313–2328. doi:10.1007/s00726-012-1309-8
126. Chi, X.; Pahari, P.; Nonaka, K.; Van Lanen, S. G. *J. Am. Chem. Soc.* **2011,** *133,* 14452–14459. doi:10.1021/ja206304k
127. Yang, Z.; Chi, X.; Funabashi, M.; Baba, S.; Nonaka, K.; Pahari, P.; Unrine, J.; Jacobsen, J. M.; Elliott, G. I.; Rohr, J.; Van Lanen, S. G. *J. Biol. Chem.* **2011,** *286,* 7885–7892. doi:10.1074/jbc.M110.203562
128. Barnard-Britson, S.; Chi, X.; Nonaka, K.; Spork, A. P.; Tibrewal, N.; Goswami, A.; Pahari, P.; Ducho, C.; Rohr, J.; Van Lanen, S. G. *J. Am. Chem. Soc.* **2012,** *134,* 18514–18517. doi:10.1021/ja308185q
129. Funabashi, M.; Baba, S.; Takatsu, T.; Kizuka, M.; Ohata, Y.; Tanaka, M.; Nonaka, K.; Spork, A. P.; Ducho, C.; Chen, W.-C. L.; Van Lanen, S. G. *Angew. Chem., Int. Ed.* **2013,** *52,* 11607–11611. doi:10.1002/anie.201305546
Angew. Chem. **2013,** *125,* 11821–11825. doi:10.1002/ange.201305546

License and Terms

BEILSTEIN JOURNAL OF ORGANIC CHEMISTRY

Marine-derived myxobacteria of the suborder Nannocystineae: An underexplored source of structurally intriguing and biologically active metabolites

Antonio Dávila-Céspedes‡, Peter Hufendiek‡, Max Crüsemann‡, Till F. Schäberle and Gabriele M. König*

Review

Open Access

Address:
Institute for Pharmaceutical Biology, University of Bonn, Nussallee 6, 53115 Bonn, Germany

Email:
Gabriele M. König* - g.koenig@uni-bonn.de

* Corresponding author ‡ Equal contributors

Keywords:
Enhygromyxa; genome mining; myxobacteria; Nannocystineae; natural products

Beilstein J. Org. Chem. **2016,** *12,* 969–984.
doi:10.3762/bjoc.12.96

Received: 22 February 2016
Accepted: 25 April 2016
Published: 13 May 2016

This article is part of the Thematic Series "Natural products in synthesis and biosynthesis II".

Guest Editor: J. S. Dickschat

Abstract

Myxobacteria are famous for their ability to produce most intriguing secondary metabolites. Till recently, only terrestrial myxobacteria were in the focus of research. In this review, however, we discuss marine-derived myxobacteria, which are particularly interesting due to their relatively recent discovery and due to the fact that their very existence was called into question. The to-date-explored members of these halophilic or halotolerant myxobacteria are all grouped into the suborder Nannocystineae. Few of them were chemically investigated revealing around 11 structural types belonging to the polyketide, non-ribosomal peptide, hybrids thereof or terpenoid class of secondary metabolites. A most unusual structural type is represented by salimabromide from *Enhygromyxa salina*. In silico analyses were carried out on the available genome sequences of four bacterial members of the Nannocystineae, revealing the biosynthetic potential of these bacteria.

Review

Taxonomy and ecology of myxobacteria

Bacteria from the order Myxococcales, commonly known as myxobacteria, are Gram-negative, rod-shaped δ-proteobacteria, comprising compared to many other bacteria large genomes. The 14,782,125 bp large genome of *Sorangium cellulosum* So0157-2 is the largest bacterial genome reported to date [1]. Myxobacteria are able to glide over surfaces in swarms in order to facilitate heterotrophic nutrition on macromolecules as well as on whole microorganisms, a distinctive trait of these bacteria

[2]. Additionally, under adverse environmental conditions, e.g., nutrient shortages, high temperature and dryness, individuals cooperate to create intercommunicated multicellular myxospore-containing fruiting bodies in order to ensure the distribution of nutrients they can still harness, allowing germination as soon as conditions are favorable for the vegetative phase again [3]. Based on our experience in the laboratory, fruiting bodies can occur on solid surfaces like agar plates, as well as in liquid cultures. These adaptive strategies play a fundamental role on how these organisms are able to endure under unfavorable conditions [2,4]. In terms of oxygen demand for growth, myxobacteria were thought to be strictly aerobic until the only anaerobic genus known to date, *Anaeromyxobacter*, was reported in 2002 [5]. Also, for many years myxobacteria were considered to typically occur only in terrestrial habitats and much has been published in terms of their morphology, physiology and ecology [2,4,6,7].

Recently, ever more myxobacteria from intertidal and marine environments were reported. According to salt requirements for growth, a straightforward classification of these bacteria has been provided [8]: (I) halotolerant strains are capable to grow with or without NaCl; and (II) halophilic bacteria are unable to grow without sea salt. Bacteria of group (I) may be derived from terrestrial organisms, which have adapted to saline conditions, whereas those of group (II) may be of truly marine origin.

A typical halotolerant myxobacterium, originally obtained from coastal samples, is the *Myxococcus fulvus* strain HW-1 (suborder Cystobacterineae). In this case, it was demonstrated that salt concentration not only affects growth, but also myxobacterial motility systems as well as fruiting body formation [9]. In the absence of salt, both capabilities were diminished. Mutational studies imply that the single, probably horizontally transferred gene *hdsp*, which was found in five halotolerant *Myxococcus* strains, but not in soil-derived *Myxococcus* strains, leads among other changes to sea water tolerance [10].

Only few myxobacteria dwelling in sea habitats are considered as halophilic, that is, of true marine origin. Indeed, early isolates from marine environments were thought to be halotolerant terrestrial myxobacteria whose myxospores had been washed into the ocean [11]. This opinion prevailed until Fudou and Iizuka [12-15] discovered the first strictly halophilic myxobacteria within the suborder Nannocystineae, namely *Enhygromyxa*, *Haliangium*, and *Plesiocystis*, which strictly require sea-like salinity conditions in order to grow. Whether the adaptation to the marine environment was acquired independently several times, or if these entire marine clades share one common ancestor, is not clarified yet due to the relatively low number of species known to date.

Regarding the strategies employed by these bacteria to cope with salt and desiccation stress, the accumulation of organic osmolytes instead of the salt-in strategy can be expected. This hypothesis is supported by the fact that all strains investigated so far can grow within a relatively wide range of salinity. Also, the terrestrial strain *M. xanthus*, which is slightly halotolerant, uses organic osmolytes, i.e., glycine betaine to combat osmotic stress [16]. Analyses on the osmoprotective strategies of *Enhygromyxa salina* SWB007 and *Plesiocystis pacifica* SIR-1 revealed that both closely related strains rely on organic osmolytes. For instance, *E. salina* SWB007 biosynthesizes the osmolytes betaine, ectoine, and especially hydroxyectoine under high salt concentrations. In contrast, *P. pacifica* SIR-1 does not synthesize specialized compatible solutes; this strain rather accumulates amino acids as osmoprotective agents [17]. Of course, further mechanisms may be involved for osmoregulation, but are not known to date for myxobacteria. A list of general bacterial osmoregulation processes is given elsewhere [18].

Secondary metabolites from myxobacteria

Members of the order Myxococcales are famous for their ability to produce secondary metabolites of diverse chemical nature with the capability to exert different biological effects [19,20]. Detailed descriptions of myxobacteria-derived metabolites can be found in various detailed reports [19-23]. The majority of these metabolites are either non-ribosomal peptides, e.g., cystobactamids **1–3** (Figure 1) [24], polyketides, e.g., aurafuron A (**4**) [25], or hybrids thereof, e.g., corallopyronin A (**5**, Figure 2) [26].

Interestingly, an ample amount of them was shown to work as antimicrobial agents, above all corallopyronin A. This is probably a reflection of their predatory habits [27,28]. A comprehensive description of antibiotics obtained from myxobacteria can be found in a previous review [21]. One outstanding example of a biologically active PKS/NRPS-derived compound produced by the terrestrial *S. cellulosum* is the microtubule stabilizer epothilone B, of which the lactam analogue ixabepilone (**6**) is currently used together with capecitabine (**7**, Figure 3) in cancer therapy to improve the effectiveness of taxane-resistant metastatic breast cancer treatment, demonstrating the therapeutic potential of myxobacterial secondary metabolites [29-31]. This drug has also been assessed as chemotherapeutic agent in pancreatic lymphoma showing promising results and tolerable toxicity [32].

Over time, different strategies have been designed to tackle the sometimes cumbersome task of finding bioactive secondary metabolites of bacterial origin, i.e., mainly bioactivity- or chemistry-guided methods. An additional approach, complementary

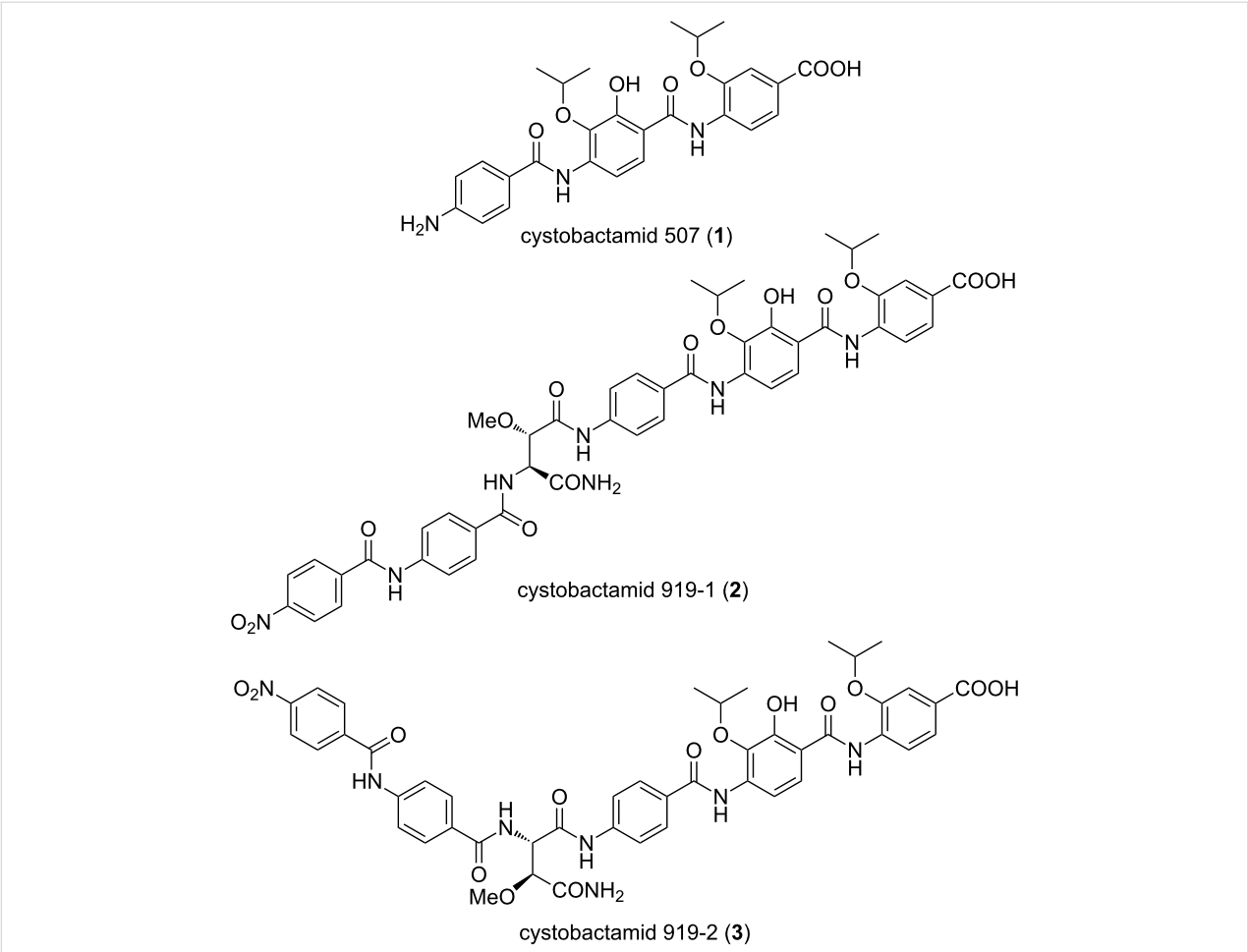

Figure 1: Structures of cystobactamids 507, 919-1 and 919-2.

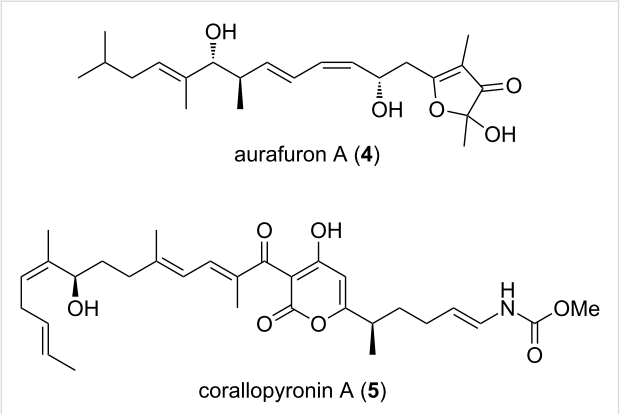

Figure 2: Structures of aurafuron A and corallopyronin A.

to the latter, arose in the late 1990s, when the first microbial genomes were sequenced, allowing genome mining. Thus, knowledge derived from bioinformatic analysis of microbial genomes paved the way to gain detailed insights into bacterial secondary metabolism. Since then, in silico methods for genome mining have enormously advanced and effective experimental approaches for connecting genomic and metabolic information have been developed [33-35].

The terrestrial *Myxococcus xanthus* strain DK1622 was the first myxobacterium to have its 9.14 Mb genome sequenced, with the initial aim to study its swarming motility and fruiting body formation [36]. At the same time, this work reinforced the notion that large genomes often correlate with the potential for prolific secondary metabolite production by revealing almost 8.6% of the genome to be possibly involved in the biosynthesis of secondary metabolites [36]. Mining this genome for the presence of PKS and NRPS genes exposed 18 biosynthetic clusters, with a predominance of hybrid PKS-NRPS systems [37]. *M. xanthus* strain DK1622 is responsible for the synthesis of metabolites like DKxanthene-534 (**8**, Figure 4), a pigment required for fruiting body formation and sporulation processes [37] and the siderophore myxochelin A (**9**), which belongs to a class of compounds that have recently been shown to have antiproliferative effects on leukemic K-562 cells [27].

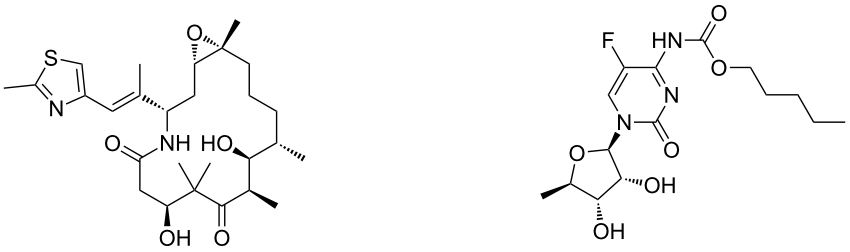

Figure 3: Structures of ixabepilone and capecitabine.

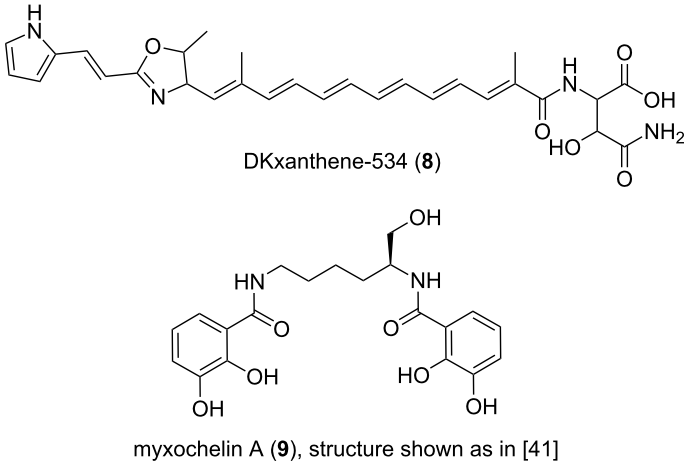

Figure 4: Structures of DKxanthene-534 and myxochelin A.

Halotolerant and halophilic marine myxobacteria are poorly investigated regarding secondary metabolite production. Therefore, the pool of secondary metabolites isolated from organisms of this kind is very low to date, when compared to that of their terrestrial counterparts. This is mainly due to the difficulties that are encountered during isolation and cultivation processes of marine myxobacteria. However, herein we intend to show that these organisms are a great research niche, which offers the opportunity to find novel bioactive compounds with the potential to become drug leads.

Regarding halotolerant myxobacteria, the 9 Mb genome of the *Myxococcus fulvus* strain HW-1 (ATCC BAA-855, suborder Cystobacterineae) was the first-of-its-kind to be sequenced [38]. Genome mining performed in our group revealed that this organism displays, analogous to the previously discussed example *M. xanthus* strain DK1622, a plethora of cryptic gene clusters, e.g., five NRPS, four hybrid PKS-NRPS, one PKS-NRPS-lantipeptide, three lantipeptide and numerous bacteriocin- and terpene-encoding gene loci. A more detailed comparison revealed that both strains share the majority of their gene clusters, among them the aforementioned DKxanthene, the myxochromide [39] and myxoprincomide [40] pathways, besides other, yet uncharacterized loci. It is worth mentioning that no gene clusters involved in synthesis of osmolytes like betaine and ectoine were detected in the halotolerant bacterium.

Taxonomy, cultivation and secondary metabolite chemistry of marine-derived myxobacteria (Nannocystineae)

The following sections summarize features of three halotolerant and three marine-derived bacterial taxa clustered in the suborder Nannocystineae: *Nannocystis, Haliangium, Enhygromyxa, Plesiocystis,* Myxobacterium SMH-27-4 (i.e., *Paraliomyxa*) and *Pseudenhygromyxa* (see Figure 5).

Information on strain isolation, culture conditions, phylogeny, genetics and hitherto isolated molecules will be provided, with an emphasis on structural details and biological activity of the metabolites. Additionally, putative gene clusters for secondary

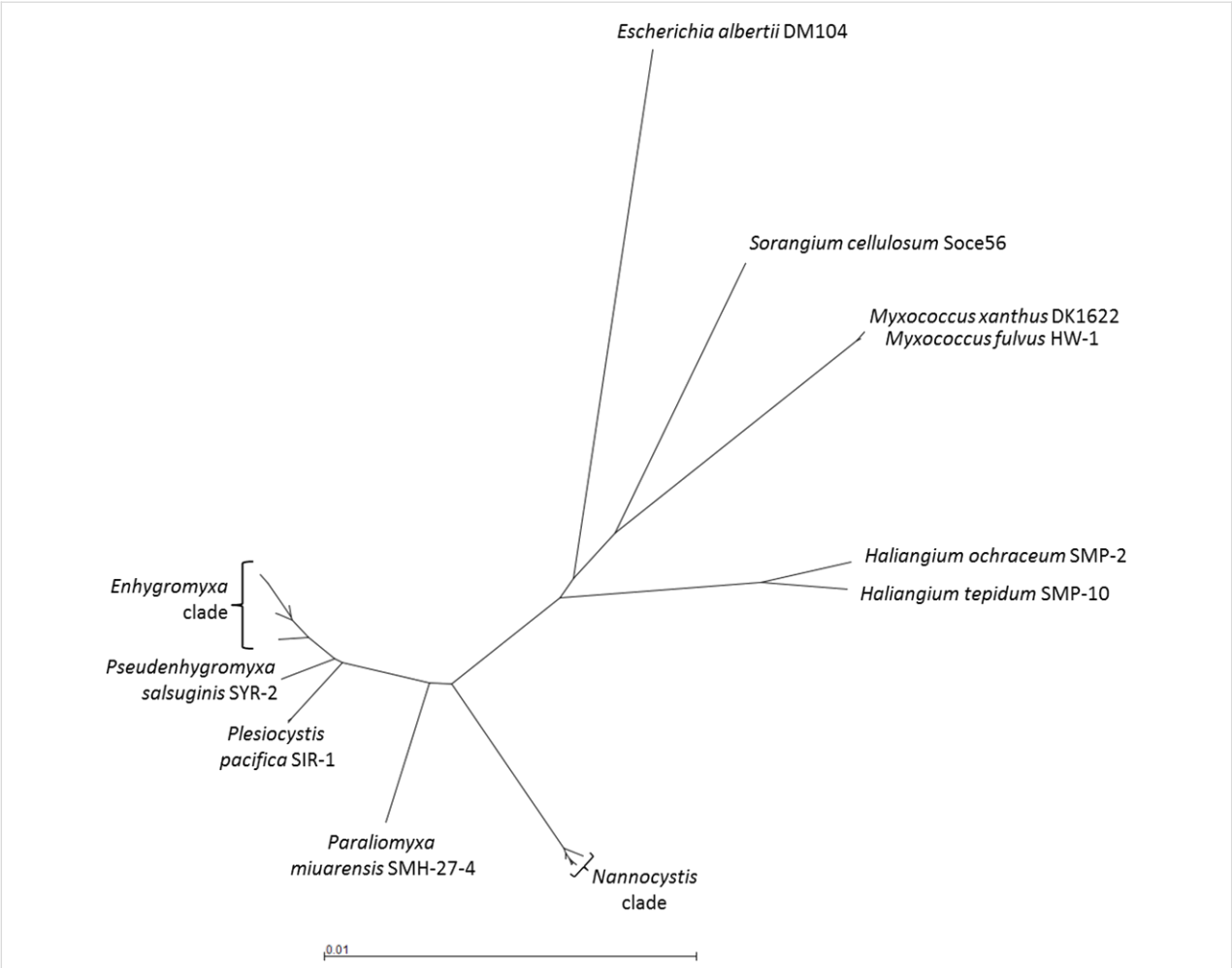

Figure 5: Phylogenetic tree of halotolerant and halophilic myxobacteria. The neighbor-joining tree is based on a multiple sequence alignment (MSA) of the 16S rDNA sequences. The terrestrial myxobacteria *Myxococcus xanthus* DK1622 and *Sorangium cellulosum* Soce56 as well as *Escherichia albertii* DM104 are included for comparison (see Supporting Information File 1 for the sequences used; the MSA was computed using Clustal Omega).

metabolite biosynthesis are included in this review. For this reason we were mining the four available genomes from bacteria of the Nannocystineae using the antiSMASH 3 tool [41] (see Table 1). The genome mining results are generated by feeding the software with the INSDC code of the annotated sequences. The databases are continuously updated, thus, results presented in this part of the review may vary in ulterior analyses. Our data, however, present a useful guide for future projects. For detailed information on terrestrial myxobacteria and other predatory bacteria, readers are referred to the review article from Korp et al. in this thematic series [42].

The genus *Nannocystis*

Bacteria of the genus *Nannocystis* are merely halotolerant and frequently isolated from terrestrial or intertidal regions. Back in the 1970s, the Reichenbach group informed on the isolation of a widely distributed soil-dwelling myxobacterium similar to members of the genus *Sorangium* in terms of cytology and growth pattern [43]. After taxonomic studies, they proposed a new genus and species, i.e., *Nannocystis exedens.* Only recently it was recognized that members of this genus have a great potential as producers of metabolites with relevant biological activities. One striking example is the 2015 described nannocystin A (**10**, Figure 6), a macrocyclic compound of NRPS-PKS origin with strong antiproliferative properties isolated from the terrestrial *Nannocystis* sp. ST201196 (DSM 18870) [44].

It was subsequently shown that nannocystin A targets the eukaryotic translation elongation factor 1α, a promising novel target for cancer therapy [44]. Regarding metabolites from halotolerant *Nannocystis* strains, the most outstanding examples are the phenylnannolones A–C (**11**–**13**, Figure 7), molecules of polyketide nature with a phenylalanine-derived starter unit [45].

Table 1: Summary of antiSMASH analysis (version 3.0.4) of the four available genomes of myxobacteria of the suborder Nannocystineae.

	halophilic/halotolerant			terrestrial
	Enhygromyxa salina DSM 15201	*Plesiocystis pacifica* SIR 1	*Haliangium ochraceum* DSM 14365	*Nannocystis exedens* ATCC 25963
genome size (Mb)	10.44	10.59	9.45	11.61
GC %	67.4	70.7	69.5	72.2
number of contigs	330	237	1	174
% of genome involved in secondary metabolism[a]	9.2	6.4	10.1	8.2
total number of clusters	38	28	25	31
NRPS	2	1	3	1
PKS (including PKS hybrids)	13	11	2	2
NRPS/PKS hybrids	2	0	3	6
terpene	7	6	3	10
bacteriocin	6	6	5	3
ribosomal peptides	0	0	4	1
siderophore	2	1	0	2
indole	1	0	0	0
arylpolyene	2	1	0	2
phenazine	0	0	0	2
ectoine	0	0	1	0
other	3	2	4	2

[a]Total bases of all detected antiSMASH secondary metabolite gene clusters divided by number of bases in the genome.

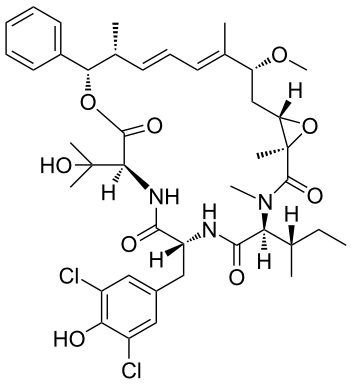

Figure 6: Structure of nannocystin A.

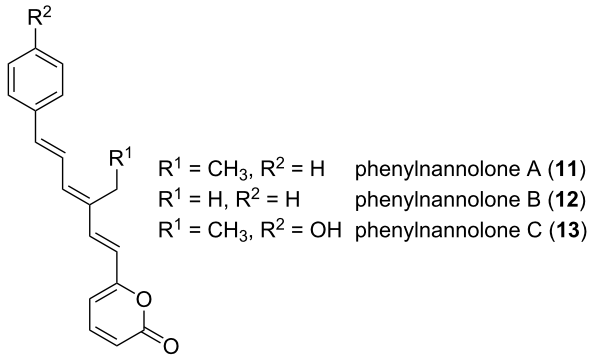

Figure 7: Structure of phenylnannolones A–C.

These compounds are synthesized by *N. exedens* strain 150, later reassigned to *N. pusilla,* isolated from the intertidal region of a beach in Crete [45]. Cultivation of the regarding organism was carried out in liquid medium with addition of adsorber resin. The adsorbed metabolites were then extracted and isolated via different chromatographic techniques. Phenylnannolone A (**11**) was found to be the main metabolite, which is accompanied by only minute amounts of the other derivatives **12** and **13**. Phenylnannolone A was proven to restore daunorubicin sensitivity in cancer cells by inhibiting P-glycoprotein (P-gp), an ATP-binding cassette transporter (ABC transporter). In tumor cells, P-gp serves as an efflux transporter of drugs, ultimately leading to treatment failure [46].

Apart from these polyketides, an array of nitrogen-containing metabolites was published recently by Jansen et al. [47]. They investigated three strains of *N. pusilla* isolated from coastal sediment samples – deemed halotolerant for this reason – for their secondary metabolite production. Two strains, Ari7 and Na a174 yielded a new class of halogenated pyrrole–oxazole compounds **14–18** (Figure 8). Pyrronazols A (**14**), A2 (**15**) and

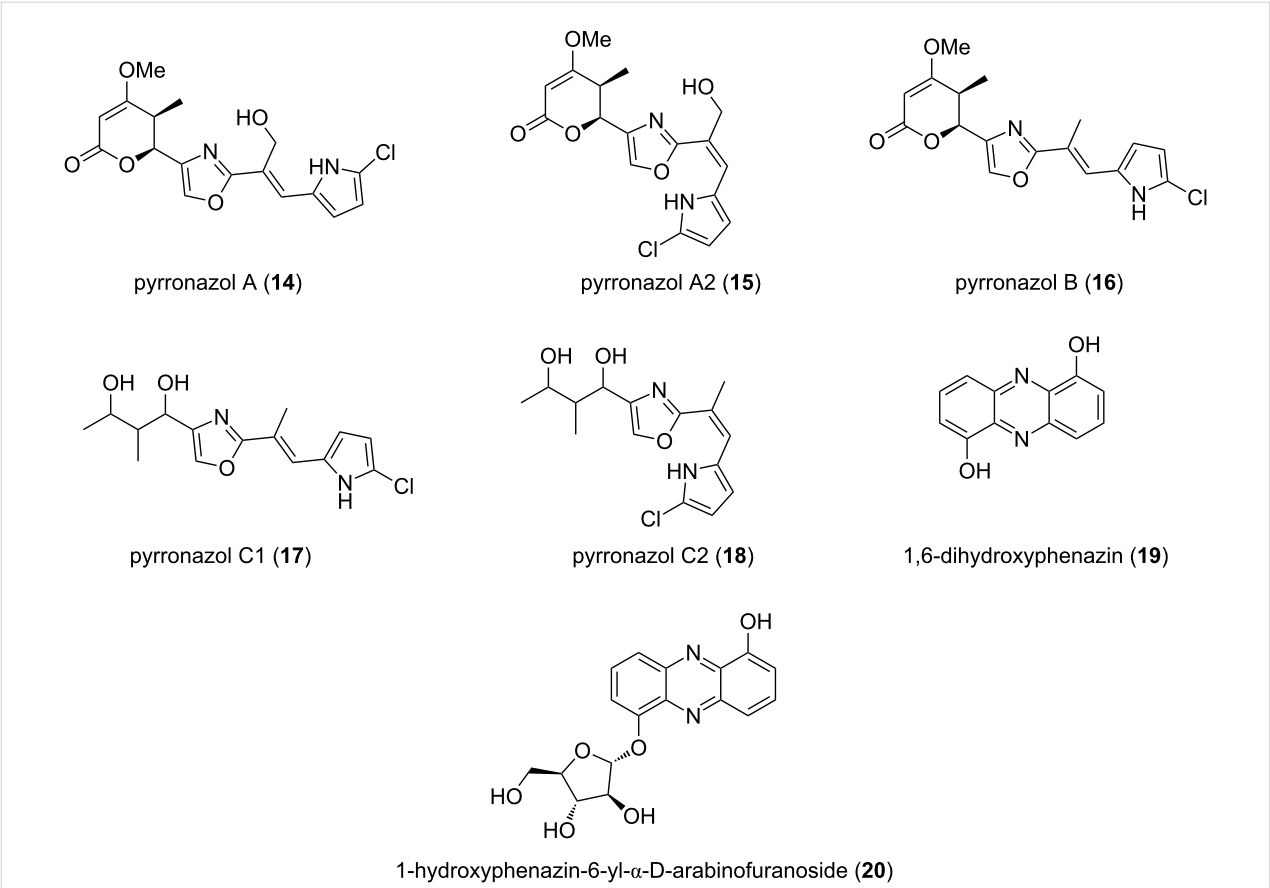

Figure 8: Structures of the pyrronazols, dihydroxyphenazin and 1-hydroxyphenazin-6-yl-α-D-arabinofuranoside.

B (**16**), synthesized by Ari7, additionally include an α-pyrone moiety [48].

This is worth noting, since the non-cyclic alkyl moiety in the pyrronazols C1 (**17**) and C2 (**18**), found in strain Na a174, is supposed to be a result of degradation processes due to long-time cultivation. Additionally, the known compound 1,6-dihydroxyphenazin (**19**) and its arabinofuranoside **20** were obtained.

To date, **14** has shown marginal antifungal activity towards *Mucor hiemalis* (DSM 2656, MIC: 33.3 µg/mL) and **19** proved to have cytotoxic effects in the lower micromolar range against different cancer cell lines [47].

Nannozinones A (**21**) and B (**22**, Figure 9) are produced by *N. pusilla* strain MNa10913, isolated from a soil sample, collected in Mallorca, Spain [49]. They represent novel pyrazinone type molecules. Additionally, the siderophore nannochelin A (**23**) also from other myxobacteria was isolated [50].

All three compounds were tested against a broad range of microorganisms and mammalian cell lines. The most relevant

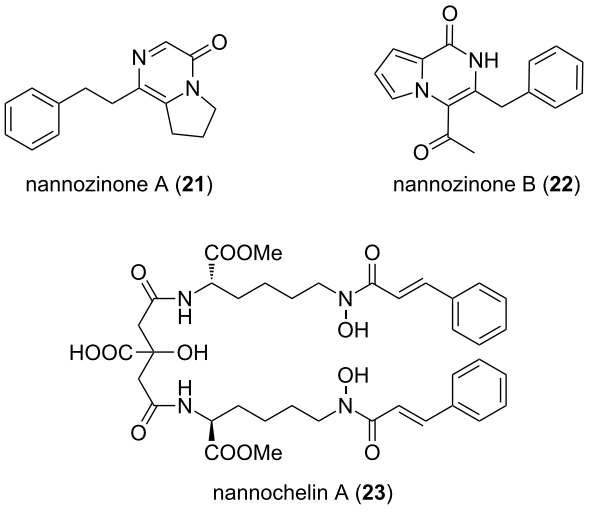

Figure 9: Structures of nannozinones A + B and nannochelin A from *N. pusilla* strain MNa10913.

antimicrobial activity was shown by **21** towards *Mycobacterium diernhoferi* (DSM 43542), *Candida albicans* (DSM 1665) and *Mucor hiemalis* (DSM 2656, 33.3 µg mL^{-1} in each

case). Significant cytotoxic activity was revealed for **22** towards SKOV-3 (IC_{50} = 2.4 μM), KB3-1 (IC_{50} = 5.3 μM), as well as A431 (IC_{50} = 8.45 μM), while **23** showed remarkable cytotoxicity against cell lines HUVEC and KB3-1 (IC_{50} = 50 nM).

So far, no genome sequence is publicly available for halotolerant strains of this genus. The only sequence found in the databases belongs to the terrestrial *N. exedens* ATCC 25963 (see Table 1). Remarkably, this genome encodes, among a considerable number of NRPS/PKS hybrids, 10 different terpene biosynthesis gene clusters.

The genus *Haliangium*

Haliangium ochraceum sp. nov. (initially termed *H. luteum*, DSM 14365^T) and *H. tepidum* sp. nov. (DSM 14436^T) were isolated from seaweed and sea grass, respectively, with both samples being obtained from a sandy beach in Miura, Japan by Fudou et al. in 2002 [12]. The species were proposed to be of true marine origin according to their salt requirement for growth. Indeed, 2 to 3% NaCl (w/v) and a pH of 7.5 are optimal for growth on yeast medium with artificial seawater solution. These conditions were established for routine isolation and cultivation. One particular feature worth mentioning is that the species have rather different optimal growth temperature intervals: 30–34 °C for *H. ochraceum* and 37–40 °C for *H. tepidum*. According to the original report, both strains share 95.5% of 16S rDNA sequence identity and have the terrestrial *Kofleria flava* (DSM 14601) as their closest relative (16S rDNA sequence identity lower than 95%). The GC content of *H. ochraceum* and *H. tepidum* is 67 and 69 mol %, respectively.

H. ochraceum was found by Fudou et al. [51] to be a producer of secondary metabolites with antibacterial and antifungal activities. Further investigation led to the isolation and structure elucidation of the bioactive polyketide haliangicin (**24**, Figure 10), which was the first myxobacterial metabolite of true marine origin.

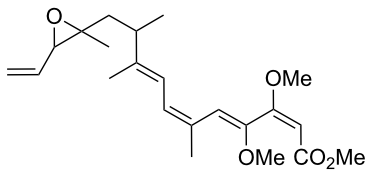

haliangicin (**24**)

Figure 10: Structure of haliangicin from *H. ochraceum*.

It was found that this molecule comprised a β-methoxyacrylate subunit including a conjugated tetraene moiety [52]. The complete structure was elucidated via 2D NMR techniques, while NOESY correlations were used to study the configuration of the double bonds. However, the configuration at the epoxide bearing carbon atoms could not be resolved at that time. In further work, Kundim et al. [53] published three new haliangicin stereoisomers, which differed in the configuration of the three terminal double bonds in the tetraene moiety. Each of the isomers haliangicin, haliangicin B, haliangicin C and haliangicin D happened to be present with two different configurations around the epoxy group. The NOESY spectra showed correlations for the *cis*- and *trans*-configuration. However, the absolute configuration of the chiral centers could not be resolved yet. Moreover, the origin of the different isomers is not clear. Due to their alleged instability upon exposure to air and light, one could speculate that isomerization occurs during the purification process. Interestingly, the authors found a NaCl-dependent production of haliangicin [51]. The optimal production range is at 2–3% NaCl (w/v) in the medium, which is the same range as for optimal growth. Haliangicin showed activity against some fungal organisms, e.g., *Aspergillus niger* (AJ117374, MIC: 12.5 μg mL^{-1}) and *Fusarium* sp. (AJ177167, MIC: 6.3 μg mL^{-1}). These MIC values were in a similar range as those of known antifungal compounds such as amphotericin B or nystatin against the same fungi (MIC: 3.1 μg mL^{-1} for both compounds).

Recently, the 9.4 Mb genome of *H. ochraceum* (DSM 14365^T) was completely sequenced and published [54]. This was the first marine-derived myxobacterium to have its genome fully determined. We performed an antiSMASH analysis on the genome of *H. ochraceum* (DSM 14365^T, INSDC: CP001804.1). The results revealed the presence of 25 secondary metabolite gene clusters, among them three NRPS, two PKS, three NRPS/PKS and four ribosomal peptides (see Table 1). Apart from homologies to geosmin (100%), aurafuron (71%) and paneibactin (50%) biosynthetic genes, the gene clusters display a large degree of novelty. Recently, the biosynthetic gene cluster of haliangicin was heterologously expressed in *Myxococcus xanthus*, leading to tenfold higher haliangicin production than in the native producer. Insights into its biosynthesis were gained by feeding studies with labeled precursors and in vitro experiments. Additionally, unnatural haliangicin analogues that provided insights into the structure–activity relationship of haliangicin were generated in this study [55]. The huge potential to synthesize novel metabolites in the genus *Haliangium* is further corroborated by a PCR screening-based study for PKS sequences in *H. tepidum* among other myxobacteria [56]. The authors found *H. tepidum* to contain the highest amount of novel PKS sequences in this array. Additionally, the indications at the genetic level are reinforced by the very recent discovery of a new compound produced by *H. ochraceum* SMP-2, i.e., haliamide (**25**, Figure 11). The authors also

describe the corresponding hybrid PKS-NRPS machinery responsible for metabolite biosynthesis [57]. The molecule was shown to have cytotoxic effects towards HeLa-S3 cells (IC_{50} = 12 μM).

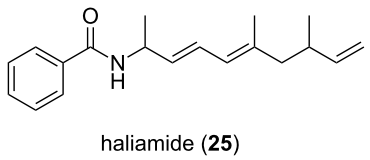

haliamide (**25**)

Figure 11: Structure of haliamide from *H. ochraceum* SMP-2.

The genus *Enhygromyxa*

All *Enhygromyxa* species isolated to date are halophilic and considered as truly marine myxobacteria. The initial report on isolation, characterization and taxonomic classification of six strains of *E. salina,* SHK-1^T, SMK-1-1, SMK-1-3, SMK-10, SKK-2, and SMP-6, was published in 2003 by Iizuka et al. [14]. These organisms were obtained respectively from mud, sand and algal samples collected in marine environments around Japan. Later, four additional strains of *E. salina* were isolated by the group of König from marine-intertidal sediment samples collected at the West Coast of the USA, at German coasts and the Netherlands [58,59]. As judged from these varied geographical occurrences a world-wide distribution of *Enhygromyxa* species is likely.

The prior mentioned groups reported 1–2% NaCl (w/v) and a pH interval of 7.0–8.5 for optimal growth on yeast medium. The optimal temperature for growth was determined as 28–30 °C. In terms of gliding motility, fruiting body and myxospore formation, these bacteria show the typical features of terrestrial myxobacteria. A salt-dependency and high G + C content ranging from 65.6 to 67.4 mol % [14] and 63.0 to 67.3 mol % [59] were also observed. Based on 16S rDNA sequence alignments, *E. salina* SHK-1^T (NR_024807) from Iizuka [14] was found to be most closely related to the *E. salina* strains from the König group [59]. The 16SrDNA sequences of these strains share between 98% (SWB004, AN: HM769727) and 99% (SWB005, AN: HM769728; SWB006, AN: HM769729; SWB007, AN: KC818422) identity.

Some of the bacterial isolates were originally evaluated for their ability to produce PKS-type metabolites and for the biosynthesis of antimicrobials [59]. In these studies, PKS genes could be amplified, sequenced and compared with known sequences in the BLAST database. The potential of producing active molecules was established by using disc diffusion antibiotic activity testing of the bacterial extracts, whereby an inhibitory effect of the extracts of *E. salina* SWB005 on various test organisms, including the clinically relevant MRSA (methicillin resistant *Staphylococcus aureus*) strains LT1334, LT1338 and MRSE methicillin resistant *Staphylococcus epidermidis strain* LT1324 was observed [59].

To date, five structures of putative polyketide, shikimate and terpenoid origin have been described and classified as salimabromide (**26**, Figure 12) [58], produced by *E. salina* SWB007, enhygrolides **27** and **28** and salimyxins **29** and **30** produced by *E. salina* SWB005 [60].

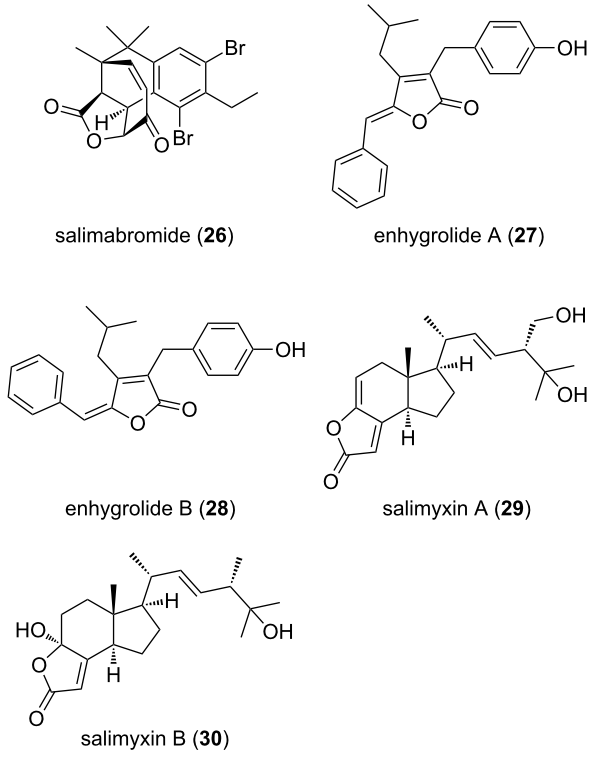

salimabromide (**26**) enhygrolide A (**27**)

enhygrolide B (**28**) salimyxin A (**29**)

salimyxin B (**30**)

Figure 12: Structures of salimabromide, enhygrolides A + B and salimyxins A + B.

Salimabromide (**26**) is particularly interesting due to its unique halogenated tetracyclic core structure. Its biosynthesis is postulated to be carried out by a type III-PKS. Pure PKS-derived compounds are rare in myxobacteria, which together with the new carbon skeleton and the high bromination level makes this structure even more fascinating. Structure elucidation was achieved via extensive NMR measurements. The absolute configuration of the chiral centers could be resolved through comparison of the experimental CD spectrum with calculated data. This metabolite showed inhibitory activity towards the bacterium *Arthrobacter crystallopoietes* with an MIC value of 16 μg mL^{-1}. Further bioactivity assays were impossible to carry

out due to the minute amounts in which this metabolite is produced. Consequently, a synthetic approach has been utilized in order to overcome this problem, leading so far to the synthesis of the tricyclic core structure of the molecule. However, the complete natural product has not yet been synthesized [61].

The enhygrolide group of compounds comprises enhygrolide A (**27**) and B (**28**). These molecules resemble cyanobacteria-derived metabolites, known as nostoclides and cyanobacterin, which also have a γ-lactone-moiety with a similar substitution pattern. In the myxobacterial metabolites an *E*-configuration was found at the benzylidene unit, whereas the nostoclides and cyanobacterin have a *Z*-configuration. Only the anhydro form of cyanobacterin was found to isomerize from the *Z*- to the *E*-configured isomer in organic solvents upon light exposure [62].

The salimyxins represent the third group of compounds, i.e., salimyxin A (**29**) and B (**30**). These belong to a subgroup of terpenoids named incisterols, which were first discovered from the sponge *Dictyonella incisa* [63]. Their biosynthesis presumably involves oxidative degradation of a sterol, leading to the tricyclic core structure. Compounds **27** and **30** have shown inhibitory activity towards *A. crystallopoietes* (MIC value of 8 and 4 μg mL^{-1}, respectively).

Since salimabromide is a novel structure of putatively assigned PKS origin, our research group sequenced the genome of the producing strain SWB007. The results revealed a PKS III gene cluster adjacent to a halogenase sequence (unpublished data). Upon sequencing, primers for these genes were designed. Given the genetic proximity among the *E. salina* isolates, strains SWB004, SWB005 and SWB006 were screened with the PKS III and halogenase primers specific for the SWB007 sequence revealing the presence of close-to-identical sequences in their genomes (unpublished data), a clear suggestion that similar molecules may be also produced by the related strains.

Bioinformatic analysis was performed by us on the available genome of *E. salina* (DSM 15201, INSDC: JMCC00000000.2) of which as to date, no reports on the isolation of compounds are available. However, the screening with antiSMASH revealed an ample amount of uncharacterized biosynthetic gene clusters, among them 17 gene clusters putatively responsible for the synthesis of NRPS, PKS and hybrid NRPS-PKS products (see Table 1). Apart from the geosmin biosynthesis genes, no gene cluster or fragment thereof shares an identity higher than 33% to any known gene cluster in the MiBIG database [64]. It should be noted that since this is a draft genome sequence, the actual amount of gene clusters might be slightly smaller, since small contigs display only fragments of gene clusters.

The genus *Plesiocystis*

In 2003 Iizuka et al. [13] proposed the genus and the species *Plesiocystis pacifica* for the myxobacterial strains SHI-1 (JCM 11592, DSM 14876) and SIR-1^T (JCM 11591^T, DSM 14875T). SHI-1 was retrieved from a sand sample of a Japanese coastal area, whilst strain SIR-1^T was isolated from a piece of dried marine grass (*Zostera* sp.). These strains require 2–3% NaCl (w/v) and a pH of 7.4 for optimal growth on yeast medium with artificial seawater solution at 28 °C.

According to Iizuka et al. [13] the isolates are closely related, sharing 99.5% 16S rDNA sequence identity between them. Their closest relative was reported to be *Nannocystis exedens* DSM 71T, with 89.3% sequence identity to SIR-1T and 89.4% to SHI-1. Regarding GC content, SIR-1T and SHI-1 were reported to have 69.3 and 70.0 mol %, respectively. Such a high GC content is a distinctive trait of all myxobacteria. To date, no reports on biological testing of extracts or of any metabolites isolated from these organisms have been published.

The antiSMASH analysis was performed on the available draft genome of *P. pacifica* strain SIR-1 (INSDC: ABCS00000000.1). The analysis revealed the presence of 12 NRPS, PKS and hybrid NRPS-PKS gene clusters amongst many others (see Table 1), which should encourage researchers to isolate some of the predicted metabolites. Here, no gene clusters sharing more than 28% identity to pathways of characterized molecules were detected. Again, many of the PKS and NRPS gene cluster appear to be fragmented to smaller contigs.

Myxobacterium SMH-27-4 (*Paraliomyxa miuraensis*)

In 2006, as a result of the remarkable efforts of Iizuka et al. [65] a novel myxobacterium was isolated from a soil sample of a seashore area in Miura, Japan. After genetic analysis, the new isolate was classified as strain SMH-27-4, tentatively named *Paraliomyxa miuraensis*. This strain is considered slightly halophilic.

Yeast medium with only a low sea salt concentration was selected for isolation, whereas cultivation in NaBr-containing medium was selected for antibiotic production. The diminished strength of salinity in the medium implies an optimal salt range concentration for growth of 0.5–1% (w/v), at pH 7.2 and a temperature of 27 °C. Fermentation and the production of antibiotic compounds were performed at 27 °C at pH 7.3.

Surprisingly, the authors do not report fruiting body formation during the cultivation of myxobacterium SMH-27-4, which usually is a hallmark feature of myxobacteria. Phylogenetic analyses carried out by Iizuka et al. [65] revealed that this or-

ganism shares 93.0% identity with *Nannocystis exedens* DSM 71^T (AB084253), 93.2 to 93.3% with *Enhygromyxa salina* JCM 11769^T (AB097590), and 91.3 to 91.5% with *Plesiocystis pacifica* JCM 11591^T (AB083432). No information on the GC content of the bacterial genome has been found.

Myxobacterium SMH-27-4 (AN: AB252740) was investigated for the production of secondary metabolites [65]. This work led to the isolation and structure elucidation of two compounds of peptidic nature called miuraenamide A (**31**) and B (**32**, Figure 13). Two years later, the same research group published the structures of four additional derivatives, named miuraenamides C–F (**33–36**) [66].

The cyclic core structure of this compound class represents a halogenated depsipeptide with an additional polyketide-derived moiety. As in haliangicin, all miuraenamides, except E, contain a methoxyacrylate structural motif, which surely is important for the biological activity. For miuraenamide A (**31**) the absolute configuration was determined. Marfey´s method was employed to show that L-alanine and *N*-methyl-D-tyrosine are present. Furthermore, after acid hydrolysis, methylation and application of modified Mosher´s method the absolute configuration at the oxygen bearing C-9 was deduced as *S*. For miuraenamide F (**36**) the configuration at C-3 was found to be *R*, again using Mosher's method. For all the other chiral centers in compounds **32–36** the authors conclude that they have the same configuration as determined for **31**. Further work led to semisynthetic derivatives, which upon activity testing, revealed that the lactone moiety and the configuration of the methoxyacrylate partial structure are crucial for antifungal activity. The latter structural motif is well known from a range of antifungal compounds produced by fungi and myxobacteria, e.g., the strobilurins and the melithiazols [67,68].

Miuraenamide A (**31**) was assayed against various fungal, yeast and bacterial organisms. It showed a remarkable inhibitory effect toward the fungal phytopathogen *Phytophthora capsici* NBRC 8386 (MIC: 0.4 mg mL^{-1}) and *Candida rugosa* AJ 14513 (MIC: 12.5 mg mL^{-1}). No inhibitory effect on selected bacteria was detected. The mode of action is proposed to be similar to other antifungals with a methoxyacrylate partial structure, i.e., inhibition of the mitochondrial cytochrome bc1 complex. Additionally, miuraenamide A was shown to act as actin filament stabilizer in HeLa cells [69]. The activity of miuraenamide B (**32**) was not assessed due to the minute amounts of the metabolite available.

To date, there is no genome sequence available for this organism.

The genus *Pseudenhygromyxa*

Pseudenhygromyxa salsuginis is the latest example of a halotolerant myxobacterium, published in 2013 by Iizuka et al. [70]. This organism was retrieved from mud samples of an estuarine marsh in a coastal area in Japan and termed SYR-2^T. Even though it is able to grow in the absence of salt, optimal growth was shown to occur within a concentration range of 0.2–1.0% NaCl (w/v) and pH values from 7.0–7.5 on CY-S agar (bacto casitone, bacto yeast extract) in a temperature range of

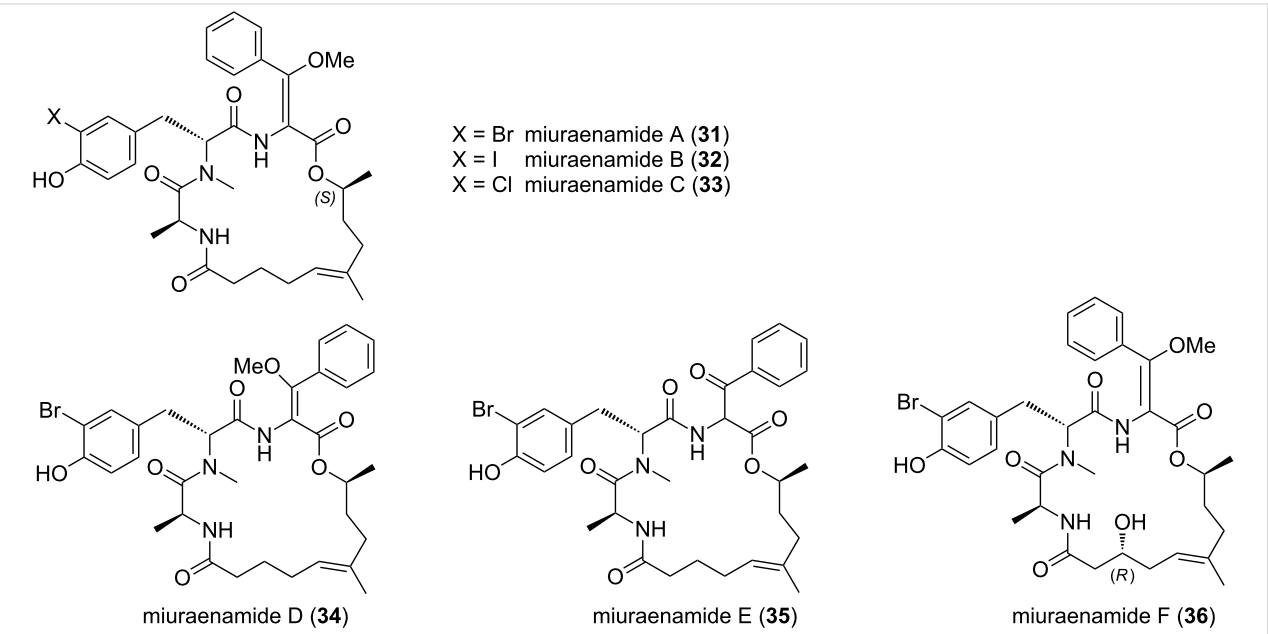

Figure 13: Structures of miuraenamides A–F from *P. miuraensis*.

30–35 °C. After alignment of 16S rDNA sequences, Iizuka et al. [70] found that *P. salsuginis* SYR-2^T showed 96.5% and 96.0% identity to *Enhygromyxa salina* SHK-1^T (NR_024807) and *Plesiocystis pacifica* SIR-1^T (NR_024795), respectively. The G + C content is 69.7 mol %, and thus slightly higher than for various *E. salina* strains described above.

To date, no reports on biological activities or any metabolites derived from *P. salsuginis* have been published. Nevertheless, the genetic proximity to *E. salina* and the fact that it belongs to the group of myxobacteria suggests that this organism may also possess a high potential as a producer of active molecules. To date no genome sequence has been published.

Conclusion

Geographically, halophilic and halotolerant myxobacteria are widely distributed as evidenced by some of the above described bacterial isolates, originating, e.g., from German, Japanese and US American marine environments. This observation is supported by the investigation of myxobacteria-enriched libraries of 16S rRNA gene sequences revealing myxobacteria-related sequences in mud samples taken around Japan. The latter sequences were phylogeographically clearly distinct from those of terrestrial myxobacteria [71]. A further report also states that myxobacteria capable of thriving in ocean-like conditions exhibit a worldwide distribution [72].

The quantitative presence of myxobacteria in marine environments can hardly be judged. Based on the isolation success one may suggest that the frequency is much lower (e.g., only 6 isolates from 90 coastal samples [12,14]) than in terrestrial habitats, but this may simply represent the less than perfect isolation and cultivation conditions used today. Indeed, the currently applied isolation protocols for marine myxobacteria are only slightly altered in terms of the addition of sea salt, when compared to those for terrestrial strains, e.g., terrestrial

Table 2: Metabolites reported to date from myxobacteria grouped into the suborder Nannocystineae and their bioactivities.

genus	classification according to salt requirements for growth	metabolites	metabolite [No] bioactivity
Nannocystis	terrestrial	nannocystin A (**10**)	**10** antiproliferative activity, MDA-MB231 and its related drug resistant MDA-A1 (IC_{50} = 6.5 and 12 nM respectively), HCT116 (IC_{50} = 1.2 nM) and PC3 (IC_{50} = 1.0 nM)
	halotolerant	phenylnannolone A, B, C (**11**–**13**), pyrronazol A, A2, B, C1, C2 (**14**–**18**), nannozinone A, B (**21**, **22**), nannochelin A (**23**)	**11** reversing drug-resistance of tumor cells **21** *Mycobacterium diernhoferi*, *Candida albicans*, *Mucor hiemalis*, MICs: 33.3 µg mL^{-1} in each case **22** cytotoxicity, SKOV-3 IC_{50} = 2.4 µM, KB3-1 IC_{50} = 5.3 µM and A431 IC_{50} = 8.45 µM **23** cytotoxicity, HUVEC and KB3-1 IC_{50} = 50 nM
Haliangium	moderately halophilic	haliangicin (**24**) haliamide (**25**)	**24** *Aspergillus niger*, MIC: 12.5 µg mL^{-1}, *Phytophthora capsici,* MIC: 0.4 µg mL^{-1}; **25** Cytotoxicity, HeLa-S3, IC_{50} 12 µM
Enhygromyxa	halophilic	salimabromide (**26**) enhygrolide A, B (**27**, **28**) salimyxin A, B (**29**, **30**)	**26**, **27**, **30** *Arthrobacter crystallopoietes*, MICs: 16, 8 and 4 µg mL^{-1}, respectively
Myxobacterium SMH-27-4 (*Paraliomyxa*)	slightly halophilic	miuraenamide A–F (**31**–**36**)	**31** *Trichophyton mentagrophytes*, MIC: 12.5 µg mL^{-1}
Plesiocystis	halophilic	no metabolites described	–
Pseudenhygromyxa	halotolerant	no metabolites described	–

Escherichia coli is still used as prey. In addition, it surely is difficult to recognize marine myxobacterial colonies after isolation, since their morphological features may deviate from the ones of terrestrial strains and are not well known. Thus, in order to use marine-derived myxobacteria as a source of bioactive metabolites, in-depth studies of their morphology and physiology are necessary.

From the available genetic and chemical data, the potential of halotolerant and halophilic myxobacteria as producers of chemically diverse secondary metabolites is out of question. Salimabromide (**26**) from *E. salina* is an outstanding example of such a molecule having a most unusual new carbon skeleton [58]. The number of molecules obtained so far however is very low (Table 2), especially when compared with the expected metabolites envisioned after bioinformatic analysis of the four available genomes of myxobacteria in the suborder Nannocystineae. All strains harbor at least 25 biosynthetic gene clusters (Table 1), most of them bearing no or very little homology to known biosynthetic genes. Compared to *Myxococcus xanthus* DK1622, the so far sequenced strains dedicate a similar or even larger portion of their genome of up to 10% to secondary metabolism.

These “cryptic” or “silent” gene clusters may be addressed with different strategies [73], e.g., the OSMAC (one strain, many compounds) approach [74] or co-culturing and elicitation techniques [75-77]. Mass spectrometric analysis [78-81], dereplication procedures [35,79], bioinformatic analysis and genetic experiments allow a direct connection of metabolites and gene clusters [33,34,80]. On the other hand, recent advances in the direct cloning of gene clusters and their heterologous expression [82-85] may enable researchers to select their “favorite” gene cluster and express and manipulate it in heterologous hosts for rational secondary metabolite discovery. These techniques offer the chance for an effective metabolomics-guided natural product and genome mining platform.

In conclusion, the application of these promising state-of-the-art approaches to marine myxobacteria should expand our knowledge on novel secondary metabolites in these organisms, and help to systematically unveil the chemistry encoded in their genomes.

Supporting Information

Supporting Information File 1

List of 16S rDNA sequences used for Figure 5.
[http://www.beilstein-journals.org/bjoc/content/supplementary/1860-5397-12-96-S1.pdf]

Acknowledgements

This work was supported by scholarships from the Mexican Council of Science and Technology (CONACyT), the Mexican Secretary of Foreign Affairs (SRE) and the German Academic Exchange Service (DAAD). The authors hold the copyright of the pictures shown in the graphical abstract.

References

1. Han, K.; Li, Z.-f.; Peng, R.; Zhu, L.-p.; Zhou, T.; Wang, L.-g.; Li, S.-g.; Zhang, X.-b.; Hu, W.; Wu, Z.-h.; Qin, N.; Li, Y.-z. *Sci. Rep.* **2013,** *3,* 2101. doi:10.1038/srep02101
2. Reichenbach, H. *Environ. Microbiol.* **1999,** *1,* 15–21. doi:10.1046/j.1462-2920.1999.00016.x
3. Cao, P.; Dey, A.; Vassallo, C. N.; Wall, D. *J. Mol. Biol.* **2015,** *427,* 3709–3721. doi:10.1016/j.jmb.2015.07.022
4. Reichenbach, H. Myxobacteria: A Most Peculiar Group of Social Prokaryotes. In *Myxobacteria;* Rosenberg, E., Ed.; Springer Series in Molecular Biology; Springer: New York, NY, 1984; pp 1–50. doi:10.1007/978-1-4613-8280-5_1
5. Sanford, R. A.; Cole, J. R.; Tiedje, J. M. *Appl. Environ. Microbiol.* **2002,** *68,* 893–900. doi:10.1128/AEM.68.2.893-900.2002
6. Rosenberg, E. *Myxobacteria. Development and Cell Interactions;* Springer Series in Molecular Biology; Springer: New York, NY, 1984. doi:10.1007/978-1-4613-8280-5
7. Dworkin, M. *Microbiol. Rev.* **1996,** *60,* 70–102.
8. Zhang, Y.-Q.; Li, Y.-z.; Wang, B.; Wu, Z.-h.; Zhang, C.-Y.; Gong, X.; Qiu, Z.-J.; Zhang, Y. *Appl. Environ. Microbiol.* **2005,** *71,* 3331–3336. doi:10.1128/AEM.71.6.3331-3336.2005
9. Wang, B.; Hu, W.; Liu, H.; Zhang, C.-Y.; Zhao, J.-y.; Jiang, D.-m.; Wu, Z.-h.; Li, Y.-z. *Microb. Ecol.* **2007,** *54,* 43–51. doi:10.1007/s00248-006-9169-y
10. Pan, H.-w.; Tan, Z.-g.; Liu, H.; Li, Z.-f.; Zhang, C.-Y.; Li, C.-y.; Li, J.; Li, Y.-z. *ISME J.* **2010,** *4,* 1282–1289. doi:10.1038/ismej.2010.52
11. Li, Y.-Z.; Hu, W.; Zhang, Y.-Q.; Qiu, Z.-j.; Zhang, Y.; Wu, B.-H. *J. Microbiol. Methods* **2002,** *50,* 205–209. doi:10.1016/S0167-7012(02)00029-5
12. Fudou, R.; Jojima, Y.; Iizuka, T.; Yamanaka, S. *J. Gen. Appl. Microbiol.* **2002,** *48,* 109–115. doi:10.2323/jgam.48.109
13. Iizuka, T.; Jojima, Y.; Fudou, R.; Hiraishi, A.; Ahn, J.-W.; Yamanaka, S. *Int. J. Syst. Evol. Microbiol.* **2003,** *53,* 189–195. doi:10.1099/ijs.0.02418-0
14. Iizuka, T.; Jojima, Y.; Fudou, R.; Tokura, M.; Hiraishi, A.; Yamanaka, S. *Syst. Appl. Microbiol.* **2003,** *26,* 189–196. doi:10.1078/072320203322346038
15. Iizuka, T.; Jojima, Y.; Fudou, R.; Yamanaka, S. *FEMS Microbiol. Lett.* **1998,** *169,* 317–322. doi:10.1016/S0378-1097(98)00473-X
16. Kimura, Y.; Kawasaki, S.; Yoshimoto, H.; Takegawa, K. *J. Bacteriol.* **2010,** *192,* 1467–1470. doi:10.1128/JB.01118-09
17. Moghaddam, J. A.; Boehringer, N.; Burdziak, A.; Kunte, H.-J.; Galinski, E. A.; Schäberle, T. F. *Microbiology (London, U. K.)* **2016,** *162,* 651–661. doi:10.1099/mic.0.000250
18. Sleator, R. D.; Hill, C. *FEMS Microbiol. Rev.* **2002,** *26,* 49–71. doi:10.1111/j.1574-6976.2002.tb00598.x
19. Still, P. C.; Johnson, T. A.; Theodore, C. M.; Loveridge, S. T.; Crews, P. *J. Nat. Prod.* **2014,** *77,* 690–702. doi:10.1021/np500041x
20. Wenzel, S. C.; Müller, R. *Curr. Opin. Drug Discovery Dev.* **2009,** *12,* 220–230.

21. Schäberle, T. F.; Lohr, F.; Schmitz, A.; König, G. M. *Nat. Prod. Rep.* **2014,** *31,* 953–972. doi:10.1039/c4np00011k
22. Weissman, K. J.; Müller, R. *Bioorg. Med. Chem.* **2009,** *17,* 2121–2136. doi:10.1016/j.bmc.2008.11.025
23. Weissman, K. J.; Müller, R. *Nat. Prod. Rep.* **2010,** *27,* 1276–1295. doi:10.1039/c001260m
24. Baumann, S.; Herrmann, J.; Raju, R.; Steinmetz, H.; Mohr, K. I.; Hüttel, S.; Harmrolfs, K.; Stadler, M.; Müller, R. *Angew. Chem., Int. Ed.* **2014,** *53,* 14605–14609. doi:10.1002/anie.201409964
25. Frank, B.; Wenzel, S. C.; Bode, H. B.; Scharfe, M.; Blöcker, H.; Müller, R. *J. Mol. Biol.* **2007,** *374,* 24–38. doi:10.1016/j.jmb.2007.09.015
26. Erol, Ö.; Schäberle, T. F.; Schmitz, A.; Rachid, S.; Gurgui, C.; El Omari, M.; Lohr, F.; Kehraus, S.; Piel, J.; Müller, R.; König, G. M. *ChemBioChem* **2010,** *11,* 1253–1265. doi:10.1002/cbic.201000085
27. Schieferdecker, S.; König, S.; Koeberle, A.; Dahse, H.-M.; Werz, O.; Nett, M. *J. Nat. Prod.* **2015,** *78,* 335–338. doi:10.1021/np500909b
28. Xiao, Y.; Wei, X.; Ebright, R.; Wall, D. *J. Bacteriol.* **2011,** *193,* 4626–4633. doi:10.1128/JB.05052-11
29. Thomas, E.; Tabernero, J.; Fornier, M.; Conté, P.; Fumoleau, P.; Lluch, A.; Vahdat, L. T.; Bunnell, C. A.; Burris, H. A.; Viens, P.; Baselga, J.; Rivera, E.; Guarneri, V.; Poulart, V.; Klimovsky, J.; Lebwohl, D.; Martin, M. *J. Clin. Oncol.* **2007,** *25,* 3399–3406. doi:10.1200/JCO.2006.08.9102
30. Thomas, E. S.; Gomez, H. L.; Li, R. K.; Chung, H.-C.; Fein, L. E.; Chan, V. F.; Jassem, J.; Pivot, X. B.; Klimovsky, J. V.; de Mendoza, F. H.; Xu, B.; Campone, M.; Lerzo, G. L.; Peck, R. A.; Mukhopadhyay, P.; Vahdat, L. T.; Roché, H. H. *J. Clin. Oncol.* **2007,** *25,* 5210–5217. doi:10.1200/JCO.2007.12.6557
31. Hunt, J. T. *Mol. Cancer Ther.* **2009,** *8,* 275–281. doi:10.1158/1535-7163.MCT-08-0999
32. Smaglo, B. G.; Pishvaian, M. J. *Drug Des., Dev. Ther.* **2014,** *8,* 923–930. doi:10.2147/DDDT.S52964
33. Kersten, R. D.; Yang, Y.-L.; Xu, Y.; Cimermancic, P.; Nam, S.-J.; Fenical, W.; Fischbach, M. A.; Moore, B. S.; Dorrestein, P. C. *Nat. Chem. Biol.* **2011,** *7,* 794–802. doi:10.1038/nchembio.684
34. Kersten, R. D.; Ziemert, N.; Gonzalez, D. J.; Duggan, B. M.; Nizet, V.; Dorrestein, P. C.; Moore, B. S. *Proc. Natl. Acad. Sci. U. S. A.* **2013,** *110,* E4407–E4416. doi:10.1073/pnas.1315492110
35. Nguyen, D. D.; Wu, C.-H.; Moree, W. J.; Lamsa, A.; Medema, M. H.; Zhao, X.; Gavilan, R. G.; Aparicio, M.; Atencio, L.; Jackson, C.; Ballesteros, J.; Sanchez, J.; Watrous, J. D.; Phelan, V. V.; van de Wiel, C.; Kersten, R. D.; Mehnaz, S.; de Mot, R.; Shank, E. A.; Charusanti, P.; Nagarajan, H.; Duggan, B. M.; Moore, B. S.; Bandeira, N.; Palsson, B. Ø.; Pogliano, K.; Gutiérrez, M.; Dorrestein, P. C. *Proc. Natl. Acad. Sci. U. S. A.* **2013,** *110,* E2611–E2620. doi:10.1073/pnas.1303471110
36. Goldman, B. S.; Nierman, W. C.; Kaiser, D.; Slater, S. C.; Durkin, A. S.; Eisen, J. A.; Ronning, C. M.; Barbazuk, W. B.; Blanchard, M.; Field, C.; Halling, C.; Hinkle, G.; Iartchuk, O.; Kim, H. S.; Mackenzie, C.; Madupu, R.; Miller, N.; Shvartsbeyn, A.; Sullivan, S. A.; Vaudin, M.; Wiegand, R.; Kaplan, H. B. *Proc. Natl. Acad. Sci. U. S. A.* **2006,** *103,* 15200–15205. doi:10.1073/pnas.0607335103
37. Krug, D.; Zurek, G.; Revermann, O.; Vos, M.; Velicer, G. J.; Müller, R. *Appl. Environ. Microbiol.* **2008,** *74,* 3058–3068. doi:10.1128/AEM.02863-07
38. Li, Z.-F.; Li, X.; Liu, H.; Liu, X.; Han, K.; Wu, Z.-H.; Hu, W.; Li, F.-f.; Li, Y.-Z. *J. Bacteriol.* **2011,** *193,* 5015–5016. doi:10.1128/JB.05516-11
39. Wenzel, S. C.; Gross, F.; Zhang, Y.; Fu, J.; Stewart, A. F.; Müller, R. *Chem. Biol.* **2005,** *12,* 349–356. doi:10.1016/j.chembiol.2004.12.012
40. Cortina, N. S.; Krug, D.; Plaza, A.; Revermann, O.; Müller, R. *Angew. Chem., Int. Ed.* **2012,** *51,* 811–816. doi:10.1002/anie.201106305
41. Weber, T.; Blin, K.; Duddela, S.; Krug, D.; Kim, H. U.; Bruccoleri, R.; Lee, S. Y.; Fischbach, M. A.; Müller, R.; Wohlleben, W.; Breitling, R.; Takano, E.; Medema, M. H. *Nucleic Acids Res.* **2015,** *43,* W237–W243. doi:10.1093/nar/gkv437
42. Korp, J.; Vela Gurovic, M. S.; Nett, M. *Beilstein J. Org. Chem.* **2016,** *12,* 594–607. doi:10.3762/bjoc.12.58
43. Reichenbach, H. *Arch. Microbiol.* **1970,** *70,* 119–138. doi:10.1007/BF00412203
44. Hoffmann, H.; Kogler, H.; Heyse, W.; Matter, H.; Caspers, M.; Schummer, D.; Klemke-Jahn, C.; Bauer, A.; Penarier, G.; Debussche, L.; Brönstrup, M. *Angew. Chem., Int. Ed.* **2015,** *54,* 10145–10148. doi:10.1002/anie.201411377
45. Ohlendorf, B.; Leyers, S.; Krick, A.; Kehraus, S.; Wiese, M.; König, G. M. *ChemBioChem* **2008,** *9,* 2997–3003. doi:10.1002/cbic.200800434
46. Bouhired, S. M.; Crüsemann, M.; Almeida, C.; Weber, T.; Piel, J.; Schäberle, T. F.; König, G. M. *ChemBioChem* **2014,** *15,* 757–765. doi:10.1002/cbic.201300676
47. Jansen, R.; Sood, S.; Huch, V.; Kunze, B.; Stadler, M.; Müller, R. *J. Nat. Prod.* **2014,** *77,* 320–326. doi:10.1021/np400877r
48. Schäberle, T. F. *Beilstein J. Org. Chem.* **2016,** *12,* 571–588. doi:10.3762/bjoc.12.56
49. Jansen, R.; Sood, S.; Mohr, K. I.; Kunze, B.; Irschik, H.; Stadler, M.; Müller, R. *J. Nat. Prod.* **2014,** *77,* 2545–2552. doi:10.1021/np500632c
50. Kunze, B.; Trowitzsch-Kienast, W.; Höfle, G.; Reichenbach, H. *J. Antibiot.* **1992,** *45,* 147–150. doi:10.7164/antibiotics.45.147
51. Fudou, R.; Iizuka, T.; Yamanaka, S. *J. Antibiot.* **2001,** *54,* 149–152. doi:10.7164/antibiotics.54.149
52. Fudou, R.; Iizuka, T.; Sato, S.; Ando, T.; Shimba, N.; Yamanaka, S. *J. Antibiot.* **2001,** *54,* 153–156. doi:10.7164/antibiotics.54.153
53. Kundim, B. A.; Itou, Y.; Sakagami, Y.; Fudou, R.; Iizuka, T.; Yamanaka, S.; Ojika, M. *J. Antibiot.* **2003,** *56,* 630–638. doi:10.7164/antibiotics.56.630
54. Ivanova, N.; Daum, C.; Lang, E.; Abt, B.; Kopitz, M.; Saunders, E.; Lapidus, A.; Lucas, S.; Glavina Del Rio, T.; Nolan, M.; Tice, H.; Copeland, A.; Cheng, J.-F.; Chen, F.; Bruce, D.; Goodwin, L.; Pitluck, S.; Mavromatis, K.; Pati, A.; Mikhailova, N.; Chen, A.; Palaniappan, K.; Land, M.; Hauser, L.; Chang, Y.-J.; Jeffries, C. D.; Detter, J. C.; Brettin, T.; Rohde, M.; Göker, M.; Bristow, J.; Markowitz, V.; Eisen, J. A.; Hugenholtz, P.; Kyrpides, N. C.; Klenk, H.-P. *Stand. Genomic Sci.* **2010,** *2,* 96–106. doi:10.4056/sigs.69.1277
55. Sun, Y.; Feng, Z.; Tomura, T.; Suzuki, A.; Miyano, S.; Tsuge, T.; Mori, H.; Suh, J.-W.; Iizuka, T.; Fudou, R.; Ojika, M. *Sci. Rep.* **2016,** *6,* 22091. doi:10.1038/srep22091
56. Komaki, H.; Fudou, R.; Iizuka, T.; Nakajima, D.; Okazaki, K.; Shibata, D.; Ojika, M.; Harayama, S. *Appl. Environ. Microbiol.* **2008,** *74,* 5571–5574. doi:10.1128/AEM.00224-08
57. Sun, Y.; Tomura, T.; Sato, J.; Iizuka, T.; Fudou, R.; Ojika, M. *Molecules* **2016,** *21,* 59. doi:10.3390/molecules21010059
58. Felder, S.; Dreisigacker, S.; Kehraus, S.; Neu, E.; Bierbaum, G.; Wright, P. R.; Menche, D.; Schäberle, T. F.; König, G. M. *Chemistry* **2013,** *19,* 9319–9324. doi:10.1002/chem.201301379
59. Schäberle, T. F.; Goralski, E.; Neu, E.; Erol, O.; Hölzl, G.; Dörmann, P.; Bierbaum, G.; König, G. M. *Mar. Drugs* **2010,** *8,* 2466–2479. doi:10.3390/md8092466

60. Felder, S.; Kehraus, S.; Neu, E.; Bierbaum, G.; Schäberle, T. F.; König, G. M. *ChemBioChem* **2013,** *14,* 1363–1371. doi:10.1002/cbic.201300268
61. Schmalzbauer, B.; Menche, D. *Org. Lett.* **2015,** *17,* 2956–2959. doi:10.1021/acs.orglett.5b01231
62. Pignatello, J. J.; Porwoll, J.; Carlson, R. E.; Xavier, A.; Gleason, F. K.; Wood, J. M. *J. Org. Chem.* **1983,** *48,* 4035–4038. doi:10.1021/jo00170a032
63. Ciminiello, P.; Fattorusso, E.; Magno, S.; Mangoni, A.; Pansini, M. *J. Am. Chem. Soc.* **1990,** *112,* 3505–3509. doi:10.1021/ja00165a039
64. Medema, M. H.; Kottmann, R.; Yilmaz, P.; Cummings, M.; Biggins, J. B.; Blin, K.; de Bruijn, I.; Chooi, Y. H.; Claesen, J.; Coates, R. C.; Cruz-Morales, P.; Duddela, S.; Düsterhus, S.; Edwards, D. J.; Fewer, D. P.; Garg, N.; Geiger, C.; Gomez-Escribano, J. P.; Greule, A.; Hadjithomas, M.; Haines, A. S.; Helfrich, E. J. N.; Hillwig, M. L.; Ishida, K.; Jones, A. C.; Jones, C. S.; Jungmann, K.; Kegler, C.; Kim, H. U.; Kotter, P.; Krug, D.; Masschelein, J.; Melnik, A. V.; Mantovani, S. M.; Monroe, E. A.; Moore, M.; Moss, N.; Nützmann, H.-W.; Pan, G.; Pati, A.; Petras, D.; Reen, F. J.; Rosconi, F.; Rui, Z.; Tian, Z.; Tobias, N. J.; Tsunematsu, Y.; Wiemann, P.; Wyckoff, E.; Yan, X.; Yim, G.; Yu, F.; Xie, Y.; Aigle, B.; Apel, A. K.; Balibar, C. J.; Balskus, E. P.; Barona-Gómez, F.; Bechthold, A.; Bode, H. B.; Borriss, R.; Brady, S. F.; Brakhage, A. A.; Caffrey, P.; Cheng, Y.-Q.; Clardy, J.; Cox, R. J.; De Mot, R.; Donadio, S.; Donia, M. S.; van der Donk, W. A.; Dorrestein, P. C.; Doyle, S.; Driessen, A. J. M.; Ehling-Schulz, M.; Entian, K.-D.; Fischbach, M. A.; Gerwick, L.; Gerwick, W. H.; Gross, H.; Gust, B.; Hertweck, C.; Höfte, M.; Jensen, S. E.; Ju, J.; Katz, L.; Kaysser, L.; Klassen, J. L.; Keller, N. P.; Kormanec, J.; Kuipers, O. P.; Kuzuyama, T.; Kyrpides, N. C.; Kwon, H.-J.; Lautru, S.; Lavigne, R.; Lee, C. Y.; Linquan, B.; Liu, X.; Liu, W.; Luzhetskyy, A.; Mahmud, T.; Mast, Y.; Méndez, C.; Metsä-Ketelä, M.; Micklefield, J.; Mitchell, D. A.; Moore, B. S.; Moreira, L. M.; Müller, R.; Neilan, B. A.; Nett, M.; Nielsen, J.; O'Gara, F.; Oikawa, H.; Osbourn, A.; Osburne, M. S.; Ostash, B.; Payne, S. M.; Pernodet, J.-L.; Petricek, M.; Piel, J.; Ploux, O.; Raaijmakers, J. M.; Salas, J. A.; Schmitt, E. K.; Scott, B.; Seipke, R. F.; Shen, B.; Sherman, D. H.; Sivonen, K.; Smanski, M. J.; Sosio, M.; Stegmann, E.; Süssmuth, R. D.; Tahlan, K.; Thomas, C. M.; Tang, Y.; Truman, A. W.; Viaud, M.; Walton, J. D.; Walsh, C. T.; Weber, T.; van Wezel, G. P.; Wilkinson, B.; Willey, J. M.; Wohlleben, W.; Wright, G. D.; Ziemert, N.; Zhang, C.; Zotchev, S. B.; Breitling, R.; Takano, E.; Glöckner, F. O. *Nat. Chem. Biol.* **2015,** *11,* 625–631. doi:10.1038/nchembio.1890
65. Iizuka, T.; Fudou, R.; Jojima, Y.; Ogawa, S.; Yamanaka, S.; Inukai, Y.; Ojika, M. *J. Antibiot.* **2006,** *59,* 385–391. doi:10.1038/ja.2006.55
66. Ojika, M.; Inukai, Y.; Kito, Y.; Hirata, M.; Iizuka, T.; Fudou, R. *Chem. – Asian J.* **2008,** *3,* 126–133. doi:10.1002/asia.200700233
67. Bartlett, D. W.; Clough, J. M.; Godwin, J. R.; Hall, A. A.; Hamer, M.; Parr-Dobrzanski, B. *Pest Manage. Sci.* **2002,** *58,* 649–662. doi:10.1002/ps.520
68. Böhlendorf, B.; Herrmann, M.; Hecht, H.-J.; Sasse, F.; Forche, E.; Kunze, B.; Reichenbach, H.; Höfle, G. *Eur. J. Org. Chem.* **1999,** *1999,* 2601–2608. doi:10.1002/(SICI)1099-0690(199910)1999:10<2601::AID-EJOC2601>3.0.CO;2-#
69. Sumiya, E.; Shimogawa, H.; Sasaki, H.; Tsutsumi, M.; Yoshita, K.; Ojika, M.; Suenaga, K.; Uesugi, M. *ACS Chem. Biol.* **2011,** *6,* 425–431. doi:10.1021/cb1003459
70. Iizuka, T.; Jojima, Y.; Hayakawa, A.; Fujii, T.; Yamanaka, S.; Fudou, R. *Int. J. Syst. Evol. Microbiol.* **2013,** *63,* 1360–1369. doi:10.1099/ijs.0.040501-0
71. Jiang, D.-M.; Kato, C.; Zhou, X.-W.; Wu, Z.-H.; Sato, T.; Li, Y.-Z. *ISME J.* **2010,** *4,* 1520–1530. doi:10.1038/ismej.2010.84
72. Brinkhoff, T.; Fischer, D.; Vollmers, J.; Voget, S.; Beardsley, C.; Thole, S.; Mussmann, M.; Kunze, B.; Wagner-Döbler, I.; Daniel, R.; Simon, M. *ISME J.* **2012,** *6,* 1260–1272. doi:10.1038/ismej.2011.190
73. Zarins-Tutt, J. S.; Barberi, T. T.; Gao, H.; Mearns-Spragg, A.; Zhang, L.; Newman, D. J.; Goss, R. J. M. *Nat. Prod. Rep.* **2016,** *33,* 54–72. doi:10.1039/C5NP00111K
74. Bode, H. B.; Bethe, B.; Höfs, R.; Zeeck, A. *ChemBioChem* **2002,** *3,* 619–627. doi:10.1002/1439-7633(20020703)3:7<619::AID-CBIC619>3.0.CO;2-9
75. Pimentel-Elardo, S. M.; Sørensen, D.; Ho, L.; Ziko, M.; Bueler, S. A.; Lu, S.; Tao, J.; Moser, A.; Lee, R.; Agard, D.; Fairn, G.; Rubinstein, J. L.; Shoichet, B. K.; Nodwell, J. R. *ACS Chem. Biol.* **2015,** *10,* 2616–2623. doi:10.1021/acschembio.5b00612
76. Seyedsayamdost, M. R. *Proc. Natl. Acad. Sci. U. S. A.* **2014,** *111,* 7266–7271. doi:10.1073/pnas.1400019111
77. Derewacz, D. K.; Covington, B. C.; McLean, J. A.; Bachmann, B. O. *ACS Chem. Biol.* **2015,** *10,* 1998–2006. doi:10.1021/acschembio.5b00001
78. Watrous, J.; Roach, P.; Alexandrov, T.; Heath, B. S.; Yang, J. Y.; Kersten, R. D.; van der Voort, M.; Pogliano, K.; Gross, H.; Raaijmakers, J. M.; Moore, B. S.; Laskin, J.; Bandeira, N.; Dorrestein, P. C. *Proc. Natl. Acad. Sci. U. S. A.* **2012,** *109,* E1743–52. doi:10.1073/pnas.1203689109
79. Yang, J. Y.; Sanchez, L. M.; Rath, C. M.; Liu, X.; Boudreau, P. D.; Bruns, N.; Glukhov, E.; Wodtke, A.; de Felicio, R.; Fenner, A.; Wong, W. R.; Linington, R. G.; Zhang, L.; Debonsi, H. M.; Gerwick, W. H.; Dorrestein, P. C. *J. Nat. Prod.* **2013,** *76,* 1686–1699. doi:10.1021/np400413s
80. Johnston, C. W.; Skinnider, M. A.; Wyatt, M. A.; Li, X.; Ranieri, M. R. M.; Yang, L.; Zechel, D. L.; Ma, B.; Magarvey, N. A. *Nat. Commun.* **2015,** *6,* No. 8421. doi:10.1038/ncomms9421
81. Duncan, K. R.; Crüsemann, M.; Lechner, A.; Sarkar, A.; Li, J.; Ziemert, N.; Wang, M.; Bandeira, N.; Moore, B. S.; Dorrestein, P. C.; Jensen, P. R. *Chem. Biol.* **2015,** *22,* 460–471. doi:10.1016/j.chembiol.2015.03.010
82. Tang, X.; Li, J.; Millán-Aguiñaga, N.; Zhang, J. J.; O'Neill, E. C.; Ugalde, J. A.; Jensen, P. R.; Mantovani, S. M.; Moore, B. S. *ACS Chem. Biol.* **2015,** *10,* 2841–2849. doi:10.1021/acschembio.5b00658
83. Yamanaka, K.; Reynolds, K. A.; Kersten, R. D.; Ryan, K. S.; Gonzalez, D. J.; Nizet, V.; Dorrestein, P. C.; Moore, B. S. *Proc. Natl. Acad. Sci. U. S. A.* **2014,** *111,* 1957–1962. doi:10.1073/pnas.1319584111
84. Jiang, W.; Zhao, X.; Gabrieli, T.; Lou, C.; Ebenstein, Y.; Zhu, T. F. *Nat. Commun.* **2015,** *6,* 8101. doi:10.1038/ncomms9101
85. Ongley, S. E.; Bian, X.; Neilan, B. A.; Müller, R. *Nat. Prod. Rep.* **2013,** *30,* 1121–1138. doi:10.1039/c3np70034h

License and Terms

BEILSTEIN JOURNAL OF ORGANIC CHEMISTRY

Cyclisation mechanisms in the biosynthesis of ribosomally synthesised and post-translationally modified peptides

Andrew W. Truman

Review

Open Access

Address:
Department of Molecular Microbiology, John Innes Centre, Colney Lane, Norwich, NR4 7UH, UK

Email:
Andrew W. Truman - andrew.truman@jic.ac.uk

Keywords:
biosynthesis; cyclisation; enzymes; peptides; RiPPs

Beilstein J. Org. Chem. **2016,** *12,* 1250–1268.
doi:10.3762/bjoc.12.120

Received: 14 March 2016
Accepted: 02 June 2016
Published: 20 June 2016

This article is part of the Thematic Series "Natural products in synthesis and biosynthesis II".

Guest Editor: J. S. Dickschat

Abstract

Ribosomally synthesised and post-translationally modified peptides (RiPPs) are a large class of natural products that are remarkably chemically diverse given an intrinsic requirement to be assembled from proteinogenic amino acids. The vast chemical space occupied by RiPPs means that they possess a wide variety of biological activities, and the class includes antibiotics, co-factors, signalling molecules, anticancer and anti-HIV compounds, and toxins. A considerable amount of RiPP chemical diversity is generated from cyclisation reactions, and the current mechanistic understanding of these reactions will be discussed here. These cyclisations involve a diverse array of chemical reactions, including 1,4-nucleophilic additions, [4 + 2] cycloadditions, ATP-dependent heterocyclisation to form thiazolines or oxazolines, and radical-mediated reactions between unactivated carbons. Future prospects for RiPP pathway discovery and characterisation will also be highlighted.

Introduction

Nature employs a number of routes to produce peptidic secondary metabolites, including non-ribosomal peptide synthetases [1,2] (NRPSs) and diketopiperazine-forming cyclases [3,4]. Alternatively, peptides synthesised by the ribosome can be post-translationally modified into secondary metabolites [5]. These are termed ribosomally synthesised and post-translationally modified peptides (RiPPs), and they are prevalent throughout nature. Massive advances in genome sequencing has revolutionised the discovery of new natural products from all biosynthetic classes [6-8], and it has been particularly beneficial for the discovery of new RiPP pathways, which are often small and lacking in homology to one another [9]. There has therefore been a massive increase in the study of their biosynthesis in recent years.

RiPPs usually originate from a larger precursor peptide that consists of an N-terminal leader sequence and a core peptide that contains the natural product precursor (Figure 1). The

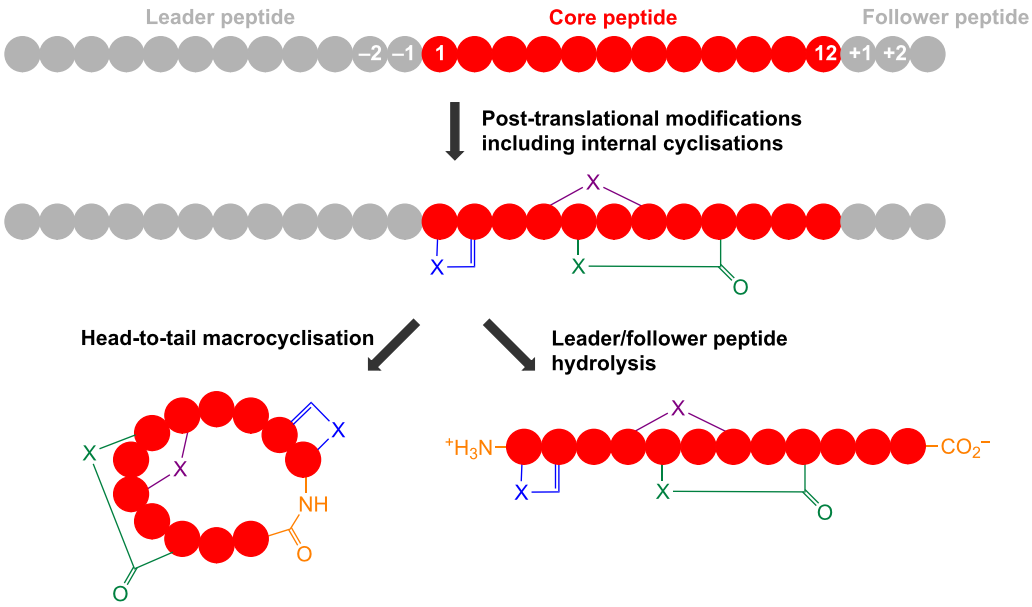

Figure 1: Schematic of RiPP biosynthesis. Thiazole/oxazole formation is represented by the blue heterocycle (X = S, O), lanthionine formation is represented by the purple cross-link (X = S) and macrolactam (X = N) or macrolactone (X = O) formation is represented by the green cyclisation.

bottromycin precursor peptide represents a notable exception as it features an N-terminal core peptide and a C-terminal follower peptide [10-13]. The core peptide is post-translationally modified and cleaved from the leader peptide to yield a biologically active peptide natural product (Figure 1 and Figure 2). A huge variety of RiPP post-translational modifications have been identified [5,14]; some are specific to certain classes of RiPP while others occur across the entire RiPP spectrum. These modifications can range from leader peptide hydrolysis and disulphide bond formation through to the complex remodelling of almost every amino acid in a molecule. For example, thiopeptide antibiotics [15] and the marine toxin polytheonamide [16] were both believed to be non-ribosomal peptides for a number of years, while the bacterial cofactor pyrroloquinoline quinone (PQQ, Figure 2) has a ribosomal origin [17] but has been modified so that no peptide bonds remain. This demonstrates that a huge amount of structural diversity can be introduced into RiPPs, despite an intrinsic requirement to be assembled from the 20 regular proteinogenic amino acids (possibly 21, as RiPPs containing selenocysteine were proposed in a recent bioinformatic study [18]). Excitingly, the ribosomal origin of RiPPs means that significant chemical changes to complex natural products can be achieved by simple site-directed mutagenesis. This requires the associated tailoring enzymes to tolerate a modified substrate, and there are many examples of pathways whose precursor peptides can be extensively mutagenised [19-23]. This is a powerful tool for the generation of natural product analogues and means that RiPP libraries can be generated much more rapidly and predictably than molecules made from multi-domain megasynthases such as polyketides and non-ribosomal peptides.

Cyclisation is a common post-translational modification in RiPP pathways and includes a multitude of transformations. These modifications are usually essential for the proper biological activity of the RiPP, as they fundamentally change the shape of a molecule, which can be critical for receptor binding or for protection from proteolysis. Examples include amide bonds, heterocyclisation to form thiazolines or oxazolines [24] (Figure 2), oxidative carbon–carbon bond formation [25] and thioether cross-links [26]. Fascinatingly, a significant number of these modifications are unique to RiPPs [27]. This review will focus on cyclisations that have been mechanistically characterised, as well as reactions where a mechanism can be confidently postulated. Disulphide bond formation is common in RiPP pathways but is found across proteins of all sizes so will not be discussed here.

Review

Thiazole and oxazoles

Thiazoles and oxazoles are found in a huge number of bacterial RiPPs, which are often loosely defined as thiazole/oxazole-modified microcins [24] (TOMMs), although these can be subdivided more accurately into a variety of structural classes, including linear azol(in)e-containing peptides (LAPs, e.g., microcin B17 [28], Figure 3A), thiopeptides (e.g., TP1161 [29], Figure 2) and cyanobactins [30] (e.g., patellamide A [31], Figure 2). In each class, the biosynthetic route to generate

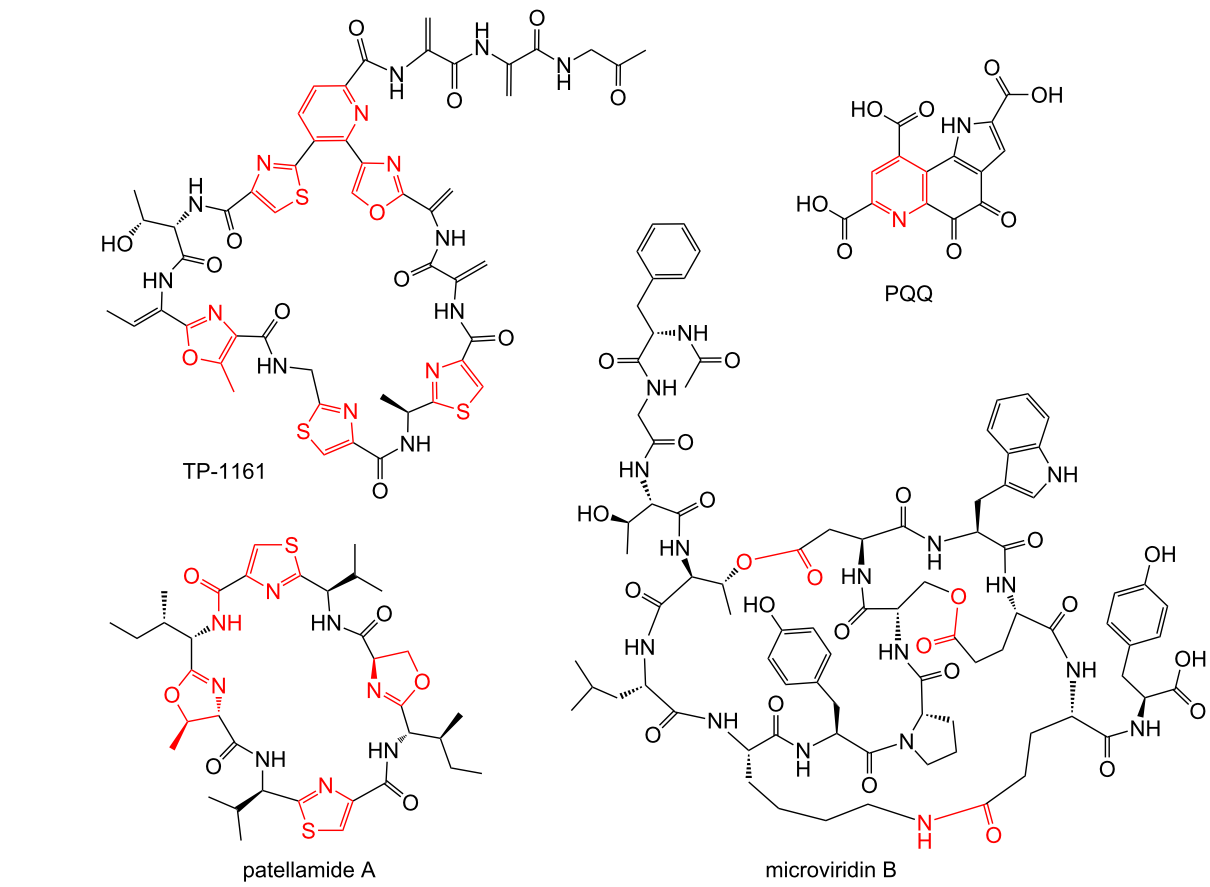

Figure 2: Examples of heterocycles in RiPPs alongside the precursor peptides that these molecules derive from. The red features on the molecules indicate where cyclisation has taken place, while the sections of the sequences highlighted in red correspond to the core peptides for each of these molecules. The sequence highlighted in blue in PatE corresponds to the core peptide for patellamide C, another macrocyclic RiPP that contains thiazoles and oxazolines.

azol(in)es is highly similar, and is distinct from their generation in non-ribosomal peptides. The first in vitro reconstitution of a TOMM was carried out with microcin B17 [28,32,33], which showed that there are four essential proteins for its biosynthesis: the precursor peptide (the "A" protein McbA) that is post-translationally modified into the final product, and a heterotrimeric complex that is responsible for both heterocyclisation of serine and cysteine residues, and subsequent oxidation of (ox/thi)azolines into (ox/thi)azoles (Figure 3A). This catalytic complex consists of "C" and "D" proteins (annotated as McbB and McbD, respectively, for microcin B17) that cooperate to catalyse heterocyclisation of specific serine and cysteine residues in McbA, and a flavin-dependent dehydrogenase (the "B-protein", McbC for microcin B17) that oxidises these heterocycles. These early in vitro studies indicated that the "C-protein" was a zinc-containing cyclase, and the "D-protein" possesses ATPase activity. The requirement for ATP turnover during cyclisation led to the hypothesis that the D-protein was a docking protein that regulates heterocyclase activity [33], while the presence of zinc in the C-protein pointed towards a catalytic role for this metal [33]. However, this role was later demonstrated to be structural rather than catalytic [34].

The Mitchell group showed [35] that the D-protein is actually directly involved in catalysis and uses ATP to activate the backbone amide bond for cyclodehydration, thus explaining the hydrolysis of ATP. A stoichiometric ratio of 1:1 between azole formation and ATP hydrolysis was demonstrated, and [^{18}O]H_2O was used in the reaction to show that oxygen incorporated into phosphate following ATP turnover was not derived

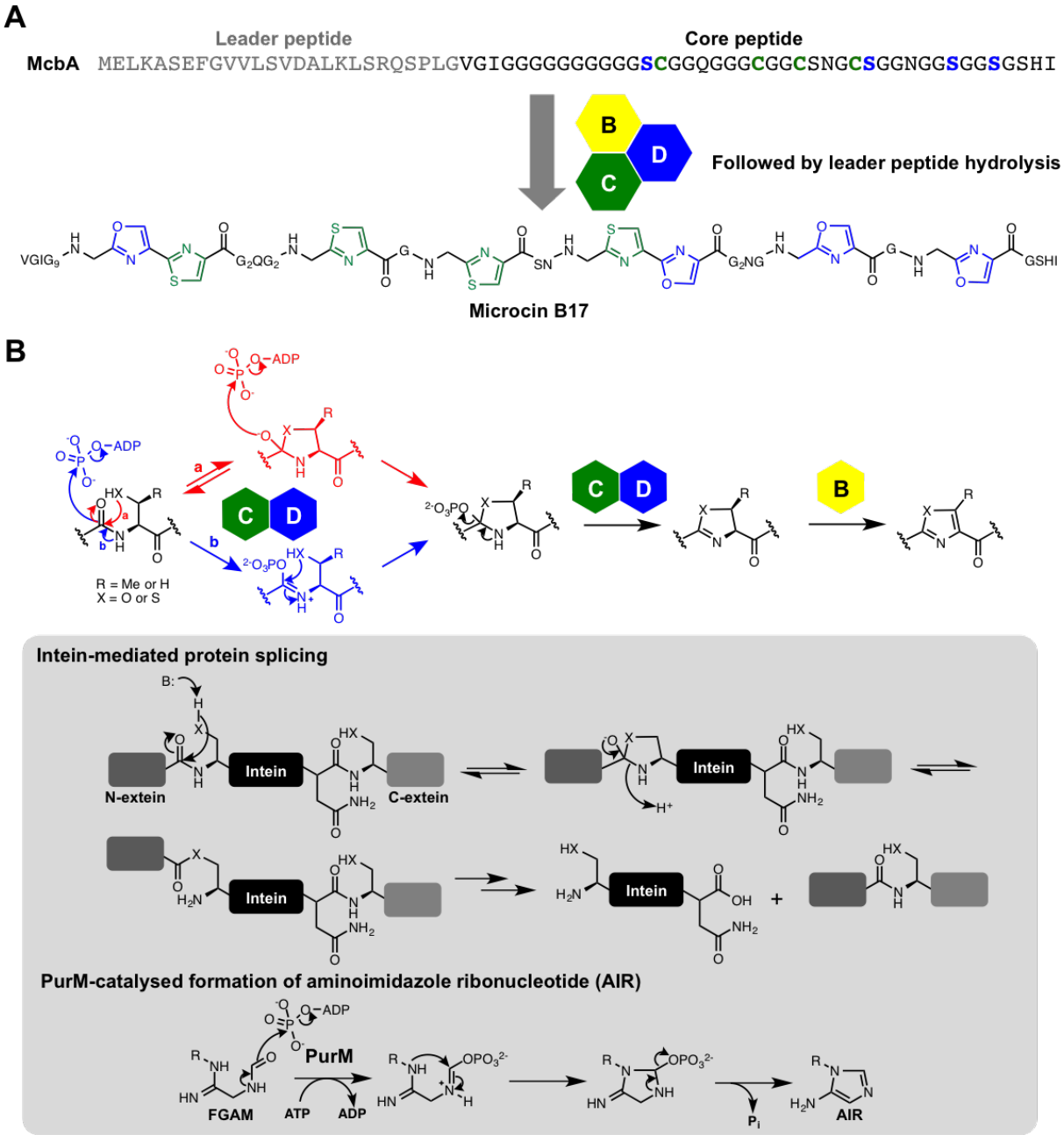

Figure 3: Formation of thiazoles and oxazoles in RiPPs. A) Biosynthesis of microcin B17. B) Mechanistic models for the introduction of azol(in)es into microcin, where pathway a was reported by the authors as the likely order of steps. An analogous mechanism was proposed in the biosynthesis of trunkamide, but with the transfer of AMP instead of phosphate. Inset: partial mechanism of intein-mediated protein splicing, which proceeds via a reversible hemiorthoamide, and the proposed mechanism of PurM-catalysed conversion of formylglycinamide ribonucleotide (FGAM) into aminoimidazole ribonucleotide (AIR), which involves activation of an amide by ATP and a 5-*endo*-trig cyclisation.

from bulk water. This led to a mechanistic model where a reversible hemiorthoamide is first formed by side-chain *S*- or *O*-attack onto the amide carbonyl [35] (Figure 3B, pathway a), which is analogous to a step proposed for protein autoproteolysis [36] (Figure 3, inset). The exocyclic oxygen in this intermediate then attacks the α-phosphate of ATP to displace ADP and generate a phosphorylated hemiorthoamide. This highly reactive intermediate ensures that the rapid elimination of phosphate to generate (ox/thi)azolines is thermodynamically favourable. [^{18}O]-labeled precursor peptide was subsequently used to further substantiate this proposal [37].

A similar heterocyclisation mechanism was proposed by the Naismith group for the cyanobactin heterocyclase TruD, which

contains fused C- and D-proteins [38]. Interestingly, this revealed a notable difference with the microcin pathway, as cyclisation was accompanied by the generation of AMP and pyrophosphate (PP_i), instead of ADP and phosphate. This points to an adenylation-type mechanism, and the authors also proposed a hemiorthoamide mechanism to account for the absence of wasted ATP hydrolysis (Figure 3B, pathway a). An alternative mechanism that would also account for the [^{18}O]-labelling results involves direct activation of the amide carbonyl by ATP (Figure 3B, pathway b), which is analogous to a reaction catalysed by PurM family enzymes (aminoimidazole ribonucleotide synthetases) in the biosynthesis of aminoimidazole ribonucleotide as part of the purine biosynthetic pathway [39] (Figure 3, inset). This activated amide would then be attacked by an adjacent serine or cysteine side chain, thus releasing phosphate/AMP and generating the heterocycle. This order of steps was not advocated by either the Naismith or Mitchell groups as it requires a disfavoured 5-*endo*-trig cyclisation, although this mode of cyclisation is postulated to be catalysed by PurM, and Baldwin disfavoured cyclisations do occur in other biosynthetic pathways [40,41].

Curiously, members of the D-protein family are commonly annotated as YcaO domain proteins [35], where YcaO is an *E. coli* protein (Ec-YcaO) of unknown function that has been implicated in the β-methylthiolation of ribosomal protein S12 [42]. Crystallographic analysis has demonstrated that Ec-YcaO is structurally homologous to RiPP D-proteins and that ATP-binding residues are conserved across the superfamily [38,43]. Furthermore, biochemical studies showed that Ec-YcaO hydrolyses ATP to AMP and pyrophosphate [43]. The function of this highly conserved "non-TOMM" protein has yet to be identified, but it indicates that amide activation by ATP may not be confined to the biosynthesis of secondary metabolites or purines. Ec-YcaO also lacks a partner C-protein, which is also the case for a number of characterised secondary metabolite pathways. For example, the bottromycin gene cluster encodes two stand-alone YcaO domain proteins that have been postulated to participate in heterocyclisation reactions [10-13].

Lanthionine bond formation in lanthipeptides

Lanthipeptides (alternatively named lantipeptides [44]) are large bacterial RiPPs, and the first member to be reported was nisin (Figure 4A) from *Lactococcus lactis* in 1928 [45]. Many members of this family have antibacterial activity and these are termed lantibiotics [46]; nisin itself is used as a food preservative as it suppresses bacterial spoilage. Lanthipeptides are characterised by *meso*-lanthionine (Lan) and (2*S*,3*S*,6*R*)-3-methyllanthionine (MeLan) residues. Lanthionine consist of two alanine residues linked via a thioether that connects their β-carbons, while MeLan contains an additional methyl group (Figure 4B). These crosslinks are formed via a two-stage process. Firstly, serine (for Lan) and threonine (for MeLan) residues are dehydrated to 2,3-didehydroalanine (Dha) and (*Z*)-2,3-didehydrobutyrine (Dhb), respectively (Figure 4B). This is followed by 1,4-nucleophilic additions onto these didehydro

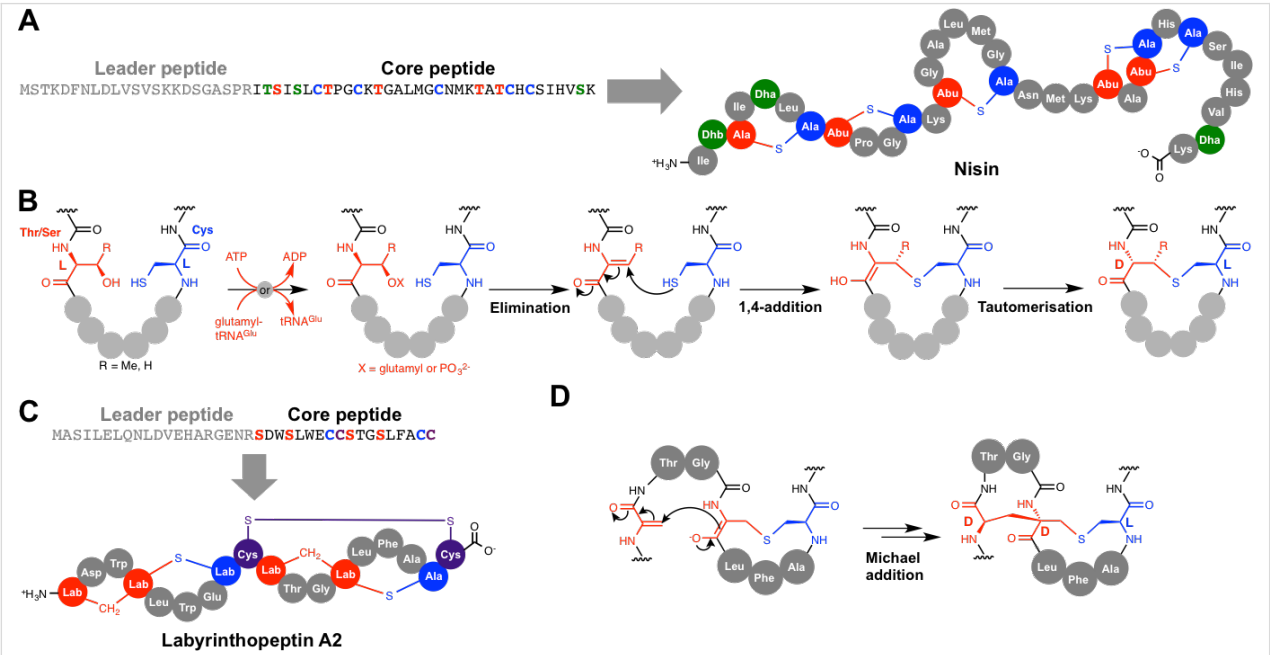

Figure 4: Lanthionine bond formation. A) Nisin and its precursor peptide. B) Mechanism of lanthionine bond formation for class I–IV lanthionine synthetases. GTP is used in an analogous way to ATP by some enzymes, for example in the biosynthesis of labyrinthopeptin A2. C) Labyrinthopeptin A2 and its precursor peptide. D) Mechanism for labionin formation in the biosynthesis of labyrinthopeptin A2.

amino acids by cysteine residues [47-49]. Lanthipeptides are divided into four distinct classes (I–IV) based on the differences between the biosynthetic enzymes that carry out dehydration and cyclisation [44]. Dehydration in class I lanthipeptide pathways is catalysed by a LanB dehydratase (NisB for nisin) and cyclisation is catalysed by a zinc-dependent LanC cyclase (NisC). In nisin biosynthesis, the precursor peptide, NisA, is dehydrated 8 times by NisB [50], and this has been shown to occur with directionality from the N- to C-terminus of the core peptide [51].

In vitro reconstitution of NisB activity with the nisin precursor peptide NisA showed that dehydration involves the glutamylation of Ser and Thr side chains prior to elimination of glutamate [50]. This mechanistic proposal was established due to the observation that three NisB mutants (R786A, R826A and H961A) were able to transfer multiple glutamates to NisA without subsequent elimination. Wild-type NisB was then able to convert polyglutamylated NisA to dehydrated NisA without the need for any additives that are usually necessary for NisB in vitro activity, thus demonstrating that glutamylated NisA is an authentic activated intermediate. Subsequent biochemical and structural work identified that glutamate is supplied by glutamyl-tRNA, and that glutamylation and elimination steps are catalysed by distinct domains within NisB [52]. Protein homology analysis indicated that LanB-like proteins are widespread in bacteria [52], so this unusual use of an aminoacyl-tRNA may actually be common across nature. Interestingly, a subset of these proteins lack the elimination domain and are commonly associated with NRPSs rather than RiPPs, but the function of these small LanBs is not yet known [52,53].

In contrast to class I lanthipeptides, both dehydration and cyclisation reactions are catalysed by bifunctional lanthionine synthetases for classes II–IV [47,49,54]. Furthermore, dehydration in each of these classes has been shown to proceed via phosphorylation of the amino acid side chain rather than by glutamylation [54]. Class II synthetases ("LanM") have an N-terminal dehydratase domain and a C-terminal LanC-like cyclase domain, and detailed mechanistic studies on LamM enzymes was enabled by the in vitro reconstitution of lacticin 481 synthetase, LctM [47,54-56]. Both class III ("LanKC" [57]) and IV ("LanL" [49]) synthetases feature three domains, where a central kinase domain catalyses phosphorylation and an N-terminal lyase domain catalyses elimination [58]. Both class III and IV synthetases have C-terminal LanC-like cyclase domains, but class III enzymes lack the three conserved residues that bind zinc in the other classes [57], which is surprising, given that the active site Zn^{2+} is proposed to activate the cysteine side chains for cyclisation. The identification of the labyrinthopeptins [59] (Figure 4C) led to the discovery of a subset of class III lanthipeptides that contain an additional carbocyclic ring, which features the labionin (Lab) amino acid (Figure 4C). This is formed by sequential Michael-type cyclisations [57,60], where a conventional lanthionine thioether is first formed by the attack of cysteine onto Dha. The resulting enolate then attacks another Dha residue to stereospecifically form the carbocycle (Figure 4D), and the stereochemical outcome of this cyclisation is equivalent to lanthionine formation [59]. Both S–C and C–C crosslinks are formed by the same enzyme, LabKC, which also catalyses the formation of the Dha residues. An elegant experiment using a series of peptides with α-deuterated serine residues demonstrated that LabKC dehydrates the precursor peptide with C- to N-terminal directionality [61], which is in contrast to NisB from the nisin pathway, which processes its peptide in the opposite direction [51].

Aminovinylcysteine-containing peptides

A structural variation on the lanthionine linkage is the C-terminal aminovinylcysteine [62] (AviCys, Figure 5A). This is found in a variety of RiPPs that also feature conventional lanthionine rings, such as epidermin [63] (Figure 5A), mersacidin [64] and cypemycin [65]. In epidermin, a *S*-[(*Z*)-2-aminovinyl]-D-cysteine (AviCys) residue is formed by the 1,4-nucleophilic addition of an oxidatively decarboxylated cysteine residue onto a Dha residue derived from serine (Figure 5A). Extensive in vitro experiments indicate that decarboxylation of cysteine precedes 1,4-addition and is catalysed by a flavoprotein (EpiD) in epidermin biosynthesis [66,67], which uses flavin mononucleotide (FMN) to oxidise the cysteine. A mechanistic proposal based on structural data involves the oxidation of the thiol to a thioaldehyde, which then functions as an electron sink to facilitate decarboxylation to generate the double bond between C_α and C_β [66] (Figure 5A). The functional characterisation of EpiD led to the identification of homologous bacterial flavoproteins (Dfp) that catalyse the decarboxylation of 4'-phospho-*N*-pantothenoylcysteine to 4'-phosphopantetheine, which is essential for coenzyme A biosynthesis [68] (Figure 5B). This demonstrates how the mechanistic analysis of secondary metabolism can inform the characterisation of primary metabolism. Surprisingly, the gene cluster for the AviCys-containing RiPP cypemycin indicates that this pathway features an alternative way to produce dehydrated amino acids [65]. Firstly, the cluster does not encode any Lan-like dehydratases, and secondly, the Dha residue required for AviCys formation derives from cysteine rather than serine.

Pyridine and piperidine formation in thiopeptides

Thiopeptides are a widespread bacterial RiPP family that are characterised by multiple thiazoles, dehydrated residues and a central substituted pyridine, dehydropiperidine or piperidine

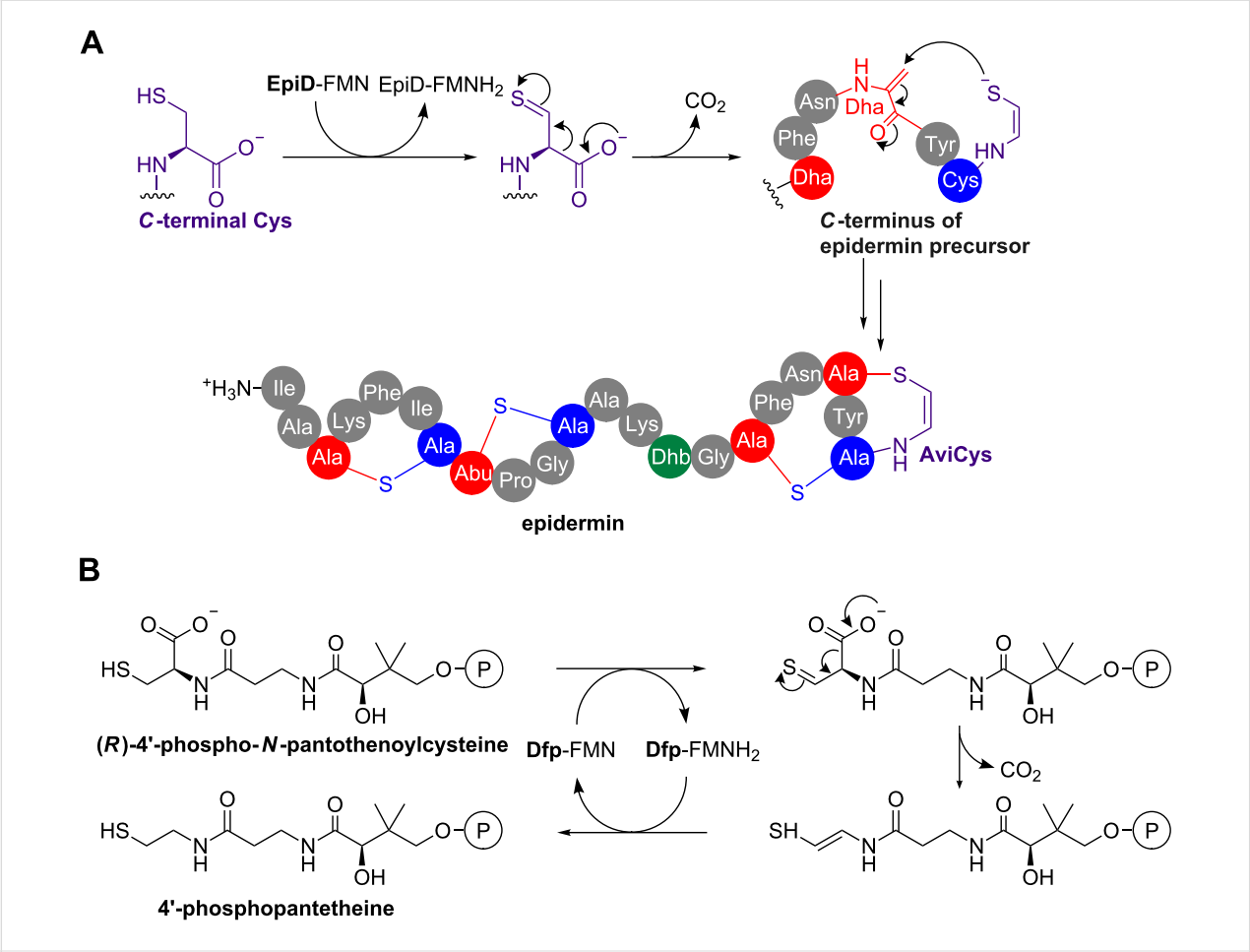

Figure 5: *S*-[(*Z*)-2-Aminovinyl]-D-cysteine (AviCys) formation in the epidermin pathway. A) Mechanisms for decarboxylation and 1,4-addition. B) Mechanism for the *E. coli* Dfp-catalysed conversion of (*R*)-4'-phospho-*N*-pantothenoylcysteine into 4'-phosphopantetheine during coenzyme A biosynthesis. The function of Dfp was discovered following the mechanistic characterisation of EpiD.

ring [69] (Figure 6A). Micrococcin was the first member to be identified [70], while the most well-studied member of the class is thiostrepton [71], whose gene cluster was the first of this class to be reported [72,73], along with the thiocillin and siomycin A gene clusters [73,74]. Thiopeptides are antibacterial towards Gram-positive species by inhibiting protein biosynthesis [75], but some members also exhibit biological activity towards a number of eukaryotic targets, which makes them promising anticancer [76,77] and antimalarial [78] compounds. Intriguingly, a recent study identified actively transcribed thiopeptide gene clusters in human microbiota from every body site assessed [6].

Thiazoles in thiopeptides are introduced by a BCD-protein system described previously, while threonine and serine residues are dehydrated by lantibiotic-like dehydratases. The formation of core pyridine, dehydropiperidine or piperidine is consistent with a [4 + 2] cycloaddition across two dehydrated serine residues [79,80]. Genetic disruption of *tclM* from the thiocillin pathway showed that TclM was responsible for this transformation [81], although the precise cyclisation mechanism (concerted or stepwise) could not be distinguished. Therefore, a synthetic peptide substrate was tested with recombinant TclM [82]. This showed that standalone TclM does function as a "hetero-Diels–Alderase" and a potential concerted mechanism has been proposed that involves the imidic acid tautomer of one amino acid residue (Figure 6B). The enzyme is also capable of catalysing aromatisation by elimination of water and the leader peptide. Aromatisation via leader peptide elimination does not happen in the biosynthesis of various thiopeptides, including thiostrepton, which indicates that TclM could have an active role in this elimination step.

Macrolactam and macrolactone formation

A diverse array of macrolactams are found in RiPPs from bacteria [31], plants [83] and mammals [84]. These can arise from a variety of routes: (i) head-to-tail cyclisation by attack of the N-terminal amine of the core peptide onto the C-terminus

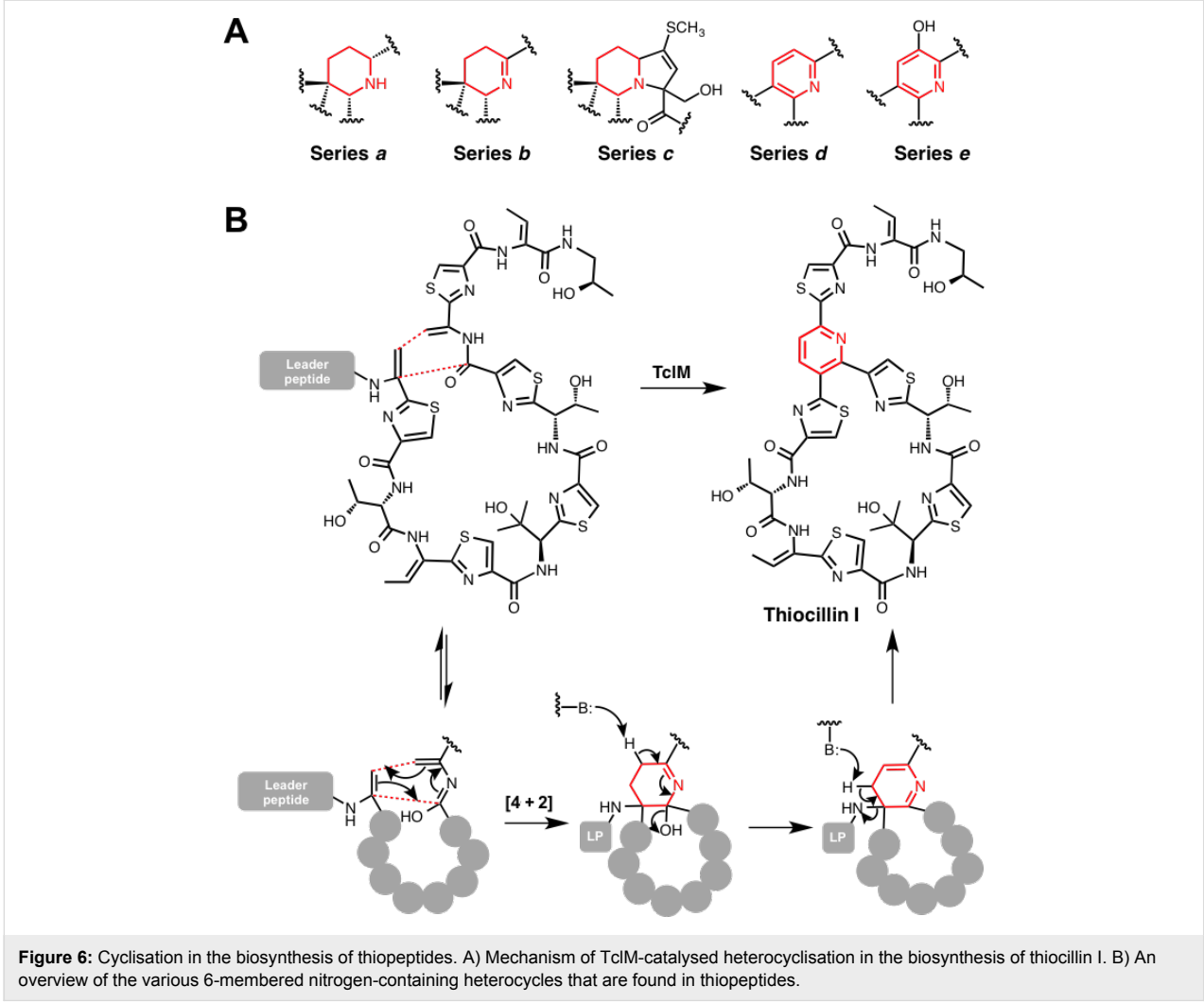

Figure 6: Cyclisation in the biosynthesis of thiopeptides. A) Mechanism of TclM-catalysed heterocyclisation in the biosynthesis of thiocillin I. B) An overview of the various 6-membered nitrogen-containing heterocycles that are found in thiopeptides.

[85]; (ii) attack of a side-chain amine onto a carbonyl [86]; (iii) condensation between the N-terminal amine of the core peptide onto a side-chain carboxylate [87]. Biochemically, these macrolactams are formed via two distinct routes: (a) ATP-dependent activation of carboxylates [88], and (b) peptidase-like cyclisation onto internal amides [85].

(a) ATP-dependent macrolactam and macrolactone formation

ATP-dependent macrolactam formation occurs in the biosynthesis of the lasso peptides [87] and the microviridins [86,89] (Figure 7). Lasso peptides are bacterial RiPPs that are characterised by their knotted structures, where a tail peptide is threaded through a macrolactam that is formed by the condensation of the N-terminal amino group with an asparatate or glutamate side-chain carboxylate. These are highly stable structures, and lasso peptides with a variety of biological activities have been identified [87,90]. The most well-studied member of the family is microcin J25 (Figure 7C) from *E. coli* AY25. Initial structural characterisation incorrectly identified microcin J25 as a conventional head-to-tail macrocyclic peptide [91], which was later revised to the lassoed structure by multiple groups [92-94]. McjC was identified as the macrolactam synthetase using both genetic inactivation in *E. coli* and in vitro analysis of purified protein [95]. McjC has homology to asparagine synthetases and the reaction they catalyse is mechanistically similar [96], although McjC lacks the N-terminal domain that catalyses the hydrolysis of glutamine to glutamic acid and ammonia [95]. The McjB peptidase first removes the leader peptide to expose an N-terminal amino group, which is usually a glycine residue, although other residues have been identified at this position [97,98]. McjC then catalyses cyclisation by activating the carboxylate of an aspartate or glutamate side chain at position 7, 8 or 9 using ATP. This generates an acyl-AMP intermediate, which is then attacked by the α-NH_2 group of the N-terminal amino acid to form the isopeptide bond. Crucially, the precursor peptide is pre-folded so that once the lactam is formed the C-terminal tail is trapped within the macrolactam due to the po-

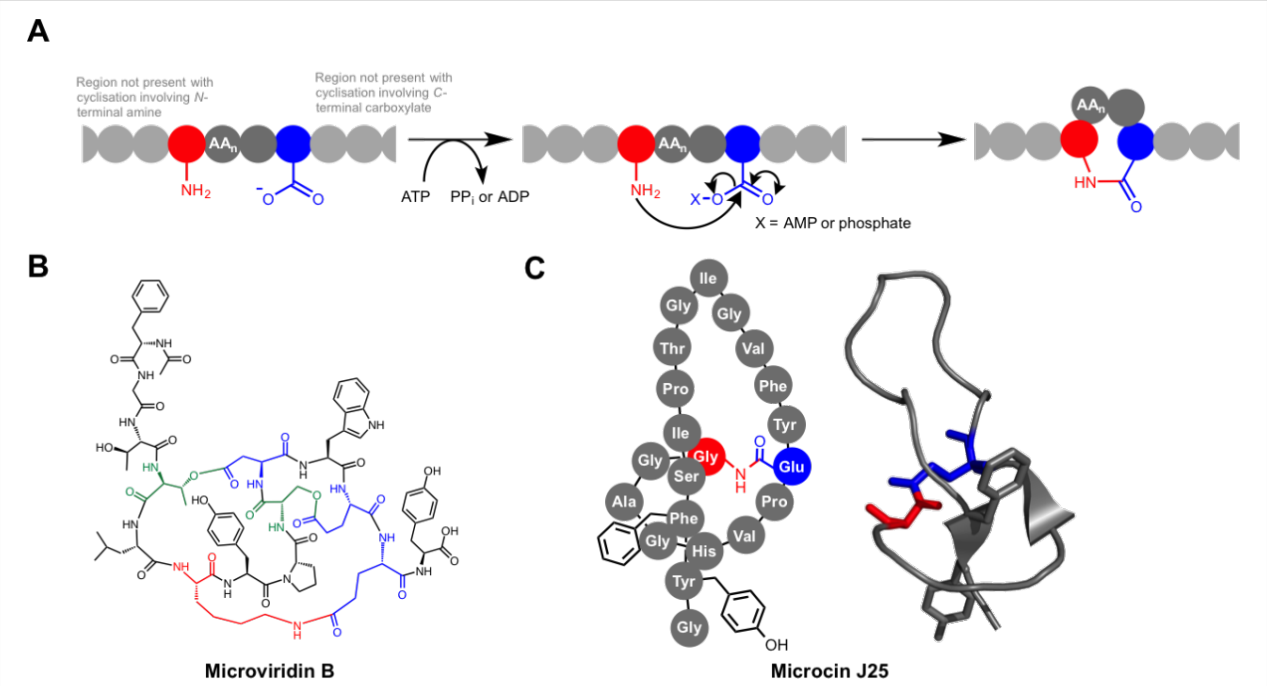

Figure 7: ATP-dependent macrocyclisation. A) General mechanism for ATP-dependent macrolactonisation or macrolactamisation in RiPPs. B) Structure of microviridin B, where the nucleophilic residues involved in the formation of cyclic esters are coloured green. C) Illustration of microcin J25 alongside a solution NMR structure [93] of this molecule (PDB: 1PP5). The Phe19 and Tyr20 side chains are shown in both structures to illustrate how the lasso peptide is conformationally restricted following cyclisation.

sition of bulky side chains on the lasso peptide tail (Phe19 and Tyr20, Figure 7C).

Microviridins constitute a much smaller family of RiPPs than lasso peptides and have only been identified from a limited number of cyanobacteria [99-103]. Members of this family can feature both macrolactams and macrolactones, and both of these are introduced by ATP-grasp ligases [88]. These macrolactams are formed by the condensation between the side chains of lysine and glutamate residues, whereas the macrolactones form from the condensation of threonine or serine side chains with aspartate or glutamate side chains. Studies on microviridin B (Figure 7B) from *Microcystis aeruginosa* NIES298 and microviridin K from *Planktothrix agardhii* CYA126/8 demonstrated that one ligase is responsible for ester formation and another catalyses amide formation [86,89]. In vitro studies on the microviridin K pathway showed that one ATP-grasp ligase catalyses the formation of two macrolactone rings, which precedes macrolactam formation [88]. The stoichiometric generation of phosphate during lactonisation indicates that the acid side chains are activated as carboxylate-phosphate mixed anhydrides, which are then attacked by serine or threonine to release phosphate. The sequence similarity between the ligases in the microviridin pathway points towards an equivalent mechanism for lactam formation, although this has not yet been demonstrated experimentally.

(b) Peptidase-like macrolactam formation

An alternative route to macrolactams involves the use of protease-like proteins that catalyse cyclisation via a ping-pong mechanism [85,104,105] (Figure 8A). In fact, protease-mediated ligation is a well-established concept and early studies showed that peptide bond formation could be achieved by modulating protease reaction conditions accordingly [106]. This has since been found to happen in the biosynthesis of cyclic RiPPs from a wide range of hosts, including cyclic peptides from both plants [105] and bacteria [104] (Figure 8B and C). Mechanistically, these cyclases function in an analogous way to either cysteine proteases or serine proteases, and these RiPP cyclases often belong to these peptidase superfamilies. The PatG cyclase from the patellamide cyanobactin pathway [31] has been very well characterised to show that one of its domains (PatGmac) possesses similarity to subtilisin-like peptidases [104,107]; accordingly, this catalyses macrocyclisation via a serine protease-like mechanism. PatG features a canonical serine protease-like catalytic triad (Asp548, His618 and Ser783), which cuts before an AYDG motif on the precursor peptide. This generates an acyl–enzyme intermediate, where the C-terminus of the peptide is bound to Ser783 as an ester. The N-terminal amino group then attacks this intermediate to generate a cyclic octapeptide. This is mechanistically similar to thioesterase-catalysed macrocyclisation found in NRP biosynthesis, although the energetic demands of breaking an amide

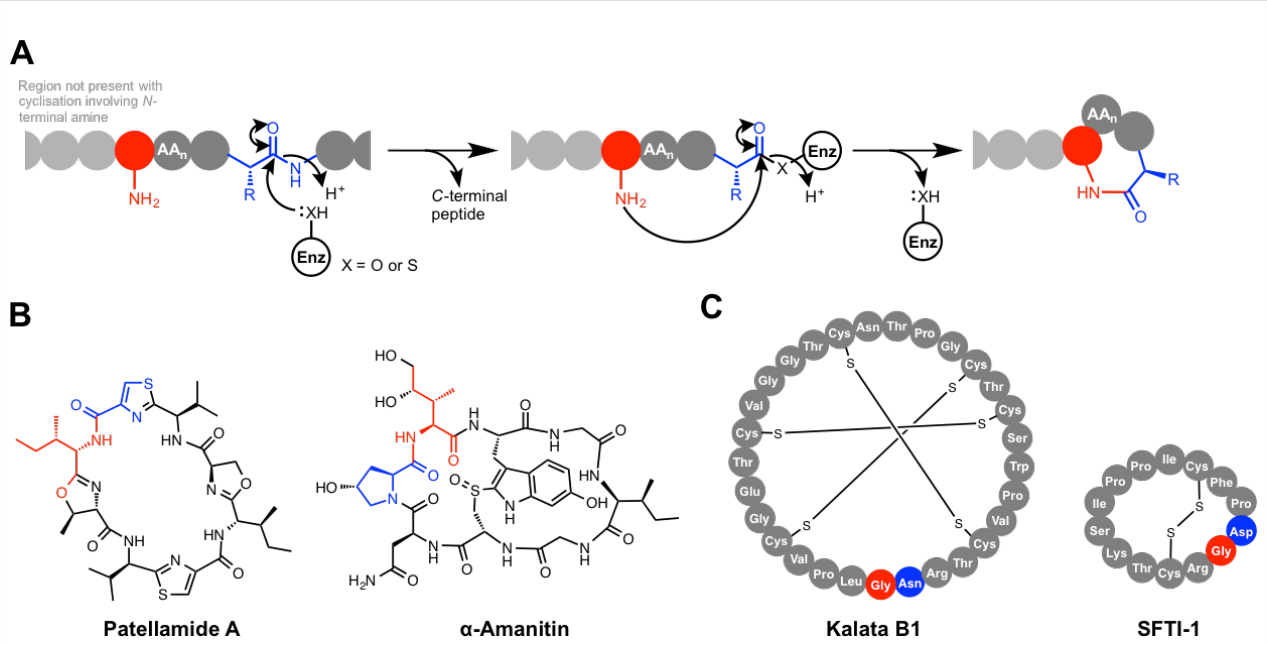

Figure 8: Peptidase-like macrolactam formation. A) General mechanism. B) Examples of RiPPs cyclised by serine protease-like enzymes. C) Examples of RiPPs cyclised by cysteine protease-like enzymes.

bond versus a thioester bond are notably different. PatG may have synthetic utility, as studies with unnatural substrates have shown that macrocycles of between 5–22 residues can be produced [108], despite it naturally producing a cyclic octapeptide.

A serine protease-like cyclase (PCY1) is also found in the biosynthesis of Caryophyllaceae-type cyclic peptides in *Saponaria vaccaria* [109]. This cyclase functions in an analogous way to PatG, although PCY1 has structural similarity to S9a family serine peptidases, whereas PatG belongs to the S8 family. Another S9a family serine protease-like cyclase features in the biosynthesis of α-amanitin (Figure 8B), an amatoxin produced by the fungus *Amanita phalloides* and related fungi [110]. Amatoxins are responsible for many of the fatalities caused by mushroom poisoning of humans, where they function by inhibiting RNA polymerase II [111]. In the α-amanitin pathway [112], a prolyl oligopeptidase-like enzyme catalyses both hydrolysis of the leader peptide and transpeptidation to yield a backbone macrolactam [113]. No distinguishing features have been identified to indicate how it preferentially catalyses cyclisation over hydrolysis.

Given the discovery of serine protease-like cyclisation in RiPP biosynthesis, it is not surprising that cysteine protease-like enzymes have also evolved the ability to cyclise ribosomal peptides. A well-characterised cysteine protease-like macrocyclase is found in the biosynthesis of the 14-residue sunflower trypsin inhibitor 1 (SFTI-1, Figure 8C), where asparaginyl endopeptidase (AEP) employs a catalytic triad of Asn, His and Cys to catalyse both proteolysis and cyclisation [105,114,115]. SFTI-1 is found in sunflower seeds and its precursor peptide, prealbumin, is processed into both SFTI-1 and albumin [115]. Evidence towards the mechanism of AEP-catalysed cyclisation was provided by an in situ assay that used the enzyme isolated from sunflower seeds [115]. This showed that the enzyme is directly responsible for cyclisation and that the reaction does not involve full hydrolysis of the precursor peptide; this indicates that it catalyses cyclisation by amine attack onto an acyl–enzyme intermediate. Furthermore, AEP is a broad specificity peptidase that can also catalyse regular peptide hydrolysis, including excision of the SFTI-1 core peptide from prealbumin. This means that macrolactam formation is somewhat inefficient and a significant amount of acyclic SFTI-1 is also produced, but this is masked by the rapid in vivo degradation of this unwanted side-product [105].

Gene silencing experiments have linked AEP-like proteins to the macrocylisation of other cyclic plant RiPPs, including kalata-type cyclotides [85] (Figure 8C) and cyclic knottins [116], especially because the ligation site almost always features an Asx residue. *Clitoria ternatea* is a tropical plant that produces cylotides, and a remarkably efficient peptide ligase, butelase 1, was identified from this plant that is capable of cyclising a range of native and non-native peptides of between 14 to 58 residues [117]. This enzyme belongs to the AEP family, but in contrast to sunflower seed AEP, it preferentially

catalyses cyclisation over hydrolysis and is actually the fastest known peptide ligase or cyclase. The variety of unrelated cyclic peptides from phylogenetically distant plant families that are processed by AEP family proteins has led to the theory that this reflects evolutionary parallelism, where AEP functions as a constraining evolutionary channel due to its capacity to catalyse cyclisation [116]. Butelase 1 can also catalyse peptide ligation when a short C-terminal sequence motif of NHV is used as the acceptor, where N is the site of ligation. Conversely, the well-characterised peptide ligase sortase A (SrtA) has been employed to catalyse cyclisation using a cysteine protease-like mechanism [118]. In vivo, this staphylococcal protein ligates proteins with a C-terminal LPXTG motif to the peptidoglycan, via the formation of an enzyme bound thioester on the threonine residue, and has been used widely as an enzymatic tool for ligation to proteins with an LPXTG tag. Cyclisation can be achieved using SrtA by the same principle, although this does require oligo-Gs at the N-terminus for efficient cyclisation [119].

A cysteine protease-like cyclase is proposed in the biosynthesis of autoinducing peptide [120] (AIP). However, its function differs from the above pathways as a thiolactone is generated in AIP biosynthesis (Figure 9). Autoinducing peptides are secreted molecules that form part of a quorum-sensing system in *Staphylococcus* [121]. Heterologous expression in *E. coli* showed that only AgrD (precursor peptide) and AgrB (peptidase) are required for AIP biosynthesis, although AgrD contains an N-terminal signal peptide that is cleaved by an endogenous peptidase [120]. Unlike other macrocyclisation peptidases, AgrB does not belong to a well-characterised peptidase family, but mutagenesis experiments on Cys86 infer that a cysteine protease-like mechanism acts to generate a thioester acyl–enzyme intermediate that is then attacked by Cys28 of AgrD to generate a 16-membered thiolactone [120] (Figure 9).

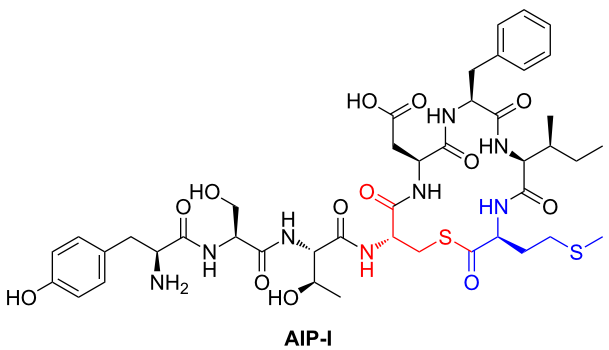

Figure 9: Structure of autoinducing peptide AIP-I from *Staphylococcus aureus* and the sequence of the corresponding precursor peptide AgrD.

Radical SAM-catalysed oxidative cross-linking

The majority of characterised cyclic RiPPs are generated by standard ionic reactions. In contrast, radical mechanisms permit reactions between unactivated atoms [122], and this exotic chemistry is employed in a number of RiPP cyclisations. In each case, cyclisation is catalysed by members of the SPASM protein family [123,124]. These are radical SAM (*S*-adenosylmethionine) proteins that contain two [4Fe–4S] binding domains, and the highly reactive iron–sulphur clusters in these proteins make them capable of carrying out complex oxidative chemistry. This protein family has been named after currently characterised pathways (SPASM = subtilosin, PQQ, anaerobic sulfatase, and mycofactocin), although the mycofactocin pathway has only been described bioinformatically [123]. Subtilosin is a *Bacillus* RiPP antibiotic that belongs to the sactipeptide family of natural products that are defined by the presence of one or more sulphur to α-carbon bonds [125]. Three thioethers in subtilosin are formed by a single SPASM protein, AlbA, and a mechanism was proposed by the Marahiel group based following detailed in vitro studies [26] (Figure 10A). The first [4Fe–4S] cluster accepts an electron from an external source to generate an active reduced form. This electron is transferred to a coordinated SAM, which is reductively cleaved to generate a 5'-deoxyadenosyl radical (5'-dA•). The formation of 5'-dA• is common to all radical SAM proteins. The second [4Fe-4S] cluster coordinates the peptide substrate via a deprotonated thiol group of a cysteine. The 5'-dA• abstracts a hydrogen from a specific α-carbon, which then attacks the thiol bound to the second [4Fe–4S] cluster. To facilitate sulphur to α-carbon bond formation, the second cluster accepts an electron. It is possible that the electron accepted by the second [4Fe–4S] cluster can be transferred to the first cluster by intramolecular electron channeling to convert both clusters into their active forms. A study on thioether bond formation during the biosynthesis of sporulation killing factor, another *Bacillus* sactipeptide, was in agreement with this mechanistic model [126].

Another SPASM protein involved in RiPP cyclisation is found in the biosynthesis of streptide, a streptococcal RiPP that is involved in bacterial communication [127]. Here, StrB catalyses the formation of a carbon–carbon bond between lysine and tryptophan side chains [25]. This is proposed to be mechanistically similar to thioether bond formation, although the role of the second [4Fe–4S] cluster is likely to differ slightly as it is unlikely that either carbon initially bonds to this cluster (Figure 10B). Instead, a radical on the lysine β-carbon (generated by 5'-dA• hydrogen abstraction) attacks C-7 on the tryptophan ring. This generates an indolyl radical that can lose an electron to the second [4Fe–4S] cluster along with simultaneous loss of a proton to rearomatise. An analogous reaction

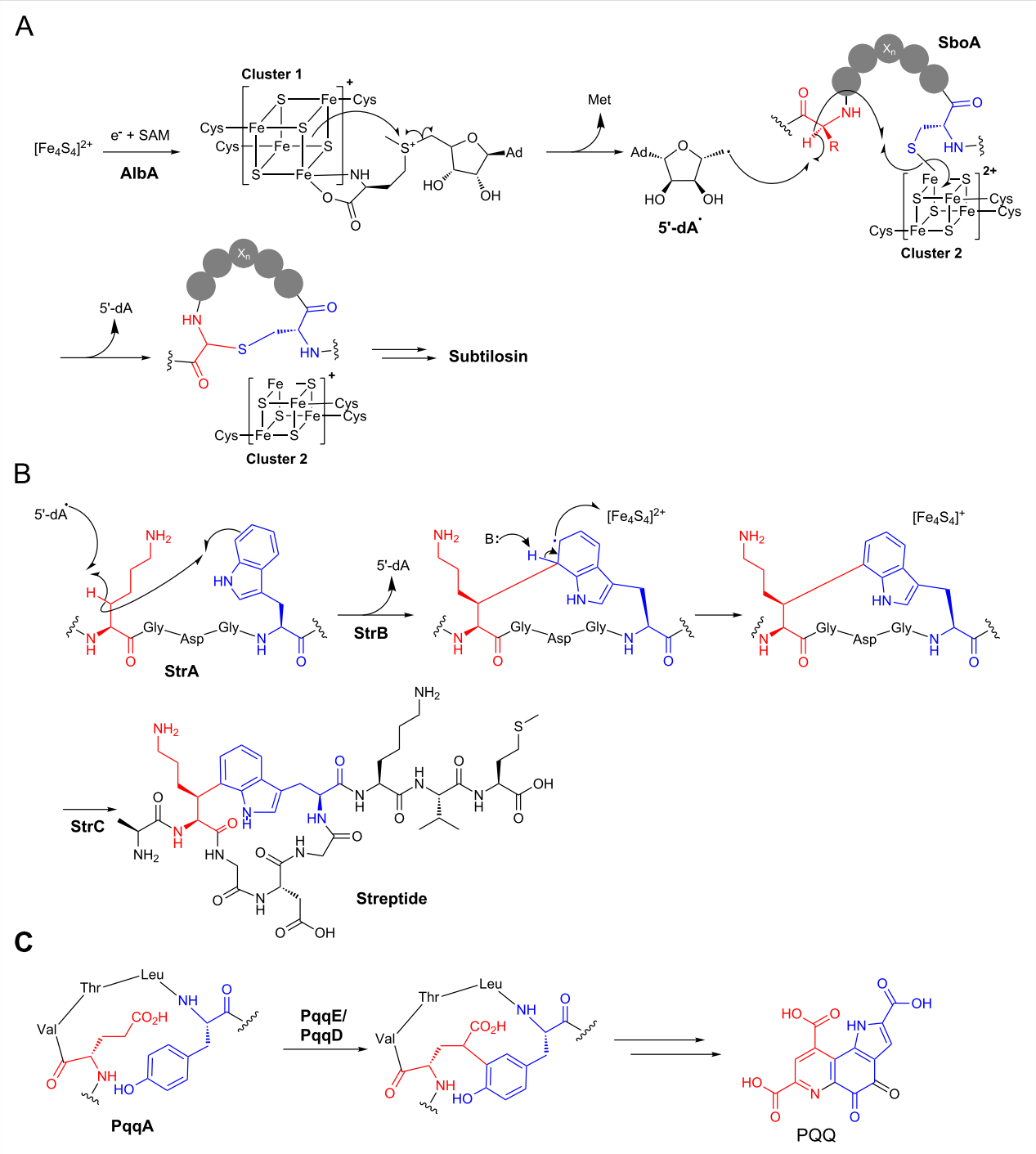

Figure 10: Radical cyclisation in RiPP biosynthesis. A) AlbA-catalysed formation of thioethers in the biosynthesis of subtilosin. The mechanism for deoxyadenosine radical formation is consistent throughout most radical SAM enzymes. B) Mechanism of carbon–carbon cross-linking in streptide biosynthesis. C) Proposed carbon–carbon bond formation by SPASM protein PqqE in the biosynthesis of pyrroloquinoline quinone (PQQ).

takes place in the biosynthesis of the bacterial cofactor pyrroloquinoline quinone (PQQ), where the SPASM protein PqqE was proposed to catalyse the oxidative cross-linking of carbon bonds on glutamate and tyrosine side chains [17] (Figure 10C). This proposal was confirmed by in vitro reconstitution of PqqE activity with PqqA [128]. Interestingly, PqqE activity is dependent on PqqD, a 10 kDa protein that functions as a chaperone that tightly binds PqqA [129]. This key interaction promotes an association with PqqE, which then catalyses cross-linking. A number of SPASM proteins actually have a PqqD-like domain at their N-terminus, including AlbA and ThnB [130]. ThnB catalyses thioether bridge formation in thurincin H biosynthesis,

and in vitro analysis demonstrated that its PqqD-like domain is essential for catalysing thioether formation, but not for SAM cleavage activity [130].

Notable uncharacterised RiPP cyclisations

Despite the huge progress that has been made over the past couple of decades on RiPP cyclisation, there still exist a number of notable pathways where key cyclisation mechanisms have not yet been determined. This is often due to the lack of suitable candidate enzymes, especially in eukaryotic pathways where gene clustering is less common. Otherwise, it could reflect the challenges associated with expression of functional soluble protein or the generation of a suitable substrate for candidate enzymes. A number of these cyclisations are found in partially characterised pathways, such as the S–C cross-link in α-amanitin (Figure 8B) that is formed between cysteine and tryptophan residues (the tryptathionine linkage [131]). The ComQXPA quorum sensing (QS) system [132] found in *Bacillus* species represents another partially characterised pathway that features an unusual cyclised RiPP [133]. Mature ComX is a secreted RiPP that functions as a signal in this QS system, and the cyclised residue is crucial for its bioactivity [134]. The precursor peptide ComX is modified by a isoprenyl transferase (ComQ), which transfers an isoprenyl group to position 3 of the indole side chain of a conserved tryptophan residue [135]. This directly generates a tricyclic structure, presumably via attack of the main chain amide nitrogen onto the iminium intermediate that is generated following prenylation (Figure 11).

Class IV bacteriocins

Class IV bacteriocins are a broad class of cyclic bacterial RiPP where their N- and C-termini are linked by a peptide bond [136]. This broad class consists of globular, α-helical and thermostable cyclic peptides, and includes molecules whose pathways are poorly understood, such as enterocin AS-48 [137,138] (also known as bacteriocin 21 [139]). AS-48 is a 70-residue cyclic antibiotic produced by *Enterococcus faecalis* and was recently shown to enhance the ability of the strain to colonise the mammalian gastrointestinal tract by outcompeting bacteria that are sensitive to AS-48 [140]. A gene cluster has been identified [141], and site-directed mutagenesis has been used to identify key residues in the precursor peptide that are critical for cyclisation [142], but the actual cyclase has not been characterised. One explanation for the limited understanding of this

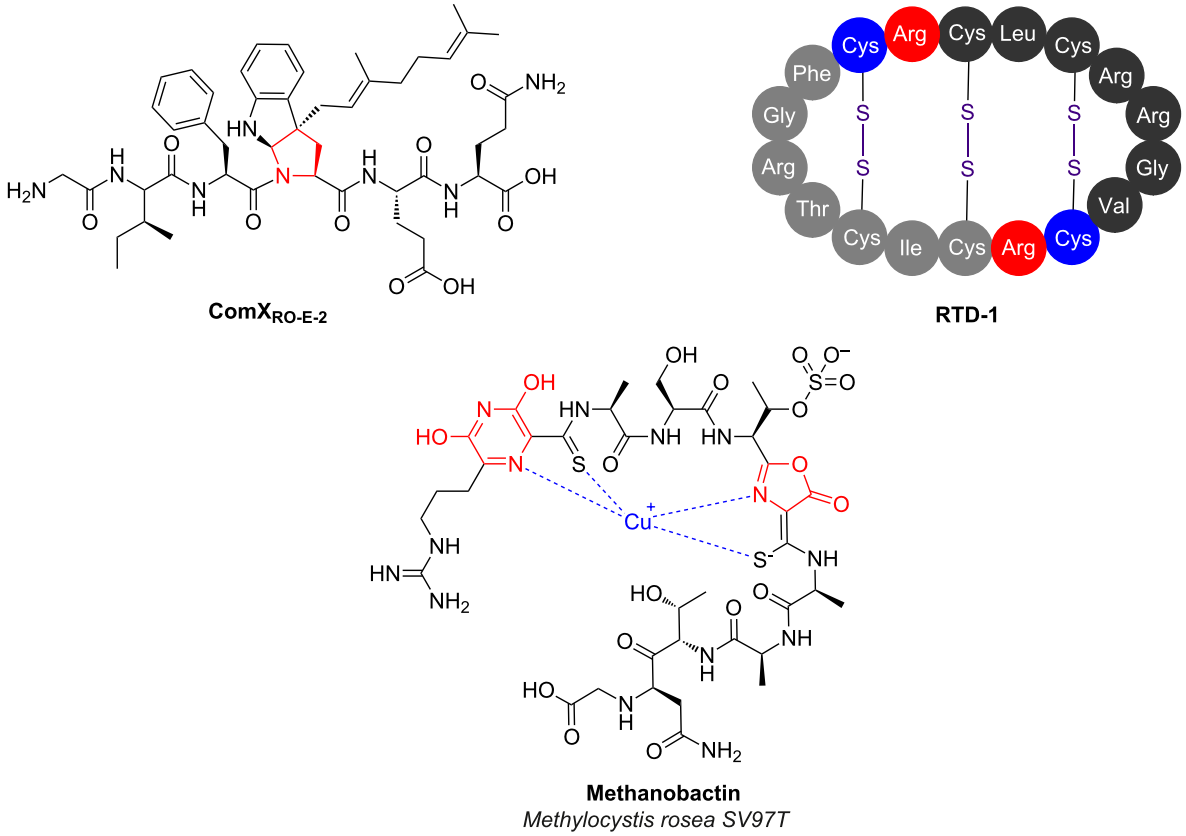

Figure 11: RiPPs with uncharacterised mechanisms of cyclisation. Unusual heterocycles in ComX and methanobactin are indicated in red. RTD-1 is formed by the head-to-tail dimerisation of precursor peptides encoded on two separate genes.

pathway is that the leader peptide removal and cyclisation could be catalysed by membrane associated proteins (perhaps as a complex), which hinders biochemical characterisation. Alternatively, these biosynthetic proteins may exist elsewhere in the *Enterococcus* genome.

Defensins

Mammals produce various antimicrobial peptides (AMPs) that have important roles in the mammalian immune system [143], including in humans [144], and these AMPs often exist as a cocktail of compounds. Many of these are unmodified linear peptides, such as the human peptide cathelicidin LL-37 [145], or are cyclised by disulphide bonds, such as human β-defensin hBD-2 [146]. However, there is one class of backbone-cyclised AMP in mammals, the θ-defensins [84]. These are found in Old World monkeys and orangutans, but are not made by New World monkeys or humans. θ-Defensins, such as RTD-1 (Figure 11), are 18-residue peptides that are formed by the head-to-tail cyclisation of two nonapeptides that are themselves derived from the C-terminal region of precursor peptides, and both heterodimers or homodimers can be formed in this process [84,144]. Along with their antimicrobial activity, these peptides can inhibit fusion of HIV-1 to host cells [147]. Surprisingly, the human genome contains six θ-defensin pseudogenes that are actually expressed [148]. However, these contain premature stop codons that prevent the proper expression of these precursor peptides. Remarkably, aminoglycoside-induced stop codon readthrough of these genes in human-tissue cultures leads to the production of properly cyclised θ-defensins that possess antimicrobial activity [148], indicating that humans have retained the proteins required for processing and cyclisation. The identity of these genes in either humans or monkeys has not been found, although a peptidase-like mechanism can be speculated.

Methanobactins

Methanobactins are copper-binding RiPPs produced by methanotrophic bacteria [149,150]. A methane monooxygenase (MMO) used by these bacteria requires copper as a cofactor, so the requirement for copper with these methanotrophs is much higher than in other bacteria [151]. Therefore, methanobactins assist with copper uptake for these bacteria and have been shown to participate in the control of the "copper-switch" that regulates whether copper-containing or copper-free MMO is expressed [152]. Thus far, methanobactins have been identified that contain oxazolones and pyrazinediones [150,153,154], which are found alongside thioamides in these molecules (Figure 11). These post-translational modifications are critical for copper binding but the mechanisms of these heterocyclisation steps have not yet been determined for any pathway, despite the identification of various gene clusters [150,154]. A bioinformatic analysis showed that methanobactin-like pathways are found in non-methanotrophic bacteria [154], although the products and roles of these gene clusters are currently unknown.

Future challenges

There have been stunning advances in the discovery and characterisation of RiPP post-translational modifications in recent years [5,14]. Much of this has been led by genomics, which has informed both the study of established molecules whose biosynthetic origins were previously unknown (e.g., thiostrepton [72]) and the discovery of new pathways via genome mining [155-157]. However, gene cluster identification does not provide detailed mechanistic information about post-translational modifications and there are numerous examples where key steps in pathways with sequenced gene clusters have not been characterised (see examples above). More widely, it is clear that there are a vast number of uncharacterised pathways encoded in sequenced genomes [8,158]. Many of these are homologous to known RiPP classes, such as uncharacterised lasso peptide and lanthipeptide pathways that are highly prevalent in many bacterial genomes [49,87,159], although it is evident that many novel classes of RiPP await characterisation [7].

Despite the successes reported above, genome mining for novel RiPP clusters is hindered by a number of factors. Firstly, RiPP "gene clusters" can be as small as two genes: a precursor peptide and a tailoring protein, especially when further hydrolytic processing can be carried out by endogenous peptidases [120]. The prevalence of putative small peptides encoded throughout genomes [160] make it difficult to predict which of these are post-translationally processed, and some small genes are overlooked by automated gene annotation software, which means that some putative RiPP precursors are not even listed in databases. Furthermore, novel classes are difficult to identify precisely due to their novelty compared to known pathways. This is in contrast to terpenes, polyketide synthases or NRPSs, whose pathways are all clearly identified by signature protein domains. Finally, many RiPPs do not possess antimicrobial or cytotoxic activity, so are not identified by classical activity-based screens.

Mass spectrometry (MS) represents a relatively unbiased approach to screening for the production of novel RiPPs, although this is non-trivial due to the variety of unusual post-translational modifications that could take place. This means that product masses and fragmentation patterns are very difficult to predict, especially when peptides are cyclised [161]. Despite these issues, significant progress has been made to develop methods to correlate MS data with RiPP genomic data [162], although these methods still have focused on known

RiPP classes with relatively predictable modifications [155-157,161]. The use of ultra-tolerant search terms does allow for the identification of peptides with unexpected post-translational modifications [163], although this method has not been applied to bacterial RiPPs.

To overcome these barriers to discovery, various search algorithms have been developed or adopted to identify truly novel RiPP gene clusters. For example partial phylogenetic profiling was used to propose the currently uncharacterised "mycofactocin" family of gene clusters [123]. A similar approach was also used to propose a family of selenocysteine-containing RiPPs [18]. An alternative approach is to screen for homology to tailoring proteins from known pathways, which can be particularly effective when RiPP-specific protein classes are assessed. For example, thousands of gene clusters with limited homology to TOMMs were identified by searching for clusters associated with YcaO domain proteins [43,164], which are essential for heterocyclisation. These pathways may have some mechanistic similarities with known TOMM pathways, but the diversity of precursor peptide sequences identified, along with novel combinations of predicted tailoring enzymes, indicates that the products of these pathways will be significantly different to known RiPPs. Similar results were obtained when mining for lanthipeptide-like gene clusters [7,53], and widespread searches for pathways with RiPP-like tailoring enzymes can be carried out using BAGEL3 [9]. More generally, a hidden Markov model-based probabilistic algorithm, ClusterFinder, identified hundreds of putative new classes of RiPP alongside novel clusters for the biosynthesis of other natural product classes [8,158]. These bioinformatic analyses all indicate that a vast amount of the RiPP landscape remains unexplored, and a major future challenge will be to determine the both identity and the biological function of these putative metabolites.

Conclusion

A remarkable array of RiPP cyclisation steps have been identified and subsequently mechanistically characterised. These biosynthetic steps enable producing organisms to convert simple ribosomal precursor peptides into complex molecules with exquisite biological activities. There is a degree of commonality between the modification steps that have been characterised for both RiPPs and for other secondary metabolite pathways, but it is interesting to note that there are a significant number of biochemical modifications that, thus far, appear to be unique to RiPP biosynthesis. For example, lanthionine formation, YcaO protein-catalysed heterocyclisation and radical SAM-catalysed thioether cross-links are only found in RiPP biosynthetic pathways. Much recent work on RiPP biosynthesis has been assisted by the rapid identification of gene clusters by next generation sequencing technologies, and this widespread genome sequencing also indicates that there remains a wealth of unexplored pathways to discover and characterise.

Acknowledgements

The author would like to thank Prof. Mervyn Bibb and Dr Javier Santos-Aberturas for helpful comments. This work was supported by a Royal Society University Research Fellowship.

References

1. Marahiel, M. A. *Nat. Prod. Rep.* **2016,** *33,* 136–140. doi:10.1039/C5NP00082C
2. Walsh, C. T. *Nat. Prod. Rep.* **2016,** *33,* 127–135. doi:10.1039/C5NP00035A
3. Lautru, S.; Gondry, M.; Genet, R.; Pernodet, J.-L. *Chem. Biol.* **2002,** *9,* 1355–1364. doi:10.1016/S1074-5521(02)00285-5
4. Gondry, M.; Sauguet, L.; Belin, P.; Thai, R.; Amouroux, R.; Tellier, C.; Tuphile, K.; Jacquet, M.; Braud, S.; Courçon, M.; Masson, C.; Dubois, S.; Lautru, S.; Lecoq, A.; Hashimoto, S.-i.; Genet, R.; Pernodet, J.-L. *Nat. Chem. Biol.* **2009,** *5,* 414–420. doi:10.1038/nchembio.175
5. Arnison, P. G.; Bibb, M. J.; Bierbaum, G.; Bowers, A. A.; Bugni, T. S.; Bulaj, G.; Camarero, J. A.; Campopiano, D. J.; Challis, G. L.; Clardy, J.; Cotter, P. D.; Craik, D. J.; Dawson, M.; Dittmann, E.; Donadio, S.; Dorrestein, P. C.; Entian, K.-D.; Fischbach, M. A.; Garavelli, J. S.; Göransson, U.; Gruber, C. W.; Haft, D. H.; Hemscheidt, T. K.; Hertweck, C.; Hill, C.; Horswill, A. R.; Jaspars, M.; Kelly, W. L.; Klinman, J. P.; Kuipers, O. P.; Link, A. J.; Liu, W.; Marahiel, M. A.; Mitchell, D. A.; Moll, G. N.; Moore, B. S.; MUller, R.; Nair, S. K.; Nes, I. F.; Norris, G. E.; Olivera, B. M.; Onaka, H.; Patchett, M. L.; Piel, J.; Reaney, M. J. T.; Rebuffat, S.; Ross, R. P.; Sahl, H.-G.; Schmidt, E. W.; Selsted, M. E.; Severinov, K.; Shen, B.; Sivonen, K.; Smith, L.; Stein, T.; Süssmuth, R. D.; Tagg, J. R.; Tang, G.-L.; Truman, A. W.; Vederas, J. C.; Walsh, C. T.; Walton, J. D.; Wenzel, S. C.; Willey, J. M.; van der Donk, W. A. *Nat. Prod. Rep.* **2013,** *30,* 108–160. doi:10.1039/C2NP20085F
6. Donia, M. S.; Cimermancic, P.; Schulze, C. J.; Wieland Brown, L. C.; Martin, J.; Mitreva, M.; Clardy, J.; Linington, R. G.; Fischbach, M. A. *Cell* **2014,** *158,* 1402–1414. doi:10.1016/j.cell.2014.08.032
7. Doroghazi, J. R.; Albright, J. C.; Goering, A. W.; Ju, K.-S.; Haines, R. R.; Tchalukov, K. A.; Labeda, D. P.; Kelleher, N. L.; Metcalf, W. W. *Nat. Chem. Biol.* **2014,** *10,* 963–968. doi:10.1038/nchembio.1659
8. Weber, T.; Blin, K.; Duddela, S.; Krug, D.; Kim, H. U.; Bruccoleri, R.; Lee, S. Y.; Fischbach, M. A.; Müller, R.; Wohlleben, W.; Breitling, R.; Takano, E.; Medema, M. H. *Nucleic Acids Res.* **2015,** *43,* W237–W243. doi:10.1093/nar/gkv437
9. van Heel, A. J.; de Jong, A.; Montalbán-López, M.; Kok, J.; Kuipers, O. P. *Nucleic Acids Res.* **2013,** *41,* W448–W453. doi:10.1093/nar/gkt391
10. Crone, W. J. K.; Leeper, F. J.; Truman, A. W. *Chem. Sci.* **2012,** *3,* 3516–3521. doi:10.1039/c2sc21190d
11. Gomez-Escribano, J. P.; Song, L.; Bibb, M. J.; Challis, G. L. *Chem. Sci.* **2012,** *3,* 3522–3525. doi:10.1039/c2sc21183a
12. Huo, L.; Rachid, S.; Stadler, M.; Wenzel, S. C.; Müller, R. *Chem. Biol.* **2012,** *19,* 1278–1287. doi:10.1016/j.chembiol.2012.08.013

13. Hou, Y.; Tianero, M. D. B.; Kwan, J. C.; Wyche, T. P.; Michel, C. R.; Ellis, G. A.; Vazquez-Rivera, E.; Braun, D. R.; Rose, W. E.; Schmidt, E. W.; Bugni, T. S. *Org. Lett.* **2012,** *14,* 5050–5053. doi:10.1021/ol3022758
14. Ortega, M. A.; van der Donk, W. A. *Cell. Chem. Biol.* **2016,** *23,* 31–44. doi:10.1016/j.chembiol.2015.11.012
15. Mocek, U.; Knaggs, A. R.; Tsuchiya, R.; Nguyen, T.; Beale, J. M.; Floss, H. G. *J. Am. Chem. Soc.* **1993,** *115,* 7557–7568. doi:10.1021/ja00070a001
16. Hamada, T.; Matsunaga, S.; Fujiwara, M.; Fujita, K.; Hirota, H.; Schmucki, R.; Güntert, P.; Fusetani, N. *J. Am. Chem. Soc.* **2010,** *132,* 12941–12945. doi:10.1021/ja104616z
17. Puehringer, S.; Metlitzky, M.; Schwarzenbacher, R. *BMC Biochem.* **2008,** *9,* 8. doi:10.1186/1471-2091-9-8
18. Haft, D. H.; Basu, M. K. *J. Bacteriol.* **2011,** *193,* 2745–2755. doi:10.1128/JB.00040-11
19. Deane, C. D.; Melby, J. O.; Molohon, K. J.; Susarrey, A. R.; Mitchell, D. A. *ACS Chem. Biol.* **2013,** *8,* 1998–2008. doi:10.1021/cb4003392
20. Young, T. S.; Dorrestein, P. C.; Walsh, C. T. *Chem. Biol.* **2012,** *19,* 1600–1610. doi:10.1016/j.chembiol.2012.10.013
21. Cotter, P. D.; Deegan, L. H.; Lawton, E. M.; Draper, L. A.; O'Connor, P. M.; Hill, C.; Ross, R. P. *Mol. Microbiol.* **2006,** *62,* 735–747. doi:10.1111/j.1365-2958.2006.05398.x
22. Ruffner, D. E.; Schmidt, E. W.; Heemstra, J. R. *ACS Synth. Biol.* **2015,** *4,* 482–492. doi:10.1021/sb500267d
23. Li, B.; Sher, D.; Kelly, L.; Shi, Y.; Huang, K.; Knerr, P. J.; Joewono, I.; Rusch, D.; Chisholm, S. W.; van der Donk, W. A. *Proc. Natl. Acad. Sci. U. S. A.* **2010,** *107,* 10430–10435. doi:10.1073/pnas.0913677107
24. Melby, J. O.; Nard, N. J.; Mitchell, D. A. *Curr. Opin. Chem. Biol.* **2011,** *15,* 369–378. doi:10.1016/j.cbpa.2011.02.027
25. Schramma, K. R.; Bushin, L. B.; Seyedsayamdost, M. R. *Nat. Chem.* **2015,** *7,* 431–437. doi:10.1038/nchem.2237
26. Flühe, L.; Knappe, T. A.; Gattner, M. J.; Schäfer, A.; Burghaus, O.; Linne, U.; Marahiel, M. A. *Nat. Chem. Biol.* **2012,** *8,* 350–357. doi:10.1038/nchembio.798
27. McIntosh, J. A.; Donia, M. S.; Schmidt, E. W. *Nat. Prod. Rep.* **2009,** *26,* 537. doi:10.1039/b714132g
28. Sinha Roy, R.; Belshaw, P. J.; Walsh, C. T. *Biochemistry* **1998,** *37,* 4125–4136. doi:10.1021/bi9728250
29. Engelhardt, K.; Degnes, K. F.; Zotchev, S. B. *Appl. Environ. Microbiol.* **2010,** *76,* 7093–7101. doi:10.1128/AEM.01442-10
30. Donia, M. S.; Ravel, J.; Schmidt, E. W. *Nat. Chem. Biol.* **2008,** *4,* 341–343. doi:10.1038/nchembio.84
31. Schmidt, E. W.; Nelson, J. T.; Rasko, D. A.; Sudek, S.; Eisen, J. A.; Haygood, M. G.; Ravel, J. *Proc. Natl. Acad. Sci. U. S. A.* **2005,** *102,* 7315–7320. doi:10.1073/pnas.0501424102
32. Kelleher, N. L.; Belshaw, P. J.; Walsh, C. T. *J. Am. Chem. Soc.* **1998,** *120,* 9716–9717. doi:10.1021/ja9822097
33. Milne, J. C.; Roy, R. S.; Eliot, A. C.; Kelleher, N. L.; Wokhlu, A.; Nickels, B.; Walsh, C. T. *Biochemistry* **1999,** *38,* 4768–4781. doi:10.1021/bi982975q
34. Zamble, D. B.; McClure, C. P.; Penner-Hahn, J. E.; Walsh, C. T. *Biochemistry* **2000,** *39,* 16190–16199. doi:10.1021/bi001398e
35. Dunbar, K. L.; Melby, J. O.; Mitchell, D. A. *Nat. Chem. Biol.* **2012,** *8,* 569–575. doi:10.1038/nchembio.944
36. Perler, F. B.; Allewell, N. M. *J. Biol. Chem.* **2014,** *289,* 14488–14489. doi:10.1074/jbc.R114.570531
37. Dunbar, K. L.; Mitchell, D. A. *J. Am. Chem. Soc.* **2013,** *135,* 8692–8701. doi:10.1021/ja4029507
38. Koehnke, J.; Bent, A. F.; Zollman, D.; Smith, K.; Houssen, W. E.; Zhu, X.; Mann, G.; Lebl, T.; Scharff, R.; Shirran, S.; Botting, C. H.; Jaspars, M.; Schwarz-Linek, U.; Naismith, J. H. *Angew. Chem., Int. Ed.* **2013,** *52,* 13991–13996. doi:10.1002/anie.201306302
39. Li, C.; Kappock, T. J.; Stubbe, J.; Weaver, T. M.; Ealick, S. E. *Structure* **1999,** *7,* 1155–1166. doi:10.1016/S0969-2126(99)80182-8
40. Gallimore, A. R.; Spencer, J. B. *Angew. Chem., Int. Ed.* **2006,** *45,* 4406–4413. doi:10.1002/anie.200504284
41. Tosin, M.; Smith, L.; Leadlay, P. F. *Angew. Chem., Int. Ed.* **2011,** *50,* 11930–11933. doi:10.1002/anie.201106323
42. Strader, M. B.; Costantino, N.; Elkins, C. A.; Chen, C. Y.; Patel, I.; Makusky, A. J.; Choy, J. S.; Court, D. L.; Markey, S. P.; Kowalak, J. A. *Mol. Cell. Proteomics* **2011,** *10,* M110. doi:10.1074/mcp.M110.005199
43. Dunbar, K. L.; Chekan, J. R.; Cox, C. L.; Burkhart, B. J.; Nair, S. K.; Mitchell, D. A. *Nat. Chem. Biol.* **2014,** *10,* 823–829. doi:10.1038/nchembio.1608
44. Knerr, P. J.; van der Donk, W. A. *Annu. Rev. Biochem.* **2012,** *81,* 479–505. doi:10.1146/annurev-biochem-060110-113521
45. Rogers, L. A.; Whittier, E. O. *J. Bacteriol.* **1928,** *16,* 211–229.
46. Field, D.; Hill, C.; Cotter, P. D.; Ross, R. P. *Mol. Microbiol.* **2010,** *78,* 1077–1087. doi:10.1111/j.1365-2958.2010.07406.x
47. Xie, L.; Miller, L. M.; Chatterjee, C.; Averin, O.; Kelleher, N. L.; van der Donk, W. A. *Science* **2004,** *303,* 679–681. doi:10.1126/science.1092600
48. Li, B.; Yu, J. P. J.; Brunzelle, J. S.; Moll, G. N.; van der Donk, W. A.; Nair, S. K. *Science* **2006,** *311,* 1464–1467. doi:10.1126/science.1121422
49. Goto, Y.; Li, B.; Claesen, J.; Shi, Y.; Bibb, M. J.; van der Donk, W. A. *PLoS Biol.* **2010,** *8,* e1000339. doi:10.1371/journal.pbio.1000339
50. Garg, N.; Salazar-Ocampo, L. M. A.; van der Donk, W. A. *Proc. Natl. Acad. Sci. U. S. A.* **2013,** *110,* 7258–7263. doi:10.1073/pnas.1222488110
51. Lubelski, J.; Khusainov, R.; Kuipers, O. P. *J. Biol. Chem.* **2009,** *284,* 25962–25972. doi:10.1074/jbc.M109.026690
52. Ortega, M. A.; Hao, Y.; Zhang, Q.; Walker, M. C.; van der Donk, W. A.; Nair, S. K. *Nature* **2015,** *517,* 509–512. doi:10.1038/nature13888
53. Zhang, Q.; Doroghazi, J. R.; Zhao, X.; Walker, M. C.; van der Donk, W. A. *Appl. Environ. Microbiol.* **2015,** *81,* 4339–4350. doi:10.1128/AEM.00635-15
54. Chatterjee, C.; Miller, L. M.; Leung, Y. L.; Xie, L.; Yi, M.; Kelleher, N. L.; van der Donk, W. A. *J. Am. Chem. Soc.* **2005,** *127,* 15332–15333. doi:10.1021/ja0543043
55. You, Y. O.; van der Donk, W. A. *Biochemistry* **2007,** *46,* 5991–6000. doi:10.1021/bi602663x
56. Paul, M.; Patton, G. C.; van der Donk, W. A. *Biochemistry* **2007,** *46,* 6268–6276. doi:10.1021/bi7000104
57. Müller, W. M.; Schmiederer, T.; Ensle, P.; Süssmuth, R. D. *Angew. Chem., Int. Ed.* **2010,** *49,* 2436–2440. doi:10.1002/anie.200905909
58. Goto, Y.; Ökesli, A.; van der Donk, W. A. *Biochemistry* **2011,** *50,* 891–898. doi:10.1021/bi101750r
59. Meindl, K.; Schmiederer, T.; Schneider, K.; Reicke, A.; Butz, D.; Keller, S.; Gühring, H.; Vértesy, L.; Wink, J.; Hoffmann, H.; Brönstrup, M.; Sheldrick, G. M.; Süssmuth, R. D. *Angew. Chem., Int. Ed.* **2010,** *49,* 1151–1154. doi:10.1002/anie.200905773

60. Müller, W. M.; Ensle, P.; Krawczyk, B.; Süssmuth, R. D. *Biochemistry* **2011,** *50,* 8362–8373. doi:10.1021/bi200526q
61. Krawczyk, B.; Ensle, P.; Müller, W. M.; Süssmuth, R. D. *J. Am. Chem. Soc.* **2012,** *134,* 9922–9925. doi:10.1021/ja3040224
62. Sit, C. S.; Yoganathan, S.; Vederas, J. C. *Acc. Chem. Res.* **2011,** *44,* 261–268. doi:10.1021/ar1001395
63. Schnell, N.; Engelke, G.; Augustin, J.; Rosenstein, R.; Ungermann, V.; Götz, F.; Entian, K. D. *Eur. J. Biochem.* **1992,** *204,* 57–68. doi:10.1111/j.1432-1033.1992.tb16605.x
64. Majer, F.; Schmid, D. G.; Altena, K.; Bierbaum, G.; Kupke, T. *J. Bacteriol.* **2002,** *184,* 1234–1243. doi:10.1128/JB.184.5.1234-1243.2002
65. Claesen, J.; Bibb, M. *Proc. Natl. Acad. Sci. U. S. A.* **2010,** *107,* 16297–16302. doi:10.1073/pnas.1008608107
66. Blaesse, M.; Kupke, T.; Huber, R.; Steinbacher, S. *EMBO J.* **2000,** *19,* 6299–6310. doi:10.1093/emboj/19.23.6299
67. Schmid, D. G.; Majer, F.; Kupke, T.; Jung, G. *Rapid Commun. Mass Spectrom.* **2002,** *16,* 1779–1784. doi:10.1002/rcm.780
68. Kupke, T.; Uebele, M.; Schmid, D.; Jung, G.; Blaesse, M.; Steinbacher, S. *J. Biol. Chem.* **2000,** *275,* 31838–31846. doi:10.1074/jbc.M004273200
69. Zhang, Q.; Liu, W. *Nat. Prod. Rep.* **2013,** *30,* 218–226. doi:10.1039/C2NP20107K
70. Su, T. L. *Br. J. Exp. Pathol.* **1948,** *29,* 473–481.
71. Dutcher, J. D.; Vandeputte, J. *Antibiot. Annu.* **1955,** *3,* 560–561.
72. Kelly, W. L.; Pan, L.; Li, C. *J. Am. Chem. Soc.* **2009,** *131,* 4327–4334. doi:10.1021/ja807890a
73. Liao, R.; Duan, L.; Lei, C.; Pan, H.; Ding, Y.; Zhang, Q.; Chen, D.; Shen, B.; Yu, Y.; Liu, W. *Chem. Biol.* **2009,** *16,* 141–147. doi:10.1016/j.chembiol.2009.01.007
74. Wieland Brown, L. C.; Acker, M. G.; Clardy, J.; Walsh, C. T.; Fischbach, M. A. *Proc. Natl. Acad. Sci. U. S. A.* **2009,** *106,* 2549–2553. doi:10.1073/pnas.0900008106
75. Pucci, M. J.; Bronson, J. J.; Barrett, J. F.; DenBleyker, K. L.; Discotto, L. F.; Fung-Tomc, J. C.; Ueda, Y. *Antimicrob. Agents Chemother.* **2004,** *48,* 3697–3701. doi:10.1128/AAC.48.10.3697-3701.2004
76. Kwok, J. M.-M.; Myatt, S. S.; Marson, C. M.; Coombes, R. C.; Constantinidou, D.; Lam, E. W.-F. *Mol. Cancer Ther.* **2008,** *7,* 2022–2032. doi:10.1158/1535-7163.MCT-08-0188
77. Hegde, N. S.; Sanders, D. A.; Rodriguez, R.; Balasubramanian, S. *Nat. Chem.* **2011,** *3,* 725–731. doi:10.1038/nchem.1114
78. Rogers, M. J.; Cundliffe, E.; McCutchan, T. F. *Antimicrob. Agents Chemother.* **1998,** *42,* 715–716.
79. Bycroft, B. W.; Gowland, M. S. *J. Chem. Soc., Chem. Commun.* **1978,** 256–258. doi:10.1039/c39780000256
80. Houck, D. R.; Chen, L. C.; Keller, P. J.; Beale, J. M.; Floss, H. G. *J. Am. Chem. Soc.* **1987,** *109,* 1250–1252. doi:10.1021/ja00238a048
81. Bowers, A. A.; Walsh, C. T.; Acker, M. G. *J. Am. Chem. Soc.* **2010,** *132,* 12182–12184. doi:10.1021/ja104524q
82. Wever, W. J.; Bogart, J. W.; Baccile, J. A.; Chan, A. N.; Schroeder, F. C.; Bowers, A. A. *J. Am. Chem. Soc.* **2015,** *137,* 3494–3497. doi:10.1021/jacs.5b00940
83. Gillon, A. D.; Saska, I.; Jennings, C. V.; Guarino, R. F.; Craik, D. J.; Anderson, M. A. *Plant J.* **2008,** *53,* 505–515. doi:10.1111/j.1365-313X.2007.03357.x
84. Tang, Y.-Q.; Yuan, J.; Ösapay, G.; Ösapay, K.; Tran, D.; Miller, C. J.; Ouellette, A. J.; Selsted, M. E. *Science* **1999,** *286,* 498–502. doi:10.1126/science.286.5439.498
85. Saska, I.; Gillon, A. D.; Hatsugai, N.; Dietzgen, R. G.; Hara-Nishimura, I.; Anderson, M. A.; Craik, D. J. *J. Biol. Chem.* **2007,** *282,* 29721–29728. doi:10.1074/jbc.M705185200
86. Ziemert, N.; Ishida, K.; Liaimer, A.; Hertweck, C.; Dittmann, E. *Angew. Chem., Int. Ed.* **2008,** *47,* 7756–7759. doi:10.1002/anie.200802730
87. Hegemann, J. D.; Zimmermann, M.; Xie, X.; Marahiel, M. A. *Acc. Chem. Res.* **2015,** *48,* 1909–1919. doi:10.1021/acs.accounts.5b00156
88. Philmus, B.; Guerrette, J. P.; Hemscheidt, T. K. *ACS Chem. Biol.* **2009,** *4,* 429–434. doi:10.1021/cb900088r
89. Philmus, B.; Christiansen, G.; Yoshida, W. Y.; Hemscheidt, T. K. *ChemBioChem* **2008,** *9,* 3066–3073. doi:10.1002/cbic.200800560
90. Knappe, T. A.; Manzenrieder, F.; Mas-Moruno, C.; Linne, U.; Sasse, F.; Kessler, H.; Xie, X.; Marahiel, M. A. *Angew. Chem., Int. Ed.* **2011,** *50,* 8714–8717. doi:10.1002/anie.201102190
91. Blond, A.; Péduzzi, J.; Goulard, C.; Chiuchiolo, M. J.; Barthélémy, M.; Prigent, Y.; Salomón, R. A.; Farías, R. N.; Moreno, F.; Rebuffat, S. *Eur. J. Biochem.* **1999,** *259,* 747–755. doi:10.1046/j.1432-1327.1999.00085.x
92. Rosengren, K. J.; Clark, R. J.; Daly, N. L.; Göransson, U.; Jones, A.; Craik, D. J. *J. Am. Chem. Soc.* **2003,** *125,* 12464–12474. doi:10.1021/ja0367703
93. Bayro, M. J.; Mukhopadhyay, J.; Swapna, G. V. T.; Huang, J. Y.; Ma, L.-C.; Sineva, E.; Dawson, P. E.; Montelione, G. T.; Ebright, R. H. *J. Am. Chem. Soc.* **2003,** *125,* 12382–12383. doi:10.1021/ja036677e
94. Wilson, K.-A.; Kalkum, M.; Ottesen, J.; Yuzenkova, J.; Chait, B. T.; Landick, R.; Muir, T.; Severinov, K.; Darst, S. A. *J. Am. Chem. Soc.* **2003,** *125,* 12475–12483. doi:10.1021/ja036756q
95. Duquesne, S.; Destoumieux-Garzón, D.; Zirah, S.; Goulard, C.; Peduzzi, J.; Rebuffat, S. *Chem. Biol.* **2007,** *14,* 793–803. doi:10.1016/j.chembiol.2007.06.004
96. Scofield, M. A.; Lewis, W. S.; Schuster, S. M. *J. Biol. Chem.* **1990,** *265,* 12895–12902.
97. Detlefsen, D. J.; Hill, S. E.; Volk, K. J.; Klohr, S. E.; Tsunakawa, M.; Furumai, T.; Lin, P. F.; Nishio, M.; Kawano, K.; Oki, T.; Lee, M. S. *J. Antibiot.* **1995,** *48,* 1515–1517. doi:10.7164/antibiotics.48.1515
98. Metelev, M.; Tietz, J. I.; Melby, J. O.; Blair, P. M.; Zhu, L.; Livnat, I.; Severinov, K.; Mitchell, D. A. *Chem. Biol.* **2015,** *22,* 241–250. doi:10.1016/j.chembiol.2014.11.017
99. Ishitsuka, M. O.; Kusumi, T.; Kakisawa, H.; Kaya, K.; Watanabe, M. M. *J. Am. Chem. Soc.* **1990,** *112,* 8180–8182. doi:10.1021/ja00178a060
100. Okino, T.; Matsuda, H.; Murakami, M.; Yamaguchi, K. *Tetrahedron* **1995,** *51,* 10679–10686. doi:10.1016/0040-4020(95)00645-O
101. Murakami, M.; Sun, Q.; Ishida, K.; Matsuda, H.; Okino, T.; Yamaguchi, K. *Phytochemistry* **1997,** *45,* 1197–1202. doi:10.1016/S0031-9422(97)00131-3
102. Rohrlack, T.; Christoffersen, K.; Hansen, P. E.; Zhang, W.; Czarnecki, O.; Henning, M.; Fastner, J.; Erhard, M.; Neilan, B. A.; Kaebernick, M. *J. Chem. Ecol.* **2003,** *29,* 1757–1770. doi:10.1023/A:1024889925732
103. Ziemert, N.; Ishida, K.; Weiz, A.; Hertweck, C.; Dittmann, E. *Appl. Environ. Microbiol.* **2010,** *76,* 3568–3574. doi:10.1128/AEM.02858-09
104. Lee, J.; McIntosh, J.; Hathaway, B. J.; Schmidt, E. W. *J. Am. Chem. Soc.* **2009,** *131,* 2122–2124. doi:10.1021/ja8092168
105. Bernath-Levin, K.; Nelson, C.; Elliott, A. G.; Jayasena, A. S.; Millar, A. H.; Craik, D. J.; Mylne, J. S. *Chem. Biol.* **2015,** *22,* 571–582. doi:10.1016/j.chembiol.2015.04.010

106. Bergmann, M.; Behrens, O. K. *J. Biol. Chem.* **1938,** *124,* 7–10.
107. Koehnke, J.; Bent, A.; Houssen, W. E.; Zollman, D.; Morawitz, F.; Shirran, S.; Vendome, J.; Nneoyiegbe, A. F.; Trembleau, L.; Botting, C. H.; Smith, M. C. M.; Jaspars, M.; Naismith, J. H. *Nat. Struct. Mol. Biol.* **2012,** *19,* 767–772. doi:10.1038/nsmb.2340
108. Sardar, D.; Lin, Z.; Schmidt, E. W. *Chem. Biol.* **2015,** *22,* 907–916. doi:10.1016/j.chembiol.2015.06.014
109. Barber, C. J. S.; Pujara, P. T.; Reed, D. W.; Chiwocha, S.; Zhang, H.; Covello, P. S. *J. Biol. Chem.* **2013,** *288,* 12500–12510. doi:10.1074/jbc.M112.437947
110. Wieland, T.; Faulstich, H.; Fiume, L. *CRC Crit. Rev. Biochem.* **1978,** *5,* 185–260. doi:10.3109/10409237809149870
111. Bushnell, D. A.; Cramer, P.; Kornberg, R. D. *Proc. Natl. Acad. Sci. U. S. A.* **2002,** *99,* 1218–1222. doi:10.1073/pnas.251664698
112. Hallen, H. E.; Luo, H.; Scott-Craig, J. S.; Walton, J. D. *Proc. Natl. Acad. Sci. U. S. A.* **2007,** *104,* 19097–19101. doi:10.1073/pnas.0707340104
113. Luo, H.; Hong, S.-Y.; Sgambelluri, R. M.; Angelos, E.; Li, X.; Walton, J. D. *Chem. Biol.* **2014,** *21,* 1610–1617. doi:10.1016/j.chembiol.2014.10.015
114. Mulvenna, J. P.; Foley, F. M.; Craik, D. J. *J. Biol. Chem.* **2005,** *280,* 32245–32253. doi:10.1074/jbc.M506060200
115. Mylne, J. S.; Colgrave, M. L.; Daly, N. L.; Chanson, A. H.; Elliott, A. G.; McCallum, E. J.; Jones, A.; Craik, D. J. *Nat. Chem. Biol.* **2011,** *7,* 257–259. doi:10.1038/nchembio.542
116. Mylne, J. S.; Chan, L. Y.; Chanson, A. H.; Daly, N. L.; Schaefer, H.; Bailey, T. L.; Nguyencong, P.; Cascales, L.; Craik, D. J. *Plant Cell* **2012,** *24,* 2765–2778. doi:10.1105/tpc.112.099085
117. Nguyen, G. K. T.; Wang, S.; Qiu, Y.; Hemu, X.; Lian, Y.; Tam, J. P. *Nat. Chem. Biol.* **2014,** *10,* 732–738. doi:10.1038/nchembio.1586
118. van 't Hof, W.; Hansenová Maňásková, S.; Veerman, E. C. I.; Bolscher, J. G. M. *Biol. Chem.* **2015,** *396,* 283–293. doi:10.1515/hsz-2014-0260
119. Wu, Z.; Guo, X.; Guo, Z. *Chem. Commun.* **2011,** *47,* 9218–9220. doi:10.1039/c1cc13322e
120. Thoendel, M.; Horswill, A. R. *J. Biol. Chem.* **2009,** *284,* 21828–21838. doi:10.1074/jbc.M109.031757
121. Dunman, P. M.; Murphy, E.; Haney, S.; Palacios, D.; Tucker-Kellogg, G.; Wu, S.; Brown, E. L.; Zagursky, R. J.; Shlaes, D.; Projan, S. J. *J. Bacteriol.* **2001,** *183,* 7341–7353. doi:10.1128/JB.183.24.7341-7353.2001
122. Shisler, K. A.; Broderick, J. B. *Curr. Opin. Struct. Biol.* **2012,** *22,* 701–710. doi:10.1016/j.sbi.2012.10.005
123. Haft, D. H. *BMC Genomics* **2011,** *12,* 21. doi:10.1186/1471-2164-12-21
124. Grell, T. A. J.; Goldman, P. J.; Drennan, C. L. *J. Biol. Chem.* **2015,** *290,* 3964–3971. doi:10.1074/jbc.R114.581249
125. Kawulka, K.; Sprules, T.; McKay, R. T.; Mercier, P.; Diaper, C. M.; Zuber, P.; Vederas, J. C. *J. Am. Chem. Soc.* **2003,** *125,* 4726–4727. doi:10.1021/ja029654t
126. Flühe, L.; Burghaus, O.; Wieckowski, B. M.; Giessen, T. W.; Linne, U.; Marahiel, M. A. *J. Am. Chem. Soc.* **2013,** *135,* 959–962. doi:10.1021/ja310542g
127. Ibrahim, M.; Guillot, A.; Wessner, F.; Algaron, F.; Besset, C.; Courtin, P.; Gardan, R.; Monnet, V. *J. Bacteriol.* **2007,** *189,* 8844–8854. doi:10.1128/JB.01057-07
128. Barr, I.; Latham, J. A.; Iavarone, A. T.; Chantarojsiri, T.; Hwang, J. D.; Klinman, J. P. *J. Biol. Chem.* **2016,** *291,* 8877–8884. doi:10.1074/jbc.C115.699918
129. Latham, J. A.; Iavarone, A. T.; Barr, I.; Juthani, P. V.; Klinman, J. P. *J. Biol. Chem.* **2015,** *290,* 12908–12918. doi:10.1074/jbc.M115.646521
130. Wieckowski, B. M.; Hegemann, J. D.; Mielcarek, A.; Boss, L.; Burghaus, O.; Marahiel, M. A. *FEBS Lett.* **2015,** *589,* 1802–1806. doi:10.1016/j.febslet.2015.05.032
131. May, J. P.; Perrin, D. M. *Biopolymers* **2007,** *88,* 714–724. doi:10.1002/bip.20807
132. Oslizlo, A.; Stefanic, P.; Dogsa, I.; Mandic-Mulec, I. *Proc. Natl. Acad. Sci. U. S. A.* **2014,** *111,* 1586–1591. doi:10.1073/pnas.1316283111
133. Okada, M.; Sato, I.; Cho, S. J.; Iwata, H.; Nishio, T.; Dubnau, D.; Sakagami, Y. *Nat. Chem. Biol.* **2005,** *1,* 23–24. doi:10.1038/nchembio709
134. Tsuji, F.; Kobayashi, K.; Okada, M.; Yamaguchi, H.; Ojika, M.; Sakagami, Y. *Bioorg. Med. Chem. Lett.* **2011,** *21,* 4041–4044. doi:10.1016/j.bmcl.2011.04.123
135. Tsuji, F.; Ishihara, A.; Kurata, K.; Nakagawa, A.; Okada, M.; Kitamura, S.; Kanamaru, K.; Masuda, Y.; Murakami, K.; Irie, K.; Sakagami, Y. *FEBS Lett.* **2012,** *586,* 174–179. doi:10.1016/j.febslet.2011.12.012
136. Maqueda, M.; Sánchez-Hidalgo, M.; Fernández, M.; Montalbán-López, M.; Valdivia, E.; Martínez-Bueno, M. *FEMS Microbiol. Rev.* **2008,** *32,* 2–22. doi:10.1111/j.1574-6976.2007.00087.x
137. González, C.; Langdon, G. M.; Bruix, M.; Gálvez, A.; Valdivia, E.; Maqueda, M.; Rico, M. *Proc. Natl. Acad. Sci. U. S. A.* **2000,** *97,* 11221–11226. doi:10.1073/pnas.210301097
138. Sánchez-Hidalgo, M.; Montalbán-López, M.; Cebrián, R.; Valdivia, E.; Martínez-Bueno, M.; Maqueda, M. *Cell. Mol. Life Sci.* **2011,** *68,* 2845–2857. doi:10.1007/s00018-011-0724-4
139. Tomita, H.; Fujimoto, S.; Tanimoto, K.; Ike, Y. *J. Bacteriol.* **1997,** *179,* 7843–7855.
140. Kommineni, S.; Bretl, D. J.; Lam, V.; Chakraborty, R.; Hayward, M.; Simpson, P.; Cao, Y.; Bousounis, P.; Kristich, C. J.; Salzman, N. H. *Nature* **2015,** *526,* 719–722. doi:10.1038/nature15524
141. Martínez-Bueno, M.; Valdivia, E.; Gálvez, A.; Coyette, J.; Maqueda, M. *Mol. Microbiol.* **1998,** *27,* 347–358. doi:10.1046/j.1365-2958.1998.00682.x
142. Cebrián, R.; Maqueda, M.; Neira, J. L.; Valdivia, E.; Martínez-Bueno, M.; Montalbán-López, M. *Appl. Environ. Microbiol.* **2010,** *76,* 7268–7276. doi:10.1128/AEM.01154-10
143. Ganz, T. *Nat. Rev. Immunol.* **2003,** *3,* 710–720. doi:10.1038/nri1180
144. Wiesner, J.; Vilcinskas, A. *Virulence* **2010,** *1,* 440–464. doi:10.4161/viru.1.5.12983
145. Ciornei, C. D.; Sigurdardóttir, T.; Schmidtchen, A.; Bodelsson, M. *Antimicrob. Agents Chemother.* **2005,** *49,* 2845–2850. doi:10.1128/AAC.49.7.2845-2850.2005
146. Harder, J.; Bartels, J.; Christophers, E.; Schröder, J.-M. *Nature* **1997,** *387,* 861. doi:10.1038/43088
147. Cole, A. M.; Hong, T.; Boo, L. M.; Nguyen, T.; Zhao, C.; Bristol, G.; Zack, J. A.; Waring, A. J.; Yang, O. O.; Lehrer, R. I. *Proc. Natl. Acad. Sci. U. S. A.* **2002,** *99,* 1813–1818. doi:10.1073/pnas.052706399
148. Venkataraman, N.; Cole, A. L.; Ruchala, P.; Waring, A. J.; Lehrer, R. I.; Stuchlik, O.; Pohl, J.; Cole, A. M. *PLoS Biol.* **2009,** *7,* e1000095. doi:10.1371/journal.pbio.1000095
149. Kim, H. J.; Graham, D. W.; DiSpirito, A. A.; Alterman, M. A.; Galeva, N.; Larive, C. K.; Asunskis, D.; Sherwood, P. M. A. *Science* **2004,** *305,* 1612–1615. doi:10.1126/science.1098322

150. Krentz, B. D.; Mulheron, H. J.; Semrau, J. D.; DiSpirito, A. A.; Bandow, N. L.; Haft, D. H.; Vuilleumier, S.; Murrell, J. C.; McEllistrem, M. T.; Hartsel, S. C.; Gallagher, W. H. *Biochemistry* **2010,** *49,* 10117–10130. doi:10.1021/bi1014375
151. El Ghazouani, A.; Baslé, A.; Firbank, S. J.; Knapp, C. W.; Gray, J.; Graham, D. W.; Dennison, C. *Inorg. Chem.* **2011,** *50,* 1378–1391. doi:10.1021/ic101965j
152. Semrau, J. D.; Jagadevan, S.; DiSpirito, A. A.; Khalifa, A.; Scanlan, J.; Bergman, B. H.; Freemeier, B. C.; Baral, B. S.; Bandow, N. L.; Vorobev, A.; Haft, D. H.; Vuilleumier, S.; Murrell, J. C. *Environ. Microbiol.* **2013,** *15,* 3077–3086. doi:10.1111/1462-2920.12150
153. Behling, L. A.; Hartsel, S. C.; Lewis, D. E.; DiSpirito, A. A.; Choi, D. W.; Masterson, L. R.; Veglia, G.; Gallagher, W. H. *J. Am. Chem. Soc.* **2008,** *130,* 12604–12605. doi:10.1021/ja804747d
154. Kenney, G. E.; Rosenzweig, A. C. *BMC Biol.* **2013,** *11,* 17. doi:10.1186/1741-7007-11-17
155. Kersten, R. D.; Yang, Y.-L.; Xu, Y.; Cimermancic, P.; Nam, S.-J.; Fenical, W.; Fischbach, M. A.; Moore, B. S.; Dorrestein, P. C. *Nat. Chem. Biol.* **2011,** *7,* 794–802. doi:10.1038/nchembio.684
156. Mohimani, H.; Kersten, R. D.; Liu, W.-T.; Wang, M.; Purvine, S. O.; Wu, S.; Brewer, H. M.; Pasa-Tolic, L.; Bandeira, N.; Moore, B. S.; Pevzner, P. A.; Dorrestein, P. C. *ACS Chem. Biol.* **2014,** *9,* 1545–1551. doi:10.1021/cb500199h
157. Medema, M. H.; Paalvast, Y.; Nguyen, D. D.; Melnik, A.; Dorrestein, P. C.; Takano, E.; Breitling, R. *PLoS Comput. Biol.* **2014,** *10,* e1003822. doi:10.1371/journal.pcbi.1003822
158. Cimermancic, P.; Medema, M. H.; Claesen, J.; Kurita, K.; Wieland Brown, L. C.; Mavrommatis, K.; Pati, A.; Godfrey, P. A.; Koehrsen, M.; Clardy, J.; Birren, B. W.; Takano, E.; Sali, A.; Linington, R. G.; Fischbach, M. A. *Cell* **2014,** *158,* 412–421. doi:10.1016/j.cell.2014.06.034
159. Maksimov, M. O.; Pelczer, I.; Link, A. J. *Proc. Natl. Acad. Sci. U. S. A.* **2012,** *109,* 15223–15228. doi:10.1073/pnas.1208978109
160. Rey, J.; Deschavanne, P.; Tuffery, P. *Database* **2014,** No. bau106. doi:10.1093/database/bau106
161. Mohimani, H.; Liu, W.-T.; Mylne, J. S.; Poth, A. G.; Colgrave, M. L.; Tran, D.; Selsted, M. E.; Dorrestein, P. C.; Pevzner, P. A. *J. Proteome Res.* **2011,** *10,* 4505–4512. doi:10.1021/pr200323a
162. Mohimani, H.; Pevzner, P. A. *Nat. Prod. Rep.* **2016,** *33,* 73–86. doi:10.1039/C5NP00050E
163. Chick, J. M.; Kolippakkam, D.; Nusinow, D. P.; Zhai, B.; Rad, R.; Huttlin, E. L.; Gygi, S. P. *Nat. Biotechnol.* **2015,** *33,* 743–749. doi:10.1038/nbt.3267
164. Cox, C. L.; Doroghazi, J. R.; Mitchell, D. A. *BMC Genomics* **2015,** *16,* 778. doi:10.1186/s12864-015-2008-0

License and Terms

BEILSTEIN JOURNAL OF ORGANIC CHEMISTRY

Biosynthesis of oxygen and nitrogen-containing heterocycles in polyketides

Franziska Hemmerling[1,2] and Frank Hahn[*1,2]

Review

Open Access

Address:
[1]Institut für Organische Chemie and Zentrum für Biomolekulare Wirkstoffe, Gottfried Wilhelm Leibniz Universität Hannover, Schneiderberg 38, 30167 Hannover, Germany and [2]Fakultät für Biologie, Chemie und Geowissenschaften, Universität Bayreuth, Universitätsstraße 30, 95440 Bayreuth, Germany

Email:
Frank Hahn[*] - frank.hahn@uni-bayreuth.de

* Corresponding author

Keywords:
biosynthesis; chemoenzymatic synthesis; enzymology; heterocycles; polyketides

Beilstein J. Org. Chem. **2016,** *12,* 1512–1550.
doi:10.3762/bjoc.12.148

Received: 01 April 2016
Accepted: 22 June 2016
Published: 20 July 2016

This article is part of the Thematic Series "Natural products in synthesis and biosynthesis II".

Guest Editor: J. S. Dickschat

Abstract

This review highlights the biosynthesis of heterocycles in polyketide natural products with a focus on oxygen and nitrogen-containing heterocycles with ring sizes between 3 and 6 atoms. Heterocycles are abundant structural elements of natural products from all classes and they often contribute significantly to their biological activity. Progress in recent years has led to a much better understanding of their biosynthesis. In this context, plenty of novel enzymology has been discovered, suggesting that these pathways are an attractive target for future studies.

Introduction

Heterocycles

Heterocycles are important structural elements, which are present in natural products from all classes and also in many biologically active synthetic compounds. They often contribute significantly to their structural and physical properties as well as to their biological activity [1-3]. Heterocycles can for example be involved in cation complexation as known for ionophoric polyethers or introduce conformational rigidity into a molecule, which is crucial for target binding [4].

Oxygen heterocycles are mainly found in carbohydrates, polyketides, peptides and terpenoids. Nitrogen heterocycles are part of peptides and alkaloids. Both can of course also occur in the respective hybrid natural products. Sulphur-containing heterocycles are present in few polyketides and more widespread in peptidic natural products of both, non-ribosomal and post-ribosomal modified origin [5].

The biosynthetic mechanisms for heterocycle formation are numerous, and range from simple addition or condensation reactions to oxidative ring closures. The large number of mechanistically different cyclisation modes triggers the interest on the responsible enzymes. Due to the relevance of heterocycles, under-

standing the enzymology of heterocycle formation is also an important milestone on the way to using the enzymes as chemoenzymatic tools in natural product synthesis and medicinal chemistry [6,7].

Polyketides

Polyketide natural products are biosynthesised by polyketide synthases (PKSs) of the types I–III. Type I PKS are multimodular megaenzyme complexes that produce linear, reduced polyketides in an assembly line process that uses acyl carrier proteins (ACP), ketosynthase (KS) and acyl transferase (AT) domains as well as ketoreductase (KR), dehydratase (DH), enoyl reductase (ER) and thioesterase (TE) domains [6,8]. The PKS intermediates remain tethered to the megaenzyme via a thioester linkage during the whole process.

Among these domains, only TE domains participate in cyclisation reactions as part of their standard catalytic repertoire (Scheme 1). They transacylate the thioester of a PKS-bound polyketide onto a nucleophile. If the nucleophile is water, this leads to carboxylic acids. The reactions of backbone hydroxy groups or amines consequently give lactones and lactams. TE domains mostly form macrocycles or more rarely medium-sized and small cycles with defined size.

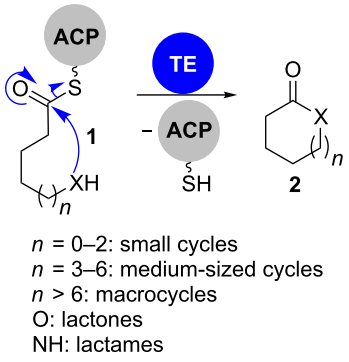

Scheme 1: Schematic description of the cyclisation reaction catalysed by TE domains. In most cases, the nucleophile "X" represents oxygen or nitrogen leading to lactones or lactams, respectively.

Type II and type III PKS are mono-modular and form aromatic structures. Their gene clusters can contain additional cyclase/aromatase domains and a chain-length factor that together force particular folding patterns of a polyketone precursor and thus particular ring systems [9-11].

Most heterocycles in polyketides are formed by specialised PKS domains and tailoring enzymes. These can be active during assembly of the nascent PKS precursor (as for example in the case of pyran/furan formation via oxa-Michael addition, see chapters 1.1.1 and 1.2.1), during the cleavage of the fully elongated precursor from the PKS (as for example for tetronates, tetramates and pyridinones, see chapters 1.7.1, 2.2.1 and 2.1.3) or during post-PKS tailoring (as for example during oxidative cyclisation in aureothin biosynthesis, see chapter 1.2.2).

This review intends to give an overview on the mechanisms involved in heterocycle formation during polyketide biosynthesis. A focus will be placed on oxygen and nitrogen-containing heterocycles due to their abundance and relevance.

Although the genuine polyketide biosynthesis machinery does not harbour enzymatic units that introduce nitrogen, we expanded the scope of this article to those products of polyketide synthase–non ribosomal peptide synthetase (NRPS) hybrid systems in which the polyketide portion strongly dominates the overall structure and in which the amino acid nitrogens are incorporated into the respective heterocycles.

We will not cover medium-sized and macrocyclic lactones and lactams, but concentrate on small heterocycles with ring sizes between 3 and 6 atoms (for a review about macrolactones see reference [12]).

Review

1 Oxygen-containing heterocycles

Oxygen-containing heterocycles are biosynthesised in seven principal ways (Scheme 2). Those comprise nucleophilic addition of a hydroxy group to electrophiles like epoxides **4**, carbonyl groups **6** or Michael acceptors **9**, potentially followed by further processing (a–c in Scheme 2).

Lactones **12** are formed by transacylation of a thioester to a hydroxy group (d in Scheme 2). A Michael addition–lactonisation cascade leads to pyranones with a substituent in the 4-position **16** (e in Scheme 2). 3-Acylfuran-2-ones (**19**, 3-acyltetronates) are formed by acylation–Dieckmann condensation between 2-hydroxythioesters **18** and β-ketothioesters **17** (f in Scheme 2). The oxidative cyclisation after C–H activation of alkyl carbons is known for the formation of furan rings **21** (g in Scheme 2).

1.1 Pyrans

1.1.1 oxa-Michael addition: The oxa-Michael addition on an α,β-unsaturated thioester intermediate leads to oxygen heterocycles along with the formation of up to two new stereocentres. Its appearance in several polyketide biosynthetic pathways was proposed for a decade based on gene cluster analysis. An in vitro characterisation of responsible catalytic units has however only recently been achieved. Two pyran-forming cyclase domains were characterised in the pederin (**24**) and the ambru-

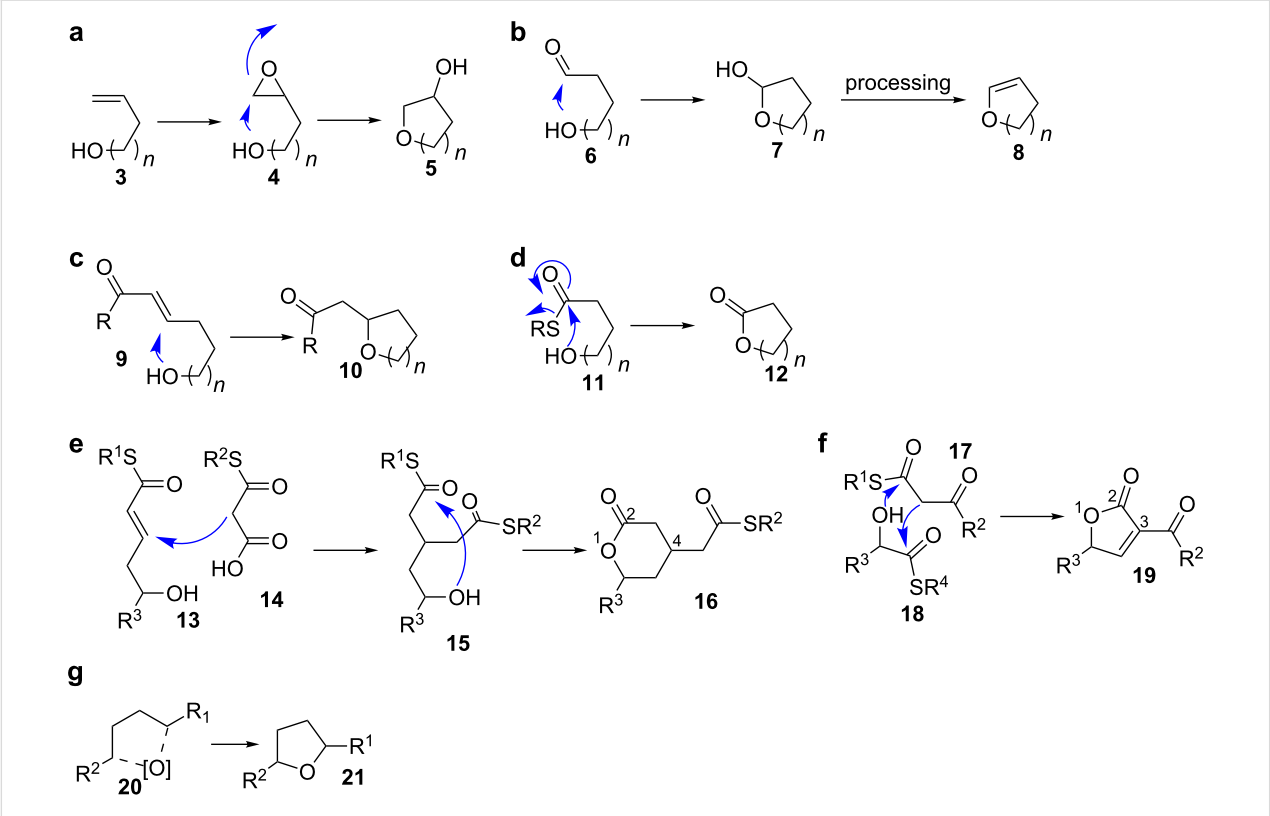

Scheme 2: Mechanisms for the formation of oxygen heterocycles. The degree of substitution can differ from that shown in the scheme. In b, other modes of processing are possible in the second step. Partially redrawn from [13].

ticin (**28**) biosynthetic pathways (Scheme 3 and Scheme 4) [14,15].

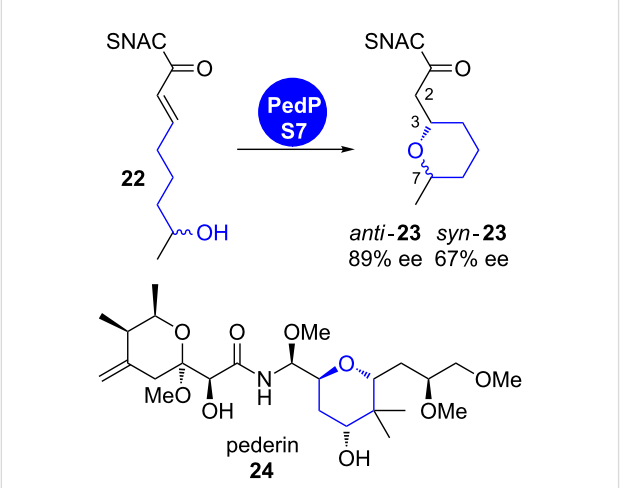

Scheme 3: Pyran-ring formation in pederin (**24**) biosynthesis. Incubation of recombinant PedPS7 with substrate surrogate **22** gave conversion into cyclic stereoisomers *anti*-**23** and *syn*-**23** [14].

PedPS7 is a monofunctional pyran synthase (PS) domain that was predicted to catalyse ring formation from an α,β-unsaturated intermediate in the biosynthesis of the PKS–NRPS hybrid product pederin (**24**) [16,17]. The recombinant, isolated domain transformed both enantiomers of the structurally simplified tetraketidic precursor surrogate **22** into cyclised products *anti*-**23** and *syn*-**23** (Scheme 3a) [14]. The in vitro reaction with PedPS7 proceeds with moderate stereoselectivity irrespective of the configuration of the substrate at C7.

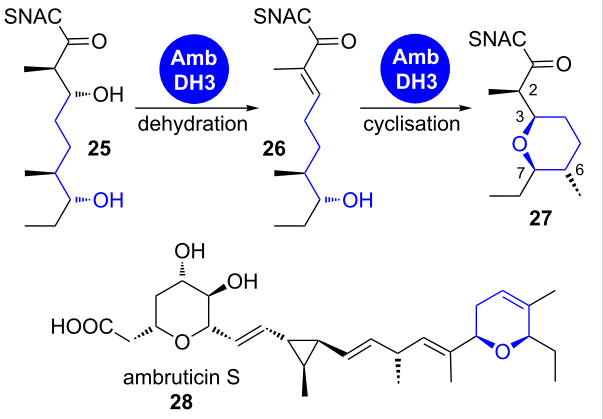

Scheme 4: The domain AmbDH3 from ambruticin biosynthesis catalyses the dehydration of **25** and subsequent cyclisation to tetrahydropyran **27** with high stereoselectivity [15].

PS domains are common in *trans*-AT PKS clusters and participate in the biosynthesis of such important compounds as bryostatin and sorangicin. They are related to DH domains on the amino acid sequence level, but show a significant mutation of a DH-characteristic aspartic acid to a histidine or an asparagine residue in their active site. This exchange avoids the dehydration reaction and might facilitate the activation of the hydroxy group for nucleophilic attack on the Michael system by proton abstraction. PS domains also form a distinct phylogenetic clade compared to DH domains. Within a module, PS domains are usually located adjacent to DH domains and act on their transiently formed dehydration product [14].

The arrangement is somewhat different in the case of AmbDH3 from ambruticin biosynthesis (Scheme 4) [15]. This bifunctional domain catalyses both steps, dehydration of a 3-hydroxythioester intermediate **25** and subsequent cyclisation to a tetrahydropyran ring **27**. AmbDH3 is currently the only known case of a pyran-forming domain in a *cis*-AT PKS.

Hahn et al. showed that AmbDH3 catalyses dehydration of only the 2-D,3-D-configured precursor **25** to the *E*-configured olefin intermediate **26** and subsequent cyclisation to **27** (Scheme 4). The C6 epimers of compounds **25** and **26** were also accepted, but with much lower conversion. In both cases, the configuration at C2 in the cyclic product was exclusively D, highlighting the high stereoselectivity of the domain-catalysed reaction. The ambruticins contain a second hydropyran ring that is established by epoxide opening (see chapter 1.1.3).

A further enzyme with similar dehydratase–cyclase activity was recently discovered by Leadlay et al. in the biosynthesis of the polyether ionophore salinomycin (**31**, Scheme 5) [18]. SalBIII is a pyran-forming cyclase that was originally annotated as an epoxide hydrolase/cyclase.

The putative biosynthetic precursor **29** was isolated from a gene knockout strain and used in an in vitro assay. The recombinant enzyme converted this compound into the cyclised salinomycin precursor **30**. The proposed mechanism also proceeds via a dehydration–oxa-Michael addition cascade. A crystal structure revealed two crucial aspartic acid residues as candidates for the acid–base catalysis occurring in the active site [18].

1.1.2 Processing of hemiacetals: Reduction or alkylation of hemiacetals in the presence of Lewis acids is a common synthetic strategy for making pyrans and furans. Hemiacetals are also biosynthesis intermediates where they are transformed into individually functionalised heterocycles or acetals. In many cases, these hemiacetals are also appropriately activated to react further spontaneously. The involvement of individual enzymes in these reactions has only been shown in a few cases.

Pyranonaphtoquinones. Pyranonaphtoquinones are a subclass of bacterial and fungal polyketides with an aglycone core, which is built up of a naphthalenedione and an annelated pyran ring (Figure 1) [19,20].

Their biosynthesis can be divided into three parts: the assembly of the PKS carbon backbone by a type II PKS including formation of the carbocyclic aromatic core, post-PKS modifications leading to the installation of the oxygen heterocycle and third, its modification by diverse tailoring enzymes [21,22].

The actinorhodin (**34**) PKS is probably the best studied type II PKS and has been used as a model system for understanding basic features of such iterative bacterial systems. The respective biosynthetic gene cluster had already been cloned in 1984 and the genes were sequenced in 1992 (Scheme 6) [23,24].

As for most pyranonaphtoquinones, seven rounds of chain extensions followed by controlled cyclisation yield the reactive intermediate **38** after release from the PKS [25,26]. The intermediate is prepared for the action of ActVI-1, which is annotated as a 3-hydroxyacyl-coenzyme A (CoA) dehydrogenase (3HAD). Enzymes of this family catalyse the

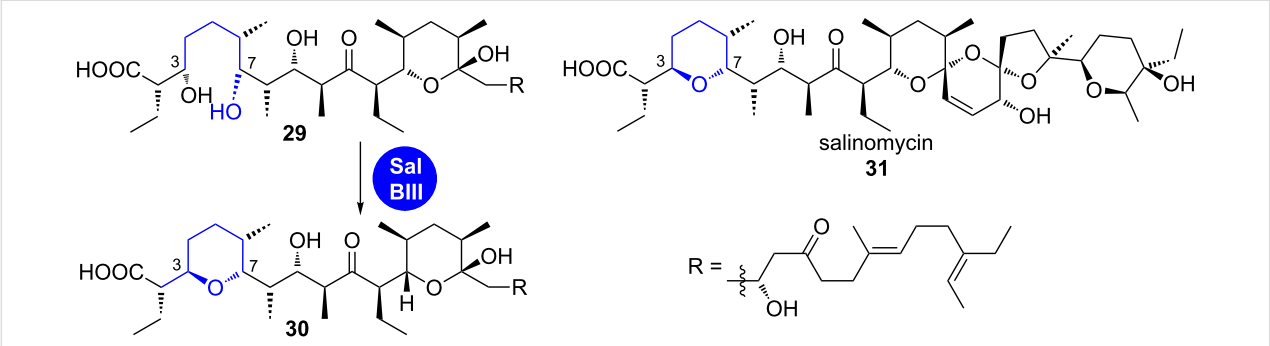

Scheme 5: SalBIII catalyses dehydration of **29** and subsequent cyclisation to tetrahydropyran **30** [18].

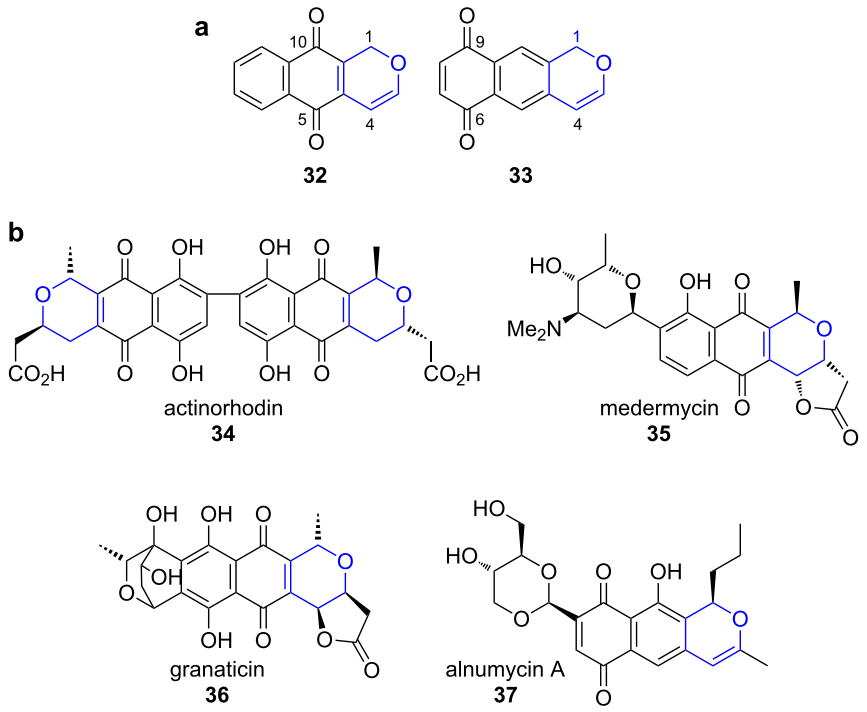

Figure 1: All pyranonaphtoquinones contain either the naphtha[2,3-*c*]pyran-5,10-dione (**32**) or the regioisomeric naphtha[2,3-*c*]pyran-6,9-dione (**33**) unit. Representative examples are actinorhodin (**34**), medermycin (**35**), granaticin (**36**) and alnumycin A (**37**) [21].

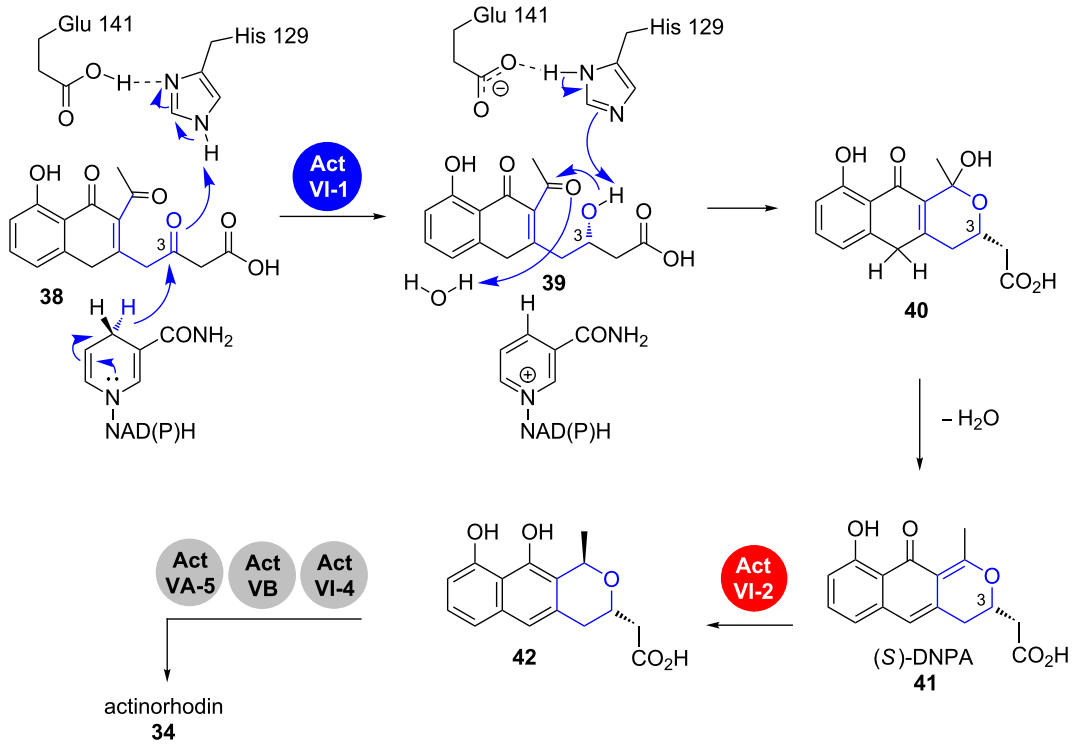

Scheme 6: Pyran-ring formation in actinorhodin (**34**) biosynthesis. DNPA: 4-dihydro-9-hydroxy-1-methyl-10-oxo-3*H*-naphto[2,3-*c*]pyran-3-acetic acid. Modified from [27-29].

dehydration of L-3-hydroxyacyl-CoA during β-oxidation of fatty acids.

In this case, it acts as a ketoreductase that installs the secondary hydroxy group in **39**. The catalytic mechanism has been proposed using a homologous 3HAD from the human heart as a model and was verified by mutagenesis and kinetic studies. In the active site, Glu141 and His129 activate the C3 keto group by protonation. The pro-*S* hydride of the reduced nicotinamide adenine dinucleotide (phosphate) (NAD(P)H) is then transferred to the C3. The resulting hydroxy group participates in the formation of a cyclic hemiacetal that subsequently undergoes vinylogous dehydration to yield (*S*)-4-dihydro-9-hydroxy-1-methyl-10-oxo-3*H*-naphto[2,3-*c*]pyran-3-acetic acid (**41**, (*S*)-DNPA) [27]. Whether the enzyme actively participates in the post-reduction steps is still in debate. It was proposed that dehydration takes place while the substrate is still bound in the active site, but it is also known that this and the analogous reaction in similar systems like medermycin (**35**) can occur spontaneously [27,30].

In vitro studies with recombinant ActVI-1 and synthetic substrate analogues showed a preference of the enzymes for a free acid substrate analogue over *N*-acetylcysteamine (SNAC)-bound substrates, suggesting that the polyketide is cleaved from the PKS prior to keto reduction [31]. The dehydration product **41** is reduced by Act VI-2 to the dihydropyran **42**, which undergoes tailoring to finally yield actinorhodin (**34**).

In granaticin (**36**) biosynthesis, the pyran-forming enzyme Gra-6 belongs to the short chain dehydrogenase/reductase (SDR) family and shows the highly conserved catalytic triad of Ser-Tyr-Lys (Scheme 7).

It was suggested that the Ser144 hydrogen bond to the C3 keto group in **38** is essential for stereocontrol, while Tyr157 and Lys161 participate in pre-orienting NADPH for transfer of its pro-*S* proton [27,32]. The resulting secondary alcohol **43** is processed similar to its enantiomer **39** in actinorhodin biosynthesis to give (*R*)-DNPA (**46**) and finally graniticin (**36**) after tailoring.

It has been proposed that already at the stage of the first post-PKS modifications, the alnumycin (**37**) pathway differs from the above mentioned routes (Scheme 8). Prior to pyran cyclisation, the lateral ring of precursor **48** is hydroxylated by the combined action of the two-component flavin-containing monooxygenase (FMO) AlnT and the flavin reductase AlnH [33].

No 3HAD homolog is present in the gene cluster that could catalyse a similar reaction as in the above mentioned examples. Instead, the oxidoreductase AlnO was proposed to catalyse the

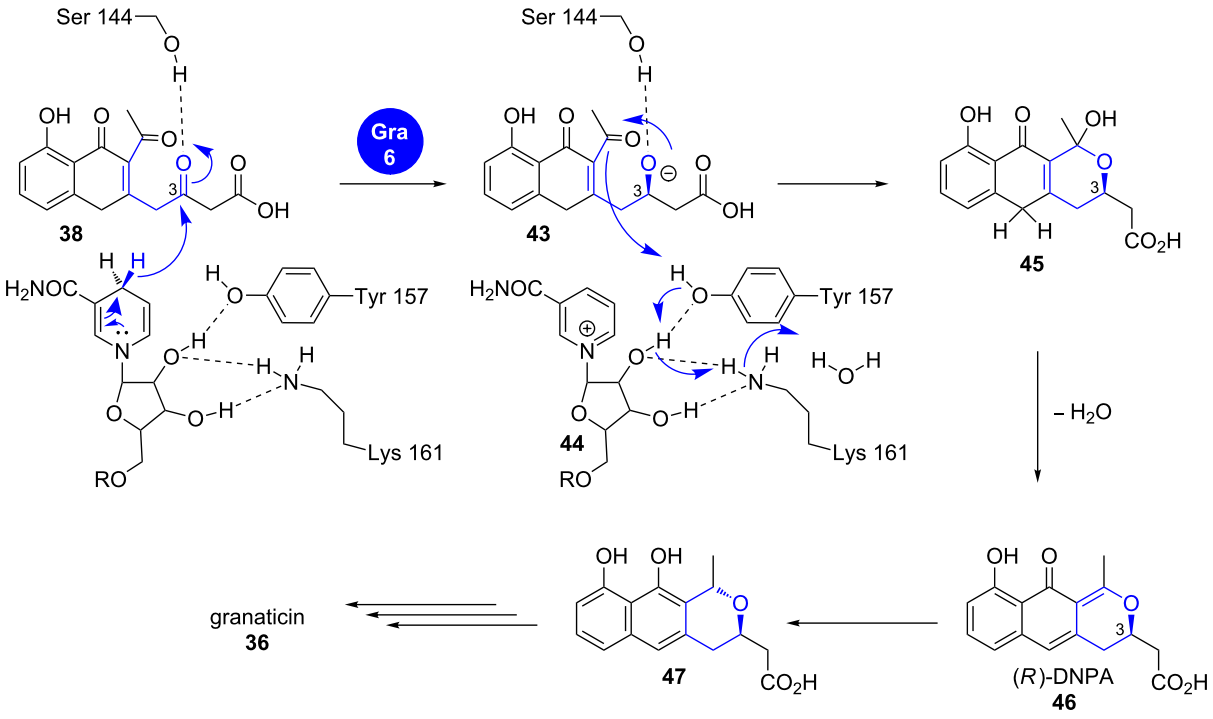

Scheme 7: Pyran formation in granaticin (**36**) biosynthesis. DNPA: 4-dihydro-9-hydroxy-1-methyl-10-oxo-3*H*-naphto[2,3-*c*]pyran-3-acetic acid. Modified from [27].

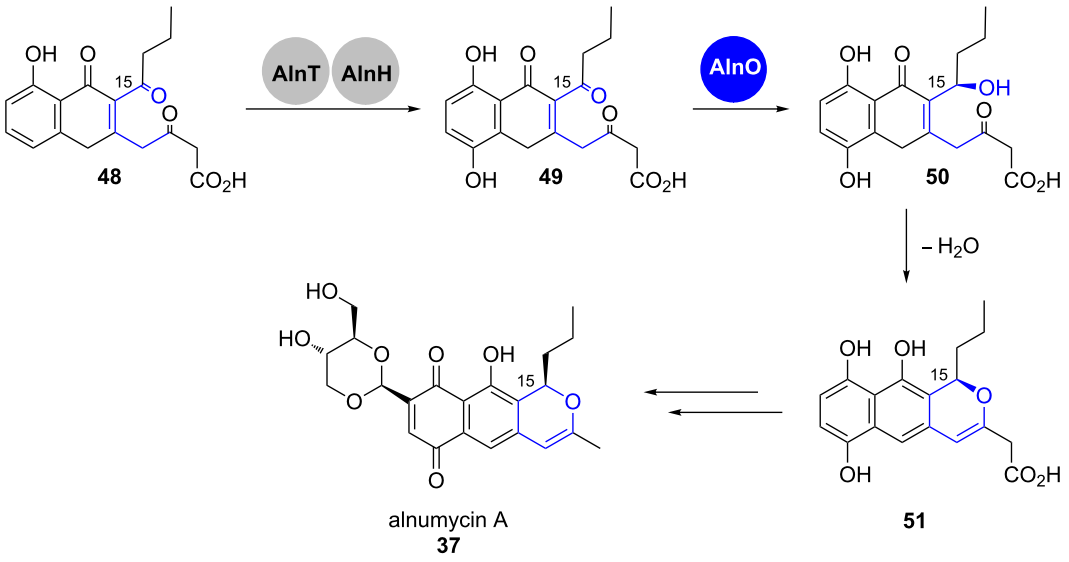

Scheme 8: Pyran formation in alnumycin (**37**) biosynthesis. Adapted from [21].

stereoselective reduction of the ketone at C15 in **49**. The pyran **51** would then be obtained by spontaneous or enzyme-supported hemiacetalisation followed by dehydration [34]. The tricyclic core unit is oxidised further and heavily decorated by tailoring enzymes, also involving an unusual rearrangement leading to the dioxane unit, whose carbon atoms originally derive from a sugar building block [34-36].

1.1.3 Epoxide opening: The nucleophilic opening of epoxides is probably the most abundant type of reaction leading to furans and pyrans. It, for example, plays an important role in the biosynthesis of ionophoric terrestrial and marine polyethers (see chapter 1.3). In this chapter, we will focus on two examples in which one pyran ring is formed. Both characteristically deviate from the typical polyether-specific interplay between one epoxidase and one or a few epoxide hydrolases that collaboratively set up multiple oxygen heterocycles.

Pseudomonic acid A. Mupirocin is a clinically important antibiotic against Gram-positive bacteria, which consists of a mixture of pseudomonic acids from *Pseudomonas fluorescens* NCIMB 10586 with pseudomonic acid A (**61**) being the main compound (Scheme 9) [37-44]. It belongs to the group of *trans*-AT-PKS products and the gene cluster harbours genes that code for a β-hydroxymethylglutaryl-CoA synthase (HCS) cassette (*mupG*, *mupH*, *mupJ*, *mupK* and *macpC*) and an iteratively acting type I fatty acid synthase (FAS) (*mmpB*).

During the biosynthesis of the pseudomonic acids, the initially formed PKS product **52** undergoes a complex tailoring pathway (Scheme 9) [45]. A remarkable feature is the tightly regulated steps that lead to the formation and decoration of the pyran-ring-containing region between C5 and C11 in **61** [46-49]. This has been studied by a series of fermentation and gene deletion–intermediate isolation experiments.

The process starts by oxidoreductase domain MmpE-catalysed epoxidation of the double bond between C10 and C11. Olefin **53** is thus a branching point from which two series of analogous C10–C11 epoxides (**53**–**61**) and C10–C11 (not shown) olefins arise (Scheme 9). The fact that the wild-type titers of the respective olefins are much lower than the analogous epoxides **53**–**61** suggests that epoxidation has a strong influence on the performance of the downstream enzymes.

The dioxygenase MupW together with its associated ferredoxin dioxygenase MupT then catalyse dehydrogenation and epoxidation on C8 and C16 of **53**. Whether the pyran-ring closure is also mediated by an enzymatic activity or if this reaction is a spontaneous process could not be clarified yet and may be subject for in vitro studies with the purified enzymes.

The net-deoxygenation on C8 of pseudomonic acid B (**57**) is obtained by a multistep process (Scheme 9). After elongation by the iterative type I fatty acid synthase MmpB, redox transformations and a dehydration on the MacpE-bound substrate **58** finally lead to pseudomonic acid A (**61**) with a 3,4-dihydroxy-2,5-disubstituted pyran ring. The reason for the elaborate oxidation–reduction on the C6 and C7 hydroxy groups during this biosynthetic endgame remains enigmatic [46].

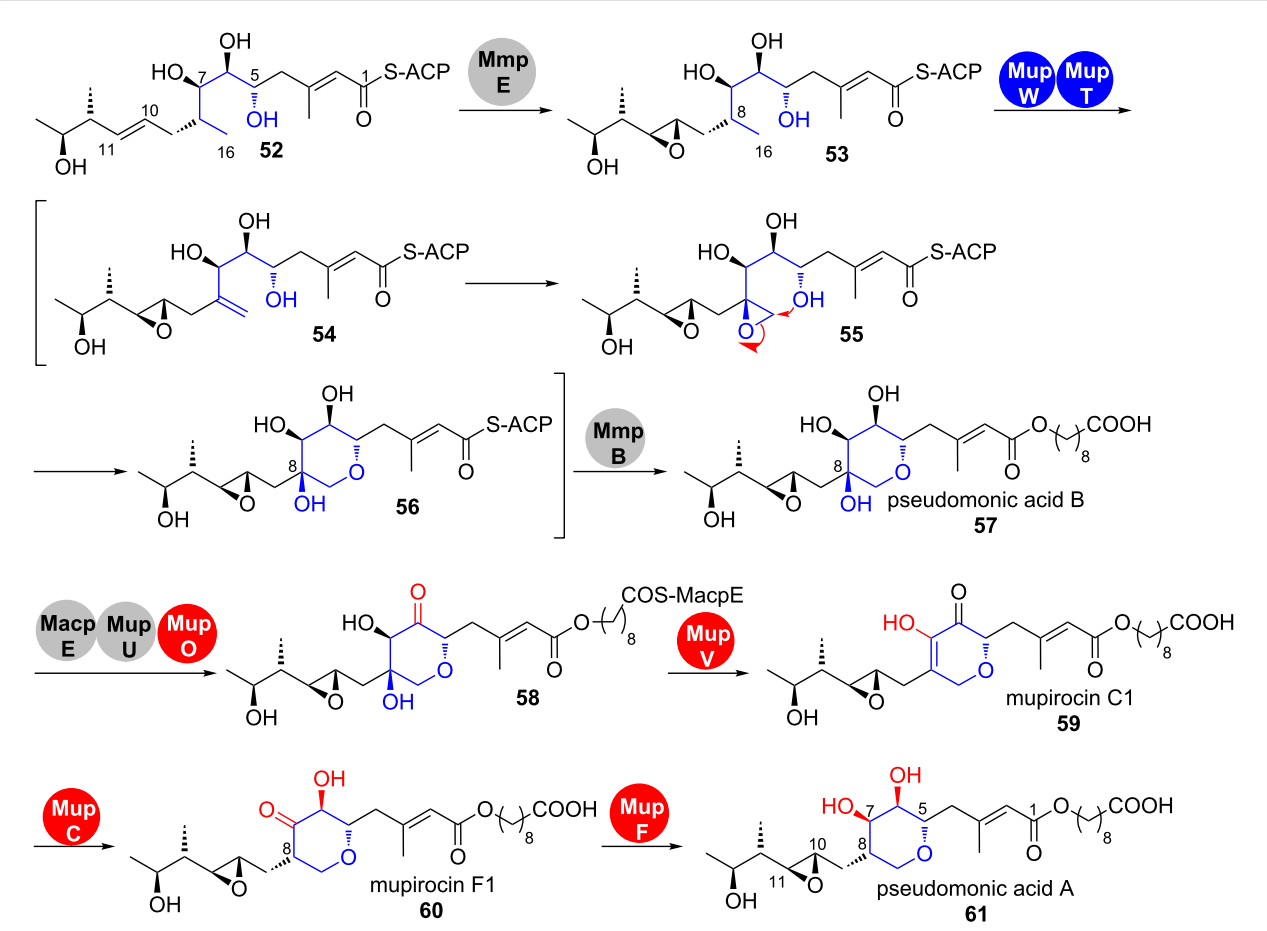

Scheme 9: Biosynthesis of pseudomonic acid A (**61**). The pyran ring is initially formed in **57** after dehydrogenation, epoxidation and ring opening by the ferredoxin dioxygenase MupT and the dioxygenase MupW and then formally deoxygenated [46].

Ambruticin. Another example in which a single epoxide opening event leads to the installation of an individual ring is the formation of the western tetrahydropyran ring in the biosynthesis of the ambruticins (Scheme 10) [50].

Their gene cluster contains a single epoxidase gene but no epoxide hydrolase, suggesting that the epoxidase is either multifunctional or that epoxide opening occurs spontaneously. The latter hypothesis is supported by the fact that allylic epoxides have been shown in synthetic experiments to be much more susceptible to nucleophilic attack than the respective 3,4-saturated analogues and that 6-*endo*-tet attack can override the 5-*exo*-tet cyclisation, which is favoured according to Baldwin's rules [51,52].

Scheme 10: Epoxidation–cyclisation leads to the formation of the tetrahydropyran ring in the western part of the ambruticins [50].

1.2 Furans

1.2.1 oxa-Michael addition: Similar to the PS domains described in chapter 1.1.1, furan rings can also be biosynthesised via oxa-Michael additions.

Nonactin. Nonactin (**70**) is the smallest homolog of the macrotetrolides, a family of cyclic polyethers that commonly have activity as ionophore antibiotics (Scheme 11a). It is produced by *Streptomyces griseus* subsp. *griseus* ETH A7796 as well as by *Streptomyces fulvissimus* and consists of four nonactic acid units, which are assembled in a head-to-tail fashion giving a C_2-symmetric (−)-(+)-(−)-(+) macrocycle [53].

Nonactin (**70**) biosynthesis has been extensively studied and shows multiple unusual features. Genes of an ACP-less, non-iteratively acting type II PKS are involved in the formation of the nonactoyl-CoA (**69a** and **69b**) backbone. The biosynthesis starts from succinyl-CoA (**65**) and malonyl-CoA (**66**), which are condensed to a 3-oxothioester and further processed to the 4,6-dioxothioester **68** (Scheme 11a) [54]. This achiral intermediate is the precursor for two enantiospecific pathways [55].

After stereoselective reduction to the (6*S*,8*S*) or the (6*R*,8*R*, **71a**) enantiomer of (*E*)-6,8-dihydroxy-2-methylnon-2-enoyl-CoA, respectively, the nonactate synthase NonS catalyses stereospecific oxa-Michael addition [56,57]. This enzyme is proposed to convert both enantiomers, finally giving the nonactic acid monomers **69a** and **69b**.

Priestley et al. showed that the cell lysate of a recombinant *Streptomyces lividans* strain overexpressing the *nonS* gene was able to convert the *N*-caprylcysteamine thioester (**71b**) into the respective cyclic compound **72** (Scheme 11b) [56]. This result has been confirmed by in vivo experiments of Shen et al. [59]. NonS was annotated as an enoyl-CoA hydratase and shows a high degree of up to complete identity amino acid homology to mostly uncharacterised enzymes in several other clusters of *Streptomyces* strains.

Pamamycins. Recently, the gene cluster of the macrodiolide antibiotic group of the pamamycins **73** was sequenced and the function of some of the genes studied (Figure 2) [60].

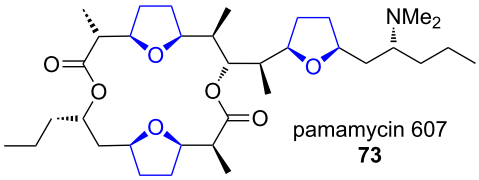

Figure 2: Pamamycins (**73**) are macrodiolide antibiotics containing three tetrahydrofuran moieties, which are all proposed to be formed by the NonS homolog PamS [60].

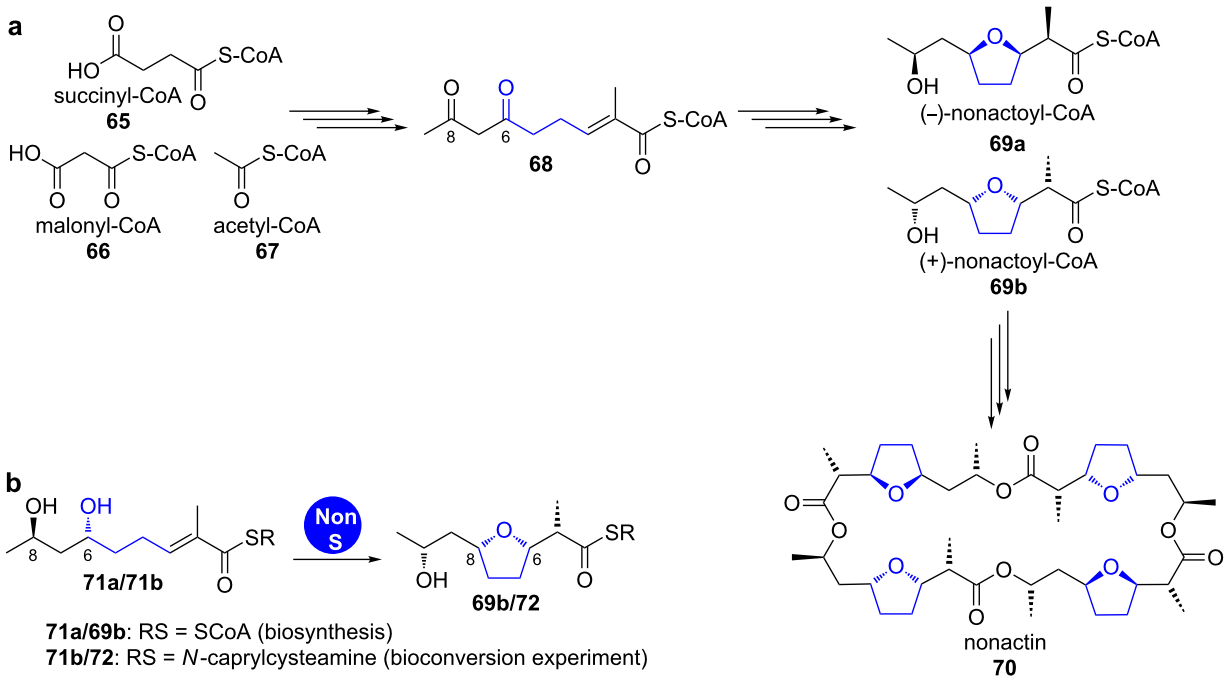

Scheme 11: a) Nonactin (**70**) is formed from heterodimers of (−)(+)-dimeric nonactic acid and (+)(−)-dimeric nonactic acid. b) The product of the *nonS* gene catalyses the cyclisation of (6*R*,8*R*,*E*)-6,8-dihydroxy-2-methylnon-2-enoic acid thioester (**71a** and **71 b**) to (+)-nonactic acid thioester (**69b**/**72**) [53,56,58].

This cluster contains a NonS homolog, PamS, that was proposed to catalyse all three oxa-Michael additions that lead to tetrahydrofuran formation during biosynthesis. As the enzyme must act on biosynthetic intermediates of strongly varying size, this attributes a remarkably broad substrate tolerance to PamS. No detailed characterisation of PamS has been carried out yet.

Oocydin. Homologs of *trans*-AT-PKS-characteristic pyran synthase (PS) domains are also proposed to be involved in the biosynthesis of furan-containing compounds (see chapter 1.1.1).

In module 7 of the oocydin A (**76**)-PKS, a DH domain and a PS domain are present that were proposed to first dehydrate a 3-hydroxythioester intermediate and then cyclise the resulting enoyl intermediate **74**, similar to the reaction in sorangicin or pederin (**24**) biosynthesis (Scheme 12) [61].

1.2.2 Oxidative cyclisation: (+)-Aureothin. Furan rings can also be directly formed by oxidative cyclisation. The best studied example is the biosynthesis of (+)-aureothin (**79**), a reduced polyketide with potent antitumor, antifungal, antiparasitic, pesticidal and antitrypanosomal activities (Scheme 13).

In its biosynthesis, the furan-ring formation occurs on a late stage, catalysed in an unprecedented fashion by the cytochrome P450 oxidase AurH [13,62-67]. This enzyme accomplishes two consecutive CH activations at the positions 7 and 9a of the biosynthetic precursor deoxyaureothin (**77**), finally leading to oxidative cyclisation. The authors could reconstitute the enzymatic reaction in vitro and showed that stereospecific oxidation of **77** occurs first at the 7-position, which is followed by allylic oxidation at the 9a-position in **78** and cyclisation [13]. This reaction was exploited in the chemoenzymatic total synthesis of (+)-aureothin (**79**) [67,68].

The molecule also contains a pyran-4-one. Reminiscent of type II and type III-PKS, this results from elimination–tautomerisation of the 3,5-dioxothioester formed by the final two elongation steps of the aureothin-PKS.

Leupyrrins. The leupyrrins (leupyrrin A_2 (**80**) is shown in Scheme 14) are remarkable hybrid natural products consisting of PKS, NRPS and isoprenoid-originating portions. They contain several heterocyclic elements, like a pyrrolidine, a furan-2-one, an oxazolidinone and particularly a 3,4-furylidene moiety in the polyketide part.

An analysis of the gene cluster as well as feeding experiments with isotope-labelled precursors led to a proposal for the formation of the furan ring [69,70]. The anticipated mechanism is reminiscent of the formation of a tetrahydropyridine ring by the berberine bridge enzyme in plant alkaloid biosynthesis. It starts with *S*-adenosyl-L-methionine (SAM)-dependent methylation of the secondary hydroxy group in **81** by the *O*-methyltrans-

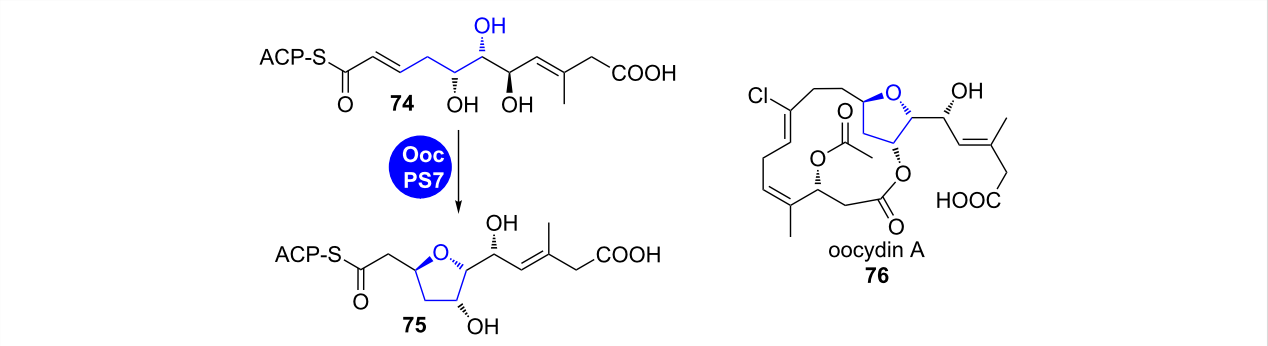

Scheme 12: A PS domain homolog in oocydin A (**76**) biosynthesis is proposed to catalyse furan formation via an oxa-Michael addition [61].

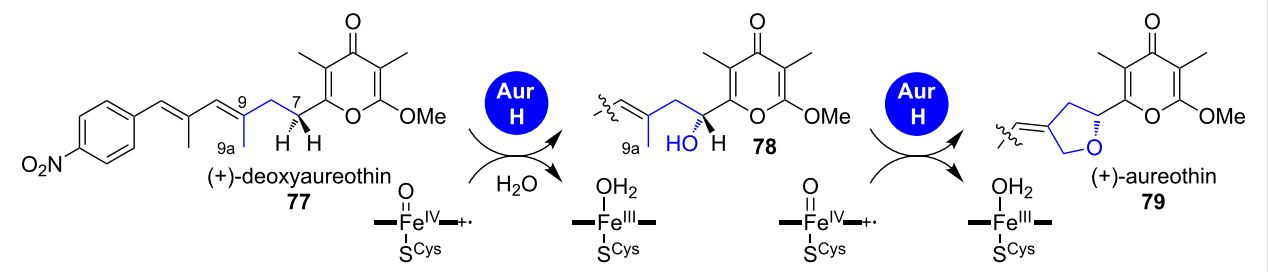

Scheme 13: Mechanism of oxidation–furan cyclisation by AurH, which converts (+)-deoxyaureothin (**77**) into (+)-aureothin (**79**) [13].

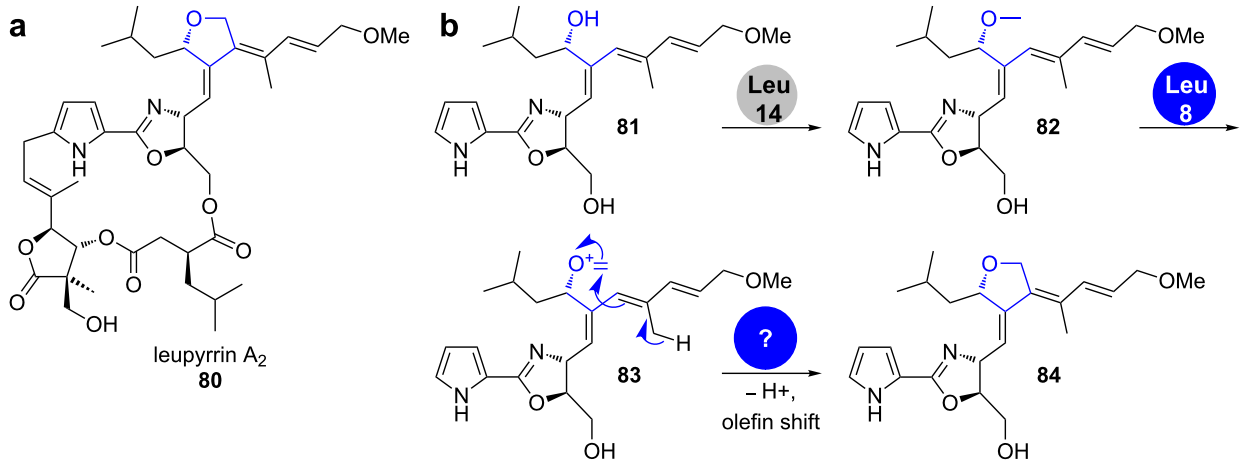

Scheme 14: Leupyrrin A_2 (**80**) and the proposed biosynthesis of its furylidene moiety [69,70].

ferase Leu14 (Scheme 14a) [71-74]. Oxidation of the methoxy group in **82** by the cluster-encoded dehydrogenase Leu8 is followed by a Prins-type cyclisation. No enzyme candidate for the cyclisation reaction to **84** could be identified in the cluster.

1.2.3 Processing of hemiacetals: Asperfuranone. Asperfuranone (**93**) consists of a polyketide side chain, attached to the C3 of an oxidised isobenzofuran (Scheme 15). The respective biosynthetic cluster contains seven genes and has been identi-

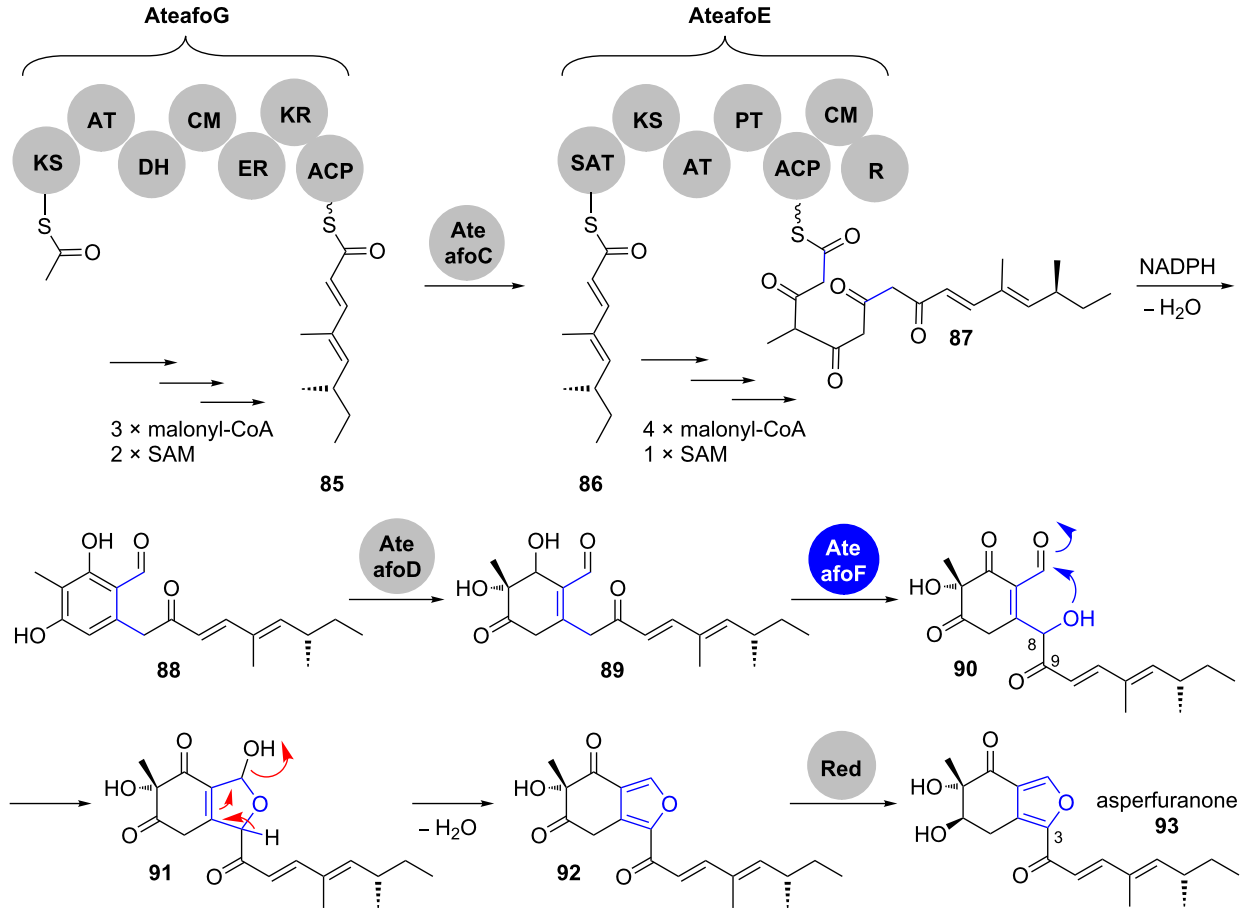

Scheme 15: Asperfuranone (**93**) biosynthesis, adapted from [75].

fied by Wang and co-workers through a genome mining approach in *Aspergillus nidulans* [76]. Later on, the same group annotated a highly homologous gene cluster in *Aspergillus terreus* and elucidated the timing and mechanism of asperfuranone biosynthesis by step-wise heterologous expression of the individual genes in *A. nidulans* [77]. Thus, genes involved in asperfuranone biosynthesis have been renamed from "*afo*" to "*ateafo*".

This bipartite azaphilone structure corresponds to its assembly by the highly reducing (HR)-PKS AteafoG, followed by a non-reducing (NR)-PKS AteafoE. The product of the HR-PKS AteafoG, tetraketide **85**, is transferred to the starter unit:ACP transacylase (SAT) domain of the NR-PKS AteafoE. After the elongation by four further ketide units, reductive PKS release and Knoevenagel condensation yield the benzaldehyde intermediate **88**. Oxidative dearomatisation of **88** catalysed by the salicylate monooxygenase AteafoD gives **89**, which is hydroxylated at C8 by the oxygenase AteafoF. The positioning of this newly formed hydroxy group forces the formation of a five-membered ring hemiacetal in **91**. Spontaneous dehydration installs the furan moiety and after keto reduction by an endogenous reductase, asperfuranone (**93**) is obtained.

Aflatoxins. Aflatoxins **94**–**99** are highly toxic carcinogens produced in several *Aspergillus* species (Figure 3). The respective pathway gene clusters have been identified and homologies between *Aspergillus* species were compared for example by the groups of Bennett and Ehrlich [78,79]. Structurally, aflatoxins belong to the group of furanocoumarins and consist of a pentacyclic system in which a benzobisfuran is annelated with a δ-lactone and a cyclopentanone or oxidation products of the latter.

Aflatoxin biosynthesis has been studied since the late 1960s and has attracted attention, because the polyketide undergoes a series of oxidative rearrangements, which drastically alter the molecular scaffold. Due to the complexity of these processes, we will focus on the steps directly associated with heterocycle formation [82-84].

Aflatoxin B1 (**94**) is considered as the most toxic aflatoxin. It is derived in multiple enzymatic conversions from norsolorinic acid anthrone **100**, which is produced by the norsolorinic acid synthase (NorS) (Scheme 16) [83,85]. NorS is a complex of a NR-PKS PksA and a pair of yeast-like fatty acid synthases HexA/HexB, which provide an unusual hexanoyl-CoA starter unit [86]. Norsolorinic acid (**100**) undergoes three oxidative rearrangements towards aflatoxin B1 (**94**): The first rearrangement sets up the benzobisfuran motif in **106**, the second rearranges the anthraquinone in **106** to the xanthone in **107** and the third is an oxidative ring contraction towards the cyclopentanone in **94** (Scheme 16).

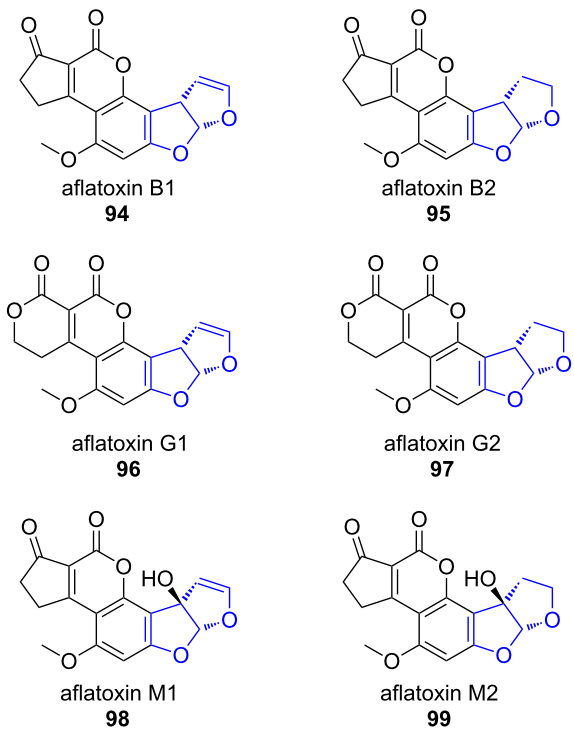

Figure 3: The four major aflatoxins produced by *Aspergilli* are the types B1, B2, G1 and G2 (**94**–**97**). In the digestive tract of animals, aflatoxins B1 and B2 (**94** and **95**) are oxidized to M1 and M2 (**98** and **99**), respectively [80,81].

After several enzymatic post-PKS modifications, the oxoaverantin (OAVN) cyclase transforms 5'-oxoaverantin (**101**) into averufin (**102**) by intramolecular acetal formation [87]. To date, it is not clear, how exactly the OAVN cyclase participates in this process [88]. Interestingly, the OAVN cyclase operates cofactor-free, although it contains a $NAD(P)^+$-binding Rossman fold. Furthermore, this enzyme is also capable of catalysing the later conversion of versiconal (**105**) to versicolorin B (**106**) [88].

Averufin (**102**) is the starting point for the first oxidative rearrangement. Feeding experiments with isotope-labelled averufins (**102**) showed that their C5' and C6'-carbons (pink) are excised on the way to aflatoxin B1 (**94**) and that the oxidation state of C1' (green) changes from that of an alcohol to an aldehyde, implying that the rearrangement must be oxidative [82,89,91,92,107].

The biosynthetic mechanims of the conversion of averufin (**102**) into 1'-hydroxyversicolorone (**103**) has been the subject of intensive studies. Gene disruption experiments in the aflatoxi-

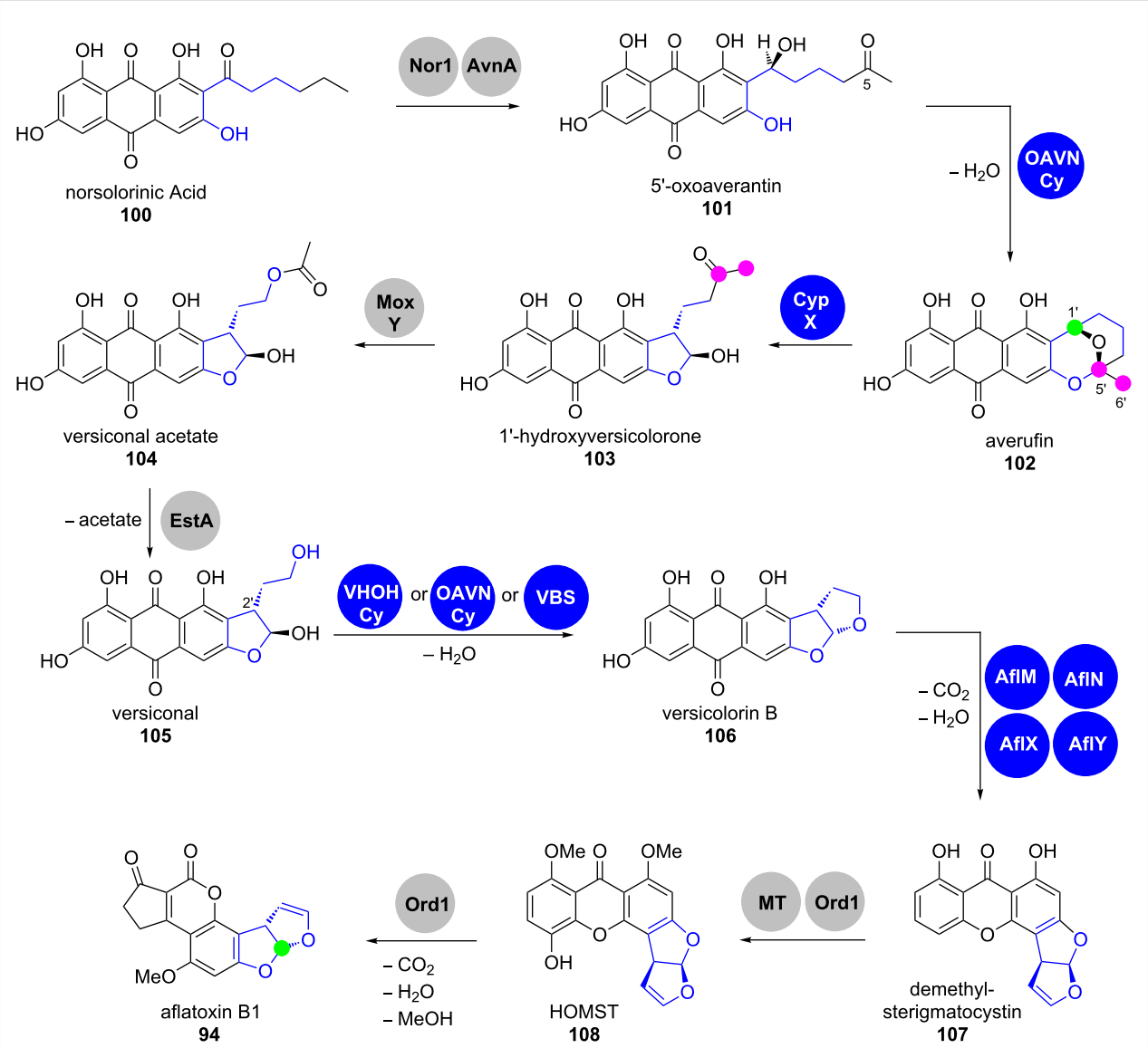

Scheme 16: Overview on aflatoxin B1 (**94**) biosynthesis. HOMST = 11-hydroxy-*O*-methylsterigmatocystin [78,79,82-106].

genic strain *A. parasiticus* NRRL 2999 revealed that this step is in fact catalysed by the cytochrome P450 enzyme AVR monooxygenase via an undeciphered mechanism (encoded by the gene *cypX*, see Scheme 16) [93]. The same study also revealed the participation of the FMO MoxY in a Baeyer–Villiger oxidation, which yields versiconal acetate (**104**) [93,94]. This is then hydrolysed by a cytosolic esterase (putatively also coded in the aflatoxin gene cluster as *estA*) to versiconal (**105**) [95]. The bisfuran moiety of versicolorin B (**106**), which is crucial for the mutagenic DNA binding, is then set up stereospecifically by the versiconal cyclase, which accepts both enantiomers (2'*R* and 2'*S*) of versiconal (**105**) [96,108]. Heterologous expression and characterisation by Townsend and co-workers revealed that the versicolorin B synthase (VBS) does not require any cofactors, in spite of its flavin adenine dinucleotide (FAD) binding site [98,99].

The reaction mechanisms and biosynthetic enzymes involved in the rearrangement of versicolorin B (**106**) to demethylsterigmatocystin (**107**) have also been discussed controversely. Up to four genes (*aflM*, *aflN*, *aflX* and *aflY*) have been implied in biosynthetic studies to code for enzymes that are participating in this complex conversion [100]. Henry and Townsend suggested an oxidation–reduction–oxidation sequence mediated by putative NADPH-dependent oxidoreductase AflM and cytochrome P450 enzyme AflN [101]. Gene disruption experiments by Cary et al. have shown that the NADH-dependent oxidoreductase AflX also takes part in the conversion [102].

Furthermore, the putative Baeyer–Villiger oxidase AflY was shown to be essential for demethylsterigmatocystin (**107**) formation and has been rationalised to form an intermediate lactone that is decarboxylated towards the xanthone [103]. Studies with recombinant AflM and a lack of isolatable intermediates however made it clear that the order of steps in demethylsterigmatocystin (**107**) formation needs to be carefully re-evaluated [100].

Methylation by an *O*-methyltransferase and subsequent oxidation by the cytochrome P450 monooxygenase Ord1 yields HOMST (**108**), which is the starting point for the final rearrangement towards aflatoxin B1 (**94**) [104,105]. Consequently, the Ord1 enzyme alone catalyses the final steps towards aflatoxin B1 (**94**) [106].

1.2.4 Epoxide opening: See chapter 1.1.3.

1.3 Polycyclic systems

During the biosynthesis of ionophoric terrestrial and marine polyethers, polyolefinic PKS products are first polyepoxidised and these epoxides are then opened in a so-called zipper mechanism that installs furan and/or pyran rings as well as cyclic acetals, if carbonyl groups are involved (shown for monensin in Scheme 17) [109-111]. While polyepoxidation is usually effected by only one epoxidase, one or more epoxide hydrolases mediate regioselective epoxide opening and following controlled cyclisation.

As the topic polyether biosynthesis is highly complex and a detailed discussion of further examples would go beyond the scope of this article, we would like to refer the reader to appropriate review literature [4,109].

Aurovertin B. The 2,6-dioxabicyclo[3.2.1]octane (DBO) ring system is present in several plant and microbial natural products, like decurrenside A from the goldenrod plant, sorangicin A from myxobacteria as well as the marine toxin palytoxin from zoanthids [112-114]. It was proposed that a complex epoxide opening cascade is involved in its formation (Scheme 18) [115].

Tang et al. were recently able to show that the interplay of one FMO and one epoxide hydrolase in the biosynthesis of the fungal polyketide aurovertin B (**118**) is sufficient to form this complex structural motif starting from a polyene-α-pyrone precursor (Scheme 18) [116]. The diene between C3 and C6 in **113** is first expoxidised by the FMO AurC. The epoxide hydrolase AurD then regioselectively hydrolyses the epoxide at the C4 position of **114** and initiates a cascade that leads to the formation of the dihydroxyfuran intermediate **115**. AurC becomes active for a second time and epoxidises the C7–C8 double bond, which is then attacked by the *syn*-positioned hydroxy group on

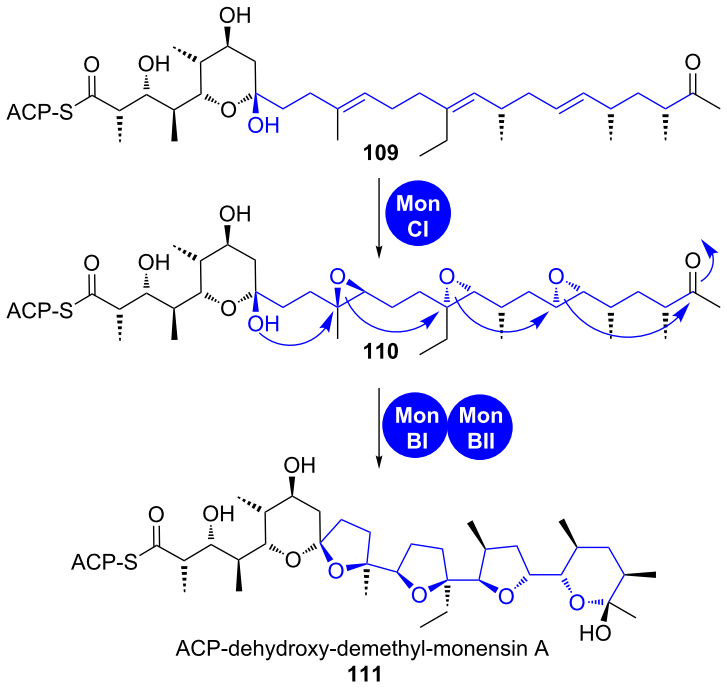

Scheme 17: A zipper mechanism leads to the formation of oxygen heterocycles in monensin biosynthesis [109-111].

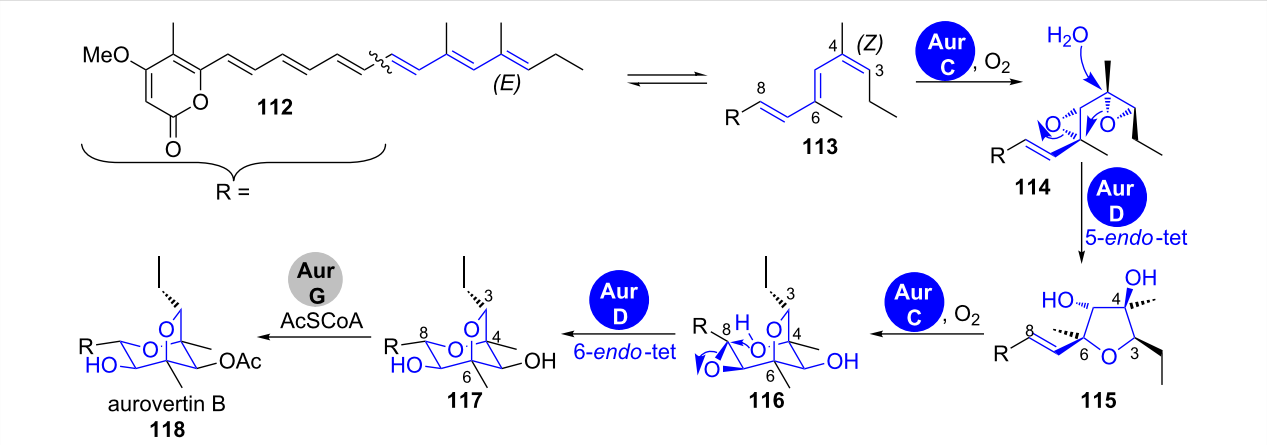

Scheme 18: Formation of the 2,6-dioxabicyclo[3.2.1]octane (DBO) ring system in aurovertin B (**118**) biosynthesis [116].

C4 to give the pyran ring. This terminal 6-*endo*-tet cyclisation is likewise facilitated by AurD, overriding the 5-*exo*-tet pathway that should be favoured in spontaneous reaction according to Baldwin's rules. Density functional theory calculations suggested that this reaction pathway is favoured, if the hydroxy-epoxide **116** is simultaneously activated by acidic and basic residues [116].

1.4 Oxetans

Oxetans are present in several isoprenoid natural products with important biological activity, like the anticancer drug paclitaxel or merrilactone A [117-122]. However, to the best of our knowledge, no information on the biosynthesis of polyketides containing this structural motif is known yet.

1.5 Epoxides

Epoxides are frequently occurring structural motifs in natural products and are often sites of covalent interaction with target proteins. Prominent compounds that contain epoxides are for example epothilone A (**119**) and oleandomycin (**120**) (Figure 4) [123-125].

Epoxides result from oxidation of olefins by oxidoreductases, mostly cytochrome P450 monooxygenases or FMOs. Alternative mechanisms, such as reactions between carbenes and carbonyls (analogous to the synthetic Corey–Chaykovsky epoxidation) are not known in biosynthetic pathways. Epoxides are abundant as biosynthetic intermediates that are further processed in downstream processes. Examples are discussed in the respective chapters 1.1.3 and 1.2.4.

1.6 Pyranones

1.6.1 TE-catalysed lactonisation: Most pyranones occurring in polyketides are pyran-2-ones that result from the attack of 5-hydroxy groups or enols on the thioester of a PKS-bound intermediate. For a general introduction into this reaction in type II and type III PKS, we would like to refer the reader to the review article from Schäberle et al. published in this issue [126]. In type I PKS, cyclisation to pyran-2-ones usually occurs TE-catalysed after full assembly of the PKS product and is often followed by tailoring steps. Examples are the biosynthesis of jerangolid A (**122**) and of phoslactomycin B (**121**) (Scheme 19).

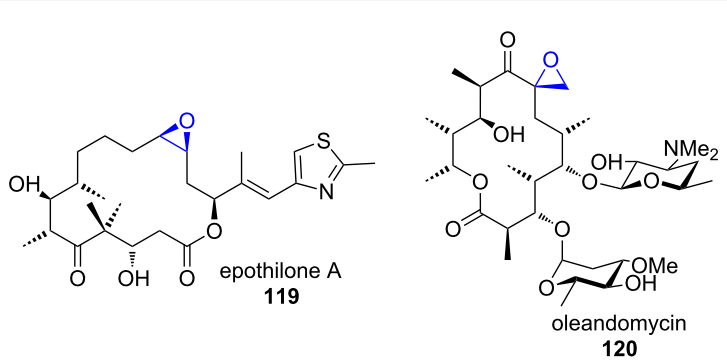

Figure 4: Structures of the epoxide-containing polyketides epothilone A (119) and oleandomycin (**120**) [123-125].

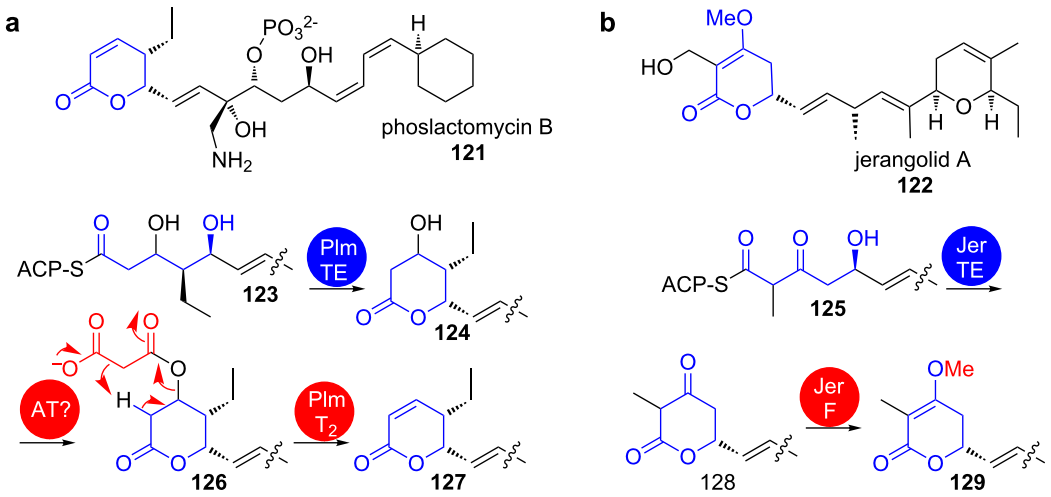

Scheme 19: Structures of phoslactomycin B (**121**) (a) and jerangolid A (**122**) (b). The heterocycle-forming steps in their biosynthesis are shown on the bottom [50,127].

In phoslactomycin B (**121**) biosynthesis, the 4-hydroxytetrahydro-2*H*-pyran-2-one **124** is formally dehydrated by consecutive malonylation–elimination to finally give a 5,6-dihydro-2*H*-pyran-2-one **127** [127]. The tailoring enzyme $PlmT_2$ was proposed to catalyse the decarboxylative elimination of malonoyl halfester **126**. It is not clear, whether the initial malonylation was catalysed by an AT domain or another enzyme in the cluster. Similar chemistry occurs during the biosynthesis of related compounds like fostriecin and leptomycin [128,129].

In jerangolid A biosynthesis, the dihydro-2*H*-pyran-2,4(3*H*)-dione **128** is transformed into a 4-methoxy-5,6-dihydro-2*H*-pyran-2-one **129** by action of the *O*-methyltransferase JerF [50].

1.6.2 Michael addition–lactonisation: A novel mechanism for the integration of pyran-2-ones into polyketide backbones has recently been discovered.

Rhizoxin. In 2013, Hertweck and co-workers provided detailed insight into the unprecedented enzyme catalysis involved in the formation of 4-substituted δ-lactones and the structurally closely related glutarimides, respectively (Scheme 20) [130].

The assembly of both moieties includes a β-branching event of the polyketide carbon backbone that is mechanistically different from that occurring during isoprenoid biosynthesis. The designated branching modules of lactone and glutarimide-producing PKS show similar designs: a branching domain (B or X), which is flanked by a KS and an ACP domain (Scheme 20b and c).

In vitro reconstitution experiments with the branching module of the macrolide rhizoxin (**130**) (*rhi*PKS) and synthetic SNAC-thioesters revealed that the chain branch originates from a *syn*-selective Michael addition of an ACP-bound malonate unit **133** to a KS-bound α,β-unsaturated thioester **132** (Scheme 20b) [130]. This results in an intermediate **134** in which the ACP and the KS domain are covalently linked by the branched polyketide. Subsequent nucleophilic attack of the δ-hydroxy group on the thioester then yields the ACP-bound δ-lactone **135** and the polyketide chain can be passed downstream on the assembly line.

When testing the substrate scope of the rhizoxin (**130**) branching module, C3-substituted as well as amino and carboxamide nucleophiles in lieu of a hydroxy group in **132** were accepted, yielding δ-lactam and glutarimide moieties, respectively [131,132]. When the B-domain of the *rhi*PKS was exchanged with an X-domain of glutarimide-producing PKS from the 9-methylstreptimidone PKS of *S. himastatinicus*, both, glutarimides and lactones were obtained from respective substrate conversions. Thus, the domains can be seen as functionally equivalent [133]. Supported by kinetic analyses and mutational studies it was shown that B-domains, neither have an influence on the substrate selectivity nor on the turnover and furthermore do not catalytically take part in the branching or heterocyclisation event. Solely their double-hotdog fold is structurally essential for the branching module. Consequently, the B-domain has even been mimicked with a dehydratase domain that bears the same folding motif. It is thus most interesting that the branching KS domain alone mediates the entire catalytic sequence and represents a unique family of ligase-cyclase.

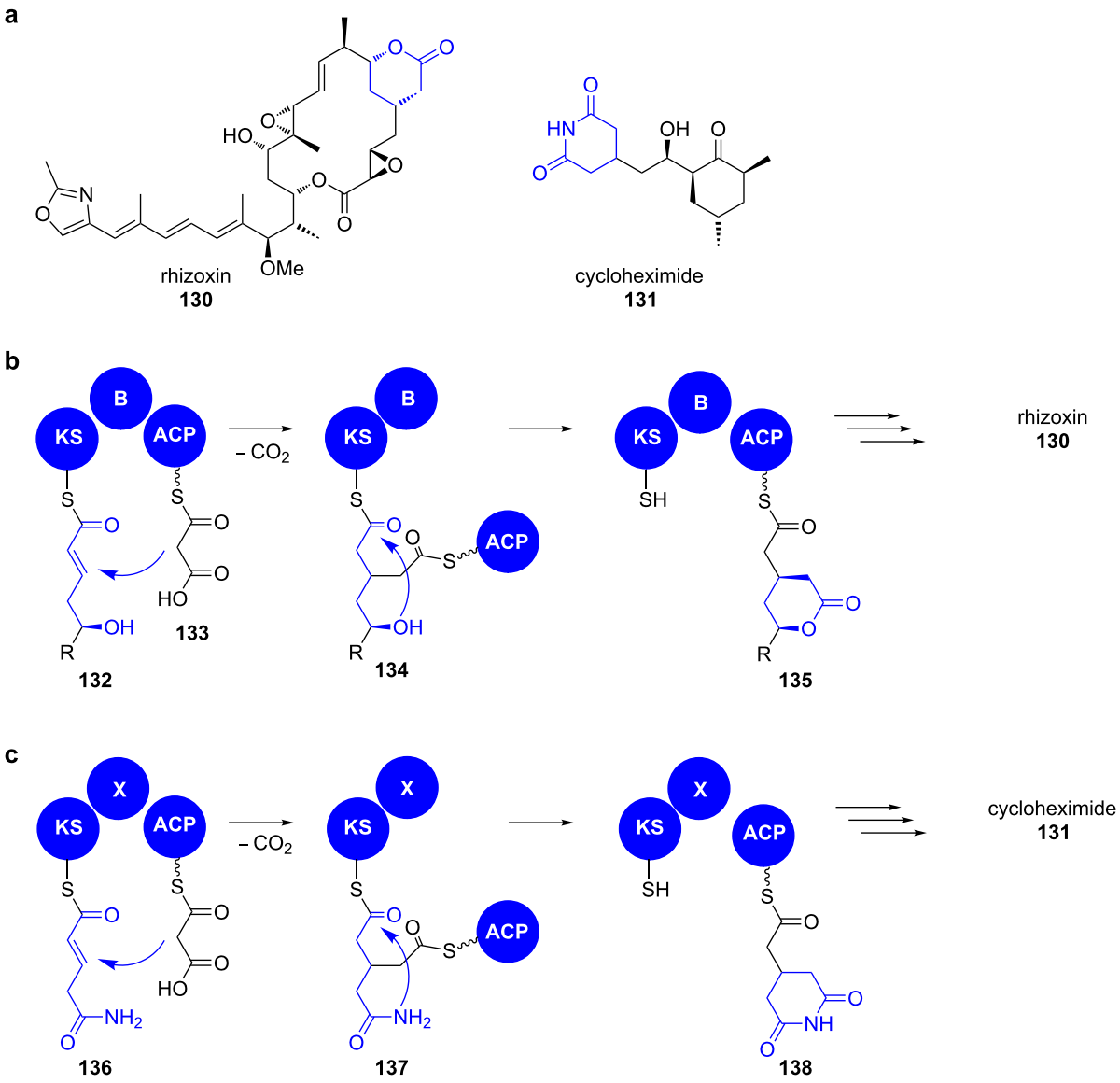

Scheme 20: a) Structures of rhizoxin (**130**) and cycloheximide (**131**). Model for the formation of δ-lactones (b) or glutarimides (c), respectively. Adapted from [133].

1.6.3 Favorskii rearrangement: Enterocin. Another mechanism applies for the δ-lactone embedded in the tricyclic, caged core of the bacteriostatic agent enterocin that is produced in *Streptomyces* species [134,135]. The respective biosynthetic pathway has been fully reconstituted in an in vitro one-pot reaction [136]. The flavoprotein EncM transforms the C12 methylene group of the octaketidic PKS type II product **139** in a two-step oxidation sequence using the unprecedented, enzyme-bound flavin-N^5-oxide **144** (Scheme 21) [137].

The resulting ketone **141** undergoes a Favorskii rearrangement, finally leading to the formation of the δ-lactone moiety. EncM has also been rationalised to participate in the stereoselectivity of the subsequent aldol condensations and the final lactonisation yielding the pyran-2-one attached to the caged ring system [137].

1.7 Furanones

1.7.1 Acylation–Dieckmann condensation: Tetronates. Tetronates (4-hydroxyfuran-2(5*H*)-ones, **145a**/**145b**) are an abundant type of heterocycles with a broad spectrum of biological activities (Figure 5) [138,139]. In polyketides, they mostly appear in form of 3-acyltetronates and it was proposed that this structural motif is able to mimic corresponding anions of acidic functional groups like phosphates, sulphates or carboxylates. In fact, tetronates often act by inhibiting enzymes that process the

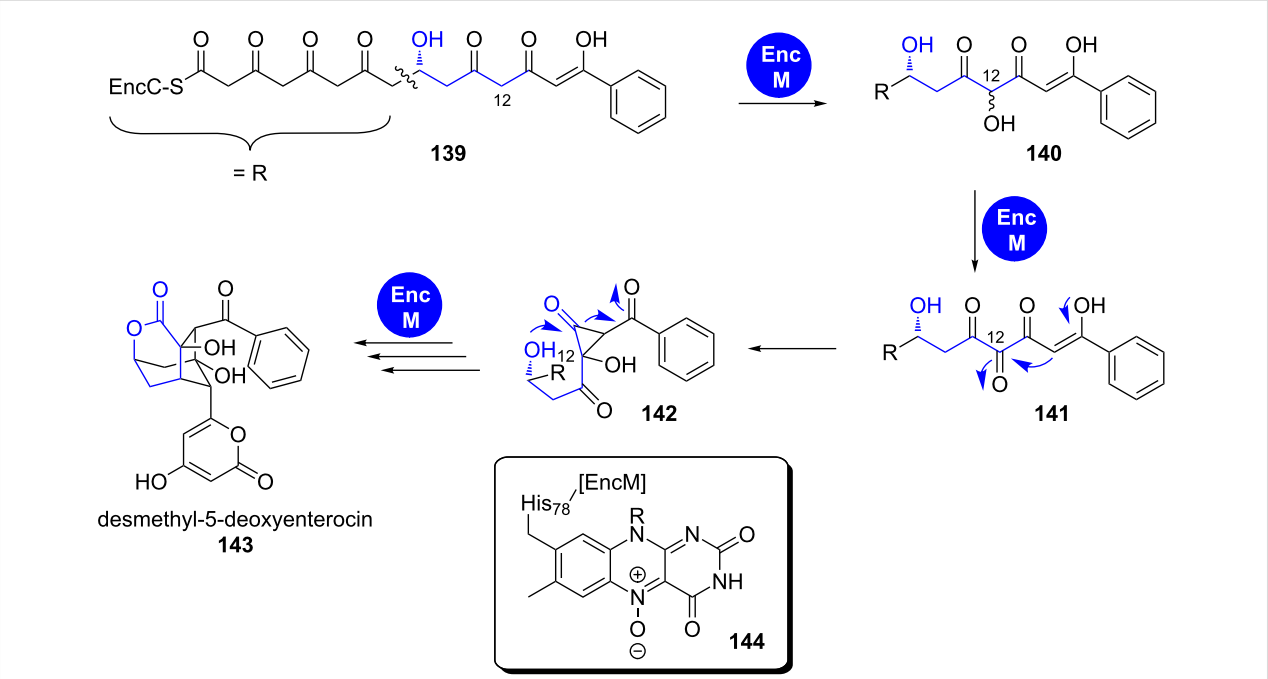

Scheme 21: EncM catalyses a dual oxidation sequence and following processing of the highly reactive intermediate **141** in enterocin biosynthesis. EncC is an ACP. Adapted from [137].

respective functional groups. Besides a common antibacterial activity, many tetronates also have further attractive bioactivities that triggered interest in their research [139,140].

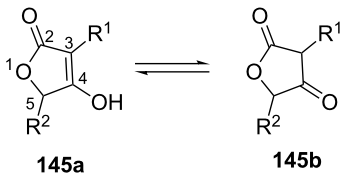

Figure 5: Mesomeric structures of tetronates [138,139].

Tetronates and their biosynthesis have recently been extensively reviewed and a classification based on structural characteristics was devised [138,139]. With the exception of a few terpenoids, most tetronates are of polyketide origin, either being completely biosynthesised by a PKS or by hijacking intermediates from fatty acid biosynthesis (Figure 6).

Although the larger body of tetronates is produced by *Actinobacteria*, they are abundant in organisms from different classes. Their origin often goes along with characteristic structural elements. Furylidene tetronates are for example exclusively produced by fungi and spirotetronates by *Actinobacteria* [139].

The biosynthetic studies that were launched since genetic information on more and more tetronates became available revealed that the formation and the decoration of the ring structure are straight forward and well-conserved among clusters and organisms.

Tetronate cyclisation. In all tetronate clusters sequenced until now, a conserved set of genes is present that codes for a glycerate-activating FkbH-like protein, an acyl carrier protein (ACP) that intermediately carries the glycerate unit and a FabH-like protein that condenses the ACP-bound glycerate with an ACP-bound β-ketothioester in an acylation–Dieckmann condensation reaction cascade (Scheme 22) [139]. This scenario has been confirmed by partial in vivo and in vitro reconstruction of tetronomycin (Tmn, **149**), RK-682 (**146**) and agglomerin A (**147**) biosynthesis [141-144]. It is however not clear, in which order the two sub-steps occur.

Tetronate processing. Spirotetronates like abyssomycin C (**148**), quartromycin D1 (**151**) or versipelostatin A (**153**) result from formal [4 + 2] cycloaddition reactions between *exo*-methylene groups and conjugated dienes. The required *exo*-methylene groups are installed by formal dehydration of 5-hydroxymethyltetronates.

Leadlay et al. have confirmed that the respective reaction in agglomerin A (**147**) biosynthesis proceeds as a two-step process

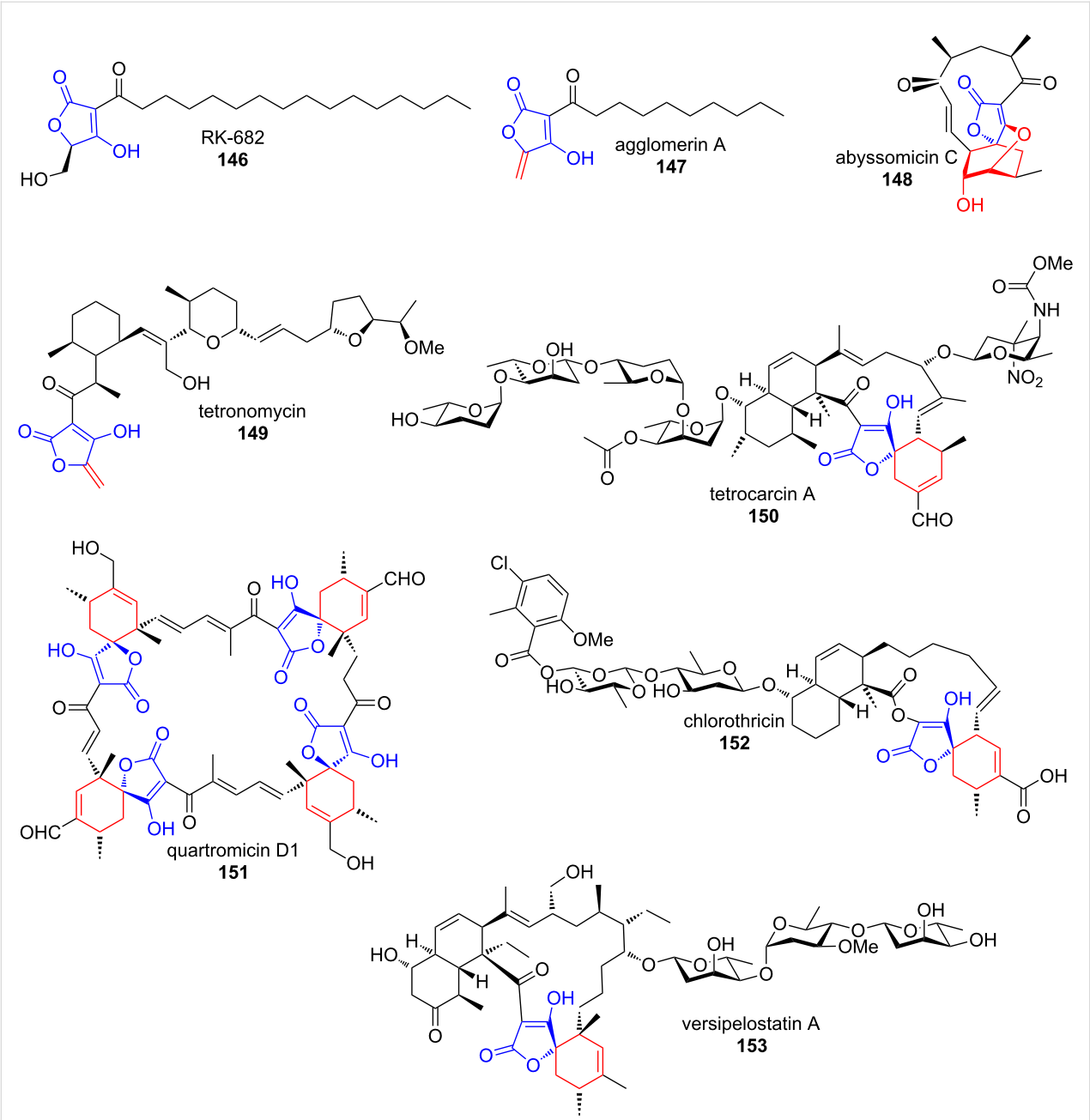

Figure 6: Structures of tetronates for which gene clusters have been sequenced. The tetronate moiety is shown in blue. All structural elements that derive from tailoring processes on the tetronate are shown in red. Kijanimicin is not shown [138,139].

[143]. An initial acyl transferase Agg4-catalysed acetylation of the primary hydroxy group in **158** is followed by dehydratase Agg5-catalysed acetic acid elimination, leading to olefin **147** (Scheme 22). This mechanism was confirmed by gene knockout and complementation experiments as well as by in vitro reconstitution using purified enzymes. Agg4 and Agg5 showed substrate tolerance and also accepted RK-682 as a substrate, thereby generating a novel agglomerin derivative. Similar genes are coded in all known clusters of spirotetronates. An analogous acetylation–elimination process was experimentally confirmed for quartromicin D1 (**151**) biosynthesis (Scheme 22) [145].

VstJ has been identified as a probable candidate for the enzyme-catalysed [4 + 2] cycloaddition in versipelostatin A (**153**) biosynthesis by heterologous expression, gene knockout experiments and in vitro reaction with the purified enzyme (Scheme 23) [146].

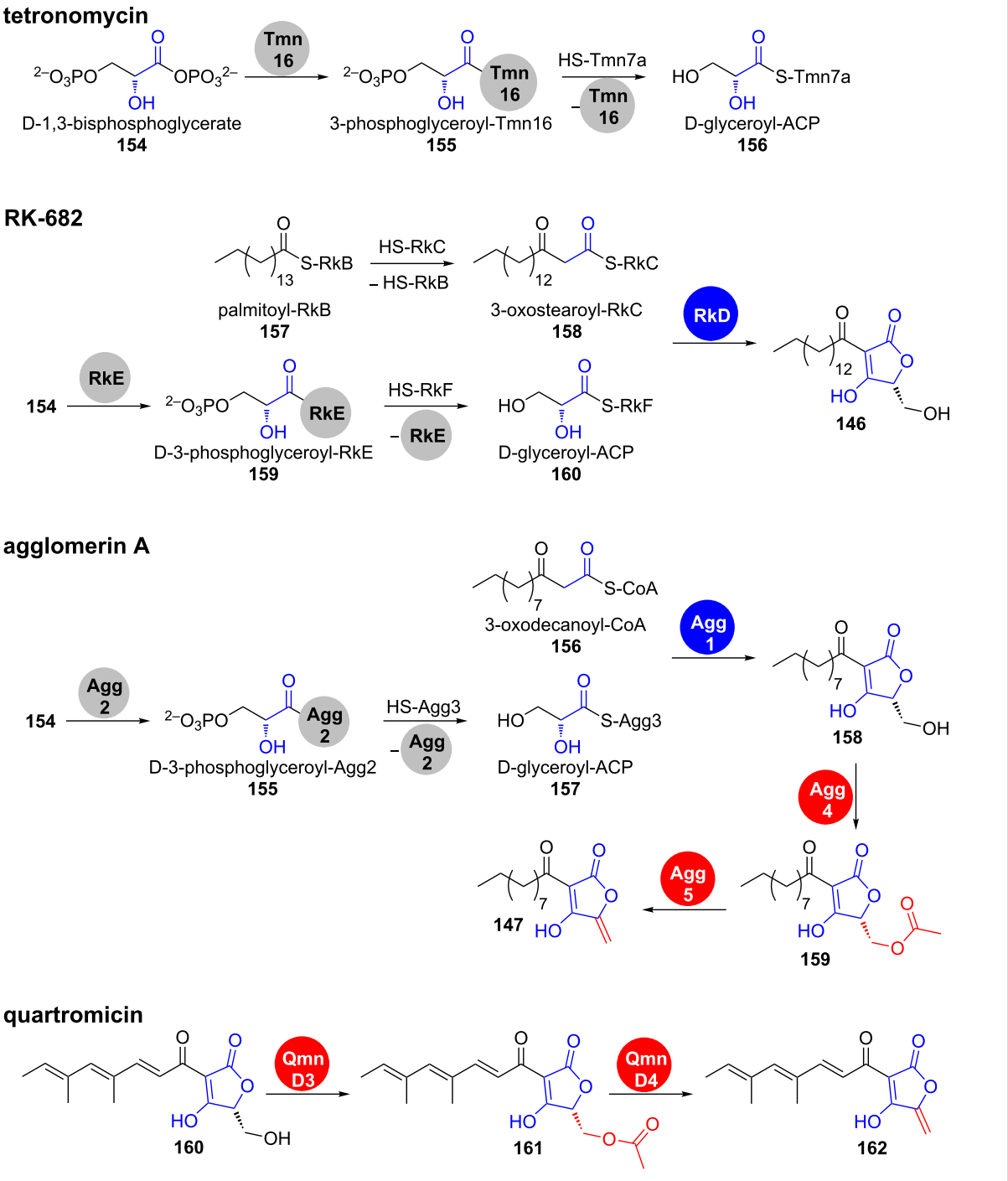

Scheme 22: Conserved steps for formation and processing in several 3-acyl-tetronate biosynthetic pathways were confirmed by in vitro studies. Tmn7a, RkC, RkF and Agg3 are ACPs. Fragments, which are established by tetronate processing are shown in red [139,141-143].

Interestingly, homologs of *vstJ* are also present in the biosynthetic gene clusters of the spirotetronate-containing polyketides abissomycin C (**148**), tetrocarcin (**150**), quartromicin D1 (**151**), chlorothricin (**152**), lobophorin and kijanimicin. All these genes are remarkably small in size (*vstJ* for example codes for only 142 amino acids) and have no significant sequence similarity to other characterised proteins [146,147].

The homologous *qmnH* from quartromicin D1 (**151**) biosynthesis contains two tandem-*vstJ* sequences in agreement with the

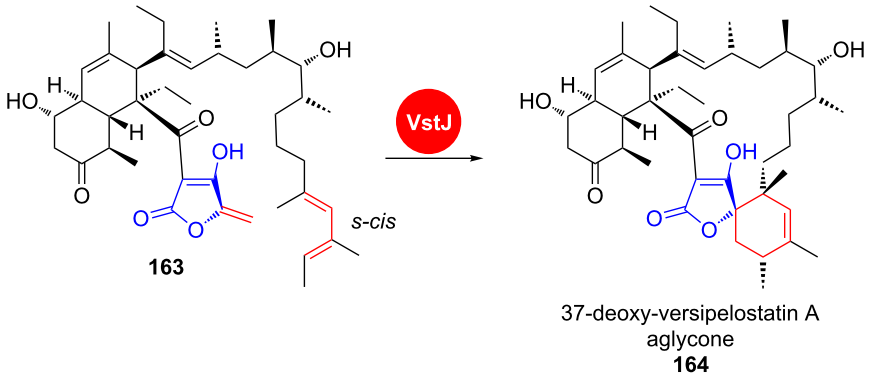

Scheme 23: In versipelostatin A (**153**) biosynthesis, VstJ is a candidate enzyme for catalysing the [4 + 2] cycloaddition. VST: versipelostatin A [146].

fact that four [4 + 2] cycloaddition events need to take place to assemble the four monomers into the highly symmetrical natural product [147].

Thiotetronates. Recently, Leadlay et al. presented their findings on the biosynthesis of thiotetronate antibiotics (Scheme 24) [148]. These small heterocyclic compounds are produced by a range of actinomycetes and a deeper understanding of their biosynthesis was for a long time hampered by the inability to identify their biosynthetic genes.

Those were finally discovered by a comparative genomics approach in which the clusters of thiolactomycin (**165**), thiotetromycin (**166**), 834-B1 (**167**) and Tü 3010 (**168**) were sequenced and genetically manipulated (Scheme 24a). Gene knockout experiments and heterologous expression of the whole clusters as well as versions devoid of key genes revealed an unprecedented mechanism for heterocycle formation (shown for thiolactomycin (**165**) in Scheme 24b).

For thiolactomycin (**165**), an iteratively acting PKS module produces a tetraketide **169** that contains all backbone carbon atoms of the natural product and which is regioselectively epoxidised at the C4 and C5 carbons by the cytochrome P450 monooxygenase TlmD1 to give **170**. The peptidyl carrier protein (PCP) of the downstream NRPS module is loaded with an L-cysteine, which serves as a sulphur donor. From **177**, sulphur is transferred by the NifS-like cysteine desulphurase TlmS to the tRNA-specific and adenosine triphosphate (ATP)-dependent 2-thiouridylase TlmJ, which is thereby converted into its disulphide form **171**.

Disulphide attack on the C5 position of **170**, activation of the resulting secondary hydroxy group as the adenosine monophosphate (AMP) ester **172** and nucleophilic attack of the sulphur on the C4 position leads to thiirane **173** formation. The cyclase domain of the NRPS module would be responsible for double-bond shift and ring opening of the thiirane **173** with concomitant nucleophilic attack of the thiolate on the thioester, leading to thiolactone **165** formation along with the cleavage from the multienzyme.

As all key genes are also present in the clusters of the other thiotetronates **166**–**168**, it was postulated that this mechanism is general for the formation of this type of heterocycle.

1.7.2 Oxidative cyclisation: Aurones. Aurones are yellow coloured pigments of ornamental flowers that belong to the flavonoids. They are structurally closely related to chalcones, from which they differ by a central, annelated furan-3-one moiety instead of an acrylate unit (Scheme 25) [149]. Their biosynthesis proceeds from chalcones by an oxidation–conjugate addition cascade catalysed by plant phenol oxidases (PPOs) [150,151].

The PPO aureusidin synthase plays a central role in aurone biosynthesis in *Antirrhinum majus* [152,153]. It catalyses the oxidation of phenols **180** and *o*-catechols **181** to *o*-quinones **182** and concomitant conjugate addition of a phenolic hydroxy group, leading to the formation of the central furan-3-one unit [154]. This enzyme is flavin-dependent and acts under consumption of hydrogen peroxide.

It has been shown that the AS is substrate tolerant and accepts different hydroxylation patterns as well as glycosylations on the chalcone A and B rings [154]. However, the oxidative half-reaction only occurs with chalcones and not with other aryl substrates like L-tyrosine, 3,4-dihydroxy-L-phenylalanine (L-DOPA), 4-coumaric acid or caffeic acid.

Grisanes. Many fungal spirobenzofuranones contain the grisane (**191**) moiety as the central structural motif

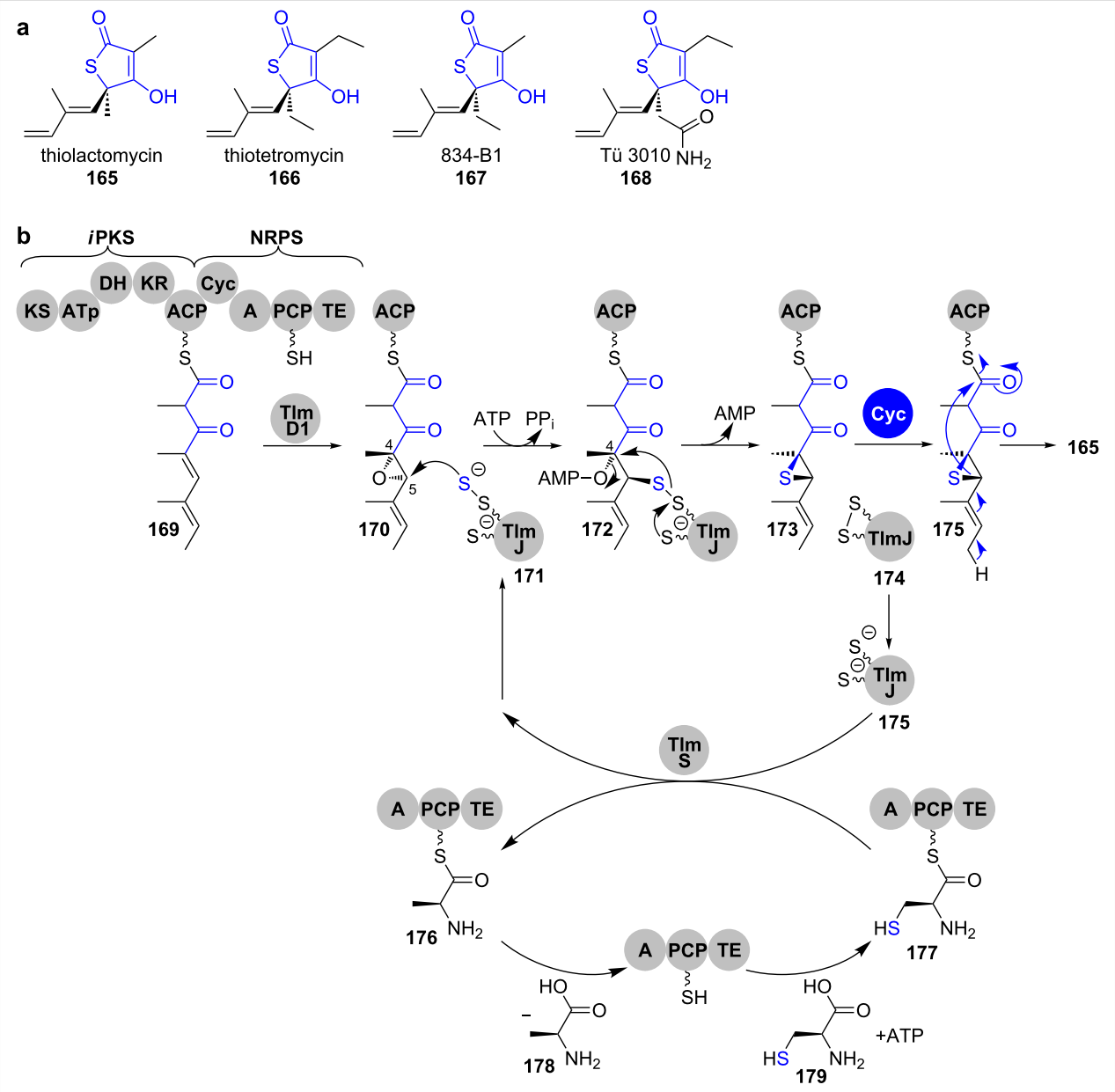

Scheme 24: a) Structures of some thiotetronate antibiotics. b) Biosynthesis of thiolactomycin (**165**) as proposed by Leadlay and co-workers. The configuration of the stereocentres in the PKS intermediates is postulated based on the assumption that all reactions on the way to the structurally fully elucidated product **165** are occurring stereospecifically. Cyc: cyclase domain, A: adenylation domain, PCP: peptidyl carrier protein [148].

(Scheme 26a). The spiro linkage between the B and C rings is installed by oxidative phenol coupling starting from type II-PKS-derived anthraquinone precursors [155].

(+)-Geodin (**189**) was the first chlorinated compound isolated from fungi [156]. During its biosynthesis in *Aspergillus terreus*, the furan-3-one ring is closed by action of the multicopper blue protein dihydrogeodin oxidase on dihydrogeodin (**186**) (Scheme 26a) [157,158]. The direct precursor of dihydrogeodin (**186**) in this pathway, sulochrin (**185**), is also a substrate for a close homologue of dihydrogeodin oxidase (DHO). Sulochrin oxidase (SO) converts sulochrin (**185**) into (+)-bisdechlorogeodin (**188**), which then spontaneously hydrates to asterric acid (**192**), the end product of this pathway in *Penecillium frequentans* [158].

In 2010, the gene cluster of griseofulvin (**193**) was sequenced and analysed [159]. This cluster does not contain a multicopper blue protein, but instead the cytochrome P450 oxygenase GsfF. This enzyme has no other obvious role in biosynthesis and was proposed to catalyse the stereospecific oxidative radical-coupling reaction of griseophenone C (**187**, Scheme 26b).

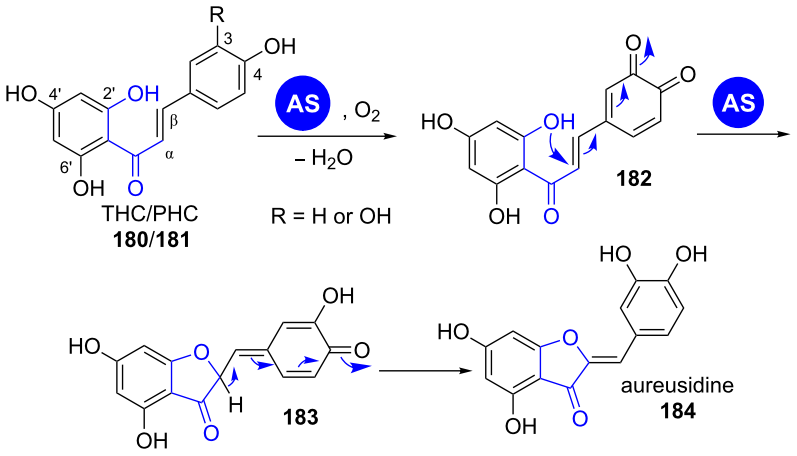

Scheme 25: Aureusidine synthase (AS) catalyses phenolic oxidation and conjugate addition of chalcones leading to aureusidine (**184**). THC: 2',4,4',6'- tetrahydroxychalcone; PHC: 2',3,4,4',6'- pentahydroxychalcone [154].

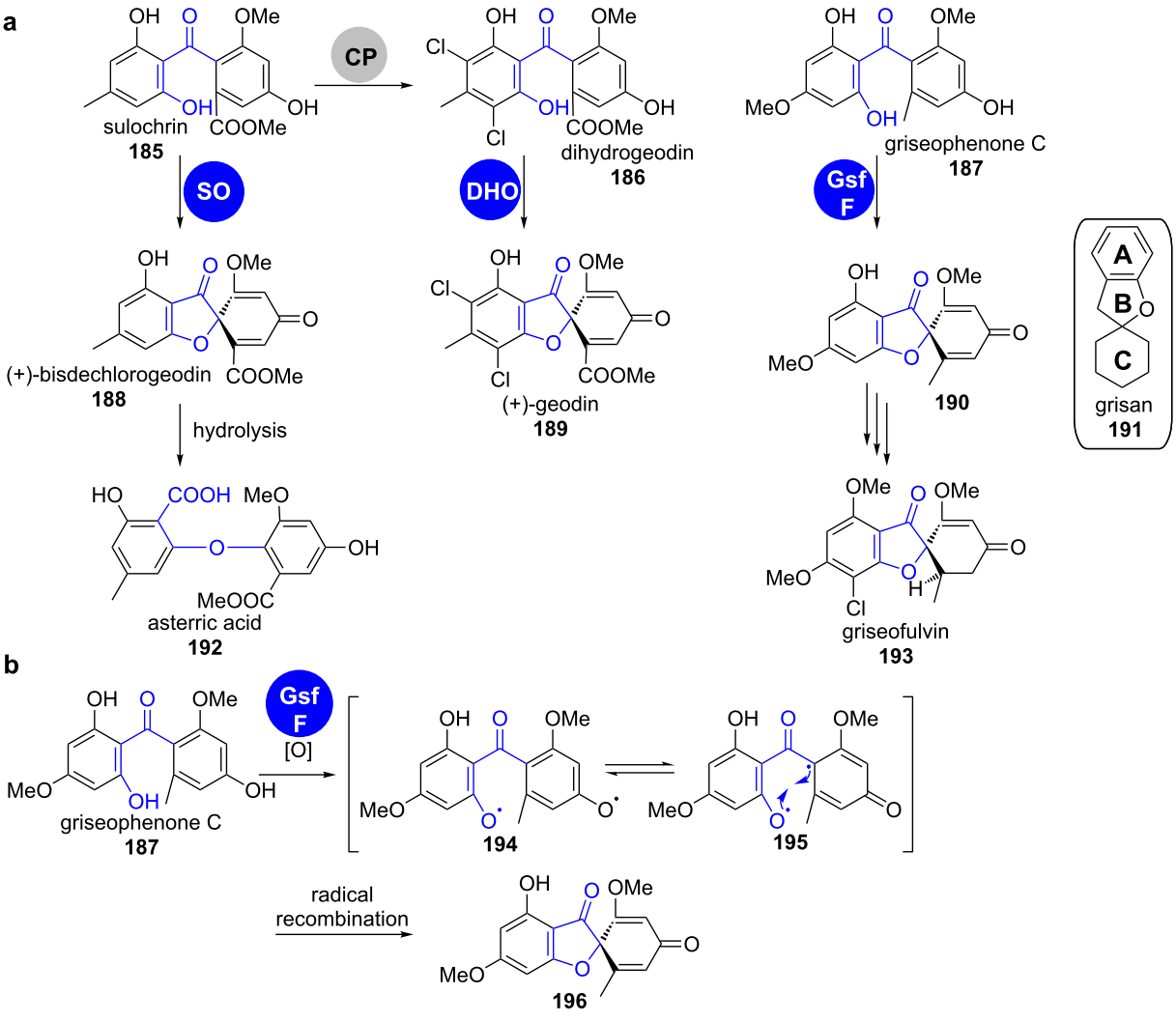

Scheme 26: a) Oxidative cyclisation is a key step in the biosynthesis of spirobenzofuranes **189**, **192** and **193**. b) Mechanism of the proposed cytochrome P450-catalysed stereospecific radical coupling in the biosynthesis of griseofulvin (**193**). CP: chloroperoxidase; SO: sulochrin oxidase; DHO: dihydrogeodin oxidase [157-159].

1.8 Oxetanones

Salinosporamide. Oxetanones are rare structures and highly reactive due to their ring strain. One of the most prominent examples is the proteasome inhibitor salinosporamide A (**199**) (Scheme 27) [160,161].

Based on gene cluster analysis, it was proposed that both heterocycles of this PKS–NRPS hybrid product, an oxetan-2-one and a pyrrolidin-2-one, are formed by a bicyclisation mechanism. Aldol addition of the amino acid α-position on the carbonyl gives the pyrrolidin-2-one. Concomitant attack of the intermediately formed hydroxylate on the thioester closes the β-lactone and releases salinosporamide A (**199**) from the assembly line.

Ebelactone A. Ebelactone A (**201**) is an esterase inhibitor of PKS type I origin that is produced by *Streptomyces aburaviensis* ATCC 31 860 [162]. Similar to salinosporamide A (**199**), the respective biosynthetic gene cluster neither encodes a modular nor a lone-standing thioesterase domain. Instead, in vitro studies with the SNAC-thioester bound acyclic intermediate demonstrated the spontaneous heterocyclisation by nucleophilic attack of the β-hydroxy group on the thioester of **200**, resulting in the off-loaded ebelactone A (**201**) (Scheme 28) [163].

The β-lactone moiety of the human pancreatic lipase inhibitor lipstatin is also formed in a similar fashion.

2 Nitrogen-containing heterocycles

Nitrogen-containing heterocycles are established in four principal ways (Scheme 29).

The biosynthesis of pyridinones (**203**, **207**, **211** or **213**) is mechanistically particularly diverse. It occurs via condensation reactions between carbonyl groups and nitrogen-containing functionalities, Michael addition–lactamisation cascades (similar to the mechanism for 4-substituted pyran-2-ones shown in Scheme 2e), Dieckmann condensations as well as oxidative ring expansion of tetramates (**212**, a–d in Scheme 29). Tetramates **209** are formed by Dieckmann condensation (c in Scheme 29).

2.1 Pyridinones

2.1.1 Condensation between carbonyl groups and nitrogen nucleophiles: Piericidin. Highly substituted α-pyridinones that carry the polyketide chain in the 6-position are assembled by type I PKS. In 2007, Grond et al. isolated the iromycins **214** from *Streptomyces bottropensis* sp. Gö Dra 17 and provided initial information on their biosynthesis by feeding studies with istope-labelled precursors (Scheme 30a) [164]. These experi-

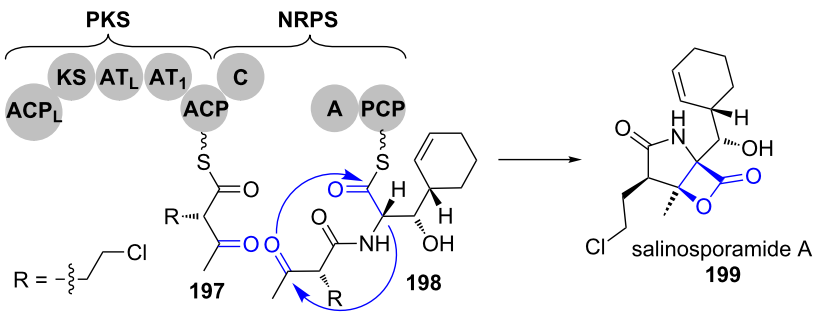

Scheme 27: A bicyclisation mechanism forms a β-lactone and a pyrrolidinone and removes the precursor from the assembly line in salinosporamide A (**199**) biosynthesis [160,161].

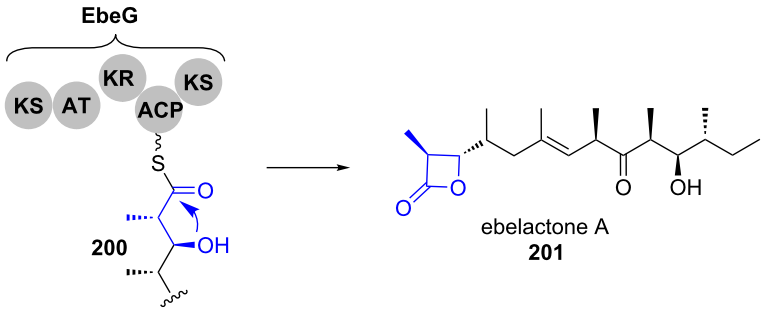

Scheme 28: Spontaneous cyclisation leads to off-loading of ebelactone A (**201**) from the PKS machinery [163].

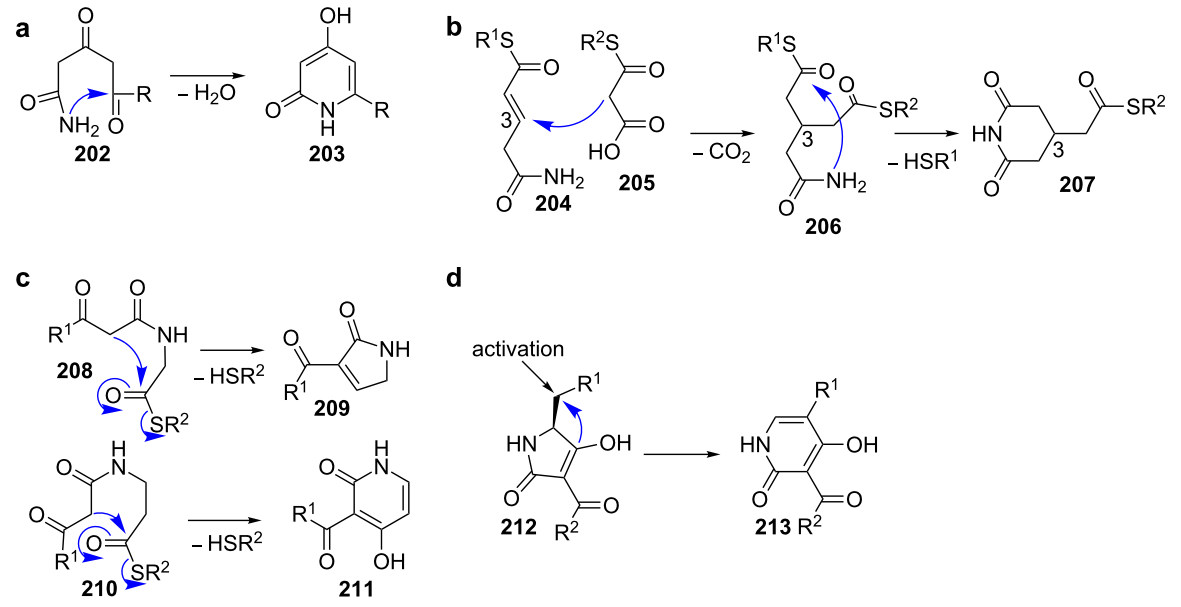

Scheme 29: Mechanisms for the formation of nitrogen heterocycles.

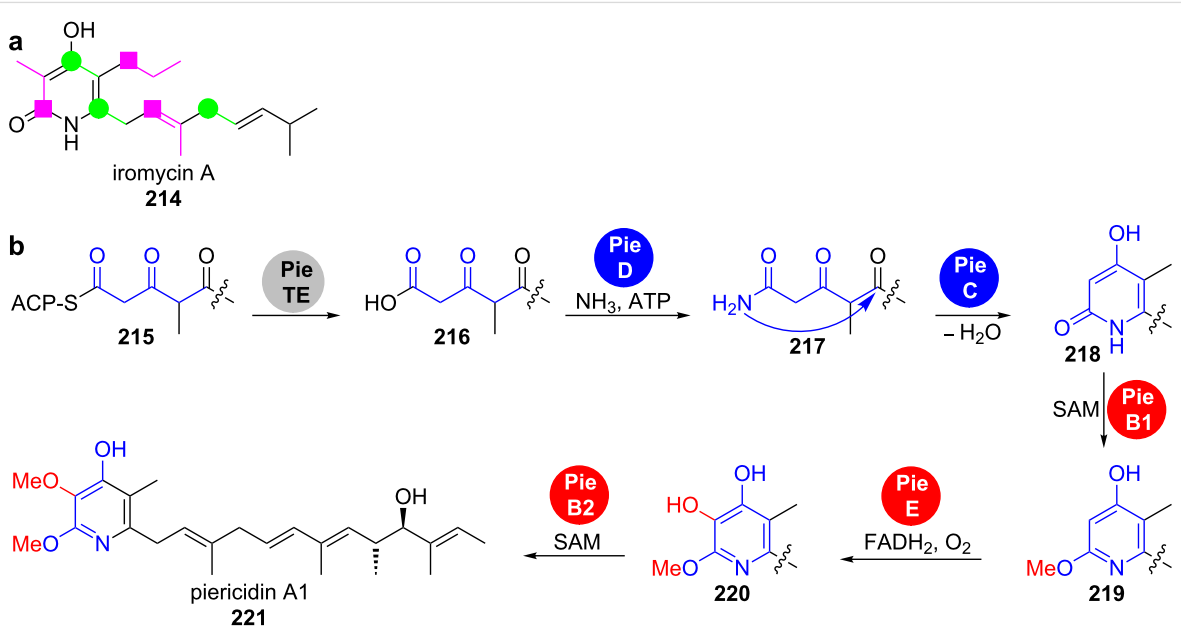

Scheme 30: Biosynthesis of highly substituted α-pyridinones. a) Feeding experiments confirmed the polyketide origin of iromycin A (**214**). b) The heterocycle in piericidin A1 (**221**) is formed by condensation between an amide and a ketone [164-166].

ments revealed that all carbon atoms of the heterocycle are derived from acetate or propionate units and that no amino acid is incorporated. The nitrogen thus originates from transamination.

More detailed information about the mechanism became available from the gene cluster analysis of the *O*-methylated, highly substituted α-pyridinone piericidin A1 (**221**) from *Streptomyces piomogeues* var. Hangzhouwanensis (Scheme 30b) [165,166]. Apart from the genes that code for a modular type I PKS as well as *O*-methyltransferases and an oxygenase, the cluster contains *pieC* and *pieD* whose gene products were annotated as a hypothetical protein and an asparagine synthase, respectively.

While inactivation of *pieD* led to complete abolishment of piericidin A1 (**221**) production, inactivation of *pieC* only led to a de-

crease in titre to about 35–50% of the wild-type levels, suggesting that *pieC* is not essential for biosynthesis [164]. PieC belongs to the SRPBCC superfamily, which has previously been shown to be involved in the controlled cyclisation events catalysed by type II PKS [167,168]. These enzymes have a deep hydrophobic ligand-binding pocket, which templates particular cyclisation patterns.

The fact that PieC was dispensable for piericidin A1 (**221**) biosynthesis was explained by that it could either be complemented by other endogenous cyclases in *S. piomogeues* or that the thermodynamically favoured formation of the six-membered heterocycle occurs spontaneously in the absence of the enzyme.

Acridones. The acridones are pyridin-4(1*H*)-one-containing metabolites of *Rutaceae*, which serve for UV protection and antimicrobial defense [169,170]. They are produced by various acridone synthases (ACSs), which are expressed depending on external triggers like irradiation or fungal elicitation (Scheme 31).

ACSs are plant type III PKSs that catalyse condensation between *N*-methylanthraniloyl-CoA (**222**) and three units of malonyl-CoA (**66**) to yield 1,3-dihydroxy-*N*-methylacridone (**224**, Scheme 31). The cyclisation mechanism passes hemiaminal **223** that then undergoes dehydrative aromatisation. ACSs show high similarity on the amino acid level to other type III PKS systems like chalcone synthases and benzalacetone synthases, but their strict substrate specificity for nitrogen-containing starter units avoids mispriming with precursors of the latter group of enzymes [172]. Altering of synthase specificity and thus interconversion into each other has been demonstrated [173].

2.1.2 Michael addition–lactamisation: Glutarimides. The biosynthesis of the glutarimides proceeds similar to δ-lactone biosynthesis and has been described in chapter 1.6.

2.1.3 Dieckmann condensation: Actinomycete-derived pyridinone natural products are formed in a similar fashion as tetramates (see chapter 2.2.1) [174]. Elaborate polyketide intermediates are condensed to the amine functionality of a PCP-bound β-alanine on the terminal module of a PKS–NRPS assembly line (Scheme 32). The resulting *N*-β-ketoacyl-β-alanyl-*S*-PCP (3-(3-oxoalkylamido)propanoyl-*S*-PCP, **225**) is then processed by a Dieckmann cyclase to give the heterocycle **226** that tautomerises to the 4-hydroxy-3-acylpyridin-2-one (**227**) [174].

The elfamycin antibiotics kirromycin (**228**) and factumycin (**229**) from *Streptomyces collinus* Tü 365 and WAC5292, respectively, are formed via this mechanism. For kirromycin (**228**) biosynthesis, it has been shown by in vitro activity testing that the Dieckmann cyclase KirHI condenses *N*-acetoacetyl β-alanyl-SNAC as well as *N*-acetoacetyl D-alanyl-SNAC and *N*-acetoacetyl glycyl-SNAC to the corresponding pyridinones and tetramates (see also chapter 2.2.1). The factumycin gene cluster was recently sequenced and contains a close homolog of KirHI, FacHI, which is supposed to catalyse the analogous reaction in its biosynthesis.

In accordance with the release from the assembly line by Dieckmann condensation, both clusters do not contain a TE domain [175]. In contrast, the cluster of the pyridinone-less elfamycin antibiotic L-681217 from *Streptomyces cattleya* does not harbour a Dieckmann cyclase homolog, but a conventional TE domain [175-177].

2.1.4 Oxidative ring expansion: The oxidative ring expansion is an alternative biosynthetic strategy that leads to pyridinone rings in fungal systems. The precursors of these expansion reactions are tetramic acids, whose biosynthetic characteristics are highlighted in chapter 2.2.1.

The backbone of the tenellins from the insect pathogen *Beauveria bassiana* is assembled by an *i*PKS–NRPS hybrid and the resulting *N*-β-ketoacyl-β-tyrosinyl-*S*-PCP intermediate **231** is

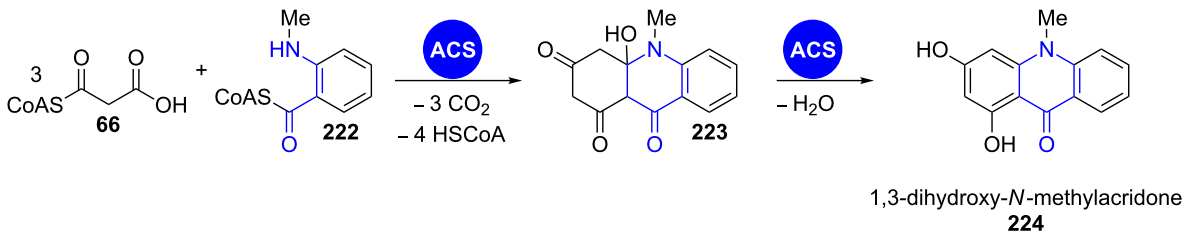

Scheme 31: Acridone synthase (ACS) catalyses the formation of 1,3-dihydroxy-*N*-methylacridone (**224**) by condensation of *N*-methylanthraniloyl-CoA (**222**) and three units of malonyl-CoA (**66**) [171].

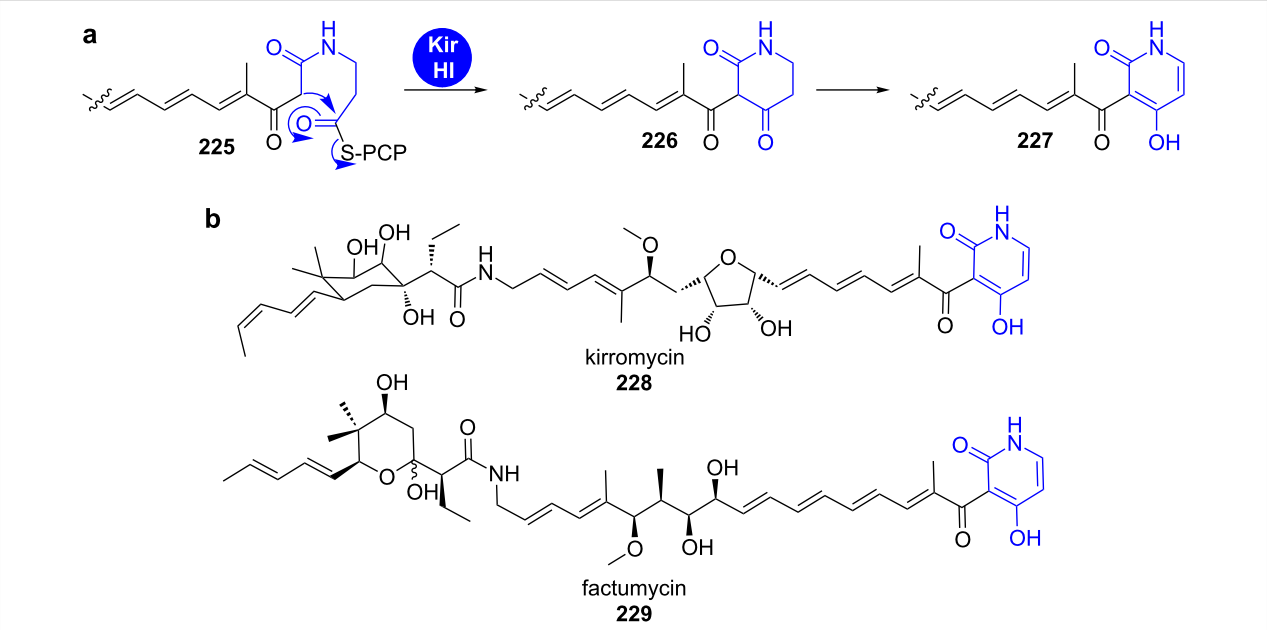

Scheme 32: A Dieckmann condensation leads to the formation of a 3-acyl-4-hydroxypyridin-2-one **227** and removes the biosynthetic precursor from the PKS–NRPS hybrid assembly line during kirromycin (**228**) biosynthesis [174].

cyclised by an R* domain to yield the tetramic acid pretenellin A (**232**, Scheme 33a). Two cytochrome P450 monooxygenases then catalyse the consecutive ring expansion to the pyridinone and *N*-hydroxylation. TenA was annotated as the ring expandase responsible for pyridinone formation.

The mechanism of this unusual ring-expansion reaction remains unclear in detail. The authors however presented preliminary indications that point towards a radical mechanism without isolable intermediates (Scheme 33b) [178]. This was supported by the presence of the shunt product prototenellin D (**240**) in the wild-type strain and in several knockout transformants. Conversion experiments with cell-free extracts showed that **240** is not a competent substrate of the tailoring enzymes in the cluster. It was suggested that other oxidising enzymes with appropriate substrate specificity must be encoded in the *Beauveria bassiana* genome and responsible for prototenellin (**240**) formation. A similar situation must be given for compounds **238**, **239** and **241**–**243**, whose clusters contain ring expandase candidates with high identity to TenA and for which similarly hydroxylated metabolites were isolated (Scheme 33c). Other authors suggested mechanisms that pass a quinonemethide intermediate [179].

The *N*-hydroxylation reaction occurring from pretenellin B (**233**) to tenellin (**234**) is catalysed by the second cytochrome P450 monooxygenase TenB. This type of reaction is usually rather catalysed by FAD-dependent monooxygenases and nonheme iron-containing monooxygenases [181-185].

The cytochrome P450 monooxygenase ApdE (48% amino acid identity to TenA) was shown to catalyse a similar ring-expansion reaction in aspyridone A (**238**) biosynthesis (Scheme 33c). This enzyme, however, shows a more diverse oxidation chemistry leading not only to the pyridinone, but also to a β-hydroxytetramic acid as well as a dephenylated product.

Oxazoles. Natural products featuring oxazole moieties are predominantly derived from the nucleophilic attack of a serine side chain hydroxy group on a carbonyl carbon of the peptide backbone. This has been shown for the oxazoles in thiazole/oxazole-modified microcins (TOMMs) which are a group of ribosomally synthesised and posttranslationally modified peptides as well as for NRPS-derived natural products [186]. In the case of NRPS, the assembly is accomplished by a modified condensation domain (designated as heterocyclisation domain) and the resulting oxazoline is often subsequently aromatised to the oxazole by a flavin-dependent oxygenase domain [187]. However, some PKS–NRPS derived oxazoles originate from a different biosynthetic route.

Oxazolomycin (**244**) is a polyene spiro-linked γ-lactam/β-lacton antibiotic that was originally isolated from *Streptomyces albus* (Scheme 34a) [188,189].

Isotope-labelling studies have shown that instead of serine, three molecules of glycine are incorporated into its carbon backbone. The analysis of the respective biosynthetic gene cluster revealed the absence of canonical heterocyclisation or

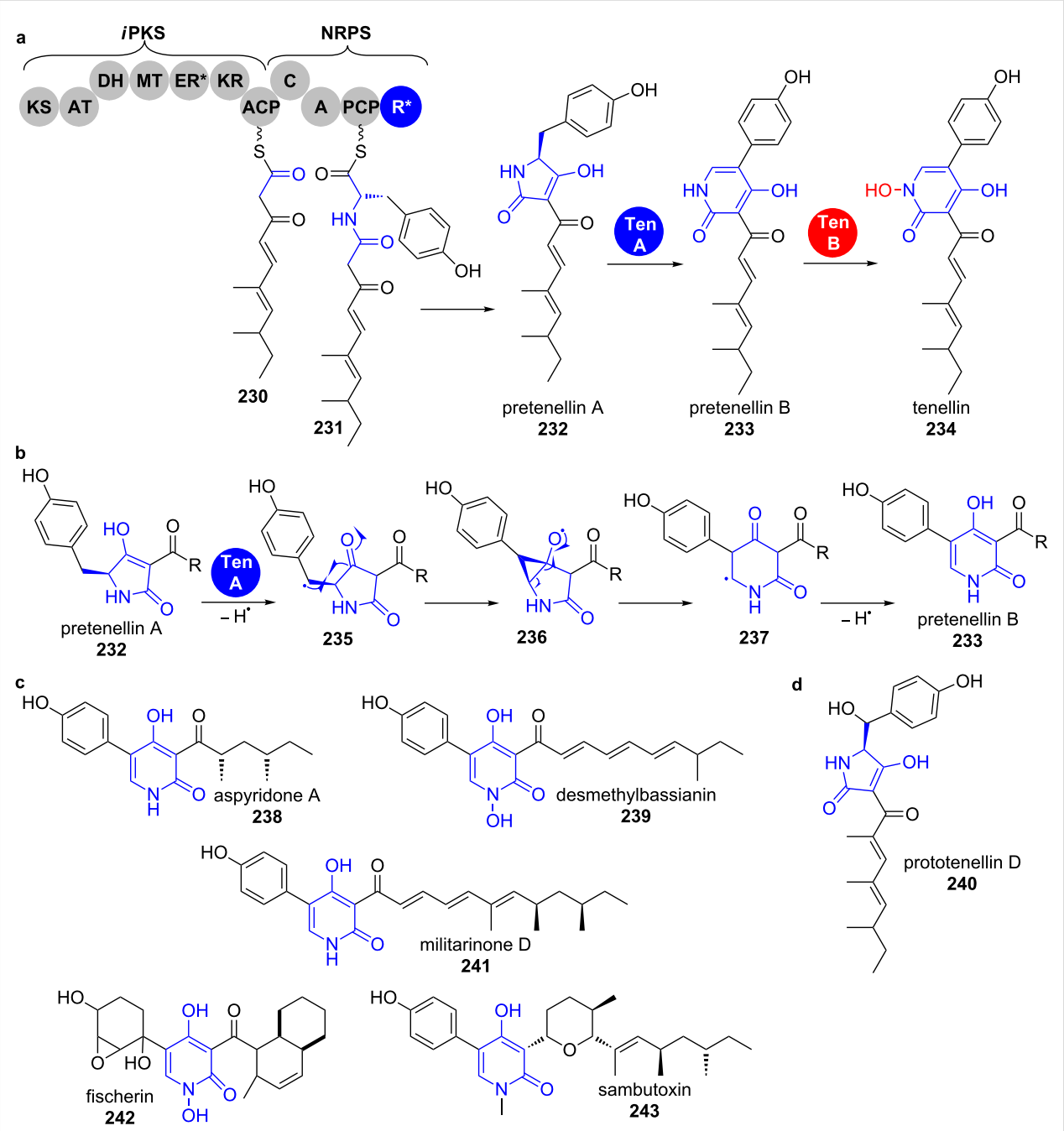

Scheme 33: a) Biosynthesis of the pyridinone tenellin (**234**). b) A radical mechanism was proposed for the ring-expansion reaction catalysed by TenA. c) Other fungal pyridinone-containing hybrid *i*PKS–NRPS natural products [178,180].

oxidation domains [190]. Instead, the loading module OzmO contains a formylation domain that transfers the formyl group of formyl-tetrahydrofolate onto glycin-*S*-PCP (Scheme 34b) [191]. The resulting formyl-glycin-*S*-PCP **246** serves as the precursor for cyclisation.

Recently, Leadlay and co-workers proposed a mechanism for oxazole formation in the biosynthesis of the *C*2-symmetrical macrodiolide conglobatin (**245**) that was isolated from *Streptomyces conglobatus* ATCC 31005 [192,193]. In the biosynthetic gene cluster, a putative cyclodehydratase CongE is coded that is homologous to OzmP from the oxazolomycin (**244**) gene cluster. Molecular modelling studies suggested, that CongE belongs to the family of N-type ATP (pyro)phosphohydrolases and contains the conserved ATP-binding motif SGGKDS. In analogy to a mechanism previously reported by Dunbar and

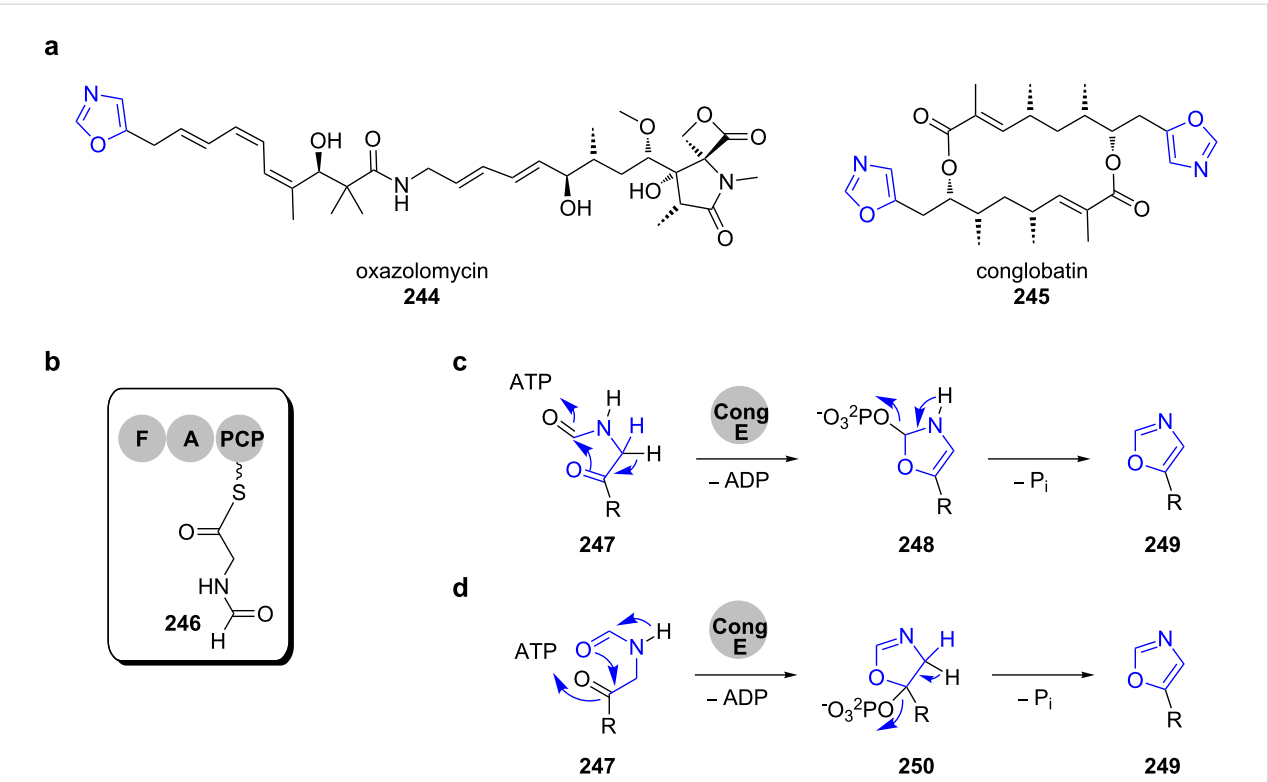

Scheme 34: a) Oxazole-containing PKS–NRPS-derived natural products oxazolomycin (**244**) and conglobatin (**245**). b) Formylglycyl-*S*-PCP precursor for oxazole formation. c) and d) Proposed mechanisms for oxazole formation as suggested by Leadlay and co-workers [192].

co-workers, Leadlay and co-workers hypothesised that CongE promotes oxazole formation by activation of one of the carbonyl amide oxygens by either phosphorylation or adenyl transfer followed by nucleophilic attack and elimination (Scheme 34c and d) [192,194].

2.2 Pyrrolidinones

2.2.1 Dieckmann condensation: Tetramates. Natural products featuring a tetramic acid moiety (pyrrolidine-2,4-dione **251**, Scheme 35) have been isolated from terrestrial and marine organisms, including fungi, bacteria and sponges. Due to different oxidation states of the five-membered heterocyclic core and diversified downstream processing, tetramates display a high structural complexity.

This chemically rich diversity results in a wide range of biological activities, including antimicrobial, antitumor and antiviral properties [195-199]. The pharmacologically most relevant tetramates are – as in the case of their corresponding oxygen-analogues tetronates (see chapter 1.7) – those featuring 3-acyl residues. Tetramic acids are usually present in their 2,4-diketo form **251** and 3-acyltetramic acids can in principle form nine different tautomers, of which typically four are detectable in solution (**252a**–**d**, Scheme 35b).

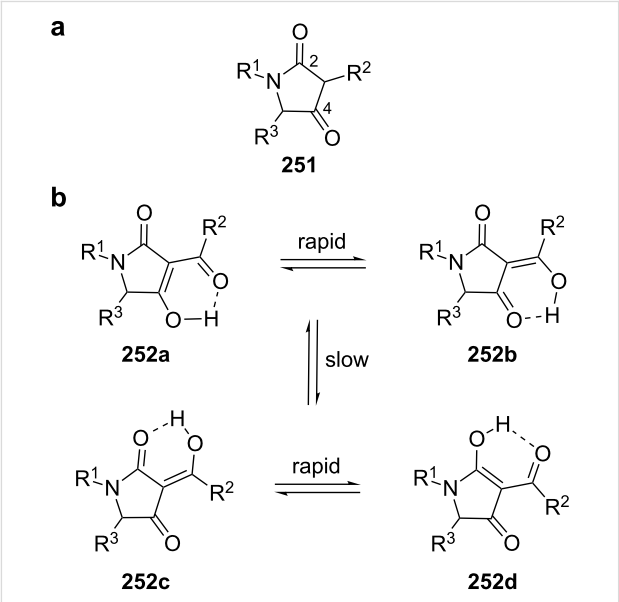

Scheme 35: Structure of tetramic acids **251** (a) and major tautomers of 3-acyltetramic acids **252a–d** (b). Adapted from [195].

Tetramate cores are typically derived from PKS–NRPS hybrid assembly lines, yielding linear 3-(β-ketoamide)propanoyl-thioester intermediates. The subsequent Dieckmann cyclisation

releases the tetramate from the megasynthetase. There are basically four different types of enzymatic units responsible for this process, which are described to date: module-embedded R*- and TE-domains, as well as lone-standing PyrD3/PyrD4-homologs and Dieckmann cyclases.

In fungal *i*PKS–NRPS systems, a terminal reductive domain (R*) directly catalyses the tetramate cyclisation without intermediacy of a free aldehyde intermediate [179]. Studies of Schmidt et al. provided the first evidence for this biosynthetic route, utilising the R* domain of the equisetin (**255**) pathway from *Fusarium* strains (Scheme 36) [200,201].

The reaction required no cofactor, despite a conserved N-terminal NAD(P)H binding motif that is characteristic for the SDR superfamily. In addition, phylogenetic analyses revealed that R*-domains represent a distinct branch in the SDR superfamily tree. Subsequent studies showed that the equisetin synthetase genes had been misidentified as the fusaridione A synthetase genes and the cluster was reassigned correctly [202]. Sequence alignments in the same study also identified corresponding R*-domains in the biosynthetic pathways of the spiro-tetramates.

Pseurotins are *Aspergillal* natural products from the group of the 3-spirotetramates, which display a wide array of biological activities (Scheme 37a).

Their spiro centre is installed by epoxidation of the C3–C4 double bond of the tetramate ring in **264** and subsequent epoxide opening by the 3'-enol oxygen of the side chain. Interestingly, it was shown that the bifunctional epoxidase/C-MT PsoF also catalyses a gate-keeping methylation in *trans* on the stage of the nascent tetraketide (Scheme 37, highlighted in boxes). This modification is crucial for the acyl-chain transfer from PKS (**261**) to NRPS (**263**) as well as the epoxidation reaction that yields the final spiro structure in **265** and pseurotin A (**256**). Multiple methylation and oxidation steps give rise to a high chemical diversity in the pseurotin compound family [203,204]. This gate-keeping methylation was also proposed for other fungal tetramates (Scheme 37b).

For the polycyclic tetramate macrolactams (PTMs), a module-embedded TE domain that belongs to the α/β-hydrolase family adopts the function of the fungal R*-domain [205,206]. The tetramic acid is incorporated into a macrolactam ring, which is fused to a set of two or three carbacycles of varying size, cyclization pattern and oxidation level (Figure 7). This rich structural diversity of PTMs, which are produced in phylogenetically diverse bacteria results in a broad spectrum of biological activities, including compounds with antifungal, antibiotic, and antitumoural properties [207].

Ikarugamycin (**267**) is a PTM produced by various *Streptomyces* species that shows a broad spectrum of biological activity including antimicrobial and cytotoxic properties [208]. Its biosynthesis has been reconstituted in *E. coli* and has shown to be remarkably streamlined, utilising only the three enzymes IkaABC to build up its highly complex structure (Scheme 38) [209,210].

IkaA is a mixed *i*PKS–NRPS, in which the *i*PKS provides two ACP-bound hexaketides **271** and **273**. The condensation domain of the NRPS attaches these two polyketide chains to the amine

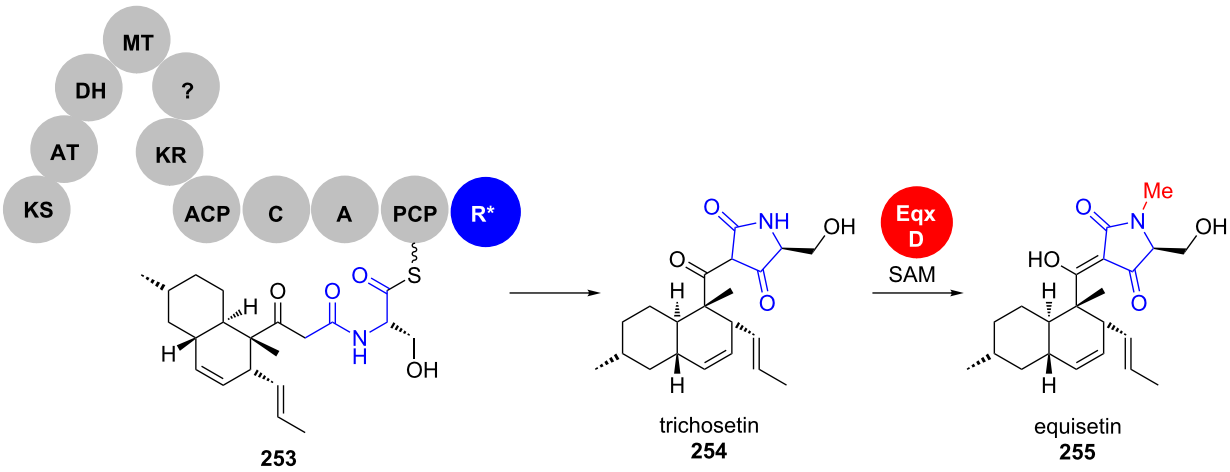

Scheme 36: Equisetin biosynthesis. R*: terminal reductive domain. Adapted from [202].

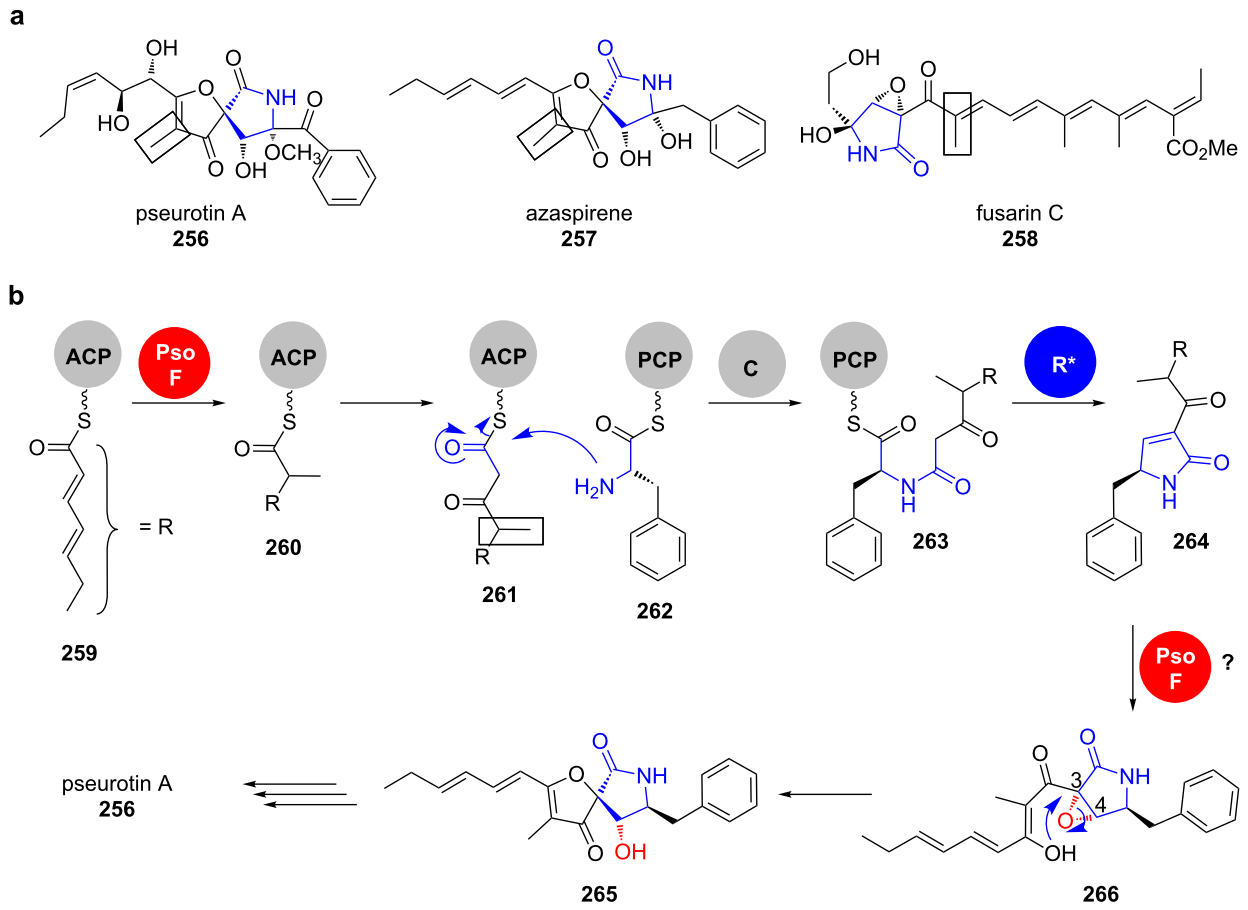

Scheme 37: a) Polyketides for which a similar biosynthetic logic was suggested. b) Pseurotin A (**256**) biosynthesis. Modified from [203].

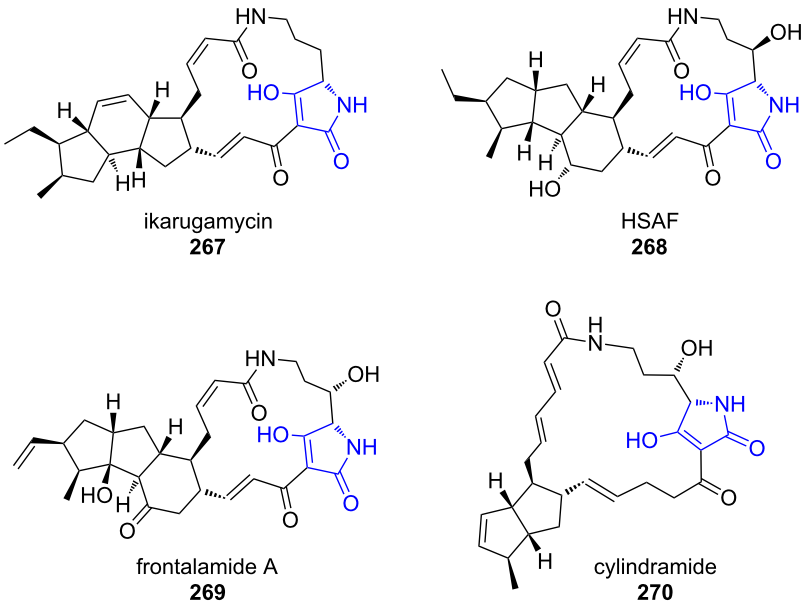

Figure 7: Representative examples of PTMs with varying ring sizes and oxidation patterns [205,206].

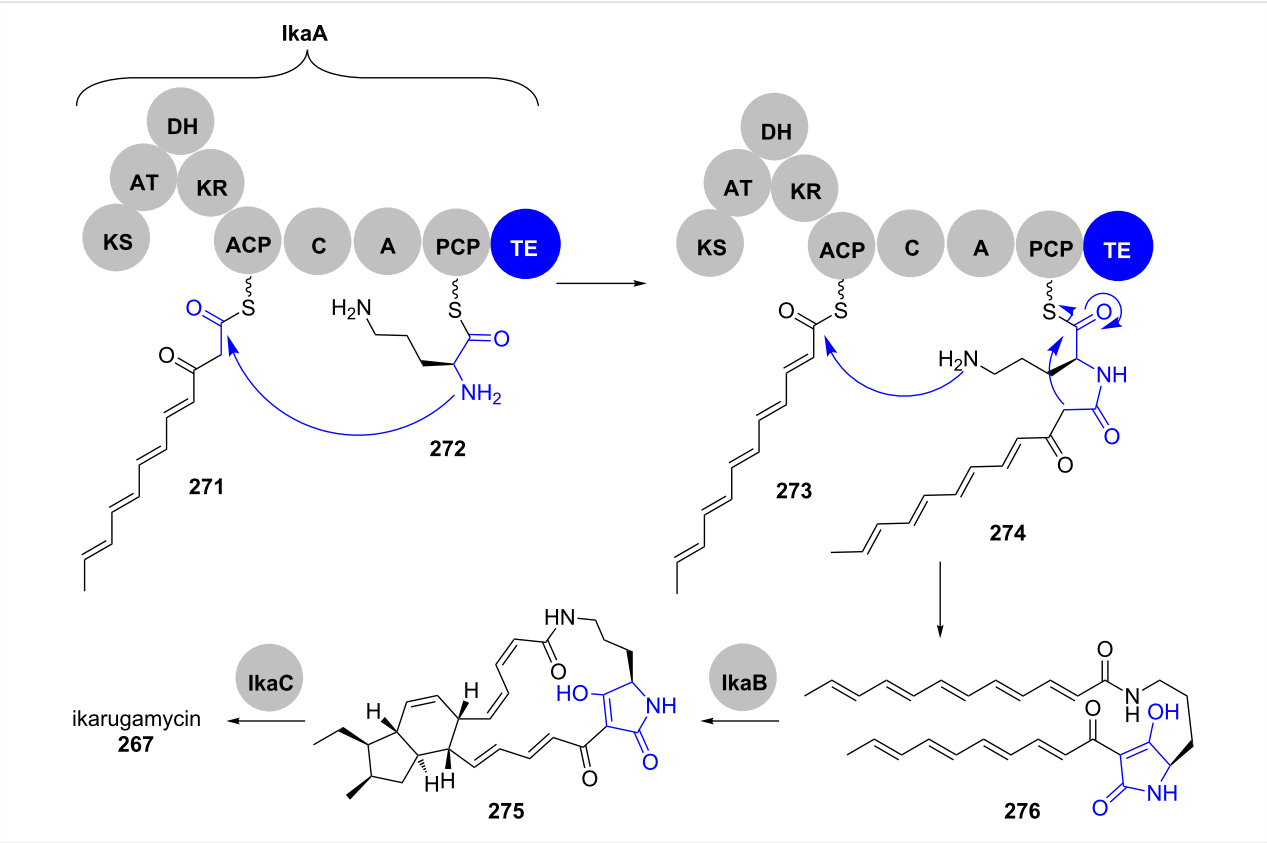

Scheme 38: Ikarugamycin biosynthesis. Adapted from [209-211].

functionalities of PCP-bound ornithine **272**. The tetramate **276** is released by the TE domain and further processed towards ikarugamycin (**267**) [212].

Isolated in a screening against various drug-resistant pathogens, the pyrroindomycins A and B from *Streptomyces rugosporus* LL-42D005 (NRRL 21084) were the first discovered natural products containing a cyclohexene spiro-linked tetramate moiety combined with a *trans*-dialkyldecalin system in their aglycone (**279**) (Scheme 39) [213,214].

The linear carbon backbone is assembled by the modular PKS type I system PyrA1-A8 in a colinear manner and passed to the NRPS PyrB, which catalyses an aminoacyl extension with

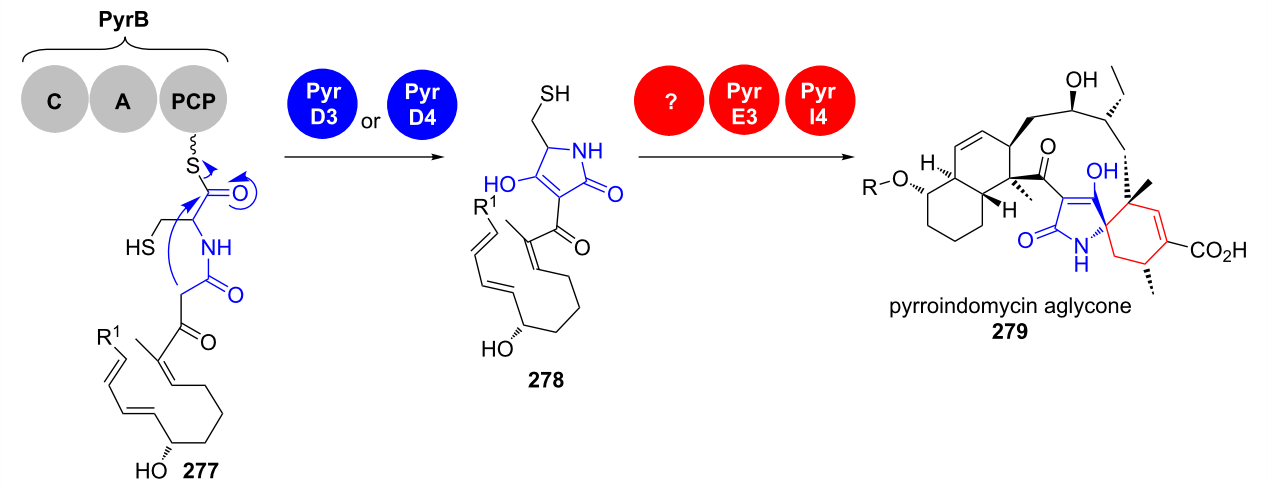

Scheme 39: Tetramate formation in pyrroindomycin aglycone (**279**) biosynthesis [213-215].

L-cysteine [215]. This linear precursor **277** is then cleaved off the megaenzyme by a Dieckmann condensation yielding the tetramate moiety in **278**. Gene deletion experiments and in vitro assays revealed that this reaction is catalysed individually by the two phylogenetically distinct enzymes PyrD3 and PyrD4. Their respective biosynthetic genes are closely clustered and located centrally in the PKS gene cluster. Homologs of PyrD3 and PyrD4 were found in biosynthetic gene clusters of the structurally related spirotetronates. The introduction of *chlD4* from the spirotetronate chlorothricin (**152**) biosynthesis even partially restored pyrroindomycin production in a Δ*pyrD3-D4* deletion mutant, highlighting the similarities in the tetronate/tetramate formation chemistry in these natural products.

Surprisingly, in some actinomycete-derived tetramic acid-containing natural products, R* or TE domains as well as PyrD3/PyrD4-homologs are absent in the respective gene clusters. On the contrary, recent in vitro studies revealed conserved dedicated Dieckmann cyclases as catalysts in the biosynthetic pathways towards tirandamycin B (**281**), streptoylydigin (**282**) and α-lipomycin (**283**), respectively (Scheme 40) [174].

In all these pathways, homologous genes are found directly upstream of the NRPS genes and in their deletion mutants, tetramate formation was abolished. In in vitro reactions, simplified SNAC thioester substrate surrogates were converted into tetramates and mutational studies revealed a conserved catalytic triad consisting of Cys_{88}-Asp_{115}-His_{253}. The respective Dieckmann cyclases are phylogenetically distinct from fungal R* domains, bacterial TE domains and PyrD3/PyrD4. Interestingly, this paradigm also applies for bacterially derived 2-pyridone scaffolds such as kirromycin (**228**) (see chapter 2.1.3).

Conclusion

Due to their attractive biological activity and abundance, oxygen and nitrogen heterocycles-containing polyketides are highly relevant. Recent years have seen a steady progress in the understanding of their biosynthesis and plenty of novel enzymology has been uncovered in this context. It is now clear that heterocycle formation occurs by an exceptionally broad range of mechanisms. Nevertheless, there is still plenty of room for future studies on the biosynthesis of other types of heterocycles as well as on the catalytic mechanisms and the structures of

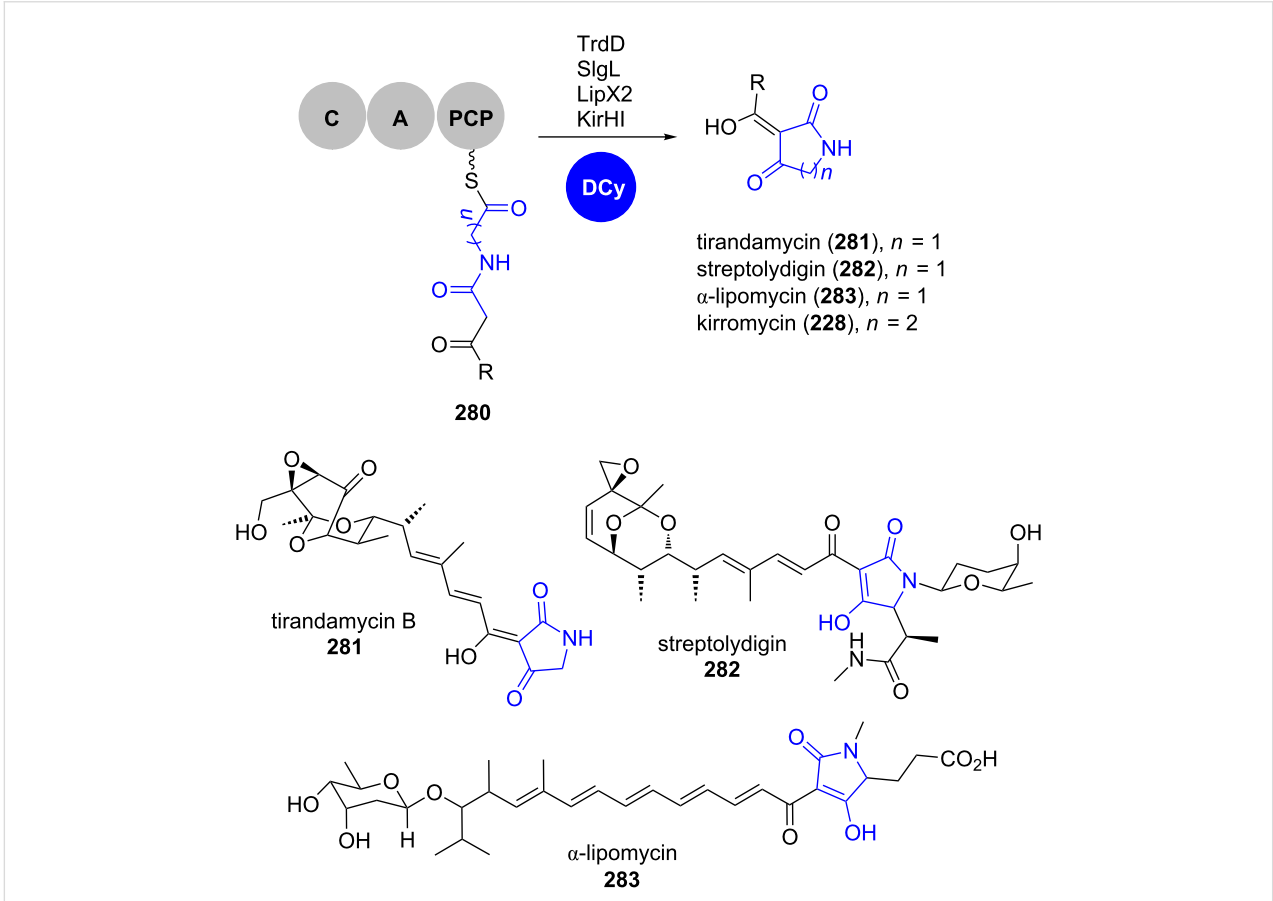

Scheme 40: Dieckmann cyclases catalyse tetramate or 2-pyridone formation in the biosynthesis of, for example, tirandamycin B (**281**), streptolyldigin (**282**), α-lipomycin (**283**) and kirromycin (**228**), respectively. DCy: Dieckmann cyclase. Adapted from [174].

cyclising enzymes. In principle, all these enzymes also represent future candidates for the development of novel types of biocatalysts for chemoenzymatic synthesis.

Acknowledgements

We thank the Deutsche Forschungsgemeinschaft for funding by the Emmy Noether program as well as the European Union for a Career Integration Grant.

References

1. Taylor, R. D.; MacCoss, M.; Lawson, A. D. G. *J. Med. Chem.* **2014,** *57,* 5845–5859. doi:10.1021/jm4017625
2. Pozharskii, A. F.; Soldatenkov, A. T.; Katritzky, A. R. *Heterocycles in Life and Society: An Introduction to Heterocyclic Chemistry, Biochemistry and Applications,* 2nd ed.; Wiley-VCH: Weinheim, 2011. doi:10.1002/9781119998372
3. Dua, R.; Shrivastava, S.; Sonwane, S. K.; Shrivastava, S. K. *Adv. Biol. Res.* **2011,** *5,* 120–144.
4. Liu, T.; Cane, D. E.; Deng, Z. The Enzymology of Polyether Biosynthesis. In *Complex Enzymes in Microbial Natural Product Biosynthesis, Part B: Polyketides, Aminocoumarins and Carbohydrates;* Hopwood, D. A., Ed.; *Methods in Enzymology*, Vol. 459; Academic Press, 2009; pp 187–214.
5. Fischbach, M. A.; Walsh, C. T. *Chem. Rev.* **2006,** *106,* 3468–3496. doi:10.1021/cr0503097
6. Friedrich, S.; Hahn, F. *Tetrahedron* **2015,** *71,* 1473–1508. doi:10.1016/j.tet.2014.12.026
7. Lechner, H.; Pressnitz, D.; Kroutil, W. *Biotechnol. Adv.* **2015,** *33,* 457–480. doi:10.1016/j.biotechadv.2015.01.012
8. Hertweck, C. *Angew. Chem., Int. Ed.* **2009,** *48,* 4688–4716. doi:10.1002/anie.200806121
9. Tang, Y.; Tsai, S.-C.; Khosla, C. *J. Am. Chem. Soc.* **2003,** *125,* 12708–12709. doi:10.1021/ja0378759
10. Weissman, K. J.; Leadlay, P. F. *Nat. Rev. Microbiol.* **2005,** *3,* 925–936. doi:10.1038/nrmicro1287
11. Staunton, J.; Weissman, K. J. *Nat. Prod. Rep.* **2001,** *18,* 380–416. doi:10.1039/a909079g
12. Parenty, A.; Moreau, X.; Campagne, J.-M. *Chem. Rev.* **2006,** *106,* 911–939. doi:10.1021/cr0301402
13. Richter, M. E. A.; Traitcheva, N.; Knüpfer, U.; Hertweck, C. *Angew. Chem., Int. Ed.* **2008,** *47,* 8872–8875. doi:10.1002/anie.200803714
14. Pöplau, P.; Frank, S.; Morinaka, B. I.; Piel, J. *Angew. Chem., Int. Ed.* **2013,** *52,* 13215–13218. doi:10.1002/anie.201307406
15. Berkhan, G.; Hahn, F. *Angew. Chem., Int. Ed.* **2014,** *53,* 14240–14244. doi:10.1002/anie.201407979
16. Sudek, S.; Lopanik, N. B.; Waggoner, L. E.; Hildebrand, M.; Anderson, C.; Liu, H.; Patel, A.; Sherman, D. H.; Haygood, M. G. *J. Nat. Prod.* **2007,** *70,* 67–74. doi:10.1021/np060361d
17. Piel, J. *Proc. Natl. Acad. Sci. U. S. A.* **2002,** *99,* 14002–14007. doi:10.1073/pnas.222481399
18. Luhavaya, H.; Dias, M. V. B.; Williams, S. R.; Hong, H.; de Oliveira, L. G.; Leadlay, P. F. *Angew. Chem., Int. Ed.* **2015,** *54,* 13622–13625. doi:10.1002/anie.201507090
19. Bieber, B.; Nüske, J.; Ritzau, M.; Gräfe, U. *J. Antibiot.* **1998,** *51,* 381–382. doi:10.7164/antibiotics.51.381
20. Naruse, N.; Goto, M.; Watanabe, Y.; Terasawa, T.; Dobashi, K. *J. Antibiot.* **1998,** *51,* 545–552. doi:10.7164/antibiotics.51.545
21. Metsä-Ketelä, M.; Oja, T.; Taguchi, T.; Okamoto, S.; Ichinose, K. *Curr. Opin. Chem. Biol.* **2013,** *17,* 562–570. doi:10.1016/j.cbpa.2013.06.032
22. Das, A.; Khosla, C. *Acc. Chem. Res.* **2009,** *42,* 631–639. doi:10.1021/ar8002249
23. Malpartida, F.; Hopwood, D. A. *Nature* **1984,** *309,* 462–464. doi:10.1038/309462a0
24. Fernández-Moreno, M. A.; Martínez, E.; Boto, L.; Hopwood, D. A.; Malpartida, F. *J. Biol. Chem.* **1992,** *267,* 19278–19290.
25. Keatinge-Clay, A. T.; Maltby, D. A.; Medzihradszky, K. F.; Khosla, C.; Stroud, R. M. *Nat. Struct. Mol. Biol.* **2004,** *11,* 888–893. doi:10.1038/nsmb808
26. McDaniel, R.; Ebert-Khosla, S.; Hopwood, D. A.; Khosla, C. *J. Am. Chem. Soc.* **1993,** *115,* 11671–11675. doi:10.1021/ja00078a002
27. Taguchi, T.; Kunieda, K.; Takeda-Shitaka, M.; Takaya, D.; Kawano, N.; Kimberley, M. R.; Booker-Milburn, K. I.; Stephenson, G. R.; Umeyama, H.; Ebizuka, Y.; Ichinose, K. *Bioorg. Med. Chem.* **2004,** *12,* 5917–5927. doi:10.1016/j.bmc.2004.08.026
28. Caballero, J. L.; Martinez, E.; Malpartida, F.; Hopwood, D. A. *MGG, Mol. Gen. Genet.* **1991,** *230,* 401–412. doi:10.1007/BF00280297
29. Cole, S. P.; Rudd, B. A.; Hopwood, D. A.; Chang, C.-J.; Floss, H. G. *J. Antibiot.* **1987,** *40,* 340–347. doi:10.7164/antibiotics.40.340
30. He, Q.; Li, L.; Yang, T.; Li, R.; Li, A. *PLoS One* **2015,** *10,* e0132431. doi:10.1371/journal.pone.0132431
31. Itoh, T.; Taguchi, T.; Kimberley, M. R.; Booker-Milburn, K. I.; Stephenson, G. R.; Ebizuka, Y.; Ichinose, K. *Biochemistry* **2007,** *46,* 8181–8188. doi:10.1021/bi700190p
32. Taguchi, T.; Ebizuka, Y.; Hopwood, D. A.; Ichinose, K. *J. Am. Chem. Soc.* **2001,** *123,* 11376–11380. doi:10.1021/ja015981+
33. Grocholski, T.; Oja, T.; Humphrey, L.; Mäntsälä, P.; Niemi, J.; Metsä-Ketelä, M. *J. Bacteriol.* **2012,** *194,* 2829–2836. doi:10.1128/JB.00228-12
34. Oja, T.; Palmu, K.; Lehmussola, H.; Leppäranta, O.; Hännikäinen, K.; Niemi, J.; Mäntsälä, P.; Metsä-Ketelä, M. *Chem. Biol.* **2008,** *15,* 1046–1057. doi:10.1016/j.chembiol.2008.07.022
35. Oja, T.; Klika, K. D.; Appassamy, L.; Sinkkonen, J.; Mäntsälä, P.; Niemi, J.; Metsä-Ketelä, M. *Proc. Natl. Acad. Sci. U. S. A.* **2012,** *109,* 6024–6029. doi:10.1073/pnas.1201530109
36. Oja, T.; Niiranen, L.; Sandalova, T.; Klika, K. D.; Niemi, J.; Mäntsälä, P.; Schneider, G.; Metsä-Ketelä, M. *Proc. Natl. Acad. Sci. U. S. A.* **2013,** *110,* 1291–1296. doi:10.1073/pnas.1207407110
37. Fuller, A. T.; Mellows, G.; Woolford, M.; Banks, G. T.; Barrow, K. D.; Chain, E. B. *Nature* **1971,** *234,* 416–417. doi:10.1038/234416a0
38. Chain, E. B.; Mellows, G. *J. Chem. Soc., Chem. Commun.* **1974,** 847–848. doi:10.1039/c39740000847
39. Chain, E. B.; Mellows, G. *J. Chem. Soc., Perkin Trans. 1* **1977,** 294–309. doi:10.1039/p19770000294
40. Clayton, J. P.; O'Hanlon, P. J.; Rogers, N. H. *Tetrahedron Lett.* **1980,** *21,* 881–884. doi:10.1016/S0040-4039(00)71533-4
41. Shiozawa, H.; Shimada, A.; Takahashi, S. *J. Antibiot.* **1997,** *50,* 449–452. doi:10.7164/antibiotics.50.449
42. Hughes, J.; Mellows, G. *Biochem. J.* **1978,** *176,* 305–318. doi:10.1042/bj1760305
43. Hughes, J.; Mellows, G. *J. Antibiot.* **1978,** *31,* 330–335. doi:10.7164/antibiotics.31.330

44. Hughes, J.; Mellows, G. *Biochem. J.* **1980,** *191,* 209–219. doi:10.1042/bj1910209
45. El-Sayed, A. K.; Hothersall, J.; Cooper, S. M.; Stephens, E.; Simpson, T. J.; Thomas, C. M. *Chem. Biol.* **2003,** *10,* 419–430. doi:10.1016/S1074-5521(03)00091-7
46. Gao, S.-S.; Hothersall, J.; Wu, J.; Murphy, A. C.; Song, Z.; Stephens, E. R.; Thomas, C. M.; Crump, M. P.; Cox, R. J.; Simpson, T. J.; Willis, C. L. *J. Am. Chem. Soc.* **2014,** *136,* 5501–5507. doi:10.1021/ja501731p
47. Cooper, S. M.; Laosripaiboon, W.; Rahman, A. S.; Hothersall, J.; El-Sayed, A. K.; Winfield, C.; Crosby, J.; Cox, R. J.; Simpson, T. J.; Thomas, C. M. *Chem. Biol.* **2005,** *12,* 825–833. doi:10.1016/j.chembiol.2005.05.015
48. Hothersall, J.; Wu, J.; Rahman, A. S.; Shields, J. A.; Haddock, J.; Johnson, N.; Cooper, S. M.; Stephens, E. R.; Cox, R. J.; Crosby, J.; Willis, C. L.; Simpson, T. J.; Thomas, C. M. *J. Biol. Chem.* **2007,** *282,* 15451–15461. doi:10.1074/jbc.M701490200
49. Cooper, S. M.; Cox, R. J.; Crosby, J.; Crump, M. P.; Hothersall, J.; Laosripaiboon, W.; Simpson, T. J.; Thomas, C. M. *Chem. Commun.* **2005,** 1179–1181. doi:10.1039/b414781b
50. Julien, B.; Tian, Z.-Q.; Reid, R.; Reeves, C. D. *Chem. Biol.* **2006,** *13,* 1277–1286. doi:10.1016/j.chembiol.2006.10.004
51. Nicolaou, K. C.; Prasad, C. V. C.; Somers, P. K.; Hwang, C. K. *J. Am. Chem. Soc.* **1989,** *111,* 5335–5340. doi:10.1021/ja00196a044
52. Nicolaou, K. C.; Prasad, C. V. C.; Somers, P. K.; Hwang, C. K. *J. Am. Chem. Soc.* **1989,** *111,* 5330–5334. doi:10.1021/ja00196a043
53. Shen, B.; Kwon, H.-J. *Chem. Rec.* **2002,** *2,* 389–396. doi:10.1002/tcr.10042
54. Nelson, M. E.; Priestley, N. D. *J. Am. Chem. Soc.* **2002,** *124,* 2894–2902. doi:10.1021/ja016965f
55. Ashworth, D. M.; Robinson, J. A.; Turner, D. L. *J. Chem. Soc., Perkin Trans. 1* **1988,** 1719–1727. doi:10.1039/p19880001719
56. Woo, A. J.; Strohl, W. R.; Priestley, N. D. *Antimicrob. Agents Chemother.* **1999,** *43,* 1662–1668.
57. Earle, M. J.; Priestley, N. D. *Bioorg. Med. Chem. Lett.* **1997,** *7,* 2187–2192. doi:10.1016/S0960-894X(97)00393-4
58. Rong, J.; Nelson, M. E.; Kusche, B.; Priestley, N. D. *J. Nat. Prod.* **2010,** *73,* 2009–2012. doi:10.1021/np100421v
59. Smith, W. C.; Xiang, L.; Shen, B. *Antimicrob. Agents Chemother.* **2000,** *44,* 1809–1817. doi:10.1128/AAC.44.7.1809-1817.2000
60. Rebets, Y.; Brötz, E.; Manderscheid, N.; Tokovenko, B.; Myronovskyi, M.; Metz, P.; Petzke, L.; Luzhetskyy, A. *Angew. Chem., Int. Ed.* **2015,** *54,* 2280–2284. doi:10.1002/anie.201408901
61. Matilla, M. A.; Stöckmann, H.; Leeper, F. J.; Salmond, G. P. C. *J. Biol. Chem.* **2012,** *287,* 39125–39138. doi:10.1074/jbc.M112.401026
62. Müller, M.; Kusebauch, B.; Liang, G.; Beaudry, C. M.; Trauner, D.; Hertweck, C. *Angew. Chem., Int. Ed.* **2006,** *45,* 7835–7838. doi:10.1002/anie.200602840
63. He, J.; Müller, M.; Hertweck, C. *J. Am. Chem. Soc.* **2004,** *126,* 16742–16743. doi:10.1021/ja046104h
64. He, J.; Hertweck, C. *Chem. Biol.* **2003,** *10,* 1225–1232. doi:10.1016/j.chembiol.2003.11.009
65. He, J.; Hertweck, C. *J. Am. Chem. Soc.* **2004,** *126,* 3694–3695. doi:10.1021/ja039328t
66. Werneburg, M.; Busch, B.; He, J.; Richter, M. E. A.; Xiang, L.; Moore, B. S.; Roth, M.; Dahse, H.-M.; Hertweck, C. *J. Am. Chem. Soc.* **2010,** *132,* 10407–10413. doi:10.1021/ja102751h
67. Werneburg, M.; Hertweck, C. *ChemBioChem* **2008,** *9,* 2064–2066. doi:10.1002/cbic.200800301
68. Henrot, M.; Richter, M. E. A.; Maddaluno, J.; Hertweck, C.; De Paolis, M. *Angew. Chem., Int. Ed.* **2012,** *51,* 9587–9591. doi:10.1002/anie.201204259
69. Bode, H. B.; Wenzel, S. C.; Irschik, H.; Höfle, G.; Müller, R. *Angew. Chem., Int. Ed.* **2004,** *43,* 4163–4167. doi:10.1002/anie.200454240
70. Kopp, M.; Irschik, H.; Gemperlein, K.; Buntin, K.; Meiser, P.; Weissman, K. J.; Bode, H. B.; Müller, R. *Mol. BioSyst.* **2011,** *7,* 1549–1563. doi:10.1039/c0mb00240b
71. Winkler, A.; Łyskowski, A.; Riedl, S.; Puhl, M.; Kutchan, T. M.; Macheroux, P.; Gruber, K. *Nat. Chem. Biol.* **2008,** *4,* 739–741. doi:10.1038/nchembio.123
72. Winkler, A.; Motz, K.; Riedl, S.; Puhl, M.; Macheroux, P.; Gruber, K. *J. Biol. Chem.* **2009,** *284,* 19993–20001. doi:10.1074/jbc.M109.015727
73. Winkler, A.; Hartner, F.; Kutchan, T. M.; Glieder, A.; Macheroux, P. *J. Biol. Chem.* **2006,** *281,* 21276–21285. doi:10.1074/jbc.M603267200
74. Gaweska, H. M.; Roberts, K. M.; Fitzpatrick, P. F. *Biochemistry* **2012,** *51,* 7342–7347. doi:10.1021/bi300887m
75. Guo, C.-J.; Wang, C. C. C. *Front. Microbiol.* **2014,** *5,* No. 717. doi:10.3389/fmicb.2014.00717
76. Chiang, Y.-M.; Szewczyk, E.; Davidson, A. D.; Keller, N.; Oakley, B. R.; Wang, C. C. C. *J. Am. Chem. Soc.* **2009,** *131,* 2965–2970. doi:10.1021/ja8088185
77. Chiang, Y.-M.; Oakley, C. E.; Ahuja, M.; Entwistle, R.; Schultz, A.; Chang, S.-L.; Sung, C. T.; Wang, C. C. C.; Oakley, B. R. *J. Am. Chem. Soc.* **2013,** *135,* 7720–7731. doi:10.1021/ja401945a
78. Yu, J.; Chang, P.-K.; Ehrlich, K. C.; Cary, J. W.; Bhatnagar, D.; Cleveland, T. E.; Payne, G. A.; Linz, J. E.; Woloshuk, C. P.; Bennett, J. W. *Appl. Environ. Microbiol.* **2004,** *70,* 1253–1262. doi:10.1128/AEM.70.3.1253-1262.2004
79. Ehrlich, K. C.; Yu, J.; Cotty, P. J. *J. Appl. Microbiol.* **2005,** *99,* 518–527. doi:10.1111/j.1365-2672.2005.02637.x
80. Asao, T.; Büchi, G.; Abdel-Kader, M. M.; Chang, S. B.; Wick, E. L.; Wogan, G. N. *J. Am. Chem. Soc.* **1965,** *87,* 882–886. doi:10.1021/ja01082a031
81. Holzapfel, C. W.; Steyn, P. S.; Purchase, I. F. H. *Tetrahedron Lett.* **1966,** *7,* 2799–2803. doi:10.1016/S0040-4039(01)99863-6
82. Cox, R. *Nat. Prod. Rep.* **2014,** *31,* 1405–1424. doi:10.1039/C4NP00059E
83. Minto, R. E.; Townsend, C. A. *Chem. Rev.* **1997,** *97,* 2537–2556. doi:10.1021/cr960032y
84. Townsend, C. A. *Nat. Prod. Rep.* **2014,** *31,* 1260–1265. doi:10.1039/C4NP00092G
85. Crawford, J. M.; Thomas, P. M.; Scheerer, J. R.; Vagstad, A. L.; Kelleher, N. L.; Townsend, C. A. *Science* **2008,** *320,* 243–246. doi:10.1126/science.1154711
86. Watanabe, C. M. H.; Townsend, C. A. *Chem. Biol.* **2002,** *9,* 981–988. doi:10.1016/S1074-5521(02)00213-2
87. Sakuno, E.; Yabe, K.; Nakajima, H. *Appl. Environ. Microbiol.* **2003,** *69,* 6418–6426. doi:10.1128/AEM.69.11.6418-6426.2003
88. Sakuno, E.; Wen, Y.; Hatabayashi, H.; Arai, H.; Aoki, C.; Yabe, K.; Nakajima, H. *Appl. Environ. Microbiol.* **2005,** *71,* 2999–3006. doi:10.1128/AEM.71.6.2999-3006.2005
89. Simpson, T. J.; de Jesus, A. E.; Steyn, P. S.; Vleggaar, R. *J. Chem. Soc., Chem. Commun.* **1982,** 631–632. doi:10.1039/C39820000631

90. Townsend, C. A.; Christensen, S. B.; Davis, S. G. *J. Am. Chem. Soc.* **1982,** *104,* 6154–6155. doi:10.1021/ja00386a070
91. Townsend, C. A.; Christensen, S. B. *J. Am. Chem. Soc.* **1985,** *107,* 270–271. doi:10.1021/ja00287a059
92. Townsend, C. A.; Christensen, S. B.; Davis, S. G. *J. Chem. Soc., Perkin Trans. 1* **1988,** 839–861. doi:10.1039/p19880000839
93. Wen, Y.; Hatabayashi, H.; Arai, H.; Kitamoto, H. K.; Yabe, K. *Appl. Environ. Microbiol.* **2005,** *71,* 3192–3198. doi:10.1128/AEM.71.6.3192-3198.2005
94. McGuire, S. M.; Townsend, C. A. *Bioorg. Med. Chem. Lett.* **1993,** *3,* 653–656. doi:10.1016/S0960-894X(01)81247-6
95. Chang, P.-K.; Yabe, K.; Yu, J. *Appl. Environ. Microbiol.* **2004,** *70,* 3593–3599. doi:10.1128/AEM.70.6.3593-3599.2004
96. Lin, B.-K.; Anderson, J. A. *Arch. Biochem. Biophys.* **1992,** *293,* 67–70. doi:10.1016/0003-9861(92)90366-5
97. Yabe, K.; Matsuyama, Y.; Ando, Y.; Nakajima, H.; Hamasaki, T. *Appl. Environ. Microbiol.* **1993,** *59,* 2486–2492.
98. McGuire, S. M.; Silva, J. C.; Casillas, E. G.; Townsend, C. A. *Biochemistry* **1996,** *35,* 11470–11486. doi:10.1021/bi960924s
99. Silva, J. C.; Minto, R. E.; Barry, C. E., III; Holland, K. A.; Townsend, C. A. *J. Biol. Chem.* **1996,** *271,* 13600–13608. doi:10.1074/jbc.271.23.13600
100. Conradt, D.; Schätzle, M. A.; Haas, J.; Townsend, C. A.; Müller, M. *J. Am. Chem. Soc.* **2015,** *137,* 10867–10869. doi:10.1021/jacs.5b06770
101. Henry, K. M.; Townsend, C. A. *J. Am. Chem. Soc.* **2005,** *127,* 3724–3733. doi:10.1021/ja0455188
102. Cary, J. W.; Ehrlich, K. C.; Bland, J. M.; Montalbano, B. G. *Appl. Environ. Microbiol.* **2006,** *72,* 1096–1101. doi:10.1128/AEM.72.2.1096-1101.2006
103. Ehrlich, K. C.; Montalbano, B.; Boué, S. M.; Bhatnagar, D. *Appl. Environ. Microbiol.* **2005,** *71,* 8963–8965. doi:10.1128/AEM.71.12.8963-8965.2005
104. Yabe, K.; Matsushima, K.; Koyama, T.; Hamasaki, T. *Appl. Environ. Microbiol.* **1998,** *64,* 166–171.
105. Prieto, R.; Woloshuk, C. P. *Appl. Environ. Microbiol.* **1997,** *63,* 1661–1666.
106. Udwary, D. W.; Casillas, L. K.; Townsend, C. A. *J. Am. Chem. Soc.* **2002,** *124,* 5294–5303. doi:10.1021/ja012185v
107. Townsend, C. A.; Christensen, S. B.; Davis, S. G. *J. Am. Chem. Soc.* **1982,** *104,* 6152–6153. doi:10.1021/ja00386a069
108. Yabe, K.; Hamasaki, T. *Appl. Environ. Microbiol.* **1993,** *59,* 2493–2500.
109. Liu, T.; Cane, D. E.; Deng, Z. *Methods Enzymol.* **2009,** *459,* 187–214. doi:10.1016/S0076-6879(09)04609-6
110. Bhatt, A.; Stark, C. B. W.; Harvey, B. M.; Gallimore, A. R.; Demydchuk, Y. A.; Spencer, J. B.; Staunton, J.; Leadlay, P. F. *Angew. Chem., Int. Ed.* **2005,** *44,* 7075–7078. doi:10.1002/anie.200501757
111. Gallimore, A. R.; Stark, C. B. W.; Bhatt, A.; Harvey, B. M.; Demydchuk, Y.; Bolanos-Garcia, V.; Fowler, D. J.; Staunton, J.; Leadlay, P. F.; Spencer, J. B. *Chem. Biol.* **2006,** *13,* 453–460. doi:10.1016/j.chembiol.2006.01.013
112. Shiraiwa, K.; Yuan, S.; Fujiyama, A.; Matsuo, Y.; Tanaka, T.; Jiang, Z.-H.; Kouno, I. *J. Nat. Prod.* **2012,** *75,* 88–92. doi:10.1021/np2007582
113. Smith, A. B., III; Dong, S.; Brenneman, J. B.; Fox, R. J. *J. Am. Chem. Soc.* **2009,** *131,* 12109–12111. doi:10.1021/ja906115a
114. Moore, R. E.; Scheuer, P. J. *Science* **1971,** *172,* 495–498. doi:10.1126/science.172.3982.495
115. Steyn, P. S.; Vleggaar, R. *J. Chem. Soc., Chem. Commun.* **1985,** 1796–1798. doi:10.1039/c39850001796
116. Mao, X.-M.; Zhan, Z.-J.; Grayson, M. N.; Tang, M.-C.; Xu, W.; Li, Y.-Q.; Yin, W.-B.; Lin, H.-C.; Chooi, Y.-H.; Houk, K. N.; Tang, Y. *J. Am. Chem. Soc.* **2015,** *137,* 11904–11907. doi:10.1021/jacs.5b07816
117. Huang, J.-m.; Yokoyama, R.; Yang, C.-s.; Fukuyama, Y. *Tetrahedron Lett.* **2000,** *41,* 6111–6114. doi:10.1016/S0040-4039(00)01023-6
118. Inoue, M.; Lee, N.; Kasuya, S.; Sato, T.; Hirama, M.; Moriyama, M.; Fukuyama, Y. *J. Org. Chem.* **2007,** *72,* 3065–3075. doi:10.1021/jo0700474
119. Holton, R. A.; Somoza, C.; Kim, H. B.; Liang, F.; Biediger, R. J.; Boatman, P. D.; Shindo, M.; Smith, C. C.; Kim, S. *J. Am. Chem. Soc.* **1994,** *116,* 1597–1598. doi:10.1021/ja00083a066
120. Holton, R. A.; Kim, H. B.; Somoza, C.; Liang, F.; Biediger, R. J.; Boatman, P. D.; Shindo, M.; Smith, C. C.; Kim, S. *J. Am. Chem. Soc.* **1994,** *116,* 1599–1600. doi:10.1021/ja00083a067
121. Wender, P. A.; Badham, N. F.; Conway, S. P.; Floreancig, P. E.; Glass, T. E.; Gränicher, C.; Houze, J. B.; Jänichen, J.; Lee, D.; Marquess, D. G.; McGrane, P. L.; Meng, W.; Mucciaro, T. P.; Mühlebach, M.; Natchus, M. G.; Paulsen, H.; Rawlins, D. B.; Satkofsky, J.; Shuker, A. J.; Sutton, J. C.; Taylor, R. E.; Tomooka, K. *J. Am. Chem. Soc.* **1997,** *119,* 2755–2756. doi:10.1021/ja9635387
122. Wender, P. A.; Badham, N. F.; Conway, S. P.; Floreancig, P. E.; Glass, T. E.; Houze, J. B.; Krauss, N. E.; Lee, D.; Marquess, D. G.; McGrane, P. L.; Meng, W.; Natchus, M. G.; Shuker, A. J.; Sutton, J. C.; Taylor, R. E. *J. Am. Chem. Soc.* **1997,** *119,* 2757–2758. doi:10.1021/ja963539z
123. Montemiglio, L. C.; Parisi, G.; Scaglione, A.; Sciara, G.; Savino, C.; Vallone, B. *Biochim. Biophys. Acta, Gen. Subj.* **2016,** *1860,* 465–475. doi:10.1016/j.bbagen.2015.10.009
124. Nagano, S.; Li, H.; Shimizu, H.; Nishida, C.; Ogura, H.; Ortiz de Montellano, P. R.; Poulos, T. L. *J. Biol. Chem.* **2003,** *278,* 44886–44893. doi:10.1074/jbc.M308115200
125. Ogura, H.; Nishida, C. R.; Hoch, U. R.; Perera, R.; Dawson, J. H.; Ortiz de Montellano, P. R. *Biochemistry* **2004,** *43,* 14712–14721. doi:10.1021/bi048980d
126. Schäberle, T. F. *Beilstein J. Org. Chem.* **2016,** *12,* 571–588. doi:10.3762/bjoc.12.56
127. Palaniappan, N.; Alhamadsheh, M. M.; Reynolds, K. A. *J. Am. Chem. Soc.* **2008,** *130,* 12236–12237. doi:10.1021/ja8044162
128. Hu, Z.; Reid, R.; Gramajo, H. *J. Antibiot.* **2005,** *58,* 625–633. doi:10.1038/ja.2005.86
129. Liu, X.-j.; Kong, R.-x.; Niu, M.-s.; Qiu, R.; Tang, L. *J. Nat. Prod.* **2013,** *76,* 524–529. doi:10.1021/np300667r
130. Bretschneider, T.; Heim, J. B.; Heine, D.; Winkler, R.; Busch, B.; Kusebauch, B.; Stehle, T.; Zocher, G.; Hertweck, C. *Nature* **2013,** *502,* 124–128. doi:10.1038/nature12588
131. Heine, D.; Bretschneider, T.; Sundaram, S.; Hertweck, C. *Angew. Chem., Int. Ed.* **2014,** *53,* 11645–11649. doi:10.1002/anie.201407282
132. Heine, D.; Sundaram, S.; Bretschneider, T.; Hertweck, C. *Chem. Commun.* **2015,** *51,* 9872–9875. doi:10.1039/C5CC03085D
133. Sundaram, S.; Heine, D.; Hertweck, C. *Nat. Chem. Biol.* **2015,** *11,* 949–951. doi:10.1038/nchembio.1932

134. Piel, J.; Hertweck, C.; Shipley, P. R.; Hunt, D. M.; Newman, M. S.; Moore, B. S. *Chem. Biol.* **2000,** *7,* 943–955. doi:10.1016/S1074-5521(00)00044-2
135. Teufel, R.; Miyanaga, A.; Michaudel, Q.; Stull, F.; Louie, G.; Noel, J. P.; Baran, P. S.; Palfey, B.; Moore, B. S. *Nature* **2013,** *503,* 552–556. doi:10.1038/nature12643
136. Cheng, Q.; Xiang, L.; Izumikawa, M.; Meluzzi, D.; Moore, B. S. *Nat. Chem. Biol.* **2007,** *3,* 557–558. doi:10.1038/nchembio.2007.22
137. Teufel, R.; Stull, F.; Meehan, M. J.; Michaudel, Q.; Dorrestein, P. C.; Palfey, B.; Moore, B. S. *J. Am. Chem. Soc.* **2015,** *137,* 8078–8085. doi:10.1021/jacs.5b03983
138. Tao, W.; Zhu, M.; Deng, Z.; Sun, Y. *Sci. China: Chem.* **2013,** *56,* 1364–1371. doi:10.1007/s11426-013-4921-x
139. Vieweg, L.; Reichau, S.; Schobert, R.; Leadlay, P. F.; Süssmuth, R. D. *Nat. Prod. Rep.* **2014,** *31,* 1554–1584. doi:10.1039/C4NP00015C
140. Lacoske, M. H.; Theodorakis, E. A. *J. Nat. Prod.* **2015,** *78,* 562–575. doi:10.1021/np500757w
141. Demydchuk, Y.; Sun, Y.; Hong, H.; Staunton, J.; Spencer, J. B.; Leadlay, P. F. *ChemBioChem* **2008,** *9,* 1136–1145. doi:10.1002/cbic.200700715
142. Sun, Y.; Hahn, F.; Demydchuk, Y.; Chettle, J.; Tosin, M.; Osada, H.; Leadlay, P. F. *Nat. Chem. Biol.* **2010,** *6,* 99–101. doi:10.1038/nchembio.285
143. Kanchanabanca, C.; Tao, W.; Hong, H.; Liu, Y.; Hahn, F.; Samborskyy, M.; Deng, Z.; Sun, Y.; Leadlay, P. F. *Angew. Chem., Int. Ed.* **2013,** *52,* 5785–5788. doi:10.1002/anie.201301680
144. Sun, Y.; Hong, H.; Gillies, F.; Spencer, J. B.; Leadlay, P. F. *ChemBioChem* **2008,** *9,* 150–156. doi:10.1002/cbic.200700492
145. Wu, L.-F.; He, H.-Y.; Pan, H.-X.; Han, L.; Wang, R.; Tang, G.-L. *Org. Lett.* **2014,** *16,* 1578–1581. doi:10.1021/ol500111n
146. Hashimoto, T.; Hashimoto, J.; Teruya, K.; Hirano, T.; Shin-ya, K.; Ikeda, H.; Liu, H.-w.; Nishiyama, M.; Kuzuyama, T. *J. Am. Chem. Soc.* **2015,** *137,* 572–575. doi:10.1021/ja510711x
147. Tian, Z.; Sun, P.; Yan, Y.; Wu, Z.; Zheng, Q.; Zhou, S.; Zhang, H.; Yu, F.; Jia, X.; Chen, D.; Mándi, A.; Kurtán, T.; Liu, W. *Nat. Chem. Biol.* **2015,** *11,* 259–265. doi:10.1038/nchembio.1769
148. Tao, W.; Yurkovich, M. E.; Wen, S.; Lebe, K. E.; Samborskyy, M.; Liu, Y.; Yang, A.; Liu, Y.; Ju, Y.; Deng, Z.; Tosin, M.; Sun, Y.; Leadlay, P. F. *Chem. Sci.* **2016,** *7,* 376–385. doi:10.1039/C5SC03059E
149. Harborne, J. B., Ed. *The Flavonoids: Advances in Research Since 1986;* Chapman & Hall: London, U.K., 1993.
150. Vaughn, K. C.; Lax, A. R.; Duke, S. O. *Physiol. Plant.* **1988,** *72,* 659–665. doi:10.1111/j.1399-3054.1988.tb09180.x
151. Mayer, A. M. *Phytochemistry* **1986,** *26,* 11–20. doi:10.1016/S0031-9422(00)81472-7
152. Sato, T.; Nakayama, T.; Kikuchi, S.; Fukui, Y.; Yonekura-Sakakibara, K.; Ueda, T.; Nishino, T.; Tanaka, Y.; Kusumi, T. *Plant Sci.* **2001,** *160,* 229–236. doi:10.1016/S0168-9452(00)00385-X
153. Nakayama, T.; Yonekura-Sakakibara, K.; Sato, T.; Kikuchi, S.; Fukui, Y.; Fukuchi-Mizutani, M.; Ueda, T.; Nakao, M.; Tanaka, Y.; Kusumi, T.; Nishino, T. *Science* **2000,** *290,* 1163–1166. doi:10.1126/science.290.5494.1163
154. Nakayama, T.; Sato, T.; Fukui, Y.; Yonekura-Sakakibara, K.; Hayashi, H.; Tanaka, Y.; Kusumi, T.; Nishino, T. *FEBS Lett.* **2001,** *499,* 107–111. doi:10.1016/S0014-5793(01)02529-7
155. Lin, Z.; Zachariah, M. M.; Marett, L.; Hughen, R. W.; Teichert, R. W.; Concepcion, G. P.; Haygood, M. G.; Olivera, B. M.; Light, A. R.; Schmidt, E. W. *J. Nat. Prod.* **2014,** *77,* 1224–1230. doi:10.1021/np500155d
156. Raistrick, H.; Smith, G. *Biochem. J.* **1936,** *30,* 1315–1322. doi:10.1042/bj0301315
157. Fujii, I.; Iijima, H.; Tsukita, S.; Ebizuka, Y.; Sankawa, U. *J. Biochem.* **1987,** *101,* 11–18.
158. Huang, K.; Yoshida, Y.; Mikawa, K.; Fujii, I.; Ebizuka, Y.; Sankawa, U. *Biol. Pharm. Bull.* **1996,** *19,* 42–46. doi:10.1248/bpb.19.42
159. Chooi, Y.-H.; Cacho, R.; Tang, Y. *Chem. Biol.* **2010,** *17,* 483–494. doi:10.1016/j.chembiol.2010.03.015
160. Udwary, D. W.; Zeigler, L.; Asolkar, R. N.; Singan, V.; Lapidus, A.; Fenical, W.; Jensen, P. R.; Moore, B. S. *Proc. Natl. Acad. Sci. U. S. A.* **2007,** *104,* 10376–10381. doi:10.1073/pnas.0700962104
161. Gulder, T. A. M.; Moore, B. S. *Angew. Chem., Int. Ed.* **2010,** *49,* 9346–9367. doi:10.1002/anie.201000728
162. Umezawa, H.; Aoyagi, T.; Uotani, K.; Hamada, M.; Takeuchi, T.; Takahashi, S. *J. Antibiot.* **1980,** *33,* 1594–1596. doi:10.7164/antibiotics.33.1594
163. Wyatt, M. A.; Ahilan, Y.; Argyropoulos, P.; Boddy, C. N.; Magarvey, N. A.; Harrison, P. H. M. *J. Antibiot.* **2013,** *66,* 421–430. doi:10.1038/ja.2013.48
164. Surup, F.; Wagner, O.; von Frieling, J.; Schleicher, M.; Oess, S.; Müller, P.; Grond, S. *J. Org. Chem.* **2007,** *72,* 5085–5090. doi:10.1021/jo0703303
165. Liu, Q.; Yao, F.; Chooi, Y. H.; Kang, Q.; Xu, W.; Li, Y.; Shao, Y.; Shi, Y.; Deng, Z.; Tang, Y.; You, D. *Chem. Biol.* **2012,** *19,* 243–253. doi:10.1016/j.chembiol.2011.12.018
166. Chen, Y.; Zhang, W.; Zhu, Y.; Zhang, Q.; Tian, X.; Zhang, S.; Zhang, C. *Org. Lett.* **2014,** *16,* 736–739. doi:10.1021/ol4034176
167. Zhang, W.; Tang, Y. In Vitro Analysis of Type II Polyketide Synthase. In *Complex Enzymes in Microbial Natural Product Biosynthesis, Part B: Polyketides, Aminocoumarins and Carbohydrates;* Hopwood, D. A., Ed.; *Methods in Enzymology*, Vol. 459; Academic Press, 2009; pp 367–393.
168. Kendrew, S. G.; Katayama, K.; Deutsch, E.; Madduri, K.; Hutchinson, C. R. *Biochemistry* **1999,** *38,* 4794–4799. doi:10.1021/bi9827924
169. Maier, W.; Baumert, A.; Schumann, B.; Furukawa, H.; Gröger, D. *Phytochemistry* **1993,** *32,* 691–698. doi:10.1016/S0031-9422(00)95155-0
170. Junghanns, K. T.; Kneusel, R. E.; Baumert, A.; Maier, W.; Gröger, D.; Matern, U. *Plant Mol. Biol.* **1995,** *27,* 681–692. doi:10.1007/BF00020222
171. Lukačin, R.; Springob, K.; Urbanke, C.; Ernwein, C.; Schröder, G.; Schröder, J.; Matern, U. *FEBS Lett.* **1999,** *448,* 135–140. doi:10.1016/S0014-5793(99)00355-5
172. Lukačin, R.; Schreiner, S.; Silber, K.; Matern, U. *Phytochemistry* **2005,** *66,* 277–284. doi:10.1016/j.phytochem.2004.11.023
173. Lukačin, R.; Schreiner, S.; Matern, U. *FEBS Lett.* **2001,** *508,* 413–417. doi:10.1016/S0014-5793(01)03061-7
174. Gui, C.; Li, Q.; Mo, X.; Qin, X.; Ma, J.; Ju, J. *Org. Lett.* **2015,** *17,* 628–631. doi:10.1021/ol5036497
175. Thaker, M. N.; García, M.; Koteva, K.; Waglechner, N.; Sorensen, D.; Medina, R.; Wright, G. D. *MedChemComm* **2012,** *3,* 1020–1026. doi:10.1039/c2md20038d
176. Brötz, E.; Kulik, A.; Vikineswary, S.; Lim, C.-T.; Tan, G. Y. A.; Zinecker, H.; Imhoff, J. F.; Paululat, T.; Fiedler, H.-P. *J. Antibiot.* **2011,** *64,* 257–266. doi:10.1038/ja.2010.170

177. Kempf, A. J.; Wilson, K. E.; Hensens, O. D.; Monaghan, R. L.; Zimmerman, S. B.; Dulaney, E. L. *J. Antibiot.* **1986,** *39,* 1361–1367. doi:10.7164/antibiotics.39.1361
178. Halo, L. M.; Heneghan, M. N.; Yakasai, A. A.; Song, Z.; Williams, K.; Bailey, A. M.; Cox, R. J.; Lazarus, C. M.; Simpson, T. J. *J. Am. Chem. Soc.* **2008,** *130,* 17988–17996. doi:10.1021/ja807052c
179. Boettger, D.; Hertweck, C. *ChemBioChem* **2013,** *14,* 28–42. doi:10.1002/cbic.201200624
180. Schmidt, K.; Riese, U.; Li, Z.; Hamburger, M. *J. Nat. Prod.* **2003,** *66,* 378–383. doi:10.1021/np020430y
181. Rydberg, P.; Ryde, U.; Olsen, L. *J. Chem. Theory Comput.* **2008,** *4,* 1369–1377. doi:10.1021/ct800101v
182. Choi, Y. S.; Zhang, H.; Brunzelle, J. S.; Nair, S. K.; Zhao, H. *Proc. Natl. Acad. Sci. U. S. A.* **2008,** *105,* 6858–6863. doi:10.1073/pnas.0712073105
183. Krithika, R.; Marathe, U.; Saxena, P.; Ansari, M. Z.; Mohanty, D.; Gokhale, R. S. *Proc. Natl. Acad. Sci. U. S. A.* **2006,** *103,* 2069–2074. doi:10.1073/pnas.0507924103
184. Yamada, O.; Nan, S. N.; Akao, T.; Tominaga, M.; Watanabe, H.; Satoh, T.; Enei, H.; Akita, O. *J. Biosci. Bioeng.* **2003,** *95,* 82–88. doi:10.1016/S1389-1723(03)80153-6
185. Lee, J.; Simurdiak, M.; Zhao, H. *J. Biol. Chem.* **2005,** *280,* 36719–36727. doi:10.1074/jbc.M505334200
186. Metelev, M. V.; Ghilarov, D. A. *Mol. Biol.* **2014,** *48,* 29–45. doi:10.1134/S0026893314010105
187. Roy, R. S.; Gehring, A. M.; Milne, J. C.; Belshaw, P. J.; Walsh, C. T. *Nat. Prod. Rep.* **1999,** *16,* 249–263. doi:10.1039/a806930a
188. Mori, T.; Takahashi, K.; Kashiwabara, M.; Uemura, D.; Katayama, C.; Iwadare, S.; Shizuri, Y.; Mitomo, R.; Nakano, F.; Matsuzaki, A. *Tetrahedron Lett.* **1985,** *26,* 1073–1076. doi:10.1016/S0040-4039(00)98515-0
189. Gräfe, U.; Kluge, H.; Thiericke, R. *Liebigs Ann. Chem.* **1992,** 429–432. doi:10.1002/jlac.199219920178
190. Zhao, C.; Ju, J.; Christenson, S. D.; Smith, W. C.; Song, D.; Zhou, X.; Shen, B.; Deng, Z. *J. Bacteriol.* **2006,** *188,* 4142–4147. doi:10.1128/JB.00173-06
191. Zhao, C.; Coughlin, J. M.; Ju, J.; Zhu, D.; Wendt-Pienkowski, E.; Zhou, X.; Wang, Z.; Shen, B.; Deng, Z. *J. Biol. Chem.* **2010,** *285,* 20097–20108. doi:10.1074/jbc.M109.090092
192. Zhou, Y.; Murphy, A. C.; Samborskyy, M.; Prediger, P.; Dias, L. C.; Leadlay, P. F. *Chem. Biol.* **2015,** *22,* 745–754. doi:10.1016/j.chembiol.2015.05.010
193. Westley, J. W.; Liu, C.-M.; Evans, R. H.; Blount, J. F. *J. Antibiot.* **1979,** *32,* 874–877. doi:10.7164/antibiotics.32.874
194. Dunbar, K. L.; Chekan, J. R.; Cox, C. L.; Burkhart, B. J.; Nair, S. K.; Mitchell, D. A. *Nat. Chem. Biol.* **2014,** *10,* 823–829. doi:10.1038/nchembio.1608
195. Schobert, R.; Schlenk, A. *Bioorg. Med. Chem.* **2008,** *16,* 4203–4221. doi:10.1016/j.bmc.2008.02.069
196. Mo, X.; Li, Q.; Ju, J. *RSC Adv.* **2014,** *4,* 50566–50593. doi:10.1039/C4RA09047K
197. Ghisalberti, E. L. Bioactive tetramic acid metabolites. In *Biactive Natural Products (Part I);* Atta-ur-Rahman, Ed.; *Studies in Natural Products Chemistry*, Vol. 28; Elsevier, 2003; pp 109–163. doi:10.1016/s1572-5995(03)80140-0
198. Gossauer, A. In *Monopyrrolic Natural Compounds Including Tetramic Acid Derivatives;* Herz, W.; Falk, H.; Kirby, G. W., Eds.; *Progress in the Chemistry of Organic Natural Products*, Vol. 86; Springer Verlag: Wien, 2003. doi:10.1007/978-3-7091-6029-9
199. Royles, B. J. L. *Chem. Rev.* **1995,** *95,* 1981–2001. doi:10.1021/cr00038a009
200. Sims, J. W.; Schmidt, E. W. *J. Am. Chem. Soc.* **2008,** *130,* 11149–11155. doi:10.1021/ja803078z
201. Singh, S. B.; Zink, D. L.; Goetz, M. A.; Dombrowski, A. W.; Polishook, J. D.; Hazuda, D. J. *Tetrahedron Lett.* **1998,** *39,* 2243–2246. doi:10.1016/S0040-4039(98)00269-X
202. Kakule, T. B.; Sardar, D.; Lin, Z.; Schmidt, E. W. *ACS Chem. Biol.* **2013,** *8,* 1549–1557. doi:10.1021/cb400159f
203. Zou, Y.; Xu, W.; Tsunematsu, Y.; Tang, M.; Watanabe, K.; Tang, Y. *Org. Lett.* **2014,** *16,* 6390–6393. doi:10.1021/ol503179v
204. Tsunematsu, Y.; Fukutomi, M.; Saruwatari, T.; Noguchi, H.; Hotta, K.; Tang, Y.; Watanabe, K. *Angew. Chem., Int. Ed.* **2014,** *53,* 8475–8479. doi:10.1002/anie.201404804
205. Du, L.; Lou, L. *Nat. Prod. Rep.* **2010,** *27,* 255–278. doi:10.1039/B912037H
206. Lou, L.; Qian, G.; Xie, Y.; Hang, J.; Chen, H.; Zaleta-Rivera, K.; Li, Y.; Shen, Y.; Dussault, P. H.; Liu, F.; Du, L. *J. Am. Chem. Soc.* **2011,** *133,* 643–645. doi:10.1021/ja105732c
207. Blodgett, J. A. V.; Oh, D.-C.; Cao, S.; Currie, C. R.; Kolter, R.; Clardy, J. *Proc. Natl. Acad. Sci. U. S. A.* **2010,** *107,* 11692–11697. doi:10.1073/pnas.1001513107
208. Jomon, K.; Kuroda, Y.; Ajisaka, M.; Sakai, H. *J. Antibiot.* **1972,** *25,* 271–280. doi:10.7164/antibiotics.25.271
209. Zhang, G.; Zhang, W.; Zhang, Q.; Shi, T.; Ma, L.; Zhu, Y.; Li, S.; Zhang, H.; Zhao, Y.-L.; Shi, R.; Zhang, C. *Angew. Chem., Int. Ed.* **2014,** *53,* 4840–4844. doi:10.1002/anie.201402078
210. Antosch, J.; Schaefers, F.; Gulder, T. A. M. *Angew. Chem., Int. Ed.* **2014,** *53,* 3011–3014. doi:10.1002/anie.201310641
211. Greunke, C.; Antosch, J.; Gulder, T. A. M. *Chem. Commun.* **2015,** *51,* 5334–5336. doi:10.1039/C5CC00843C
212. Li, Y.; Chen, H.; Ding, Y.; Xie, Y.; Wang, H.; Cerny, R. L.; Shen, Y.; Du, L. *Angew. Chem., Int. Ed.* **2014,** *53,* 7524–7530. doi:10.1002/anie.201403500
213. Ding, W.; Williams, D. R.; Northcote, P.; Siegel, M. M.; Tsao, R.; Ashcroft, J.; Morton, G. O.; Alluri, M.; Abbanat, D.; Maiese, W. M.; Ellestad, G. A. *J. Antibiot.* **1994,** *47,* 1250–1257. doi:10.7164/antibiotics.47.1250
214. Singh, M. P.; Petersen, P. J.; Jacobus, N. V.; Mroczenski-Wildey, M. J.; Maiese, W. M.; Greenstein, M.; Steinberg, D. A. *J. Antibiot.* **1994,** *47,* 1258–1265. doi:10.7164/antibiotics.47.1258
215. Wu, Q.; Wu, Z.; Qu, X.; Liu, W. *J. Am. Chem. Soc.* **2012,** *134,* 17342–17345. doi:10.1021/ja304829g

BEILSTEIN JOURNAL OF ORGANIC CHEMISTRY

The direct oxidative diene cyclization and related reactions in natural product synthesis

Juliane Adrian‡, Leona J. Gross‡ and Christian B. W. Stark*

Review

Open Access

Address:
Fachbereich Chemie, Institut für Organische Chemie, Universität Hamburg, Martin-Luther-King-Platz 6, 20146 Hamburg, Germany

Email:
Christian B. W. Stark* - stark@chemie.uni-hamburg.de

* Corresponding author ‡ Equal contributors

Keywords:
asymmetric synthesis; natural products; oxidation catalysis; tetrahydrofurans; total synthesis

Beilstein J. Org. Chem. **2016,** *12,* 2104–2123.
doi:10.3762/bjoc.12.200

Received: 04 June 2016
Accepted: 07 September 2016
Published: 30 September 2016

This article is part of the Thematic Series "Natural products in synthesis and biosynthesis II".

Guest Editor: J. S. Dickschat

Abstract

The direct oxidative cyclization of 1,5-dienes is a valuable synthetic method for the (dia)stereoselective preparation of substituted tetrahydrofurans. Closely related reactions start from 5,6-dihydroxy or 5-hydroxyalkenes to generate similar products in a mechanistically analogous manner. After a brief overview on the history of this group of transformations and a survey on mechanistic and stereochemical aspects, this review article provides a summary on applications in natural product synthesis. Moreover, current limitations and future directions in this area of chemistry are discussed.

Introduction

Scope of this article

After a concise introduction on the history and mechanistic aspects of the title reaction, the primary aim of the present review article is to summarize all relevant applications in natural product synthesis. The main text of this article is ordered by compound classes, so that tactics can easily be analysed and compared and similar applications can be condensed (both in the text and in the corresponding schemes). Methodology driven investigations as well as mechanistic studies are not the main focus of this review but may be mentioned in the introductory section. Likewise, syntheses of fragments of natural products applying an oxidative cyclization protocol [1,2] and sequential epoxidation/cyclization procedures [3] are not in the scope of this article and are therefore not covered. Previous review articles concerning oxidative diene cyclization chemistry can be considered in complement [4-6].

Oxidative cyclization – Historical background

In 1924 Kötz and Steche reported on an investigation of the constitution of the monoterpene geraniol (**1**, R = H) [7]. Though the overall structure was known at that time, the position of one

of the two C–C-double bonds within that natural product was in dispute (Scheme 1). Thus, the authors subjected a derivative (geranyl acetate (**1**, R = Ac), Scheme 1) to an aqueous solution of permanganate to dihydroxylate both double bonds in order to elucidate the structure. Elemental analysis of the crystalline reaction product ("*Der reine Stoff bildet prächtige Krystalle …*" [7]) revealed that not one of the expected tetrols **2a** or **2b** (Scheme 1) but rather a cyclic anhydro compound seemed to be the result. Though a set of further reactions were carried out on this oxidation product, it proved not possible to establish its structure. It was not until 1965 when Klein and Rojahn at the flavours and fragrance company DRAGOCO (now Symrise AG) in Holzminden, northern Germany, reinvestigated the conversion of geranyl acetate (**1b**, R = Ac) with permanganate and were able to determine that the actual product is a 2,5-bis(hydroxymethyl) THF (**3** in Scheme 1, the general structure of which is today often as a simplification referred to as "THF diol") [8]. In addition, they found that this reaction proceeds with high stereoselectivity (vide infra) and demonstrated that the reaction is not only limited to terpenes such as geranyl- (**1b**, R = Ac) or neryl acetate but seemed to be fairly general to other 1,5-diene substrates. Finally, they speculated on possible intermediates which may account for the outcome and the overall stereoselectivity of this unusual reaction. A mechanism, however, was not provided (vide infra).

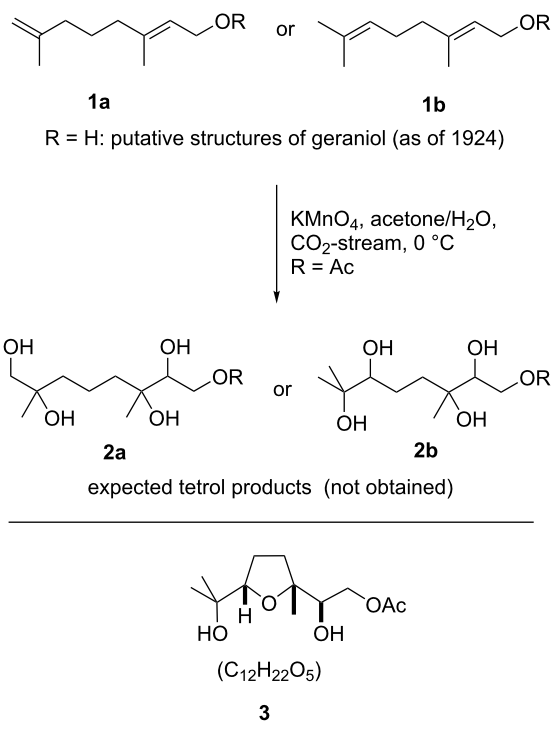

Scheme 1: Putative structures of geraniol **1a** (R = H) or **1b** (R = H) (in 1924), their expected dihydroxylation products **2a** or **2b** and the true structure **3** as determined by Klein and Rojahn in 1965 [8].

To date it is firmly established that in addition to the permanganate-mediated reaction, both ruthenium- as well as osmium tetroxide mediate the same transformation (cf. Scheme 3) and that these reactions can, contrary to the original permanganate-promoted process, be run in a catalytic fashion. All published protocols using the three different d^0-metals are highly diastereoselective (vide infra) and have been shown over the past decades to be applicable to a broad range of starting materials.

Mechanistic aspects, stereochemistry and substrate scope of the direct oxidative diene cyclization

Intrigued by the unique chemistry reported by Klein and Rojahn [8], several research groups initiated programs in order to shed light on the stereochemical course and mechanism of what appeared to be a direct oxidative diene cyclization. After a controversial debate from the early years of the discovery until the 1980s, it was finally broadly accepted that the overall reaction is a result of two consecutive *syn*-stereospecific [3 + 2]-oxidative cycloadditions (cf. type A mechanism; Scheme 3) [9-11]. Therefore, the double bond geometry of each of the two reacting double bonds translates directly to the relative stereochemistry of the vicinal hydroxy ether motif of the product (Scheme 2). The stereochemistry across the THF ring is set in the cyclization event. As a result of geometrical constraints it is usually predominantly or even exclusively *cis* (Scheme 2) – a fact that has recently been corroborated through density functional theory calculations both by Strassner and co-workers (Mn(VII) and Os(VIII)) [12,13] and by Kirchner and co-workers (Ru(VIII)) [14]. Reasonable fractions of the *trans*-THF isomer can be produced using ruthenium tetroxide in specifically optimized solvent compositions [15] (for other means to obtain the *trans*-isomer from *cis*-THFs see the examples section below).

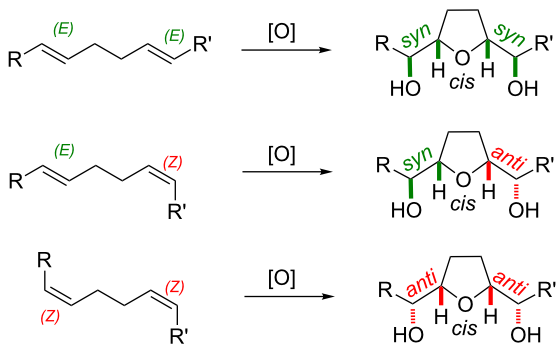

Scheme 2: Correlation between the substrate double bond geometry and relative stereochemistry of the corresponding THF diol products.

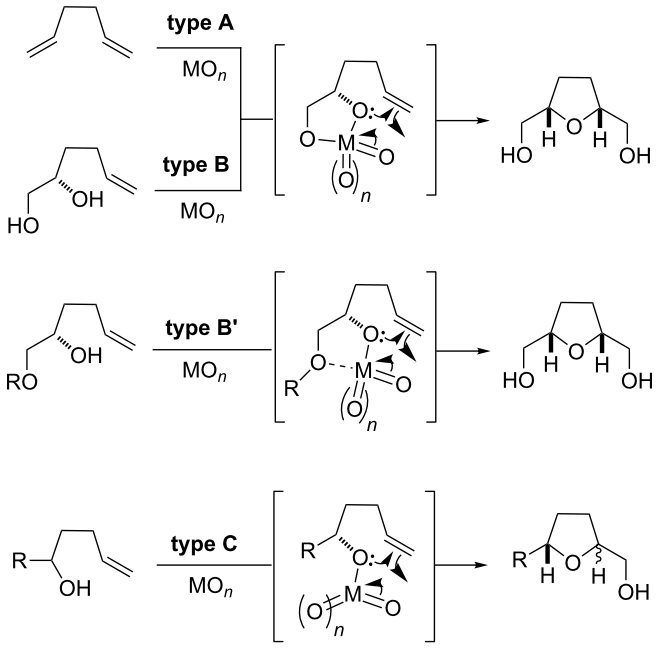

Scheme 3: Mechanisms and classification for the metal-mediated oxidative cyclizations to form 2,5-disubstituted THFs.

For all three procedures (using Mn(VII), Ru(VIII) and Os(VIII)) the scope of the reaction is very broad and a large number of 1,5-dienes with any kind of substitution pattern and double bond geometry have been used as substrates [4-6,16,17]. In addition, for Ru(VIII) [17-19] and Mn(VII) [21] it has been shown that also 1,6-dienes serve as substrates and can thus be directly converted to tetrahydropyrans [20-22]; ruthenium tetroxide even oxidizes 1,7-dienes to oxepans [23]. However, it has to be noted that the latter transformations do not have the same broad substrate spectrum as has been demonstrated for 1,5-diene precursors and there are no applications to natural product synthesis thus far.

A particularly fruitful extension of the direct 1,5-diene oxidation methodology (and due to mechanistic similarities also within the scope of this review) is the oxidative cyclization of 5,6-dihydroxyalkenes. This reaction has been reported to be catalyzed by Os(VI), Ru(VII) and Cr(VI) [24-26] and can be termed type B oxidative cyclization (as opposed to the direct oxidative cyclization of 1,5-dienes, referred to as type A reaction; cf. Scheme 3). In this case the diol and the metal oxide form a glycol ester intermediate which then undergoes an intramolecular oxidative addition to a remote double bond. Thereby, type B oxidative cyclizations converge to the same (or very similar) reactive intermediate as is passed through in type A reactions (Scheme 3). A relevant advantage of this approach is that enantiomerically pure products can be obtained when enantiomerically pure diol starting materials are used. A subgroup of closely related starting materials may contain an alkyl ether instead of a free hydroxy group at C6 (R ≠ H in Scheme 3). The key intermediate and cyclization precursor may then involve a coordinative bond of that ether oxygen to the strongly Lewis acidic metal center. Due to the close relation to type B cyclizations, they can be classified as type B' (Scheme 3). Reagents that mediate this type of reaction are Re(VII), Cr(VI) and Co(II) complexes [26-29]. Again, the observed efficiency and stereoselectivity for this class of oxidative cyclization reactions is high.

Another set of substrates are 5-hydroxyalkenes, starting materials, completely lacking the 6-OH-group (or ether oxygen donor). These compounds can only form mono-esters with the metal oxidant (Scheme 3). Therefore, they exhibit a different reactivity and a less ordered transition geometry in the oxygen transfer reaction and are thus categorized as a distinct class of oxidative cyclization, referred to as type C reaction. In fact, in these cases, mostly a *trans*-selectivity for the cyclization event is observed, due to the loose coordination. The most prominent oxidants to promote such type C reactions are Co(II) and Re(VII) complexes [27-29]. Reactions where a 5- and/or 6-(di)hydroxy group directs an oxidizing reagent to an internal alkene to form an epoxide followed by a subsequent cyclization are not covered in this article as these are different in mechanism since the oxidation and cyclization are two distinct events and do not occur in the same step [3].

The attraction to generate up to four chiral centers from a simple 1,5-diene precursor or up to two stereogenic centers

when starting from 5,6- or 5-(di)hydroxyalkenes has progressively drawn the attention of synthetic organic chemists. These efforts have so far yielded some beautiful and persuasive results in the synthesis of natural products. The aim of the present review is to assemble key results of these applications and illustrate scope and limitations.

Review

Oxidative cyclizations in the synthesis of carbohydrates, amino acids and polyketide natural products

(+)-Anhydro-D-glucitol and (+)-D-chitaric acid

(+)-Anhydro-D-glucitol (**6**) was isolated from the mould fungus *Fusarium solani* as a phytotoxin against barnyardgrass and duckweed in 1996 [30]. The Donohoe group presented a total synthesis in 2003 using an Os(VIII)-catalyzed oxidative cyclization as the key step [31] (Scheme 4). Several other total syntheses of that natural product did already exist or followed [32-39].

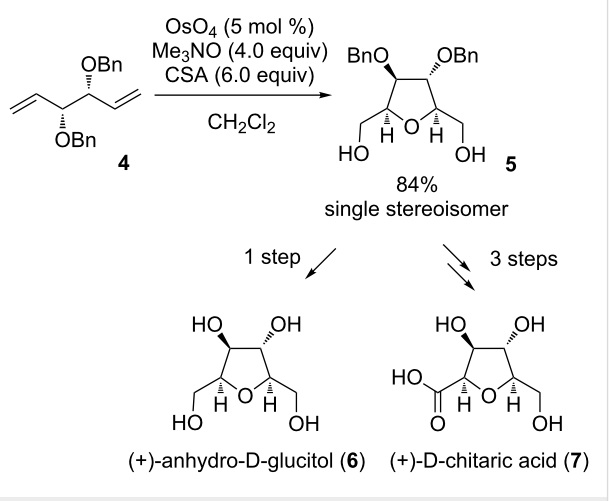

Scheme 4: Synthesis of (+)-anhydro-D-glucitol and (+)-D-chitaric acid using an OsO_4-mediated oxidative cyclization.

Starting from the readily available C_2-symmetric 1,5-diene **4** the 2,3,4,5-tetra-substituted THF diol **5** was obtained as a single stereoisomer with a yield of 84%, following the type A cyclization. Deprotection led to natural (+)-anhydro-D-glucitol (**6**) (Scheme 4). It was also possible to produce another carbohydrate using the same synthetic pathway. Thus, mono-protection of THF diol **5** followed by oxidation of the remaining free primary hydroxy group to the carboxylic acid and a final hydrogenolysis gave (+)-D-chitaric acid (**7**) with a yield of 30% over three steps (Scheme 4). Additional to the synthesis of Donohoe described above [31], two other total syntheses of (+)-D-chitaric acid have been reported [40,41].

Neodysiherbaine A

In 2001, the excitatory amino acid neodysiherbaine A (**14**) has been found in the marine sponge *Dysidea herbacea* by Sakai et al. together with the already known and closely related dysiherbaine [42]. Neodysiherbaine A (**14**) is a neurologically active compound that acts as a glutamate receptor agonist and shows epileptogenic properties. Contiguous to the isolation, the first synthesis has been carried out by the same research group [42] and several other syntheses followed [43-47].

The Lygo group chose an approach using a Ru(VIII)-catalyzed type A oxidative cyclization to form the THF motif of the natural product (Scheme 5, left) [48,49]. Starting from diacetyl-L-arabinal (**8**), 1,5-diene **9** was obtained, which was subsequently cyclized. The reaction yielded the desired THF diol **10a** in 61% as a single diastereoisomer together with over-oxidized **10b** as side product. The total synthesis was finally achieved from **10a** via some protecting group operations and an oxidation of the primary alcohol to the carboxylic acid [50,51].

In 2011, the Donohoe group developed a total synthesis of neodysiherbaine A (**14**) using an Os(VI)-catalyzed type B oxidative cyclization of a 5,6-dihydroxyalkene (Scheme 5, right) [52]. Commercially available β-D-ribopyranose tetraacetate (**11**) was converted to **12** via a Negishi coupling [53,54]. The oxidative cyclization diastereoselectively led to the THF diol **13** in 88% yield from which neodysiherbaine A (**14**) was obtained in a further three steps.

Ionomycin

Ionomycin (**19**), an ionophore antibiotic isolated from *Streptomyces conglobatus* in 1978 [55-57], has a high affinity for divalent cations. It is commonly used to both modify intracellular Ca^{2+} concentrations and to investigate Ca^{2+} transport across biological membranes [58]. In 2011, Kocienski and co-workers reported on a formal synthesis of ionomycin using an auxiliary-directed, diastereoselective permanganate-mediated oxidative cyclization to introduce the THF ring A and four of its stereogenic centers in a single step (Scheme 6) [59]. A related approach had previously been featured as a key step in their synthesis of salinomycin, a commercially significant coccidiostat [2].

The required (*Z*,*Z*)-diene **16** was prepared from commercially available neryl acetate (**15**). The auxiliary-controlled, permanganate-promoted oxidation of diene **16** proceeded selectively at low temperatures, affording the corresponding diastereomeric THF diols as an inseparable mixture (dr 7:1, major stereoisomer shown in Scheme 6). Compound **17** could successfully be converted into alcohol **18**, an intermediate in the previously reported total synthesis of ionomycin (**19**) by Kocienski and

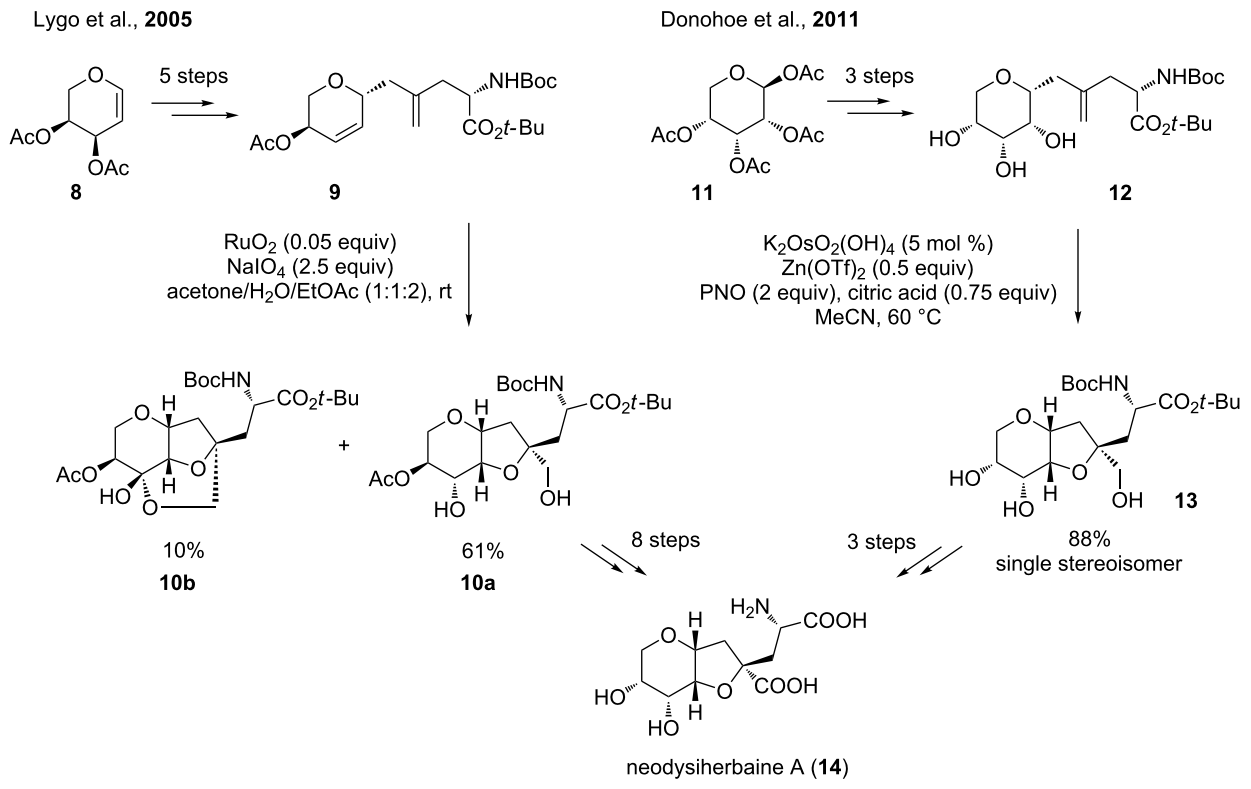

Scheme 5: Total synthesis of neodysiherbaine A via a Ru(VIII)- and an Os(VI)-catalyzed oxidative cyclization, respectively.

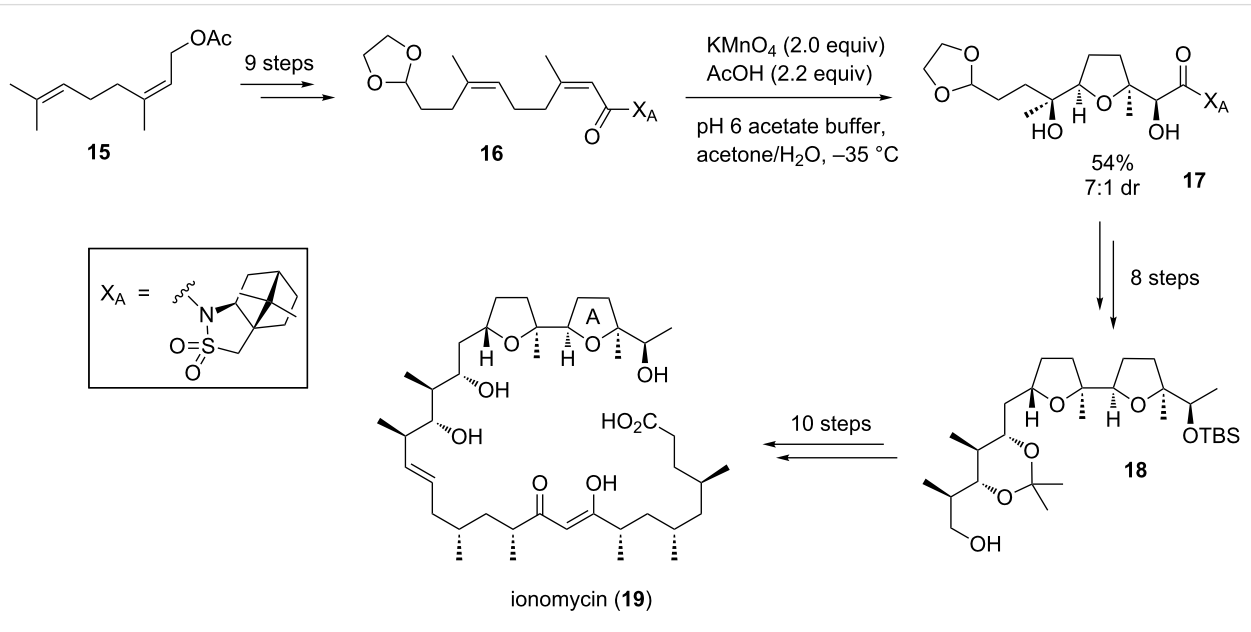

Scheme 6: Formal synthesis of ionomycin by Kocienski and co-workers.

co-workers [60] and also in the preceding syntheses developed by the group of Evans [61] and the Hanessian group [62], thus completing a formal synthesis of this polyketide. At this point it has to be mentioned that in 1987 the group of Weiler also used such a permanganate-promoted oxidative cyclization for the stereoselective synthesis of the THF unit in ionomycin [63]. Similarly, in 1980 Walba et al. reported on the B/C-ring fragment synthesis of monensin A, another well-known ionophore

antibiotic, applying an oxidative cyclization approach using potassium permanganate [64].

Amphidinolide F

Amphidinolide F (**24**) is a marine natural product isolated from the dinoflagellate *Amphidinium* sp. in 1991 [65]. The macrocyclic core of these highly cytotoxic secondary metabolites contains two 2,5-*trans*-substituted THF ring systems (Scheme 7) [66,67]. Despite significant efforts from various research groups, it took more than two decades from its isolation and characterization to the publication of its first total synthesis by Carter and co-workers in 2012 [67,68].

In 2013, the Fürstner group published a successful approach to amphidinolide F (**24**) applying an oxidative type C Mukaiyama cyclization reaction for the THF segment **22** (Scheme 7) [69,70]. Therefore, enantiomerically pure epoxide **20** was converted to 5-hydroxyalkene **21**, the oxidative cyclization precursor in this total synthesis. The subsequent cobalt-catalyzed cyclization reaction proceeded chemoselectively in the presence of the alkyne moiety and provided the *trans*-disubstituted THF **22** in high yield [69-71]. Finally, building block **23**, one important fragment in the total synthesis of amphidinolide F (**24**), was accessible in good overall yield and high diastereoselectivity (dr ≈ 95:5) in only four steps (Scheme 7).

Oxidative cyclizations in the synthesis of annonaceous acetogenins

cis-Solamin A

cis-Solamin represents a typical mono-THF acetogenin, originally isolated from the roots of the tropical fruit tree *Annona muricata* in 1998 [72]. The relative stereochemistry within the THF diol core was assigned as *threo*-*cis*-*threo*, whereas the absolute configuration present in *cis*-solamin was not established at the time of isolation. Then in 2006, the groups of Figadère and Brown were able to show that natural *cis*-solamin actually occurs as a mixture of two tetra-epimeric diastereoisomers *cis*-solamin A (**29**, Scheme 8) and *cis*-solamin B [73]. It therefore has to be noted that structure **29** was referred to as "*cis*-solamin" in the literature, up to that important discovery by Figadère and Brown. Its diverse biological activities [72] together with its broadly unexplored biogenesis [73,74] motivated many synthetic groups to develop total syntheses of *cis*-solamin A (**29**) [75-83] and B [76,78,83].

In 2002, Brown and co-workers achieved concise total syntheses of *cis*-solamin A (**29**) and B using the diastereoselective, auxiliary-controlled, permanganate-promoted type A oxidative cyclization of 1,5-dienes to create the THF diol backbone and to introduce four of the five stereogenic centers present in these mono-THF acetogenins (left, Scheme 8) [76,78]. Starting from commercially available aldehyde **25**, diene **27** was obtained in few steps and subsequently cyclized. Previously established standard conditions using acetone–water delivered THF-diol **28a** in only 18% yield. Better results were achieved when the oxidative cyclization was carried out under phase-transfer conditions [84]. Thus, the corresponding THF diols were obtained in 55% yield. In addition to the desired THF diol **28a** for the total synthesis of *cis*-solamin A (**29**), small amounts of its diastereoisomer **28b** were isolated (dr 10:1, Scheme 8 left). Similar permanganate-mediated oxidative cyclizations were also successfully applied to the total syntheses of two more mono-THF acetogenins, *cis*-uvariamicin I and *cis*-reticulatacin, by the Brown group [85].

A formal synthesis of *cis*-solamin A (**29**) was published in 2005 by the Donohoe group, employing their Os(VI)-catalyzed oxidative cyclization of 5,6-dihydroxyalkenes as the key step

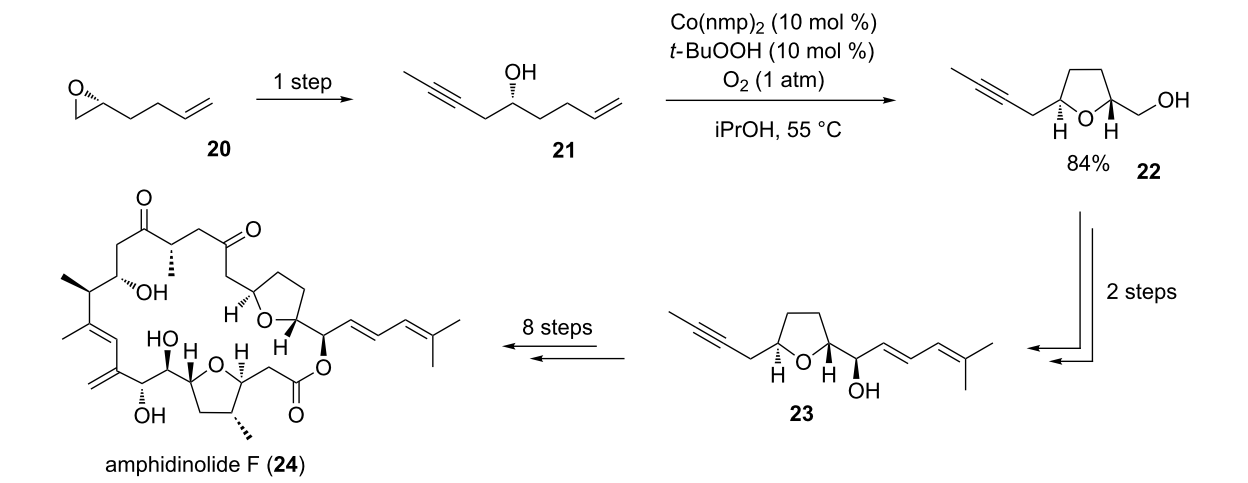

Scheme 7: Total synthesis of amphidinolide F by Fürstner and co-workers.

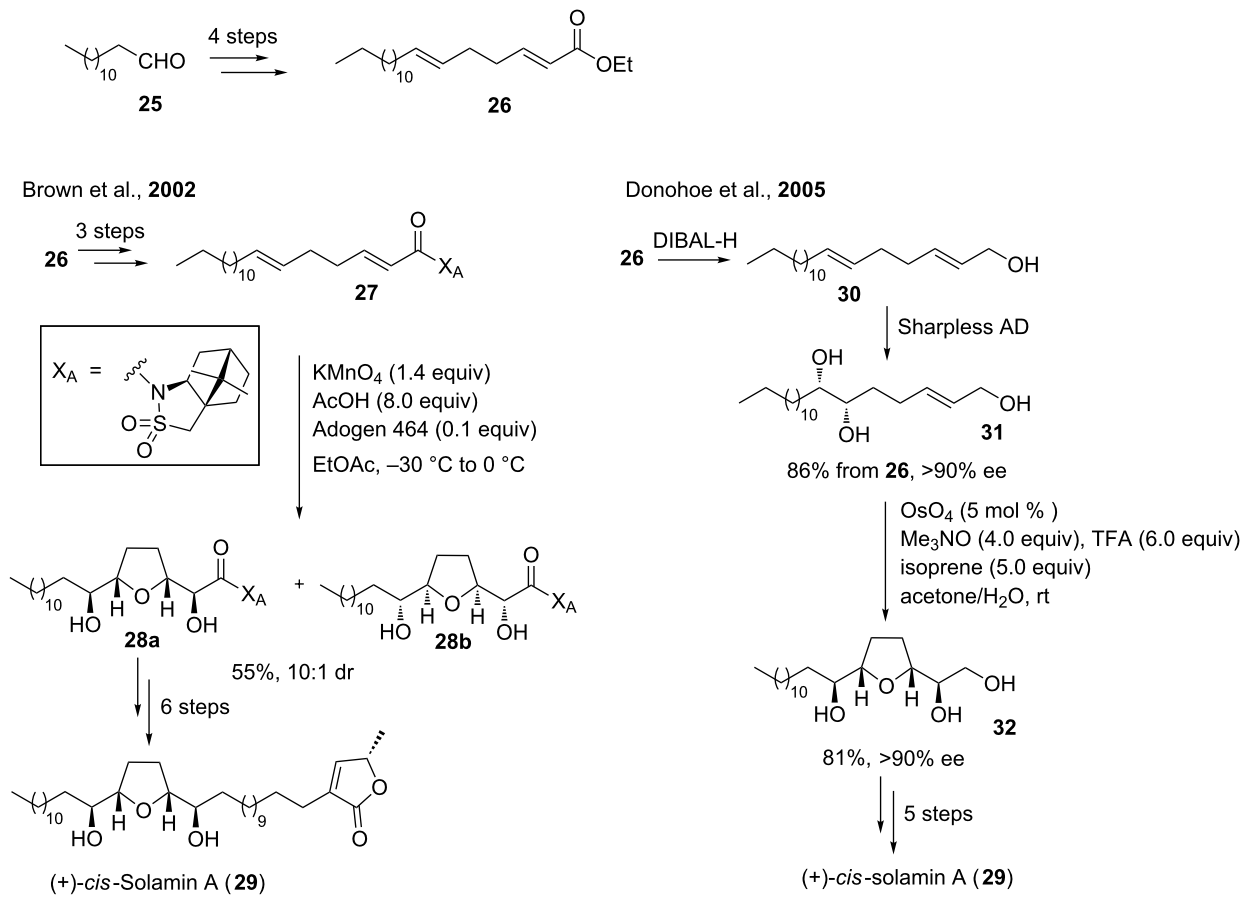

Scheme 8: Brown`s and Donohoe`s oxidative cyclization approach to *cis*-solamin A.

(right, Scheme 8) [79]. After reduction of the ester **26**, a Sharpless asymmetric dihydroxylation (AD) [86-88] reaction furnished diol **31** with a high degree of both regio- and enantioselectivity. Osmium-promoted oxidative type B cyclization of **31** proceeded in high yield (81%) and with high stereoselectivity (ee >90%) to give THF diol **32**. The latter could be almost quantitatively converted to the corresponding tosylate, an intermediate in Brown`s synthesis of *cis*-solamin A (**29**) [76,78], thus completing a formal synthesis of this natural product (Scheme 8).

In 2006, our group succeeded in synthesizing *cis*-solamin A (**29**) utilizing a ruthenium tetroxide-catalyzed type A oxidative cyclization approach (Scheme 9) [80]. Silyl-protected dienediol **34**, the oxidative cyclization precursor, was synthesized from *all-trans*-cyclododecatriene **33** in four steps including dihydroxylation, glycol cleavage [89], subsequent borohydride reduction and protection of the resulting diol. The Ru(VIII)-catalyzed oxidative cyclization in the presence of sodium periodate on wet silica [90] as the oxidizing agent delivered the THF diol **35** in high yield (83%). The product was formed with excellent diastereocontrol (dr >98:2). Subsequent enzymatic desymmetrization [91] using lipase Amano AK gave the enantiomerically pure acetate **36** in 81% yield (ee >99%). A further three transformations then delivered *cis*-solamin A (**29**). Crucial to the success of this approach and its high efficiency is that it takes advantage of the *meso*-geometry of the central THF diol moiety [80].

cis-Sylvaticin

cis-Sylvaticin (**40**), a non-adjacent bis-THF acetogenin [92] (Scheme 10), was discovered in dried fruits of *Rollinia sylvatica* [93] and leafs of *Rollinia mucosa* [94]. It has been shown to be cytotoxic against several cancer cell lines at nanomolar concentrations [93,94]. Two different synthetic approaches to *cis*-sylvaticin (**40**) were reported, utilizing an oxidative cyclization to stereoselectively establish the *cis*-configured 2,5-disubstituted THF rings.

The first total synthesis of *cis*-sylvaticin (**40**) has been accomplished in 2006 by the Donohoe group, using an osmium-catalyzed double type B oxidative cyclization strategy (Scheme 10)

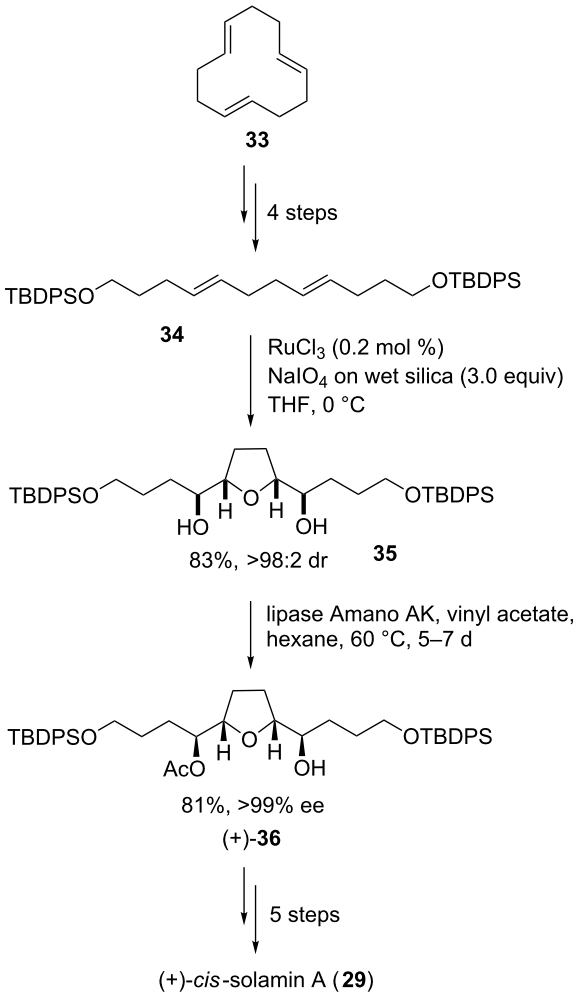

Scheme 9: Total synthesis of *cis*-solamin A using a Ru(VIII)-catalyzed oxidative cyclization and enzymatic desymmetrization as the key steps.

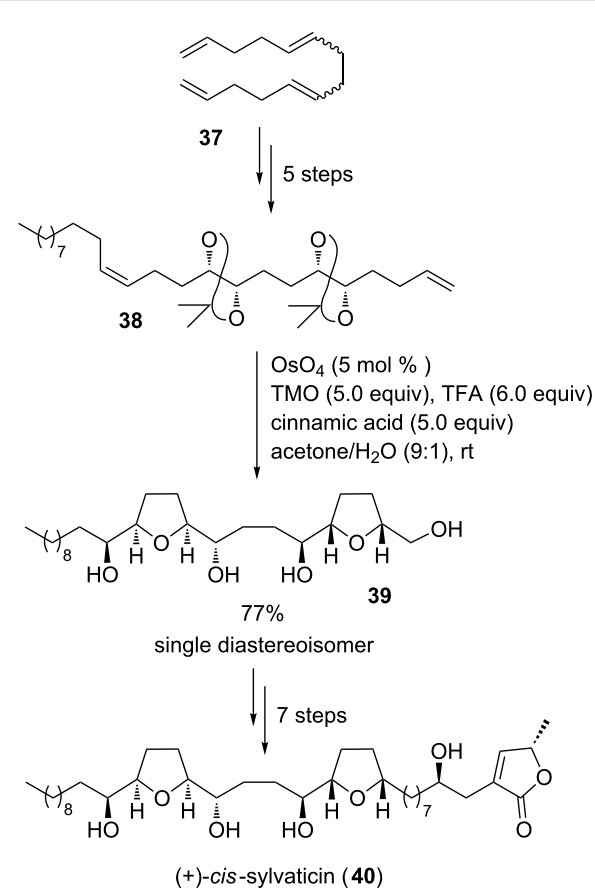

Scheme 10: Donohoe´s double oxidative cyclization approach to *cis*-sylvaticin.

[5,95]. The protected precursor **38** was synthesized from tetraene **37** in five steps involving a highly position- and stereoselective Sharpless AD reaction [86-88] (ee >98%, de >90% for the all *syn*-isomer). Subsequent osmium tetroxide-catalyzed oxidative cyclization under acidic reaction conditions resulted in bis-THF **39** which was isolated in 77% yield and as a single diastereoisomer. Thus, both THF rings of the natural product were established at the same time (Scheme 10) [5,95]. Based on this approach, in 2009, Donohoe and co-workers also reported the first total synthesis of (+)-sylvaticin [92,96], the C12-epimer of *cis*-sylvaticin (**40**) using oxidative cyclization chemistry to establish both the 2,5-*cis*- and the 2,5-*trans*-substituted THF ring of the natural product. However, it has to be noted that the *trans*-THF was not directly formed in an oxidative cyclization reaction but rather through a subsequent sequential solvolysis/hydride shift/intramolecular reduction cascade.

Another total synthesis of *cis*-sylvaticin (**40**) has been published by Brown and co-workers in 2008 [92,97]. In this case, two permanganate-promoted type A oxidative cyclization reactions were used to establish the two THF rings of this acetogenin (Scheme 11). Both THF diols **43** and **47** were isolated as pure diastereoisomers with high diastereocontrol (dr 9:1 for **43** and dr 8.7:1 for **47**, respectively) and then successfully connected in a silicon-tethered ring closing metathesis (RCM) [98] to provide the main backbone of *cis*-sylvaticin (**40**). Moreover, in 2009, Brown and co-workers reported on a short synthesis of the non-adjacent bis-THF core of *cis*-sylvaticin (**40**) making use of a permanganate-mediated bidirectional oxidative cyclization approach [99].

Membranacin and membrarollin

Membranacin (**55**) and membrarollin (**62**) are typical adjacent bis-THF acetogenins having a *threo-cis-threo-cis-erythro* configured core (Scheme 12 and Scheme 13). They were isolated from the seeds of the fruit tree *Rollinia membranaceae* by the Cortes group [100,101]. Previous studies demonstrated, that particularly adjacent bis-THF acetogenins exhibit highly potent

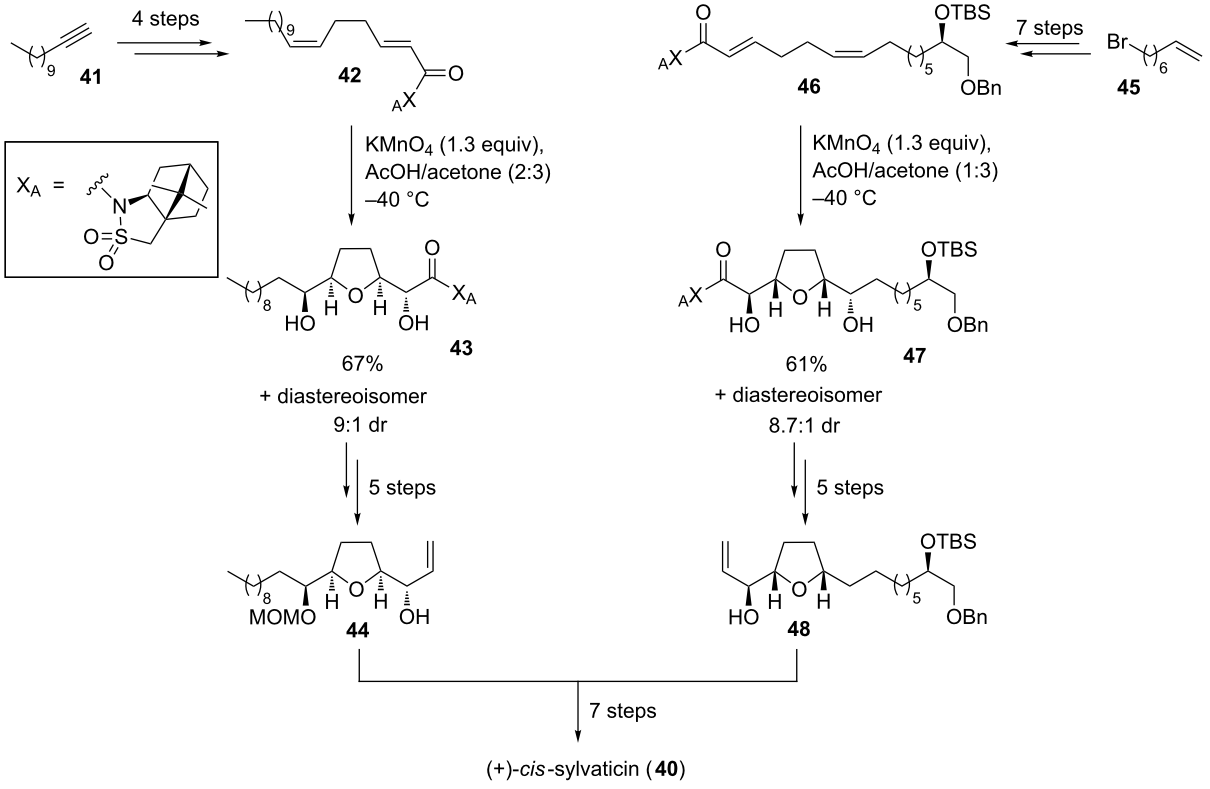

Scheme 11: Permanganate-mediated approach to *cis*-sylvaticin by Brown and co-workers.

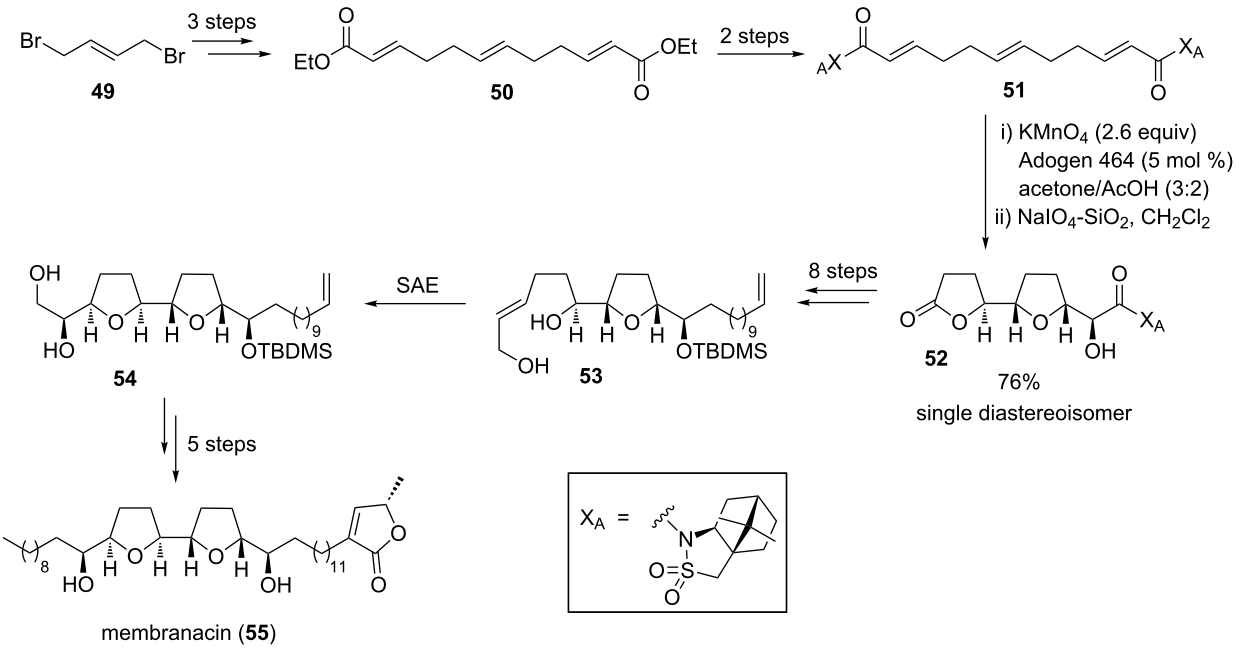

Scheme 12: Total synthesis of membranacin using a $KMnO_4$-mediated oxidative cyclization.

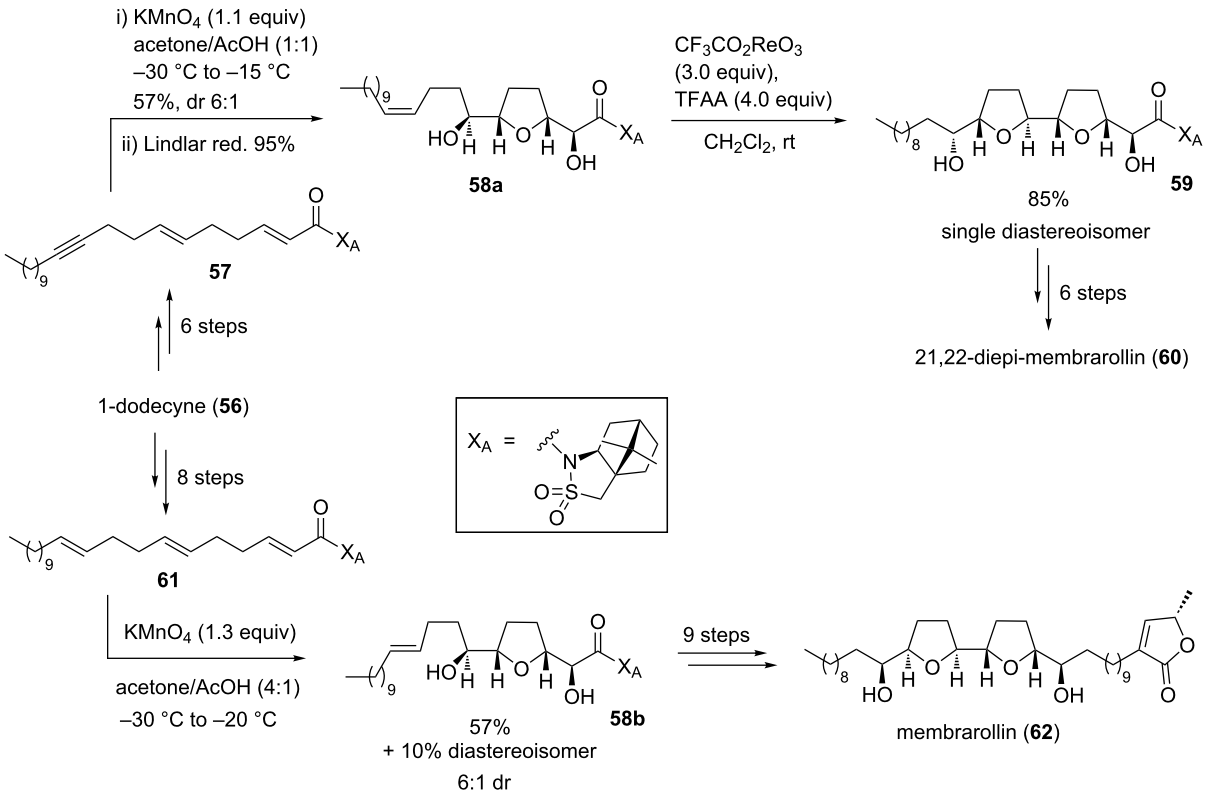

Scheme 13: Total synthesis of membrarollin and its analogue 21,22-diepi-membrarollin.

tumor growth inhibitory activity. Detailed investigations into the mode of action revealed that acetogenins inhibit cancer cell growth through the blockage of the mitochondrial NADH-ubiquinone oxidoreductase of complex I of the respiratory chain. In fact, membranacin (**55**) and membrarollin (**62**) are amongst the most potent complex I inhibitors identified to date [101]. As part of their studies towards the synthesis of adjacent bis-THF acetogenins including membranacin (**55**) and membrarollin (**62**), Brown and co-workers considered a two-stage cyclization approach to control the stereochemistry within the THF backbone ring system.

The total synthesis of membranacin (**55**), developed in 2004 by Brown and co-workers, comprised metal-oxo and metal-peroxy-mediated oxidative cyclizations as the key steps [102] (Scheme 12). Thus, permanganate oxidation of triene **51**, which can be synthesized in a few steps from (*E*)-1,4-dibromobut-2-ene (**49**), followed by treatment of the crude reaction mixture with $NaIO_4$–SiO_2 proceeded efficiently to afford the single isolated diastereoisomeric lactone **52** in 76% yield. This lactone (**52**) was converted to enediol **53** in a further few steps. The second THF ring was then established using an epoxidation–cyclization sequence. Thus, asymmetric Sharpless epoxidation (SAE) [103,104] yielded an intermediary oxirane (not shown in Scheme 12) which was intramolecularly trapped by attack of the remote hydroxy group to afford bis-THF **54**, a key intermediate *en route* to membranacin (**55**) (Scheme 12) [102].

One year later, in 2005, Brown and co-workers achieved a total synthesis of 21,22-diepi-membrarollin (**60**) [105], possessing an adjacent bis-THF motif present in various acetogenins (e.g. carolin A [106]), by applying sequential metal-oxo mediated oxidative cyclizations to introduce six of the seven stereogenic centers (Scheme 13). The required dienyne **57** was prepared from commercially available 1-dodecyne (**56**). Permanganate-promoted oxidation of dienyne **57** proceeded rapidly and selectively at low temperatures, affording the corresponding diastereomeric THF diols as a separable mixture (dr 6:1, major stereoisomer shown in Scheme 13). Semi hydrogenation of the triple bond using the Lindlar catalyst gave the bis-homoallylic alcohol **58a**, which underwent an efficient acyl perrhenate-mediated hydroxy-directed oxidative cyclization to afford a single isolated bis-THF **59** in excellent yield. A few subsequent steps were required to finish the synthesis of 21,22-diepi-membrarollin (**60**), notably avoiding the requirement for any hydroxy protecting groups.

The first total synthesis of membrarollin (**62**, Scheme 13) was finally disclosed by Brown and co-workers in 2009 [107]. Similarly starting from 1-dodecyne (**56**), triene system **61** was selectively oxidized using a permanganate-mediated oxidative cyclization affording two separable diastereoisomeric THF diols in 67% yield (only major isomer **58b** shown in Scheme 13). It is worth noting that this oxidative cyclization proceeded with high chemoselectivity leaving the remote C–C-double bond unreacted. For the formation of the adjacent THF ring different and stereodivergent strategies were studied [107]. The relative and absolute stereochemistry required to prepare natural membrarollin (**62**) was obtained using a perrhenate-mediated type B' cyclization of THF diol **58b** (not shown in Scheme 13).

Rollidecin C and D

Rollidecin C (**69**) and D (**70**) belong to the class of adjacent bis-THF acetogenins. In contrast to other representatives of this subgroup of acetogenins they are lacking one of the secondary alcohols usually framing the bis-THF core (Scheme 14). They were isolated from the leaves of *Rollinia mucosa* [108] and shown to exhibit cytotoxicity against six human tumor cell lines. Rollidecin C (**69**) was found to be more potent than rollidecin D (**70**) with selectivity toward the colon cell line HT-29 [108]. In 2001, the groups of Sinha and Keinan reported on a stereoselective synthesis of rollidecin C (**69**) and D (**70**) [109] using the tandem oxidative polycyclization reaction with trifluoro-acetylperrhenate, a synthetic method first reported in 1995 [110,111]. Bis-homoallylic dienols **65** and **66** were synthesized from *trans*-ethyl heptadec-4-enoate (**63**) via diene **64**. A Re(VII)-mediated type C oxidative cyclization furnished the bis-THF products **67** and **68** in 49% and 29% yield, respectively. Both THF rings were introduced with excellent diastereoselectivity in a single step transformation at the final stages of the total syntheses of rollidecin C (**69**) and D (**70**) (Scheme 14).

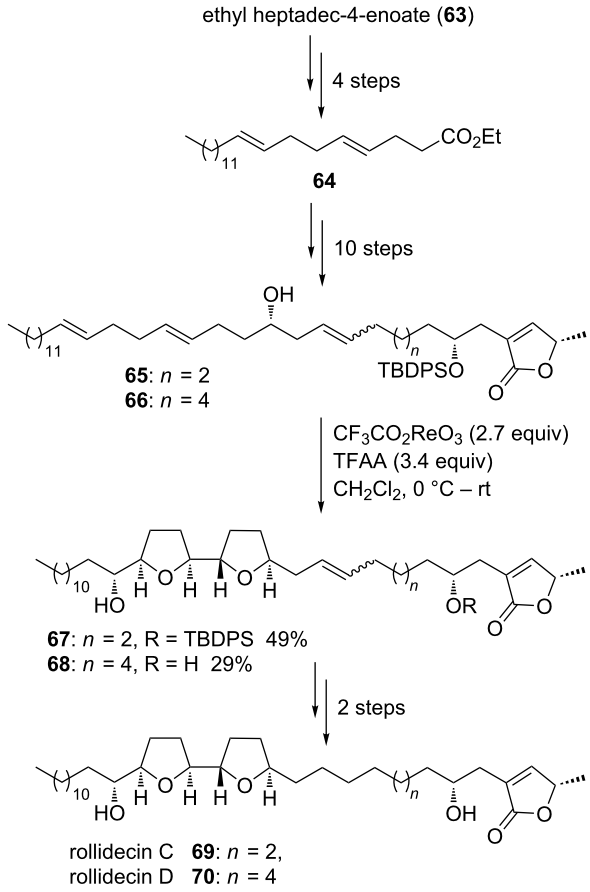

Scheme 14: Total synthesis of rollidecin C and D using a late stage Re(VII)-catalyzed oxidative polycyclization.

Similar rhenium-mediated type C oxidative cyclizations were also successfully applied in total syntheses of further acetogenins by Sinha and Keinan, e.g., asimicin [112,113], bullatacin [112-114], trilobacin [115] and even to the tris-THF acetogenins goniocin [116] and cyclogoniodenin T [116].

Asimilobin and gigantetrocin A

Asimilobin (**74**) is a bis-THF acetogenin containing two 2,5-*trans*-configured THFs [117]. It has originally been isolated from the seeds of *Asimina triloba* [118] but has also been found in extracts of the bark of *Goniothalamus giganteus* (Annonaceae) [119] by McLaughlin and co-workers [120,121]. In 1999, Wang and Shi et al. disclosed the first total synthesis of (–)-asimilobin (**74**) and its diastereomer using a highly efficient and stereocontrolled synthetic strategy to construct the desired bis-THF ring building block **73** in two steps (Scheme 15) [120,121]. Thus, starting from commercially available *trans*-1,5,9-decatriene (**71**) a stereo- and positionselective Sharpless AD reaction [86-88] provided C_2-symmetric diol **72** (R = H) in high selectivity (ee >94%). Subsequent Co(II)-mediated oxidative type B' cyclization of dienediol **72** (R = H) proceeded in good yield (78%) and with high diastereoselectivity (de 96%) to give C_2-symmetric bis-THF product **73** (Scheme 15). The natural product was then assembled in a further 10 steps (Scheme 15) [120,121].

Subsequently, Shi and co-workers successfully applied their synthetic strategy to the first total synthesis of gigantetrocin A (**76**) [122,123], a mono-THF acetogenin, isolated from *Goniothalamus giganteus* by McLaughlin and co-workers [124]. This time, mono-protected dienediol **72** (R = MOM) was cyclized to form *trans*-THF compound **75** in 74% yield (de >95%) using $Co(modp)_2$ as a catalyst under oxygen atmosphere (Scheme 15). Finally, the synthesis of gigantetrocin A (**76**) has been achieved in seventeen steps from chiral mono-protected dienediol **72** (R = MOM) [122,123].

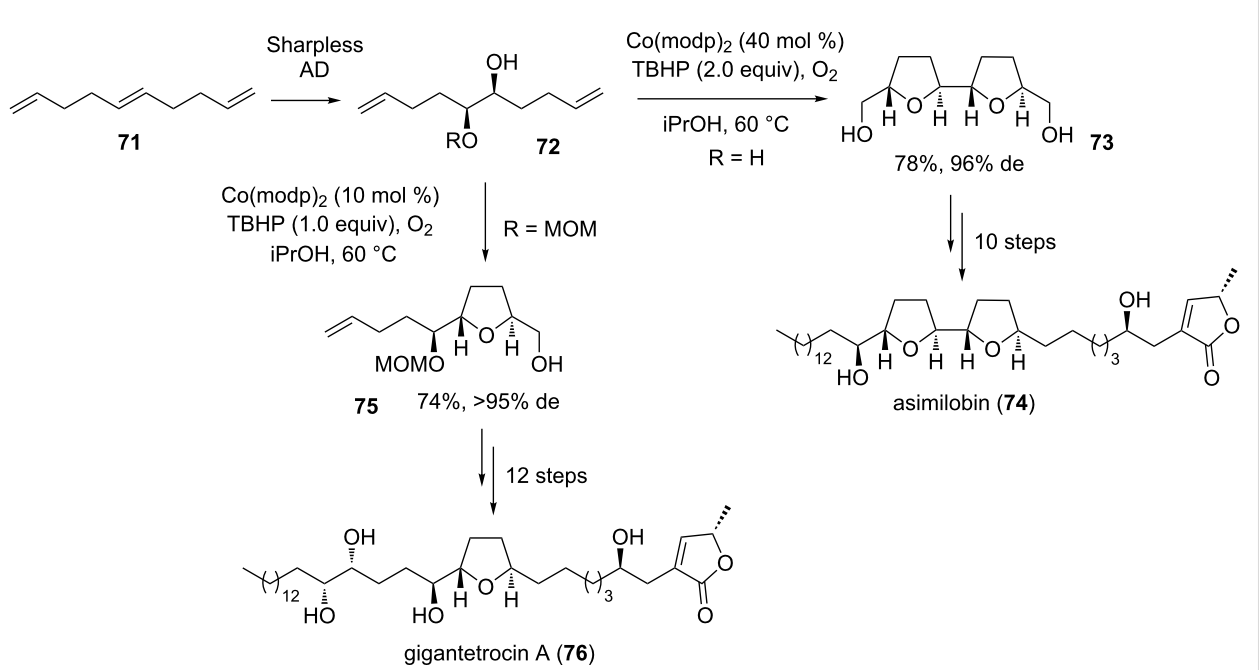

Scheme 15: Co(II)-catalyzed oxidative cyclization in the total synthesis of asimilobin and gigantetrocin A.

Further acetogenins which have been synthesized through Co(II)-mediated type B' oxidative cyclizations include mucocin, a known mono-THF representative, by Evans et al. [125] and the bis-THF acetogenin bullatacin by Pagenkopf and co-workers [126]. The latter group also employed this methodology in the total synthesis of aplysiallene [127], and more recently to bovidic acid [128] and cyclocapitelline [129].

Oxidative cyclizations in the synthesis of terpenoid natural products

Linalool oxide

The monoterpenoid *trans*-(+)-linalool oxide (**79**), containing a 2,2,5-trisubstituted THF ring, can be found in food and beverages as well as essential oils and is used as powerful sweet-woody penetrating aroma component in the perfume and flavoring industry [130]. Several syntheses have been published between 1981 and 2010 using a range of different strategies (e.g. enzymatic procedures, Sn- and Pd-catalyzed methods or even anodic oxidations) [131-136]. In 2014 the Brown group proposed an auxiliary-controlled synthesis of *trans*-(+)-linalool oxide (**79**) using a permanganate-mediated type A oxidative cyclization as the key step (Scheme 16) [137]. Thus, 1,5-diene **77** was subjected to an oxidative cyclization using stoichiometric amounts of sodium permanganate to furnish *trans*-THF diol **78** in 73% yield with an excellent diastereomeric ratio of 97:3 induced by a cyclohexanol derived chiral auxiliary. This key intermediate was subsequently converted to natural *trans*-(+)-linalool oxide (**79**) in a further few steps.

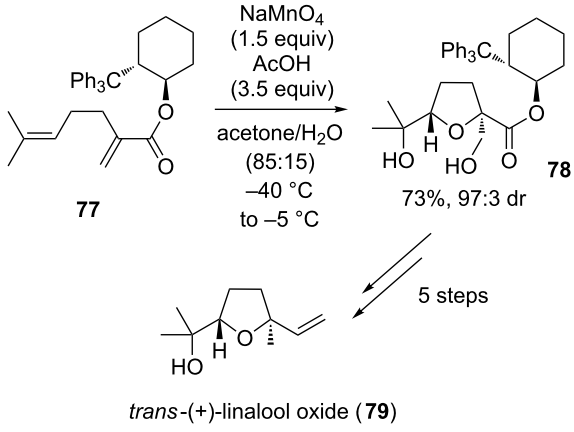

Scheme 16: Mn(VII)-catalyzed oxidative cyclization of a 1,5-diene in the synthesis of *trans*-(+)-linalool oxide.

Teurilene

Teurilene (**82**) is a squalene-derived cytotoxic polyether which was originally extracted from the red algae *Laurencia obtusa* by Suzuki et al. [138,139]. Though it is C_S-symmetric, it is structurally closely related to pentacyclic C_2-symmetric glabrescol [140], another triterpene natural product found in Jamaican endemic plant *Spathelia glabrescens* (Rutaceae) [141]. In 1999, Morimoto and co-workers reported on a stereoselective synthesis of the *meso*-tris-THF natural product teurilene (**82**) [142,143] (several previous total syntheses existed [144-151]) using an elegant two-directional approach (Scheme 17).

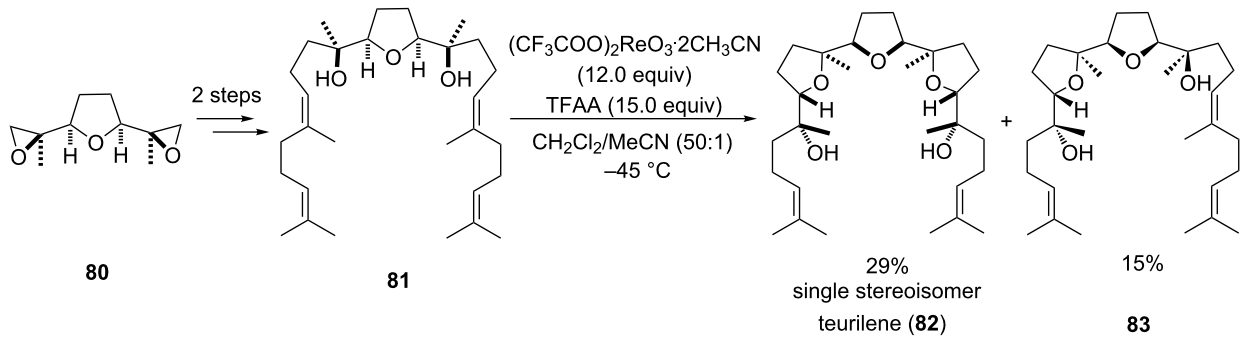

Scheme 17: Re(VII)-catalyzed oxidative cyclization in the total synthesis of teurilene.

Thus, starting from a central THF diol **81** with a fully established carbon framework, which was derived from C_S-symmetric bis-epoxide precursor **80**, a double oxidative cyclization using Re(VII)-catalysis furnished the natural product in 29% yield (Scheme 17). This (supposedly) type B' ring forming reaction occurred with high stereoselectivity for the *trans*-isomer and in addition a minor amount of the mono-cyclization product **83** was obtained.

Eurylene

Eurylene (**87**) represents yet another oxasqualenoid triterpene, sharing some structural similarity with teurilene and glabrescol, but other than the latter two, eurylene (**87**) is neither C_S- nor C_2-symmetric (Scheme 18). It has been isolated from the wood of *Eurycoma longifolia* by Itokawa et al. in 1991 [152] and was shown to exhibit cytotoxic properties against lymphocytic leukemia. The first total synthesis by Ujihara et al. [153] followed five years after its original discovery.

In 2000, the Morimoto group developed a total synthesis using two type B' cyclization steps (Re(VII) and Cr(VI) catalysis) to form the THF-heterocycles of the natural product (Scheme 18) [154]. The linear precursor **84** was cyclized diastereoselectively to the mono-THF intermediate **85** with an oxorhenium(VII) complex and was subsequently subjected to the second oxidative cyclization using stoichiometric amounts of pyridinium chlorochromate (PCC) to give the bis-THF compound **86**, which was easily converted to enantiomerically pure (+)-eurylene (**87**) (Scheme 18).

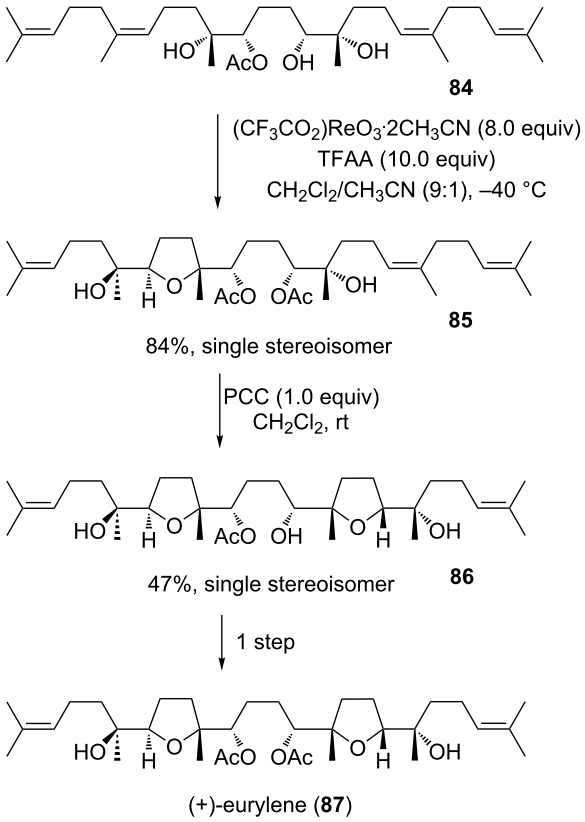

Scheme 18: Total synthesis of (+)-eurylene via Re(VII)- and Cr(VI)-mediated oxidative cyclizations.

The Brown group published an enantioselective synthesis of the *cis*- and *trans*-THF fragments of eurylene (**87**) in 2010 [155] using an auxiliary controlled Mn(VII)-promoted oxidative cyclization to form THFs **90** and **93** (Scheme 19). Both THF-derivatives had previously been prepared in a different approach and used as intermediates in a total synthesis of eurylene (**87**) by Kodama and co-workers [156]. Brown's permanganate mediated oxidative cyclization of precursor **88** gave a yield of 78% and a diastereomeric ratio of 6.7:1 in favor for the desired product **89a**. Though this reaction is *cis*-selective, cunningly, deoxygenation ultimately leads to the *trans*-THF fragment **90**. The other THF subunit **93** of the natural product **87** was prepared via an oxidative mono-cyclization of triene **91**. Thus, the desired *cis*-product **92a** was obtained in 51% yield together with 8% of its diastereoisomer **92b** and a minor amount of the double cyclized product **92c**. Both synthesized

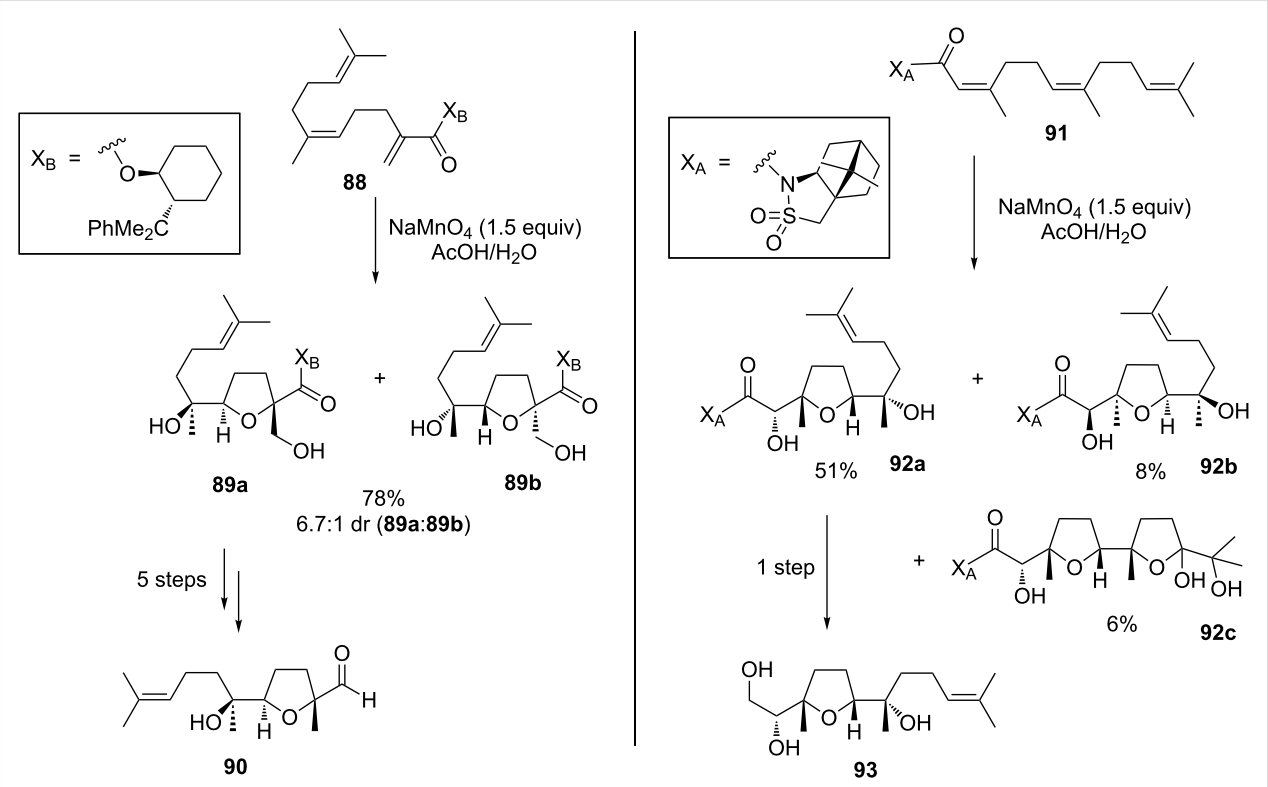

Scheme 19: Synthesis of *cis*- and *trans*-THF Rings of eurylene via Mn(VII)-mediated oxidative cyclizations.

THF fragments were consistent with those reported by Kodama [156] (Scheme 19).

Venustatriol

The tetracyclic oxasqualenoid venustatriol (**96**) was isolated in 1986 by Sakemi et al. from the red algae *Laurentia venustra* and exhibited antiviral activity against vesicular stomatitis virus (VSV) and herpes simplex virus type 1 (HSV-1) [157]. Hashimoto et al. reported a total synthesis of the natural product in 1988 [158,159] employing a vanadium-catalyzed epoxidation as a key step in the stereoselective formation of the THF ring, whilst the Corey group achieved a total synthesis using a PCC-mediated oxidative type B cyclization in the same year (Scheme 20) [160].

Diol **94**, derived from geraniol, was diastereoselectively converted into the THF derivative **95** in a yield of 43% using an oxochromium(VI) complex. Venustatriol (**96**) could then be obtained by C–C-coupling with the corresponding THP fragment in an enantioselective fashion.

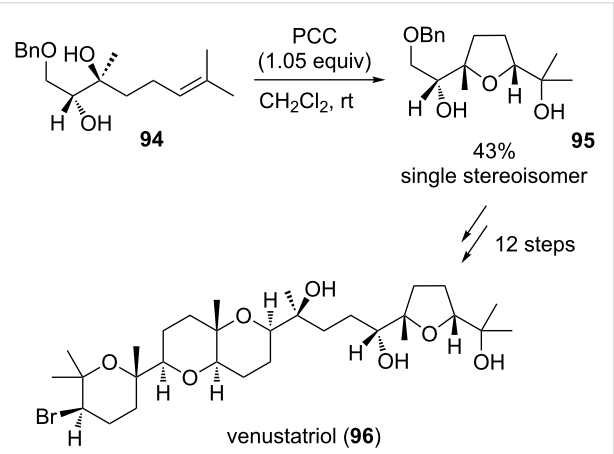

Scheme 20: Cr(VI)-catalyzed oxidative cyclization in the total synthesis of venustatriol by Corey et al.

Glaciapyrrol A

Glaciapyrrol A (**100**), B and C form a family of pyrrolo sesquiterpenoids which have been isolated in 2005 from a marine *Streptomyces sp.* (NPS008187) by Macherla et al. [161].

The only established total synthesis has been developed by the Dickschat group in 2011 [162] using a type A Ru(VIII)-catalyzed oxidative cyclization as the key step (Scheme 21).

Both neryl benzoate (**97**) as well as geranyl benzoate (**98**) have been converted into the corresponding THF diols **99** using an established oxidative cyclization protocol [15,163,164]. The diastereoselectivity of the reaction varied depending on the sol-

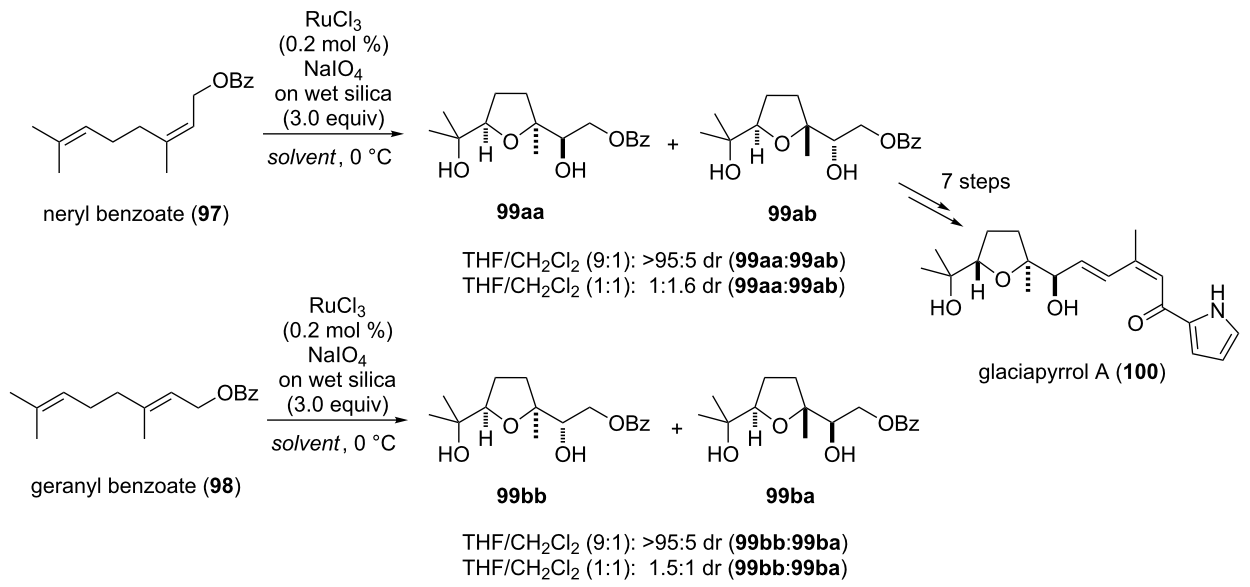

Scheme 21: Ru(VIII)-catalyzed oxidative cyclization of a 1,5-diene in the synthesis and evaluation of its stereochemistry of glaciapyrrol A.

vent composition used [15]. Therefore, reaction of **97** using THF/dichloromethane (9:1) as the solvent mixture resulted in a selective formation of *cis*-THF **99aa**, whereas a 1:1 mixture of the same solvents gave a diastereomeric ratio of 1:1.6 in favor for the *trans*-isomer **99ab**. Oxidative cyclization of *trans*-configured starting material **98** proceeded with similar efficiency. In this case a 9:1 solvent ratio gave **99bb** selectively and a 1:1 solvent mixture resulted in a diastereomeric ratio of 1.5:1, favoring **99bb** (Scheme 21). Glaciapyrrol A (**100**) was finally obtained from **99ab** by deprotection of the benzoyl group and an olefination to connect the pyrrole subunit of the natural product.

Leucosceptroids A–D

Leucosceptroids A (**105a**) and B (**105b**) have been isolated in 2010 by Luo et al. from the Chinese shrub *Leucosceptrum canum* [165]. One year later the same group was able to isolate two additional leucosceptroids C (**105c**) and D (**105d**) from the leaves of the same plant [166]. This family of sesterterpenoids is believed to be beneficial to the plant as part of a defense mechanism against herbivores. The first total synthesis of leucosceptroid B (**105b**) was established in 2013 by Huang et al. [167] and two other total syntheses of leucosceptroids A (**105a**) and B (**105b**) followed two years later [168,169]. The common tricyclic core structure of the natural products had already been synthesized in 2011 by the Horne group [170], using a TPAP-catalyzed type B oxidative cyclization to form the densely substituted THF diol motif following a protocol of our group [25] (Scheme 22).

The 5,6-dihydroxyalkene **101** was obtained from D-mannitol diacetonide via oxidation and C-C-bond formation. The oxidative cyclization catalyzed by Ru(VII) yielded THF diol **102** in 55% yield as a single diastereoisomer, without considering the configuration of the protected alcohol, as this position was subsequently oxidized to enable a Sonogashira cross-coupling to access **103**. The tricyclic core structure **104** could be obtained via an intramolecular Diels–Alder reaction, epoxidation and protection (Scheme 22) [170].

Conclusion

The direct oxidative cyclization of 1,5-dienes is known for more than 90 years, since the early finding by Kötz and Steche in 1924. While mechanistic and stereochemical aspects were in the center of research for many years, during the last two or three decades this unusual reaction has been advanced to a powerful and reliable strategy to establish 2,5-disubstituted *cis*-THF diols from very simple (often achiral) diene substrates. The reaction proceeds with a substantial increase in structural and stereochemical complexity from the starting material to the product. A similar development can be stated for the mechanistically closely related oxidative cyclizations of 5,6-dihydroxyalkenes and 5-hydroxyalkenes. All these processes are stereochemically predictable and the double bond geometry dictates the relative vicinal hydroxy ether stereochemistry at both sides adjacent to the THF-oxygen. 2,5-Disubstituted *trans*-THFs are still significantly harder to prepare using these strategies or require specific procedures. Similarly, the control of the absolute stereochemistry remains a challenge to be solved in future investigations.

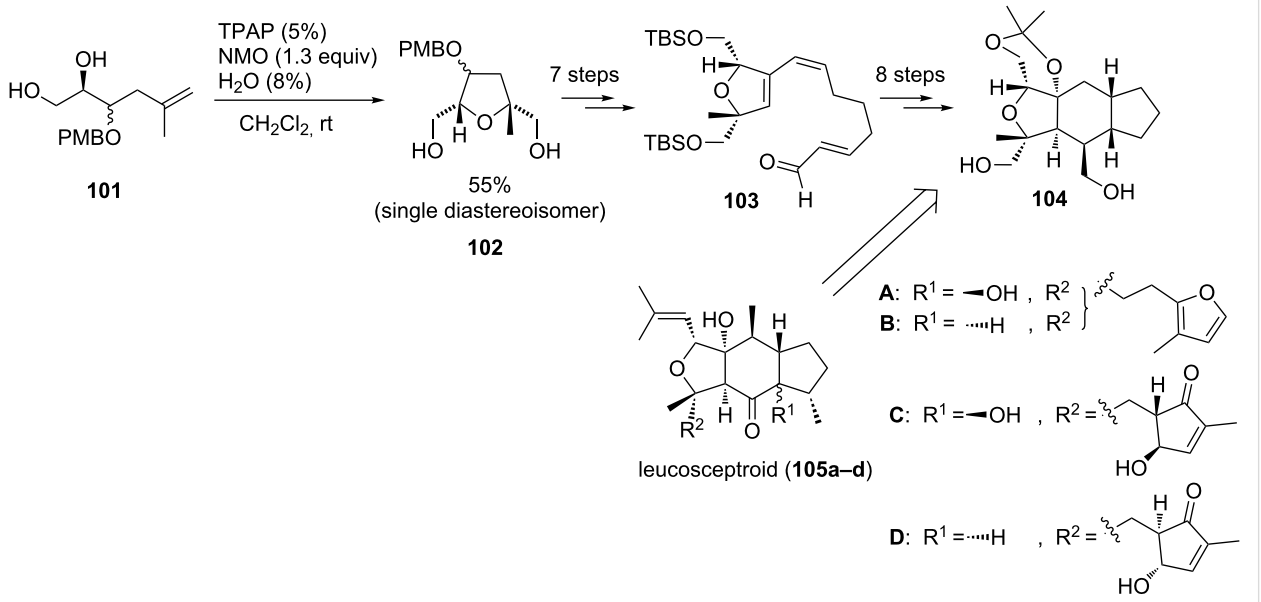

Scheme 22: Ru(VII)-catalyzed oxidative cyclization of a 5,6-dihydroxy alkene in the synthesis of the core structure of the leucosceptroids A-D.

To date there is only a single report on an enantioselective oxidative cyclization of a 1,5-diene using permanganate together with a chiral counter ion. Other strategies use either a chiral auxiliary, a subsequent desymmetrization or start from a chiral 5,6-dihydroxy alkene or 5-hydroxy alkene substrate and proceed in a diastereoselective fashion to yield optically pure products. Though the latter procedures are quite powerful, the development of a catalytic asymmetric oxidative diene cyclization appears still a worthwhile task to be solved. Moreover, one can expect that future applications in target-oriented and natural product synthesis will also apply the same reaction methodology for the construction of THP or even oxepan compounds.

Overlooking these future directions, the direct oxidative cyclization of 1,5-dienes and mechanistically related oxidative THF forming reactions seem now to be firmly established methods for the application in complex total synthesis and are expected to deliver further exciting examples. More than 25 successful examples from the past three decades from different classes of natural products (including carbohydrates, polyketides, amino acids, fatty acids as well as acetogenins and terpenoids) are summarized in this review article.

Acknowledgements

Our research in this area is generously funded by the Deutsche Forschungsgemeinschaft (DFG) and the Fonds der Chemischen Industrie (FCI). In addition, individual fellowships by the Ernst-Schering-Stiftung, the Dierks-von-Zweck-Stiftung and the Deutsche Bundesstiftung Umwelt (DBU) are gratefully acknowledged.

References

1. Walba, D. M.; Edwards, P. D. *Tetrahedron Lett.* **1980,** *21,* 3531–3534. doi:10.1016/0040-4039(80)80226-7
2. Kocieński, P. J.; Brown, R. C. D.; Pommier, A.; Procter, M.; Schmidt, B. *J. Chem. Soc., Perkin Trans. 1* **1998,** 9–40. doi:10.1039/a705385a
3. Hartung, J.; Greb, M. *J. Organomet. Chem.* **2002,** *661,* 67–84. doi:10.1016/S0022-328X(02)01807-7
4. Piccialli, V. *Synthesis* **2007,** 2585–2607. doi:10.1055/s-2007-983835
5. Pilgrim, B. S.; Donohoe, T. J. *J. Org. Chem.* **2013,** *78,* 2149–2167. doi:10.1021/jo302719y
6. Sheikh, N. S. *Org. Biomol. Chem.* **2014,** *12,* 9492–9504. doi:10.1039/C4OB01491J
7. Kötz, A.; Steche, T. *J. Prakt. Chem.* **1924,** *107,* 193–210. doi:10.1002/prac.19241070509
8. Klein, E.; Rojahn, W. *Tetrahedron* **1965,** *21,* 2353–2358. doi:10.1016/S0040-4020(01)93889-X
9. Baldwin, J. E.; Crossley, M. J.; Lehtonen, E.-M. M. *J. Chem. Soc., Chem. Commun.* **1979,** 918–920. doi:10.1039/c39790000918
10. Walba, D. M.; Wand, M. D.; Wilkes, M. C. *J. Am. Chem. Soc.* **1979,** *101,* 4396–4397. doi:10.1021/ja00509a069
11. Wolfe, S.; Ingold, C. F. *J. Am. Chem. Soc.* **1981,** *103,* 940–941. doi:10.1021/ja00394a038
12. Poething, A.; Strassner, T. *Collect. Czech. Chem. Commun.* **2007,** *72,* 715–727. doi:10.1135/cccc20070715
13. Poething, A.; Strassner, T. *J. Org. Chem.* **2010,** *75,* 1967–1973. doi:10.1021/jo100147e
14. di Dio, P. J.; Zahn, S.; Stark, C. B. W.; Kirchner, B. *Z. Naturforsch.* **2010,** *65b,* 367–375. doi:10.1515/znb-2010-0321
15. Roth, S.; Göhler, S.; Cheng, H.; Stark, C. B. W. *Eur. J. Org. Chem.* **2005,** 4109–4118. doi:10.1002/ejoc.200500052
16. Jalce, G.; Franck, X.; Figadère, B. *Tetrahedron: Asymmetry* **2009,** *20,* 25372581. doi:10.1016/j.tetasy.2009.10.034

17. Piccialli, V. *Molecules* **2014,** *19,* 6534–6582. doi:10.3390/molecules19056534
18. Plietker, B. *Synthesis* **2005,** *15,* 2453–2472. doi:10.1055/s-2005-872172
19. Murahashi, S.-I.; Komiya, N. In *Ruthenium Catalyzed Oxidation for Organic Synthesis in Modern Oxidation Methods;* Bäckvall, J.-E., Ed.; Wiley-VCH: Weinheim, Germany, 2010; pp 241–245.
20. Roth, S.; Stark, C. B. W. *Angew. Chem., Int. Ed.* **2006,** *45,* 6218–6221. doi:10.1002/anie.200504572
21. Cecil, A. R. L.; Brown, R. C. D. *Tetrahedron Lett.* **2004,** *45,* 7269–7271. doi:10.1016/j.tetlet.2004.08.023
22. Piccialli, V. *Tetrahedron Lett.* **2000,** *41,* 3731–3733. doi:10.1016/S0040-4039(00)00476-7
23. Piccialli, V.; Borbone, N.; Oliviero, G. *Tetrahedron Lett.* **2007,** *48,* 5131–5135. doi:10.1016/j.tetlet.2007.05.078
24. Donohoe, T. J.; Butterworth, S. *Angew. Chem., Int. Ed.* **2003,** *42,* 948–951. doi:10.1002/anie.200390253
25. Cheng, H.; Stark, C. B. W. *Angew. Chem., Int. Ed.* **2010,** *49,* 1587–1590. doi:10.1002/anie.200903090
26. Walba, D. M.; Stoudt, G. S. *Tetrahedron Lett.* **1982,** *23,* 727–730. doi:10.1016/S0040-4039(00)86932-4
27. Shen, Z.; Sinha, S. C. *Tetrahedron* **2008,** *64,* 1603–1611. doi:10.1016/j.tet.2007.11.089
28. Wang, Z.-M.; Tian, S.-K.; Shi, M. *Tetrahedron: Asymmetry* **1999,** *10,* 667–670. doi:10.1016/S0957-4166(99)00039-7
29. Menéndez Pérez, B.; Schuch, D.; Hartung, J. *Org. Biomol. Chem.* **2008,** *6,* 3532–3541. doi:10.1039/B804588G
30. Tanaka, T.; Hatano, K.; Watanabe, M.; Abbas, H. K. J. *Nat. Toxins* **1996,** *5,* 317–329.
31. Donohoe, T. J.; Butterworth, S. *Angew. Chem., Int. Ed.* **2003,** *42,* 948–951. doi:10.1002/anie.200390253
32. Koerner, T. A. W., Jr.; Voll, R. J.; Younathan, E. S. *Carbohydr. Res.* **1977,** *59,* 403–416. doi:10.1016/S0008-6215(00)83181-X
33. Bennek, J. A.; Gray, G. R. *J. Org. Chem.* **1987,** *52,* 892–897. doi:10.1021/jo00381a030
34. van Delft, F. L.; van der Marel, G. A.; van Boom, H. J. *Tetrahedron Lett.* **1994,** *35,* 1091–1094. doi:10.1016/S0040-4039(00)79973-4
35. van Delft, F. L.; Rob, A.; Valentijn, P. M.; van der Marel, G. A.; van Boom, J. H. *J. Carbohydr. Chem.* **1999,** *18,* 165–190. doi:10.1080/07328309908543989
36. Persky, R.; Albeck, A. *J. Org. Chem.* **2000,** *65,* 5632–5638. doi:10.1021/jo0003908
37. Das, B.; Kumar, D. N. *Tetrahedron Lett.* **2010,** *51,* 6011–6013. doi:10.1016/j.tetlet.2010.09.049
38. Aragão-Leoneti, V.; Carvalho, I. *Tetrahedron Lett.* **2013,** *54,* 1087–1089. doi:10.1016/j.tetlet.2012.12.062
39. Yuan, C.; Hollingsworth, I. R. *Lett. Org. Chem.* **2013,** *10,* 77–84. doi:10.2174/1570178611310020002
40. Kiss, J.; Furter, H.; Lohse, F.; Hardegger, E. *Helv. Chim. Acta* **1961,** *44,* 141–147. doi:10.1002/hlca.19610440119
41. Hardegger, E.; Furter, H.; Kiss, J. *Helv. Chim. Acta* **1958,** *41,* 2401–2410. doi:10.1002/hlca.19580410750
42. Sakai, R.; Koike, T.; Sasaki, M.; Shimamoto, K.; Oiwa, C.; Yano, A.; Suzuki, K.; Tachibana, K.; Kamiya, H. *Org. Lett.* **2001,** *3,* 1479–1482. doi:10.1021/ol015798l
43. Lee, H.-Y.; Lee, S.-S.; Kim, H. S.; Lee, K. M. *Eur. J. Org. Chem.* **2012,** 4192–4199. doi:10.1002/ejoc.201200439
44. Sasaki, M.; Tsubone, K.; Aoki, K.; Akiyama, N.; Shoji, M.; Oikawa, M.; Sakai, R.; Shimamoto, K. *J. Org. Chem.* **2008,** *73,* 264–273. doi:10.1021/jo702116c
45. Shoji, M.; Akiyama, N.; Tsubone, K.; Lash, L. L.; Sanders, J. M.; Swanson, G. T.; Sakai, R.; Shimamoto, K.; Oikawa, M.; Sasaki, M. *J. Org. Chem.* **2006,** *71,* 5208–5220. doi:10.1021/jo0605593
46. Sasaki, M.; Tsubone, K.; Shoji, M.; Oikawa, M.; Shimamoto, K.; Sakai, R. *Bioorg. Med. Chem. Lett.* **2006,** *16,* 5784–5787. doi:10.1016/j.bmcl.2006.08.082
47. Takahashi, K.; Matsumura, T.; Corbin, G. R. M.; Ishihara, J.; Hatakeyama, S. *J. Org. Chem.* **2006,** *71,* 4227–4231. doi:10.1021/jo060410r
48. Lygo, B.; Slack, D.; Wilson, C. *Tetrahedron Lett.* **2005,** *46,* 6629–6632. doi:10.1016/j.tetlet.2005.07.159
49. Albarella, L.; Musumeci, D.; Sica, D. *Eur. J. Org. Chem.* **2001,** 997–1003. doi:10.1002/1099-0690(200103)2001:5<997::AID-EJOC997>3.0.CO;2-7
50. Ratcliffe, R.; Rodehorst, R. *J. Org. Chem.* **1970,** *35,* 4000–4002. doi:10.1021/jo00836a108
51. Schmidt, A.-K. C.; Stark, C. B. W. *Org. Lett.* **2011,** *13,* 4164–4167. doi:10.1021/ol2014335
52. Donohoe, T. J.; Winship, P. C. M.; Tatton, M. R.; Szeto, P. *Angew. Chem., Int. Ed.* **2011,** *50,* 7604–7606. doi:10.1002/anie.201102525
53. Jana, R.; Pathak, T. P.; Sigman, M. S. *Chem. Rev.* **2011,** *111,* 1417–1492. doi:10.1021/cr100327p
54. Heravi, M. M.; Hashemi, E.; Nazari, N. *Mol. Diversity* **2014,** *18,* 441–472. doi:10.1007/s11030-014-9510-1
55. Liu, C.; Hermann, T. E. *J. Biol. Chem.* **1978,** *253,* 5892–5894.
56. Liu, W.-C.; Slusarchyk, D. S.; Astle, G.; Trejo, W. H.; Brown, W. E.; Meyers, E. *J. Antibiot.* **1978,** *31,* 815–819. doi:10.7164/antibiotics.31.815
57. Toeplitz, B. K.; Cohen, A. I.; Funke, P. T.; Parker, W. L.; Gougoutas, J. Z. *J. Am. Chem. Soc.* **1979,** *101,* 3344–3353. doi:10.1021/ja00506a035
58. Putney, J. W., Ed. *Calcium Signaling;* CRC/Taylor & Francis: Boca Raton, Florida, 2006.
59. Li, Y.; Cooksey, J. P.; Gao, Z.; Kocieński, P. J.; McAteer, S. M.; Snaddon, T. N. *Synthesis* **2011,** 104–108. doi:10.1055/s-0030-1258327
60. Gao, Z.; Li, Y.; Cooksey, J. P.; Snaddon, T. N.; Schunk, S.; Viseux, E. M. E.; McAteer, S. M.; Kocienski, P. J. *Angew. Chem., Int. Ed.* **2009,** *48,* 5022–5025. doi:10.1002/anie.200901608
61. Evans, D. A.; Dow, R. L.; Shih, T. L.; Takacs, J. M.; Zahler, R. *J. Am. Chem. Soc.* **1990,** *112,* 5290–5313. doi:10.1021/ja00169a042
62. Hanessian, S.; Cooke, N. G.; DeHoff, B.; Sakito, Y. *J. Am. Chem. Soc.* **1990,** *112,* 5276–5290. doi:10.1021/ja00169a041
63. Spino, C.; Weiler, L. *Tetrahedron Lett.* **1987,** *28,* 731–734. doi:10.1016/S0040-4039(01)80974-6
64. Walba, D. M.; Edwards, P. D. *Tetrahedron Lett.* **1980,** *21,* 3531–3534. doi:10.1016/0040-4039(80)80226-7
65. Kobayashi, J.; Tsuda, M.; Ishibashi, M.; Shigemori, H.; Yamasu, T.; Hirota, H.; Sasaki, T. *J. Antibiot.* **1991,** *44,* 1259–1261. doi:10.7164/antibiotics.44.1259
66. Kobayashi, J.; Kubota, T. *J. Nat. Prod.* **2007,** *70,* 451–460. doi:10.1021/np0605844
67. Mahapatra, S.; Carter, R. G. *Angew. Chem., Int. Ed.* **2012,** *51,* 7948–7951. doi:10.1002/anie.201203935

68. Mahapatra, S.; Carter, R. G. *J. Am. Chem. Soc.* **2013,** *135,* 10792–10803. doi:10.1021/ja404796n
69. Valot, G.; Regens, C. S.; O'Malley, D. P.; Godineau, E.; Takikawa, H.; Fürstner, A. *Angew. Chem., Int. Ed.* **2013,** *52,* 9534–9538. doi:10.1002/anie.201301700
70. Valot, G.; Mailhol, D.; Regens, C. S.; O'Malley, D. P.; Godineau, E.; Takikawa, H.; Philipps, P.; Fürstner, A. *Chem. – Eur. J.* **2015,** *21,* 2398–2408. doi:10.1002/chem.201405790
71. Palmer, C.; Morra, N. A.; Stevens, A. C.; Bajtos, B.; Machin, B. P.; Pagenkopf, B. L. *Org. Lett.* **2009,** *11,* 5614–5617. doi:10.1021/ol9023375
72. Gleye, C.; Duret, P.; Laurens, A.; Hocquemiller, R.; Cavé, A. *J. Nat. Prod.* **1998,** *61,* 576–579. doi:10.1021/np970494m
73. Hu, Y.; Cecil, A. R. L.; Frank, X.; Gleye, C.; Figadère, B.; Brown, R. C. D. *Org. Biomol. Chem.* **2006,** *4,* 1217–1219. doi:10.1039/b601943a
74. Adrian, J.; Stark, C. B. W. *Org. Lett.* **2014,** *16,* 5886–5889. doi:10.1021/ol502849y
75. Makabe, H.; Hattori, Y.; Tanaka, A.; Oritani, T. *Org. Lett.* **2002,** *4,* 1083–1085. doi:10.1021/ol0102803
76. Cecil, A. R. L.; Brown, R. C. D. *Org. Lett.* **2002,** *4,* 3715–3718. doi:10.1021/ol026669n
77. Makabe, H.; Hattori, Y.; Kimura, Y.; Konno, H.; Abe, M.; Miyoshi, H.; Tanaka, A.; Oritani, T. *Tetrahedron* **2004,** *60,* 10651–10657. doi:10.1016/j.tet.2004.09.011
78. Cecil, A. R. L.; Hu, Y.; Vicent, M. J.; Duncan, R.; Brown, R. C. D. *J. Org. Chem.* **2004,** *69,* 3368–3374. doi:10.1021/jo049909g
79. Donohoe, T. J.; Butterworth, S. *Angew. Chem., Int. Ed.* **2005,** *44,* 4766–4768. doi:10.1002/anie.200500513
80. Göksel, H.; Stark, C. B. W. *Org. Lett.* **2006,** *8,* 3433–3436. doi:10.1021/ol060520k
81. Konno, H.; Okuno, Y.; Makabe, H.; Nosaka, K.; Onishi, A.; Abe, Y.; Sugimoto, A.; Akaji, K. *Tetrahedron Lett.* **2008,** *49,* 782–785. doi:10.1016/j.tetlet.2007.11.190
82. Makabe, H.; Kuwabara, A.; Hattori, Y.; Konno, H. *Heterocycles* **2009,** *78,* 2369–2376. doi:10.3987/COM-09-11741
83. Konno, H.; Makabe, H.; Hattori, Y.; Nosaka, K.; Akaji, K. *Tetrahedron* **2010,** *66,* 7946–7953. doi:10.1016/j.tet.2010.08.028
84. Brown, R. C. D.; Keily, J. F. *Angew. Chem., Int. Ed.* **2001,** *40,* 4496–4498. doi:10.1002/1521-3773(20011203)40:23<4496::AID-ANIE4496>3.0.CO;2-F
85. Abdel Ghani, S. B.; Chapman, J. M.; Figadère, B.; Herniman, J. M.; Langley, G. J., II; Niemann, S.; Brown, R. C. D. *J. Org. Chem.* **2009,** *74,* 6924–6928. doi:10.1021/jo9012578
86. Hentges, S. G.; Sharpless, K. B. *J. Am. Chem. Soc.* **1980,** *102,* 4263–4265. doi:10.1021/ja00532a050
87. Jacobsen, E. N.; Marko, I.; Mungall, W. S.; Schroeder, G.; Sharpless, K. B. *J. Am. Chem. Soc.* **1988,** *110,* 1968–1970. doi:10.1021/ja00214a053
88. Kolb, H. C.; Sharpless, K. B. Asymmetric dihydroxylation. In *Transition Metals for Organic Synthesis;* Beller, M.; Bolm, C., Eds.; Wiley-VCH: Weinheim, Germany, 2004; Vol. 2, pp 275–298. doi:10.1002/9783527619405.ch5e
89. Schmidt, A.-K. C.; Stark, C. B. W. *Synthesis* **2014,** *46,* 3283–3308. doi:10.1055/s-0033-1338650
90. Zhong, Y.-L.; Shing, T. K. M. *J. Org. Chem.* **1997,** *62,* 2622–2624. doi:10.1021/jo9621581
91. Palomo, J. M.; Cabrera, Z. *Curr. Org. Synth.* **2012,** *9,* 791–805. doi:10.2174/157017912803901628
92. Spurr, I. B.; Brown, R. C. B. *Molecules* **2010,** *15,* 460–501. doi:10.3390/molecules15010460
93. Mikolajczak, K. J.; Madrigal, R. V.; Rupprecht, J. K.; Hui, Y.-H.; Liu, Y.-M.; Smith, D. L.; McLaughlin, J. L. *Experientia* **1990,** *46,* 324–327. doi:10.1007/BF01951779
94. Shi, G.; Zeng, L.; Gu, Z.-m.; MacDougal, J. M.; McLaughlin, J. L. *Heterocycles* **1995,** *41,* 1785–1796. doi:10.3987/COM-95-7117
95. Donohoe, T. J.; Harris, R. M.; Burrows, J.; Parker, J. *J. Am. Chem. Soc.* **2006,** *128,* 13704–13705. doi:10.1021/ja0660148
96. Donohoe, T. J.; Harris, R. M.; Williams, O.; Hargaden, G. C.; Burrows, J.; Parker, J. *J. Am. Chem. Soc.* **2009,** *131,* 12854–12861. doi:10.1021/ja9049959
97. Brown, L. J.; Spurr, I. B.; Kemp, S. C.; Camp, N. P.; Gibson, K. R.; Brown, R. C. D. *Org. Lett.* **2008,** *10,* 2489–2492. doi:10.1021/ol800767e
98. Grubbs, R. H.; Miller, S. J.; Fu, G. C. *Acc. Chem. Res.* **1995,** *28,* 446–452. doi:10.1021/ar00059a002
99. Bhunnoo, R. A.; Hobbs, H.; Laine, D. I.; Light, M. E.; Brown, R. C. D. *Org. Biomol. Chem.* **2009,** *7,* 1017–1024. doi:10.1039/b813201a
100. Saez, J.; Sahpaz, S.; Villaescusa, L.; Hocquemiller, R.; Cavé, A.; Cortes, D. *J. Nat. Prod.* **1993,** *56,* 351–356. doi:10.1021/np50093a007
101. González, M. C.; Lavaud, C.; Gallardo, T.; Zafra-Polo, M. C.; Cortes, D. *Tetrahedron* **1998,** *54,* 6079–6088. doi:10.1016/S0040-4020(98)00301-9
102. Head, G. D.; Whittingham, W. G.; Brown, R. C. D. *Synlett* **2004,** 1437–1439. doi:10.1055/s-2004-825624
103. Katsuki, T.; Sharpless, K. B. *J. Am. Chem. Soc.* **1980,** *102,* 5974–5976. doi:10.1021/ja00538a077
104. Heravi, M. M.; Lashaki, T. B.; Poorahmad, N. *Tetrahedron: Asymmetry* **2015,** *26,* 405–495. doi:10.1016/j.tetasy.2015.03.006
105. Hu, Y.; Brown, R. C. D. *Chem. Commun.* **2005,** 5636–5637. doi:10.1039/b512126d
106. Queiroz, E. F.; Roblot, F.; Figadère, B.; Laurens, A.; Duret, P.; Hocquemiller, R.; Cavé, A. *J. Nat. Prod.* **1998,** *61,* 34–39. doi:10.1021/np9703252
107. Morris, C. L.; Hu, Y.; Head, G. D.; Brown, L. J.; Whittingham, W. G.; Brown, R. C. D. *J. Org. Chem.* **2009,** *74,* 981–988. doi:10.1021/jo802012a
108. Gu, Z.-m.; Zhou, D.; Lewis, N. J.; Wu, J.; Shi, G.; McLaughlin, J. L. *Bioorg. Med. Chem.* **1997,** *5,* 1911–1916. doi:10.1016/S0968-0896(97)00129-6
109. D'Souza, L. J.; Sinha, S. C.; Lu, S.-F.; Keinan, E.; Sinha, S. C. *Tetrahedron* **2001,** *57,* 5255–5262. doi:10.1016/S0040-4020(01)00381-7
110. Sinha, S. C.; Sinha-Bagchi, A.; Keinan, E. *J. Am. Chem. Soc.* **1995,** *117,* 1447–1448. doi:10.1021/ja00109a037
111. Keinan, E.; Sinha, S. C. *Pure Appl. Chem.* **2002,** *74,* 93–105. doi:10.1351/pac200274010093
112. Sinha, S. C.; Sinha-Bagchi, A.; Yazbak, A.; Keinan, E. *Tetrahedron Lett.* **1995,** *36,* 9257–9260. doi:10.1016/0040-4039(95)02018-K
113. Avedissian, H.; Sinha, S. C.; Yazbak, A.; Sinha, A.; Neogi, P.; Sinha, S. C.; Keinan, E. *J. Org. Chem.* **2000,** *65,* 6035–6051. doi:10.1021/jo000500a
114. Chen, Z.; Sinha, S. C. *Tetrahedron* **2008,** *64,* 1603–1611. doi:10.1016/j.tet.2007.11.089
115. Sinha, S. C.; Sinha, A.; Yazbak, A.; Keinan, E. *J. Org. Chem.* **1996,** *61,* 7640–7641. doi:10.1021/jo961286m

116. Sinha, S. C.; Sinha, A.; Sinha, S. C.; Keinan, E. *J. Am. Chem. Soc.* **1998,** *120,* 4017–4018. doi:10.1021/ja973696d
117. Zeng, L.; Ye, Q.; Oberlies, N. H.; Shi, G.; Gu, Z.-M.; He, K.; McLaughlin, J. L. *Nat. Prod. Rep.* **1996,** *13,* 275–306. doi:10.1039/np9961300275
118. Woo, M. H.; Cho, K. Y.; Zhang, Y.; Zeng, L.; Gu, Z.-M.; McLaughlin, J. L. *J. Nat. Prod.* **1995,** *58,* 1533–1542. doi:10.1021/np50124a009
119. Zhang, Y.; Zeng, L.; Woo, M.-H.; Gu, Z.-M.; Ye, Q.; Wu, F.-E.; McLaughlin, J. L. *Heterocycles* **1995,** *41,* 1743–1755. doi:10.3987/COM-95-7101
120. Wang, Z.-M.; Tian, S.-K.; Shi, M. *Tetrahedron Lett.* **1999,** *40,* 977–980. doi:10.1016/S0040-4039(98)02577-5
121. Wang, Z.-M.; Tian, S.-K.; Shi, M. *Eur. J. Org. Chem.* **2000,** 349–356. doi:10.1002/(SICI)1099-0690(200001)2000:2<349::AID-EJOC349>3.0.CO;2-J
122. Wang, Z.-M.; Tian, S.-K.; Shi, M. *Tetrahedron: Asymmetry* **1999,** *10,* 667–670. doi:10.1016/S0957-4166(99)00039-7
123. Wang, Z.-M.; Tian, S.-K.; Shi, M. *Chirality* **2000,** *12,* 581–589. doi:10.1002/1520-636X(2000)12:7<581::AID-CHIR6>3.0.CO;2-P
124. Fang, X.-P.; Rupprecht, J. K.; Alkofahi, A.; Hui, Y.-H.; Liu, Y.-M.; Smith, D. L.; Wood, K. V.; McLaughlin, J. L. *Heterocycles* **1991,** *32,* 11–17. doi:10.3987/COM-90-5610
125. Evans, P. A.; Cui, J.; Gharpure, S. J.; Polosukhin, A.; Zhang, H.-R. *J. Am. Chem. Soc.* **2003,** *125,* 14702–14703. doi:10.1021/ja0384734
126. Zhao, H.; Gorman, J. S. T.; Pagenkopf, B. L. *Org. Lett.* **2006,** *8,* 4379–4382. doi:10.1021/ol061847o
127. Wang, J.; Pagenkopf, B. L. *Org. Lett.* **2007,** *9,* 3703–3706. doi:10.1021/ol701797e
128. Phillips, G. A.; Wright, T. B.; Stevens, A. C.; Pagenkopf, B. L. *Can. J. Chem.* **2015,** *93,* 196–198. doi:10.1139/cjc-2014-0288
129. Phillips, G. A.; Palmer, C.; Stevens, A. C.; Piotrowski, M. L.; Dekruyf, D. S. R.; Pagenkopf, B. L. *Tetrahedron Lett.* **2015,** *56,* 6052–6055. doi:10.1016/j.tetlet.2015.09.064
130. Surburg, H.; Panten,, J. *Common Fragrance and Flavour Materials: Preparation, Properties and Uses,* 5th ed.; Wiley-VCH: Weinheim, 2006. doi:10.1002/3527608214
131. Rychnovsky, S. D.; Bartlett, P. A. *J. Am. Chem. Soc.* **1981,** *103,* 3963–3964. doi:10.1021/ja00403a075
132. David, L.; Veschambre, H. *Tetrahedron Lett.* **1984,** *25,* 543–546. doi:10.1016/S0040-4039(00)99933-7
133. Méou, A.; Bovanah, N.; Archelas, A.; Zhang, X. M.; Guglielmetti, R.; Furstoss, R. *Synthesis* **1990,** 752–753. doi:10.1055/s-1990-27003
134. Mischitz, M.; Faber, K. *Synlett* **1996,** 978–980. doi:10.1055/s-1996-5638
135. Duan, S.; Moeller, K. D. *Org. Lett.* **2001,** *3,* 2685–2688. doi:10.1021/ol0162670
136. Wan, K. K.; Litz, J. P.; Vosberg, D. A. *Tetrahedron: Asymmetry* **2010,** *21,* 2425–2428. doi:10.1016/j.tetasy.2010.08.011
137. Al Hazni, A. M.; Sheikh, N. S.; Bataille, C. J. R.; Al-Hadedi, A. A. M.; Watkin, S. V.; Luker, T. J.; Camp, N. P.; Brown, R. C. D. *Org. Lett.* **2014,** *16,* 5104–5107. doi:10.1021/ol502454r
138. Suzuki, T.; Suzuki, M.; Furusaki, A.; Matsumoto, T.; Kato, A.; Imanaka, Y.; Kurosawa, E. *Tetrahedron Lett.* **1985,** *26,* 1329–1332. doi:10.1016/S0040-4039(00)94885-8
139. Morita, H.; Kishi, E.; Takeya, K.; Itokawa, H.; Iitaka, Y. *Phytochemistry* **1993,** *34,* 765–771. doi:10.1016/0031-9422(93)85356-V
140. Xiong, Z.; Corey, E. J. *J. Am. Chem. Soc.* **2000,** *122,* 9328–9329. doi:10.1021/ja0024901
141. Harding, W. W.; Lewis, P. A.; Jacobs, H.; McLean, S.; Reynolds, W. F.; Tay, L.-L.; Yang, J.-P. *Tetrahedron Lett.* **1995,** *36,* 9137–9140. doi:10.1016/0040-4039(95)01957-J
142. Morimoto, Y.; Iwai, T.; Kinoshita, T. *J. Am. Chem. Soc.* **1999,** *121,* 6792–6797. doi:10.1021/ja990154i
143. Morimoto, Y.; Kinoshita, T.; Iwai, T. *Chirality* **2002,** *14,* 578–586. doi:10.1002/chir.10083
144. Hoye, T. R.; Jenkins, S. A. *J. Am. Chem. Soc.* **1987,** *109,* 6196–6198. doi:10.1021/ja00254a056
145. Hashimoto, M.; Yanagiya, M.; Shirahama, H. *Chem. Lett.* **1988,** 645–646. doi:10.1246/cl.1988.645
146. Hashimoto, M.; Harigaya, H.; Yanagiya, M.; Shirahama, H. *Tetrahedron Lett.* **1988,** *29,* 5947–5948. doi:10.1016/S0040-4039(00)82236-4
147. Hashimoto, M.; Harigaya, H.; Yanagiya, M.; Shirahama, H. *J. Org. Chem.* **1991,** *56,* 2299–2311. doi:10.1021/jo00007a013
148. Morimoto, Y.; Iwai, T.; Yoshimura, T.; Kinoshita, T. *Bioorg. Med. Chem. Lett.* **1998,** *8,* 2005–2010. doi:10.1016/S0960-894X(98)00347-3
149. Morimoto, Y.; Iwai, T.; Nishikawa, Y.; Kinoshita, T. *Tetrahedron: Asymmetry* **2002,** *13,* 2641–2647. doi:10.1016/S0957-4166(02)00718-8
150. Rodríguez-López, J.; Chrisóstomo, F. P.; Ortega, N.; López-Rodríguez, M.; Martín, V. S.; Martín, T. *Angew. Chem., Int. Ed.* **2013,** *52,* 3659–3662. doi:10.1002/anie.201209159
151. Morimoto, Y.; Takeuchi, E.; Kambara, H.; Kodama, T.; Tachi, Y.; Nishikawa, K. *Org. Lett.* **2013,** *15,* 2966–2969. doi:10.1021/ol401081e
152. Itokawa, H.; Kishi, E.; Morita, H.; Takeya, K.; Iitaka, Y. *Tetrahedron Lett.* **1991,** *32,* 1803–1804. doi:10.1016/S0040-4039(00)74334-6
153. Ujihara, K.; Shirahama, H. *Tetrahedron Lett.* **1996,** *37,* 2039–2042. doi:10.1016/0040-4039(96)00212-2
154. Morimoto, Y.; Muragaki, K.; Iwai, T.; Morishita, Y.; Kinoshita, T. *Angew. Chem., Int. Ed.* **2000,** *39,* 4082–4084. doi:10.1002/1521-3773(20001117)39:22<4082::AID-ANIE4082>3.0.CO;2-Z
155. Sheikh, N. S.; Bataille, C. J.; Luker, T. J.; Brown, R. C. D. *Org. Lett.* **2010,** *12,* 2468–2471. doi:10.1021/ol100513y
156. Hioki, H.; Yoshio, S.; Motosue, M.; Oshita, Y.; Nakamura, Y.; Mishima, D.; Furukawa, Y.; Kodama, M.; Ueda, K.; Katsu, T. *Org. Lett.* **2004,** *6,* 961–964. doi:10.1021/ol036471i
157. Sakemi, S.; Higa, T.; Jefford, C. W.; Bernadinelli, G. *Tetrahedron Lett.* **1986,** *27,* 4287–4290. doi:10.1016/S0040-4039(00)94254-0
158. Hashimoto, M.; Kan, T.; Nozaki, K.; Yanagiya, M.; Shirahama, H.; Matsumoto, T. *Tetrahedron Lett.* **1988,** *29,* 1143–1144. doi:10.1016/S0040-4039(00)86672-1
159. Hashimoto, M.; Kan, T.; Nozaki, K.; Yanagiya, M.; Shirahama, H.; Matsumoto, T. *J. Org. Chem.* **1990,** *55,* 5088–5107. doi:10.1021/jo00304a022
160. Corey, E. J.; Ha, D.-C. *Tetrahedron Lett.* **1988,** *29,* 3171–3174. doi:10.1016/0040-4039(88)85113-X
161. Macherla, V. R.; Liu, J.; Bellows, C.; Teisan, S.; Nicholson, B.; Lam, K. S.; Potts, B. C. M. *J. Nat. Prod.* **2005,** *68,* 780–783. doi:10.1021/np049597c
162. Riclea, R.; Dickschat, J. S. *Chem. – Eur. J.* **2011,** *17,* 11930–11934. doi:10.1002/chem.201101139
163. Göhler, S.; Roth, S.; Cheng, H.; Göksel, H.; Rupp, A.; Haustedt, L. O.; Stark, C. B. W. *Synthesis* **2007,** *17,* 2751–2754. doi:10.1055/s-2007-983797

164. Adrian, J.; Roth, S.; Stark, C. B. W. *ChemCatChem* **2016,** *8,* 1679–1684. doi:10.1002/cctc.201600179
165. Luo, S.-H.; Luo, Q.; Niu, X.-M.; Xie, M.-J.; Zhao, X.; Schneider, B.; Gershenzon, J.; Li, S.-H. *Angew. Chem., Int. Ed.* **2010,** *49,* 4471–4475. doi:10.1002/anie.201000449
166. Luo, S.-H.; Wenig, L.-H.; Xie, M.-J.; Li, X.-N.; Hua, J.; Zhao, X.; Li, S.-H. *Org. Lett.* **2011,** *13,* 1864–1867. doi:10.1021/ol200380v
167. Huang, X.; Song, L.; Xu, J.; Zhu, G.; Liu, B. *Angew. Chem., Int. Ed.* **2013,** *52,* 952–955. doi:10.1002/anie.201208687
168. Guo, S.; Liu, J.; Ma, D. *Angew. Chem., Int. Ed.* **2015,** *54,* 1298–1301. doi:10.1002/anie.201410134
169. Hugelshofer, C. L.; Magauer, T. *J. Am. Chem. Soc.* **2015,** *137,* 3807–3810. doi:10.1021/jacs.5b02021
170. Xie, J.; Ma, Y.; Horne, D. A. *J. Org. Chem.* **2011,** *76,* 6169–6176. doi:10.1021/jo200899v

License and Terms

BEILSTEIN JOURNAL OF ORGANIC CHEMISTRY

Enduracididine, a rare amino acid component of peptide antibiotics: Natural products and synthesis

Darcy J. Atkinson[1,2], Briar J. Naysmith[1,2], Daniel P. Furkert[1,2] and Margaret A. Brimble[*1,2]

Review

Open Access

Address:
[1]School of Chemical Sciences, The University of Auckland, 23 Symonds Street, Auckland, New Zealand and [2]Maurice Wilkins Centre for Molecular Biodiscovery, The University of Auckland, 3 Symonds Street, Auckland, New Zealand

Email:
Margaret A. Brimble[*] - m.brimble@auckland.ac.nz

* Corresponding author

Keywords:
amino acid; bacterial resistance; enduracididine; natural products; peptide antibiotics

Beilstein J. Org. Chem. **2016,** *12,* 2325–2342.
doi:10.3762/bjoc.12.226

Received: 05 August 2016
Accepted: 20 October 2016
Published: 07 November 2016

This article is part of the Thematic Series "Natural products in synthesis and biosynthesis II".

Guest Editor: J. S. Dickschat

Abstract

Rising resistance to current clinical antibacterial agents is an imminent threat to global public health and highlights the demand for new lead compounds for drug discovery. One such potential lead compound, the peptide antibiotic teixobactin, was recently isolated from an uncultured bacterial source, and demonstrates remarkably high potency against a wide range of resistant pathogens without apparent development of resistance. A rare amino acid residue component of teixobactin, enduracididine, is only known to occur in a small number of natural products that also possess promising antibiotic activity. This review highlights the presence of enduracididine in natural products, its biosynthesis together with a review of analogues of enduracididine. Reported synthetic approaches to the cyclic guanidine structure of enduracididine are discussed, illustrating the challenges encountered to date in the development of efficient synthetic routes to facilitate drug discovery efforts inspired by the discovery of teixobactin.

Review

Introduction

The enduracididines

The enduracididines (**1**–**6**) are a rare structural class of amino acids that contain a unique five-membered cyclic guanidine moiety (blue, Figure 1). L-Enduracididine (**1**) and D-allo-enduracididine (**4**) were the first identified as amino acid components of potent depsipeptide antibiotics [1,2].

Free enduracididine (**1**) was subsequently isolated from the seeds of the legume *Lonchocarpus sericeus* [3,4]. It was found to inhibit seedling germination of lettuce [5] and did not exhibit any significant effect on the inhibition of protein production in rat hepatoma cells [6]. L-(**5**) and D-β-hydroxyenduracididine

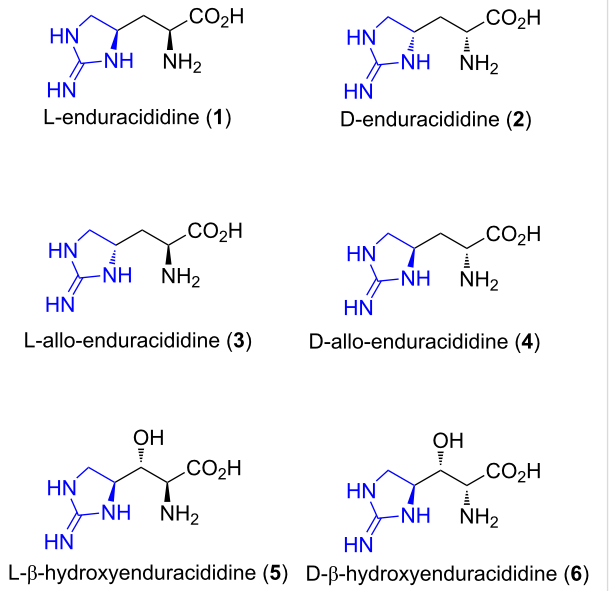

Figure 1: Structures of the enduracididine family of amino acids (**1**–**6**).

(**6**) were first resolved as components of the mannopeptimycin antibiotics, isolated from *Streptomyces hygroscopicus* LL-AC98 in 2002 [7] and to date, have not been isolated as the free amino acids or observed in any other natural products.

Natural products containing enduracididine and hydroxyenduracididine

Enduracidin A and B

Enduracidin A (**7**) and B (**8**) were first isolated from *Streptomyces fungicidicus* B 5477 from a soil sample collected in Nishinomiya, Japan (Figure 2) [1]. Detailed reports of the isolation procedures, in vivo and in vitro antimicrobial activity, physical properties and structure elucidation have been published [1,8-15]. Enduracidin A (**7**) and B (**8**) have also been isolated from *Streptomyces sp*. NJWGY366516 [16], *Streptomyces atrovirens* MGR140 [17] and along with five analogues with various halogenation patterns, from a genetically altered strain of *Streptomyces fungicidicus* [18].

Enduracidin A (**7**) and B (**8**) are depsipeptides with the same composition of seventeen amino acids, sixteen of which make up the cyclic core [11,13,19] and are structurally related to the non-enduracididine containing antibiotic, ramoplanin [19]. The enduracidins are active against Gram-positive bacteria, including resistant strains [2,9,20] and *Mycobacterium* species [21]. No activity was observed against Gram-negative bacteria (except for *Neisseria gonorrhoeae*), fungi or yeast [9]. The antibacterial activity arises through inhibition of cell wall synthesis [22] by prevention of transglycosylation during peptidoglycan synthesis [23], the same step inhibited by vancomycin [24]. Enduracidin A (**7**) and B (**8**) also exhibited inhibition of avian myeloblastosis virus reverse transcriptase but did not suppress

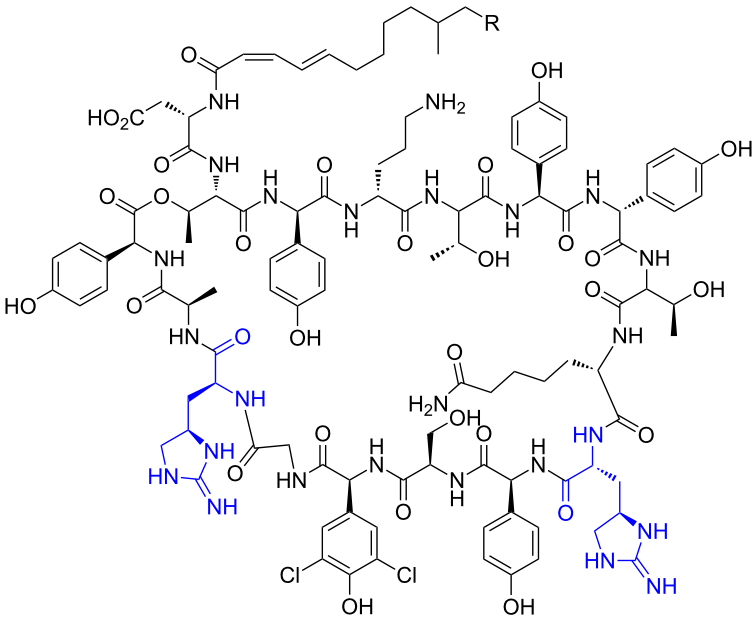

Figure 2: Enduracidin A (**7**) and B (**8**).

replication of HIV cells [25]. Enduracidin A (**7**) and B (**8**) have been produced by fermentation industrially and is used as an antibiotic feed additive for pigs [26] and chickens [27] under the trade name enradin®.

Minosaminomycin

Minosaminomycin (**9**, Figure 3) was isolated in 1974 from a culture broth of *Streptomyces* MA514-A1 [28]. It was found to be active against *Mycobacteria* (*M. smegmatis*, MIC = 15.6 µg/mL) but only weakly active against all other bacteria tested. The structure was confirmed through degradation and partial synthesis [29,30]. Minosaminomycin (**9**) inhibits protein synthesis in *E. coli* more effectively than the related antibiotic kasugamycin (**10**), however, a different mechanism is operative [31].

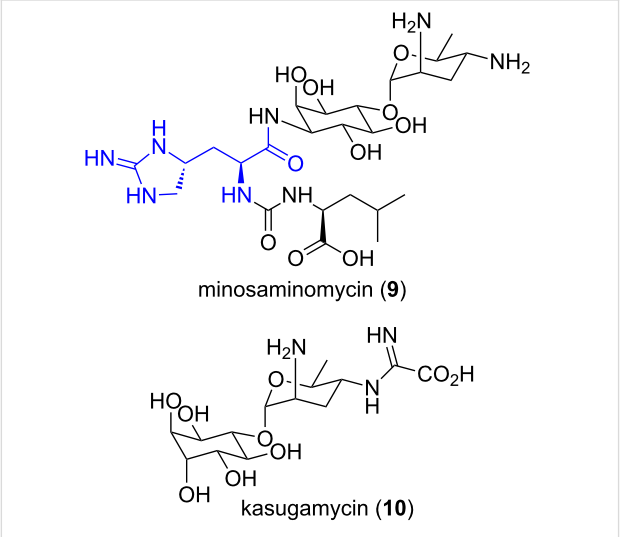

Figure 3: Minosaminomycin (**9**) and related antibiotic kasugamycin (**10**).

Indole metabolite

In 1996, during a screening program for biologically active metabolites from marine ascidians, Riguera et al. identified a small group of amino acid containing compounds in a cytotoxic extract of the ascidian *Leptoclinides dubius* [32]. Among these compounds was the unique enduracididine-containing bromoindole metabolite **11** (Figure 4). This was the first time the enduracididine motif had been isolated from a marine source. The exact compound responsible for the observed cytotoxicity was not determined.

Mannopeptimycins

Mannopeptimycins α–ε (**12**–**16**, Figure 5) were isolated from *Streptomyces hygroscopicus* LL-AC98 in 2002 [7] and their structures were elucidated using mass spectrometry and extensive NMR analysis. The absolute stereochemistry was proposed following degradation and nOe studies. The configuration of the β-methylphenylalanine stereocentre was revised from *S* to *R*, upon total synthesis [33]. The mannopeptimycins contain a unique sugar substituted hydroxyenduracididine residue (blue, Figure 5).

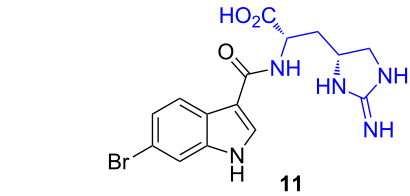

Figure 4: Enduracididine-containing compound **11** identified in a cytotoxic extract of *Leptoclinides dubius* [32].

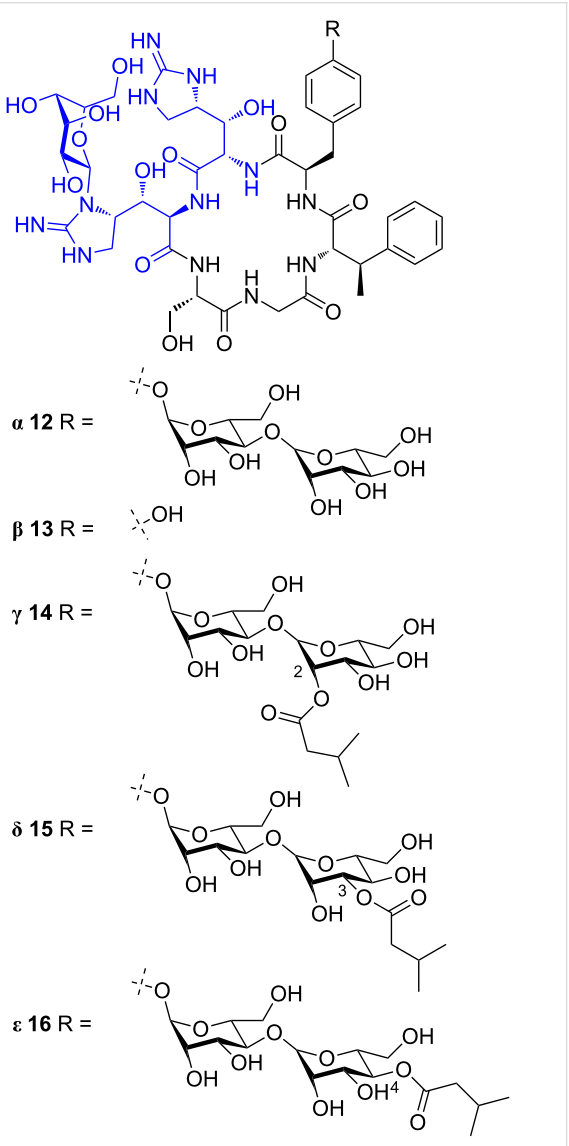

Figure 5: Mannopeptimycins α–ε (**12**–**16**).

The mannopeptimycins displayed moderate activity against Gram-positive bacteria, including MRSA, but only exhibited weak activity against Gram-negative bacteria [7] with the primary cellular target deduced to be bacterial cell wall synthesis [34]. Extensive derivatisation of both mannopeptimycin α (**12**) and β (**13**) was undertaken to improve the antibacterial activity of the parent natural products (highlighted in blue, Figure 6). An array of ether [35,36], halogenated [36], acetal [37-39], benzoxazole [40], thiobenzoxazole [40], ester and carbonate [41] analogues were synthesised and evaluated for antibacterial activity. Only the semisynthetic derivatives possessing hydrophobic groups on the terminal sugar moiety (green) exhibited comparable antibacterial activity to the parent compound and reference antibiotics [42].

Teixobactin

In early 2015, a new enduracididine-containing antibiotic named teixobactin (**17**) was reported (Figure 7) [43]. Teixobactin (**17**) was isolated using the multichannel device, the isolation chip (iChip). The iChip allows a single cell to be delivered to an individual chamber where it can grow. The chambers are covered with a semi-permeable membrane and placed into the microbe's natural environment where nutrients can diffuse into each chamber. This method gives access to cultures of

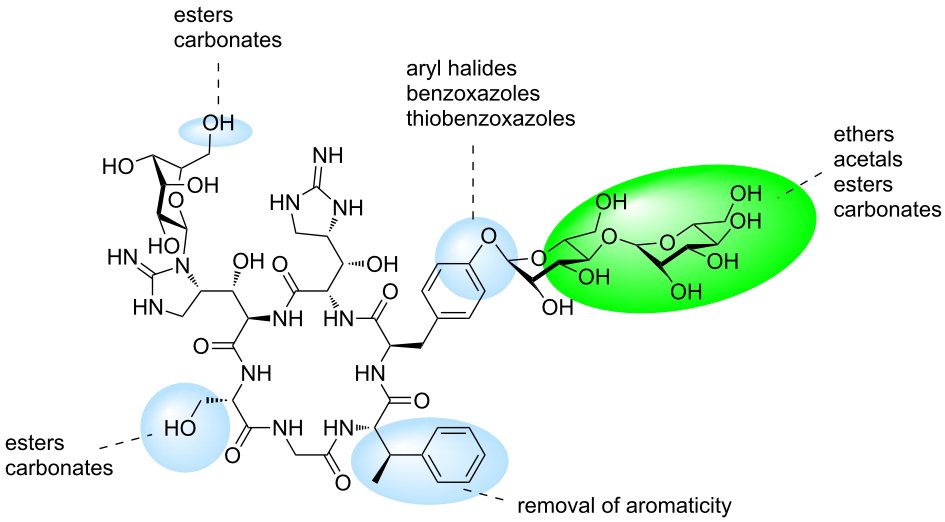

Figure 6: Regions of the mannopeptimycin structure investigated in structure–activity relationship investigations.

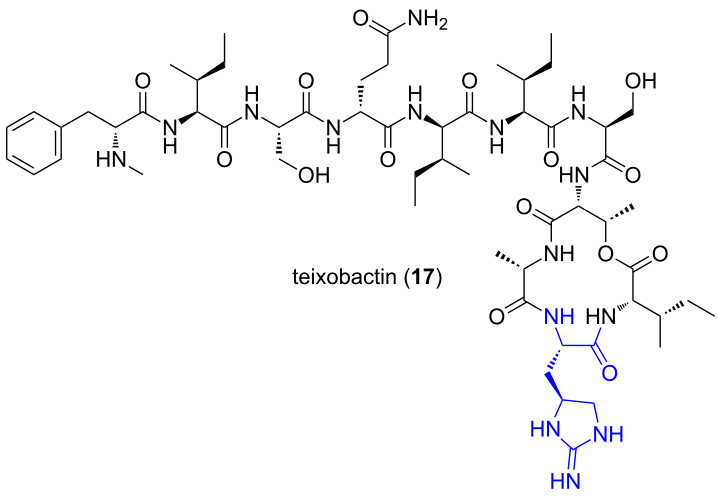

Figure 7: Teixobactin (**17**).

microbes which were previously unobtainable using traditional techniques. Teixobactin (**17**) exhibits bactericidal activity through binding of Lipid II, a precursor of peptidoglycan, and therefore shows great potential as the foundation for discovery of a new generation of antibiotics to overcome the development of antimicrobial resistance.

Teixobactin (**17**) was isolated from the β-protobacterium, *Eleftheria terrae* that belongs to a new genus. Teixobactin (**17**) demonstrated potent activity against the resistant Gram-positive bacteria, MRSA and vancomycin-resistant *Enterococci* (VRE), as well as other bacterial species including, *Mycobacterium tuberculosis* (Mtb) and *Clostridium difficile*. Remarkably, no teixobactin-resistant mutants of *Staphylococcus aureus* or *M. tuberculosis* could be detected after sub-lethal dosing of the compound over a 27 day period [43]. This lack of resistance development may possibly be attributable to the mechanism of action which involves binding to Lipid II, inhibiting one of the membrane-associated steps of peptidoglycan biosynthesis [43,44]. Analogues of teixobactin (**17**) have undergone biological testing and results show that the L-allo-enduracididine (**3**, blue, Figure 7) residue is important for potent antibacterial activity [45]. An approximately 10-fold reduction in activity was observed when the enduracididine residue is substituted for L-arginine [46] and almost complete loss of activity was observed when three of the four D-amino acids of this analogue are substituted for their L-counterparts [47].

Biosynthesis of enduracididine

In 1984, a radio-labelling study was carried out to determine the biosynthesis of enduracididine (**1**) [48]. Arginine (**18**) and its precursors ornithine and citrulline, were found to be incorporated into enduracididine (**1**), but not histidine (**19**) [48]. Between the enduracidin and mannopeptimycin gene clusters, three pairs of enzymes were found to have high sequence homology, mmpP/endP, mppR/endR and mmpQ/endQ [49,50]. MppP is a PLP-dependent hydroxylase and catalyses the conversion of L-arginine (**18**) and molecular oxygen to 2-oxo-4-hydroxy-5-guanidinovaleric acid (**20**, Scheme 1) [51]. The enzyme mppR is a pyruvate aldose that catalyses the dehydration/cyclisation of **20** to give cyclic guanidine **21** [52], where transamination by mppQ gives enduracididine (**1**). Further transformation to L-β-hydroxyenduracididine (**5**) is then catalysed by mppO [52,53].

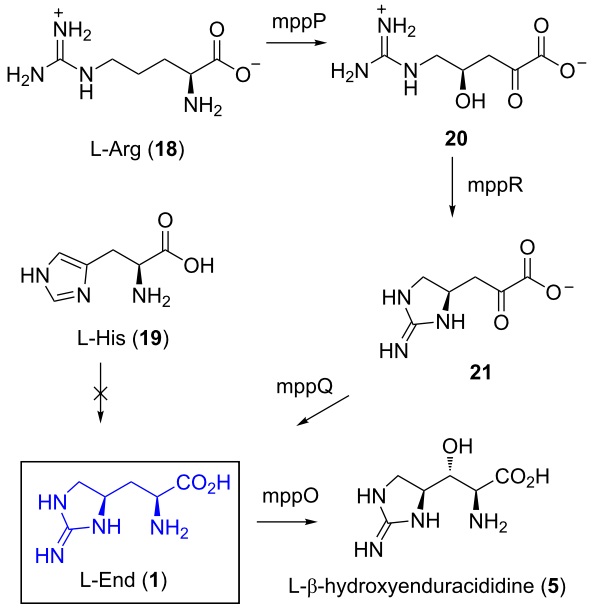

Scheme 1: Proposed biosynthesis of L-enduracididine (**1**) and L-β-hydroxyenduracididine (**5**).

Synthetic investigations

Synthesis of enduracididine

Although several synthetic approaches to enduracididine and its derivatives have been published, the discovery of teixobactin (**17**) has reignited interest in the synthesis of this unnatural amino acid.

Synthesis of enduracididine by Shiba et al.: The first diastereoselective synthesis of enduracididine (**1**) was reported by Shiba et al. in 1975 (Scheme 2) [54]. The synthesis began with

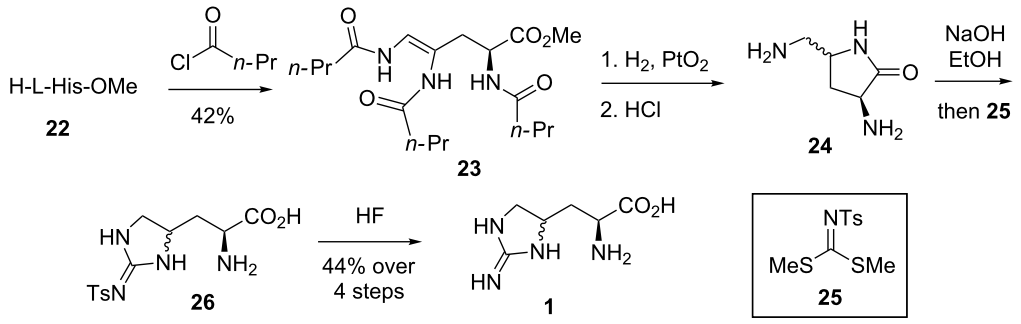

Scheme 2: Synthesis of enduracididine (**1**) by Shiba et al.

Bamberger cleavage of L-methylhistidine (**22**) to afford amide **23**. Reduction of the double bond and cleavage of the three *n*-butyryl groups afforded lactam **24**. Lactam **24** was opened with base and directly treated with guanylating agent **25** giving tosylguanidine **26** which was unstable upon standing. Immediate treatment with anhydrous HF gave L-enduracididine (**1**) as a mixture of diastereomers.

Synthesis of enduracididine and allo-enduracididine by Dodd et al.: No further synthetic investigations were reported until 2004 when Dodd et al. published a synthesis of protected enduracididine using an azide ring opening of a chiral aziridine as the key step (Scheme 3) [55]. The 9-phenylfluorenyl (PhF) protecting group was employed to help prevent undesired copper coordination during the key aziridation step.

The synthesis relied on the stereoselective formation of aziridine **27**. This key reaction proceeded from allylglycine **28** in 28% yield to give a 7:3 mixture in favour of the *S*,*S* diastereomer. Attempted optimisation of the yield and diastereoselectivity afforded no improvement. The synthesis continued with aziridine opening using sodium azide and $BF_3{\cdot}OEt_2$ in DMF at 65 °C, conditions which were key to prevent undesired intramolecular ring opening. The two diastereomers **29** and **30** could then be separated and elaborated to afford enantiopure protected L-enduracididine **31** and L-allo-enduracididine **32**.

Synthetic studies towards β-hydroxyenduracididine by Oberthür et al.: In 2009, Oberthür et al. reported a synthetic route to azide derivatives of β-hydroxyenduracididine [56]. The synthesis hinged on the use of azide **34** as a common intermediate to access both diastereomers. Diacetone D-glucose **35** was converted to azide **34** in 46% yield over twelve steps (Scheme 4). Azide **34** was easily converted to amino azide **36** via a two-step sequence, but conversion of azide **34** to amino azide **37** was more complex and required additional transformations [56].

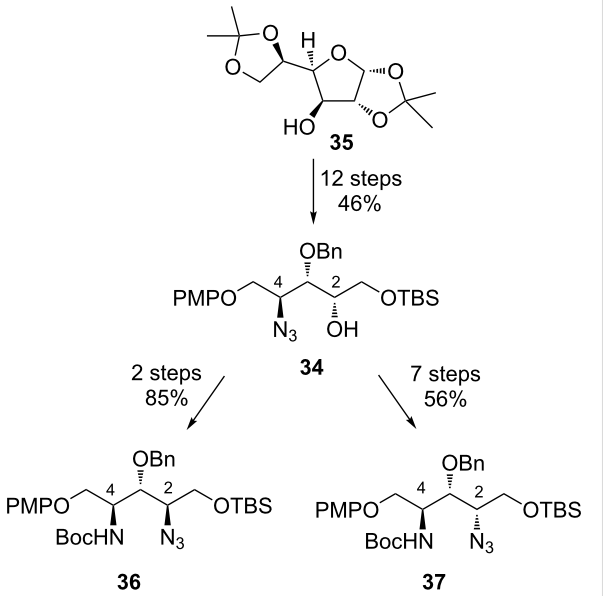

Scheme 4: Synthesis of the C-2 azido diastereomers **36** and **37**.

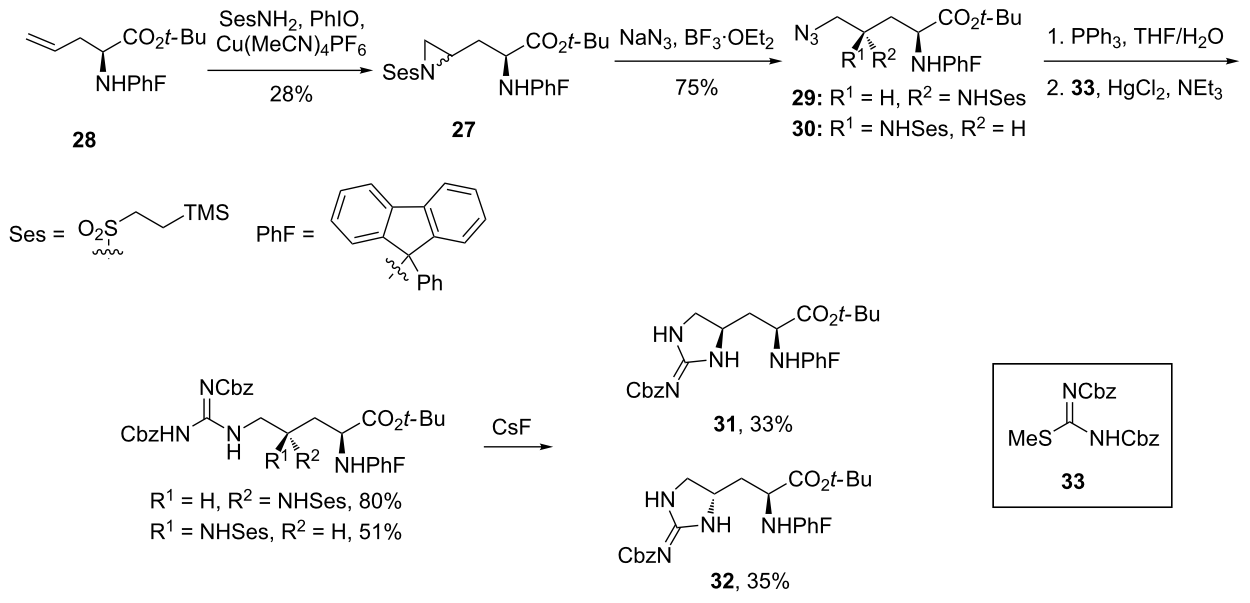

Scheme 3: Synthesis of protected enduracididine diastereomers **31** and **32**.

Conversion of both amino azides **36** and **37** to azido acids **38** and **39** began with protecting group manipulation and installation of the guanidine using *S*-methylisothiourea **33** (Scheme 5). Mitsunobu cyclisation followed by deprotection and oxidation afforded the azido acids **38** and **39** in 40% yield over 8 steps from amino azides **36** and **37**.

Synthesis of β-hydroxyenduracididine by Nieuwenhze et al.: In 2010, Nieuwenhze and Oliver reported a synthesis of protected β-hydroxyenduracididines **40** and **41** making use of intermediate nosylamine **42** (Scheme 6) [57]. The synthesis of **42** began with alkene **43**, available from (*S*)-Garner's aldehyde. Cleavage of the protecting group allowed installation of the guanidine group using isothiourea **33** before cyclisation was effected using Mitsunobu conditions. After a six-step conversion of alkene **44** to nosyl intermediate **42**, the synthesis diverged to access both C-2 diastereomers. Displacement of nosylate **42** with sodium azide followed by reduction and amine protection, afforded protected β-hydroxyenduracididine **40**. Alternatively, formation of epoxide **45** provided access to diastereomer **41**.

Synthesis of β-hydroxyenduracididine by Oberthür et al.: In 2014, Oberthür et al. reported a second generation synthesis of β-hydroxyenduracididine using a more concise route to orthogonally protected amino acids **46** and **47** (Scheme 7) [58]. Installation of the C-2 stereocentre again began with Garner's aldehyde **48** and Wittig olefination, followed by Sharpless dihydroxylation to stereoselectively afford diol **49** [59,60]. The C-2 epimer was accessed via Still–Gennari olefination of aldehyde **48** to afford the Z-olefin, which underwent dihydroxylation using potassium osmate to afford diol **50** [61,62]. With both diastereomers in hand, conversion to protected amino acids **46** and **47** was effected in four steps.

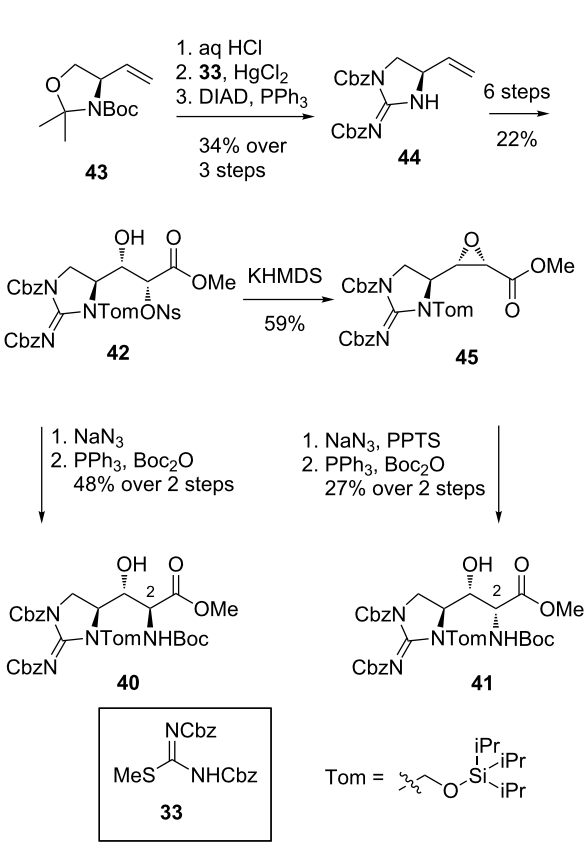

Scheme 6: Synthesis of protected β-hydroxyenduracididine derivatives **40** and **41**.

With amino acids **46** and **47** in hand, conversion to the corresponding cyclic guanidines **51** and **52** was initiated through cleavage of the *N*,*O*-acetonide and guanylation using isothiourea **33** activated with $HgCl_2$ (Scheme 8). Cyclisation of the guanidine afforded protected β-hydroxyenduracididine **51** in

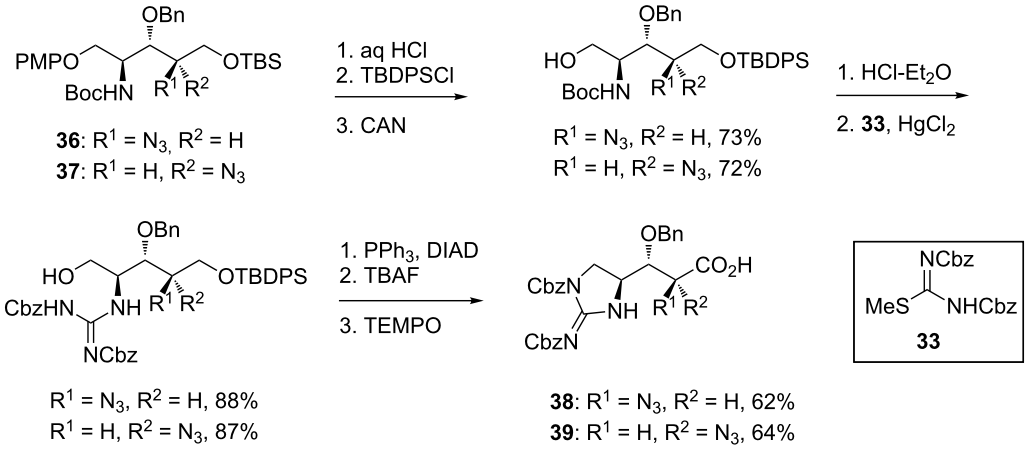

Scheme 5: Synthesis of 2-azido-β-hydroxyenduracididine derivatives **38** and **39**.

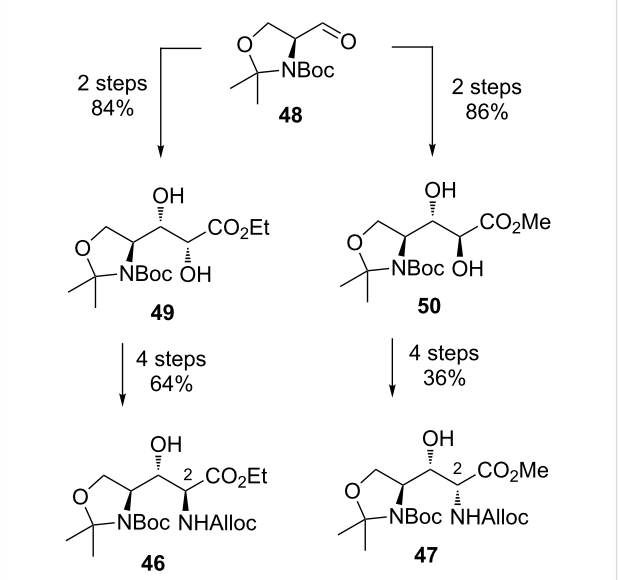

Scheme 7: Synthesis of C-2 diastereomeric amino acids **46** and **47**.

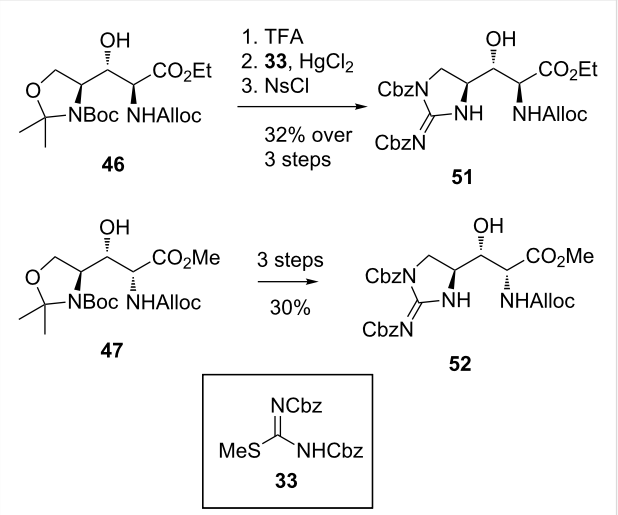

Scheme 8: Synthesis of protected β-hydroxyenduracididines **51** and **52**.

21% yield in seven steps from diol **49**. The C-2 epimer **47** was converted to β-hydroxyenduracididine **52** using the same procedure. The new route proved more efficient than the previous report and provided access to both diastereomers suitably armed with orthogonal protecting groups.

Synthesis of (±)-enduracididine and (±)-allo-enduracididine by Du Bois et al.: The synthesis of (±)-enduracididine (**1**) and (±)-allo-enduracididine (**3**) reported by Du Bois et al. arose from the methodology for the conversion of alkenes to diamines via a cyclic sulfonamide intermediate using rhodium catalysis (Scheme 9) [63]. The reaction proceeds with formation of an intermediate aziridine **53** which rearranges upon addition of sodium iodide to afford the desired cyclic sulfonamide **54**.

For the synthesis of (±)-enduracididine (**1**) and (±)-allo-enduracididine (**3**), protected (±)-allylglycine **55** was treated with $BocNHS(O)_2NH_2$, MgO, $Rh_2(esp)_2$ and $PhI(OAc)_2$ in isopropyl acetate followed by sodium iodide to afford cyclic sulfonamide **56** in 56% yield as a 1:1 mixture of diastereomers (Scheme 10). Selective deprotection of the sulfonamide Boc group allowed separation of diastereomers **57** and **58** via chromatography which were then converted to Tces (2,2,2-trichloroethoxysulfonyl) protected guanidines **59** and **60**. Global deprotection then afforded both (±)-enduracididine (**1**) and (±)-allo-enduracididine (**3**) in five steps and 6% yield from allylglycine **55**.

Synthesis of L-allo-enduracididine by Ling et al.: In 2014, Ling et al. filed a patent for their discovery of teixobactin (**17**) which included details of the structural elucidation. To confirm the configuration of the amino acids that are found in teixobactin, advanced Marfey's analysis was performed, requiring samples of known absolute stereochemistry for comparison (Scheme 11) [64]. The synthesis of L-allo-enduracididine (**3**) was reported to begin with nitro alcohol **61** and afforded the free amino acid in four steps via key intermediate 4-hydroxyarginine **62**. The synthesis of nitro alcohol **61** was not described but its preparation has been reported [65]. All four diastereomers were synthesised for comparison with the isolated enduracididine sample.

Synthesis of L-allo-enduracididine by Yuan et al.: In 2015, Yuan et al. reported their synthesis of protected L-allo-enduracididine **63** from L-4-hydroxyproline **64** (Scheme 12)

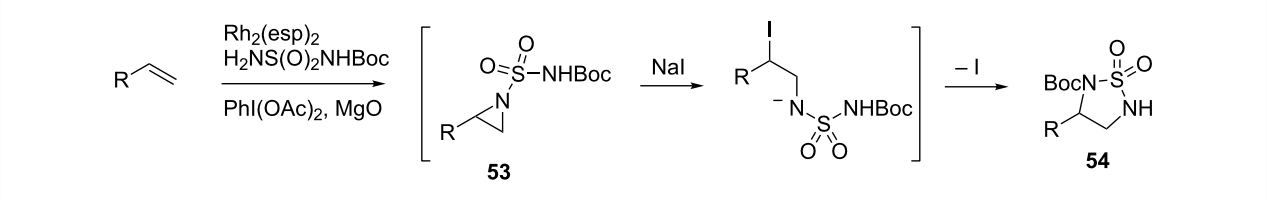

Scheme 9: General transformation of alkenes to cyclic sulfonamide **54** via aziridine intermediate **53**.

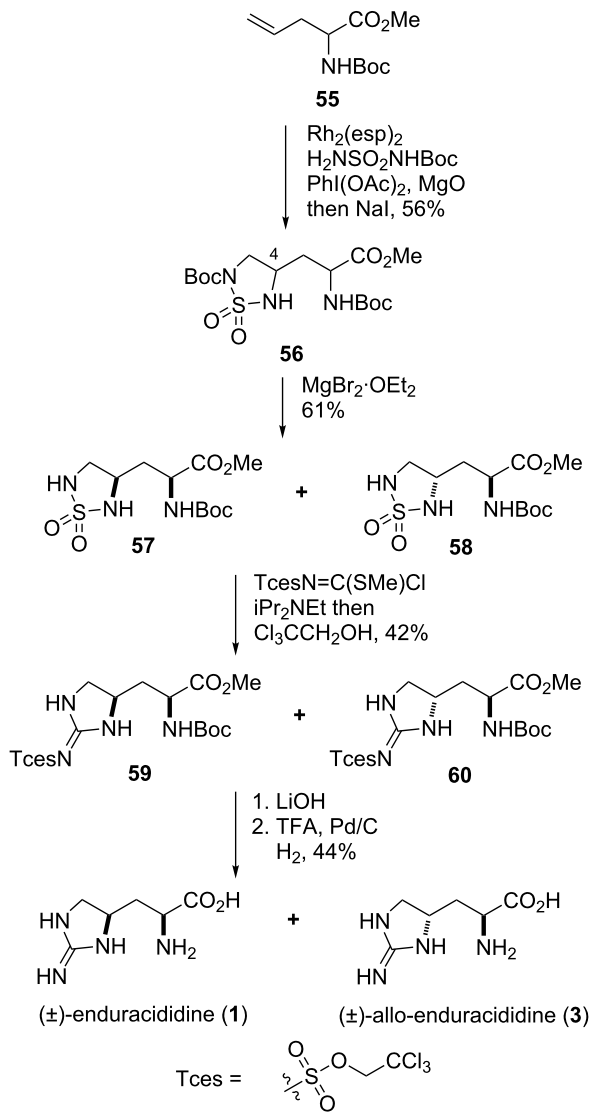

Scheme 10: Synthesis of (±)-enduracididine (**1**) and (±)-allo-enduracididine (**3**).

[66]. The C-4 stereocentre was installed through inversion of the hydroxy group of proline derivative **64** via mesylation and azide displacement to afford **65**. Oxidation installed the required carbonyl group which allowed reductive ring opening to afford alcohol **66**. Azide reduction, installation of the guanidine motif using Goodman's reagent (**67**) [67] and cyclisation afforded **68**. Protecting group manipulation then afforded protected L-allo-enduracididine **63** with a free acid moiety available for peptide coupling over nine steps in 32% overall yield.

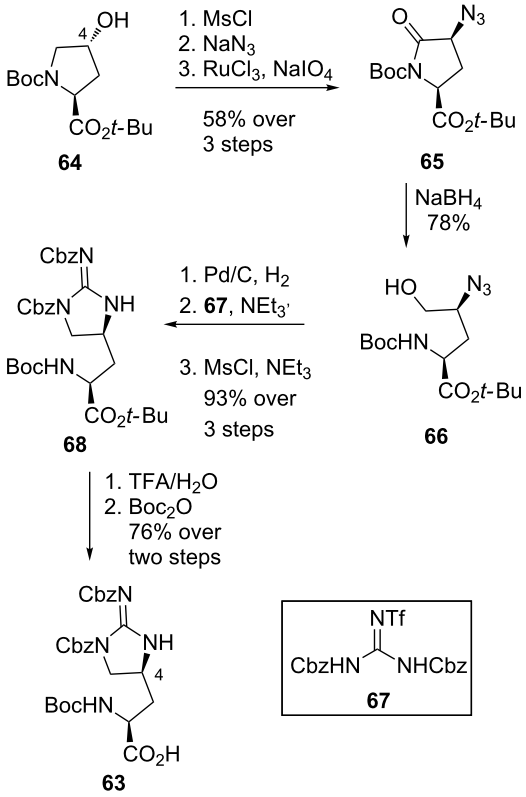

Scheme 12: Synthesis of protected L-allo-enduracididine **63**.

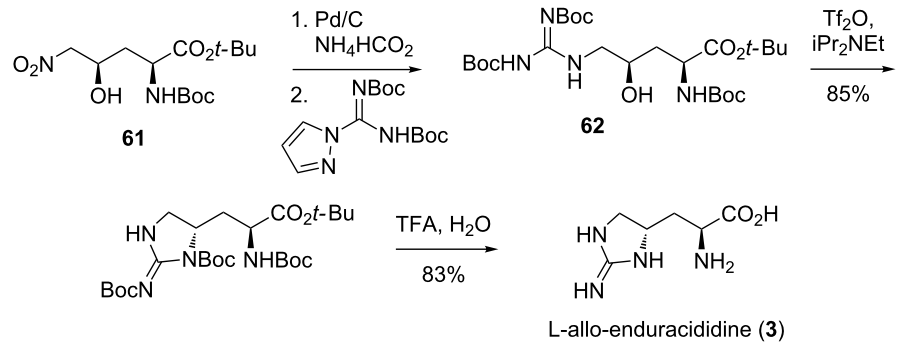

Scheme 11: Synthesis of L-allo-enduracididine (**3**).

Synthesis of a β-hydroxyenduracididine derivative by Cheng et al.: In 2016, Cheng et al. reported work towards the *N*-mannosyl-D-β-hydroxyenduracididine (**69**) residue of the mannopeptimycins (Scheme 13) [68]. Their synthetic strategy started from silylated serinol **70** to which the mannosyl unit was attached to afford glycosylamine **71**, prior to construction of the cyclic guanidine motif and amino acid functionality. With glycosylamine **71** in hand, attention turned to installation of the guanidine moiety. Treatment of **71** with isothiourea **33** followed by mesyl chloride afforded cyclic guanidine **72** in 70% yield. Silyl deprotection, Swern oxidation and Still–Gennari olefination afforded *Z*-alkene **73**. Diastereoselective dihydroxylation of **73** followed by treatment with 1,1'-thiocarbonyldiimidazole (TCDI) and sodium azide afforded azide **69** over eight steps in 5.5% from silylated serinol **70**. The reported route was the most efficient of the many investigated however, the exact sequence of functional group installation was important in order to obtain high yields.

Synthesis of enduracididine-containing antibiotics

Synthesis of Minosaminomycin by Kondo et al.: The only total synthesis of minosaminomycin (**9**) to date was reported in 1977 by Kondo et al. (Scheme 14) [69]. Enduracididine (**1**) was prepared using the method reported by Shiba et al. [54] and was coupled with the isocyanate formed in situ from protected leucine **74** affording urea **75**. Coupling of **75** with amino sugar **76** and global deprotection afforded minosaminomycin (**9**) in three steps from enduracididine (**1**). It should be noted that the diastereomer (2*R*-isomer) of **9** was also synthesised starting from D-enduracididine. Biological testing of both compounds revealed that the 2*R*-isomer exhibited 80% lower bacteriostatic activity against *Mycobacterium smegmatis* ATCC 607 compared to the parent natural product.

Synthesis of Mannopeptimycin aglycone by Doi et al.: In 2014, the total synthesis of the mannopeptimycin aglycone (**77**) was reported by Doi et al. [33]. The aglycone was synthetically broken down into tripeptides **78** and **79** (Scheme 15). Tripeptide **78** was further disconnected into protected serine **80** and protected β-hydroxyenduracididine residues **81** and **82**.

The synthesis of key amino acids **81** and **82** was based on an aldol reaction between protected aldehyde **83** and glycine **84** (Scheme 16). The reaction yielded **85** and **86** which proved to be easily separated by chromatography. The C-3 stereochemistry of the addition products **85** and **86** was rationalised by the Felkin–Ahn model, and the inability of diastereomer **85** to cyclise due to unfavourable steric interactions. Conversion of aldol products **85** and **86** to acetals **87** and **88**, respectively, was achieved using standard transformations and Goodman's reagent (**67**) [67] was used to install the guanidine moiety.

With both protected amino acids **87** and **88** in hand, the attention turned to the formation of tripeptide **78** (Scheme 17). Saponification of the ester of **88** and coupling with H-Ser(Bn)-*O*-Allyl and treatment with HCl afforded dipeptide **89**. A second peptide coupling with acid **90** then gave tripeptide **78**. With tripeptide **78** in hand, ligation with the remaining tripeptide **71** followed by cyclisation and global deprotection afforded the desired mannopeptimycin aglycone (**77**) in a further six steps and 38% yield from tripeptide **78**.

Total synthesis of mannopeptimycins α and β by Chen et al.: Chen et al. reported the first total synthesis of mannopeptimycins α (**12**) and β (**13**) in 2016 [70]. Previous biosynthetic and semisynthetic investigations had revealed that the *N*- and *O*-sugars of the natural products were essential for potent anti-

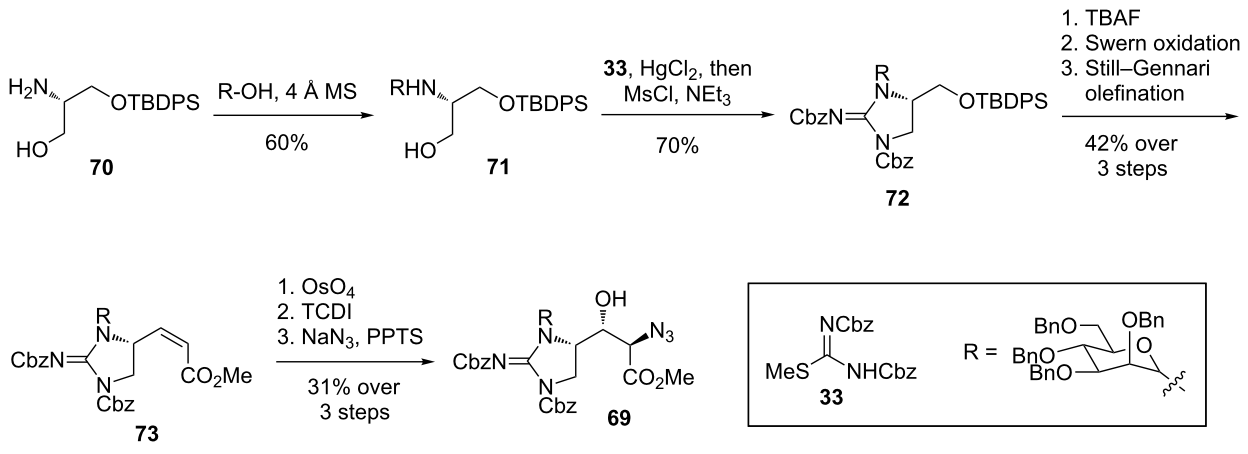

Scheme 13: Synthesis of β-hydroxyenduracididine derivative **69**.

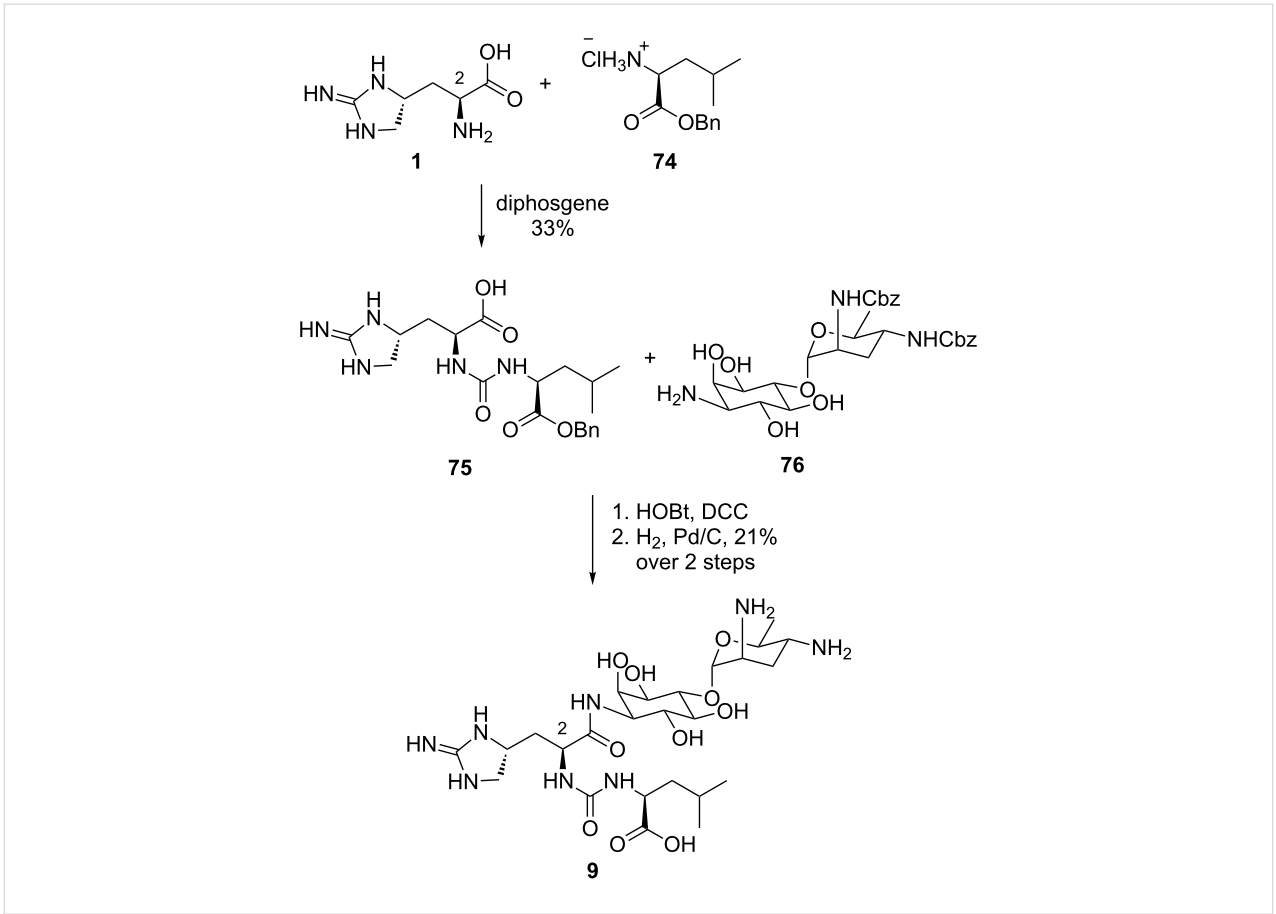

Scheme 14: Synthesis of minosaminomycin (**9**).

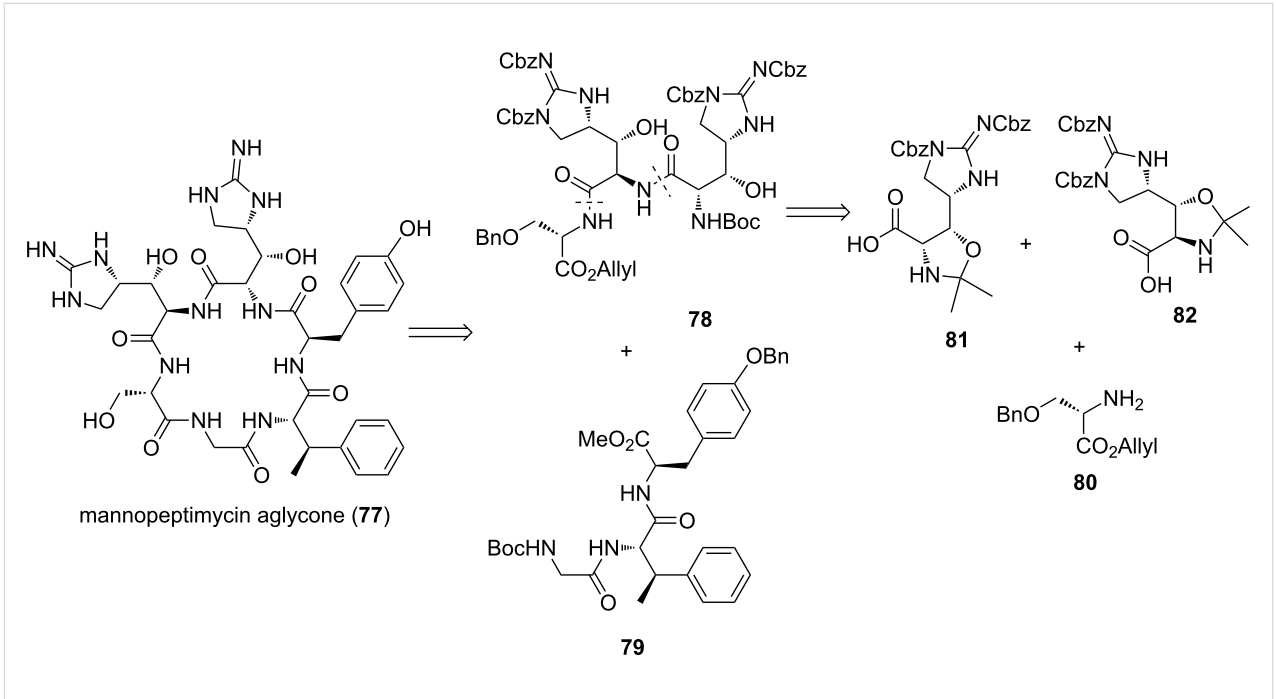

Scheme 15: Retrosynthetic analysis of mannopeptimycin aglycone (**77**).

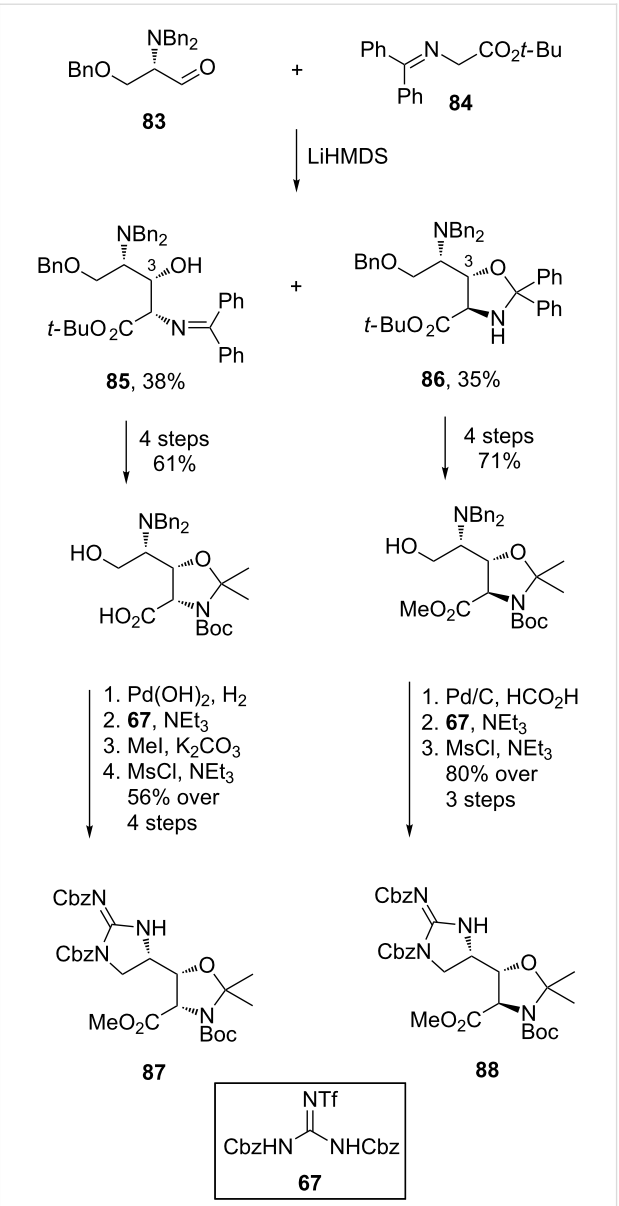

Scheme 16: Synthesis of protected amino acids **87** and **88**.

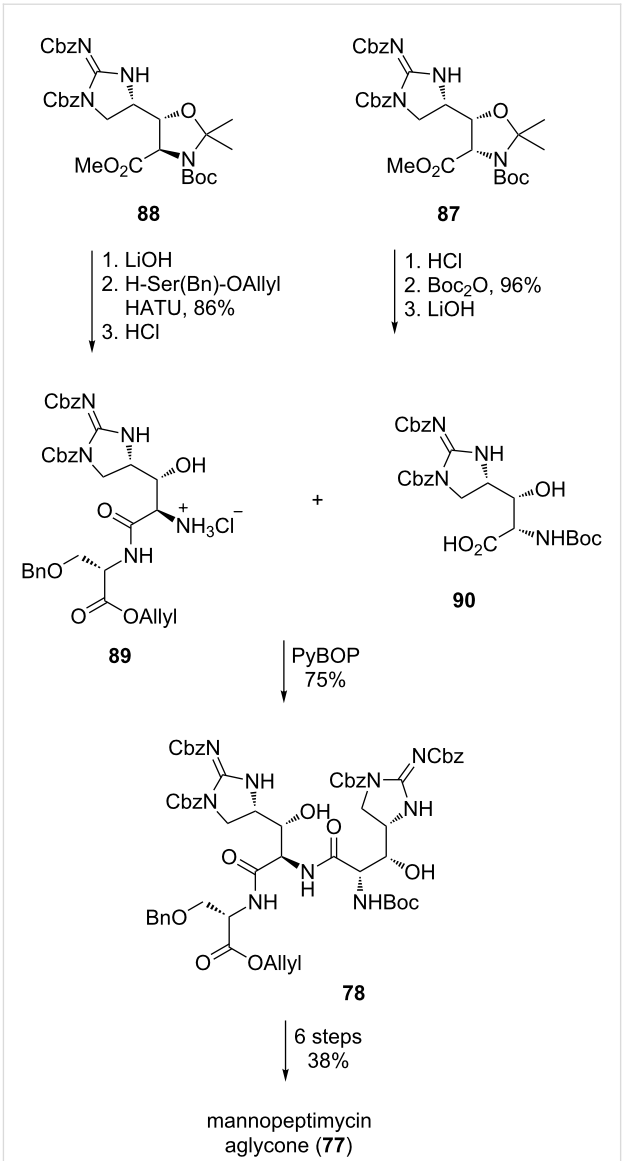

Scheme 17: Synthesis of mannopeptimycin aglycone (**77**).

bacterial activity [35,38,39,41]. The most difficult challenge involved the preparation of the *N*-α-mannosyl-D-β-hydroxyenduracididine unit. *N*-Mannosylation was complicated by steric hindrance around the reaction site and poor compatibility of the cyclic guanidine motif with Lewis acids.

Initial attempts to glycosylate cyclic guanidine **91** using an array of donors under Lewis acidic or basic conditions failed to provide access to *N*-mannosylguanidine **92** (Scheme 18). However, gold(I) mediated [71] *N*-mannosylation using *ortho*-alkynyl benzoate **93** finally afforded *N*-mannosylated **92** in 87% yield [70]. Application of these conditions to afford the fully functionalised amino acid **94** was unsuccessful. However, encouraged by the successful *N*-mannosylation of azide **95** to afford adduct **96**, Chen et al. utilised the synthesis reported by Doi et al. [33] to prepare *N*,*O*-acetonide **88**. *N*-Mannosylation of acetonide **88** was successful and afforded the desired product in 86% yield (Scheme 19). Saponification then provided the desired benzyl protected mannosyl D-β-hydroxyenduracididine **97**.

Attempts to utilise the same procedure reported by Doi et al. [33] to provide the amino acid L-β-hydroxyenduracididine **98** were unsuccessful. An alternative route to L-β-hydroxyenduracididine based on the synthesis reported by Oberthür et al. [58] afforded L-β-hydroxyenduracididine **98** in 7% yield over twelve steps from **99** (Scheme 20).

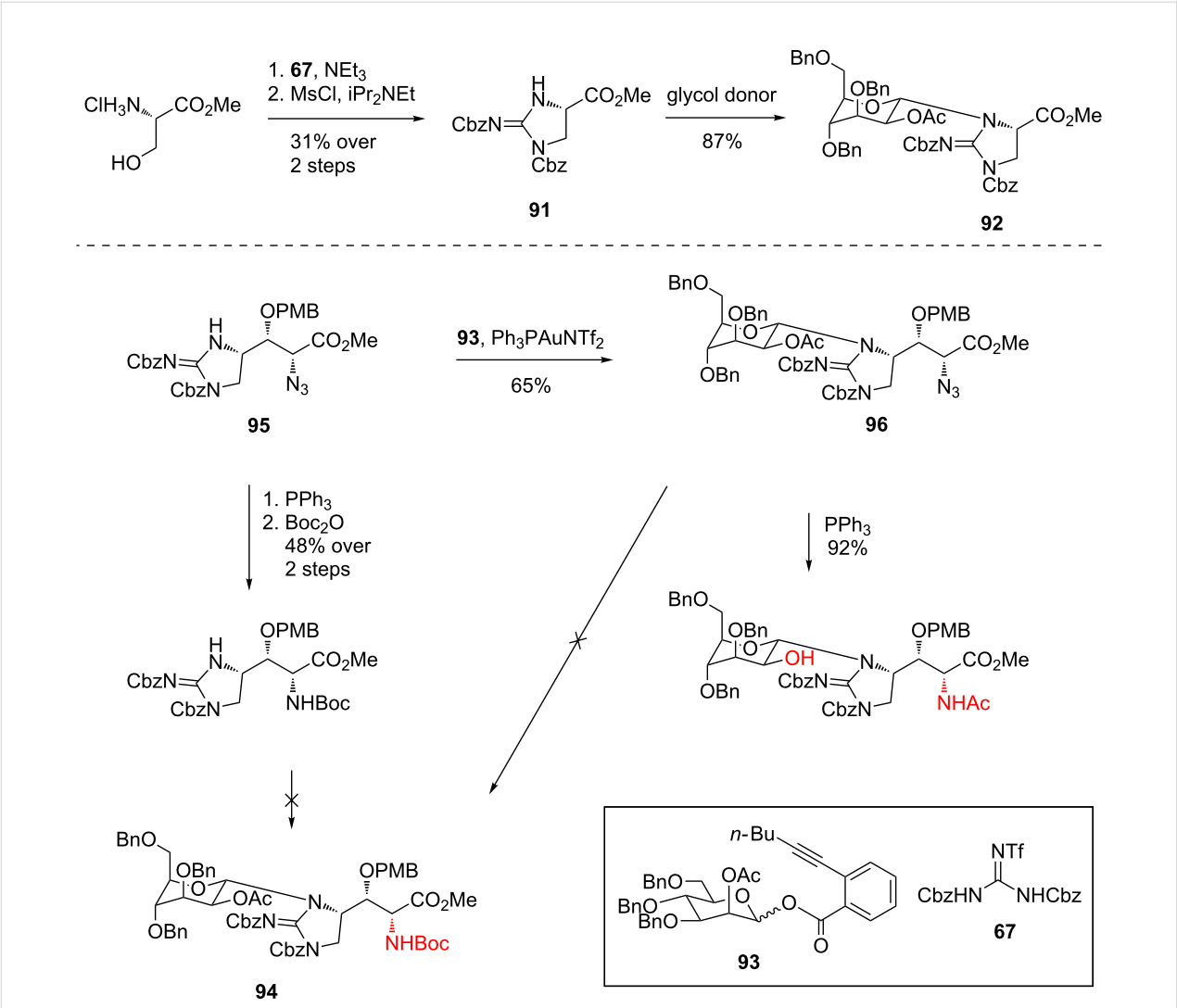

Scheme 18: Synthesis of *N*-mannosylation model guanidine **92** and attempted synthesis of benzyl protected mannosyl D-β-hydroxyenduracididine **94**.

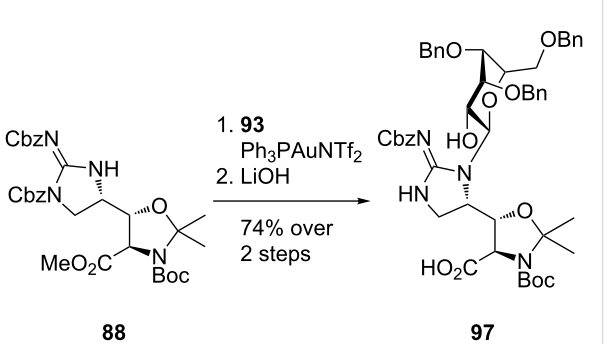

Scheme 19: Synthesis of benzyl protected mannosyl D-β-hydroxyenduracididine **97**.

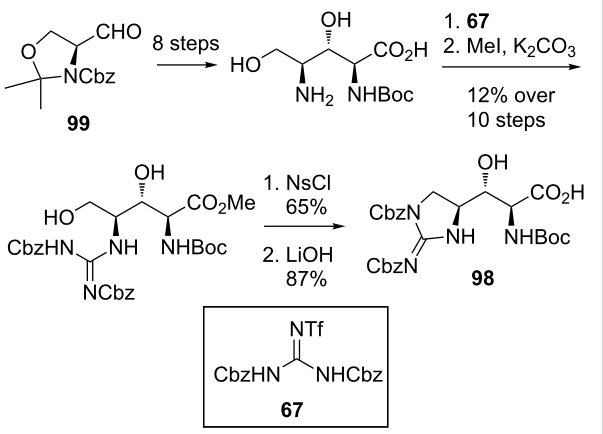

Scheme 20: Synthesis of L-β-hydroxyenduracididine **98**.

In the final stages of the synthesis (Scheme 21), benzyl protected mannosyl D-β-hydroxyenduracididine **97** was coupled with H-Ser(Bn)-*O*Allyl to afford dipeptide **100**. Unmasking of the amino and alcohol functionalities and peptide coupling with L-β-hydroxyenduracididine **98** afforded tripeptide **101** with no loss of the sugar group. This then completed the synthesis of the key fragment **101** and both mannopeptimycin α (**12**) and β (**13**) could be accessed in a further six steps.

Synthesis of teixobactin by Payne et al.: The first syntheses of the teixobactin framework were completed by Albericio et al. [46] and Singh et al. [47]. These syntheses substituted the enduracididine residue for the more readily available L-arginine. The total synthesis of the full teixobactin structure was completed in 2016 by Payne et al. [72] using Fmoc solid-phase peptide synthesis (SPPS). The key to the synthesis was access to the protected L-allo-enduracididine residue **102** (Scheme 22). The synthesis of this building block was achieved using a combination of reported procedures beginning with protected aspartic acid **103**. Using a protocol reported by Rudolph et al. [65] nitro alcohol **61** was accessed in two steps. Following procedures described in the patent filed by Ling et al. [64], alcohol **61** was converted to Boc-protected L-allo-enduracididine **68**. Protecting group exchange afforded the Fmoc protected L-allo-enduracididine **102** in seven steps and 17% yield from acid **103**.

The synthesis of the natural teixobactin (**17**) product began with Fmoc-D-Thr(TES)-OH on HMPB-NovaPEG resin. Successive couplings afforded peptide **104** (Scheme 23). Esterification with Alloc-Ile-OH and extension of the linear chain using conventional Fmoc SPPS afforded ester-peptide **105**. Deprotection of the *N*-alloc group and coupling of the key L-allo-enduracididine **102** residue proceeded smoothly giving resin bound peptide **106**. Brief (30 seconds) treatment of **106** with piperidine afforded the desired deprotected product, enabling coupling of the final amino acid. Extended exposure of

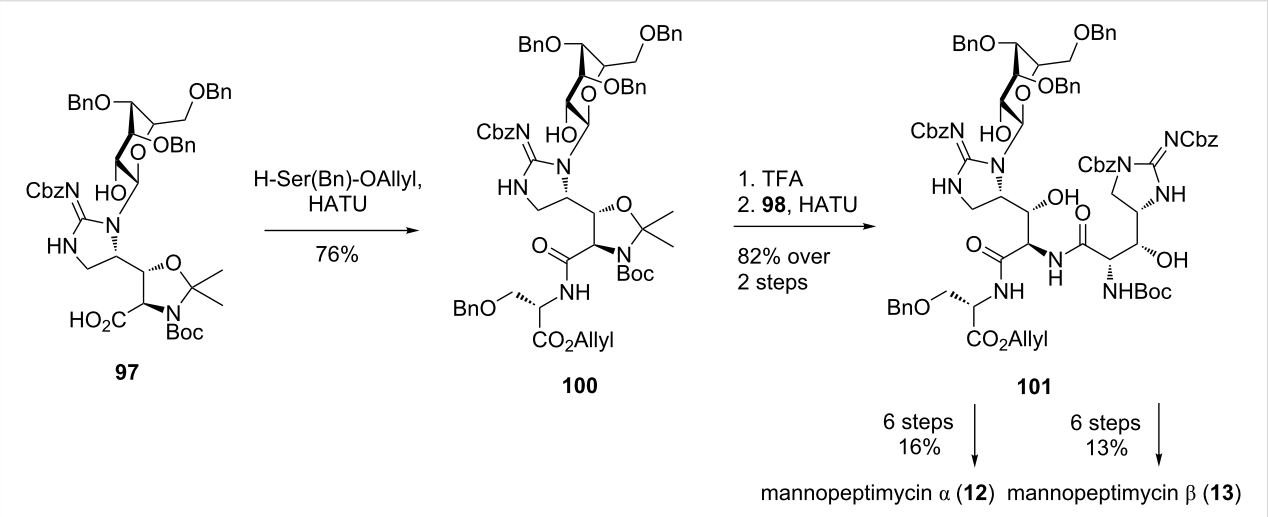

Scheme 21: Total synthesis of mannopeptimycin α (**12**) and β (**13**).

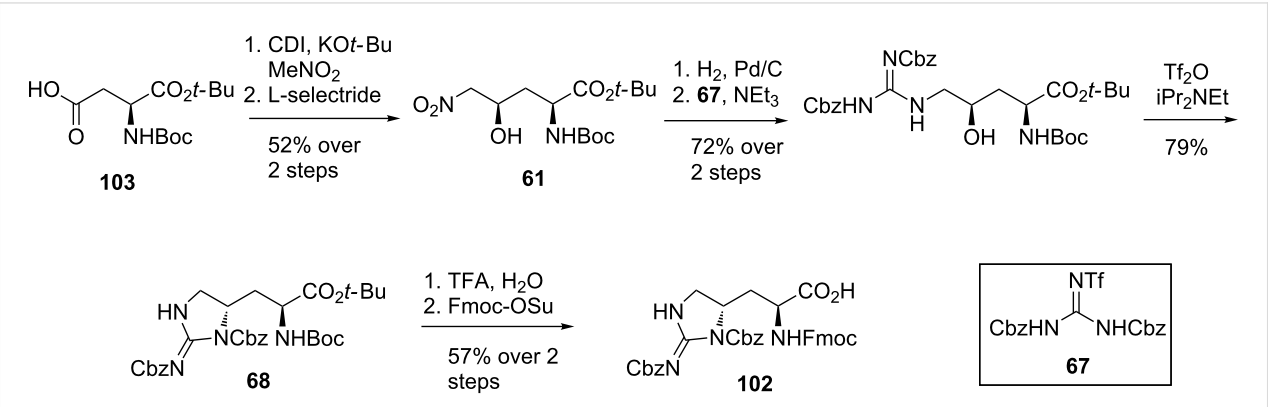

Scheme 22: Synthesis of protected L-allo-enduracididine **102**.

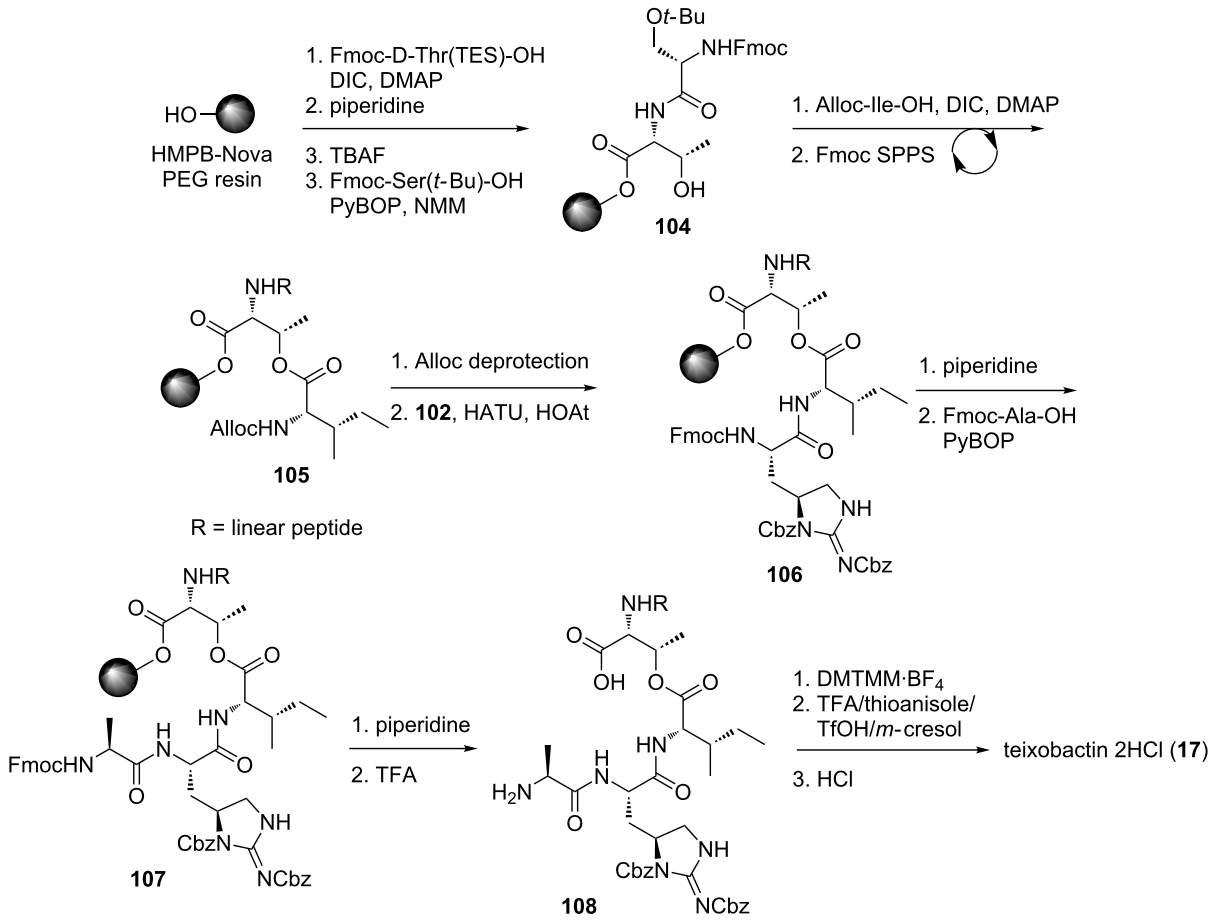

Scheme 23: The solid phase synthesis of teixobactin (**17**).

peptide **106** to piperidine led to de-esterification. Final Fmoc removal of **107** and cleavage from the resin afforded linear peptide **108** which underwent macrolactamisation using 4-(4,6-dimethoxy-1,3,5-triazin-2-yl)-4-methylmorpholinium tetrafluoroborate (DMTMM·BF_4) and acid-mediated global deprotection to afford teixobactin (**17**) in 3.3% yield over twenty four steps.

Synthesis of the macrocyclic core of teixobactin by Reddy et al.: In 2016, Reddy et al. reported their synthetic efforts towards teixobactin (**17**) with a solution-phase synthesis of the macrocyclic core **109** (Scheme 24) [73]. Their synthetic approach focused on the macrolactonisation of a linear precursor **110** differing from previous reports which employed macrolactamisation as the key ring-closing step [45-47,72].

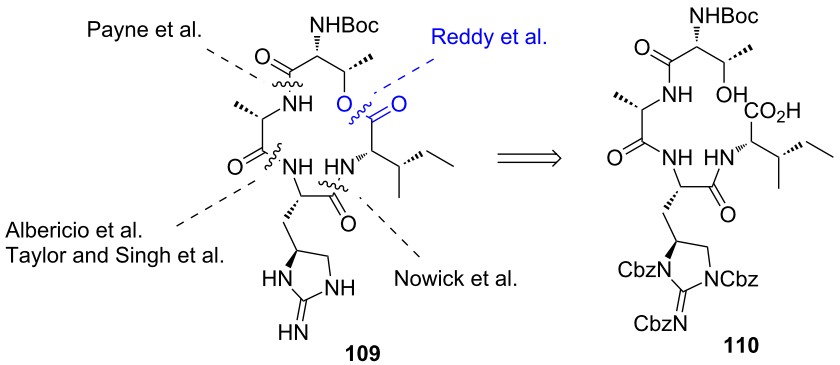

Scheme 24: Retrosynthesis of the macrocyclic core **109** of teixobactin (**17**).

The synthesis of the linear precursor **110** began with protected L-allo-enduracididine **68**, which was prepared using procedures developed by Rudolph et al. and Peoples et al. (Scheme 25) [64,65]. The remaining NH of **68** was protected using Cbz-Cl before acid **111** was afforded after a two-step, deprotection-reprotection sequence. Fully protected enduracididine **111** was then coupled with L-isoleucine methyl ester **112** to give dipeptide **113**. Cleavage of the *N*-Boc group and coupling with dipeptide **114** afforded protected linear precursor **115**. Cleavage of the TBS and methyl ester protecting groups afforded seco-acid **116**. However, during the hydrolysis step, two of the three Cbz groups were cleaved from the enduracididine residue, and the position of the remaining Cbz and CO_2H could not be determined. It was decided that final deprotection of the remaining enduracididine protecting groups would take place after formation of the macrocycle. Treatment of linear precursor **116** with modified Shiina macrolactonisation conditions reported by Batey et al. [74] of 2-methyl-6-nitrobenzoic anhydride (MNBA), DMAP and $Dy(OTf)_3$ afforded macrocycle **117** in 30–35% yield. Unfortunately efforts to remove both the Cbz and CO_2H moieties of **117** to afford macrocycle **109** under hydrogenation conditions were unsuccessful.

Conclusion

The recent interest in teixobactin has resulted from its clinically unexploited mode of action, potent activity against resistant strains of bacteria and favourable pharmacokinetics. Structure–activity relationship studies of teixobactin suggest that the rare non-proteinogenic amino acid enduracididine, is a key residue for potent antibacterial activity. This observation has driven the need for new synthetic routes to enduracididine. However, current syntheses are cumbersome and inefficient. A robust and scalable synthetic route to an orthogonally protected enduracididine derivative suitable for solid phase peptide synthesis would greatly facilitate antibiotic drug development focused on a teixobactin inspired lead structure. Efficient access

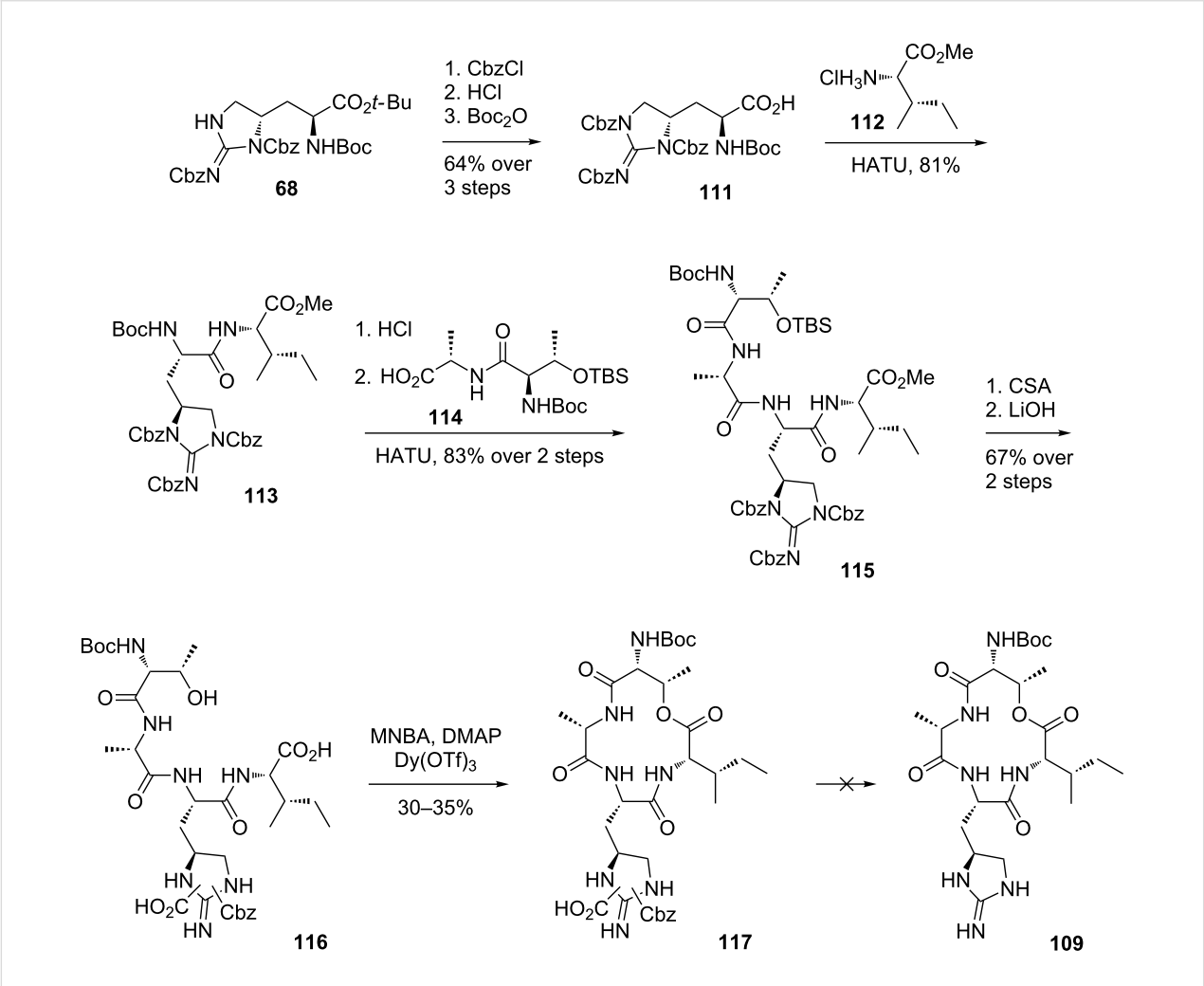

Scheme 25: Synthesis of macrocycle **117**.

to enduracididine will enable ongoing structure–activity relationship studies of teixobactin and other lead compounds, for the development of much needed antibiotic drug candidates.

Acknowledgements

The authors would like to thank the University of Auckland, the Maurice Wilkins Centre for Molecular Biodiscovery and the Roskill Freemasons Trust for financial support of this work.

References

1. Horii, S.; Kameda, Y. *J. Antibiot.* **1968,** *21,* 665–667. doi:10.7164/antibiotics.21.665
2. Higashide, E.; Hatano, K.; Shibata, M.; Nakazawa, K. *J. Antibiot.* **1968,** *21,* 126–137. doi:10.7164/antibiotics.21.126
3. Fellows, L. E.; Hider, R. C.; Bell, E. A. *Phytochemistry* **1977,** *16,* 1957–1959. doi:10.1016/0031-9422(77)80104-0
4. Evans, S. V.; Fellows, L. E.; Bell, E. A. *Biochem. Syst. Ecol.* **1985,** *13,* 271–302. doi:10.1016/0305-1978(85)90038-9
5. Wilson, M. F.; Bell, E. A. *Phytochemistry* **1979,** *18,* 1883–1884. doi:10.1016/0031-9422(79)83079-4
6. Cook, N. D.; Evans, S. V.; Fellows, L. E.; Peters, T. J. *Biochem. Soc. Trans.* **1986,** *14,* 1053–1054. doi:10.1042/bst0141053
7. He, H.; Williamson, R. T.; Shen, B.; Graziani, E. I.; Yang, H. Y.; Sakya, S. M.; Petersen, P. J.; Carter, G. T. *J. Am. Chem. Soc.* **2002,** *124,* 9729–9736. doi:10.1021/ja020257s
8. Asai, M.; Muroi, M.; Sugita, N.; Kawashima, H.; Mizuno, K.; Miyake, A. *J. Antibiot.* **1968,** *21,* 138–146. doi:10.7164/antibiotics.21.138
9. Tsuchiya, K.; Kondo, M.; Oishi, T.; Yamazaki, I. *J. Antibiot.* **1968,** *21,* 147–153. doi:10.7164/antibiotics.21.147
10. Tanayama, S.; Fugono, T.; Yamazaki, T. *J. Antibiot.* **1968,** *21,* 313–319. doi:10.7164/antibiotics.21.313
11. Hori, M.; Sugita, N.; Miyazaki, M. *Chem. Pharm. Bull.* **1973,** *21,* 1171–1174. doi:10.1248/cpb.21.1171
12. Hori, M.; Iwasaki, H.; Horii, S.; Yoshida, I.; Hongo, T. *Chem. Pharm. Bull.* **1973,** *21,* 1175–1183. doi:10.1248/cpb.21.1175
13. Iwasaki, H.; Horii, S.; Asai, M.; Mizuno, K.; Ueyanagi, J.; Miyake, A. *Chem. Pharm. Bull.* **1973,** *21,* 1184–1191. doi:10.1248/cpb.21.1184
14. Tsuchiya, K.; Takeuchi, Y. *J. Antibiot.* **1968,** *21,* 426–428. doi:10.7164/antibiotics.21.426
15. Kamiya, K.; Nishikawa, M.; Matsumaru, H.; Asai, M.; Mizuno, K. *Chem. Pharm. Bull.* **1968,** *16,* 2303–2304. doi:10.1248/cpb.16.2303
16. Hu, Y.; Yang, W.; Wan, W.; Shen, F.; Lei, Z.; Wang, D. *Appl. Biochem. Biotechnol.* **2012,** *166,* 830–838. doi:10.1007/s12010-011-9473-y
17. Li, X.-G.; Tang, X.-M.; Xiao, J.; Ma, G.-H.; Xu, L.; Xie, S.-J.; Xu, M.-J.; Xiao, X.; Xu, J. *Mar. Drugs* **2013,** *11,* 3875–3890. doi:10.3390/md11103875
18. Yin, X.; Chen, Y.; Zhang, L.; Wang, Y.; Zabriskie, T. M. *J. Nat. Prod.* **2010,** *73,* 583–589. doi:10.1021/np900710q
19. Castiglione, F.; Marazzi, A.; Meli, M.; Colombo, G. *Magn. Reson. Chem.* **2005,** *43,* 603–610. doi:10.1002/mrc.1606
20. Kawakami, M.; Nagai, Y.; Fujii, T.; Mitsuhashi, S. *J. Antibiot.* **1971,** *24,* 583–586. doi:10.7164/antibiotics.24.583
21. Hammes, W. P.; Winter, J.; Kandler, O. *Arch. Microbiol.* **1979,** *123,* 275–279. doi:10.1007/BF00406661
22. Matsuhashi, M.; Ohara, I.; Yoshiyama, Y. *Agric. Biol. Chem.* **1969,** *33,* 134–137. doi:10.1080/00021369.1969.10859291
23. Fang, X.; Tiyanont, K.; Zhang, Y.; Wanner, J.; Boger, D.; Walker, S. *Mol. BioSyst.* **2006,** *2,* 69–76. doi:10.1039/B515328J
24. Lugtenberg, E. J.; Schijndel-van Dam, A.; van Bellegem, T. H. *J. Bacteriol.* **1971,** *108,* 20–29.
25. Inouye, Y.; Take, Y.; Nakamura, S.; Nakashima, H.; Yamamoto, N.; Kawaguchi, H. *J. Antibiot.* **1987,** *40,* 100–104. doi:10.7164/antibiotics.40.100
26. Zhu, H. Disease-resistant formula feed for Tibetan pig. Japanese Patent AN2016-73355, Jan 13, 2016.
27. Chen, L. A broiler health care feed additive and its preparation method. Japanese Patent AN2016-310229, Feb 24, 2016.
28. Hamada, M.; Kondo, S.; Yokoyama, T.; Miura, K.; Iinuma, K.; Yamamoto, H.; Maeda, K.; Takeuchi, T.; Umezawa, H. *J. Antibiot.* **1974,** *27,* 81–83. doi:10.7164/antibiotics.27.81
29. Iinuma, K.; Kondo, S.; Maeda, K.; Umezawa, H. *J. Antibiot.* **1975,** *28,* 613–615. doi:10.7164/antibiotics.28.613
30. Olesker, A.; Mercier, D.; Gero, S. D.; Pearce, C. J.; Barnett, J. E. G. *J. Antibiot.* **1975,** *28,* 490–491. doi:10.7164/antibiotics.28.490
31. Suzukake, K.; Hori, M.; Uehara, Y.; IInuma, K.; Hamada, M.; Umezawa, H. *J. Antibiot.* **1977,** *30,* 132–140. doi:10.7164/antibiotics.30.132
32. García, A.; Vázquez, M. J.; Quiñoá, E.; Riguera, R.; Debitus, C. *J. Nat. Prod.* **1996,** *59,* 782–785. doi:10.1021/np9603535
33. Fuse, S.; Koinuma, H.; Kimbara, A.; Izumikawa, M.; Mifune, Y.; He, H.; Shin-ya, K.; Takahashi, T.; Doi, T. *J. Am. Chem. Soc.* **2014,** *136,* 12011–12017. doi:10.1021/ja505105t
34. Singh, M. P.; Petersen, P. J.; Weiss, W. J.; Janso, J. E.; Luckman, S. W.; Lenoy, E. B.; Bradford, P. A.; Testa, R. T.; Greenstein, M. *Antimicrob. Agents Chemother.* **2003,** *47,* 62–69. doi:10.1128/AAC.47.1.62-69.2003
35. Sum, P.-E.; How, D.; Torres, N.; Petersen, P. J.; Lenoy, E. B.; Weiss, W. J.; Mansour, T. S. *Bioorg. Med. Chem. Lett.* **2003,** *13,* 1151–1155. doi:10.1016/S0960-894X(03)00045-3
36. Sum, P.-E.; How, D.; Torres, N.; Petersen, P. J.; Ashcroft, J.; Graziani, E. I.; Koehn, F. E.; Mansour, T. S. *Bioorg. Med. Chem. Lett.* **2003,** *13,* 2805–2808. doi:10.1016/S0960-894X(03)00542-0
37. He, H.; Wang, T.-Z.; Dushin, R. G.; Feng, X.; Shen, B.; Ashcroft, J. S.; Kohn, F. E.; Carter, G. T. *Tetrahedron Lett.* **2004,** *45,* 5889–5893. doi:10.1016/j.tetlet.2004.05.155
38. Dushin, R. G.; Wang, T.-Z.; Sum, P.-E.; He, H.; Sutherland, A. G.; Ashcroft, J. S.; Graziani, E. I.; Koehn, F. E.; Bradford, P. A.; Petersen, P. J.; Wheless, K. L.; How, D.; Torres, N.; Lenoy, E. B.; Weiss, W. J.; Lang, S. A.; Projan, S. J.; Shlaes, D. M.; Mansour, T. S. *J. Med. Chem.* **2004,** *47,* 3487–3490. doi:10.1021/jm049765y
39. Petersen, P. J.; Wang, T. Z.; Dushin, R. G.; Bradford, P. A. *Antimicrob. Agents Chemother.* **2004,** *48,* 739–746. doi:10.1128/AAC.48.3.739-746.2004
40. Sum, P.-E.; How, D.; Torres, N.; Newman, H.; Petersen, P. J.; Mansour, T. S. *Bioorg. Med. Chem. Lett.* **2003,** *13,* 2607–2610. doi:10.1016/S0960-894X(03)00512-2
41. He, H.; Shen, B.; Petersen, P. J.; Weiss, W. J.; Yang, H. Y.; Wang, T.-Z.; Dushin, R. G.; Koehn, F. E.; Carter, G. T. *Bioorg. Med. Chem. Lett.* **2004,** *14,* 279–282. doi:10.1016/j.bmcl.2003.09.071
42. He, H. *Appl. Microbiol. Biotechnol.* **2005,** *67,* 444–452. doi:10.1007/s00253-004-1884-z

43. Ling, L. L.; Schneider, T.; Peoples, A. J.; Spoering, A. L.; Engels, I.; Conlon, B. P.; Mueller, A.; Schäberle, T. F.; Hughes, D. E.; Epstein, S.; Jones, M.; Lazarides, L.; Steadman, V. A.; Cohen, D. R.; Felix, C. R.; Fetterman, K. A.; Millett, W. P.; Nitti, A. G.; Zullo, A. M.; Chen, C.; Lewis, K. *Nature* **2015,** *517,* 455–459. doi:10.1038/nature14098
44. Oppedijk, S. F.; Martin, N. I.; Breukink, E. *Biochim. Biophys. Acta* **2016,** *1858,* 947–957. doi:10.1016/j.bbamem.2015.10.024
45. Yang, H.; Chen, K. H.; Nowick, J. S. *ACS Chem. Biol.* **2016,** *11,* 1823–1826. doi:10.1021/acschembio.6b00295
46. Jad, Y. E.; Acosta, G. A.; Naicker, T.; Ramtahal, M.; El-Faham, A.; Govender, T.; Kruger, H. G.; de la Torre, B. G.; Albericio, F. *Org. Lett.* **2015,** *17,* 6182–6185. doi:10.1021/acs.orglett.5b03176
47. Parmar, A.; Iyer, A.; Vincent, C. S.; Van Lysebetten, D.; Prior, S. H.; Madder, A.; Taylor, E. J.; Singh, I. *Chem. Commun.* **2016,** *52,* 6060–6063. doi:10.1039/C5CC10249A
48. Hatano, K.; Nogami, I.; Higashide, E.; Kishi, T. *Agric. Biol. Chem.* **1984,** *48,* 1503–1508.
49. Magarvey, N. A.; Haltli, B.; He, M.; Greenstein, M.; Hucul, J. A. *Antimicrob. Agents Chemother.* **2006,** *50,* 2167–2177. doi:10.1128/AAC.01545-05
50. Yin, X.; Zabriskie, T. M. *Microbiology (Reading, U. K.)* **2006,** *152,* 2969–2983. doi:10.1099/mic.0.29043-0
51. Han, L.; Schwabacher, A. W.; Moran, G. R.; Silvaggi, N. R. *Biochemistry* **2015,** *54,* 7029–7040. doi:10.1021/acs.biochem.5b01016
52. Burroughs, A. M.; Hoppe, R. W.; Goebel, N. C.; Sayyed, B. H.; Voegtline, T. J.; Schwabacher, A. W.; Zabriskie, T. M.; Silvaggi, N. R. *Biochemistry* **2013,** *52,* 4492–4506. doi:10.1021/bi400397k
53. Haltli, B.; Tan, Y.; Magarvey, N. A.; Wagenaar, M.; Yin, X.; Greenstein, M.; Hucul, J. A.; Zabriskie, T. M. *Chem. Biol.* **2005,** *12,* 1163–1168. doi:10.1016/j.chembiol.2005.09.013
54. Tsuji, S.; Kusumoto, S.; Shiba, T. *Chem. Lett.* **1975,** *4,* 1281–1284. doi:10.1246/cl.1975.1281
55. Sanière, L.; Leman, L.; Bourguignon, J.-J.; Dauban, P.; Dodd, R. H. *Tetrahedron* **2004,** *60,* 5889–5897. doi:10.1016/j.tet.2004.05.034
56. Schwörer, C. J.; Oberthür, M. *Eur. J. Org. Chem.* **2009,** 6129–6139. doi:10.1002/ejoc.200900971
57. Olivier, K. S.; Van Nieuwenhze, M. S. *Org. Lett.* **2010,** *12,* 1680–1683. doi:10.1021/ol100219a
58. Fischer, S. N.; Schwörer, C. J.; Oberthür, M. *Synthesis* **2014,** *46,* 2234–2240. doi:10.1055/s-0033-1341236
59. Devel, L.; Vidal-Cros, A.; Thellend, A. *Tetrahedron Lett.* **2000,** *41,* 299–301. doi:10.1016/S0040-4039(99)01964-4
60. Ribes, C.; Falomir, E.; Carda, M.; Marco, J. A. *J. Org. Chem.* **2008,** *73,* 7779–7782. doi:10.1021/jo8012989
61. Koskinen, A. M. P.; Chen, J. *Tetrahedron Lett.* **1991,** *32,* 6977–6980. doi:10.1016/0040-4039(91)80459-J
62. Passiniemi, M.; Koskinen, A. M. P. *Synthesis* **2010,** 2816–2822. doi:10.1055/s-0029-1218843
63. Olson, D. E.; Su, J. Y.; Roberts, D. A.; Du Bois, J. *J. Am. Chem. Soc.* **2014,** *136,* 13506–13509. doi:10.1021/ja506532h
64. Peoples, A. J.; Hughes, D.; Ling, L. L.; Millett, W.; Nitti, A.; Spoering, A.; Steadman, V. A.; Chiva, J.-Y. C.; Lazarides, L.; Jones, M. K.; Poullenec, K. G.; Lewis, K.; Epstein, S. Novel Depsipeptide and Uses Thereof. WO Patent WO2014/089053A1, June 12, 2013.
65. Rudolph, J.; Hannig, F.; Theis, H.; Wischnat, R. *Org. Lett.* **2001,** *3,* 3153–3155. doi:10.1021/ol016445p
66. Craig, W.; Chen, J.; Richardson, D.; Thorpe, R.; Yuan, Y. *Org. Lett.* **2015,** *17,* 4620–4623. doi:10.1021/acs.orglett.5b02362
67. Feichtinger, K.; Sings, H. L.; Baker, T. J.; Matthews, K.; Goodman, M. *J. Org. Chem.* **1998,** *63,* 8432–8439. doi:10.1021/jo9814344
68. Lin, C.-K.; Yun, W.-Y.; Lin, L.-T.; Cheng, W.-C. *Org. Biomol. Chem.* **2016,** *14,* 4054–4060. doi:10.1039/C6OB00644B
69. Iinuma, K.; Kondo, S.; Maeda, K.; Umezawa, H. *Bull. Chem. Soc. Jpn.* **1977,** *50,* 1850–1854. doi:10.1246/bcsj.50.1850
70. Wang, B.; Liu, Y.; Jiao, R.; Feng, Y.; Li, Q.; Chen, C.; Liu, L.; He, G.; Chen, G. *J. Am. Chem. Soc.* **2016,** *138,* 3926–3932. doi:10.1021/jacs.6b01384
71. Li, Y.; Yang, Y.; Yu, B. *Tetrahedron Lett.* **2008,** *49,* 3604–3608. doi:10.1016/j.tetlet.2008.04.017
72. Giltrap, A. M.; Dowman, L. J.; Nagalingam, G.; Ochoa, J. L.; Linington, R. G.; Britton, W. J.; Payne, R. J. *Org. Lett.* **2016,** *18,* 2788–2791. doi:10.1021/acs.orglett.6b01324
73. Dhara, S.; Gunjal, V.; Handore, K. L.; Reddy, S. D. *Eur. J. Org. Chem.* **2016,** 4289–4293. doi:10.1002/ejoc.201600778
74. Goodreid, J. D.; de Silveira dos Santos, E.; Batey, R. A. *Org. Lett.* **2015,** *17,* 2182–2185. doi:10.1021/acs.orglett.5b00781

License and Terms